

# **Physico - Chemical Studies on Micellar Properties of Selected Amphiphiles**

*Thesis Submitted for the Degree of Doctor of Philosophy  
(Science) of the University of North Bengal*

*By*

**Subrata Chakraborty**

**Supervisor**

**Professor Swapan Kumar Saha  
Department of Chemistry  
University of North Bengal**

**Department of Chemistry  
University of North Bengal  
Darjeeling, India  
August-2015**



Th  
547.84  
C435p

279287

05 AUG 2016

## DECLARATION

I declare that the thesis entitled “**Physico - Chemical Studies on Micellar Properties of Selected Amphiphiles**” has been prepared by me under the guidance of Dr. Swapan K. Saha (Supervisor), Professor of Chemistry, University of North Bengal. No part of this thesis has formed the basis for the award of any degree or fellowship previously.

*Subrata Chakraborty*  
*20/8/15*

**Subrata Chakraborty**  
Department of Chemistry  
University of North Bengal  
Darjeeling-734013  
West Bengal  
India

# University Of North Bengal



Professor S. K. Saha  
**DEPARTMENT OF CHEMISTRY**

Email: [ssahanbu@hotmail.com](mailto:ssahanbu@hotmail.com)

Ph: ( 0353 ) 2776 381  
Fax: (0353 ) 2699 001  
P.O. North Bengal University  
Raja Rammohunpur  
Dt. Darjeeling.  
PIN – 734 013  
Date-17/08/2015

Ref. No.

## CERTIFICATE

I certify that Subrata Chakraborty has prepared the thesis entitled “**Physico - Chemical Studies on Micellar Properties of Selected Amphiphiles**” for the award of Ph.D. degree of the University of North Bengal, under the guidance of myself (Supervisor). He has carried out the work at the Department of Chemistry, University of North Bengal.

**Dr. Swapan K. Saha**  
Professor of Chemistry  
Department of Chemistry  
University of North Bengal  
Darjeeling-734013  
West Bengal  
India

Date:

## ACKNOWLEDGEMENTS

*At the outset, I would like to thank my supervisor Professor Swapan K. Saha sincerely for giving me the opportunity to carry out my research work leading to Ph.D. degree under his supervision, on a research topic in the field of surface science. I enjoyed the multiple fields addressed within this Ph. D. work, I am indebted to him for his helpful guidance and interest throughout the tenure of my research, especially when precise practical problems arose. Furthermore, I am grateful for the real autonomy he gave me so that I could "explore" the topic by myself and enrich my own ideas.*

*I would like to thank University of North Bengal for providing the laboratory and other facilities. I am thankful to all the faculty members and other staff members of the Department of Chemistry for their kind help and cooperation.*

*My thanks are also due to my group members, Soumik Bardhan, Goutam Bit, Amitabha Chakraborty, Bidyut Debnath, Mrinmay Jha, Moazzam Ali, Gulmi Chakraborty and Madhurima Paul Chowdhury for the nice and academic environment we had together.*

*I am grateful to all the well-wishers who have always extended their helping hands whenever needed. I also thank them for the happy moments we shared together.*

*Finally I express my sincere thanks to my parents, my wife, my son and all the family members for their blessing and encouragement especially during the course of my Ph.D.*

**Date:**

**University of North Bengal**

**Subrata Chakraborty**

# Abstract

Surfactants form aggregates, particularly in aqueous solutions, via hydrophobic and hydrophilic interactions occurring within the same molecule. These exotic molecules have generated a great deal of interests because of their various industrial applications. While the formation of micelles is the consequence of interplay between hydrophobic and hydrophilic parts of the surfactant molecules with water, it is mainly triggered to avoid loss of entropy due to the formation of ordered water cages around hydrophobic part disrupting the hydrogen bonds between water molecules. There are many factors which influence critical micelle concentration (cmc), size, shape and the aggregation number of ionic micelles. Among these factors, the surfactant head group characteristics, including the counter ion interactions, is perhaps the least studied facet, yet one of the pivotal issues which control the shape and size of the micellar aggregate. Strong binding counter ions favorably influence aggregate formation and decrease the cmc via effective charge screening of the head groups. The formation of an ionic micelle from monomeric ions results in a balance between hydrophobic interactions between the hydrophobic part of the micelle-forming ions, electrostatic interactions between their hydrophilic charged parts, as well as with and between the counterions.

Sodiumdodecylbenzene sulfonate (SDBS) is a well known anionic surfactant widely used in the industry for manufacturing detergents, emulsions, degreaser and deinking agents and also for assisting dyeing processes in textile factories. Therefore, this work is concerned with dodecylbenzene sulfonate micelles with a view to investigate the effect of a series of alkali metal counterions, such as  $\text{Li}^+$ ,  $\text{Na}^+$ ,  $\text{K}^+$  and  $\text{NH}_4^+$  on the micellization of DBS. It may be mentioned that the cmc and other thermodynamic parameters of DBS having different counterions have not yet been reported in the literature. Therefore, the present aim is to determine the cmc of DBS with different counterions within the temperature range of  $10^\circ\text{C}$  to  $40^\circ\text{C}$  and to determine the relevant thermodynamic parameters of micellization, such as  $\Delta G_m^0$ ,  $\Delta H_m^0$ ,  $\Delta S_m^0$  and  $\Delta_m C_p^0$  along with maximum surface excess concentration ( $\Gamma_{\text{max}}$ ), and the minimum area per molecule ( $A_{\text{min}}$ ) at the surface as a function of hydrated counterion size. Symmetrical tetraalkyl ammonium counter ions with varying alkyl chain length demand special attention because one can study two opposing effects in this series of ions viz., the effect of progressively enhanced hydrophobicity and the effect of increasing dimension of the ions. Counter ion specific

interactions (hydrophobic or hydrophilic) along with change in hydration energy are also very important and this has been discussed in a number of recent reports.

To undertake an in-depth study of the effect of size of the counter ion vis-à-vis its hydrophobicity on the aggregation behaviour of sodiumdodecylbenzene sulfonate, the set of symmetrical tetraalkyl ammonium counter ions with progressively larger groups may be an excellent model which one strives to investigate. This prompted us to synthesize dodecylbenzene sulfonates with tetramethyl, tetraethyl, tetrapropyl and tetrabutyl ammonium counter ions to study their aggregation properties along with the ammonium counter ion.

This thesis contains six chapters. In the first chapter, a general introduction has been given. The second chapter contains the scope and object of the thesis. The third chapter of the thesis presents the result of the effect of alkali metal and organic counterions on the aggregation behaviour of dodecyl benzene sulfonate surfactant. The fourth chapter presents aggregation behaviour of all the surfactants containing alkali metal counter ions and organic counter ions in presence of symmetrical bromide salts and also in presence of an organic additives viz., ethylene glycol. In the fifth chapter, aggregation number has been determined for all the surfactants and dye-surfactant interaction has been studied with an oxazine dye by spectroscopic method. And in the last chapter, effect of cetyltrimethylammonium bromide on the aggregation behaviour of sodium dodecyl benzene sulfonate is presented, since compared to single surfactant, the mixed surfactant exhibits superior interfacial properties such as higher surface activity and lower critical micelle concentration (cmc).

The lithium, potassium and ammonium salts of dodecylbenzene sulfonic acid have been prepared from the pure sodium salt by applying ion-exchange technique. The critical micellization concentrations (cmc) of the surfactants with four different counterions have been determined in a temperature range 10°C to 40°C using surface tension as well as electrical conductivity measurements.

Different tetraalkylammonium viz.,  $N^+(CH_3)_4$ ,  $N^+(C_2H_5)_4$ ,  $N^+(C_3H_7)_4$ ,  $N^+(C_4H_9)_4$  along with simple ammonium salts of dodecylbenzene sulfonic acid were prepared by ion-exchange technique. The cmcs' of dodecylbenzene sulfonate salts with varied counterions were determined by electrical conductivity and surface tension measurements within the

temperature range 283 – 313 K. Counterion ionization constant,  $\alpha$ , the surface parameters  $\Gamma_{max}$  and  $A_{min}$  and also the thermodynamic parameters of micellization process viz.,  $\Delta G_m^0$ ,  $\Delta H_m^0$  and  $\Delta S_m^0$  in aqueous solution have been determined by using pseudo-phase model. The order of cmc in aqueous solution is found to be  $\text{NH}_4^+ > \text{N}^+(\text{CH}_3)_4 > \text{N}^+(\text{C}_2\text{H}_5)_4 > \text{N}^+(\text{C}_3\text{H}_7)_4 > \text{N}^+(\text{C}_4\text{H}_9)_4$  at any given temperature. On the other hand, aggregation number increases with alkyl chain length first due to increasing hydrophobic interactions and then decreases as a function of counterion size passing through a maximum for  $\text{N}^+(\text{C}_2\text{H}_5)_4$ . Spontaneity of micellization in aqueous solution is supported by large negative  $\Delta G_m^0$  as well as the positive entropy change for the micellization process for all the above counterions. At a given temperature,  $\Delta G_m^0$  for surfactant with different counterions followed the order  $\text{N}^+(\text{CH}_3)_4 > \text{NH}_4^+ > \text{N}^+(\text{C}_2\text{H}_5)_4 > \text{N}^+(\text{C}_3\text{H}_7)_4 > \text{N}^+(\text{C}_4\text{H}_9)_4$ . Electrostatic interaction along with effective charge screening and hydrophobicity of the surfactant head group together may give an explanation for the observed variation of aggregation behaviour and the energetics as a function of the nature of counterion.

To study dye-surfactant interaction as influenced by counter ion characteristics, we have taken an oxazine dye (Cresyl fast violet) with dodecylbenzene sulfonate with varying counterions. Due to the dye-surfactant interactions, the changes in spectral characteristics are observed. At concentration below the normal cmc, surfactants and dyes may interact to form a mixed micelle of the two species, lowering the resultant cmc. Above the cmc, a change in the molecular environment of the dye due to incorporation into the micelle interior is observed. The fluorescence spectra of all the surfactant show similar behaviour with the change of surfactant concentrations. The order of the ion pair formation or cluster formation for alkali metal counter ions is as follows:  $\text{Li}^+ > \text{K}^+ > \text{Na}^+$  and for tetraalkyl ammonium counter ion along with ammonium ion is as follows:  $\text{NH}_4^+ > (\text{C}_4\text{H}_9)_4\text{N}^+ > (\text{C}_3\text{H}_7)_4\text{N}^+ > (\text{C}_2\text{H}_5)_4\text{N}^+ > (\text{CH}_3)_4\text{N}^+$ . The trend can be explained as the consequences of the increased charged screening and higher counter ion binding capacity via stronger hydrophobic interactions with the micelles. Anisotropy measurement was done with the same surfactants. The value of the cmc derived from polarization value is in good agreement with the value determined by surface tension and conductometrically for each of the surfactant. In the present experiment, time resolved fluorescence studies were carried out to determine the emission decay parameters of all the surfactants with different surfactant concentrations. The concentration of the dye used was  $5 \times 10^{-6}$  (M). The lifetime values did not change significantly or in a regular manner with the change

in surfactant concentration suggesting single exponential fluorescence decay curve for all the surfactants.

Mixtures of cationic and anionic surfactants show not only synergistic effect of the aggregation properties but also triggered micellar growth in one dimension to form long worm-like micelles. In the first part, the synergistic effect of the mixing of cetyltrimethylammonium bromide (CTAB, a cationic surfactant) with SDBS (an anionic surfactant) is studied under Newtonian flow regime. In the second part, the formation of viscoelastic worm-like micelles is examined and the rheological behavior of the system is investigated under non Newtonian flow regime. Here the cmc's were determined for the mixed surfactant systems of various mole ratios at a particular temperature. The results indicate that the added cationic surfactant (CTAB in this experiment) is assisting in the micelle formation of the anionic surfactants.

The reason for the non-ideal behaviour among surfactant molecules upon mixing are then various types of molecular interactions. The purely energetic effects usually are much smaller for surfactants mixtures like CTAB and SDBS which explains comparatively lower interactions parameter. When the concentrations of the individual component of the mixtures are increased (e.g., CTAB = 100 mM and SDBS = 20 mM), a viscoelastic gel is formed and the flow becomes non-Newtonian in nature. The observed viscoelasticity is related to worm-like micelle (WLM) formation. No cross over point is displayed beyond the temperature range of 303 K - 313 K, except at 281 K.

The plots for the present system fit to a good extent to a simple Maxwell model particularly at 303 K. The large deviation from Cole - Cole plot with high angular viscosity is indicative that of a less structured system with poor viscoelastic behaviour. From the zero-shear viscosity of the surfactant mixtures, it is clear that with increase in temperature,  $\eta_0$  increases indicating an increase in the curvature energy for surfactant aggregates which leads to an increase in micellar length and the formation of wormlike micelles. In summary, all these results support a fascinating and complex rheology to exist in the present system is a structural evolution from a spherical micelle to a worm like micelle. Finally, the shift in cross over frequency  $\omega$  to higher values indicate that the relaxation time  $\tau$  decreases with temperature.

4.2.3. Results and discussion	152
References	172

## **Chapter V**

### **Aggregation number of dodecyl benzene sulfonate micelles with varying counterion and the interactions with oxazine dye in aqueous media: A fluorescence spectroscopic Study** 177-224

5.1 Introduction	177
5.2. Steady state fluorescence	178
5.3 Determination of aggregation number by fluorescence spectroscopy of dodecyl benzene sulfonate with varying counter ions	180
5.3.1. Introduction and review of the previous work	180
5.3.2. Theory	181
5.3.3. Materials and method	185
5.3.4. Results and discussion	186
5.4. Studies of interactions with oxazine dye in aqueous media	198
5.4.1. Introduction and review of the previous work	198
5.4.2 Materials and methods	199
5.4.3 Results and discussions	200
5.5 Anisotropy	212
5.5.1. Theory of anisotropy	212
5.5.2 Materials and methods	213
5.5.3 Results and discussions	213
5.6 Lifetime measurements	221
References	222

## **Chapter VI**

### **Effect of cetyltrimethylammonium bromide on the aggregation behaviour of sodiumdodecylbenzene sulfonate** 225-259

6.1. Introduction and review of the previous work	225
6.2.Theoretical models for analyzing mixing behaviour of surfactants	227
6.3. Experimental	230
6.4. Preparation of solution of SDBS-CTAB mixed micelle system	231
6.5. Results and discussion	231
References	256

## **Chapter VII**

### **Summary and conclusion** 260-273

### **List of Publications** 274

# Table of Contents

	Page No.
<b>Chapter I</b>	
<b>Surfactant Aggregation in Solution</b>	<b>1-28</b>
1.1 General introduction	1
1.2. Aggregation of surfactant molecules	3
1.3. Structure and shape micelles: The molecular packing parameters	4
1.4. Amphiphiles in aqueous medium	8
1.5 Aggregation number of micelle	15
1.6. Oxazine dye	16
1.7. Dye-surfactant interactions in aqueous medium	18
1.8. Effect of addition of a surfactant to the aggregation of another surfactant	20
References	22
<b>Chapter II</b>	
<b>Scope and object</b>	<b>29-38</b>
Scope and object	29
References	36
<b>Chapter III</b>	
<b>Physico - chemical behaviour of Dodecyl benzene sulfonate micelles as influenced by counter ion characteristics</b>	<b>39-103</b>
3.1. Introduction and review of the previous work	39
3.2 Effect of counterion in aqueous medium	43
3.3 Thermodynamics of micellization: The Mass-action model	44
3.4. Materials and methods	49
3. 5. Results and discussions	52
3. 5. 1. <i>Critical Micelle Concentrations (cmc)</i>	52
3. 5. 2. <i>Surface Parameters</i>	73
3. 5. 3. <i>Thermodynamic Parameters</i>	75
3.6. Effects on the micellization of SDBS, SDS and AOT also with different counter ions: A brief comparison	85
References	98
<b>Chapter IV</b>	
<b>Aggregation behaviour of dodecyl benzene sulfonate in presence of symmetrical bromide salts and ethylene glycol</b>	<b>104 - 176</b>
4.1. Dodecyl benzene sulfonate in presence of symmetrical bromide salts	104
4.1.1. Introduction and review of previous works	104
4.1.2. Materials and methods	107
4.1.3. Results and discussions	107
4.1.3.1. Critical micellization concentration (cmc)	107
4.1.3.2. Degree of counter ion binding ( $\beta$ )	142
4.1.3.3. Thermodynamics of micellization	144
4.1.3.4 Thermodynamic properties	148
4.2. Dodecyl benzene sulfonate in presence of Ethylene glycol in aqueous medium	149
4.2.1 Introduction and review of the previous work	149
4.2.2. Material and methods	152

# **Chapter I**

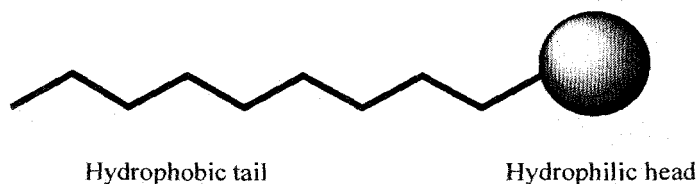
## **Surfactant aggregation in solution**

# Chapter I

## Surfactant aggregation in solution

### 1.1. General introduction

The "Surface Chemistry" is the branch of chemistry deals with the nature of the surfaces and also changes occurring on the surfaces of substances which may be liquid, gas or solid. The study of surface chemistry is not applicable for only academic interest but also for various technical applications of industry and our daily lives including different biological fields. In surface chemistry, we are concerned with the term "Surfactants" which comes from the common contraction of the term "Surface-active-agents". As the name suggest, they are the versatile chemical substances that modify the surfaces or interfaces of the systems in which they are contained. Surfactants have the ability to locate at the surfaces thereby altering significantly the physical properties of the interfaces [1, 2]. The interface at which a surfactant is adsorbed can be between two immiscible liquids, the liquid-gas (air) surface or between a solid and a liquid. This is due to the characteristics molecular structure of the surfactant molecules. Surfactant molecules have two parts in their molecular structure: a hydrophilic (polar) part which likes water or other polar molecules, and a hydrophobic (non-polar) part which does not like any other polar molecules but likes non-polar molecules. They are often also called amphiphiles. In short, the characteristic molecular structure of surfactants is amphiphilic in nature (from the Greek *amphi* meaning 'on both sides' and *philein* meaning 'to love') within the same molecular unit. The common schematic representation of the surfactant molecules is shown in **Figure 1.1**.



**Figure 1.1** A common schematic representation of a surfactant molecule.

The non-polar part (water repelling or hydrophobic part) which generally consists of long chain hydrocarbon is also called a 'tail' whereas the polar part (water attracting or hydrophilic part) is termed as 'head'.

The hydrophobic part is of many different types, viz., aliphatic, aromatic or the mixture of both which generally originates from natural fats and oils, petroleum fractions, relatively short synthetic polymers, or relatively high molecular weight synthetic alcohols. The hydrophobic part is also less often halogenated or oxygenated hydrocarbon or sometime bears siloxane chain, where as the hydrophilic part is, in general, of four types, viz., cationic, anionic, nonionic and zwitterionic [2].

- (a) *Anionic*: In anionic surfactants, generally the carboxylates (soap), sulphates, sulfonates and phosphates are present with the hydrophobic part as hydrophiles which here acts as a surface active portion, e.g.,  $\text{RCOO-Na}^+$  (soap),  $\text{RC}_6\text{H}_4\text{SO}_3\text{-Na}^+$  (alkyl benzene sulfonate). All of these still feature extensively in cleaning formulations.
- (b) *Cationic*: In cationic surfactants, generally some forms of amines are present with the hydrophobic part as hydrophiles which here act as a surface active portion, e.g.,  $\text{RNH}_3^+$  (salt of long chain amine),  $\text{RN}(\text{CH}_3)_3^+\text{Br}^-$  (quaternary ammonium bromide). The positive charge on the head group gives the surfactants a strong substantivity on negatively charged fibres, such as cotton, and they are, therefore, used in fabric.
- (c) *Non-ionic*: In non-ionic surfactants, the surface active portion bears no apparent ionic charges, e.g.,  $\text{RCOOCH}_2\text{CHOHCH}_2\text{OH}$  (monoglyceride or long chain fatty acid),  $\text{RC}_6\text{H}_4(\text{OC}_2\text{H}_4)_x\text{OH}$  (polyoxyethylenated alkyl phenol). They are used extensively in low-temperature detergency and as emulsifiers.
- (d) *Zwitterionic*: Zwitterionic surfactants often referred to as amphoteric surfactants. In this types of surfactants, there are both positive and negative part with the hydrophobic part as hydrophiles. These are often found in the form of  $-\text{N}^+(\text{CH}_3)_2\text{CH}_2\text{COO}^-$  (betaines),  $-\text{N}^+(\text{CH}_3)_2\text{CH}_2\text{SO}_3^-$  (sulphobetaines) and  $-\text{O-PO}_3\text{-CH}_2\text{CH}_2-\text{N}^+(\text{CH}_3)_3$  (lecithins/phosphatidyl cholines).

Apart from these four major types of surfactants, combinations of the above head group types are increasingly being used within a single surfactant. The most common are those that have both non-ionic and anionic groups such as the  $-(\text{OCH}_2\text{CH}_2)_n\text{OSO}_3^-$  (alkyl ethoxy sulphates). Surfactants of this type are mild on the skin and are, therefore, used in formulations where skin contact is not usually avoided.

In double chain surfactants, two hydrocarbon chains are attached to a polar head. On the other hand, Gemini surfactant contains two hydrophobic and two hydrophilic groups. Amphiphilic molecules can also have two head groups which may be both anionic, both cationic or one anionic and the other cationic, joined by hydrophobic spacer [2]. These types of molecules are termed "bola-amphiphiles" commonly known as "bolaforms" [3]. Surface activity of these molecules depends on both the hydrocarbon chain length and the nature of head group(s).

## 1.2. Aggregation of surfactant Molecules

Self-assembled surfactants or surfactant aggregates become popular to the researchers in recent years due to a huge benefit achieved in many industries producing detergents, cosmetics and pharmaceuticals which have surfactants as one of their constituents [4-6]. The spontaneous organization of molecules driven by intermolecular interactions into stable aggregates is the self-assembly of surfactants which is well recognized in biological systems, e.g., lipid bilayers, the DNA duplex, tertiary and quaternary structure of proteins. The process of spontaneous aggregation of simple molecules in solution into larger structures with a certain order is also an important phenomenon in every-day life as well as an interesting subject for scientific investigations. The best known example of aggregation in every-day life is the formation of "micelle" by surfactant or detergent molecules as has already been explained. The term micelle is used for an entity of colloidal dimension (radius of the colloid molecules  $10^{-5} - 10^{-7}$  cm), in dynamic equilibrium with the monomer solution from which it is formed. The concentration at which the ions (head groups) are pulled into the bulk of the solution and form a cluster of molecules in which hydrophobic tails are in the interior of the cluster and ionic ends are at the surface of the cluster is

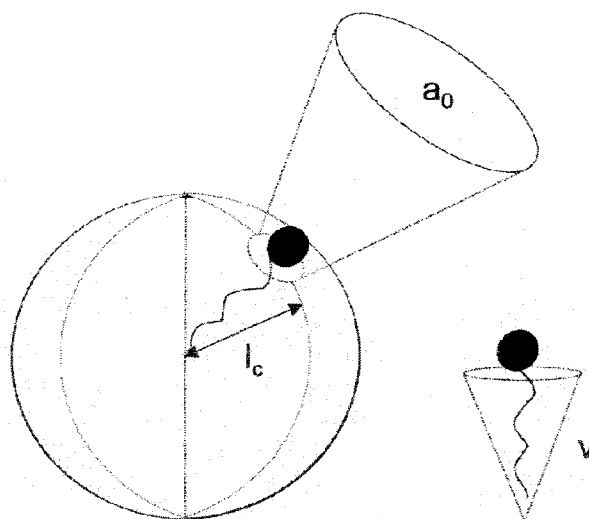
known as critical micelle concentration (cmc). Above the critical micelle concentration of the surfactant concentration, the addition of fresh monomer results in the formation of new micelles. Here the monomer concentration remains essentially constant and equal to the cmc. Due to three dimensional hydrogen bonding of water molecules, it has an open structure which permits the existence of clusters of water molecules containing cavities with specific sizes which can accommodate non-polar chains [7-9]. Creation of the cavity restricts the motions of solvent molecules in the hydration shell of a non-polar solute. This restriction leads to loss of entropy, which is exceptionally large in aqueous solution due to the small size of water molecules [8-12]. For a given surfactant, at a given temperature, only a certain amount of monomer can be accommodated in the cavities and any further addition of surfactant will result in the formation of micelles. In other words, the further addition of surfactant provides a driving force to minimize contact of the monomer hydrocarbon chains with water. Therefore, according to Langmuir's principle of differential solubility, the hydrocarbon chains cluster to form a core (micellar core) while the polar groups interact with the water [13]. Each micelle consists of a certain number of monomer molecules (aggregation number,  $n$ ) which determines its general size and shape. The exact size and shape of micelles is still uncertain but that of an ionic micelle in dilute salt-free conditions it is known to be spherical [10]. The region adjacent to the stern layer contains a high density of counter ions of the polar heads (Gouy Chapman double layer) and separates the hydrophobic interior from the bulk aqueous phase [14].

### 1.3. Structure and shape of micelles: The molecular packing parameters

In solution, a dynamic equilibrium exists between surfactant monomers and micelles. Therefore, it may be to some extent unrealistic considering them to be rigid with precise structures and shapes. The spherical shape of the micelle was conceived by Hartley [15]. The micelle having regular shape are supported by different studies of micellar solutions, viz., dynamic light scattering (DLS) studies, Small-angle neutron scattering (SANS) studies, phase diagram studies etc [16-24]. The general assumption is that the micelles at critical micelle concentration are roughly spherical. The radius of a micelle cannot be greater than the stretched-out length of the surfactant molecule. Typically micelles may have average radii of 1.2 - 3 nm and can contain 5 - 100

monomer units. Other proposed structures of micelles are rod-like [25], lamellar model [26], cylindrical model [27] etc. Added electrolyte has great influence on the shape of ionic micelles. As the counterion concentration is increased, the shape of ionic micelles changes in the sequence spherical - cylindrical - hexagonal - lamellar [17-18, 21, 28-30]

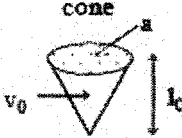


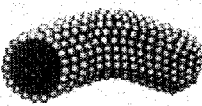

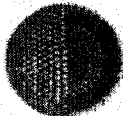

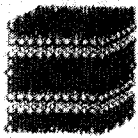


The molecular packing parameter allows a simple and also intuitive insight into the self-assembly phenomena and that is why it is most cited in different science subjects and topics [31-32]. The packing parameter approach permits indeed to relate the shape of the surfactant monomer to the aggregate morphology [33-35]. The molecular packing parameter  $P$  is defined as the ratio  $v/a_0 l_c$ , where  $v$  and  $l_c$  are the volume and the extended length of the surfactant tail, respectively and  $a_0$  is the equilibrium area per molecule at the aggregate interface (or mean cross-sectional (effective) head-group surface area), as illustrated in figure 1.2. If we consider a spherical micelle with a core radius  $R$ , made up of  $N_{agg}$  molecules, then the volume of the core is  $V = N_{agg} \times v = 4 \pi R^3/3$ , the surface area of the core  $A = N_{agg} \times a_0 = 4\pi R^2$ . Hence, it can be deduced that  $R = 3 v/a_0$ , from simple geometric relations. If the micelle core is packed with surfactants tails without any empty space, then the radius  $R$  cannot exceed the extended length  $l_c$  of the tail. Introducing this constraint in the expression for  $R$ , one obtains  $0 \leq v / a_0 l_c \leq 1/3$ , for spherical micelles. These geometrical relations, together with the constraint that at least one dimension of the aggregate (the radius of the sphere or the cylinder, or the half-bilayer thickness, all denoted by  $R$ ) cannot exceed  $l_c$ , lead to the following well-known connection between the molecular packing parameter and the aggregate shape [33], i.e.,  $0 \leq v/a_0 l_c \leq 1$  for bilayers. Inverted structures are formed when  $P > 1$ . This can be easily understood from a figure showing the critical packing parameter with head group area, extended length and the volume of the hydrophobic part of a surfactant molecule. From this figure, it can also be concluded that the radius of a micelle cannot be greater than the stretched-out length of the surfactant molecule.



**Figure 1.2.** The critical packing parameter  $P$  (or surfactant number) relates the head group area, the extended length and the volume of the hydrophobic part of a surfactant molecule into a dimensionless number  $P = v / a_0 l_c$ .

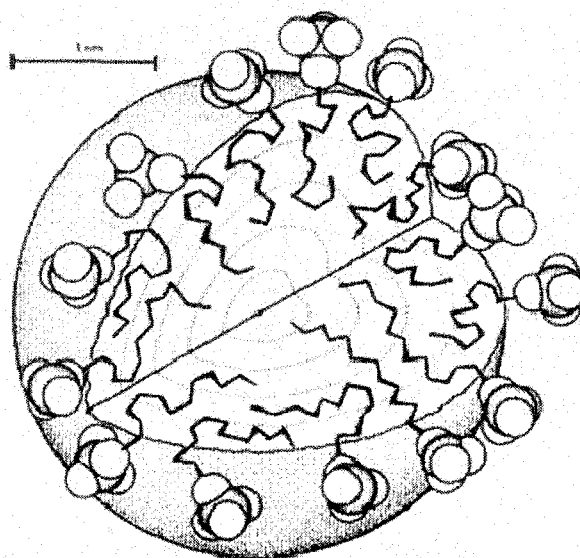
Therefore, if the molecular packing parameter is known, the shape and size of the equilibrium aggregate can be readily identified. Nagarajan showed that the tail length influences the head group area (considering the tail packing constraints) and thereby the micellar shape [32]. It is important to note that  $a_0$  is often referred to as the “headgroup area” in the literature. This has led to the erroneous identification of  $a_0$  as a simple geometrical area based on the chemical structure of the headgroup, although  $a_0$  is actually an equilibrium parameter derived from thermodynamic considerations [32]. Needless to say, that for the same surfactant molecule, the area  $a_0$  can assume widely different values depending on the solution conditions such as temperature, salt concentration, additives present, etc.; hence, it is meaningless to associate one specific area with a given head group. For example, sodium dodecyl benzene sulfonate forms micelle in aqueous solution whereas bilayers structures are formed when alkali metal chlorides are added [35] resulting different  $a_0$  values in these two cases. Moreover, the role of the surfactant tail has been virtually neglected. This is in part because the ratio  $v / l_c$  appearing in the molecular packing parameter is independent of the chain length for common surfactants ( $0.21 \text{ nm}^2$  for single tail surfactants) and the area  $a_0$  depends only on the head group interaction parameter. The predicted aggregation characteristics of surfactants are presented in Table 1.1.

**Table 1.1.** Schematic representation of surfactant structures and shapes derived from various packing parameters.

Possible surfactant type	$P (= v / a_0 l_c)$	Shape	Structure formed
Single-tail surfactants with large head groups	$< 1/3$	cone 	spherical micelles 
Single-chain surfactants with small head groups	$1/3 < P < 1/2$	truncated cone 	cylindrical micelles 
Double-chain surfactants with large head groups and flexible chains	$1/2 < P < 1$	truncated cone 	flexible bilayers, vesicles 
Double-chain surfactants with small head groups or rigid, immobile chains	$P \sim 1$	cylinder 	planar bilayers 
Double-chain surfactants with small head groups, and bulky chains	$P > 1$	inverted truncated cone or wedge 	inverted micelles 

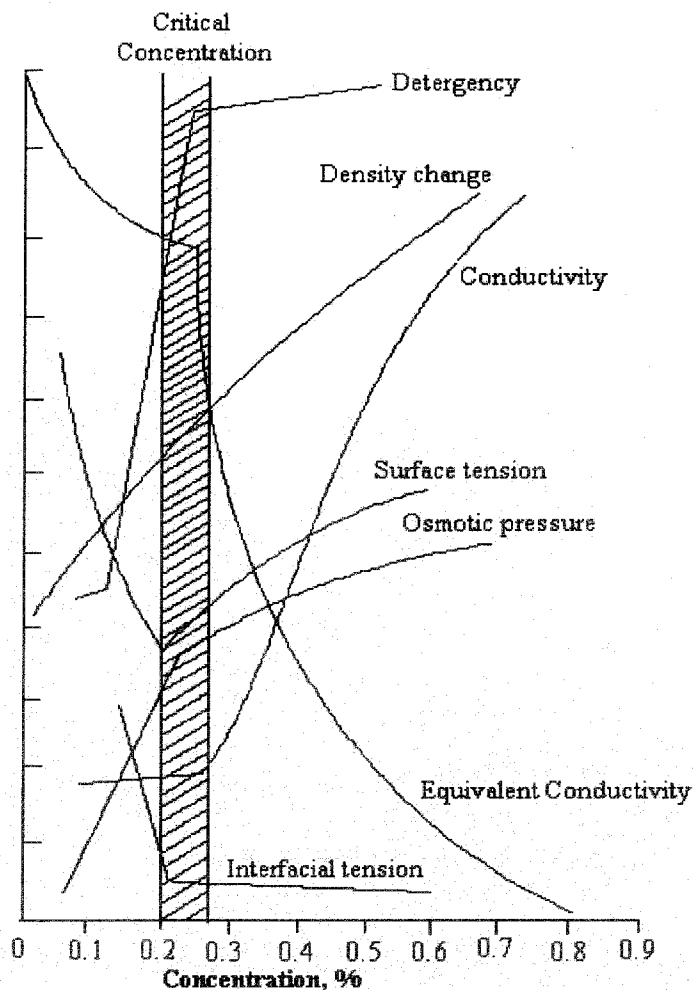
#### 1.4. Amphiphiles in aqueous medium

The most intensely studied and debated type of molecular self-assembly and perhaps the simplest in terms of the structure of the aggregate is the micelle. They are loose, mostly spherical aggregates above their critical micellization concentration (cmc) in water or organic solvents. The schematic representation of a spherical micelle in aqueous solution is shown in Figure 1.3. In this figure, the hydrophobic chains are directed towards the interior of the aggregates and the polar head-groups points towards water, hence allowing the stability/solubility of the aggregate (no phase separation) [2].



**Figure 1.3.** Schematic representation of a spherical micelle in aqueous solution.

As stated earlier, micelles are in dynamic equilibrium with the monomer from which it is formed. The physical properties of the surfactants are different in pre-micellar and post micellar region. It is interesting to note that although it is usually assumed that there are fairly well-defined water layers around the micelle surface, there is no agreement on the composition of the micellar core [36], i.e., whether it consists of pure hydrocarbon or of hydrocarbon mixed with water is not certain. The penetration of water molecules in the micellar core [37] is still a matter of controversy.



**Figure 1.4.** Schematic representation of the concentration dependency of some physical properties for solutions of a micelle forming surfactant.

All types of surfactants viz., cationic, anionic, nonionic and also zwitterionic, can form micelles in aqueous solutions. An important criterion of a versatile solvent is to form hydrogen bonds as like water molecules. When the non-polar unit of the surfactants is introduced in water, the hydrogen bonding network of water molecules is (Figure 1.5) disrupted and the water molecules order themselves around the nonpolar part to satisfy hydrogen bonds resulting in an unfavourable decrease in entropy in the bulk water phase.

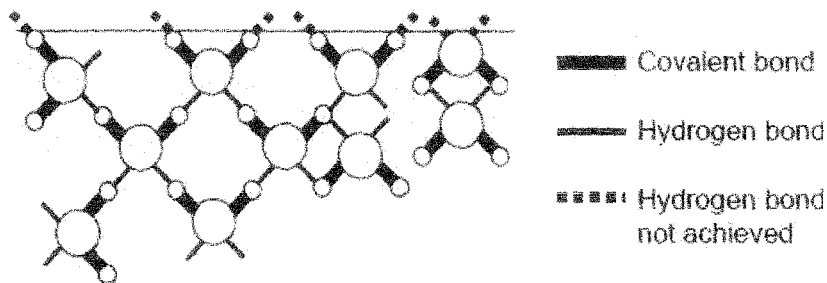


Figure 1.5. Water molecules at the liquid-air interface.

As additional non-polar units are added to the solution, they self-associate and reduce the total water-accessible surface of the complex relative to the monodisperse state. Now, fewer water molecules are required to rearrange around the collection of non-polar groups (Figure 1.6). As a result, entropy associated with the complex is less unfavourable than for the monodisperse detergents. In short, hydrophobic association and the formation of micelles is driven by the favourable thermodynamic effect on the bulk phase of water.

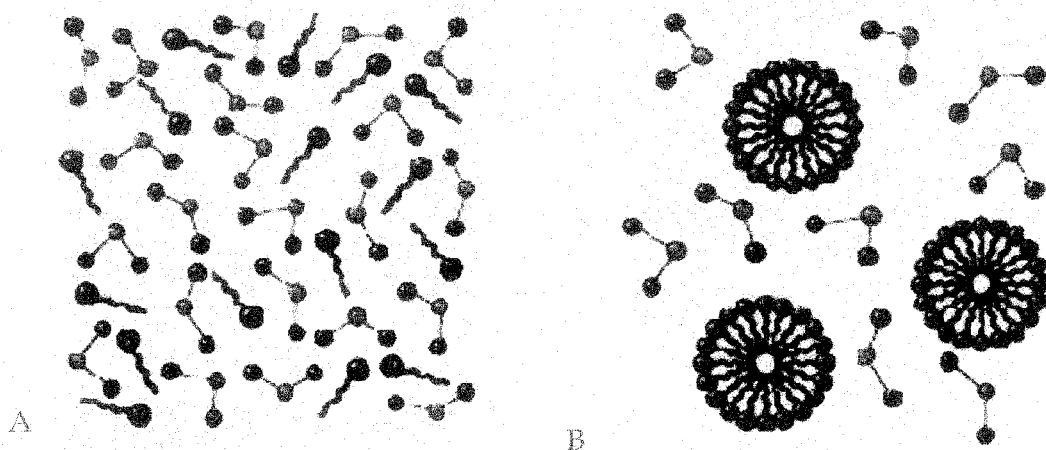


Figure 1.6. (A) Water molecules ordered around surfactant monomers. (B) Loss of total water-accessible surface as a result of micellization.

Only average shape and aggregation number of a micelle can be determined due to its short life-span in dynamic equilibrium. Micellization is the results of the hydrophobic effect present in the surfactant molecules. In micellization there are two opposing forces working together. The first is the hydrophobicity of the hydrocarbon tail, favoring the formation of micelles and second is the repulsion between the surfactant head groups. The mere fact that micelles are formed from the ionic surfactants is an indication that the hydrophobic driving force is large enough to overcome the electrostatic repulsion arising from the surfactant head groups. A large

number of theoretical and experimental researches by different methods have been carried out to understand the structure and thermodynamic and other property of the micelles employing various methods [38-40].

The controversial "water exposure of micelles" concept [41, 42] discusses in terms of predictions of the main characteristics of the molecular conformation of micelles by using "phase separation model" or "mass action model" [43-45]. These models predictions are in agreement with the experimental data with the following assumption with some principal features of micellar structure.

- (I) The micellar core is virtually devoid of water, according to Langmuir's original principle of differential solubility.
- (II) Micellar chains are randomly distributed and steric forces determine the final structure.
- (III) Contact of the hydrophobic sections of the micelle with water results from a disordered structure in which the terminal groups or chain ends are near the micellar surface and thus exposed to bulk water [46].

The mass action model along with the related thermodynamics of micelle formation is discussed in chapter III.

A lot of research work has been devoted by numerous workers to elucidate various factors responsible for cmc [47]. Among the factors that are known to affect the cmc in aqueous solutions are:

- (I) The structure of the surfactant
- (II) The presence of added electrolyte (in the case of ionic surfactants) in solution
- (III) The presence of various organic compounds in solution, and
- (IV) Temperature of the solution.

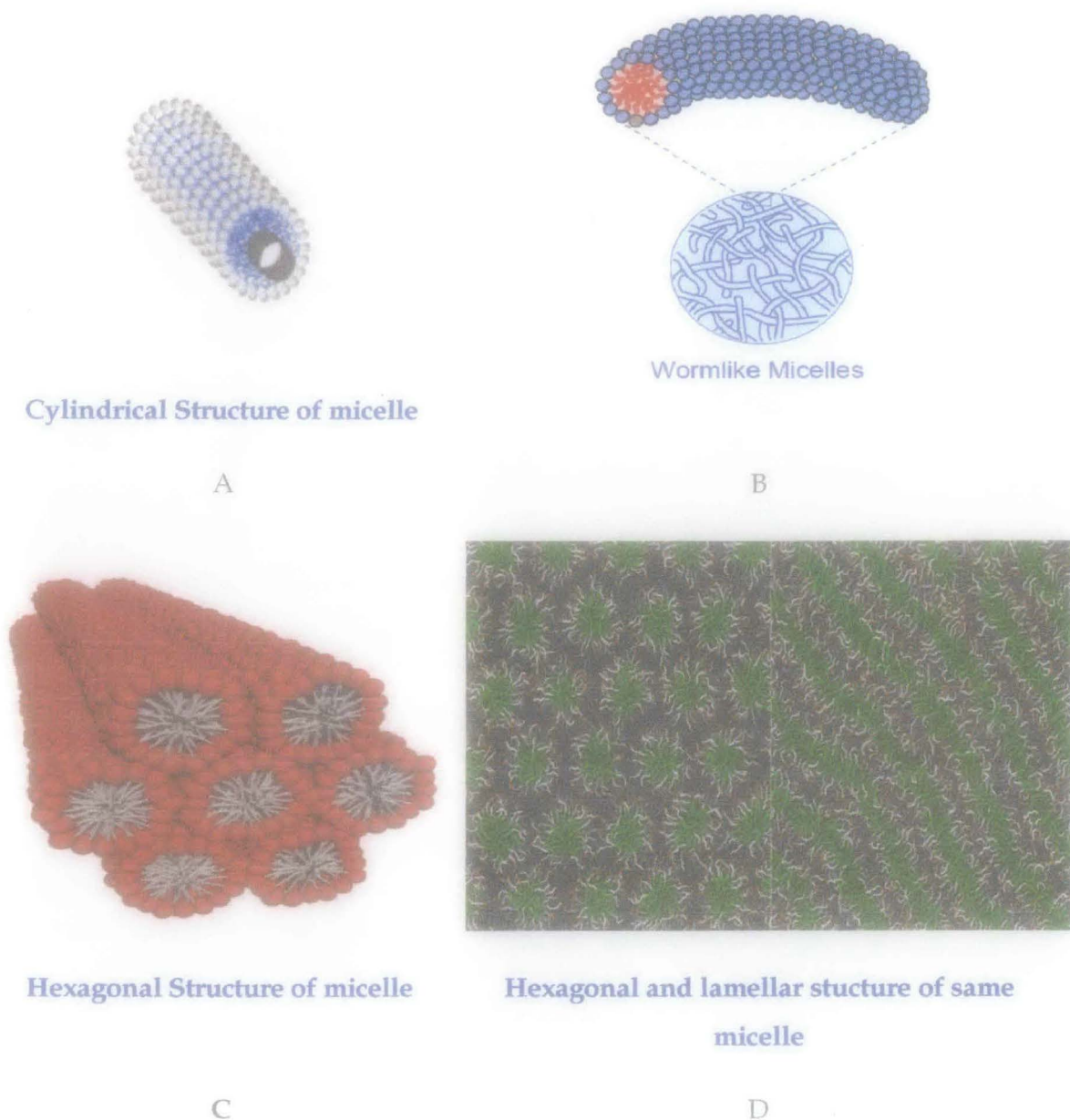
**Surfactant structure:** Generally it is known that the non-ionic surfactants have lower cmc values as compared to the ionic surfactants and this cmc value decreases with the increase in hydrophobicity of the surfactant molecules. It is also known that the cmc value becomes halved by addition of one methylene group to the hydrocarbon tail. But this decrease is not similar incase of nonionic and zwitterionic surfactants. It is known

that the cmc decreases in case of nonionic and zwitterionic surfactants to one fifth of its previous value on addition of one methylene group to the hydrocarbon tail. The unsaturation of hydrocarbon chain has also great influence on the cmc value. It is also known that the increase of unsaturation increases the cmc of the surfactant. On the other hand, introduction of a polar group such as - O or - OH to the hydrocarbon chain increases the cmc to a significant extent. However, replacement of hydrocarbon chain by a fluorocarbon chain of same length causes a decrease in cmc values. For n-alkyl ionic surfactants, the cmc decreases in the order ammonium salts > carboxylates > sulfonates > sulfates. It has also been found that in quaternary cationics, trimethylammonium compounds have higher cmc's than the corresponding pyridinium compounds.

**Counterion:** With changes of the counterion, the cmc value of the surfactant changes significantly. The degree of counterion binding plays an important role in determining the value of cmc. For alkali metal counterion and also for other counterions, with increase in the hydrated radius, cmc increases. This cmc increase is due to the weaker counterion binding with increase in hydrated radius of the counterions. In aqueous solution, the cmc values of sodium dodecyl sulfate with different counterion shows the order:  $\text{Li}^+ > \text{Na}^+ > \text{K}^+ > \text{Cs}^+ > \text{NH}_4^+ > \text{N}(\text{CH}_3)_4^+ > \text{N}(\text{C}_2\text{H}_5)_4^+$ . Also similar variation is seen for the cationic surfactants with change in anionic counterions. For cationic dodecyltrimethylammonium and dodecylpyridinium salts, the order of cmc in aqueous solution are  $\text{F}^- > \text{Cl}^- > \text{Br}^- > \text{I}^-$ .

**Electrolytes:** With addition of electrolytes to a surfactant solution, the cmc value decreases to a certain extent. But this decrease is very small for nonionic surfactant as compared to the cationic and anionic surfactants. Also for zwitterionic surfactant this decrease is much higher as compared to the anionic or cationic surfactants due to the stronger interactions of the surfactants and electrolyte present in the solution. Screening of charge by the ions of the added electrolyte to the head group of surfactant is mainly responsible for the decrease in cmc values. Added electrolyte has great influence on the shape and aggregation number of the ionic micelles. As the counterion concentration is increased, the shape of ionic micelles changes in the

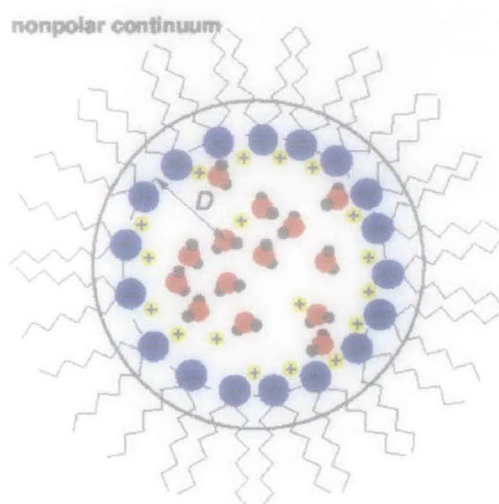
sequence spherical – cylindrical – hexagonal – lamellar. The different forms of micelle are shown in figure 1.7.



**Figure 1.7.** (A) Structure of a cylindrical micelle. (B) Microstructure of a typical wormlike micelle formed from cylindrical micelle. (C) Hexagonal shape micelle (D) Structural changes from hexagonal micelle to lamellar micelle.

But the charge screening effect is not responsible for nonionic and zwitterionic surfactants. Here, mainly "salting out" and "salting in" of the hydrophobic group in aqueous solvents are responsible for decrease in cmc.

**Organic additives:** Polar organic compounds such as alcohols with longer chains and water miscible properties generally decrease the cmc of surfactants to a much lower concentration than in aqueous solutions. But shorter chain length alcohols with high degree of polarity, the effect will be reverse. So, the effect of alcohols on the cmc of the surfactants depends on the chain length and the solubility of the alcohol present in the systems. Alcohols with short chain length are mainly adsorbed in the water-micelle interfacial region but alcohols with longer chain length are adsorbed in the outer portion of the micellar core. On the other hand, additives like urea, formamide, guanidinium salts, fructose and xylose increases the cmc to relatively higher concentrations by modifying the interaction of surfactant molecules with water. When the surfactants aggregate in non polar solvents, their polar or charged groups are located in the interior, or core, of the aggregate, while their hydrocarbon tails extend into the bulk solvent. These aggregates are referred to as reverse micelles (Figure 1.8).



**Figure 1.8.** Schematic representation of a reverse micelle formed from a double tailed surfactant.

**Temperature:** The effect of temperature on the cmc of surfactants in aqueous solution is generally first to decrease with temperature and then to increase with temperature passing through a minimum in between these two. But there are also other types of variation observed in the literature, for example, with increase in temperature the cmc of the surfactant increases. Increase of temperature causes decrease of hydration of the hydrophilic group, which favours micellization and also causes disruption of the structured water surrounding the hydrophobic group. This disfavors micellization.

The relative magnitude of these two opposing effects, therefore, determines increase or decrease of the cmc value. Pronounced effect of temperature appeared in case of double chain surfactants. It is known that turbid, liposomal dispersions of didecyldimethyl ammonium bromide at room temperature become a clear solution when heated to 60°C due to formation of small micellar aggregates [48-49].

### 1.5 Aggregation number of micelle

An aggregation number of a micelle is defined as the number of surfactant molecules present in a micelle once the critical micelle concentration (cmc) has been reached. It is one of the most important and fundamental structural parameters of micellar aggregates [50]. Different methods are employed to determine the aggregation number of the micelles. The value of the aggregation number contains information on the micellar size and shape, which may be important in determining stability and practical applications of the investigated systems [50-52]. Generally, aggregation number of a micelle can vary from 10 to 100. But in the literature, aggregation number of 3 is also reported. Further, the aggregation number changes with the solvent or electrolyte present in the systems. It has been observed by different researchers that the addition of electrolyte generally increases the aggregation number of the micelles. Among the different methods employed to determine the aggregation number, fluorescence probe method is one of the important techniques. In this method, a quencher is added from the outside to the system. And fluorescence intensity is measured with the change of quencher concentration. From these data, aggregation number can be calculated. This method is very popular due to easy availability and handling of the instruments (Fluorescence Spectrophotometer) and also simplicity of the technique. It has been found that the bile salts, which are the main products of cholesterol metabolism, has the aggregation number of 3 (three), as measured by different methods [53]. Similarly, the study of sodium dodecyl micelles in presence of aluminium salt shows the average number of 250 which is much higher than the aggregation number of the same surfactant in aqueous solution [54]. Large volume of the research has been carried out for anionic micelles with sodium dodecyl sulfate [55-58]. It is also known that surfactants with smaller aggregation numbers tend to form more spherical micelle while surfactants with larger aggregation

numbers tend to form ellipsoid micelles. In general, aggregation numbers increase as the length of the hydrocarbon chain increases. Aggregation numbers tend to decrease as the size of the hydrophilic group increases and upon the addition of hydrocarbons and polar compounds to surfactant solutions [59]. Increasing the temperature of solutions of ionic surfactants also causes an increase in the aggregation number. In short, the factors that increase the aggregation numbers are (i) increasing number of methylene groups in the alkyl chain (ii) addition of counterions (for ionic surfactants) whereas the factors that responsible for decrease in aggregation number of a surfactants are (i) increasing size of hydrophilic head group (ii) polar organic additives (iii) Addition of hydrocarbons to solution.

## 1.6. Oxazine Dye

Photo-induced electron transfer processes in surfactant solutions are potentially important for efficient energy conversion and storage because surfactant micelles help to achieve the separation of the photoproducts by hydrophilic-hydrophobic interactions of the products with the micellar interface [60-63]. The visible absorption spectra of organic dyes exhibit a strong dependence on concentration in aqueous solution because of aggregation [64-65]. Aggregation affects colour, solubility and photophysical behaviour of dyes. Self association of fluorescent dyes often leads to self quenching. It plays key roles in many technological applications such as opto-electronic devices, optical logical elements etc. Important examples include sensitization of silver halide nanocrystals in photographic processes and nonlinear optical materials [66-71]. A systematic study of the aggregation characteristics of dyes from spectrophotometric data has become a useful field of research because of its possible application in understanding such phenomena on energy transfer in biological systems, metachromatia, hypochromism, conformation of polypeptides, and staining properties of dyes for biological specimens. The force responsible for holding the component molecules in the dimer or in polymer is not yet well understood. Nevertheless, it is clear that for ionic dyes, aggregation would be possible if there exists some very strong attractive interaction, which first of all overcomes the coulombic repulsion and then brings the component molecules to a reasonable distance to form dimers and subsequently high polymers. Photochemical

systems for photoreduction of water and photoinduced electron transfer reaction in surfactant solutions are of considerable interest as models for understanding of photobiology [72-73] and the conversion of solar energy [74-75]. Compared to inorganic complexes, organic dyes have been investigated only rarely as sensitizers for the photo-reduction of water [74-76].

The properties of oxazine dye aggregates at liquid/solid interfaces have been of interest for long time. It was suggested that solar energy harvesting with wide band gap semiconducting photoconductors may be improved by covering with this dyes to expand the wave length range [68]. The oxazine dyes display surprisingly long wave length absorption and emission maxima given their small sizes and as such have been shown to be important fluorescent probe for biological systems [69-70]. They can be excited with simple laser sources such as solid state laser diodes. Oxazine dyes are also finding increasing applications in the field of electrocatalysis of electrochemical redox processes. Oxazine dye modified electrodes have been shown to be useful in electrocatalytic oxidation of coenzyme NADH in the context of enzyme based biosensors [71]. Examples of oxazine dyes are: oxazine 1, oxazine 170, cresyl fast violet etc. These types of dye have similar structure as that of methylene blue which is one of the most investigated substance in the relevant field of research. The structure of cresyl fast violet is given in figure 1.9:

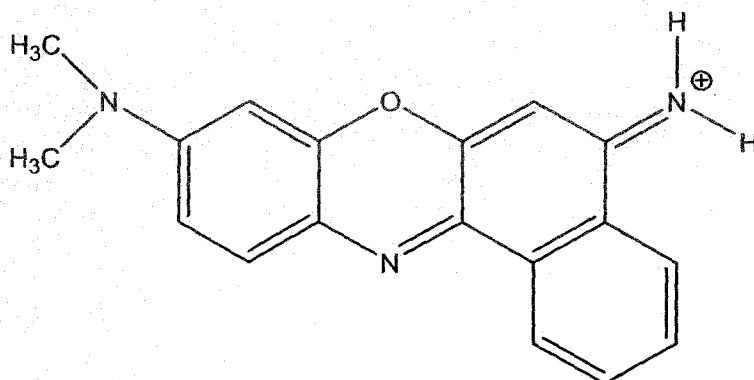


Figure 1.9.: Schematic representation of Cresyl fast violet.



Oxazine dyes are known to form non-fluorescent H-aggregates, which have the dimers stacked on top of each other ( $\pi$ -stacked dimers). In H aggregates, only transitions to the higher of the two states are allowed which means that the light

absorbed by these dimers to make this transition will be of higher energy, and therefore blue-shifted from the light absorbed by the monomer.

### 1.7. Dye-Surfactant Interactions in Aqueous Medium

Surfactants exert profound effects on many chemical reactions and interactions arise mainly from change in the local environments and concentrations of interacting species due to the interactions with the surfactant micelles. In order to elucidate the nature of effects of surfactants and to design desirable surfactant systems, it is essential to understand the nature of interactions between probe molecules and surfactants [77]. The dye-surfactant systems have attracted considerable amounts of interest in recent years. The enhanced energy transfer between dyes in dye-surfactant systems made them good model membrane systems of chloroplast [78-81]. The peculiar behavior in both absorption and fluorescence spectra of dyes in the presence of surfactants of opposite charge were attributed to the formation of a continuum of dye - surfactant aggregates: dye ratio (S/D) [82-86]. Photoinduced electron transfer processes in surfactant micelles help to achieve the separation of the photoproducts by hydrophilic-hydrophobic interactions of the products with the micellar interface. Dye surfactant interactions are generally complex [87]. In dye surfactant interactions, molecular complexes having specific and characteristics physicochemical features may be formed. Also, physico-chemical properties of the adsorbed dye can be controlled with ease by the incorporation of some oppositely charged surfactant assembly. The very high polarity (large dielectric constant) of water arises principally from the extended hydrogen bond network and mutual polarization of the water molecules in close proximity. Because of polarization, the dipole moment of water in the liquid phase (2.6 D) is higher than that in vapour (1.85 D). A water molecule bound to a dye molecule cannot polarize another water molecule. This causes a marked reduction in the dielectric constant of the hydration layer of an organized assembly compared to bulk water and hence the dye-surfactant interactions in aqueous solution is also important to know the interaction thoroughly. From early times, the colour changes of ionic dyes in presence of surfactants in aqueous solution have led many researchers to propose dimer and multimer formation of dye molecules in the surfactant micelle, this area is still important and interesting for theoretical, ecological and technological point of view [88-89]. The interest in fluorescent dyes for qualitative and quantitative assays

has increased considerably during the last few decades. The sensitivity, simplicity and selectivity of fluorescent-based techniques make them particularly attractive for *in vitro* and *in-vivo* cellular and molecular biology studies. There are several major advantages of using fluorescent dyes that absorb in the red over those that absorb at shorter blue and green wavelengths. The most important of these advantages is the reduction in background that ultimately improves the sensitivity achievable. There are three major sources of background: (I) elastic scattering, i.e., Rayleigh scattering, (ii) inelastic scattering, i.e., Raman scattering and (III) fluorescence from impurities. The efficiencies of both Rayleigh and Raman Scattering are dramatically reduced by shifting to longer wavelength excitation. Likewise, the number of fluorescent impurities is significantly reduced with longer excitation and detection wavelength. Besides reduced background, a further advantage is that of low-cost and energy efficient system. A recent report demonstrates that the use of red-absorbing fluorescent labels and diode laser excitation at 635 nm provides sufficiently low autofluorescence of biological samples so that individual antigen and antibody molecules can be detected in human serum samples [90-95]. Among other things, the investigations into the behaviour of different dyes in surfactant aqueous solutions, give useful information about the mechanisms according to which surfactants operate as leveling agents and provide information on the influence of dye-surfactant interactions on the thermodynamics and kinetics of dyeing process. This may directly affect the quality of dyeing, which is one of the goals of textile finishing. To understand the chemical equilibrium, mechanism and kinetics of surfactant sensitized colour reactions, the knowledge of dye-surfactant interaction should also be a great value. Surfactants are also used as solubilizers for dyes which are insoluble in water, to break down aggregates of the dye in order to accelerate adsorption process on fiber, as auxiliaries for improving dye adsorption and as leveling or dispersing agents [96-98]. According to the structures of dye and substrate, surfactants used as leveling agents operate by different mechanisms. It seems probable that once the electrostatic forces have brought together the oppositely charged molecules, hydrophobic interactions take place, dramatically changing the microenvironment experienced by the chromophore. Therefore, a great deal of research work focused on dye-surfactant interactions in binary mixtures including the interactions between ionic dyes and ionic surfactants of the opposite and the same charges, ionic dyes and nonionic surfactants

as well as between nonionic dyes and ionic or nonionic surfactants in the submicellar and micellar concentration ranges of surfactants have been performed [98-104].

It has been observed by Carroll et. al. that sodium dodecyl sulfate in presence of different oxazine dye displays evidences of intermolecular interactions via spectrofluorometric method. The absorption spectra and the emission spectra change with the concentration of the surfactant in different ways. Also with the change of dye, the premicellar and postmicellar spectrophotometric characteristics changes showing different types of interactions with different dyes.

### 1.8. Effect of addition of a surfactant to the aggregation of another surfactant.

Above the critical micelle concentration (cmc), hydrophilic surfactants form small globular micellar aggregates and the solutions show Newtonian flow behaviour. Compared to single surfactant, the mixed surfactant exhibits superior interfacial properties such as higher surface activity and lower critical micelle concentration (cmc). Various such surfactant mixtures have been studied including cationic/anionic, non ionic/non ionic, cationic/non ionic, anionic/non ionic, cationic/cationic surfactants etc. Surfactant mixtures are commonly preferred in medicinal and pharmaceutical formulations and industrial preparations due to the purpose of suspension, solubilization and dispersion. Ionic surfactants can also self assembled to long thread-like or worm-like micelles in presence of certain organic ions e.g., sodium salicylate. Under certain conditions such as concentration, salinity, temperature, presence of counterions, etc., the globular micelles may undergo uniaxial growth and form very long and highly flexible aggregates, referred to as "wormlike" or "threadlike" micelles [105 - 112]. Wormlike micelles [106] are long, self-assembled, semi-flexible, breakable polymers with surfactant heads on the outside and tails in the core and display a striking range of dynamical properties, including anomalous relaxation, shear banding, and rheological chaos [113-114]. Due to this reason, wormlike micelles have received considerable attention from theoretician and experimentalist during the past few decades. A dramatic influence on the viscosity of wormlike micelles in aqueous solutions of CTAB was shown for *trans-ortho*-methoxycinnamic acid [115]. Through this development it became clear that by mixing surfactants (hydrotropes) of opposite charges, cationic and anionic, but with varying chain lengths, one can control the degree of precipitation of the surfactants to produce

different supramolecular structures like vesicles and polymeric micelles [116]. The transition from one structure to another is also well known facts in recent studies. A temperature-induced vesicle to micelle transition has been claimed for a system of cationic surfactant e.g., cetyltrimethylammonium 3-hydroxy naphthalene 2-carboxylate [117].

**References:**

1. Fuhrop, J. H.; Köning, J. in *Membranes and Molecular Assemblies: the Synkinetic Approach*; The Royal Society of Chemistry: Cambridge, **1994**.
2. Clint, J. H.; *Surfactant Aggregation*; Blackie: Glasgow/ London, **1992**.
3. Fhurtherop, J. H.; Mathieu, J. J. *Chem. Soc., Chem. Commun.* **1983**, 144.
4. Madsen, T.; Boyd, H. B.; Nylén, D.; Pendersen, A. R.; Petersen, G. I.; Simonsen, F. "Environmental and Health Assessment of Substances in Household Detergents and Cosmetic Detergent Products," Environmental Project No. 615, Danish Environmental Protection Agency ([www.mst.dk](http://www.mst.dk)): Copenhagen, 2001.
5. Schramm, L. L.; *Surfactants: Fundamentals and Applications in the Petroleum Industry*, Cambridge University Press, 2000.
6. Shah, D. O., *Surface Phenomena in Enhanced Oil Recovery*, Plenum Press: New York, 1991.
7. Lindman, B.; Marie-Claude, P.; Kamenka, N.; Rymdén, R.; Stilbs, P. *J. Phys. Chem.* **1984**, 88, 5048.
8. Blokzijl, W.; Engberts, J. B. F. N. *Angew. Chem., Int. Ed. Engl.* **1993**, 32, 1545.
9. Mancera, R. L. *J. Chem. Soc., Faraday Trans.* **1996**, 92, 2547.
10. Saha, S. K.; Jha, M.; Ali, M.; Chakraborty, A.; Bit, G.; Das, S. K. *J. Phys. Chem. B.* **2008**, 112, 4642.
11. Graziano, G.; Barone, G. *J. Am. Chem. Soc.* **1996**, 118, 1831.
12. Graziano, G. *Phys. Chem. Chem. Phys.* **1999**, 1, 1877.
13. Tanford, C. *The Hydrophobic Effect*, 2<sup>nd</sup> Ed., Wiley - Interscience, New York. **1980**.
14. Fendler, J. H. and Fendler, E. J. *Catalysis in micellar and Macromolecular Systems*, Academic Press, New York, **1975**.
15. Heartley, G. S. *Aqueous Solution of Paraffin - Chain Salts*, Herman, Paris, **1936**.
16. Ranganathan, R.; Peric, M.; Medina, R.; Garcia, U.; Bales, B. L. *Langmuir*, **2001**, 17, 6765.

17. Varade, D.; Joshi, T.; Aswal, V. K.; Goyal, P. S.; Hassan, P. A.; Bahadur, P. *Colloids Surf. A.*, **2005**, 259, 95.
18. Hayashi, S.; Ikeda, S. **1980**, 84, 744.
19. Sheu, E. Y.; Chen, S. H.; Huang, J. S. *J. Phys. Chem.*, **1987**, 91, 3306.
20. Goyal, P. S.; Aswal, V. K. *Curr. Sci.*, **2001**, 80, 972.
21. Balinov, B.; Olsson, U.; Södermann, O. *J. Phys. Chem.*, **1991**, 95, 5931.
22. Ekwall, P.; Mandell, L.; Fontell, K. *J. Colloid Interface Sci.*, **1970**, 33, 215.
23. Gruen, D. W. R. *J. Phys. Chem.*, **1985**, 89, 146.
24. Hayter, J. B.; Penfold, J. J. *Chem. Soc. Faraday Trans. 1*, **1981**, 77, 1851.
25. Debye, P.; Anacker, E. W. *J. Phys. Colloid Chem.*, **1951**, 55, 644.
26. Phillipoff, W. *J. Colloidal Sci.*, **1950**, 169.
27. Harkins, W. D.; Mittelman, R.; *J. Colloid Sci.*, **1949**, 4, 367.
28. Courchene, W. L. *J. Phys. Chem.*, **1964**, 68, 1870.
29. Bendedouch, D.; Chen, S. H.; Koehler, W. C. *J. Phys. Chem.*, **1983**, 87, 2621.
30. Moroi, Y. *Micelles : Theoretical and Applied Aspects*, Plenum Press, New York, Ch. 4.
31. Ali, M. *Ph. D. Thesis*; **2010**
32. Nagarajan, R. *Langmuir*, **2002**, 18, 31.
33. Israelachvili, J. N.; Mitchel, D. J.; Ninham, B. W. *J. Chem. Soc., Faraday Trans. 2*. **1976**, 72, 1525.
34. Israelachvili, J. N. In *Intermolecular and Surface Forces*; Academic Press: London, **1994**.
35. Nagarajan, R.; Ruckenstein, E. in *Equation of State for Fluids and Fluid Mixtures*; Sengers, J. V.; Kayser, R. F.; Peters, C. J.; White Jr. H. J. Eds.; Elsevier: Amsterdam, 2000, Chapter 15.
36. Menger, F. M.; Zana, R.; Lindman, B. *J. Chem. Ed.*, **1998**, 75, 115.

37. Tsujii, K. In *Surface Activity: Principles, Phenomena and Applications*; Academic Press Ed.: San Diego, London, New York, Tokyo, **1997**.
38. Laughlin, R. G. *The aqueous phase behaviour of surfactants*; Academic Press: London, **1994**.
39. Fendler, J. H. *Membrane Mimetic Chemistry*, Wiley: New York, **1982**.
40. Fuhrhop, J. H.; Helfrich, W. *Chem. Rev.* **1993**, 93, 1565.
41. Menger, F. M. *Nature*, **1985**, 313, 603
42. Cabane, B. *Nature*, **1985**, 314, 385.
43. Myers, D., *Surfactant Science And Technology*, VCH: New York, **1992**.
44. Suarez, M. J.; Lopez-Fontan, J. L.; Sarmiento, F.; Mosquera, V. *Langmuir*, **1999**, 15, 5265.
45. González-Pérez, A.; Czapkiewicz, J.; Del Castillo, J. L.; Rodríguez, J. R. *Colloid Polym. Sci.* **2004**, 282, 1359.
46. Dill, K. A.; Flory, P. J., *Proc. Natl. Acad. Sci. USA*, **1980**, 77, 3115; **1981**, 78, 676.
47. Mukherjee, P.; Mysels, K. J. *Critical Micelle Concentrations of Aqueous Surfactant Systems*, NSRDS-NBS 36, U. S. Dept. of Commerce, Washington DC, **1971**.
48. Brady, J. E.; Evans, D. F.; Warr, G. G.; Griser, F.; Ninham, B. W. *J. Phys. Chem.* **1986**, 90, 1853.
49. Evans, D. F.; Ninham, B. W. *J. Phys. Chem.* **1983**, 87, 5025.
50. Tanford, C. 'The hydrophobic Effect: Formation of Micelles and Biological Membranes', Wiley, New York, N. Y., **1973**.
51. Rosen, M. J. *Surfactant and Interfacial Phenomena*; John Wiley: New York, **1989**.
52. Mizusaki, M.; Morishima, Y.; Dubin, P. L. *J. Phys. Chem. B* **1998**, 102, 1908.
53. Coello, A.; Mejjide, F.; Núñez, E. R.; Tato, J. V. *J. Pharm. Sci.* **1996**, 85, 9.
54. Vasilescu, M.; Angelescu, D.; Caldararu, H.; Almgren, M.; Khan, A. *Colloid. Surf. A.* **2004**, 235, 57.

55. Rafati, A. A.; Gharibi, H.; Rezaie-Sameti, M. J. *Mol. Liquids*, **2004**, 111, 109.
56. Quina, F. H.; Nassar, P. M.; Bonilha, B. S.; Bales, B. L. *J. Phys. Chem.* **1995**, 99, 17028.
57. Bales, B. L.; Messina, L.; Vidal, A.; Peric, M.; Nascimento, O. R. *J. Phys. Chem. B.* **1998**, 102, 10347.
58. Jobe, D. J. *Langmuir*, **1995**, 11, 2476.
59. Rosen, M., *Surfactants and Interfacial Phenomena*, 3rd Ed. **2004**, Hoboken: John Wiley & Sons, Inc.
60. Kalyansundaram, K. *Chem. Soc. Rev.*, **1978**, 7, 453.
61. Matsuo, T. K.; Kano, K.; Nagamura, T. *Polym. Prepr. Am. Chem. Soc. Div. Polym. Chem.* **1979**, 20, 1087.
62. Moroi, Y.; Braun, A. M.; Gratzel, M. *J. Am. Chem. Soc.* **1979**, 101, 567.
63. Moroi, Y.; Infelta, P. P.; Gratzel, M. *J. Am. Chem. Soc.* **1979**, 101, 573.
64. Valdes-Aguilera, O.; Neckers, D. C.; *J. Phys. Chem.* **1988**, 92, 4286.
65. Horng, M.; Quitevis, E. L.; *J. Chem. Educ.* **2000**, 77, 637.
66. Kamat, P. V. *Chem. Rev.* **1993**, 93, 267.
67. Hoffman, M. R.; Martin, S. T.; Choi, W.; Bahnemann, D. W. *Chem. Rev.* **1995**, 95, 69.
68. Steinhurst, D. A.; Owrutsky, J. C. *J. Phys. Chem. B.* **2001**, 105, 3062.
69. Thompson, R. B. in *Topics in Fluorescence Spectroscopy*, J. R. Lakowicz (Ed.), Plenum Press, New York, **1994**, 4, 151.
70. Lakowicz, J. R. *Principles of Fluorescence Spectroscopy*, 2nd Ed., Kluwer Academic/Plenum Publishers, New York, **1999**.
71. Malinauskas, A.; Ruzgas, T.; Gorton, L. *J. Electroanal. Chem.* **2000**, 484, 55.
72. Buryak, A.; Severin, K. *Chem. Comm.* **2007**, 2366.
73. Kwon, J. Y.; Singh, N. J.; Kim, H. N.; Kim, S. K.; Kim, K. S.; Yoon, J.; *J. Am. Chem. Soc.* **2004**, 126, 8892.

74. De Groot, M. S.; Hendriks, P. A. J. M.; Brokken-Zijp, J. C. M. *Chem. Phys. Lett.* **1983**, *97*, 521.
75. Lal, C. J. *Power Sources*, **2007**, *164*, 926.
76. Kalyansundaram, K.; Dung, D.; *J. Phys. Chem.* **1980**, *84*, 2551.
77. Park, J. W.; Chung, H. *Bull. Korean. Chem. Soc.* **1986**, *7*, 2.
78. Kusumoto, Y.; Sato, H. *Chem. Phys. Lett.* **1979**, *68*, 13.
79. Usui, Y.; Gotou, A. *Photochem. Photobiol.* **1979**, *29*, 165.
80. Sato, H.; Kusumoto, Y.; Nakashima, N.; Yoshihara, K. *Chem. Phys. Lett.*, **1980**, *71*, 326.
81. Usui, Y.; Saga, K.; *Bull. Chem. Soc. Jpn.* **1982**, *55*, 3302.
82. Mukherjee, P.; Mysels, K. J. *J. Am. Chem. Soc.*, **1955**, *77*, 2937.
83. Mataga, N.; Koizumi, M. *Bull. Chem. Soc. Jpn.*, **1954**, *27*, 197.
84. Reeves, R. L.; Harkaway, S. A. in *Micellization, Solubilization and Microemulsion*, K. Mittal Ed., Vol. 2, Plenum Press, New York, **1979**, pp. 819-834.
85. Sato, H.; Kawasaki, M.; Kasatani, Y.; Nakashima, N.; Yoshihara, K. *Chem. Phys. (Jpn.)*, **1980**, 1529.
86. Vaidyanathan, S.; Patterson, L. K.; Möbius, D.; Gruniger, H. R. *J. Phys. Chem.*, **1985**, *89*, 491.
87. Shinoda, K.; *Colloidal Surfactants*, Academic Press, New York, **1963**, 155.
88. Hiskey, C. P.; Downery, T. A. **1954**, *J. phys. Chem.* *58*, 835.
89. Cockbain, E. G. *Trans. Faraday Soc.* **1954**, *49*, 104.
90. Buschmann, V.; Weston, K. D.; Sauer, M. *Bioconjugate Chem.* **2003**, *14*, 195.
91. Waggoner, A. in *Methods in Enzymology*, **1995**, *246*, p. 362, Academic Press, San Diego, CA.

92. Daehne, S. *Near-infrared dyes for high-technology applications*, 1998, Kluwer, Dordrecht.
93. Haugland, R. P. *Handbook of Fluorescent probes and research chemicals*, 1996, Sixth Edition, Molecular Probes, Eugene.
94. Sauer, M.; Zander, C.; Müller, R.; Ullrich, B.; Drexhage, K. H.; Kaul, S.; Wolfrum, J. *Appl. Phys. B*. 1997, 65, 427.
95. Neuweiler, H.; Schulz, A.; Vaiana, A.; Smith, J.; Kaul, S.; Wolfrum, J.; Sauer, M. *Angew. Chemie*. 2002.
96. Sudbeck, E. A.; Dubin, P. L.; Curran, M. E.; Skelton, J. J. *Colloid Interface Sci.* 1991, 142, 512.
97. Missclyn-Bavduin, A. M.; Thibaut, A.; Grandjean, J.; Broze, G.; Jerome, R. *Langmuir*, 2000, 16, 4430.
98. Gou, L. N.; Arnaud, I.; Petit-Ramel, M.; Gauthier, R.; Monnet, C.; Le Perchec, P.; Chevalier, Y. *J. Colloid Interface Sci.* 1994, 163, 334.
99. Simončič, B.; Špan, J. *Dyes and Pigments*, 2000, 46, 1.
100. Bračko, S.; Špan, J. *Dyes and Pigments*, 2001, 50, 77.
101. Moulik, S. P.; Ghosh, S.; Das, A. R.; *Colloid Polym. Sci.* 1979, 257, 645.
102. Tanaka, F.; Harada, Y.; Ikeda, N.; Aratono, M.; Motomura, K. *Bull. Chem. Soc. Jpn.* 1994, 67, 2378.
103. Bhattacharya, S. C.; Das, H.; Moulik, S. P.; *J. of Photochem. Photobio. A.* 1993, 74, 239.
104. Ogino, K.; Kasuya, T.; Abe, M. *Colloid Polym. Sci.*. 1998, 266, 539.
105. S. J. Candau, E. Hirsch and R. Zana, *J. Colloid Interface Sci.*, 1985, 105, 521.
106. M. E. Cates and S. J. Candau, *J. Phys.: Condens. Matter*, 1990, 2, 6869.
107. M. E. Cates, *J. Phys. Chem.*, 1990, 94, 371.
108. S. J. Candau, A. Khatory, F. Lequeux and F. Kern, *J. Phys. IV*, 1993, 3, 197.
109. E. J. Magid, *J. Phys. Chem. B*, 1998, 102, 4064.

110. C. A. Dreiss, *Soft Matter*, **2007**, 3, 956.
111. S. Ezrahi, E. Tuval and A. Aserin, *Adv. Colloid Interface Sci.*, **2006**, 128, 77.
112. H. Rehage and H. Hoffmann, *Mol. Phys.*, **1991**, 74, 933.
113. Bandyopadhyay, R., Basappa, G and Sood, A. K., *Phys. Rev. Lett.*, **2000**, 84, 2022.
114. Ganapathy, R.; Sood, A. K. and Ramaswamy, S. *EPL*, **2007**, 77, 18007.
115. A. M. Ketner, R. Kumar, T. S. Davies, P. W. Elder and S. R. Raghavan, *J. Am. Chem. Soc.*, **2007**, 129, 1553.
116. Hassan, P. A., Narayanan, J., Manohar, C., *Curr. Sci.*, **2001**, 80, 8, 980.
117. Salkar, R. A., Hassan, P. A., Samant, S. D., Valaulikar, B. S., Kuma, R. V. V., Kern, F., Candau, S. J. and Manohar, C., *J. Chem. Soc., Chem. Comm.*, **1996**, 1223 – 1224.

# **Chapter II**

## **Scope and object**

## Chapter II

### Scope and object

In solutions of paraffin-chain salts the critical concentration for micelle formation (cmc) is determined by a number of factors. It is markedly dependent upon the size and shape of the paraffin chain and on the nature of the polar group. Temperature usually has complex effect on the cmc value [1]. Polar organic additives have been shown to alter it appreciably. In general, factors that increases cmc of a surfactants are (I) carbon-carbon double bonds (II) polar groups within the hydrophobic tail and (III) ionic head groups whereas, the factors that decreases the cmc are (I) increasing number of methylene groups in the alkyl chain (II) introduction of phenyl rings in the alkyl chain (III) fluorocarbons within the hydrophobic tail and (IV) addition of electrolytes to solutions of ionic surfactants. The solutions of these colloidal electrolytes (i.e., soaps, detergents, etc.) change their properties abruptly at critical micelle concentration. The osmotic pressure and the electrical conductivity become much lower than the values predicted by the theory of Debye-Hückel, and viscosity and the turbidity are increased. A considerable number of research works have been devoted recently about the amphiphilic aggregates mainly due to three reasons. First, one can consistently and easily prepare aqueous micellar solutions which have aggregates of colloidal dimensions with, characteristics size, shape and surface properties. Hence micellar systems have been employed as a model system in investigations concerned with understanding colloidal physico-chemical phenomena [2-3]. Second, it has been found that micelles can act as unique reaction media. And finally, the similarities between self-assembled surfactant aggregates, such as micelles and vesicles, and biological lipid membranes prompted researchers to employ micelles and vesicles as model biological systems [4-7]. Bales et al. showed that changing of counterions have great influence on the properties of micelle [8-10]. A complete understanding of the micellization phenomena, its fundamental aspects, use of related studies for technological developments, and understanding molecular behaviour requires a comprehensive knowledge of the forces and factors controlling the process. One approach that is widely being practiced for the said knowledge has been the study of the effect of additives, especially electrolytes and organic solvents, on the micellization characteristics of ionic surfactants. The recent advances in micellar

chemistry have demonstrated the effect of macromolecules in micellar systems and their major applications in the fields of oil recovery, pharmacology, medicine and the food industry [11-13]. They have major applications in surface activity, detergency, wetting, spreading, foaming etc. The effect of different kinds of additives, including various glycols on the micellization of single tail surfactants has also been widely studied [14-16]. Apart from pure water, micelle formation has also been reported in pure non-aqueous solvents such as ethylene glycol, glycerol, formamide and hydrazine [17-22]. All these solvents have high cohesive energies and considerable hydrogen-bonding capability, which favour the aggregation of surfactant monomers to micelles. These aggregates in nonaqueous media are of nanometer size and being almost spherical can solubilize large amount of water, forming water-pool, whose properties have been determined with different techniques [23-25].

The cmc value is usually determined from the abrupt change of a certain physical property over a very small concentration range. It is possible to distinguish between methods examining the behaviour of a bulk solution property such as surface tension, conductivity, light scattering etc. and those using some spectroscopic property. In most cases, the choice of the methods depends on the availability of various techniques or the personal preference of the worker. Usually, the cmc is obtained from the graphical procedures, and often one finds that it is difficult to determine the exact break point providing the cmc value. As a consequence, sometimes the reported value depends, in some measure, on the good judgment of the researcher. A frequent problem arises when the conductance method is used in the cmc determination of surfactants with a small aggregation number. In these cases, it is very difficult to determine the break in the conductance-concentration curves and, consequently, the cmc is affected by a great uncertainty. To solve this problem, the one preferred procedure is to plot differential conductance against concentration of surfactant [26]. Manabe et al. have obtained cmc at the shoulder point of the first derivative versus concentration plots [27]. Sugihara et al. used plots of the first derivative of specific conductivity versus the square root of the surfactant concentration, thus reducing the range of the independent variable where the variation of specific conductivity occurs [28-29]. The other preferred way is to determine cmc of a surfactant with small aggregation number by two or more different methods to solve the above said problem. With this viewpoint, an attempt has been made to correlate most of the cmc value of the surfactants presented here in

two or more different way to avoid the possible errors as these cmc values and systematic information regarding thermodynamics are not as readily available in the literature as sodium dodecyl sulfate, cetyl trimethyl ammonium bromide or Triton X-100 etc.

Linear alkyl benzene sulfonates are known as the work horse of the detergent industry and have good foaming property [30-31]. Alkyl benzene sulfonate contains fluorescing group as part of their molecular architecture which exhibit excimer-monomer emission [32]. The alkyl benzene sulfonate is also applied to a typical commercial petroleum sulfonate (TRS 10-80) which is one of a family of surfactants used in chemical flooding oil recovery and is obtained by direct sulfonation of a large variety of aromatic petroleum feed stocks [33]. The surfactant sodium dodecyl benzene sulfonate is also used in chemical, biochemical and industrial works, and it is an effective surface-active compound. It can conveniently interact with neutral and cationic polymers forming solutions of different constituencies. It has antifungal properties and has a low cost of production. So far, the solution properties of this surfactant have not been critically examined although few reports are available in literature [34-36]. These considerations prompted us to make elaborate and critical study of the micellization and interfacial properties of SDBS as a function of counter ion size and hydrophobicity and their interaction with cationic dye. Major advantage of the sulfonate surfactants over the carboxylates is their greater tolerance of divalent metal ions in hard water.

In recent years, attention has been focused on the interactions of surfactants with hydrophobic counter ions and to this effect symmetrical tetraalkyl ammonium cations have been considered in most of the studies. It is also true that SDS is the most well known, and widely used in industry. However, in acidic solutions or at high temperatures, SDS undergoes autocatalytic acid hydrolysis, and dodecanol and sodium hydrogen sulfate are produced. These products are believed to cause skin irritation. In contrast, ammonium dodecyl sulfate is less hydrolyzed in acidic solutions and less skin-irritative than SDS [37]. For this reasons, the use of ammonium dodecyl sulfate in the cosmetic and toiletry industry has been expanding. In view of the growing importance and very limited number of studies on different tetraalkyl ammonium dodecyl benzene sulfonates, viz. tetramethyl ammonium dodecyl benzene sulfonate, tetraethyl ammonium dodecyl benzene sulfonate, tetrapropyl ammonium dodecyl benzene sulfonate and tetrabutyl ammonium dodecyl benzene sulfonate,

investigation on their aggregation behaviour in aqueous solution have been undertaken with the other counter ions of alkali metals.

The cmc and other physico-chemical properties such as surface property, thermodynamic properties etc. change with the change in temperature of the medium. Also the stabilities of surfactant systems with respect to temperature prior to their multifold uses need to be known, especially where elevated temperature prevails. Keeping the above in view, physico-chemical properties of different surfactants are determined with varying temperature to get an overall view of the energetics of the process. Moreover, a series of work done previously in our laboratory to understand the effect of counter ions of the aggregation behaviour of sodium dodecyl sulfate and bis (2-ethylhexyl) sulfosuccinic acid. Therefore, we have undertaken the present study on the characterization of the different properties of dodecyl benzene sulfonate such that we can compare and make a generalized view of the three compounds having different hydrophobic and hydrophilic character.

Linear alkyl benzene sulfonates (ABS) are arguably the most important class of commercial surfactant, used in many industrial applications as described above. Commercial ABS surfactants are generally produced by using a process that results in a mixture of alkyl chain homologues with a range of head group positional isomers. The positional isomers have a molecular structure where the benzene sulfonate head group is attached at different positions along the alkyl chain [3]. For example, the polydispersity of one commercial linear ABS surfactant is illustrated by the numerous peaks in its HPLC chromatogram highlighting the alkyl chain length distribution and the different isomeric components produced for each chain length. Not only are such complex mixtures difficult to characterize, and hence predict functional performance, the situation is even more complex as nominally the same surfactant, manufactured by different suppliers, may contain varying proportions of the individual isomeric components. Dodecyl benzene sulfonates are known to form micelles in dilute solution and display an array of liquid crystalline phases at higher concentrations [38]. In particular, it is already known that a micelle to vesicle aggregate transition can be induced by a change in ionic strength, resulting in a reduction of the air-aqueous solution interfacial tension [39-40]. This behaviour is important from practical perspective, as the ability of surfactants to reduce interfacial tension is often key to their performance. The ability to control the self-assembly aggregate structure and related solution rheology can also be desirable from a formulation and consumer

acceptability perspective. Furthermore, added electrolytes have significant effect on the properties of surfactants with the nature of counter ions, its radius and valence [41-49]. Keeping in view of the above physico-chemical studies of all the surfactant in presence of corresponding bromides have done to understand the changes in properties as mentioned above.

The photochemistry of dyes has contributed to the understanding of the mechanism of electron transfer reactions in photo electrochemical devices [50-55]. Photo induced electron transfer processes in surfactant solutions are potentially important for efficient energy conversion and storage because surfactant micelles help to achieve the separation of the photoproducts by hydrophilic-hydrophobic interactions of the products with the micellar interface [56-59]. Dye-surfactant interactions are generally complex [60]. Molecular complexes having specific and characteristic physicochemical features may be formed. The dyes aggregation phenomena have attracted attention in the past and are nowadays receiving novel consideration [61-63] in view of possible new technical applications such as opto-electronic devices, optical logical elements, sensitizing agents in color photography, photoconductors, electroluminescent devices and electro optically active centers in photogalvanic systems, solar energy conversion, semiconductor photo catalysis, pollutant control, photodynamic therapy, pharmaceutical preparation, besides the more traditional ones. The properties of oxazine dye aggregates at liquid/solid interfaces have been of interest for long time [64]. The solar energy harvesting with wide band gap semiconducting photoconductors may be improved by covering with this dyes to expand the wave length range [65]. The oxazine dyes display surprisingly long wave length absorption and emission maxima given their small sizes and as such have been shown to be important fluorescent probe for biological systems. They can be excited with simple laser sources such as solid state laser diodes. Oxazine dye modified electrodes have been shown to be useful in electrocatalytic oxidation of coenzyme Nicotinamide Adenine Dinucleotide (NADH) in the context of enzyme-based biosensors [66]. A study of the photophysical behaviour of one of the oxazine dye, cresyl fast violet, has been carried out to understand the dye-surfactant interactions present in the system.

Surfactant mixtures are commonly preferred in medicinal and pharmaceutical formulations and industrial preparations due to the purpose of suspension, solubilization and dispersion as compared to single surfactant. The mixed surfactant

exhibits superior interfacial properties such as higher surface activity and lower critical micelle concentration (cmc). Generally, it has been observed that with anions that associate strongly with the surfactant cations, worm-like micellar growth occurs rapidly at low surfactant and salt concentrations. The rheological behaviour exhibited by these systems is viscoelastic and analogous to that observed in solution of flexible polymers. These surfactant solutions undergo similar rheological behaviour whether they are prepared directly from surfactant salts with a strongly associating anion or by addition of strongly associating anions to solutions prepared from surfactant salts with weakly associating anions. The rheological behaviour observed for wormlike micelles in the surfactant solution is similar to that for flexible polymers, and therefore, aqueous solutions of entangled wormlike micelles are often called "living polymer systems". The research of wormlike micelles has drawn considerable interest owing to their superior properties and wide applications [67 - 70].

Main objectives in this present investigation would, therefore, be

1. To investigate the self association behaviour of dodecyl benzene sulfonate with varying counter ion at different temperatures in aqueous solution to know the physico-chemical properties and to compare the same properties with the well investigated anionic surfactants SDS and AOT containing identical counter ions.
2. To extend investigation on the influence of salt or solvent on the micelle formation, especially when a third component was added and to calculate the change in heat content for the process: surfactant molecule in solution  $\rightarrow$  surfactant molecule in the micelle using different component in aqueous solution.
3. To know the aggregation number of each of the surfactant in aqueous solution, and also.
4. To know the types of interactions present with the oxazine dye, viz., cresyl fast violet.
5. To investigate the microstructural change of micelle formed in presence of mixed surfactants by using conductance, surface tensiometry and dynamic rheology.

To investigate on the above mentioned objectives, a variety of measurements including conductometry, tensiometry, rheology, spectrophotometry and spectrofluorometry measurements are made.

**References:**

1. Clint, J. H.; *Surfactant Aggregation*, Blackie Chapman and Hall, New York, 1992.
2. Nilsson, S.; Thuresson, K.; Hansson, P.; Lindman, B. *J. Phys. Chem. B*, **1998**, 102, 7099.
3. Rosen, M. J. *Surfactants and Interfacial Phenomena*, Wiley-Interscience, USA, 2004.
4. Saha, S. K.; Jha, M.; Ali, M.; Chakraborty, A.; Bit, G.; Das, S. K. *J. Phys. Chem. B*. **2008**, 112, 4642.
5. Yin, H.; Lei, S.; Zhu, S.; Huang, J.; Ye, J. *Chem. Eur. J.* **2006**, 12, 2825.
6. Hedin, N.; Sitnikov, R.; Furo, I.; Henriksson, U.; Regev, O. *J. Phys. Chem. B*. **1999**, 103, 9631.
7. Lindemuth, P. M.; Bertrand, G. L. *J. Phys. Chem.* **1993**, 97, 7769.
8. Benrraou, M.; Bales, B. L.; Zana, R. *J. Phys. Chem. B* **2003**, 107, 13432.
9. Bales, B. L. *J. Phys. Chem. B* **2001**, 105, 6798.
10. Pisărcăik, K.; Devinsky, F.; Lacko, I. *Acta. Facult. Pharm. Univ. Comenianac*, **2003**, 50, 119.
11. Karlström, G.; Carlsson, A.; Lindman, B. *J. Phys. Chem.*, **1990**, 94, 5005.
12. Goddard, E. D. *Colloid Surf.*, **1986**, 19, 255.
13. Hoffmann, H.; Ulbricht, W. *Curr. Opin. Colloid. Interface Sci.*, **1996**, 1, 726.
14. Jha, R.; Ahluwalia, J. C. *J. Phys. Chem.*, **1991**, 95, 7782.
15. Bakshi, M. S.; *J. Chem. Soc., Faraday Trans.*, **1993**, 89, 4323.
16. Collaghan, A.; Doyle, R.; Alexander, E.; Palepu, R. *Langmuir*, **1993**, 9, 3422.
17. Ray, A. *Nature (London)*, **1971**, 231, 313.
18. Evans, D. F.; Yamauchi, A.; Wei, G. J.; Bloomfield, V. A. *J. Phys. Chem.*, **1983**, 87, 3537.
19. Sjöberg, M.; Henriksson, U.; Warnheim, T. *Langmuir*, **1990**, 6, 1205.
20. Lattea, A.; Rico, I. *Colloids Surf.*, **1989**, 35, 221.
21. Ramadan, M.; Evans, D. F.; Lumry, R. *J. Phys. Chem.*, **1983**, 87, 4538.
22. Ramadan, M.; Evans, D. F.; Lumry, R.; Pillion, S. *J. Phys. Chem.*, **1985**, 89, 3405.
23. Tatikolov, A. S.; Costa, M. B. *Photochem. Photobiol. Sci.* **2002**, 1, 211.
24. Mittal, K. L. *Micellization, Solubilization and Microemulsion*, Vol. 2, USA, 1977.
25. Forley, M. S. C.; Beebay, A.; Parker, A. W.; Bishop, S. M.; Phillips, D. *J. Photochem. Photobiol. B: Bio.* **1977**, 38, 18.
26. Carpena, P.; Aguiar, J.; Bernal-Galván, P.; Ruiz, C. C. *Langmuir*, **2002**, 18, 6054.
27. Manabe, M.; Kawamura, H.; Yamashita, A.; Tokunaga, S. *J. Colloid Interface Sci.* **1987**, 115, 147.

28. Sugihara, G.; Era, Y.; Funatsu, M.; Kunitake, T.; Lee, S.; Sasaki, Y. *J. Colloid Interface Sci.* **1997**, 187, 435.
29. Fujiwara, M.; Okano, T.; Nakashima, T. -H.; Nakamura, A. A.; Sugihara, G. *Colloid Polym. Sci.* **1997**, 275, 474.
30. Berth, P.; Jeschke, P. *Tenside Deterg.* **1989**, 26, 75.
31. Richtler H. J. in *World prospects for surfactants. Proceedings of the 2nd World Surfactant Congress (CESIO), Paris, 1988.*
32. Aoudia, M.; Rodgers, M. A. J.; *J. Am. Chem. Soc.*, **1979**, 101, 6777.
33. Linfield, W. M. (Ed.), "Anionic Surfactants", Vol. 2., Dekker, New York, **1976.**
34. Bi, Z. C.; Yu, Z. Y. *Chin. Sci. Bull.* **2001**, 46 (5), 372.
35. Bahdur, P.; Chand, M.; *Tenside, Surfactants, Deterg.* **1998**, 35 (2), 134.
36. Hait, S. K.; Majhi, P. R.; Blume, A.; Moulik, S. P. *J. Phys. Chem. B.* **2003**, 107, 3650-3658.
37. Porter, M. R. *Handbook of Surfactants*; Chapman and Hall: New York, **1991**, p 73.
38. Težak, D.; Hertal, G.; Hoffmann, H. *Liq. Cryst.* **1991**, 10, 15.
39. Farquhar, K. D.; Misran, M.; Robinson, B. H.; Steytler, D. C.; Morini, P.; Garrett, P. R.; Holzwarth, J. F. *J. Phys.: Condens. Matter*, **1996**, 8, 9397-9404.
40. Brinkmann, U.; Neumann, E.; Robinson, B. H. *J. Chem. Soc.* **1998**, 94.
41. Ropers, M. H.; Czichocki, G.; Brezesinski, G. *J. Phys. Chem. B.* **2003**, 107, 5281.
42. Gaillon, L.; Lelievre, J.; Gaboriaud, R. *J. Colloid Interface Sci.* **1999**, 213, 287.
43. Zana, R.; Benraou, M.; Bales, B. L. *J. Phys. Chem. B.* **2004**, 108, 18195.
44. Bales, B. L.; Tiguída, K.; Zana, R. *J. Phys. Chem. B.* **2004**, 108, 14984.
45. Vasilescu, M.; Angelescu, D.; Caldararu, H.; Almgren, M.; Khan, A. *Colloid Surf. A.* **2004**, 235, 57.
46. Paul, A.; Griffiths, P. C.; Petersson, E.; Stilbs, P.; Bales, B. L.; Zana, R.; Heenan, R. H. *J. Phys. Chem. B.*, **2005**, 109, 15775.
47. Chatterjee, A.; Moulik, S. P.; Sanyal, S. K.; Mishra, B. K.; Puri, P. M. *J. Phys. Chem. B.* **2001**, 105, 12823.
48. Molina-Bolivar, J. A.; Aguiar, J.; Ruiz, C. C. *J. Phys. Chem. B.* **2002**, 106, 870.
49. Singh, O. G.; Ismail, K. *J. Surf. Deterg.* **2008**, 11, 89.
50. Rohatgi-Mukherjee, K. K.; Bagchi, M.; Bhowmik, B. B. *Electrochem. Acta.* **1983**, 28, 293.
51. Rohatgi-Mukherjee, K. K.; Roy, M.; Bhowmik, B. B. *Sol. Energy.* **1983**, 31, 417.
52. Bhowmik, B. B.; Roy, S.; Rohatgi-Mukherjee, K. K. *Indian. J. Chem.* **1986**, 25A, 714.

53. Calvin, M. *Photochem. Photobiol.* **1983**, 37, 349.
54. Kalyansundaram, K.; Gratzel, M. *Photochem. Photobiol.* **1984**, 40, 807.
55. Tsubomura, H.; Shimoura, Y.; Fujiwara, S. *J. Phys. Chem.* **1979**, 83, 2103.
56. Kalyansundaram, K.; *Chem. Soc. Rev.*, **1978**, 7, 453.
57. Matsuo, T. K.; Kano, K.; Nagamura, T.; *Polym. Prepr. Am. Chem. Soc. Div. Polym. Chem.* **1979**, 20, 1087.
58. Moroi, Y.; Braun, A. M.; Gratzel, M.; *J. Am. Chem. Soc.* **1979**, 101, 567.
59. Moroi, Y.; Infelta, P. P.; Gratzel, M.; *J. Am. Chem. Soc.* **1979**, 101, 573.
60. Shinoda, K. et al., *Colloidal Surfactants*, Academic Press, New York, **1963**, 155.
61. Ohline, S. M.; Lee, S.; William, S.; Chang, C. *Chem. Phys. Lett.* **2001**, 46, 9.
62. Vostiar, I.; Tkac, J.; Sturdik, E.; Gemeiner, P. *Bioelectrochemistry*, **2000**, 56, 113.
63. Usacheva, M. N.; Teichert, M. C.; Biel, M. A.; *J. Photochem. Photobiol. B: Biol.* **2003**, 71, 87.
64. Adhikari, R.; Saha, S. K. *Z. Phys. Chem.* **2005**, 219, 1373-1384.
65. Steinhurst, D. A.; Owrutsky, J. C. *J. Phys. Chem. B.* **2001**, 105, 3062.
66. Malinausks, A.; Ruzgas, T.; Gorton, L. *J. Electroanal. Chem.* **2000**, 484, 55.
67. L. M. Walker, *Curr. Opin. Colloid Interface Sci.*, **2001**, 6, 451.
68. G. C. Maitland, *Curr. Opin. Colloid Interface Sci.*, **2000**, 5, 301.
69. J. Yang, *Curr. Opin. Colloid Interface Sci.*, **2002**, 7, 276.
70. J. L. Zakin and H. W. Bewersdorff, *Rev. Chem. Eng.*, **1998**, 14, 2533.

## **Chapter III**

**Physico - chemical behaviour of dodecylbenzene  
sulfonate micelles as influenced by counter ion  
characteristics**

## Chapter III

# Physico - chemical behaviour of dodecylbenzene sulfonate micelles as influenced by counter ion characteristics

### 3.1 Introduction and review of the previous work

The study of surface chemistry is not applicable for only academic interest but also for various technological applications in industry and our daily lives including different biological fields. Surfactants modify the surfaces or interfaces of the systems in which they are contained. Surfactants have the ability to locate at the surfaces, thereby altering significantly the physical properties of the interfaces [1]. Due to characteristics molecular structure of the surfactant molecules they can be adsorbed between two immiscible liquids or between the liquid-gas or between a solid and a liquid. A surfactant molecule must contain two different parts in their structures, a hydrophilic part which likes polar molecules and a hydrophobic part which does not likes polar molecules but likes non-polar molecules. So, they are often called amphiphiles. The non-polar part which generally consists of long chain hydrocarbon is also called a 'tail' whereas the polar part is termed as "head". Their composite character is described by a property known as "hydrophobic lipophilic balance" i.e., HLB. It is the HLB which primarily decides their micellization, dispersion and emulsification activities [2-8]. Usually the long chain hydrocarbon acts as the hydrophobic part with which the hydrophilic part is attached and the latter determines the general classification of the surfactant molecules. Generally, the hydrophilic part is of four types, viz., cationic, anionic, nonionic and zwitterionic [9].

As has already been mentioned, surfactant aggregates become popular to the researchers in recent years due to a huge benefit achieved in many industries producing detergents, cosmetics and pharmaceuticals which have surfactants as one of their constituents [10-12]. Surfactant molecules in aqueous media form micelles above their critical micelle concentration (cmc), accompanying striking changes in the

various physico-chemical properties [13-14]. With increasing surfactant concentration the micelles undergo a special set of structural transitions, transforming from spherical shape into cylindrical, rodlike or long threadlike, disk-like vesicles and other supramolecular shapes [15]. The shapes of the micelles depend upon the environments of the surfactants as well.

1. Spherical micelles are formed with the interior composed of hydrocarbon chains and a surface of polar head groups facing water. Spherical micelles are characterized by a low aggregation number (critical packing parameter) and the hydrocarbon core has a radius close to the length of the extended alkyl chain.
2. Cylindrical micelles with an interior composed of the hydrocarbon chains and a surface of the polar head groups facing water. The cross section of the hydrocarbon core is similar to that of spherical micelles. The micellar length is highly variable to these micelles are polydisperse in nature.
3. Surfactant bilayers which build up lamellar liquid crystals for surfactant water systems having a hydrocarbon core with a thickness of about 80% of the length of two extended alkyl chains.
4. Reverse or inverted micelles having a water core surrounded by the surfactant polar head groups. The alkyl chains together with a non-polar solvent make up the continuous medium.
5. A bicontinuous structure with the surfactant molecules aggregated into a connected films characterized by two curvature of opposite sign. The mean curvature is small (zero for a minimal surface structure).
6. Vesicles are built from bilayers similar to those of the lamellar phase and are characterized by two distinct water components, with one forming the

core and the one the external medium. Vesicles may have different shapes and there are also reversed-type vesicles.

The shape and size of a micelle is a function of the molecular geometry of its surfactant molecules and solution conditions such as surfactant concentration, temperature,  $pH$  and ionic strength [16-17]. In water, the hydrophilic "heads" of surfactant molecules are always in contact with the solvent, regardless of whether the surfactants exist as monomers or as part of a micelle formation. However, the lipophilic "tails" of surfactant molecules have less contact with water when they are part of a micelle – this being the basis for energetic drive for micelle formation. Those micelles which are composed of ionic surfactants have an electrostatic attraction to the ions that surround them in solution, the latter known as counterions. Although the closest counterions partially mask a charged micelle, the effects of micelle charge affect the structure of the surrounding solvent at appreciable distances from the micelle. Adding salts to a colloid containing ionic micelles can decrease the strength of electrostatic interactions and lead to the formation of larger ionic micelles [18]. This is more accurately seen from the point of view of an effective charge in hydration of the system. Since surfactant solutions can have certain aggregation structures which are responsible for giving the solution its physical properties, they are sometimes defined as complex fluids. However, Gruen has described a realistic model for micelle which involves a rather sharp interface between a dry hydrophobic hydrocarbon core and a region filled with surfactant head groups, part of the counterions and water, viz., the stern region [19].

Over a very small concentration range, the cmc value is usually determined from the abrupt change in physical properties. It is possible to distinguish between methods examining the behaviour of a bulk solution property such as surface tension, conductance, light scattering etc. and those using some spectroscopic property. Counterion binding and diffusion coefficient of a micelle, compared with that of a single surfactant molecule, together explain the sudden decrease in equivalent conductivity of a surfactant solutions beyond the cmc. Micelles only form when the concentration of surfactant is greater than the cmc, and the temperature of the system is greater than the critical micelle temperature or Krafft temperature. Micelles can form spontaneously because of a balance between entropy and enthalpy. In water, the hydrophobic effect is the driving force for a micelle formation, despite the fact that

assembling surfactant molecules together reduces their entropy. Above the cmc, the entropic penalty of assembling the surfactant molecules is less than the entropic penalty of caging the surfactant monomers with water molecules. Also important are enthalpic considerations, such as the electrostatic interactions that occur between charged parts of surfactants. The parameters that illustrates the temperature dependence of hydrophobic effect is the heat capacity of micellization ( $\Delta_{mic}C_p^0$ ) which is generally highly negative and mainly reflects the amount of non-polar solvent accessible area buried on micellization [19].

Spherical micelles are formed by ionic surfactants since the electrostatic repulsion between adjacent head groups result in a large value for optimal head group area. Direct visualization was made by Bellare et al. in a cryo-TEM image of 10 mM solution of ditetradecyldimethyl-ammonium acetate with a micelle radius of  $3.0 \pm 0.3$  nm [4]. The most precise dimension of spherical micelle has been established by small angle neutron scattering technique.

There are so many different studies of counterions on the aggregation behaviour of surfactants to understand the adsorption kinetics and surface rheology [20-21]. In these studies, it has been proved that various parameters, viz., Gibbs elasticity ( $E_G$ ) etc., determined by theoretical and experimental way differs very much from each other which perhaps due to counterion bindings with the surfactant molecules. Further study proves that the effects are less important in case of non-ionic surfactants. The counterion binding alters the interactions in surfactant adsorption monolayer and the average surface charge density [20]. In the old literature, ionic micelle's counterion binding was not considered importantly [22-23]. In so many recent works, the importance of counterion bindings have been recognized as a important factor for the micellization process and the mole fraction scale have been used to evaluate the energetics of the process [24-26]. It has been shown by researchers that the counterion has also pronounced effects on the various properties of the micelles of anionic and cationic surfactants [27-29]. The study of the effect of counterions eliminates some of the complications by leaving the properties of the amphiphilic ion as a constant factor and thus simplifies some of the interpretation of the experimental results. But, it often leads to complications connected with limited stability and preparative difficulties of the surfactant containing different counterions. It has been shown that the shape of micelle of cetyltrimethyl ammonium bromide (CTAB) is spherical over a large concentration range and also in presence of additives

[30]. The most of the work for containing counterion has been carried out for the single tail anionic surfactants mainly on sodium dodecyl sulfate [31-33]. Though there is some amount of work done on the counterionic properties of double tailed surfactant, AOT [34].

Surfactant molecules show dramatic temperature dependability. For many ionic surfactants, the solubility is very low at low temperature but increases with increase in temperature by orders in a narrow temperature range. The phenomenon is generally known as Krafft Phenomenon and the temperature is known as the Krafft Temperature [13, 35]. The effects shown by the surfactant at Krafft temperature is best described as due to micellization of the surfactant molecules.

### 3.2. Effect of counter ion in aqueous medium

The aggregation number of ionic micelles depends on the counterions at a constant temperature in the aqueous phase. Surfactants having more tightly bound counterions with the hydrophobic part show more non-ionic nature than those surfactants with loosely bound counterions. As we know, the more non-ionic character, the less is the solubility in water and more non-spherical shape in aqueous solution. It was observed that most of the counterions interact with the surfactant by electrostatic interaction only; no chemical interactions are present in between surfactant molecules and counterions [24, 26-28, 36]. Zana et al. have reported that the degree of binding of counterion is related to the surface area per head group in the micelle in a number of experiments on cationic surfactants with varying counterions [14]. The surface area per head group decreases with degree of binding of counter ions. Ionic micelles grow in response to increase in the value of whether the counterions are provided by the added electrolytes or the surfactant alone [37]. Counterion binding also increases with the addition of electrolyte to the surfactant system and it will also increase with the increase of surfactant concentration because increasing concentration of the surfactants produces micellar growth in the solution [26, 28]. As stated above, the aggregation number of ionic micelle depends only upon the concentration of ionic surfactants in aqueous phase which can be defined below by the equation:

$$C_{aq} = F(S_t) [\alpha S_1 + (1 - \alpha) S_m] \quad (3.1)$$

where,  $S_t$  and  $S_m$  are the total concentration of the surfactant and monomeric concentration of the surfactant respectively. The factor  $F(S_t) = \frac{1}{(1-\theta)}$ , where  $\theta$  is related to the volume fraction occupied by the micelle.

In this present work, a series of counterionic activity of DBS moiety was measured by preparing surfactants with respective counterions in the temperature range 283 K to 313 K with an interval of 5 K. The counterions investigated are monovalent alkali metals counterion, viz.,  $\text{Li}^+$ ,  $\text{Na}^+$ ,  $\text{K}^+$  and also ammonium and different tetraalkyl ammonium counterions, viz., tetramethyl ammonium, tetraethyl ammonium, tetrapropyl ammonium and tetrabutyl ammonium counterions. The objective of this present work is to determine the cmc of the surfactant as a function of counter ion size and hydrophobicity at various temperatures in aqueous medium and to find out the different thermodynamic parameters and surface parameters, viz., standard Gibb's free energy of micellization ( $\Delta G_m^0$ ), standard enthalpy of micellization ( $\Delta H_m^0$ ), standard entropy of micellization ( $\Delta S_m^0$ ), heat capacity of micellization ( $\Delta_{mic} C_p^0$ ), minimum surface area per molecule ( $A_{min}$ ) and maximum surface excess concentration ( $\Gamma_{max}$ ) at the air / water interface. This is a part of the series of work done in our laboratory on the influence of counter ions of dodecyl sulfate, AOT and DBS moiety to understand the effect of different alkali metal ions and organic ions with hydrophobic chain length on the micelle formation. Since very little work of this type is reported in the literature [38], a comparative data for three surfactants with varying hydrophobic chain length is also presented to understand the effect.

### 3.3. Thermodynamics of micellization: The Mass-Action model

Among many theories proposed and reviewed by different researchers [39-42], mass action model has wide acceptance. In the mass-action model [34], the micelle formation is followed as a chemical equilibrium between free surfactant and micelle.

In solution, the formation of aggregates from free surfactant can be represented, as shown in equation (3.2).



where  $n$  is the number of free surfactant molecules ( $S$ ), which form a micelle ( $S_n$ ). Both micelles and free surfactants are treated as solutes in an aqueous solution. In the mass-action model, the thermodynamic formulations are slightly different for non-ionic and ionic surfactant solutions. Such thermodynamic formulations may be described as follows (Blandamer and et al.):

For non-ionic (neutral) surfactant solutions, at equilibrium, we have:

$$n_g \mu_{i,mon} = \mu_{i,micelle} \quad (3.3)$$

where  $\mu_{i,mon}$  is the chemical potential of monomer (free) surfactant  $i$ ,  $\mu_{i,micelle}$  is the chemical potential of surfactant  $i$  in the micelle form,  $n_g$  is the aggregation number. The chemical potentials of monomeric surfactant and surfactant in micelle are given as:

$$\mu_{i,mon} = \mu_{i,mon}^0 + RT \ln x_{i,mon} \gamma_{i,mon} \quad (3.4)$$

$$\mu_{i,micelle} = \mu_{i,micelle}^0 + RT \ln x_{i,micelle} \gamma_{i,micelle} \quad (3.5)$$

Now, we have

$$\Delta G_{i,m}^0 = \frac{1}{n_g} \mu_{i,micelle}^0 - \mu_{i,mon}^0 = RT \ln x_{i,mon} \gamma_{i,mon} - \frac{1}{n_g} RT \ln x_{i,micelle} \gamma_{i,micelle} \quad (3.6)$$

where  $x_{i,mon}$  and  $x_{i,micelle}$  are the mole fraction of monomeric surfactant and surfactant in micelle, respectively, where  $\gamma_{i,mon}$  and  $\gamma_{i,micelle}$  are the activity coefficients and  $\mu_{i,mon}^0$  and  $\mu_{i,micelle}^0$  are the standard state chemical potential of the same,  $\Delta G_{i,m}^0$  is the standard Gibbs energy of micellization.

For a dilute solution, the activity coefficients of monomeric surfactant and surfactant in micelle are set equal to 1. Then, equation (3.6) becomes

$$\Delta G_{i,m}^0 = RT \ln x_{i,mon} - \frac{1}{n_g} RT \ln x_{i,micelle} \quad (3.7)$$

In surfactant solution, the total concentration of surfactant,  $x_{tot}$ , which is a sum of free surfactant,  $x_{i,mon}$  and surfactants in micelles,  $x_{i,micelle}$ . Assuming a sufficiently high value for  $n_g$ , the second term in the above equation become very small and can be neglected. Then  $x_{i,mon}$  can be approximated to cmc.

But for ionic surfactants the micellization equilibrium can be expressed as:

$$xS^- + x\beta M^+ \rightleftharpoons (SM_\beta)_x^{-x(1-\beta)} \quad (3.8)$$

where  $(SM_\beta)_x$  is the micelle composed of  $x$  surfactant monomers and  $x\beta$  counterions bearing  $S^-$  and  $M^+$  as the monomer and counterion of the surfactant forming micelles. The value of  $\beta$  may corresponds the fraction of bound counterion in the micelle. But for nonionic surfactants monomers and micelles are obviously uncharged and  $M^+$  does not enter to the equation and the model approaches to a limiting case having  $\beta = 0$ . However, applying the mass action law to the monomer-micelle equilibrium for the ionic surfactant, and taking into account the charges of counterion along with the other parameters, the Standard Gibbs free energy,  $\Delta G_m^0$  can be expressed as [24, 39, 43]:

$$\Delta G_{i,m}^0 = (2 - \alpha) RT \ln x_{i,cmc} \quad (3.9)$$

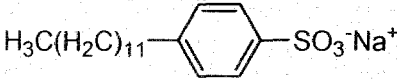
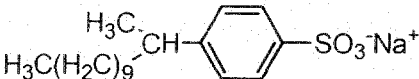
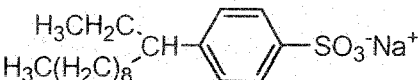
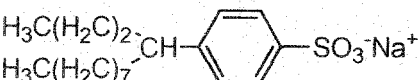
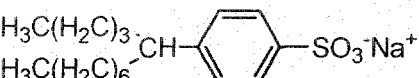
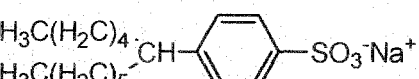
for an ionic uni-univalent surfactant. Here,  $x_{cmc}$  is the cmc expressed in mole fraction scale and  $\alpha = 1 - \beta$ .

The standard thermodynamic parameters,  $\Delta G^0$ ,  $\Delta H^0$  and  $\Delta S^0$  indicate what is happening in a process. The standard free energy change upon micellization,  $\Delta G_m^0$  tells us whether the process is spontaneous ( $\Delta G_m^0 < 0$ ) or not and the magnitude of the driving force. The standard enthalpy change upon micellization,  $\Delta H_m^0$ , on the other hand shows whether bond making ( $\Delta H_m^0 < 0$ ) or bond breaking ( $\Delta H_m^0 > 0$ ) predominates in the micellization process. The standard entropy change,  $\Delta S_m^0$ , indicates whether the system becomes more structured ( $\Delta S_m^0 < 0$ ) or more random ( $\Delta S_m^0 > 0$ ).

Because of the characteristics behaviour of surfactants to orient at surfaces and to form micelles, their applicability varies with the phase as foaming agents, emulsifiers, solubilization, suspension, wetting detergency and dispersants. The type of surfactant behaviour, whether acting as emulsifiers or dispersant or otherwise, depends on the structural groups on the molecule. So, the functions and properties of the surfactant systems depend on their structural type, concentration, and composition in addition to environmental conditions such as  $p^H$ , temperature, pressure and presence and absence of additives. It has been a long term goal of surfactant chemists to devise a quantitative way of correlating the chemical structure of surfactant molecules with their surface activity to facilitate the choice of material for a particular use.

Anionic surfactants, among which the alkyl benzene sulfonates form a major constituent of synthetic detergents, are widely used in various industrial process, such as in paper industries, electroplating, cosmetics, food processing, laundry, vehicle washing. Commercial alkyl benzene sulfonate (ABS) surfactants are generally produced by using a process that results in a mixture of alkyl chain homologues with a range of head group positional isomers. The positional isomers have a molecular structure where the benzene sulfonate head group is attached at different positions along the alkyl chain [44]. In Table 3.1 the structure of different SDBS positional isomer along with their cmc values in literature is given:

Table 3.1  
Different positional isomers of SDBS with their cmc values at 298 K

Name	Structure	cmc	Reference
Na-1-DBS <sup>a</sup> (1φC <sub>12</sub> )		-	[45]
Na-2-DBS (2φC <sub>12</sub> )		1.04	[45]
Na-3-DBS (3φC <sub>12</sub> )		1.38	[45]
Na-4-DBS (4φC <sub>12</sub> )		1.65	[45]
Na-5-DBS (5φC <sub>12</sub> )		1.94	[45]
Na-6-DBS (6φC <sub>12</sub> )		2.78	[46]
		3.10	This work

<sup>a</sup>The cmc of Na-1-DBS could not be determined due to its very high Krafft temperature rendering it insoluble at 25°C even at very low surfactant concentrations.

Sodium dodecyl benzene sulfonates are known to form micelles in dilute solution and display an array of liquid crystalline phases at higher concentrations [47]. Also, this reagent is employed in floatation application (as collectors). In this process, these reagents have a high specificity for a given mineral surface and are utilized in

relatively low dosages [48]. In particular, it is already known that a micelle to vesicle aggregate transition can be induced by a change in ionic strength, resulting in a reduction of the air-aqueous solution interfacial tension [49-50]. The ability to control the self-assembly aggregate structure can also be a desirable from a formulation and consumer accessibility perspective. Very recent developments in nanotube research indicated that the SDBS is the substance used to stabilize Single-Walled Carbon nanotubes (SWNT) dispersions with varying effectiveness [51-58]. Alkyl benzene sulfonate contains fluorescing group as part of their molecular architecture which exhibit excimer-monomer emission [59]. The alkyl benzene sulfonate is also applied to a typical commercial petroleum sulfonate (TRS 10-80) which is one of a family of surfactants used in chemical flooding oil recovery and is obtained by direct sulfonation of a large variety of aromatic petroleum feed stocks [60]. The dodecyl benzene sulfonate moiety is an effective surface-active compound. It can also conveniently interact with neutral and cationic polymers forming solutions of different constituencies. It has antifungal properties and has a low cost of production. So far, the solution properties of this surfactant have not been critically examined although few reports are available in the literature [46,61-62]. These considerations prompted us to make elaborate and critical study of the micellization and interfacial properties of DBS moiety with varying counterions.

### **3. 4. Materials and methods**

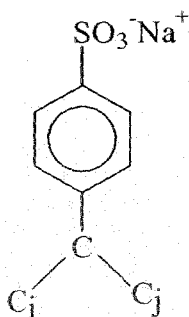
#### **3. 4. 1. Materials and ion-exchange procedure**

Surfactants with the desired counterions were prepared from a sample of purified sodium dodecyl benzene sulfonate (SDBS) (from Across Organics, 88%, USA) by the technique used by Eastoe and et al. [39] and the extended work of Temsamani and et al. [64] and Benrraou and et al. [65]. The procured sample produced no minima in surface tension vs. concentration plot indicates good purity of the sample. Surfactants with different counterions were prepared from purified SDBS by ion-exchange techniques using a strong ion-exchange resin (Amberlite IR-120, 20-50 mesh, Loba Cheme, India) using following process:

About 2 gm sample of SDBS was dissolved in 20 ml of a 1:1 (v/v) mixture of water and ethanol. The solution was passed through the column of 40 cm × 2 sq. cm size of a strong cationic ion exchanger in the H<sup>+</sup> form very slowly. The resin was put in the acid form by using a large excess of a 0.20 M aqueous hydrochloric acid solution and washed with water until the complete removal of the excess acid takes place. The free sulphonic acid formed on passing the aqueous sodium dodecyl benzene sulfonate solution through the resin was then immediately neutralized with an aqueous solution of the hydroxides of desired counterions viz., Li<sup>+</sup>, K<sup>+</sup>, NH<sub>4</sub><sup>+</sup>, (CH<sub>3</sub>)<sub>4</sub>N<sup>+</sup>, (C<sub>2</sub>H<sub>5</sub>)<sub>4</sub>N<sup>+</sup>, (C<sub>3</sub>H<sub>7</sub>)<sub>4</sub>N<sup>+</sup> and (C<sub>4</sub>H<sub>9</sub>)<sub>4</sub>N<sup>+</sup>. All the hydroxides of high purity were procured from Fluka, Switzerland and Merck, India. The solvent water was then removed first by freeze drying and then keeping under vacuum (bath temperature 313 K) for several days and the waxy solid was finally dried in vacuum over P<sub>2</sub>O<sub>5</sub>. The residual water of the sample was finally removed by the action of P<sub>2</sub>O<sub>5</sub> (from Loba Cheme, India) on a solution of surfactant in isooctane (≥ 99.5% from Merck, India). Controlling the flow rate of the solution through the ion exchange column had optimized the extent of Na<sup>+</sup>/H<sup>+</sup> ion exchange and H<sup>+</sup> content of the surfactant solution (acid form) was measured by titrating with standard NaOH to determine the extent of exchange. The extent of exchange was found to be more than 99%. Doubly distilled water having conductivity of 2 μS cm<sup>-1</sup> was used throughout experiment. Among all the ion-exchanged surfactants TBADBS did not crystallize at room temperature even after keeping at low temperature for several months. It appeared as a highly viscous, colourless semi-solid material.

Commercial SDBS may contain five different isomers viz. 2 φC<sub>12</sub>, 3 φC<sub>12</sub>, 4 φC<sub>12</sub>, 5 φC<sub>12</sub> and 6 φC<sub>12</sub> depending upon the number of carbon atoms in the branched chain [46] as stated earlier. However the supplier of the product which was used in the present study (sodium dodecyl benzene sulfonate, 88%; Acros, USA, Product Code 325912500) did not mentioned the isomeric identification of their product. While the separation of isomers from their mixtures and their identification are difficult, the cmc and other parameters indicate the presence of 6 φC<sub>12</sub> as the major component of the present surfactant system. Further, the recrystallised product of SDBS was subjected to ion exchange treatment in order to prepare surfactant with different counterions, followed by repeated recrystallization to ensure adequate purification. Therefore, it may be argued that the major component of each of SDBS, LDBS, PDBS, ADBS,

TMADBS, TEADBS, TPADBS and TBADBS was essentially  $6\phi C_{12}$  isomers as shown in Figure 3.1 [66].



**Figure 3.1.** Schematical general molecular structure of DBS ( $6\phi C_{12}$  isomer) where  $i = 5$ ,  $j = 6$ .

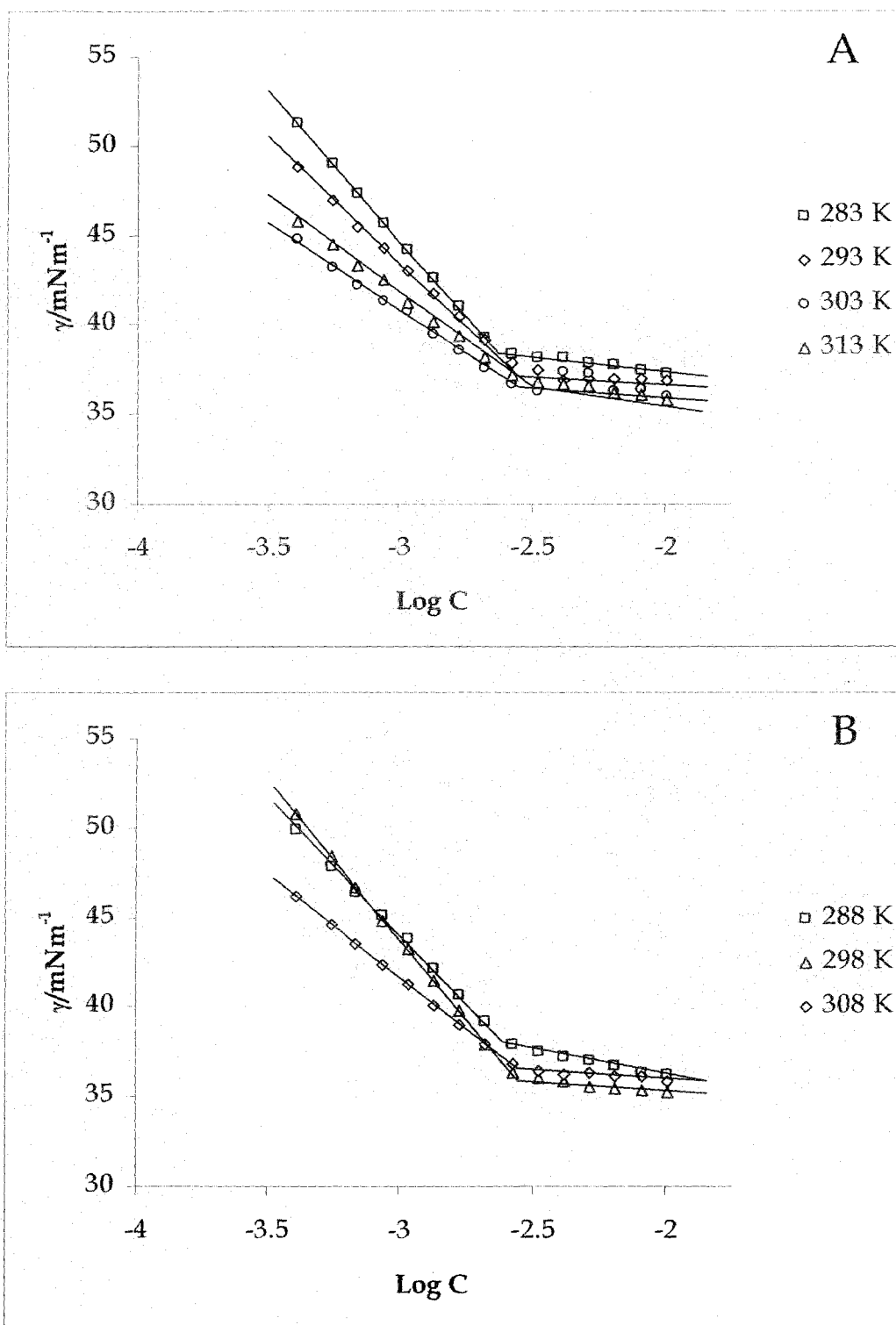
#### 3. 4. 2. Methods of measurement

The cmc and other thermodynamic parameters were determined from the surface tension as well as specific conductance data. The surface tension measurements were done by a calibrated Tensiometer (K9, KRÜSS; Germany), to measure the surface tension at the air / water interface of the solution by the platinum ring detachment methods at different temperatures. The ring was cleaned by washing with doubly distilled water followed by burning in an alcohol flame. Solutions of known concentration were progressively diluted in water solutions. The accuracy of the measurements was within  $\pm 0.1 \text{ mNm}^{-1}$ . Temperature of the system was maintained by circulating auto-thermostated water through a double-wall glass vessel containing the solution to keep the temperature constant within  $\pm 0.1 \text{ K}$ . similar studies were also done conductometrically by using an electrical conductivity bridge (METTLER TOLEDO, Switzerland). The conductance values were uncertain within the limit of  $\pm 1\%$ . Each measurement was repeated several times at each temperature in the range of 283 to 313 K. Measurements were made at 5 K intervals of temperature.

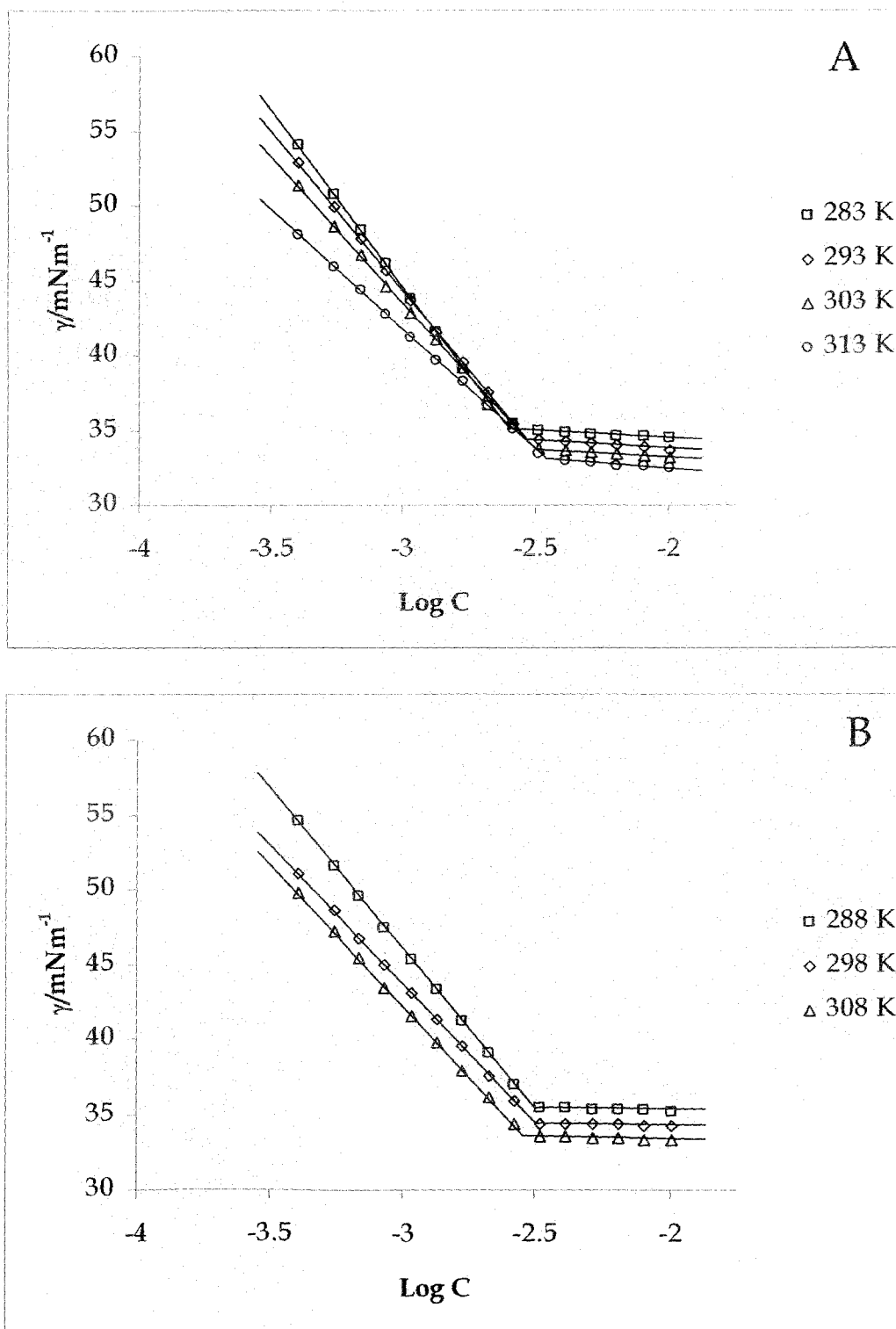
### 3. 5. Results and discussions

#### 3. 5. 1. Critical micelle concentrations (cmc)

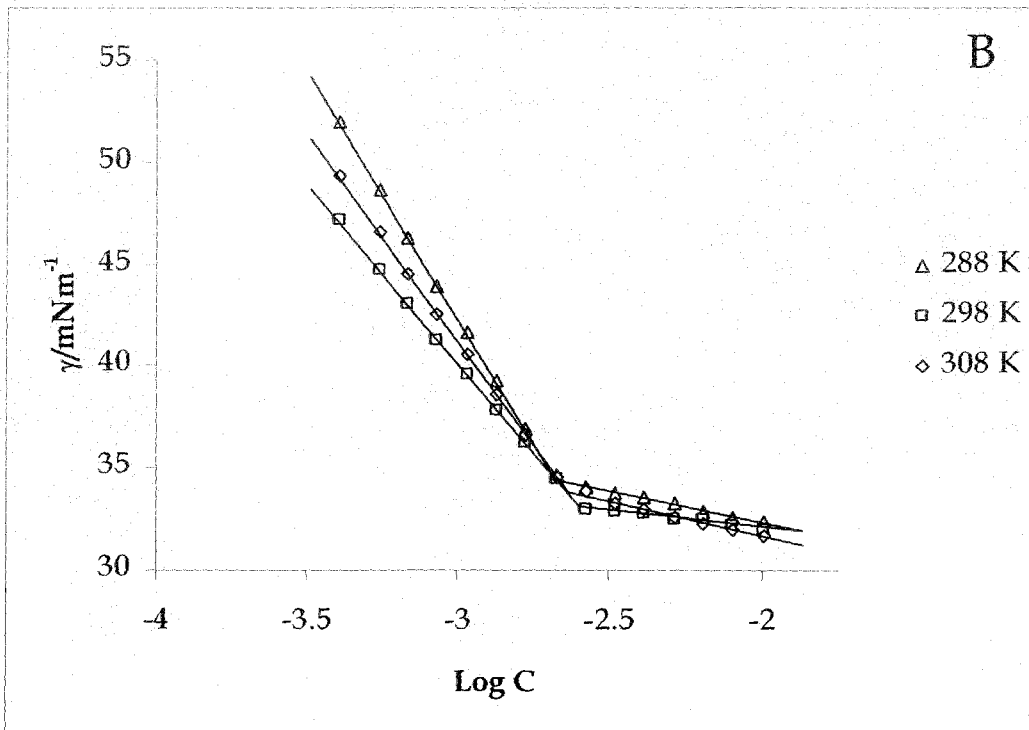
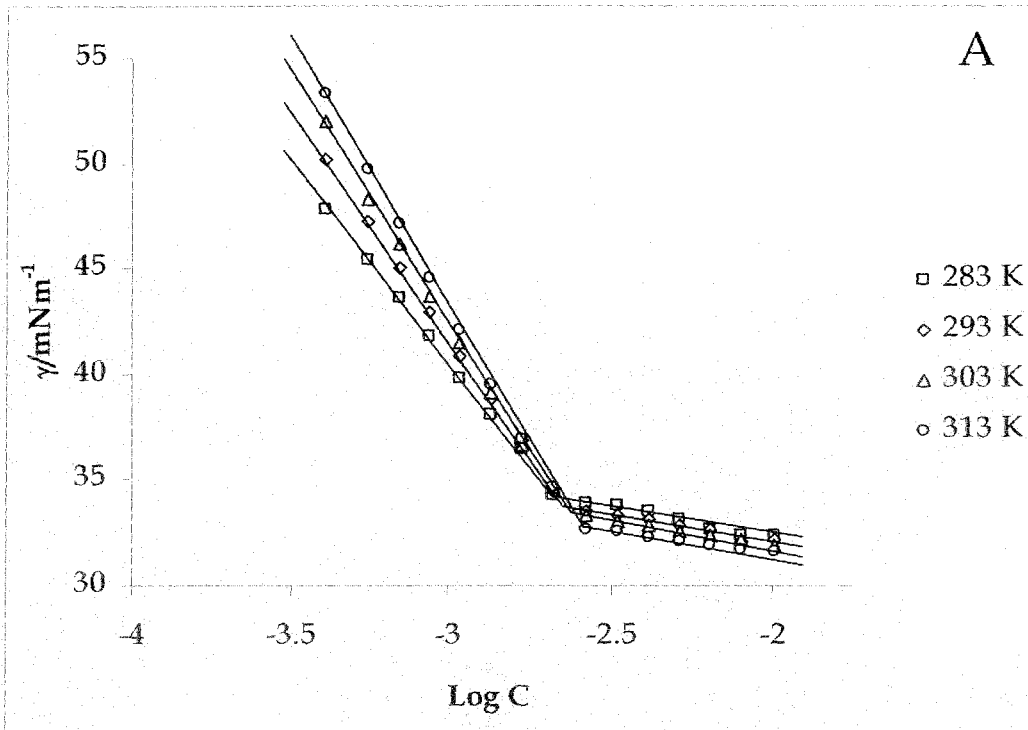
Since, the cmc data are not available in the literature (except sodium dodecyl benzene sulfonate, SDBS) for the present system and also to maintain the adequate accuracy of the results for this systems, cmc values were determined in both surface tension as well as in specific conductance methods for each surfactant with varying counter ions throughout the temperature range of 283 - 313 K at 5 K intervals (Figure 3.2 - 3.17). The value of cmc was determined from these figures at the break points of premicellar and post micellar region in the usual manner. At the intersection of almost each plot, nonlinearity in a very small range is present which may be due to traces of surface-active impurities or some small aggregation of surfactant molecules [67-68]. Ignoring this nonlinearity, the cmc values are determined by drawing two straight lines through the two straight portions of the plot. In table 3.2 and table 3.3, we present the cmc values of all the surfactant systems at various temperatures with varying counterions along with different surface parameters and degree of binding of counterions,  $\alpha$ . The changes of cmc values with varying temperatures of different surfactants are very small but clearly detectable. At a specific temperature, the cmc values of the surfactants follow the order  $\text{Na}^+ > \text{Li}^+ > \text{NH}_4^+ > \text{K}^+ > \text{N}^+(\text{CH}_3)_4 > \text{N}^+(\text{C}_2\text{H}_5)_4 > \text{N}^+(\text{C}_3\text{H}_7)_4 > \text{N}^+(\text{C}_4\text{H}_9)_4$ . So, it can be said from the results that the cmc values of the DBS moiety depends on the counterions with the above order. For the present purpose the surfactants having different counterions have been classified into two categories: one containing different alkali metal counterions along with  $\text{NH}_4^+$  and the other having various tetraalkyl ammonium counterions. It is apparent that the hydrodynamic radii along with the accessibility of the counterion towards the head group play an important role in micellization. For the tetraalkyl ammonium counterions, the binding ability of the counterions with the head group of the micelle can explain the relative cmc values of the surfactants. Among tetraalkyl ammonium cations along with ammonium cations, the binding ability is highest for  $\text{N}^+(\text{C}_4\text{H}_9)_4$  and decreases in the following order  $\text{N}^+(\text{C}_4\text{H}_9)_4 > \text{N}^+(\text{C}_3\text{H}_7)_4 > \text{N}^+(\text{C}_2\text{H}_5)_4 > \text{N}^+(\text{CH}_3)_4 > \text{NH}_4^+$ . As a result, the reduction of the electrostatic intermicellar repulsive force occurs which leads to the formation of the micelle in the lower concentration range which is shown in the figure 3.18.



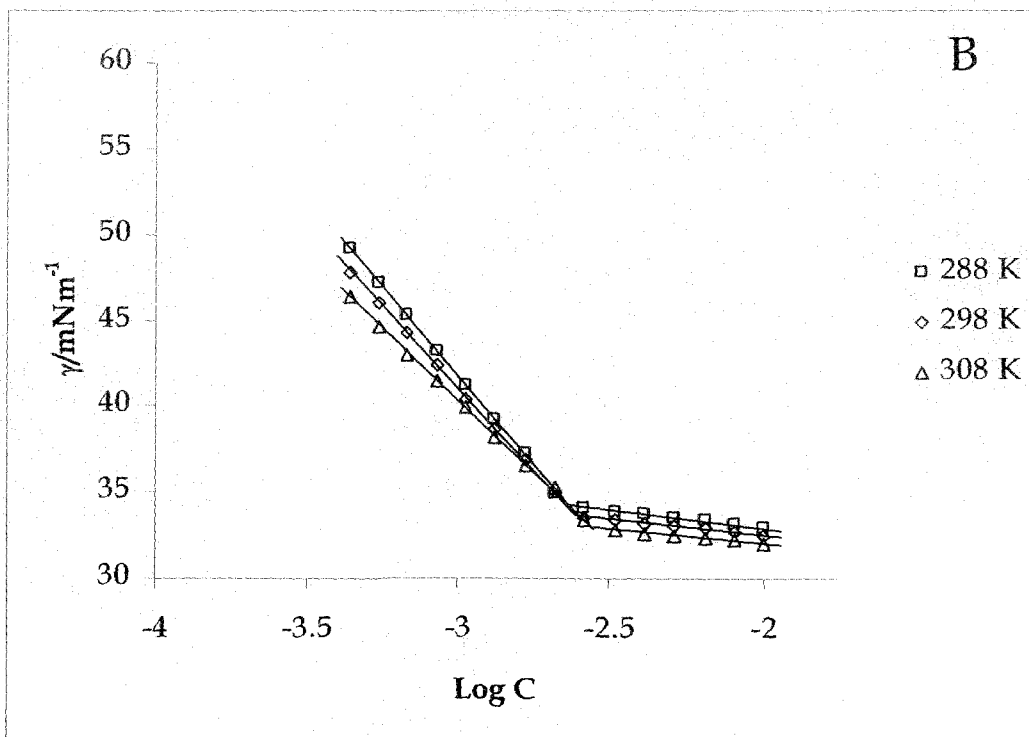
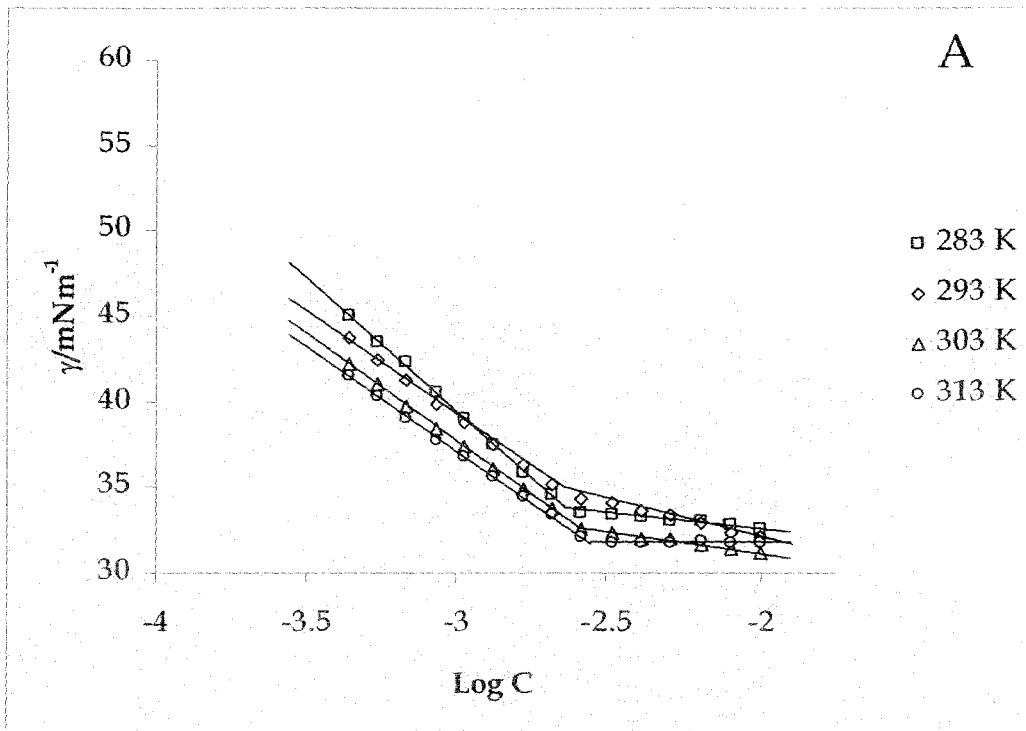
**Figure 3.2:** Surface tension,  $\gamma$ , of Lithium dodecyl benzene sulfonate (LDBS) in aqueous solution as a function of the logarithm of the surfactant concentration (mM) at different temperatures (A: temperature 283K, 293K, 303K, 313K), (B: temperature 288K, 298K, 308K).



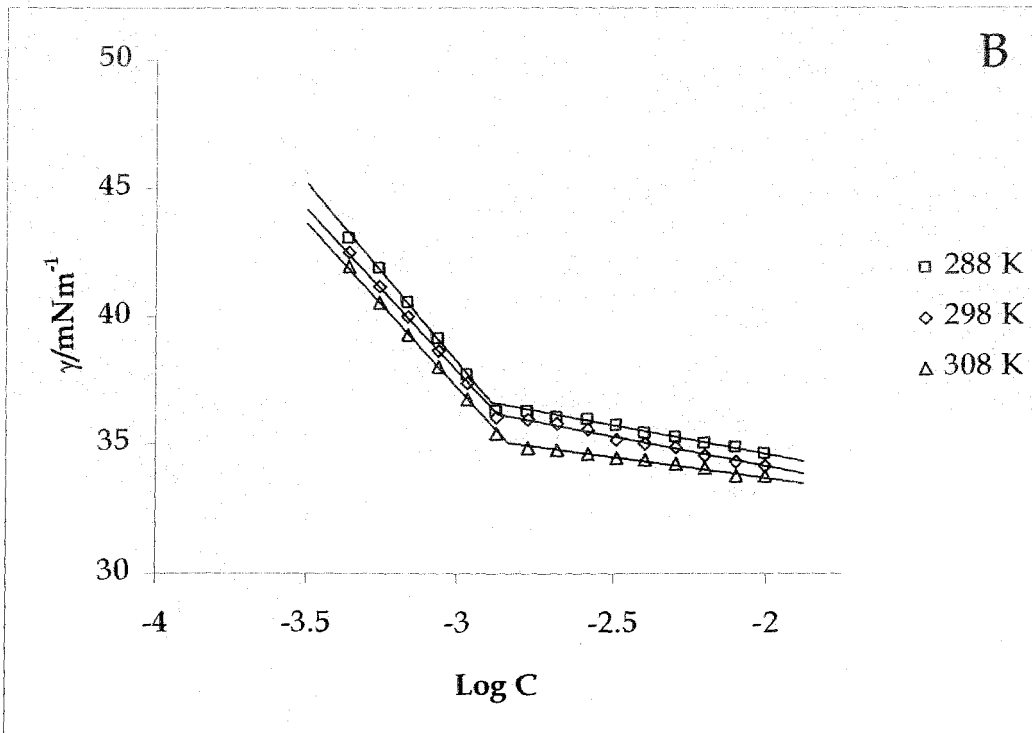
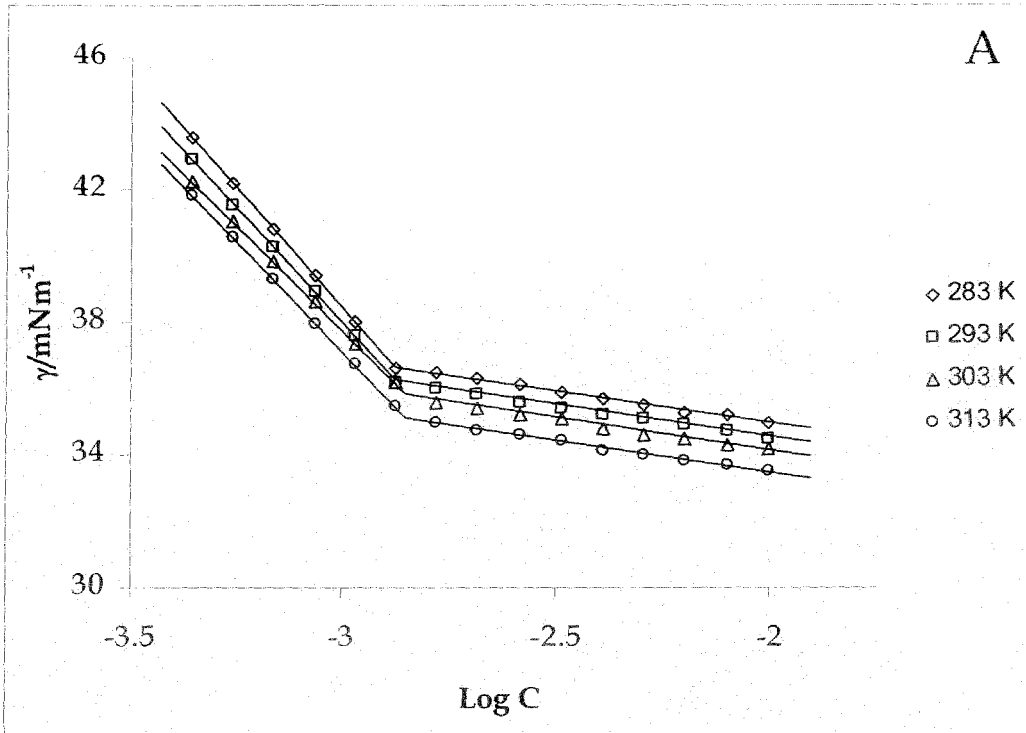
**Figure 3.3:** Surface tension,  $\gamma$ , of Sodium dodecyl benzene sulfonate (SDBS) in aqueous solution as a function of the logarithm of the surfactant concentration (mM) at different temperatures (A: temperature 283K, 293K, 303K, 313K), (B: temperature 288K, 298K, 308K).



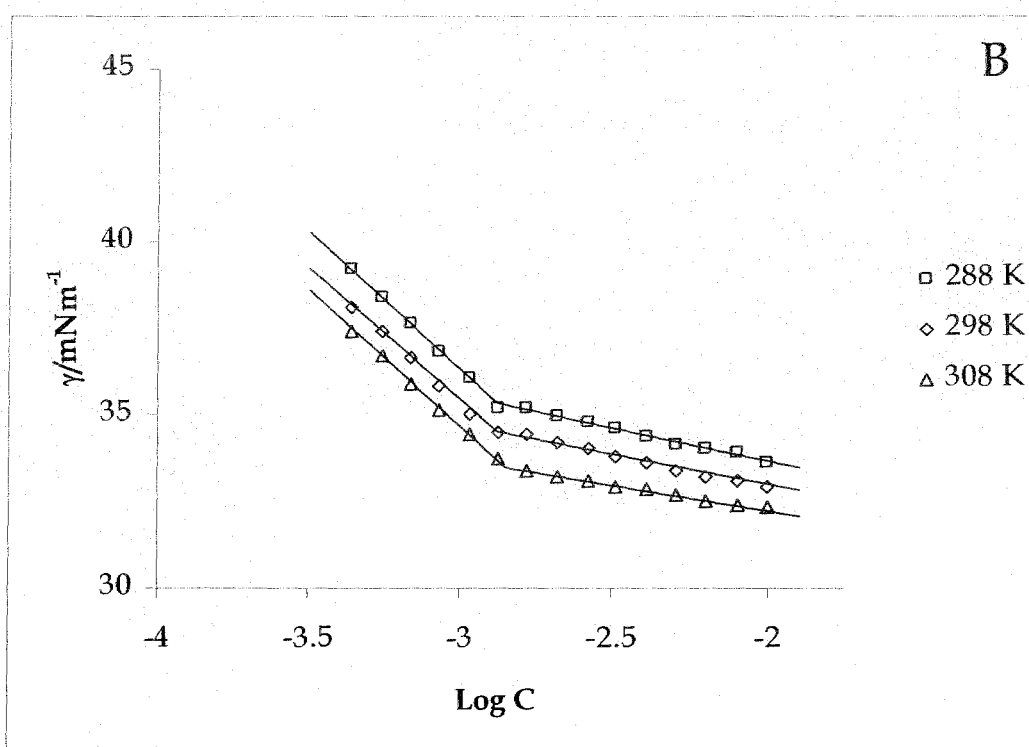
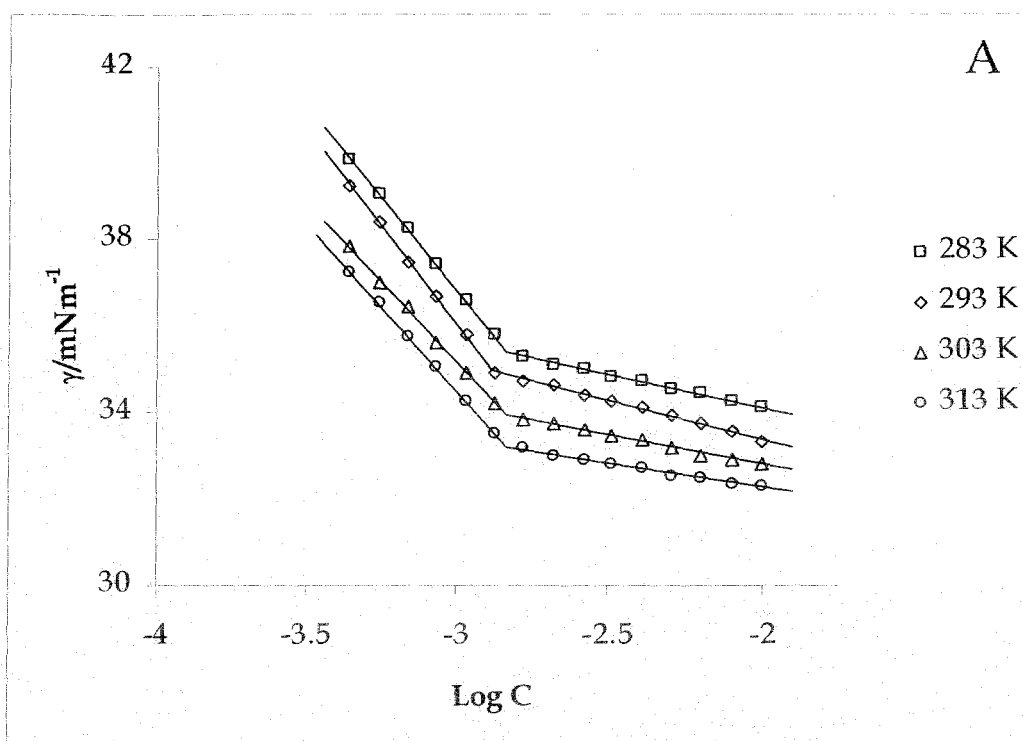
**Figure 3.4:** Surface tension,  $\gamma$ , of Potassium dodecyl benzene sulfonate (PDBS) in aqueous solution as a function of the logarithm of the surfactant concentration (mM) at different temperatures (A: temperature 283K, 293K, 303K, 313K), (B: temperature 288K, 298K, 308K).



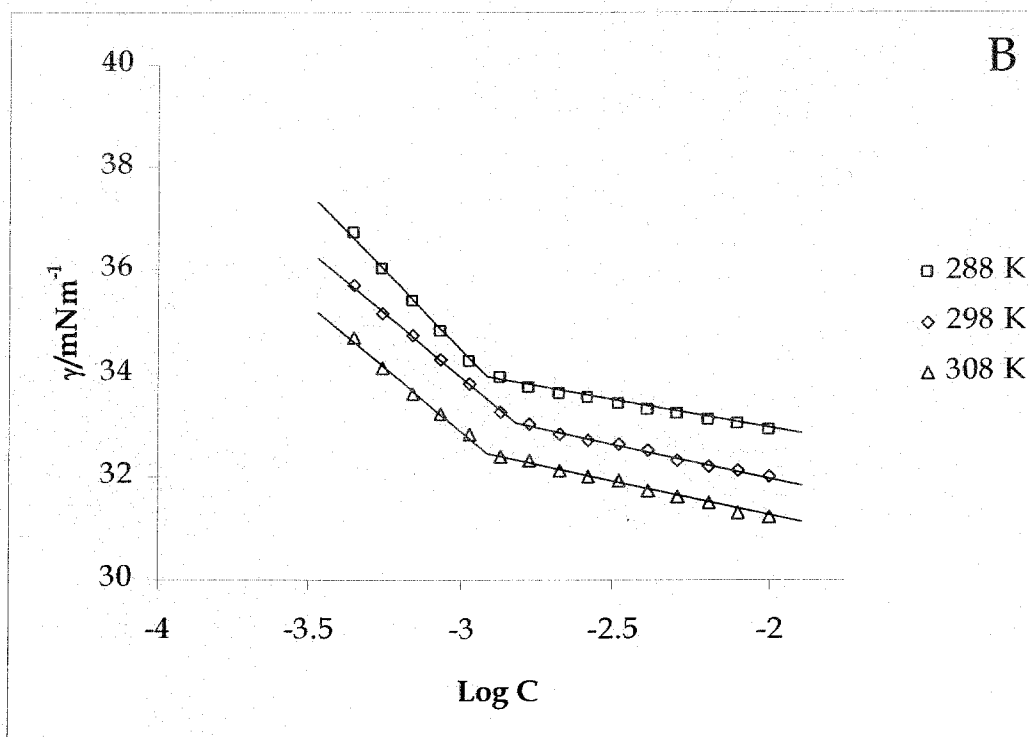
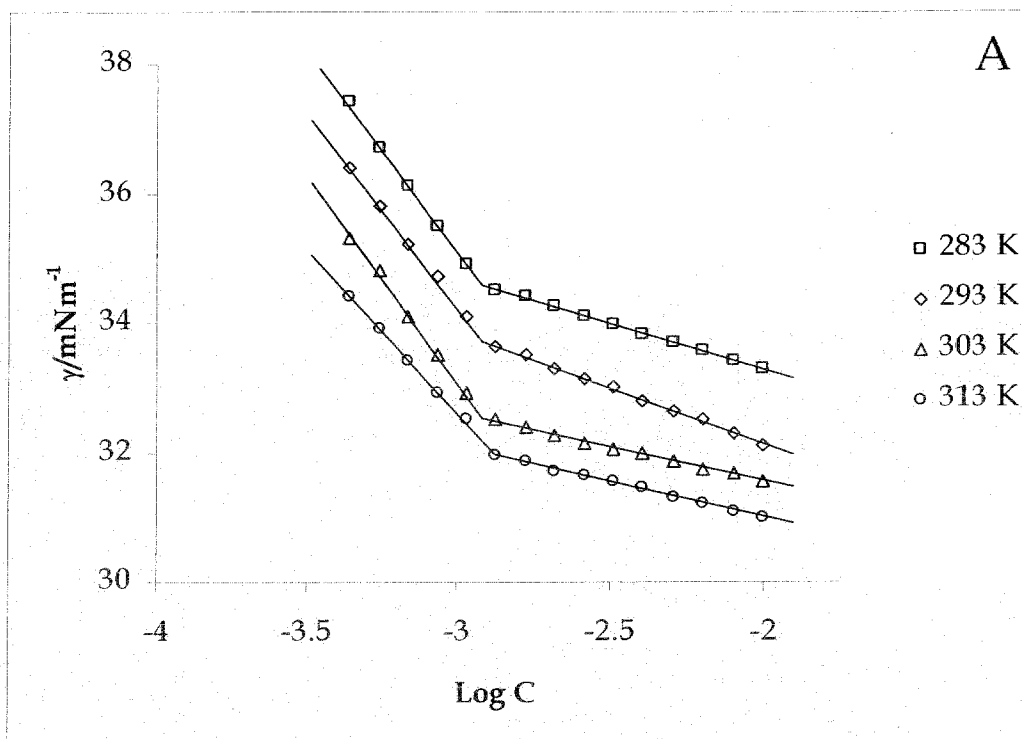
**Figure 3.5:** Surface tension,  $\gamma$ , of Ammonium dodecyl benzene sulfonate (ADDBS) in aqueous solution as a function of the logarithm of the surfactant concentration (mM) at different temperatures (A: temperature 283K, 293K, 303K, 313K), (B: temperature 288K, 298K, 308K).



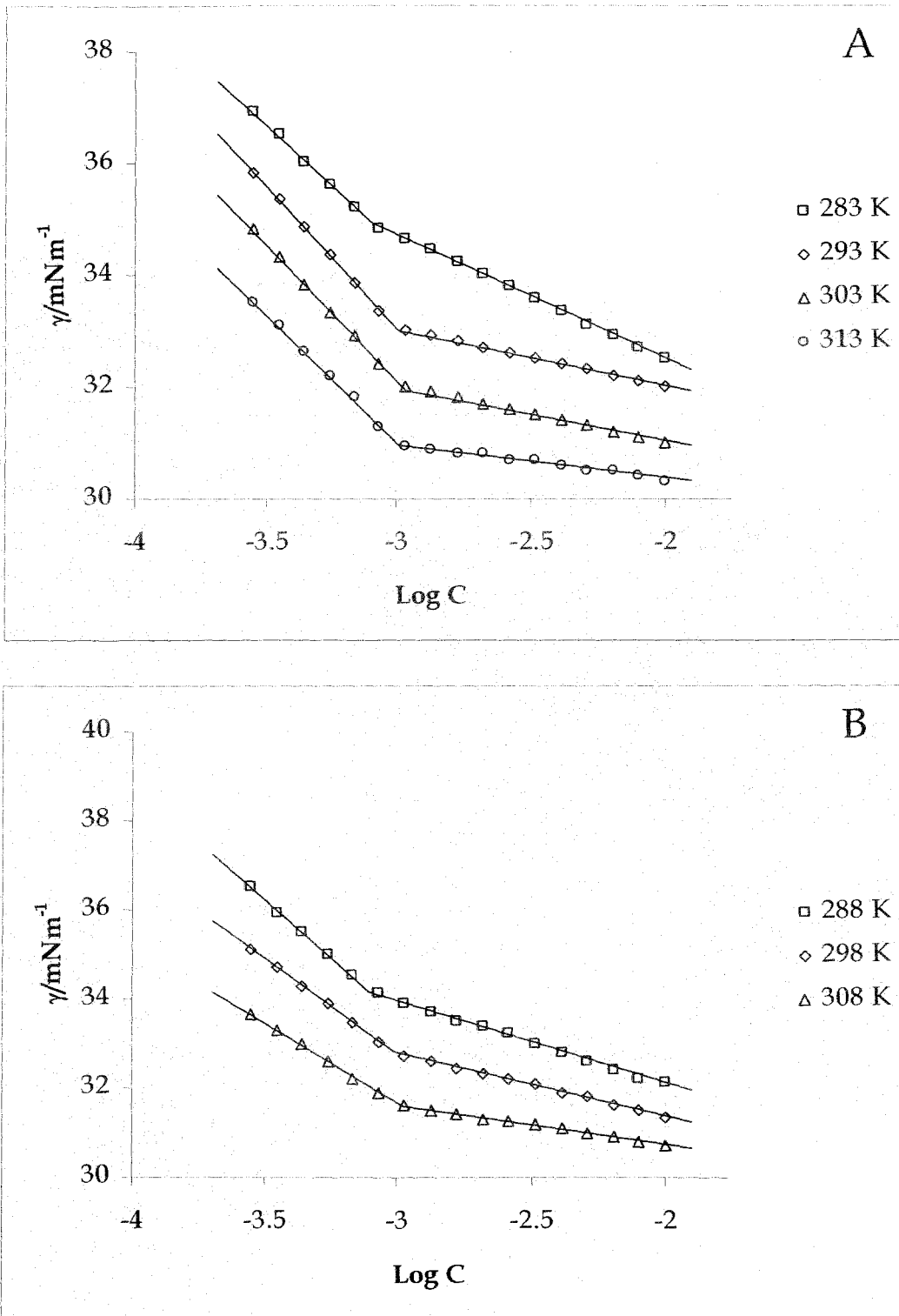
**Figure 3.6:** Surface tension,  $\gamma$ , of Tetramethylammonium dodecyl benzene sulfonate (TMADBS) in aqueous solution as a function of the logarithm of the surfactant concentration (mM) at different temperatures (A: temperature 283K, 293K, 303K, 313K), (B: temperature 288K, 298K, 308K).



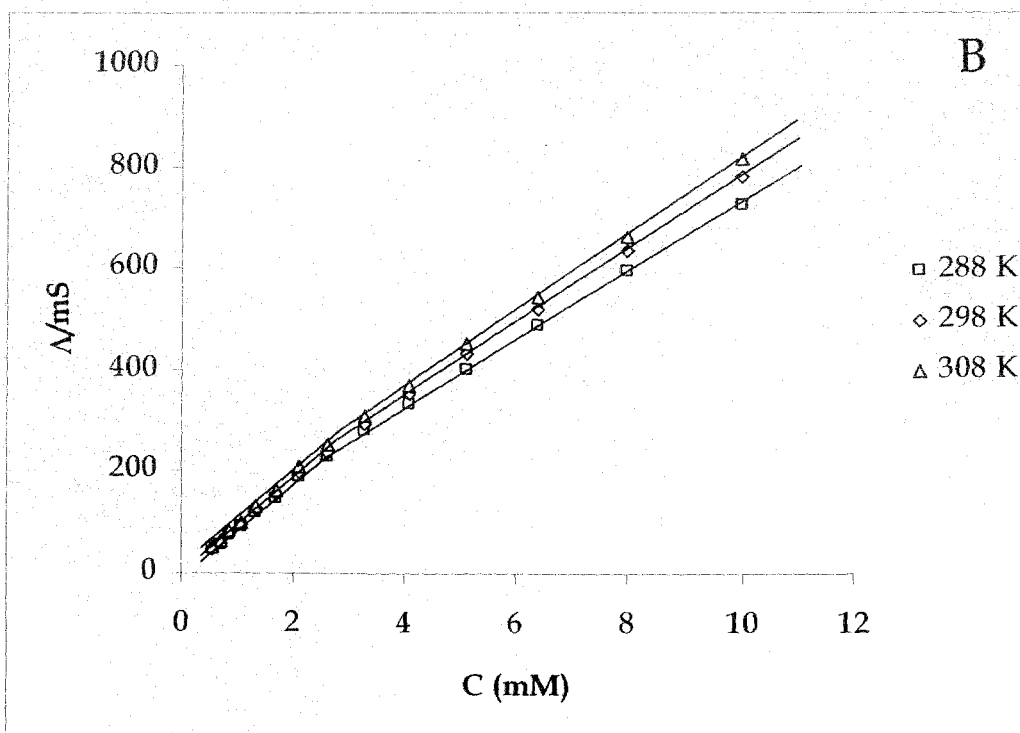
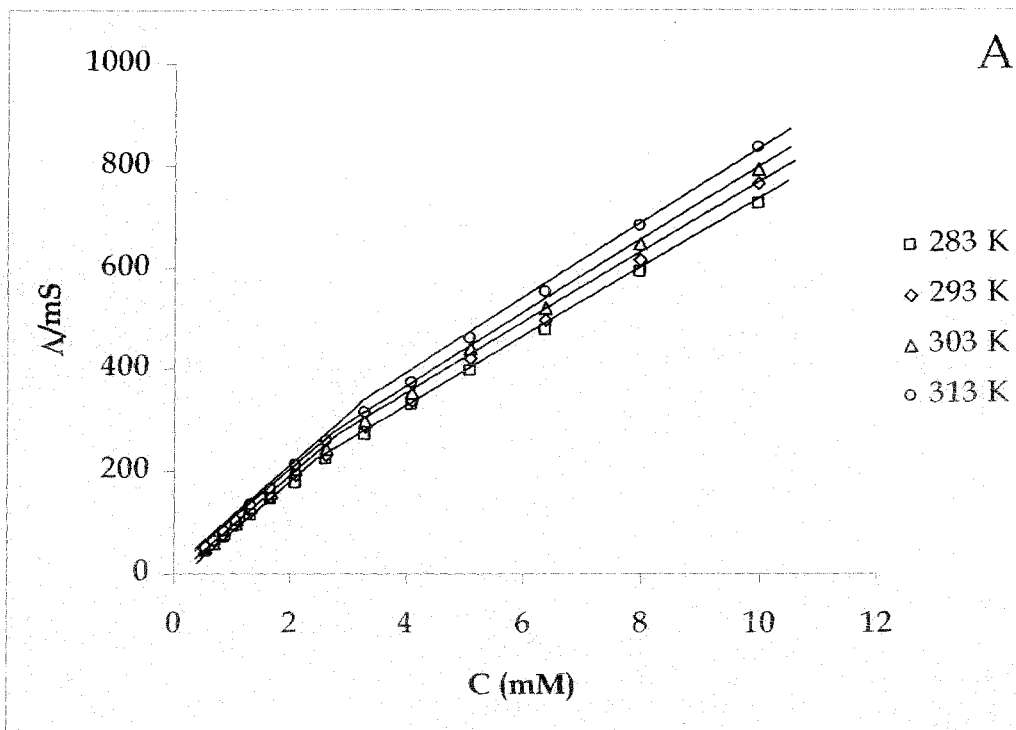
**Figure 3.7:** Surface tension,  $\gamma$ , of Tetraethylammonium dodecyl benzene sulfonate (TEADBS) in aqueous solution as a function of the logarithm of the surfactant concentration (mM) at different temperatures (A: temperature 283K, 293K, 303K, 313K), (B: temperature 288K, 298K, 308K).



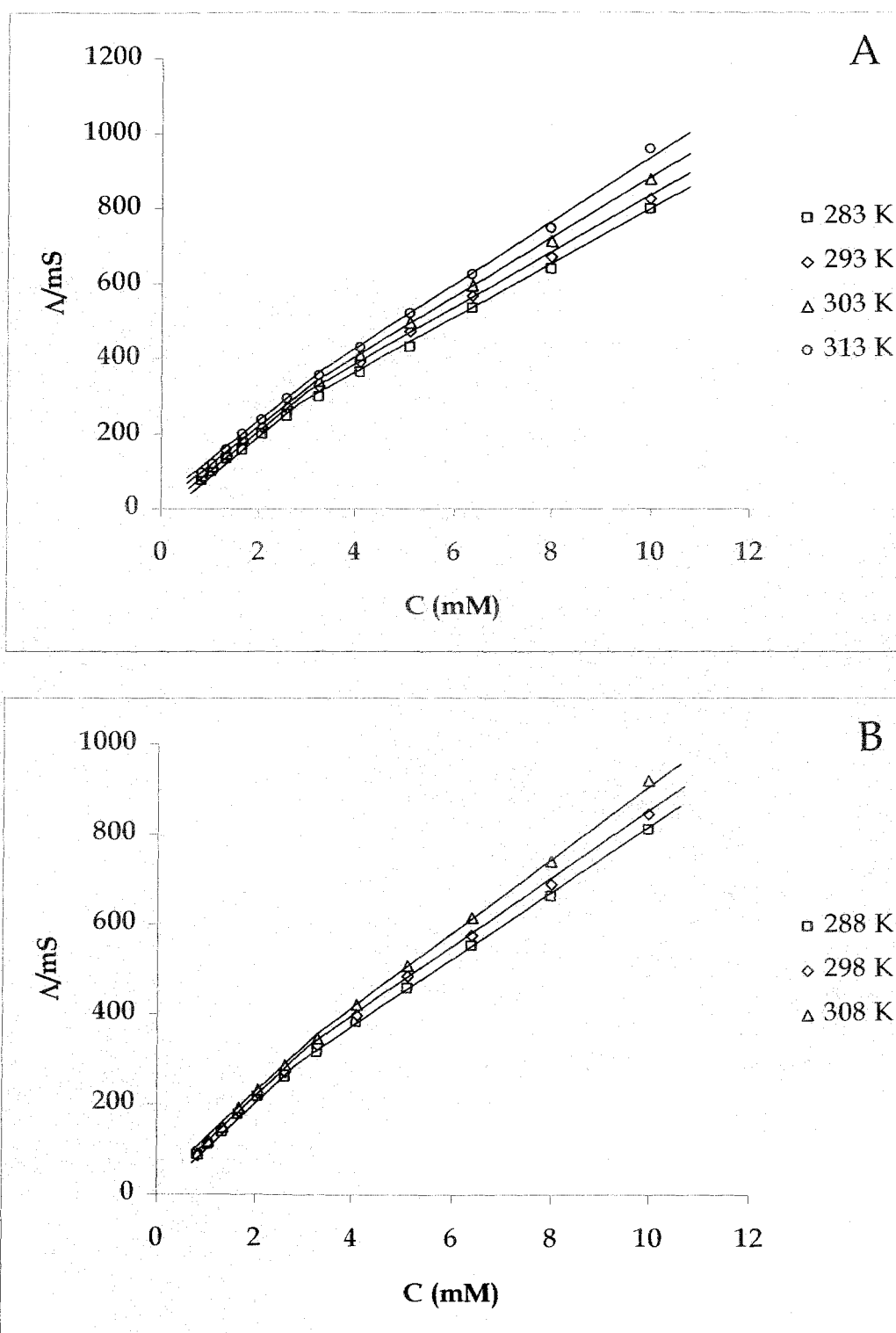
**Figure 3.8:** Surface tension,  $\gamma$ , of Tetrapropylammonium dodecyl benzene sulfonate (TPADBS) in aqueous solution as a function of the logarithm of the surfactant concentration (mM) at different temperatures (A: temperature 283K, 293K, 303K, 313K), (B: temperature 288K, 298K, 308K).



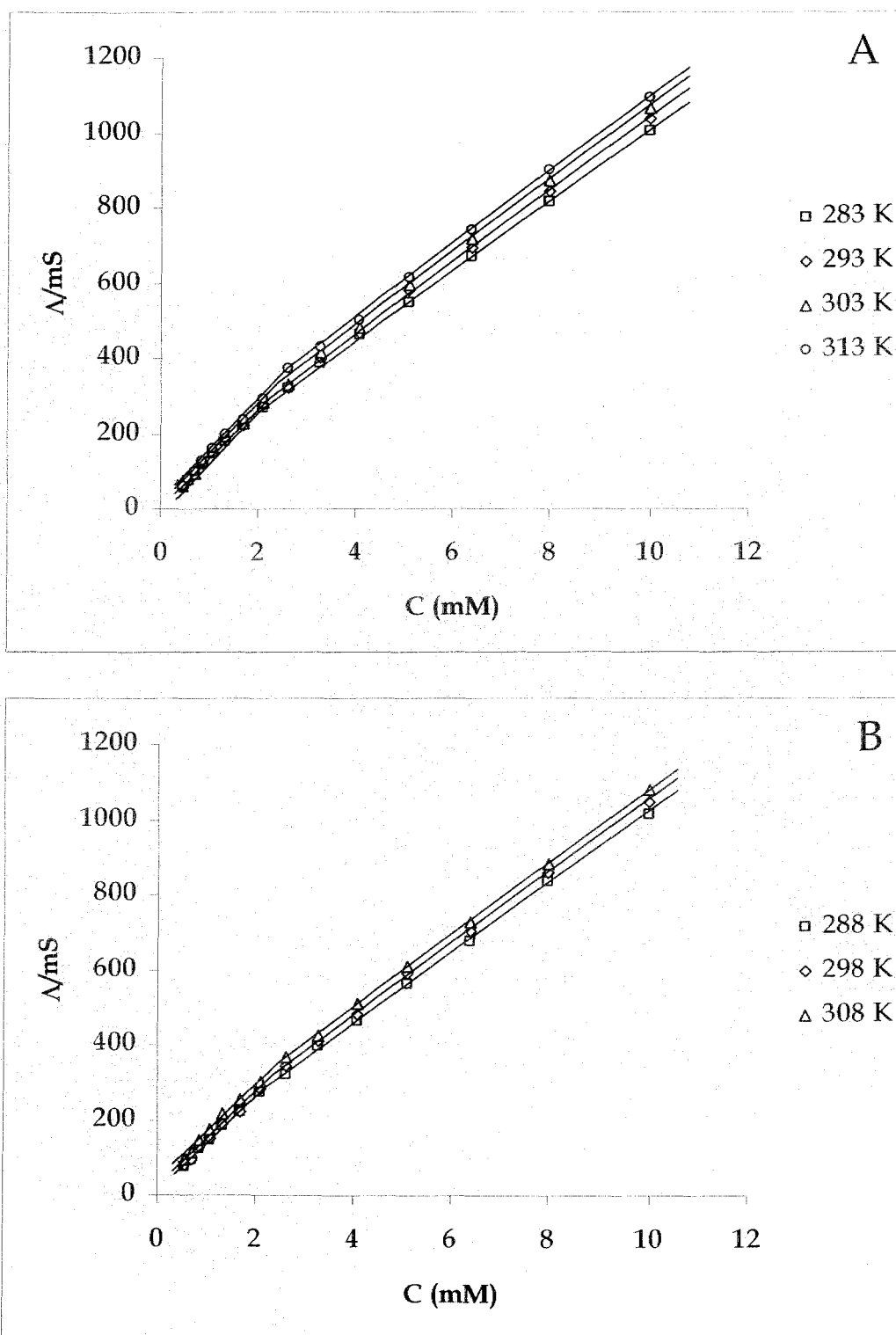
**Figure 3.9:** Surface tension,  $\gamma$ , of Tetrabutylammonium dodecyl benzene sulfonate (TBADBS) in aqueous solution as a function of the logarithm of the surfactant concentration (mM) at different temperatures (A: temperature 283K, 293K, 303K, 313K), (B: temperature 288K, 298K, 308K).



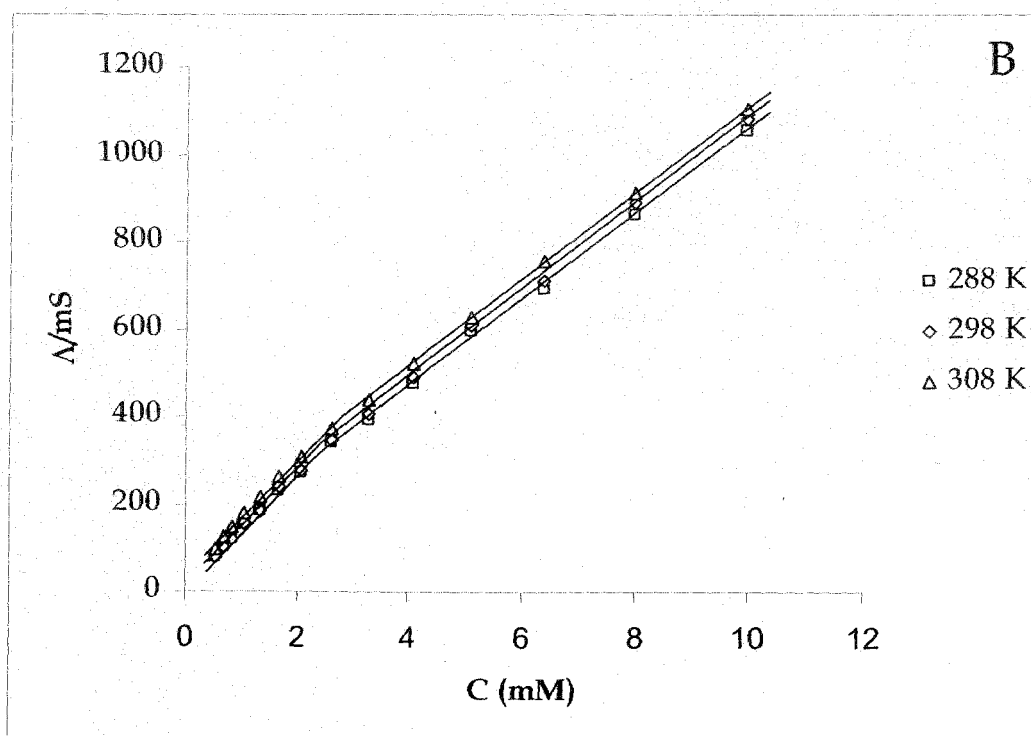
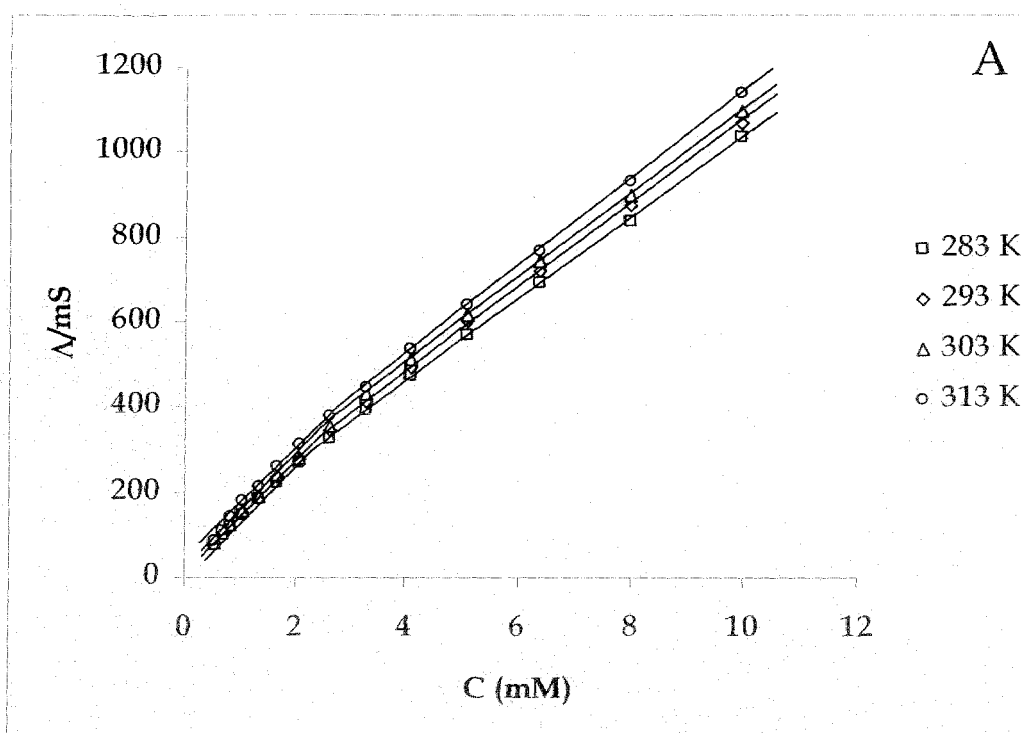
**Figure 3.10:** Conductance,  $\Lambda$ , of Lithium dodecyl benzene sulfonate (LDBS) in aqueous solution as a function of the surfactant concentration at different temperatures (A: temperature 283K, 293K, 303K, 313K), (B: temperature 288K, 298K, 308K).



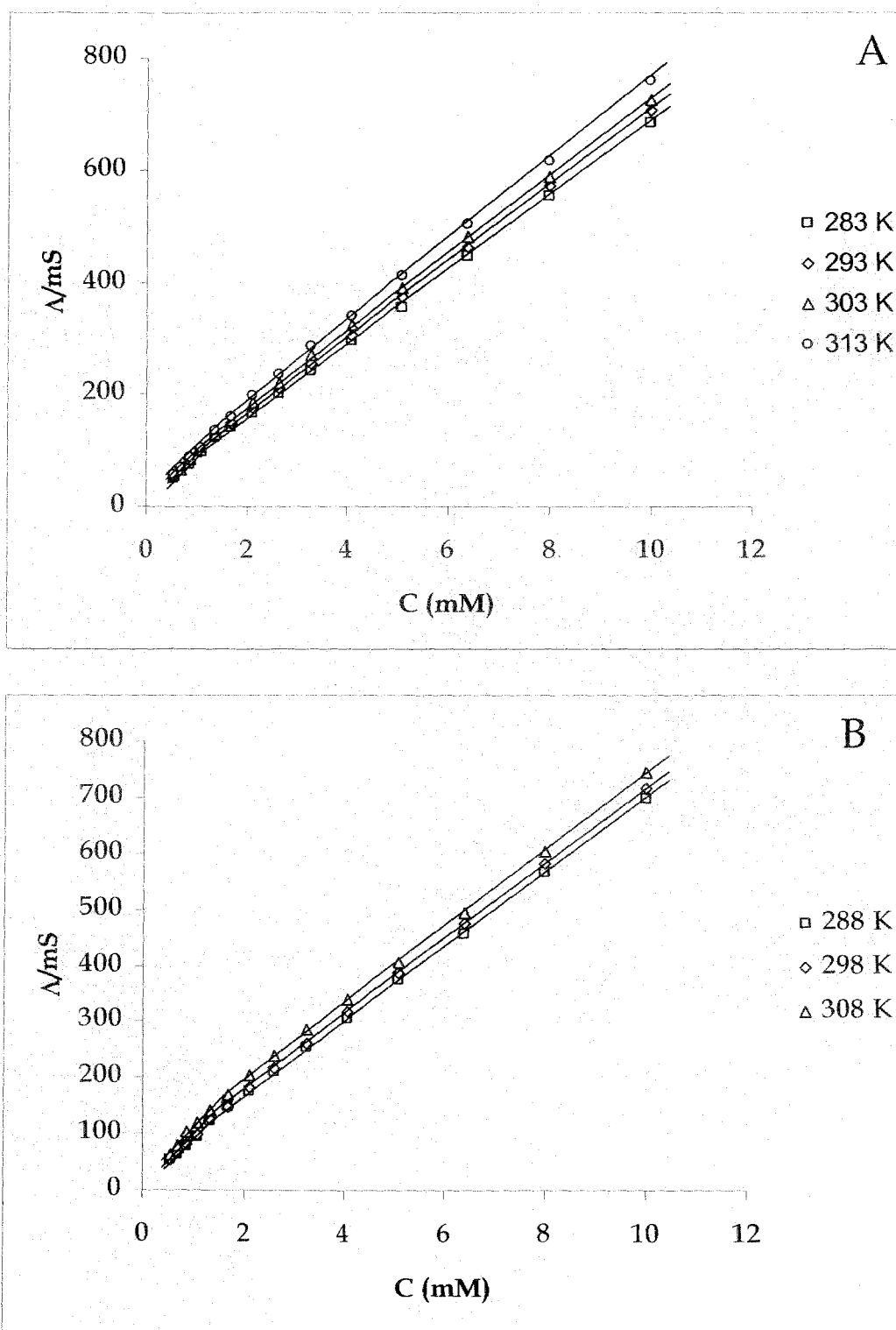
**Figure 3.11:** Conductance,  $\Delta$ , of Sodium dodecyl benzene sulfonate (SDBS) in aqueous solution as a function of the surfactant concentration at different temperatures (A: temperature 283K, 293K, 303K, 313K), (B: temperature 288K, 298K, 308K).



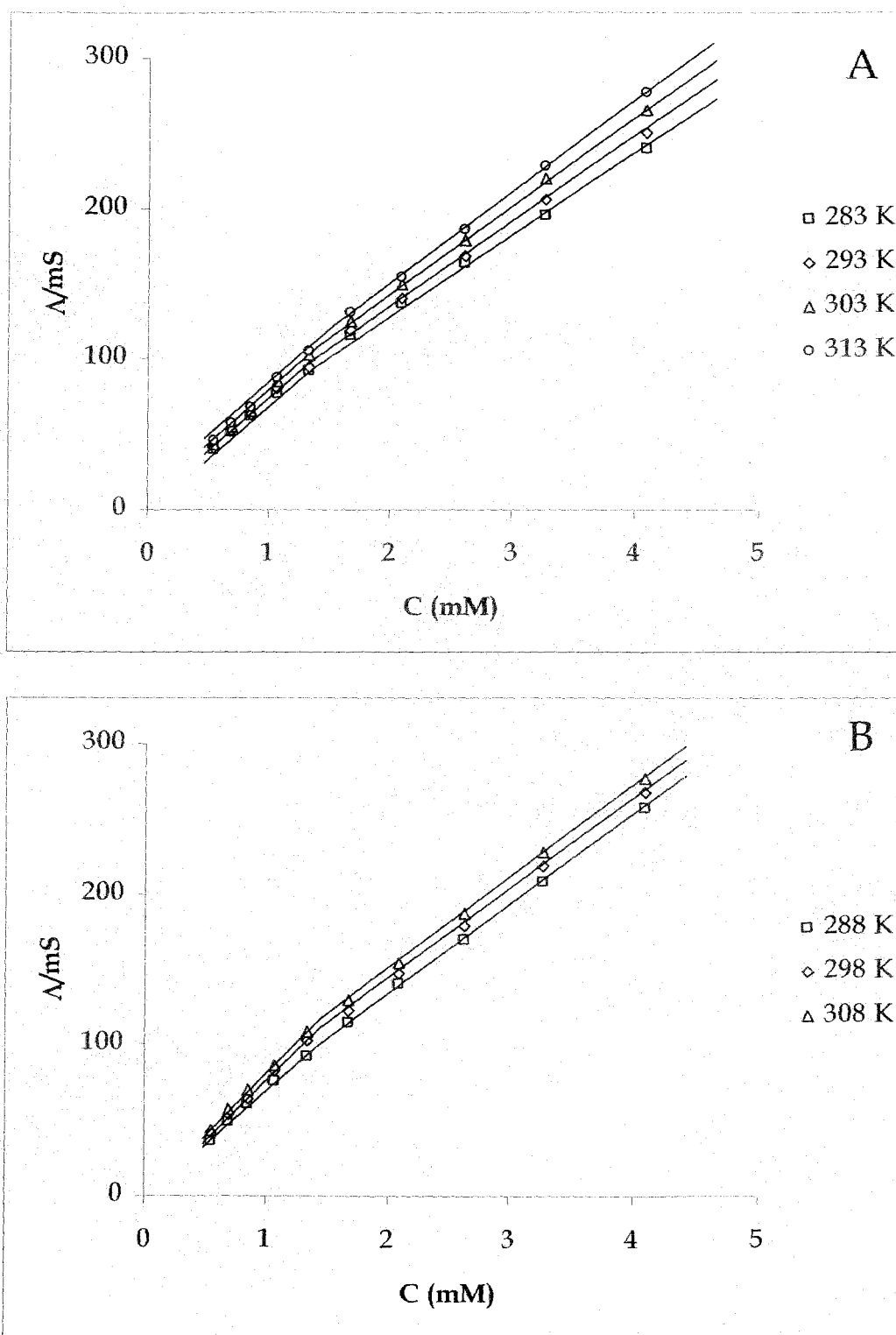
**Figure 3.12:** Conductance,  $\Lambda$ , of Potassium dodecyl benzene sulfonate (PDBS) in aqueous solution as a function of the surfactant concentration at different temperatures (A: temperature 283K, 293K, 303K, 313K), (B: temperature 288K, 298K, 308K).



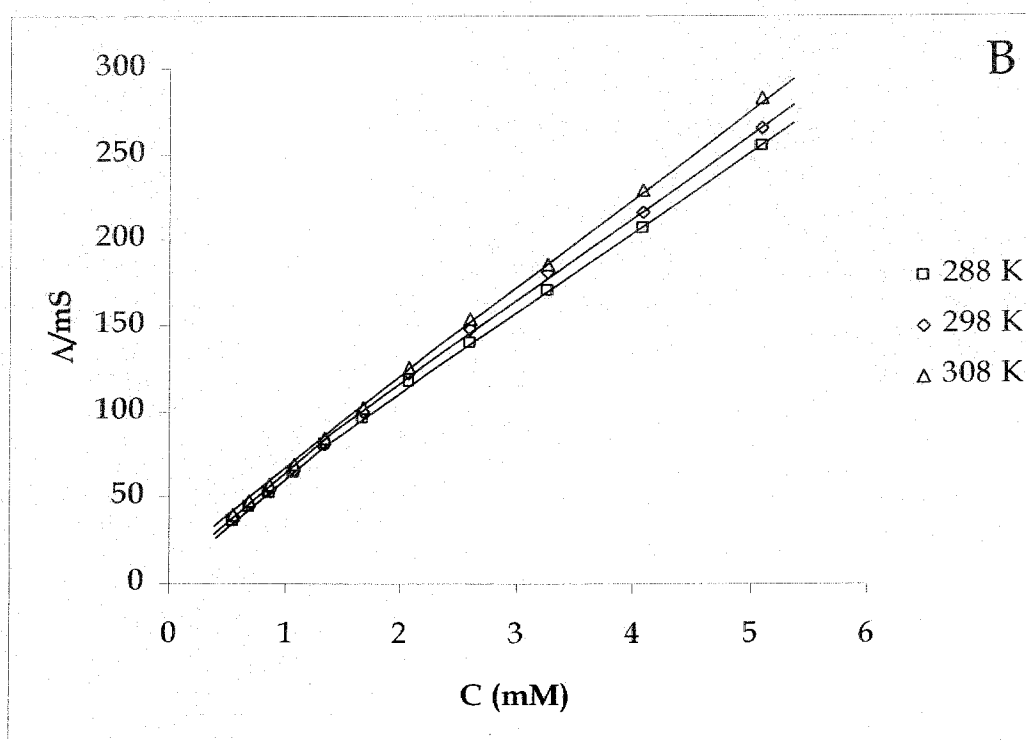
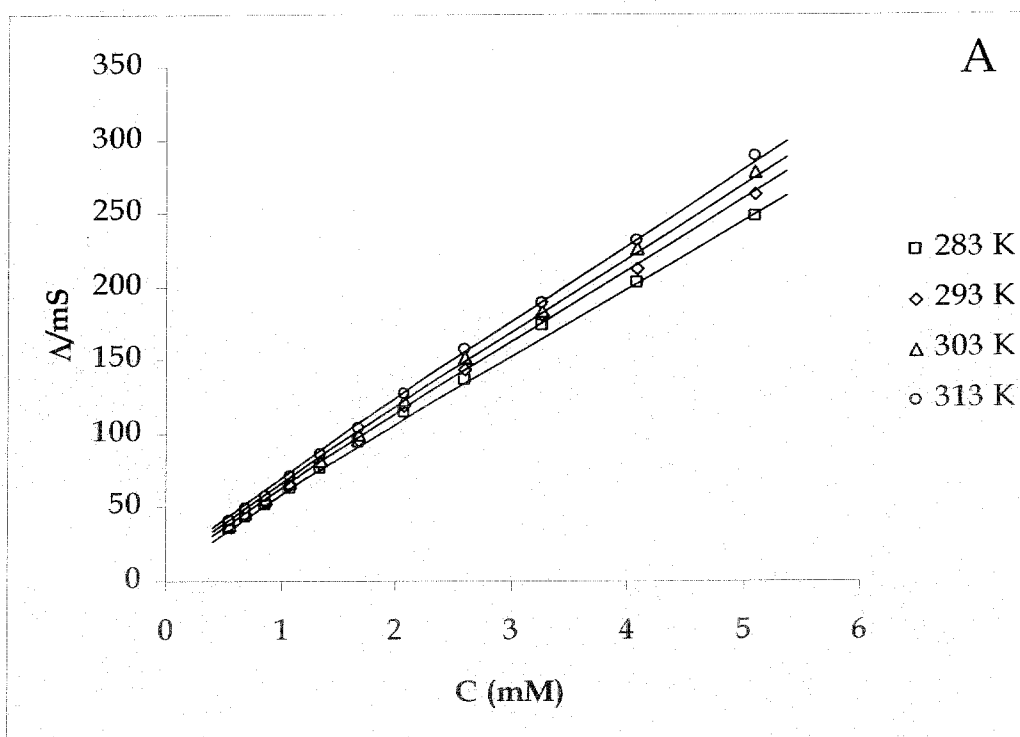
**Figure 3.13:** Conductance,  $\Lambda$ , of Ammonium dodecyl benzene sulfonate (ADBS) in aqueous solution as a function of the surfactant concentration at different temperatures (A: temperature 283K, 293K, 303K, 313K), (B: temperature 288K, 298K, 308K).



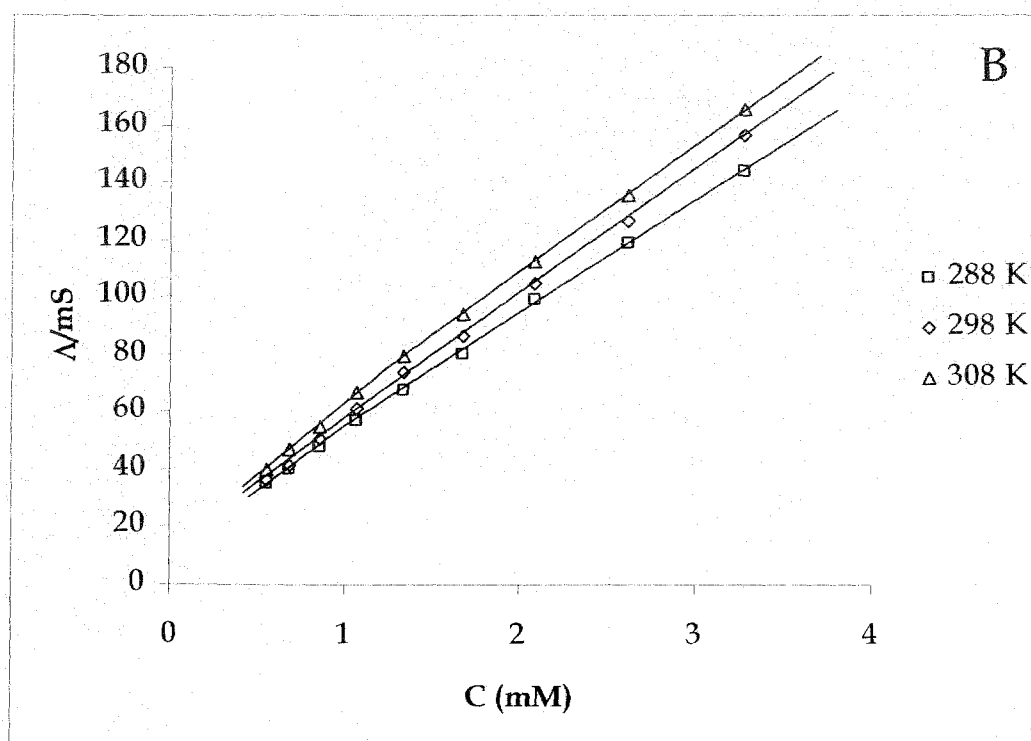
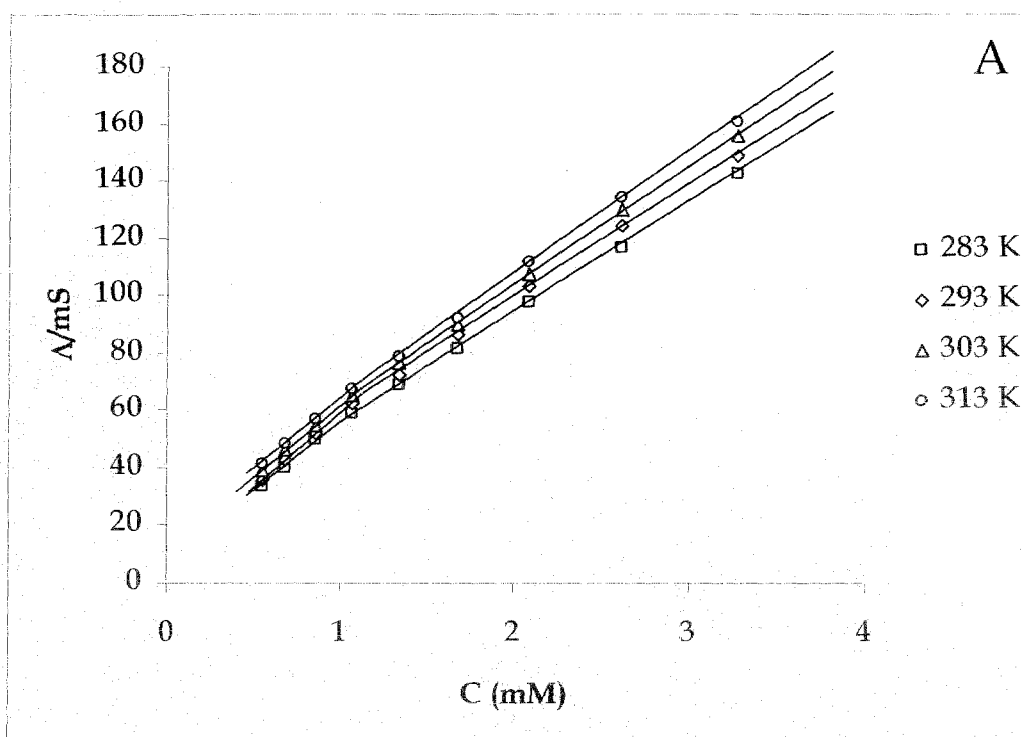
**Figure 3.14:** Conductance,  $\Delta$ , of Tetramethylammonium dodecyl benzene sulfonate (TMADBS) in aqueous solution as a function of the surfactant concentration at different temperatures (A: temperature 283K, 293K, 303K, 313K), (B: temperature 288K, 298K, 308K).



**Figure 3.15:** Conductance,  $\Delta$ , of Tetraethylammonium dodecyl benzene sulfonate (TEADBS) in aqueous solution as a function of the surfactant concentration at different temperatures (A: temperature 283K, 293K, 303K, 313K), (B: temperature 288K, 298K, 308K).



**Figure 3.16:** Conductance,  $\Lambda$ , of Tetrapropylammonium dodecyl benzene sulfonate (TPADBS) in aqueous solution as a function of the surfactant concentration at different temperatures (A: temperature 283K, 293K, 303K, 313K), (B: temperature 288K, 298K, 308K).



**Figure 3.17:** Conductance,  $\Lambda$ , of Tetrabutylammonium dodecyl benzene sulfonate (TBADBS) in aqueous solution as a function of the surfactant concentration at different temperatures (A: temperature 283K, 293K, 303K, 313K), (B: temperature 288K, 298K, 308K).

It has been also reported that the  $\text{NH}_4^+$  binds more strongly to the dodecyl head group compared to  $\text{Na}^+$  thus a lower value in cmc observed [69]. The observed cmc values are also in good agreement with the literature values [38,45-46,70-73]. The hydrated radius along with hydration number of alkali metal ions with  $\text{NH}_4^+$  ion derived from corrected ionic radii is given in the table 3.4. In the present case of dodecyl benzene sulfonate, there is a branched carbon chain in the molecular structure of the anion. Though the actual nature of dependency of hydrophobic tail on the interaction of the hydrated counterions is not still well understood, it can be said that, "branched chain molecular structure" of DBS makes the environment around more hydrophobic in nature, where  $\text{Li}^+$  along with its large hydrated volume binds more readily than that of  $\text{Na}^+$  with the hydrophobic head. But  $\text{NH}_4^+$ , which has the lowest hydration number shows anomalous behaviour towards its accessibility to the head group [74].

Table 3.2

Micellization and Surface parameters of Dodecyl benzene sulfonate having different alkali counterions along with  $\text{NH}_4^+$  ion at various temperatures (T/K): cmc, maximum surface excess concentration, minimum areas per molecule and ionization degree.

Counterion	T/K	cmc <sup>a</sup> / (mol dm <sup>-3</sup> × 10 <sup>-3</sup> )	$\Gamma_{\text{max}}$ / mol cm <sup>-2</sup> × 10 <sup>6</sup>	A <sub>min</sub> /nm <sup>2</sup> × 10 <sup>2</sup>	$\alpha$
Li <sup>+</sup>	283	2.50 (2.41)	3.10	0.54	0.75
	288	2.60 (2.54)	2.98	0.57	0.71
	293	2.83 (2.76)	3.18	0.52	0.72
	298	2.82 (2.80)	3.22	0.52	0.72
	303	2.79 (2.84)	3.22	0.51	0.72
	308	2.91 (2.90)	3.27	0.51	0.71
	313	3.21 (3.17)	3.29	0.50	0.71
Na <sup>+</sup>	283	2.82 (2.77)	2.99	0.56	0.76
	288	2.91 (2.86)	3.16	0.53	0.70
	293	2.98 (2.95)	3.21	0.52	0.71
	298	3.10 (3.13)	3.25	0.51	0.72
	303	3.21 (3.20)	3.27	0.51	0.74
	308	3.27 (3.31)	3.27	0.50	0.76
	313	3.33 (3.36)	3.32	0.48	0.77
K <sup>+</sup>	283	2.11 (2.14)	3.40	0.49	0.70
	288	2.18 (2.19)	3.46	0.48	0.70
	293	2.25 (2.24)	3.52	0.47	0.69
	298	2.38 (2.32)	3.55	0.47	0.71
	303	2.42 (2.41)	3.54	0.47	0.70
	308	2.50 (2.52)	3.58	0.46	0.71
	313	2.61 (2.60)	3.61	0.46	0.70
NH <sub>4</sub> <sup>+</sup>	283	2.28 (2.23)	3.12	0.53	0.74
	288	2.39 (2.36)	3.17	0.52	0.74
	293	2.41 (2.40)	3.23	0.51	0.73
	298	2.52 (2.48)	3.28	0.51	0.74
	303	2.68 (2.62)	3.38	0.49	0.78
	308	2.81 (2.82)	3.41	0.49	0.74
	313	2.80 (2.82)	3.49	0.47	0.74

<sup>a</sup>The values in the parenthesis represent cmc determined by conductivity method.

Table 3.3

Micellization and Surface parameters of Dodecyl benzene sulfonate having different tetraalkylammonium counterions at various temperatures (T/K): cmc, maximum surface excess concentration, minimum areas per molecule and ionization degree.

Counterion	T/K	cmc <sup>a</sup> / (mol dm <sup>-3</sup> × 10 <sup>-3</sup> )	Γ <sub>max</sub> / cm <sup>-2</sup> × 10 <sup>6</sup>	mol	A <sub>min</sub> /nm <sup>2</sup> × 10 <sup>2</sup>	α
(CH <sub>3</sub> ) <sub>4</sub> N <sup>+</sup>	283	1.31 (1.28)	3.11		0.53	0.71
	288	1.34 (1.29)	3.14		0.53	0.73
	293	1.34 (1.30)	3.17		0.52	0.74
	298	1.37 (1.31)	3.20		0.52	0.73
	303	1.39 (1.34)	3.28		0.51	0.74
	308	1.45 (1.37)	3.30		0.50	0.75
	313	1.49 (1.45)	3.36		0.49	0.73
(C <sub>2</sub> H <sub>5</sub> ) <sub>4</sub> N <sup>+</sup>	283	1.27 (1.27)	3.05		0.55	0.76
	288	1.28 (1.32)	3.03		0.55	0.77
	293	1.27 (1.22)	3.02		0.55	0.79
	298	1.30 (1.24)	3.10		0.54	0.79
	303	1.32 (1.25)	3.14		0.53	0.80
	308	1.32 (1.27)	3.19		0.52	0.79
	313	1.37 (1.29)	3.26		0.51	0.81
(C <sub>3</sub> H <sub>7</sub> ) <sub>4</sub> N <sup>+</sup>	283	1.08 (1.10)	3.02		0.55	0.79
	288	1.17 (1.15)	3.04		0.55	0.81
	293	1.18 (1.17)	3.07		0.54	0.81
	298	1.22 (1.19)	3.08		0.54	0.82
	303	1.23 (1.20)	3.11		0.53	0.82
	308	1.25 (1.23)	3.16		0.53	0.82
	313	1.31 (1.25)	3.19		0.52	0.82
(C <sub>4</sub> H <sub>9</sub> ) <sub>4</sub> N <sup>+</sup>	283	0.79 (0.75)	2.93		0.57	0.87
	288	0.84 (0.81)	2.96		0.56	0.84
	293	0.99 (0.96)	2.99		0.55	0.84
	298	1.05 (1.02)	2.99		0.56	0.83
	303	1.05 (1.03)	3.00		0.55	0.83
	308	1.10 (1.05)	3.01		0.55	0.82
	313	1.01 (0.82)	3.05		0.54	0.83

<sup>a</sup>The values in the parenthesis represent cmc determined by conductivity method.

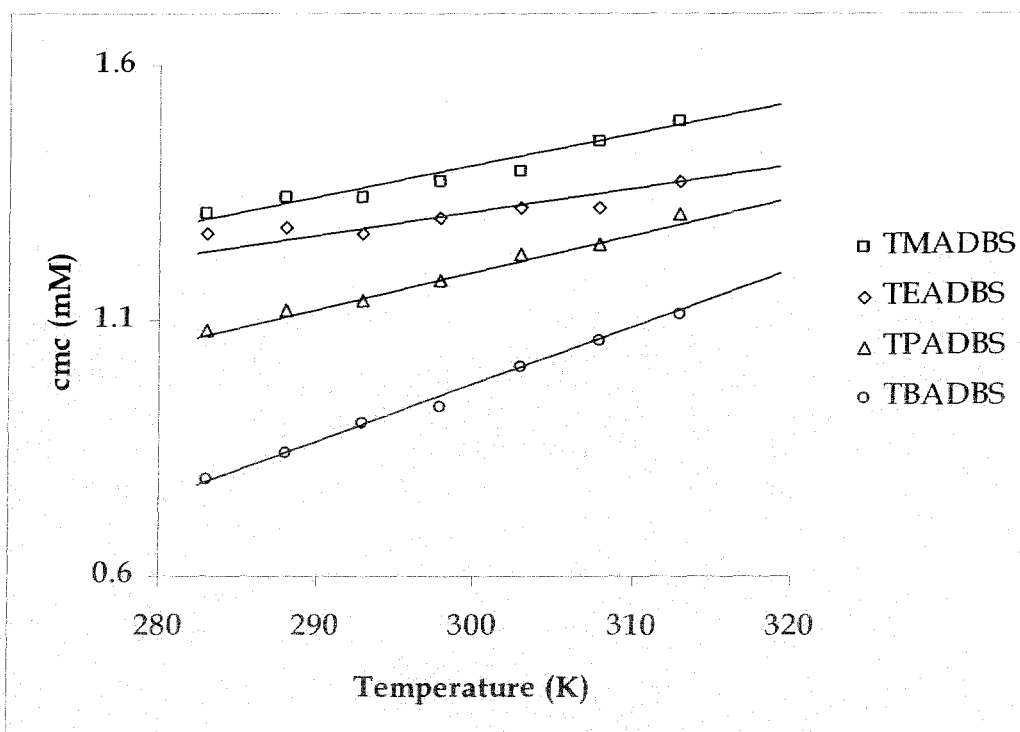


Figure 3.18. Variation of cmc with temperature of DBS having different tetra alkyl ammonium counterions.

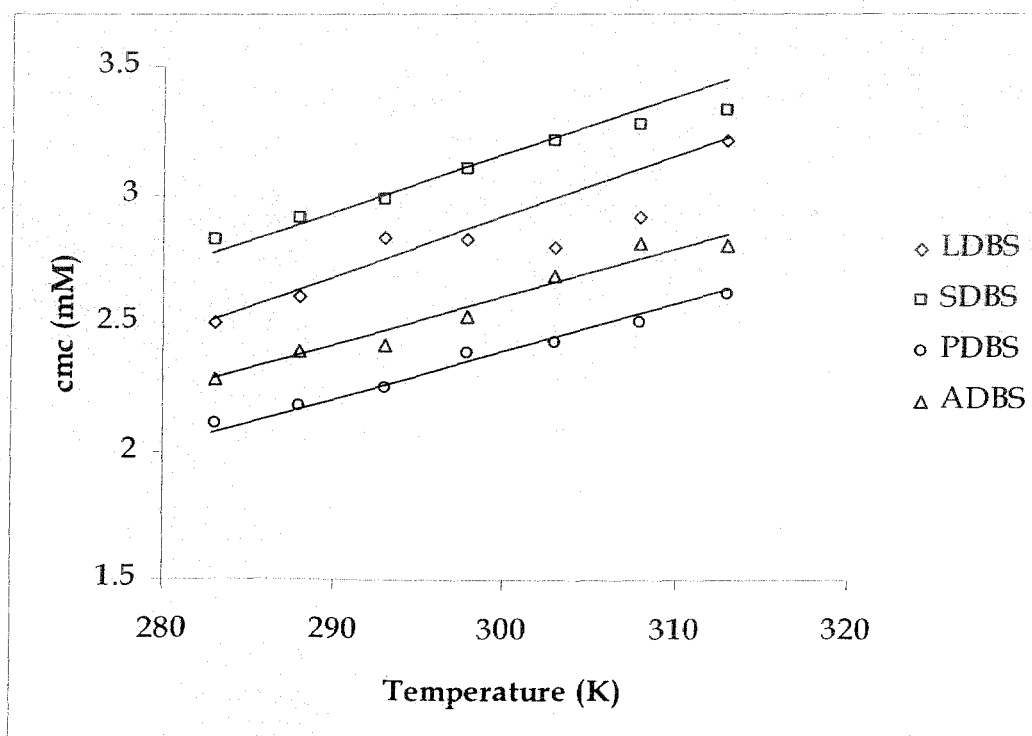


Figure 3.19. Variation of cmc with temperature of DBS having different alkali metal counterions along with  $\text{NH}_4^+$ .

**Table 3.4**  
**Ionic and Hydrated radius along with Hydration number of ions derived from corrected ionic radii**

Ion	Hydration number	Ionic Radius (Å)	Hydrated Radius (Å)
NH <sub>4</sub> <sup>+</sup>	4.6	1.48	3.31
K <sup>+</sup>	5.1	1.37	2.23
Na <sup>+</sup>	6.5	0.99	2.76
Li <sup>+</sup>	7.4	0.59	3.40

It has been also reported [75] that the binding tendency of alkali metal cations to polyethylene oxide (PEO) follows the order  $K^+ > Cs^+ > Na^+$ . However, among all the alkali ions under investigation in the present study,  $K^+$  binds most strongly to DBS resulting in the lowest cmc at a particular temperature. Figure 3.19 represents the variation of cmc with temperature for DBS containing different alkali metal counterions along with  $NH_4^+$ .

### 3.5.2. Surface parameters

The maximum surface excess concentrations ( $\Gamma_{max}$ ) in the aqueous-air interface are calculated by using Gibb's adsorption equation since the  $\Gamma_{max}$  is a useful measure of the effectiveness of adsorption of the surfactant at air-solution interface, since it is the maximum value that adsorption can attain. It is well known that the air-solution interface of a surfactant solution is well populated by the adsorbed molecules. The general trend of  $\Gamma_{max}$  with increase of temperature is a slight decrease in its value for both nonionic and anionic surfactants but there is some other cases where opposite trend is also observed [76-78]. For 1:1 ionic surfactant in the absence of any additives,  $\Gamma_{max}$  has the following expression [76-77,79]:

$$\Gamma_{max} = \left( \frac{1}{2.303n'RT} \right) \left( - \frac{\partial \gamma}{\partial \log C} \right) \quad (3.10)$$

where  $\gamma$ ,  $C$  and  $n'$  are the surface tension, molar concentration and number of particles per molecule of surfactant respectively.  $\gamma$  vs.  $\log C$  plot was fitted to a second order

polynomial to measure the  $\Gamma_{\max}$  value and also all the surfactants behave like a univalent electrolyte for which  $n'$  value is taken equal to 2.

The area per molecule at the air / water interface gives us the information on the packing degree and also the adsorbed surfactant molecules orientation when compared with the dimensions of the molecule as obtained by the use of molecular models. The minimum area per molecule ( $A_{\min}$ ) can be easily obtained from the expression of surface excess concentration by using the following relations:

$$A_{\min} = \frac{10^{14}}{(N\Gamma_{\max})} \quad (3.11)$$

where  $\Gamma_{\max}$  is in mol/cm<sup>2</sup> and  $N$  is the Avogadro's number. So, with increase in temperature, the  $A_{\min}$  value generally shows the inverse trend as that of  $\Gamma_{\max}$ .

A closer look at the table 3.2 and table 3.3 show that the  $\Gamma_{\max}$  values of all the counterions change in the opposite way from general trend. However, the result can be explained in the following way. The  $\Gamma_{\max}$  values generally decrease due to the increased thermal motion with a consequent decrease in the effective adsorption process. But for dodecyl benzene moiety with varying counterions, a slight increase may be due to the lower hydration effect of the dodecyl benzene sulfonate surfactants at higher temperature and hence increasing tendency to move the molecules to the air-liquid interface [80-84]. The benzene ring in the surfactants may also be partially responsible for this result via steric inhibition during adsorption process. Similar type of result is also reported in the literature [81]. At a particular temperature, with changes in counterions, the  $\Gamma_{\max}$  value shows some irregularities due to the enhanced hydrophobicity of the anionic part of the surfactant molecules depending upon the accessibility of their corresponding counterions. Some part of the tetraalkyl ammonium counterion in the dodecyl benzene sulfonate layer may be responsible for the gradual decrease  $\Gamma_{\max}$  value. This type of penetration is found in the literature [83] also. With increase in temperature, amphiphilic molecule tend to form a closely packed monolayer film of the hydrocarbon chain at the air / solution interface owing to the decreased repulsion between the oriented head groups indicated by the value of  $A_{\min}$ .

### 3. 5. 3. Thermodynamic parameters

The temperature dependency of DBS micelles having different counterions also enables one to determine the thermodynamic parameters of micellization. According to the pseudo-phase separation model the standard Gibbs free energy of micellization,  $\Delta G_m^0$  for ionic uni-univalent surfactant can be expressed as [21,24,85]:

$$\Delta G_m^0 = (2 - \alpha) RT \ln x_{cmc} \quad (3.12)$$

Here,  $x_{cmc}$  is the cmc expressed in mole fraction scale and  $\alpha$ , the ionization degree or counterionic ionization constant of the micelle, can be expressed by  $\alpha = \frac{p}{n}$ , where  $p$  and  $n$  are the effective charge and the aggregation number of the micelle respectively. It is well known that the value of  $\alpha$  can be determined from the ratio of the slope of the two linear fragments of conductivity-concentration plot above and below cmc [85-86].

The standard enthalpy change  $\Delta H_m^0$  can be obtained from Gibb's-Helmholtz equation [25]:

$$\Delta H_m^0 = -RT^2 \left[ (2 - \alpha) \left( \frac{\partial \ln x_{cmc}}{\partial T} \right)_p - \ln x_{cmc} \left( \frac{\partial (2 - \alpha)}{\partial T} \right)_p \right] \quad (3.13)$$

However, as the variation of  $\alpha$  with temperature is not well defined due to polydispersity of micelle and does not follow any general trend, it is difficult to estimate the second term in the parenthesis experimentally [87-88]. The term, however, is small in comparison with the first one, and therefore, to gain quantitative information regarding the thermodynamics we neglect the second term of the equation (3.13), and the expression now becomes:

$$\Delta H_m^0 = -(2 - \alpha)RT^2 \left( \frac{\partial \ln x_{cmc}}{\partial T} \right)_p \quad (3.14)$$

The enthalpy of micellization may be obtained if the dependency of the cmc on the temperature is known. The  $\Delta S_m^0$  and  $\Delta_{mic}C_p^0$  are also determined as essential thermodynamic parameters from the common expressions:

$$\Delta S_m^0 = \frac{(\Delta H_m^0 - \Delta G_m^0)}{T} \quad (3.15)$$

$$\Delta_{mic}C_p^0 = \left( \frac{\partial \Delta H_m^0}{\partial T} \right)_p \quad (3.16)$$

In table 3.5 and table 3.6, the various thermodynamic data associated with micellization are presented. These parameters are found to vary with temperature and also with the nature of the associated counterions. Negative sign of  $\Delta H_m^0$  suggests that surfactant aggregation is an endothermic process. The variation of the standard thermodynamic parameters with different counterions at a particular temperature can also be explained by the size and the hydration of the counterion. In the figure 3.20, the variation of enthalpy with the variation of counterion of alkali metals along with ammonium ion is given. From the plot, it is clear that the enthalpy first increases from LDBS to SDBS and then decreases to a very low value in all the temperatures for PDBS and after that it will further increases to the higher values close to LDBS. Similar plot of enthalpy with tetraalkyl ammonium counterions are presented in the Figure 3.21. From these two tables it is clear that the counterionic activity is more pronounced in the case of alkali metal ions. The tetraalkyl ammonium surfactants have their enthalpy of micellization relatively close to each other. The enthalpy value first decreases with increase in chain length, reaches a shallow minimum for tetrapropyl ammonium counterions and then increases.

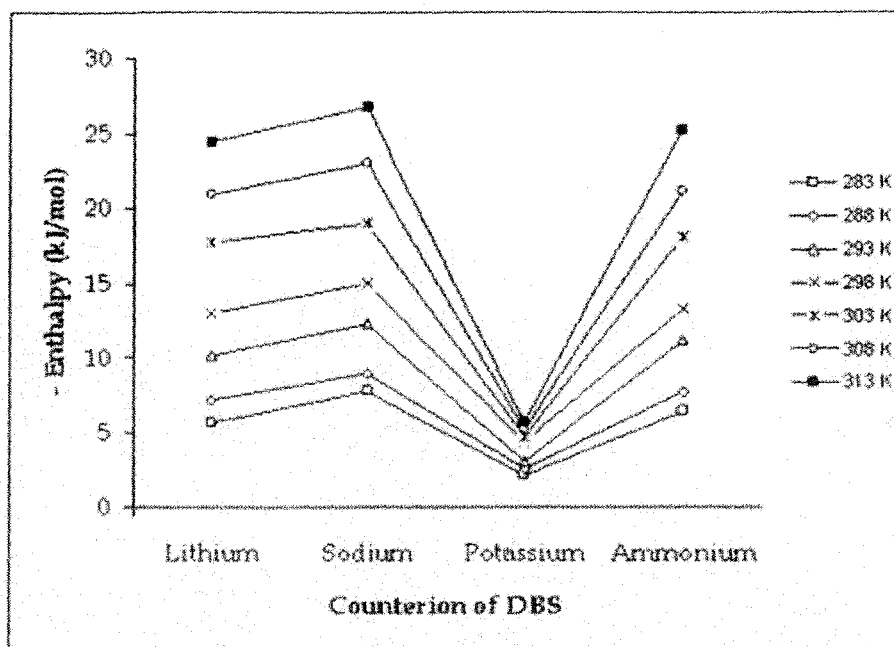


Figure 3.20. Enthalpy Change with the change in alkali metal counterions along with  $\text{NH}_4^+$  ion.

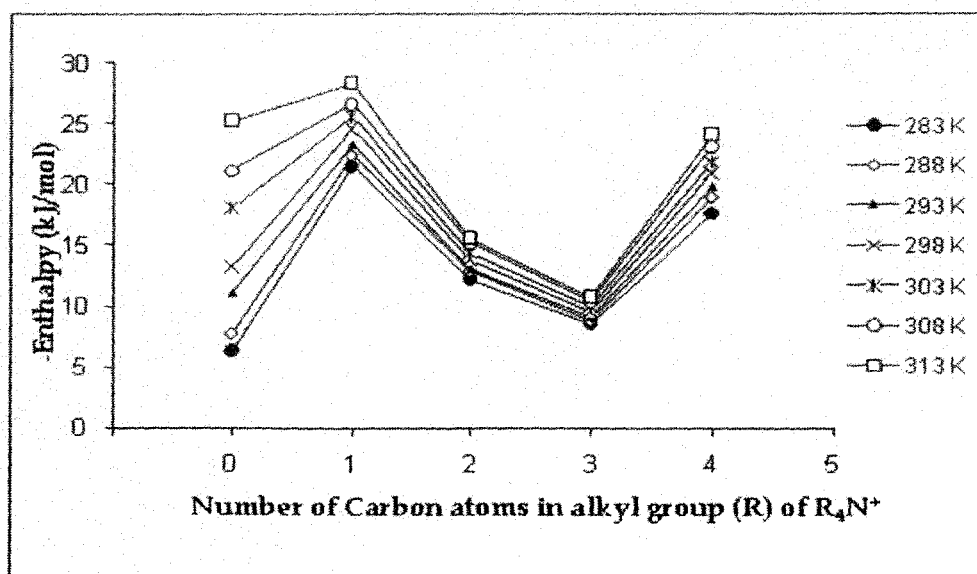


Figure 3.21. Enthalpy Change with the change in Alkyl Chain Length of R in  $\text{R}_4\text{N}^+$  counterion.

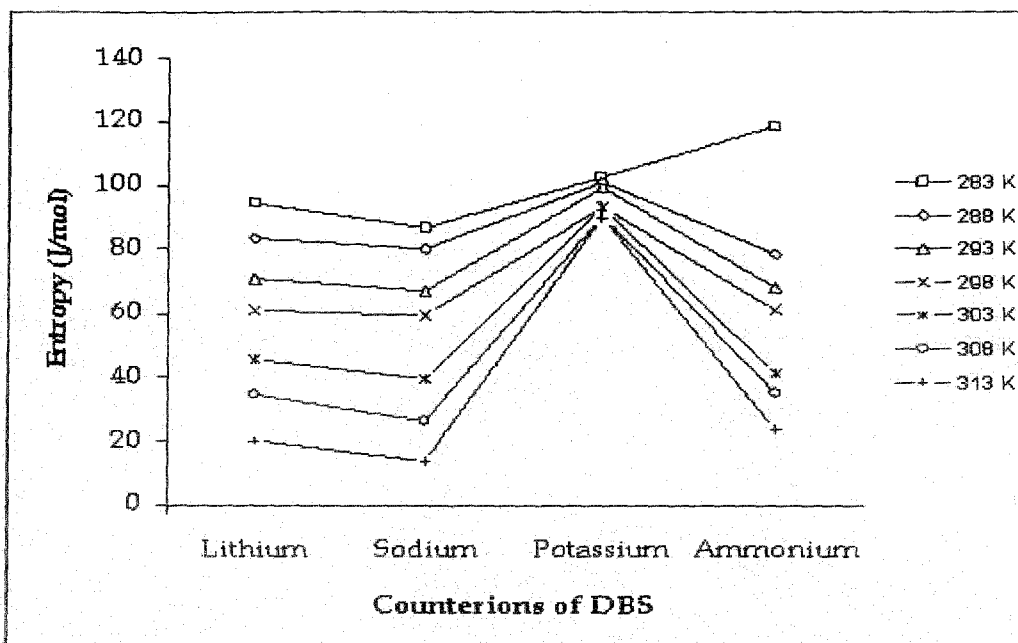


Figure 3.22. Entropy Change with the change in alkali metal counterions along with  $\text{NH}_4^+$  ion.

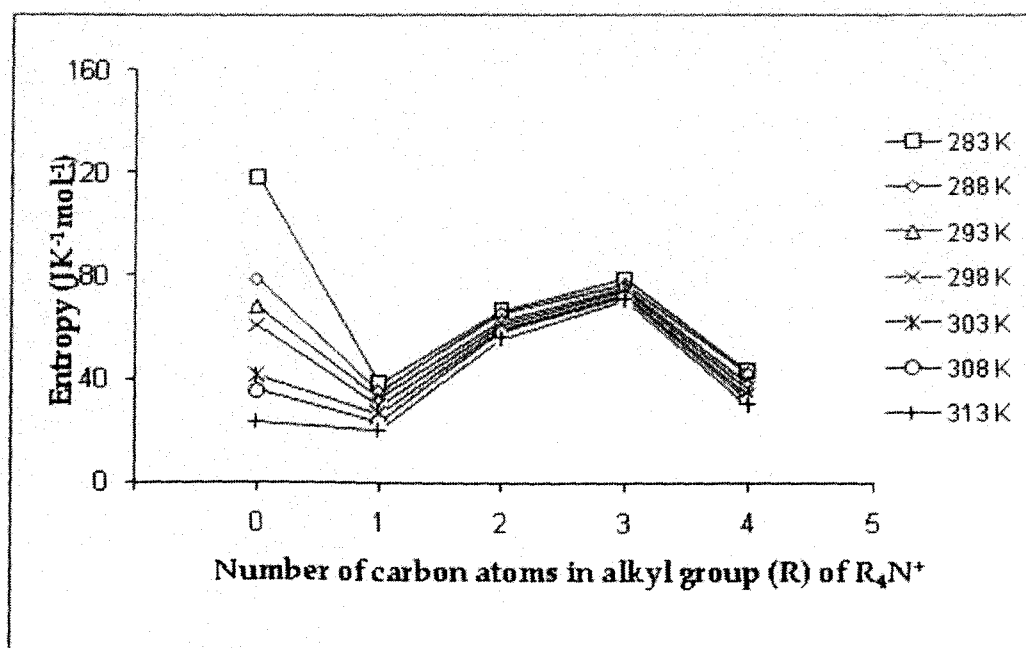


Figure 3.23. Entropy Change with the change in Alkyl Chain Length of R in  $\text{R}_4\text{N}^+$  counterion.

In figure 3.22 and 3.23, the entropy changes as a function of counterions are given. The opposite trend of what is observed in enthalpy changes is attributed to the fact that in a normal micellization process the contribution of both entropy and enthalpy ultimately makes the process spontaneous according to the Gibbs-Helmholtz equation.

Different researchers often attempted to represent the thermodynamic variables of micellization into additive contribution of two factors: (1) interactions between hydrocarbon chains with water and (2) interactions between head groups, counterions and surfaces [89-90]. It is, therefore, logical to suppose that the second factor is important for the present work. A close look on the thermodynamic parameters support the view that in order to form micelle the gain in entropy is the major factor leading to negative change in Gibb's free energy [91-92]. But for the alkali metals counterions, the fact that though the free energy changes are not very different, the entropy change is significantly higher and the enthalpy changes are much lower for  $K^+$  counterion containing DBS compared to all other systems. This suggests that the entropy contributes as a major driving force in micellization. Less hydration and higher binding capacity of  $K^+$  ion may cause higher contribution of  $\Delta S_m^0$  in aggregation process. With increasing temperature,  $\Delta S_m^0$  decreases systematically for a particular type of counterion, suggesting a disruption of ordered arrangement of water dipoles around the amphiphilic part of the surfactant molecules [5,7,44]. Conceptually,  $\Delta G_m^0$  may be imagined to be divided into an electric contribution,  $F_{el}^0$  arising from the ionic head groups and a hydrocarbon contribution,  $F_{hc}^0$ .

$$\Delta G_m^0 = F_{el}^0 + F_{hc}^0 \quad (3.17)$$

Where  $F_{el}^0$  is positive and its contribution to the total  $\Delta G_m^0$  value is generally small (about 3 ~ 4%). The  $F_{hc}^0$  value may be divided into the free energy components  $\Delta G_{-CH_2-}^0$  (contribution of  $-CH_2-$  groups) and  $\Delta G_{-CH_3}^0$  (contribution of terminal  $-CH_3$  groups).  $\Delta G_{-CH_3}^0$  is constant, however,  $\Delta G_{-CH_2-}^0$  depends upon the chain length. The reported value for ionic surfactants is approximately  $2.93 \sim 3 \text{ kJ mol}^{-1}$  [5,7,44]. Though the free energy change is not very different for all the systems, the enthalpy change is relatively higher.

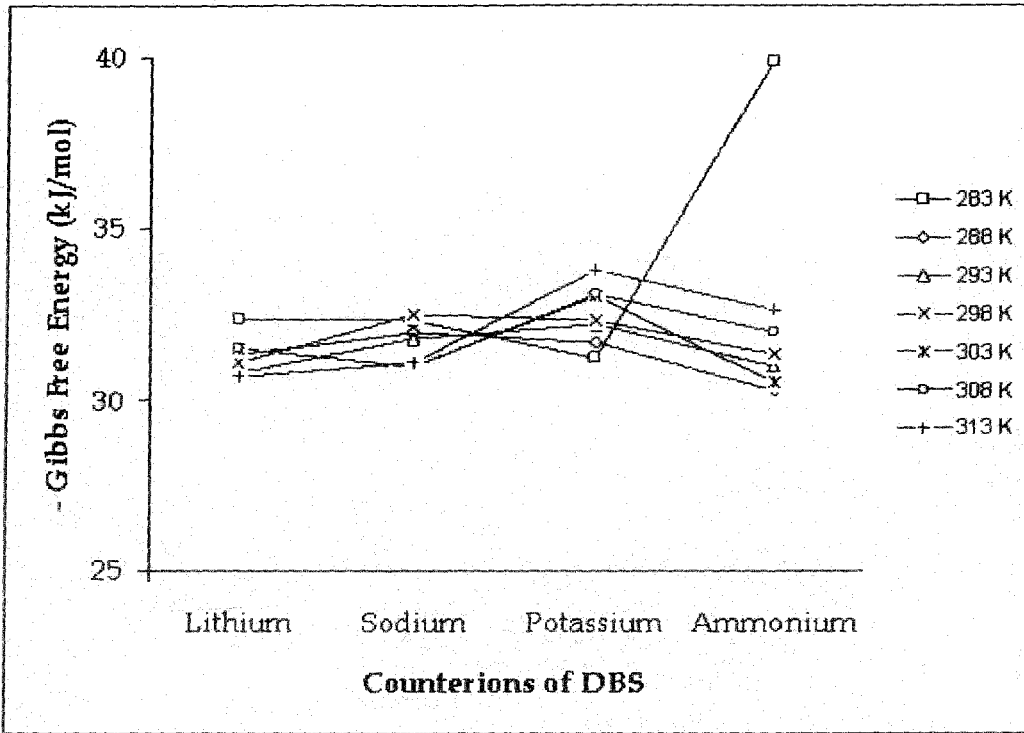


Figure 3.24. Gibbs Free Energy Change with the change in alkali metal counterions along with  $\text{NH}_4^+$  ion.

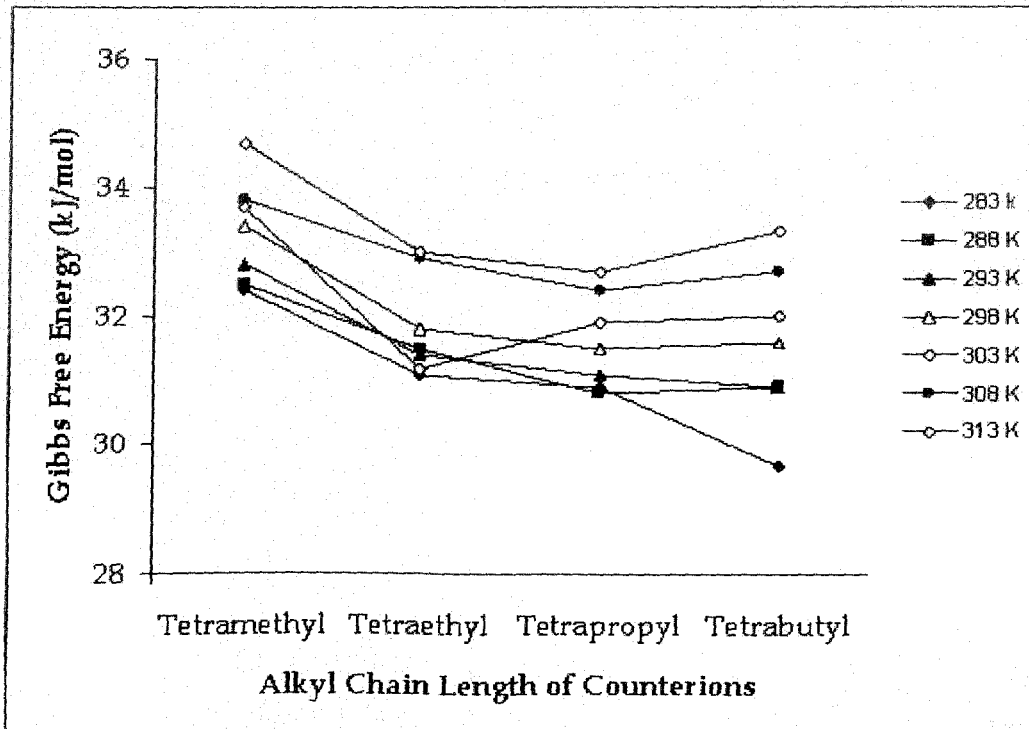


Figure 3.25. Entropy Change with the change in Alkyl Chain Length of R in  $\text{R}_4\text{N}^+$  counterion.

Table 3.5

Thermodynamic parameters of micellization for Dodecyl benzene sulfonate with different alkali counterions along with  $\text{NH}_4^+$  at various temperatures: Standard Gibb's free energy, Enthalpy, Entropy and standard heat capacity.

Counterion	T/K	$-\Delta G_m^\circ$ (kJ mol <sup>-1</sup> )	$-\Delta H_m^\circ$ (kJ mol <sup>-1</sup> )	$\Delta S_m^\circ$ (J mol <sup>-1</sup> )	$-\Delta C_{pm}^\circ$ (J mol <sup>-1</sup> K <sup>-1</sup> )
Li <sup>+</sup>	283	32.4	5.7	94.3	409
	288	31.3	7.2	83.7	480
	293	30.8	10.1	70.6	551
	298	31.1	12.9	61.1	622
	303	31.5	17.7	45.5	693
	308	31.5	20.8	34.7	764
	313	30.7	24.3	20.4	835
Na <sup>+</sup>	283	32.3	7.8	86.6	382
	288	32.0	9.0	79.9	474
	293	31.8	12.2	66.9	566
	298	32.5	14.9	59.1	658
	303	31.0	19.0	39.6	750
	308	31.0	22.9	26.3	842
	313	31.1	26.7	14.0	934
K <sup>+</sup>	283	31.2	2.1	102.8	127
	288	31.7	2.6	101.0	117
	293	32.2	3.1	99.3	107
	298	32.3	4.4	93.6	97
	303	33.0	4.7	93.4	87
	308	33.1	5.2	90.6	77
	313	33.8	5.7	89.8	67
NH <sub>4</sub> <sup>+</sup>	283	39.9	6.3	118.7	405
	288	30.3	7.7	78.5	488
	293	31.0	11.1	67.9	571
	298	31.3	13.2	60.7	654
	303	30.5	18.0	41.2	737
	308	32.0	21.1	35.4	820
313	32.6	25.2	23.6	903	

<sup>a</sup>The values in the parenthesis represent cmc determined by conductivity method.

Table 3.6

Thermodynamic parameters of micellization for Dodecyl benzene sulfonate with different tetraalkyl ammonium counterions at various temperatures: Standard Gibb's free energy, Enthalpy, Entropy and standard heat capacity.

Counterion	T/K	$-\Delta G_m^\circ$ (kJ mol <sup>-1</sup> )	$-\Delta H_m^\circ$ (kJ mol <sup>-1</sup> )	$\Delta S_m^\circ$ (J mol <sup>-1</sup> )	$-\Delta C_{pm}^\circ$ (J mol <sup>-1</sup> K <sup>-1</sup> )
(CH <sub>3</sub> ) <sub>4</sub> N <sup>+</sup>	283	32.4	21.5	38.34	141
	288	32.5	22.4	35.05	159
	293	32.8	23.3	32.21	177
	298	33.4	24.6	29.46	195
	303	33.7	25.6	26.47	213
	308	33.8	26.6	23.17	231
	313	34.7	28.3	20.41	249
(C <sub>2</sub> H <sub>5</sub> ) <sub>4</sub> N <sup>+</sup>	283	31.1	12.2	66.68	108
	288	31.5	12.8	65.09	116
	293	31.4	13.1	62.50	124
	298	31.8	13.8	60.81	132
	303	31.2	14.3	59.08	140
	308	32.9	15.1	58.02	148
	313	33.0	15.6	55.53	156
(C <sub>3</sub> H <sub>7</sub> ) <sub>4</sub> N <sup>+</sup>	283	30.9	8.5	79.05	81
	288	30.8	8.7	76.50	87
	293	31.1	9.1	75.00	93
	298	31.5	9.5	73.71	99
	303	31.9	9.9	72.76	105
	308	32.4	10.3	71.64	111
	313	32.7	10.7	70.26	117
(C <sub>4</sub> H <sub>9</sub> ) <sub>4</sub> N <sup>+</sup>	283	29.7	17.6	43.07	245
	288	30.9	18.9	41.71	241
	293	30.9	19.8	38.01	237
	298	31.6	20.9	35.79	233
	303	32.0	21.8	33.60	229
	308	32.7	23.1	31.38	225
	313	33.3	24.0	29.90	221

<sup>a</sup>The values in the parenthesis represent cmc determined by conductivity method.

for tetramethyl ammonium ion compared to the other counter ions. It can, therefore, be concluded that for the present system, enthalpy contribution is the major factor for micellization. Loosely bound water dipole with the  $N^+(CH_3)_4$  ion may cause lower contribution of  $\Delta S_m^0$  in aggregation process.

The effective interactions associated with hydrocarbon chains may be expressed by standard heat capacity of micelle formation,  $\Delta_{mic}C_p^0$ . In all the surfactant systems, the standard heat capacity changes linearly with temperature, as shown in figure 3.26.

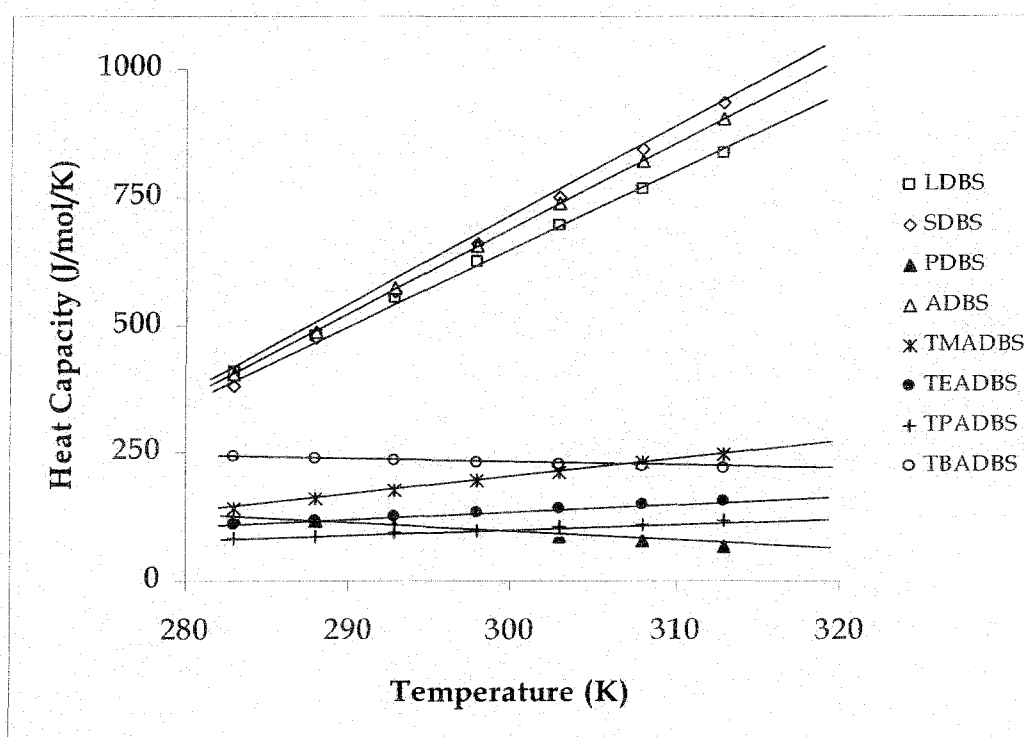


Figure 3.26. Variation of Heat capacity of the surfactants as a function of temperature.

The calculated values of  $\Delta_{mic}C_p^0$  for DBS with varying counterions fall between a wide range of value viz., -67 to -934 J mol<sup>-1</sup> K<sup>-1</sup>, for the variation of temperature between 283 K and 313 K. For all the counterions except K<sup>+</sup>,  $\Delta_{mic}C_p^0$ 's do not change significantly at lower temperatures (<25°C); but at higher temperatures,  $\Delta_{mic}C_p^0$  values follow the order Na<sup>+</sup> > NH<sub>4</sub><sup>+</sup> > Li<sup>+</sup> > K<sup>+</sup>. Potassium ion, however, shows anomalous behaviour, which may be due to its strong tendency of ion-pair formation. For the tetraalkyl ammonium counterions, the order of  $\Delta_{mic}C_p^0$  values at a particular temperature is as follows: (CH<sub>3</sub>)<sub>4</sub>N<sup>+</sup> > (C<sub>4</sub>H<sub>9</sub>)<sub>4</sub>N<sup>+</sup> > (C<sub>2</sub>H<sub>5</sub>)<sub>4</sub>N<sup>+</sup> > (C<sub>3</sub>H<sub>7</sub>)<sub>4</sub>N<sup>+</sup>. This irregularity in behaviour

may also be explained by the tendency to form ion pair with the DBS moiety. Counterion binding also reduces the number of water molecules in the solvation shell of the counterion as well as the negatively charged head groups of DBS. At high temperatures,  $\Delta_{mic}C_p^{0'}$ 's give large negative values due to solvation of ions upon demicellization, and this is quite reasonable because as the temperature is increased cmc value also increases in all the present systems.

Enthalpy and entropy change in the micellization process show a linear relationship for all the surfactant systems at a particular temperature and this is known as the enthalpy-entropy compensation and it is true for any other following processes, viz., oxidation-reduction, hydrolysis, protein unfolding etc. The entropy-enthalpy compensation plot is given in the figure 3.27 for different surfactant system at 298 K [25,77-78].

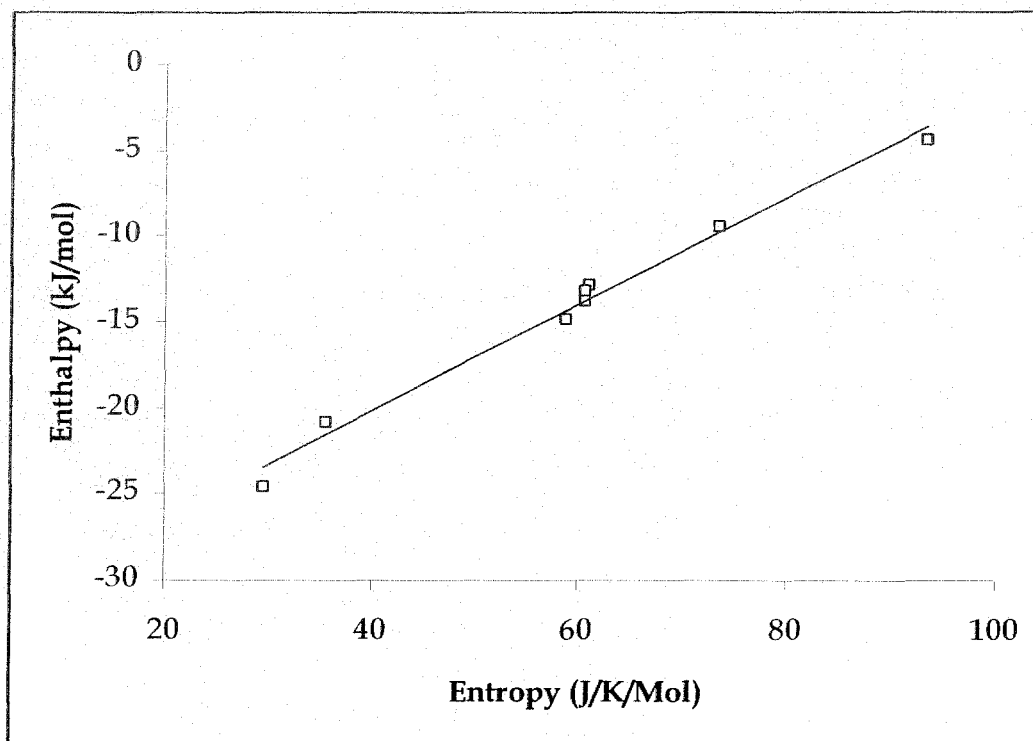


Figure 3.27. Entropy-enthalpy compensation plot of surfactant with different counterions at 298 K temperature.

The importance of this value lies in the fact with hydrophobicity of surfactant which leads to stable micelle formation. The compensation phenomenon between the enthalpy change,  $\Delta H_m^0$ , and the entropy change,  $\Delta S_m^0$ , in various processes can be described in the form of [83-84]

$$\Delta H_m^0 = \Delta H_m^* + T_c \Delta S_m^0 \quad (3.18)$$

The compensation temperature can be calculated from the slope of the enthalpy-entropy compensation plot, which is a straight line. The slope and intercept of the straight line has different meanings, slope interprets a measure of desolvation part of micellization which means a characteristic of solute-solute and solute-solvent interaction whereas the intercepts interprets solute-solute interactions. From the figure 3.27, the intercepts ( $\Delta H_m^*$ ) has been found to be  $-32.6 \text{ kJ mol}^{-1}$  for DBS which correspond to the driving force of micellization where the entropy does not contribute the process at that particular temperature.

### 3.6. Effects of counterions on the micellization of dodecyl benzene sulfonate, dodecyl sulfate and bis-(2-ethyl-1-hexyl) sulfosuccinate: A brief comparison

Present work constitutes a part of the series of research performed in our laboratory on the effect of counterions and temperature on the micellization of various anionic surfactants; some of them are already published [80 - 82]. The work has been carried out mainly on the three anionic surfactants viz., dodecyl benzene sulfonates, dodecyl sulfate and bis-(2-ethyl-1-hexyl) sulfosuccinate with varying counterions. The reason for selecting these surfactants stems from their structural differences at the hydrophobic ends. The general structure of dodecyl benzene sulfonate with sodium ion is given in figure 3.1. As discussed earlier, the DBS moiety contains a benzene ring attached with the sulfonate group and also the  $C_{12}$ -hydrocarbon tail is branched in the present system of the study. Furthermore, the literature concerning DBS surfactant is not so huge as compared to SDS or AOT. This may be due to the presence of several

isomeric forms of DBS moiety. Sodium dodecyl sulfate is probably the most researched anionic surfactants possibly due to its simple structure [36-37,74,93-94]. It shows many other properties like interactions with dyes, electrophoresis and electrokinetics or methane hydrate formation reactions [95-97]. The schematic molecular structure of SDS is in Figure 3.28.

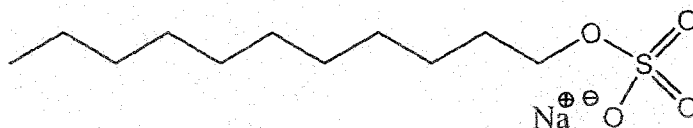


Figure 3.28: Schematic molecular structure of SDS

AOT (Aerosol-OT, sodium bis-(2-ethyl-1-hexyl) sulfosuccinate), a double tailed anionic surfactant, used mainly in medicinal and pharmaceutical purposes due to its non-toxic property, It can form microemulsion and has the rich phase behaviour in solution [98-99]. Figure 3.29 shows the schematic molecular structure of AOT.

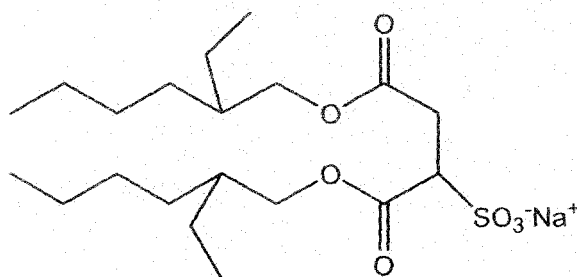


Figure 3.29: Schematic molecular structure of AOT

In tables 3.7, 3.8, 3.11 and 3.12, the cmc values were determined by surface tension and conductivity measurements, are given. The range of cmc values of the following three surfactants with varying counterions are 3.33 mM to 0.79 mM, 9.21 mM to 1.10 mM and 3.55 mM to 0.75 mM for DBS, DS and AOT respectively. The insertion of a phenyl ring and the branching of hydrophobic tail lowered the cmc values of DBS and AOT compared to DS. On the other hand, benzene ring with branching hydrocarbon chain brings more hydrophobicity to the surfactant than double strand structure of AOT and as a result, the cmc values are less than as compared to AOT.

In all the three surfactants, the change of cmc values with temperature is small but it is in detectable range. In potassium salts of DS and AOT, it was found that at a concentration of 10 times the cmc, they are immiscible in water at room temperature. The solution contains hydrated crystals dispersed in a micellar phase. So, the micellization property can be studied for K-AOT in the temperature lower than 313 K and we have studied the cmc within the temperature range 283-308 K. Potassium dodecyl sulfate has the Krafft temperature of 307 K [100-102] at the cmc. So, it is impossible to investigate the micellization process in our temperature range for KDS since the temperature leading to a clear solution was too high. But for DBS moiety, no such problem arises in the temperature range 283 - 308 K.

For all the surfactant systems with tetraalkyl ammonium counterions, cmc decreases with increase in tetraalkyl ammonium chain length. The order of alkali metal cations and ammonium ion is not same for the three surfactants. The orders are:  $\text{NH}_4^+ > \text{Li}^+ > \text{Na}^+$  for dodecyl sulfate,  $\text{NH}_4^+ > \text{Na}^+ > \text{Li}^+ > \text{K}^+$  for AOT and  $\text{Na}^+ > \text{Li}^+ > \text{NH}_4^+ > \text{K}^+$  for DBS. This trend can be explained by the counterion binding to micelles.  $\text{K}^+$  gives anomalous results owing to its tendency towards ion-pair formation in K-AOT.  $\text{Li}^+$  has the highest hydrated radius can modify the internal structure of double trailed structure of AOT micelle resulting a lower cmc values. The general tendency of cmc change with temperature is parabolic in nature [103-106]. These are true to the micelles of surfactants viz., LDS, SDS, ADS, Na-AOT,  $\text{NH}_4$ -AOT, TMA-AOT, TEA-AOT. Other surfactants of DS and AOT have very low temperature dependency. However, the present DBS with different counterions show linear types of temperature dependency.

Table 3.7\*

Surface properties of dodecyl sulfate having different alkali counterions along with  $\text{NH}_4^+$  ion at various temperatures (T/K): cmc, maximum surface excess concentration, minimum areas per molecule at the surface.

Counterion	T/K	cmc <sup>a</sup> / (mol dm <sup>-3</sup> × 10 <sup>-3</sup> )	$\Gamma_{\text{max}}$ / mol cm <sup>-2</sup> × 10 <sup>10</sup>	$A_{\text{min}}$ /nm <sup>2</sup> × 10 <sup>2</sup>	$\alpha$
Li <sup>+</sup>	283	9.11 (9.06)	3.22	0.52	0.30
	288	8.87 (8.92)	3.10	0.54	0.29
	293	8.52 (8.55)	2.98	0.55	0.31
	298	8.23 (8.18)	3.08	0.54	0.33
	303	8.43 (8.42)	2.94	0.56	0.34
	308	8.51 (8.52)	2.90	0.57	0.32
	313	8.47 (8.45)	2.91	0.57	0.33
Na <sup>+</sup>	283	8.88 (8.96)	3.12	0.53	0.28
	288	8.15 (8.17)	3.01	0.55	0.30
	293	8.05 (8.01)	3.11	0.54	0.30
	298	7.96 (7.94)	2.90	0.57	0.32
	303	8.58 (8.62)	2.88	0.58	0.35
	308	8.65 (8.67)	2.78	0.60	0.32
	313	8.77 (8.80)	2.73	0.61	0.34
NH <sub>4</sub> <sup>+</sup>	283	9.21 (9.16)	3.21	0.52	0.27
	288	9.07 (9.10)	3.18	0.52	0.29
	293	8.88 (8.90)	3.11	0.53	0.28
	298	8.51 (8.62)	3.02	0.55	0.32
	303	8.39 (8.38)	2.93	0.57	0.30
	308	8.85 (8.76)	2.87	0.58	0.31
	313	8.92 (8.88)	2.88	0.58	0.28

<sup>a</sup>The values in the parenthesis represent cmc determined by conductivity method.

Table 3.8\*

Surface properties of dodecyl sulfate having different tetraalkylammonium counterions at various temperatures (T/K): cmc, maximum surface excess concentration, minimum areas per molecule at the surface.

Counterion	T/K	cmc <sup>a</sup> / (mol dm <sup>-3</sup> × 10 <sup>-3</sup> )	Γ <sub>max</sub> / cm <sup>-2</sup> × 10 <sup>10</sup>	mol	A <sub>min</sub> /nm <sup>2</sup> × 10 <sup>2</sup>	α
(CH <sub>3</sub> ) <sub>4</sub> N <sup>+</sup>	283	5.92 (6.01)	3.34		0.50	0.21
	288	5.70 (5.66)	3.24		0.51	0.21
	293	5.58 (5.55)	3.18		0.52	0.23
	298	5.51 (5.52)	3.15		0.53	0.25
	303	5.49 (5.47)	3.20		0.52	0.22
	308	5.56 (5.60)	3.14		0.53	0.24
	313	5.80 (5.72)	3.08		0.54	0.23
(C <sub>2</sub> H <sub>5</sub> ) <sub>4</sub> N <sup>+</sup>	283	4.08 (4.10)	3.28		0.51	0.20
	288	3.98 (3.97)	3.25		0.51	0.21
	293	3.92 (3.91)	3.19		0.52	0.23
	298	3.86 (3.86)	3.11		0.53	0.24
	303	3.82 (3.85)	3.18		0.52	0.24
	308	3.87 (3.88)	3.09		0.54	0.22
	313	3.85 (3.85)	2.99		0.56	0.23
(C <sub>3</sub> H <sub>7</sub> ) <sub>4</sub> N <sup>+</sup>	283	2.32 (2.36)	3.35		0.49	0.20
	288	2.26 (2.30)	3.30		0.50	0.19
	293	2.22 (2.23)	3.22		0.51	0.20
	298	2.23 (2.24)	3.19		0.52	0.21
	303	2.18 (2.21)	3.20		0.52	0.21
	308	2.23 (2.20)	3.17		0.52	0.19
	313	2.22 (2.21)	3.11		0.53	0.19
(C <sub>4</sub> H <sub>9</sub> ) <sub>4</sub> N <sup>+</sup>	283	1.34 (1.32)	3.33		0.50	0.19
	288	1.29 (1.28)	3.28		0.50	0.18
	293	1.22 (1.24)	3.20		0.52	0.20
	298	1.17 (1.15)	3.14		0.53	0.20
	303	1.18 (1.21)	3.09		0.54	0.18
	308	1.15 (1.17)	2.91		0.57	0.18
	313	1.10 (1.11)	3.01		0.55	0.17

<sup>a</sup>The values in the parenthesis represent cmc determined by conductivity method.

Table 3.9\*

Thermodynamic parameters of micellization for Dodecyl sulfate with different alkali counterions along with  $\text{NH}_4^+$  at various temperatures: Standard Gibb's free energy, Enthalpy and Entropy.

Counterion	Temp/K	$-\Delta G_m^\circ$	$\Delta H_m^\circ$	$\Delta S_m^\circ$
Li <sup>+</sup>	283	34.9	27.2	219.2
	288	35.8	25.9	214.4
	293	36.2	24.1	205.7
	298	36.5	22.2	196.9
	303	36.8	20.3	188.3
	308	37.8	18.6	182.9
	313	38.2	16.3	174.2
Na <sup>+</sup>	283	35.4	-9.4	91.8
	288	35.9	-14.3	75.1
	293	36.6	-19.6	57.8
	298	36.8	-25.0	39.5
	303	36.5	-30.4	19.8
	308	37.7	-37.4	1.2
	313	37.8	-43.5	-18.3
NH <sub>4</sub> <sup>+</sup>	283	35.4	-15.7	69.8
	288	35.7	-19.6	56.0
	293	36.6	-24.1	42.9
	298	36.6	-28.0	28.6
	303	37.7	-33.2	14.7
	308	37.8	-38.1	-0.9
	313	39.1	-44.3	-16.5

Table 3.10\*

Thermodynamic parameters of micellization for Dodecyl sulfate with different tetraalkylammonium counterions at various temperatures: Standard Gibb's free energy, Enthalpy and Entropy.

Counterion	Temp/K	$-\Delta G_m^\circ$	$\Delta H_m^\circ$	$\Delta S_m^\circ$
(CH <sub>3</sub> ) <sub>4</sub> N <sup>+</sup>	283	38.5	-2.3	128.1
	288	39.4	-6.1	115.7
	293	39.7	-10.0	101.4
	298	40.0	-14.0	86.9
	303	41.4	-18.9	74.2
	308	41.5	-23.4	58.6
	313	42.2	-28.7	43.2
(C <sub>2</sub> H <sub>5</sub> ) <sub>4</sub> N <sup>+</sup>	283	40.3	19.0	209.8
	288	40.9	18.4	205.9
	293	41.2	17.6	200.6
	298	41.7	16.8	196.4
	303	42.5	16.0	193.0
	308	43.6	15.3	191.3
	313	44.1	14.3	186.5
(C <sub>3</sub> H <sub>7</sub> ) <sub>4</sub> N <sup>+</sup>	283	42.7	21.1	225.4
	288	43.8	20.7	224.1
	293	44.4	20.0	220.0
	298	44.9	20.0	215.4
	303	45.8	18.6	212.3
	308	46.9	18.0	210.7
	313	47.7	17.1	207.1
(C <sub>4</sub> H <sub>9</sub> ) <sub>4</sub> N <sup>+</sup>	283	45.3	14.0	209.4
	288	46.5	13.3	207.7
	293	47.0	12.3	202.6
	298	48.0	11.4	199.5
	303	49.3	10.6	197.7
	308	50.3	9.5	194.0
	313	51.6	8.3	191.4

Table 3.11\*

Micellization and Surface parameters of AOT surfactants having different alkali counterions along with  $\text{NH}_4^+$  ion at various temperatures (T/K): cmc, maximum surface excess concentration, minimum areas per molecule and ionization degree.

Counterion	T/K	cmc <sup>a</sup> / (mol dm <sup>-3</sup> × 10 <sup>-3</sup> )	$\Gamma_{\text{max}}$ / cm <sup>-2</sup> × 10 <sup>10</sup>	mol	A <sub>min</sub> /nm <sup>2</sup> × 10 <sup>2</sup>	$\alpha$
Li <sup>+</sup>	283	3.35 (3.40)	1.63		1.02	0.73
	288	2.98 (3.15)	1.60		1.04	0.51
	293	2.82 (2.90)	1.59		1.04	0.49
	298	2.66 (2.63)	1.59		1.44	0.58
	303	2.40 (2.37)	1.56		1.06	0.70
	308	2.24 (2.19)	1.61		1.03	0.68
	313	2.39 (2.23)	1.60		1.05	0.77
Na <sup>+</sup>	283	3.55 (3.53)	1.42		1.17	0.61
	288	3.16 (3.20)	1.45		1.14	0.51
	293	2.88 (2.77)	1.49		1.11	0.46
	298	2.63 (2.40)	1.57		1.06	0.70
	303	2.24 (2.20)	1.76		0.94	0.69
	308	2.37 (2.26)	1.70		0.98	0.70
	313	2.80 (2.69)	1.71		0.97	0.67
K <sup>+</sup>	283	2.97 (3.11)	1.84		0.90	0.74
	288	2.90 (3.01)	2.01		0.83	0.63
	293	2.82 (2.90)	2.22		0.75	0.58
	298	2.70 (2.62)	2.25		0.74	0.73
	303	2.44 (2.35)	2.30		0.72	0.85
	308	2.42 (2.32)	2.44		0.68	0.75
	313	-	-		-	-
NH <sub>4</sub> <sup>+</sup>	283	3.87 (3.85)	1.56		1.06	0.45
	288	3.31 (3.20)	1.58		1.05	0.58
	293	3.09 (3.12)	1.45		1.14	0.66
	298	2.70 (2.65)	1.55		1.07	0.68
	303	2.59 (2.52)	1.80		0.92	0.77
	308	2.65 (2.60)	1.72		0.96	0.66
	313	2.82 (2.75)	1.76		0.94	0.71

<sup>a</sup>The values in the parenthesis represent cmc determined by conductivity method.

Table 3.12\*

Micellization and Surface parameters of AOT surfactants having different tetraalkylammonium counterions at various temperatures (T/K): cmc, maximum surface excess concentration, minimum areas per molecule and ionization degree.

Counterion	T/K	cmc <sup>a</sup> / (mol dm <sup>-3</sup> × 10 <sup>-3</sup> )	Γ <sub>max</sub> / cm <sup>-2</sup> × 10 <sup>10</sup>	mol	A <sub>min</sub> /nm <sup>2</sup> × 10 <sup>2</sup>	α
(CH <sub>3</sub> ) <sub>4</sub> N <sup>+</sup>	283	4.76 (4.61)	1.68		0.99	0.50
	288	3.82 (4.10)	1.65		1.01	0.51
	293	3.24 (3.40)	1.53		1.08	0.67
	298	2.90 (2.90)	1.60		1.04	0.74
	303	2.05 (2.35)	1.80		0.92	0.72
	308	2.10 (2.20)	1.72		0.96	0.76
	313	2.26 (2.31)	1.67		0.99	0.74
(C <sub>2</sub> H <sub>5</sub> ) <sub>4</sub> N <sup>+</sup>	283	1.88 (2.10)	1.44		1.15	0.42
	288	1.78 (2.00)	1.33		1.25	0.56
	293	2.95 (1.85)	1.46		1.14	0.65
	298	2.45 (2.50)	1.43		1.16	0.67
	303	2.31 (2.43)	1.76		0.94	0.80
	308	2.37 (2.50)	1.31		1.27	0.69
	313	2.56 (2.63)	1.41		1.12	0.66
(C <sub>3</sub> H <sub>7</sub> ) <sub>4</sub> N <sup>+</sup>	283	1.18 (1.34)	1.67		0.99	0.56
	288	1.05 (1.20)	1.71		0.97	0.69
	293	0.93 (0.98)	1.85		0.89	0.66
	298	0.97 (0.95)	1.71		0.97	0.65
	303	0.92 (0.85)	1.77		0.94	0.68
	308	0.87 (0.90)	1.69		0.98	0.75
	313	0.74 (0.80)	1.93		0.86	0.74
(C <sub>4</sub> H <sub>9</sub> ) <sub>4</sub> N <sup>+</sup>	283	1.04 (1.11)	1.32		1.26	0.57
	288	0.87 (0.91)	1.40		1.18	0.58
	293	0.80 (0.83)	1.42		1.17	0.59
	298	0.77 (0.80)	1.63		1.02	0.76
	303	0.75 (0.78)	1.82		0.91	0.67
	308	-	-		-	-
	313	-	-		-	-

<sup>a</sup>The values in the parenthesis represent cmc determined by conductivity method.

Table 3.13\*

Thermodynamic parameters of micellization for AOT surfactants with different alkali counterions along with  $\text{NH}_4^+$  at various temperatures: Standard Gibb's free energy, Enthalpy and Entropy.

Counterion	Temp/K	$-\Delta G_m^\circ$	$\Delta H_m^\circ$	$\Delta S_m^\circ$
Li <sup>+</sup>	283	29.0	9.9	63.4
	288	35.1	12.1	80.0
	293	36.3	12.6	80.9
	298	34.9	12.3	76.0
	303	32.8	11.6	69.9
	308	34.3	12.3	71.5
	313	32.1	12.0	73.3
Na <sup>+</sup>	283	44.4	23.5	73.8
	288	37.2	25.3	41.3
	293	37.0	25.4	39.7
	298	32.1	22.1	33.3
	303	33.5	23.1	34.1
	308	33.6	23.8	32.0
	313	34.2	24.3	34.4
K <sup>+</sup>	283	29.2	5.7	83.4
	288	32.4	6.4	90.5
	293	34.1	6.8	93.2
	298	31.3	6.3	84.0
	303	29.2	5.9	76.8
	308	32.3	6.7	83.3
	313	-	-	-
NH <sub>4</sub> <sup>+</sup>	283	35.0	16.5	61.3
	288	33.0	15.6	56.9
	293	32.0	14.3	50.2
	298	32.5	15.9	56.6
	303	30.9	15.8	52.0
	308	34.1	16.0	50.0
	313	33.2	16.3	53.5

Table 3.14\*

Thermodynamic parameters of micellization for AOT surfactants with different tetraalkylammonium counterions at various temperatures: Standard Gibb's free energy, Enthalpy and Entropy.

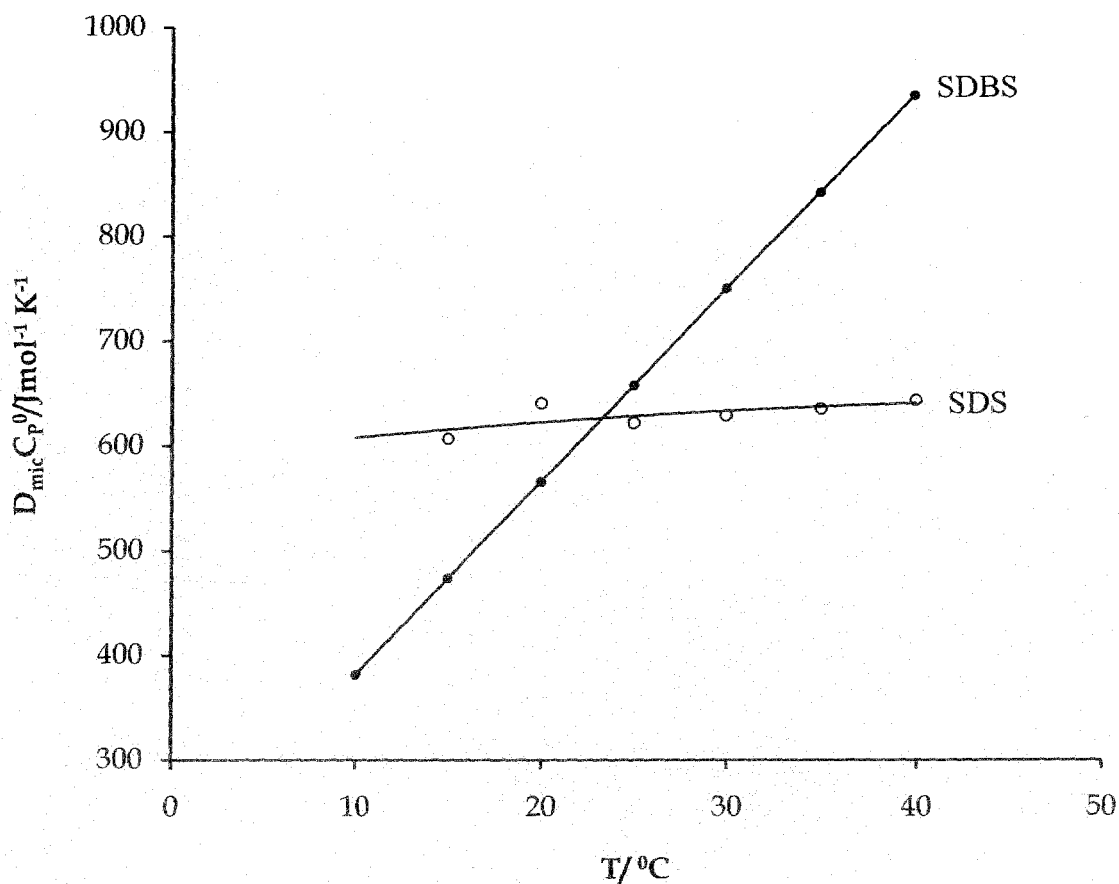
Counterion	Temp/K	$-\Delta G_m^\circ$	$\Delta H_m^\circ$	$\Delta S_m^\circ$
(CH <sub>3</sub> ) <sub>4</sub> N <sup>+</sup>	283	33.0	29.1	13.7
	288	34.2	30.0	14.6
	293	31.7	27.9	13.3
	298	30.8	27.2	12.1
	303	33.0	28.6	14.5
	308	32.3	28.5	12.2
	313	33.1	29.0	12.8
(C <sub>2</sub> H <sub>5</sub> ) <sub>4</sub> N <sup>+</sup>	283	35.0	12.2	80.6
	288	33.0	11.7	74.0
	293	32.0	12.2	67.6
	298	32.5	12.3	67.8
	303	30.9	11.9	62.7
	308	34.1	13.3	67.5
	313	35.2	13.7	67.7
(C <sub>3</sub> H <sub>7</sub> ) <sub>4</sub> N <sup>+</sup>	283	36.4	8.5	98.7
	288	34.7	8.1	92.3
	293	35.8	8.5	93.3
	298	36.6	8.8	93.1
	303	36.6	8.9	91.2
	308	35.4	8.7	86.5
	313	36.8	8.8	90.6
(C <sub>4</sub> H <sub>9</sub> ) <sub>4</sub> N <sup>+</sup>	283	36.6	14.4	78.4
	288	37.6	14.9	78.8
	293	38.2	15.3	78.2
	298	34.4	15.2	64.4
	303	37.7	15.5	73.3
	308	-	-	-
	313	-	-	-

\* Data are collected from our previous work [34,80-81].

Surface parameters are also listed in the table as mentioned above for cmc values. Among the  $\Gamma_{max}$  values of DS, DBS and AOT, only the DS follows the general trend with temperature. The order of  $\Gamma_{max}$  values is lower in the case of DBS as compared to DS and AOT suggesting weaker adsorption of this surfactant at air-solution interface is low. The lower  $A_{min}$  values for DS and AOT suggest that these amphiphiles tend to form a more closely packed monolayer film of the hydrocarbon chain at air / liquid interface as compared to DBS with same counterions.

The thermodynamic parameters have been reported in the tables 3.9, 3.10, 3.13, 3.14. From the tables, it is clear that the micellization process is spontaneous as indicated by large negative values of  $\Delta G_m^0$  for all the surfactant systems. A close look in all the systems in the table shows that at low temperature, the entropy gain is the main factor for the formation of micelle leading to the negative Gibb's free energy change. Therefore, the magnitude and the signs of  $\Delta G_m^0$  and  $\Delta S_m^0$  suggest the stability of the micelle. The  $\Delta G_m^0$  values of the three systems are almost in the same range and with increase in temperatures the  $\Delta G_m^0$  value generally increases for DS and DBS systems whereas for AOT some reverse trend is observed. The reverse trend may be due to the double trailed structure of AOT which facilitates more disruption of water structures at higher temperatures. In between the DS and DBS systems, the  $\Delta G_m^0$  value is higher for DS systems, particularly more pronounced for the alkyl ammonium counterions. The enthalpy of micellization is negative for all the counterions in case of AOT and DBS. But for DS, there are both positive and negative value of enthalpy change of micellization suggests that both exothermic and endothermic process to occur at the micellization process. The lower enthalpy values are shown by potassium counterions for both AOT and DBS surfactants with higher enthalpy values.

The effective interaction associated with hydrocarbon chains may be expressed by standard heat capacity of micelle formation,  $\Delta_{mic}C_p^0$ . The  $\Delta_{mic}C_p^0$  values for comparison are calculated for only SDBS and SDS systems due to their very similar molecular formula and also for the presence of a dodecyl moiety in hydrocarbon chains. In both the systems, the standard heat capacity changes with temperature are shown in figure 3.30.



**Figure 3.30:** Variation of standard heat capacity of micelle formation,  $\Delta_{mic}C_p^0$  as a function of temperature for SDBS and SDS.

The calculated values of  $\Delta_{mic}C_p^0$  for SDBS fall between a wide range of value viz., -381.8 to -933.8 J mol<sup>-1</sup> K<sup>-1</sup> for the temperature range 283-293 K. On the other hand, SDS which also yields  $\Delta_{mic}C_p^0$  values between -607 and -644 J mol<sup>-1</sup> K<sup>-1</sup>.

**References:**

1. Fuhrop, J. H.; Köning, J. in *Membranes and Molecular Assemblies: the Synkinetic Approach*; The Royal Society of Chemistry: Cambridge, **1994**.
2. Hiementz, P. C.; Rajagopalan, R.; *Principles of Colloidal and Surface Chemistry*, Third Edition, New York, **1997**.
3. Hoffmann, H. J. *Phys. Chem.* **1994**, 98, 1433.
4. Bellare, J. R.; Kaneko, T.; Evans, D. F.; *Langmuir*, **1988**, 4, 1066.
5. Attwood, D.; Florence, A. T.; *Surfactant Systems*, Chapman and Hall Ltd. USA, **1985**.
6. Jakobi, G.; Lohr, A. *Detergent and Textiles Washing*, VCH Publisher, Germany, P 49-63, **1987**.
7. Hartley, G. S.; *Aqueous Solutions of Paraffin Salts*, Hermann and Cie, Paris, **1936**.
8. Paul, M.; Holland, Donn, N.; Rubingh, *Mixed Surfactants System, ASC Symposium Series 501*, American Chemical Society, Washinton, DC, P 1-43.
9. Clint, J. H.; *Surfactant Aggregation*; Blackie: Glasgow/ London, **1992**.
10. Madsen, T.; Boyd, H. B.; Nylén, D.; Pendersen, A. R.; Petersen, G. I.; Simonsen, F. "Environmental and Health Assessment of Substances in Household Detergents and Cosmetic Detergent Products," Environmental Project No. 615, Danish Environmental Protection Agency (www.mst.dk): Copenhagen, 2001.
11. Schramm, L. L.; *Surfactants: Fundamentals and Applications in the Petroleum Industry*, Cambridge University Press, 2000.
12. Shah, D. O., *Surface Phenomena in Enhanced Oil Recovery*, Plenum Press: New York, 1991.
13. Bales, B. L.; Benrraou, M.; Zana, R. *J. Phys. B.* **2002**, 101, 9033.
14. Zana, R.; *Colloid Interface Sci.* **1980**, 78, 330.
15. Evans, D. F.; Wennerström, *The Colloidal Domain. Where Physics, Chemistry, Biology and Technology Meet*, Wiley-VCH, New York, **1994**.

16. Saha, S. K.; Jha, M.; Ali, M.; Chakraborty, A.; Bit, G.; Das, S. K.; *J. Phys. Chem. B.* **2008**, *112*, 4642.
17. Israelachvili, J. N. *Intermolecular and Surface Forces*, Academic Press, London, **1985**.
18. Turro, N. J.; Yekta, A. *J. Am. Chem. Soc.* **1978**, *100*, 5951.
19. Gruen, D. W. R. *Prog. Colloid Polym. Sci.* **1985**, *70*, 6.
20. Kralchevsky, P. A.; Danov, K. D.; Broze, G.; Mehreteab, A. *Langmuir*, **1999**, *15*, 2351-2365.
21. Vlahovska, P. M.; Danov, K. D.; Mehreteab, A.; Broze, G. *J. Colloid Interface Sci.* **1997**, *192*, 194.
22. stigter, D. *J. Phys. Chem. B*, **1998**, *102*, 2480.
23. Kresheck, G. C.; *J. Phys. Chem. B.* **1998**, *102*, 6596.
24. González-Pérez, A.; Czapkiewicz, J.; Del Castillo, J. L.; Rodríguez, J. R. *Colloid Polym. Sci.* **2004**, *282*, 1359.
25. Chatterjee, A.; Moulik, S. P.; Sanyal, S. K.; Mishra, B. K.; Puri, P. M. *J. Phys. Chem. B.* **2001**, *105*, 12823.
26. Asakawa, T.; Kitano, H.; Ohta, A.; Miyagishi, S. *J. Colloid Interface Sci.* **2001**, *242*, 284.
27. Rehage, H.; Hoffmann, H. *Mol. Phys.* **1991**, *74*, 933.
28. Iijima, H.; Kato, T.; Soderman, O.; *Langmuir*, **2000**, *16*, 318.
29. Hoffmann, S.; Rauscher, A.; Hoffmann, H. *Ber. Bunsen-Ges. Phys. Chem.* **1991**, *95*, 153.
30. Malliaris, A.; Lang, J.; Zana, R. *J. Chem. Soc., Faraday Trans. 1* **1986**, *82*, 109.
31. Benrraou, S.; Bales, B. L.; Zana, R. *J. Phys. Chem. B.* **2003**, *107*, 13432.
32. Lindman, B.; Puyal, M-C.; Kamenka, N.; Rymden, R.; Stilbs, P. *J. Phys. Chem.* **1984**, *88*, 5048.
33. Bales, B.L.; Benrraou, M.; Tiguida, K.; Zana, R. *J. Phys. Chem. B* **2005**, *109*, 7987.

34. Chakraborty, A. *Ph. D. Thesis*, 2008, North Bnegal University, West Bengal, India.
35. Zana, R. *Colloid Interface Sci.* **1980**, 78, 330.
36. (a) Mukherjee, P. *Adv. Colloid Interface Sci.* **1967**, 1, 241. (b) Tanford, C. *The Hydrophobic Effect: Formation of Micelles and Biological Membranes*, 1980, Vol. 2. Wiley, New York.
37. Benrrouau, M.; Bales, B. L.; Zana, R.; *J. Phys. Chem. B.* **2003**, 107, 13432.
38. Basu Ray, G.; Chakraborty, I.; Ghosh, S.; Moulik, S. P. *J. Colloid Polym. Sci.* **2007**, 285, 457-469.
39. Zana, R. *Adv. Colloid Interface Sci.* **1995**, 57, 1.
40. Blandamer, M. J.; Cullis, P. M.; Soldi, L. G.; Engbert, J. B. F.N.; Kacperska, A.; van Os, N. M.; Subha, M. C. S.; *Adv. Colloid Interface Sci.* **1995**, 58, 171.
41. Blankschtein, D.; Shiloach, A.; Zoeller, N. *Current Opinion Colloid Interface Sci.* **1997**, 2, 294.
42. Hines, J. D. *Current Opinion Colloid Interface Sci.* **2001**, 6, 350.
43. Zana, R. *Langmuir*, **1996**, 12, 1208.
44. Rosen, M. J. *Surfactants and Interfacial Phenomena*, Wiley-Interscience, USA, **2004**.
45. Ma, J. -G.; Boyd, B. J.; Drummond, C. J. *Langmuir*, **2006**, 22, 8646 - 8654.
46. Hait, S. K.; Majhi, P. R.; Blume, A.; Moulik, S. P. **2003**, *J. Phys. Chem. B*, 107: 3650-3658.
47. Težak, D.; Hertal, G.; Hoffmann, H. *Liq. Cryst.* **1991**, 10, 15.
48. Taffarel, S. R.; Rubio, J. *Minerals Engineering*, **2010**, 23, 771-779.
49. Farquhar, K. D.; Misran, M.; Robinson, B. H.; Steytler, D. C.; Morini, P.; Garrett, P. R.; Holzwarth, J. F. *J. Phys.: Condens. Matter*, **1996**, 8, 9397-9404.
50. Brinkmann, U.; Neumann, E.; Robinson, B. H. *J. Chem. Soc.* **1998**, 94.
51. Blanch, A. J.; Lenehan, C. E.; Quniton, J. S. *J. Phys. Chem. B.* **2010**, 114, 9805.

52. Clark, M. D.; Subramanian, S.; Krishnamoorti, R. *J. Colloid Interface Sci.* **2011**, 354, 144.
53. Haggemueller, R.; Rahatekar, S. S.; Fagan, J. A.; Chun, J.; Becker, M. L.; Naik, R. R.; Krauss, T.; Carlson, L.; Kadla, J. F.; Trulove, P. C.; Fox, D. F.; Delong, H. C.; Fang, Z.; Kelley, S. O.; Gilman, J. W. *Langmuir*, **2008**, 24, 5070.
54. Islam, M. F.; Rojas, E.; Bergey, D. M.; Johnson, A. T.; Yodh, A. G. *Nano Lett.* **2003**, 3, 269.
55. Matarredona, O.; Rhoads, H.; Li, Z.; Harwell, J. H.; Balzano, L.; Resasco, D. E.; *J. Phys. Chem. B.* **2003**, 107, 13357.
56. Okazaki, T.; Saito, T.; Matsuura, K.; Ohshima, S.; Yumura, M.; Iijima, S. *Nano Lett.* **2005**, 5, 2618.
57. Tan, Y.; Resasco, D. E.; *J. Phys. Chem. B.* **2005**, 109, 14454.
58. Utsumi, S.; Kanamaru, M.; Honda, H.; Kanoh, H.; Tanaka, H.; Ohkubo, T.; Sakai, H.; Abe, M.; Kaneko, K. *J. Colloid Interface Sci.* **2007**, 308, 276.
59. Aoudia, M.; Rodgers, M. A. J. *J. Am. Chem. Soc.*, **1993**, 70, 59.
60. Linfield, W. M. (Ed.), "Anionic Surfactants", Vol. 2. Dekker, New York, **1976**.
61. Bi, Z. C.; Yu, Z. Y.; *Chin. Sci. Bull.* **2001**, 46 (5), 372.
62. Bahadur, P.; Chand, M.; *Tenside, Surfactants, Deterg.*, **1998**, 35 (2), 134.
63. Eastoe, J.; Robenson, B.H.; Heenan, R.K. *Langmuir*, **1993**, 9, 2820.
64. Temsamani, M.B.; Maeck, M.; Hassani, I.E.; Hurwitz, H.D. *J. Phys. Chem. B* **1998**, 102, 3335.
65. Benrraou, M.; Bales, B.L.; Zana, R. *J. Phys. Chem. B* **2003**, 107, 13432.
66. Van Os, N. M.; Danne, D.J.; HAandrikman, G. **1991**, *J. Colloid Interface Sci.*, 141: 199-217.
67. Mei, L.; Yahya, R.; Xiaoyu, H.; Winnik, M. A. *J. Colloid Interface Sci.* **2000**, 230, 135.

68. Ruiz, C. C.; Molina-Bolívar, J. A.; Aguiar, J.; MacIsaac, G.; Moroze, S.; Palepu, R. *Langmuir*, **2001**, *17*, 6831 – 6840.
69. Dubin, P. L.; Gruber, J. H.; Xia, J.; Zhang, H. J. *Colloid Interface Sci.* **1992**, *148*, 35-41.
70. Sulthana, S. B.; Bhat, S. G. T.; Rakshit, A. K. *Bull. Chem. Soc. Jpn.*, **2000**, *73*, 281-287.
71. Šegota, S.; Heimer, S.; Težac, Đ. *Colloids and Surfaces A: Physicochem. Eng. Aspects.* **2006**, *274*, 91-99.
72. Sein, A.; Engberts, J. B. F. N. *Langmuir*, **1995**, *11*, 455-465.
73. Aoudia, M.; Wade, W. H.; Rodgers, M. A. J. *J. Colloid Interf. Sci.* **1991**, *145*, 2.
74. Paul, A.; Griffith, P. C.; Pettersson, E.; Stilbs, P.; Bales, B. L.; Zana, R.; Heenan, R. K. *J. Phys. Chem. B.* **2005**, *109*, 15775-15779.
75. Chaput, G.; Jeminet, G.; Juillard, J. *Can. J. Chem.* **1975**, *53*, 2240-2246.
76. Rosen, M. J.; Cohen, A. W.; Dahanayake, M. Hua, X. *J. Phys. Chem.*, **1982**, *86*, 541.
77. Oh, S. G.; Shah, D. O. *J. Phys. Chem.*, **1993**, *97*, 284.
78. Sulthana, S. B.; Bhat, S. G. T.; Rakshit, A. K. *Langmuir*, **1997**, *13*, 4562.
79. Umlong, I. M.; Ismail, K. *J. Colloid Interface Sci.* **2005**, *291*, 529.
80. Chakraborty, A.; Chakraborty, S.; Saha, S. K.; *J. Dispersion Sci. Technol.* **2007**, *28*, 984.
81. Chakraborty, A.; Saha, S. K.; Chakraborty, S. *Colloid Polym. Sci.* **2008**, *286*, 927.
82. Chakraborty, S.; Chakraborty, A.; Ali, M.; Saha, S. K. *J. Dispersion Sci. Technol.* **2010**, *31*, 209-215.
83. Su, T. J.; Lu, J. R.; Thomas, R. K.; Penfold, J. *J. Phys. Chem. B.* **1997**, *101*, 937.
84. Chakraborty, S.; Chakraborty, A.; Saha, S. K. *RSC Advances.* **2014**, *4*, 32579.
85. Mukhim, T.; Ismail, K. *J. Surface Sci. Technol.* **2005**, *21*, 113-127.
86. Perger, T. -M.; Bešter-Rogač, M. *J. Colloid Interface Sci.* **2007**, *313*, 288-295.
87. Kang, K.; Kim, H.; Lim, K. *Colloid Surf. A.* **2000**, *189*, 113-121.

88. Vautier-Giongo, C.; Bales, B. L. *J. Phys. Chem. B.* **2003**, *107*, 5398-5403.
89. Rodríguez, A.; Muñoz, M.; Graciaani, M. M.; Moyá, M. L. *J. Colloid Interface Sci.* **2006**, *298*, 942-951.
90. Weckström, K.; Hanu, K.; Rosenholm, J. B. *J. Chem. Soc., Faraday Trans.*, **1994**, *90*: 733-738.
91. Ninham, B. W.; Evans, D. F.; Wei, G. J. *J. Phys. Chem.*, **1983**, *87*, 5025.
92. Morori, A. *Micelles: Theoretical and Applied Aspects*; New York: Plenum Press.
93. Bales, B. L.; *J. Phys. Chem. B.* **2001**, *105*, 6798.
94. Satake, I.; Iwamatsu, I.; Hosokawa, S.; Matuura, R. *Bull. Chem. Soc. Jpn.* **1963**, *36*, 204.
95. Gao, H. -W.; Zhao, J. -F.; *J. Anal. Chem.* **2003**, *58*, 322.
96. Watanabe, K.; Imai, S.; Mori, Y.H. *Japan Chemical Engineering Science*, **2005**, *60*, 4846.
97. Apostolos, G.; Evangelos, G.; Antigoni, S. *Desalination*, **2007**, *211*, 249.
98. Paul, B. K.; Moulik, S. P. *Ind. J. Biochem. Biophys.* **1991**, *28*, 174.
99. Paul, B. K.; Moulik, S. P. *Adv. Colloid Interface Sci.* **1998**, *78*, 99.
100. Van Os, N. M.; Haak, J. R.; Rupert, L. A. M. *Physicochemical properties of Anionic, Cationic and Nonionic Surfactants*; Elsevier: New York, **1993**.
101. Mukherjee, P.; Mysels, K. J.; Kapauan, P. *J. Phys. Chem.* **1967**, *71*, 4166.
102. Romsted, L.S.; Yoon, C.O. *J. Am. Chem. Soc.* **1993**, *115*, 989.
103. Palazzesi, F.; Calvaresi, M.; Zerbetto, F. *Soft Matter*, **2011**, *7*, 9148-9156.
104. Kim, H. -U.; Lim, K. -H. *Colloids Surf. A.* **2004**, *235*, 121-128.
105. Tsubone, K.; Arkawa, Y.; Rosen, M. J. *J. Colloid Interface Sci.* **2003**, *262*, 516.
106. Tsubone, K.; Ogawa, T.; Mimura, K. *J. Surfactants Detergents*, **2003**, *6*, 39.

## **Chapter IV**

**Aggregation behaviour of dodecyl benzene  
sulfonate in presence of symmetrical bromide  
salts and ethylene glycol**

## Chapter IV

# Aggregation behaviour of dodecyl benzene sulfonate in presence of symmetrical bromide salts and ethylene glycol

### 4.1. Dodecyl Benzene Sulfonate in presence of Symmetrical Bromide Salts

#### 4.1.1. Introduction and Review of Previous Works

The self-assembly of surfactants in water into micelles is a widely studied phenomenon. These micellar systems have immense technological applications such as flow field regulators, solubilising and emulsifying agents, membrane mimetic media, nanoreactors, to name a few [1-4]. Altering or modifying important physicochemical properties of aqueous surfactant solutions is highly desirable as far as potential applications of such systems are concerned. One way to alter/modify the physicochemical properties of a given aqueous surfactant solution is to use of the external means, such as changes in temperature/pressure and/or addition of a variety of modifiers like cosolvents, cosurfactants, electrolytes and polar organics [1-12].

Added electrolytes are known to affect the aggregation behaviour of ionic surfactants. Micellization, which is a manifestation of both hydrophobic and hydrophilic effects, is likely to undergo a significant change in the presence of such additives. It has been generally observed that the addition of electrolytes, with both organic and inorganic counterions, to aqueous ionic micellar solutions increases the solubilization power of surfactant micelles [7,13]. It is thus not surprising that the effect of different kinds of electrolytes, with either organic or inorganic counterions, on the cmc, aggregation number, micellar shape and the solubilization power of aqueous aggregates have been examined in detail. The cmc value can serve as a measure of micelle stability in a given state and the thermodynamics of micellization can be determined from the study of the temperature dependence of the cmc of a surfactant system. In addition, the changes in hydration energies and specific interactions with counterions may also be important [14-18]. The strength and importance of these various interactions depend upon externally controllable factors, such as temperature

and ionic strength on the properties of the particular ions involved. Moreover, the structure of the resulting micelle, in particular, its aggregation number, its shape, and the compactness of its electrical double layer show some kind of dependency [17]. Even the molecular conformation of some dimeric surfactants (known as Gemini surfactants) affects the micellization to a large extent [18]. Obviously, the actually existing micelles correspond to the lowest free energy state of the system. Thus, the intense interest in determining the thermodynamic parameters of micelle formation in aqueous solutions, namely, the Gibbs free energy,  $\Delta G_{mic}^0$ , the enthalpy,  $\Delta H_{mic}^0$ , and the entropy,  $\Delta S_{mic}^0$ , is generated because they quantify the relative importance of hydrophobic interactions, surfactant-water contact and (for ionic surfactants) head-group repulsion. These parameters can be derived from the temperature dependence of the critical micelle concentration (cmc), though very highly accurate cmc's are required in order to achieve satisfactory values of  $\Delta H_{mic}^0$ .

Among available techniques for studying surfactant aggregation, for example, conductivity, surface tension, NMR and calorimetry has a distinct advantage, for it is possible to calculate both the cmc and  $\Delta H_{mic}^0$  directly from the experimental data. Additionally, the calculated enthalpy and entropy characterize the balance of forces involved in micelle formation. For example, whereas the aggregation is entropy-driven at room temperature, it is enthalpy-driven at higher temperatures [19]. Among the factors known to affect cmc in aqueous solution are (i) the structure of the surfactant, (ii) the presence of added electrolyte in solution, (iii) the presence of various organic compounds in solution, (iv) the presence of a second liquid phase and (v) temperature of the solution. In aqueous medium, the cmc decreases as the number of carbon atoms in the hydrophobic groups increases. For ionic surfactants it was generally found that the cmc became halved by the addition of one methylene group to a straight chain hydrophobic part attached to a single terminal hydrophilic group as has already been mentioned [20]. Also phase separation on heating is a general phenomenon that has been investigated in great detail in the context of non-ionic surfactants which is not included in our present study [21-23]. Ionic surfactant solutions are complex in nature. Since the micelles are charged, there must be an electrostatic repulsion between the micelles in addition to the van der Waals attraction force.

Over the years a considerable amount of literature on anionic surfactant-electrolyte system has been compiled, majority of which involved sodium dodecyl

sulfate (SDS) as the surfactant and NaCl as the electrolyte. However, in recent years, attention has been focused on the interactions of other surfactants with hydrophobic counterions and to this effect in many studies [7,16,24-32]. The alkali metal ions are heavily hydrated in aqueous solution and hence cannot approach to close proximity of the highly charged micellar surface [33,34]. These ions are, therefore, less effective in screening the charge on the micellar heads. Unlike the alkali metal halides the tetramethyl ammonium ion ( $\text{TAA}^+$ ) ions are weakly hydrated in aqueous solution as the positive charge is supposed to be wrapped in the paraffin shell and are thus hydrophobic in nature [24]. Therefore, the  $\text{TAA}^+$  ions, in addition to the electrostatic interaction, can interact hydrophobically with the anionic head groups of the micelle as well. This is clearly evident from the previous study where it has been shown that micelles of sodium dodecylbenzene sulfonate interact more strongly with the  $\text{TAA}^+$  ions than with the alkali metal ions [35].

In the present study, the surfactant chosen is again dodecyl benzene sulfonate (DBS) with different counterions, viz.,  $\text{Na}^+$ ,  $\text{Li}^+$ ,  $\text{K}^+$ ,  $\text{NH}_4^+$ ,  $(\text{CH}_3)_4\text{N}^+$ ,  $(\text{C}_2\text{H}_5)_4\text{N}^+$ ,  $(\text{C}_3\text{H}_7)_4\text{N}^+$  and  $(\text{C}_4\text{H}_9)_4\text{N}^+$  and the electrolytes are the symmetrical bromides and tetra alkyl bromides. The  $\text{NH}_4^+$  ion, in terms of size, is in fact an ion that stands between the largest common alkali metal ion  $\text{Cs}^+$  and the smallest tetraalkyl ammonium ion, viz.,  $\text{TMA}^+$  [36]. All the  $\text{TAA}^+$  ions are fairly surface active, while  $\text{TPA}^+$  and  $\text{TBA}^+$  show signs of self-aggregation in aqueous solution [37].  $\text{TBA}^+$  is one of the most effective additives for the occurrence of clouding in anionic surfactants. Hence the DBS with different counterions and the corresponding bromide salt systems seem to be an interesting combination in this respect as well. Present study is, therefore, undertaken on the micellization of DBS with different counter ions in aqueous bromide salt solutions mainly by surface tension measurements and also by electrical conductivity measurements. The dependence of the thermodynamic parameters of micellization of DBS with different counterions on the corresponding bromide ions has been studied. In many applications, the stability of micellar solutions at elevated temperatures is of practical importance [38,39]. Therefore, the occurrence of temperature dependent thermodynamic study has also been reported.

## 4.1.2. Materials and Methods

### Materials

A high grade purified sample of SDBS from Across Organics (New Jersey, USA) was used for the present study. Both of them produced no minima in the surface tension vs. concentration plots indicating good purity of the compounds. The samples are converted into the surfactants bearing different counterions by ion exchange technique using a strong ion exchange resin (Amberlite IR-120, 20-50 mesh, Loba Cheme, India). Surfactants with the desired counterions were prepared by following the technique of Eastoe and et al. [40] and the extended work of Tamsamani and et al. [41] and Benrraou and et al. [42]. The process is same as discussed in the chapter III. Sodium bromide is of AR grade (LOBA-CHEMIE INDOAUSTRANAL CO., India). Potassium bromide is of AR grade (Sigma-Aldrich Co., St. Louis, USA). Lithium bromide and the other tetraalkyl ammonium bromides were of puriss grade (Fluka, Switzerland) and were purified by standard procedures. The recrystallised salts were dried in vacuum for 12 hours before use.

### Methods

**Electrical conductivity measurements:** The cmc values were determined from the surface tension as well as specific conductance data as discussed in chapter III, section 3.4.2.

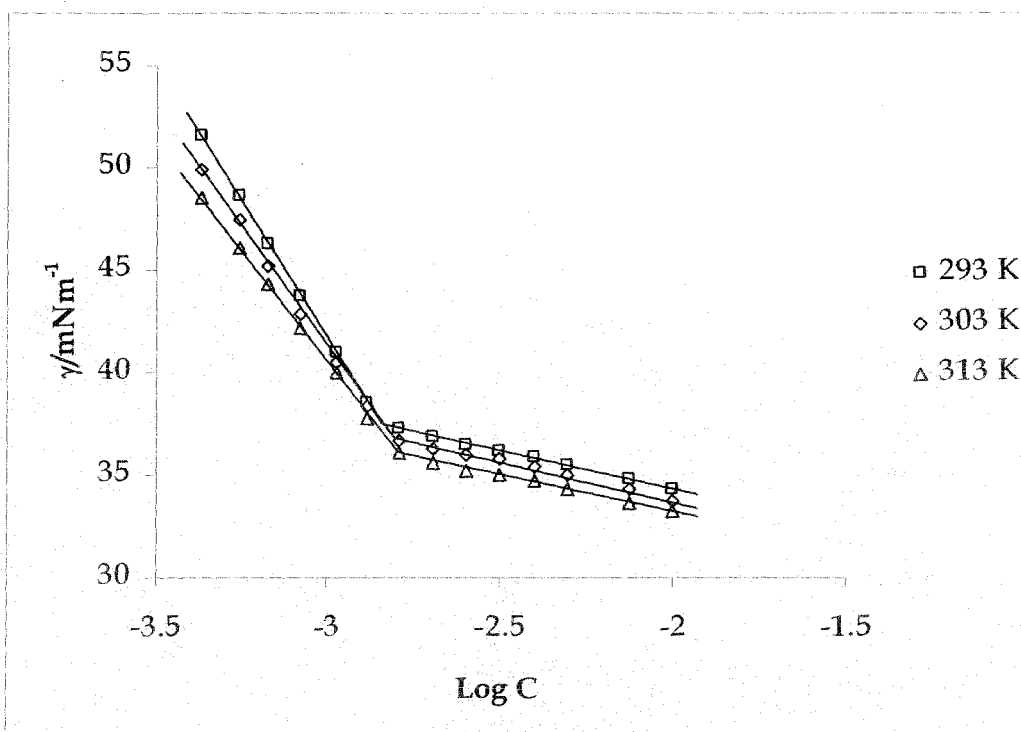
## 4.1.3. Results and discussions

### 4.1.3.1. Critical micellization concentration (cmc)

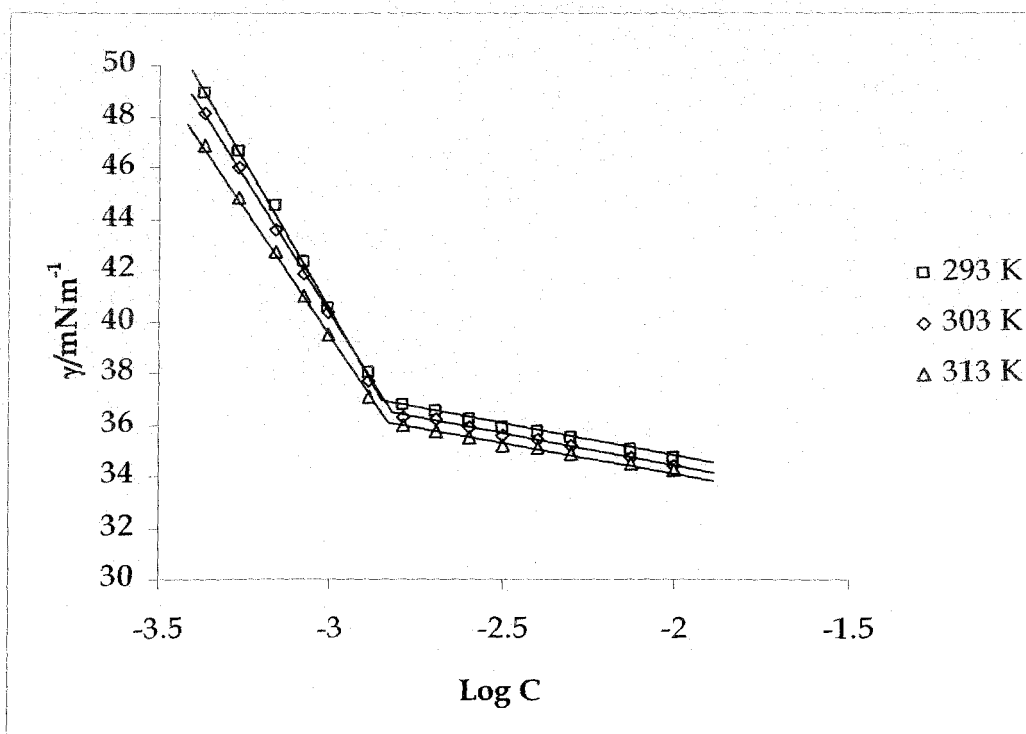
The critical micellization concentrations of DBS with different counter ions in presence of corresponding aqueous bromide salt solutions in the concentration range of (5-0.5) mM were determined mainly by surface tension and partly also by the electrical conductivity method. (Conductivity measurement in the whole salt concentration range was not done to avoid the chance of merging surfactant conductivity data by the salt conductance at high concentration.) Figure 4.1-4.48 shows

the plot of surface tension value ( $\gamma$ ) with logarithm of the concentration of the surfactant solution in presence of varying concentrations of same bromide salt as that of the counter ion and figure 4.49 - 4.56 also shows the plot of experimental values of conductivity ( $\kappa$ ) as a function of DBS concentration with different counter ions. From these figures, a substantial decrease in the cmc of DBS with all counterions with increasing concentration of bromide salt is apparent.

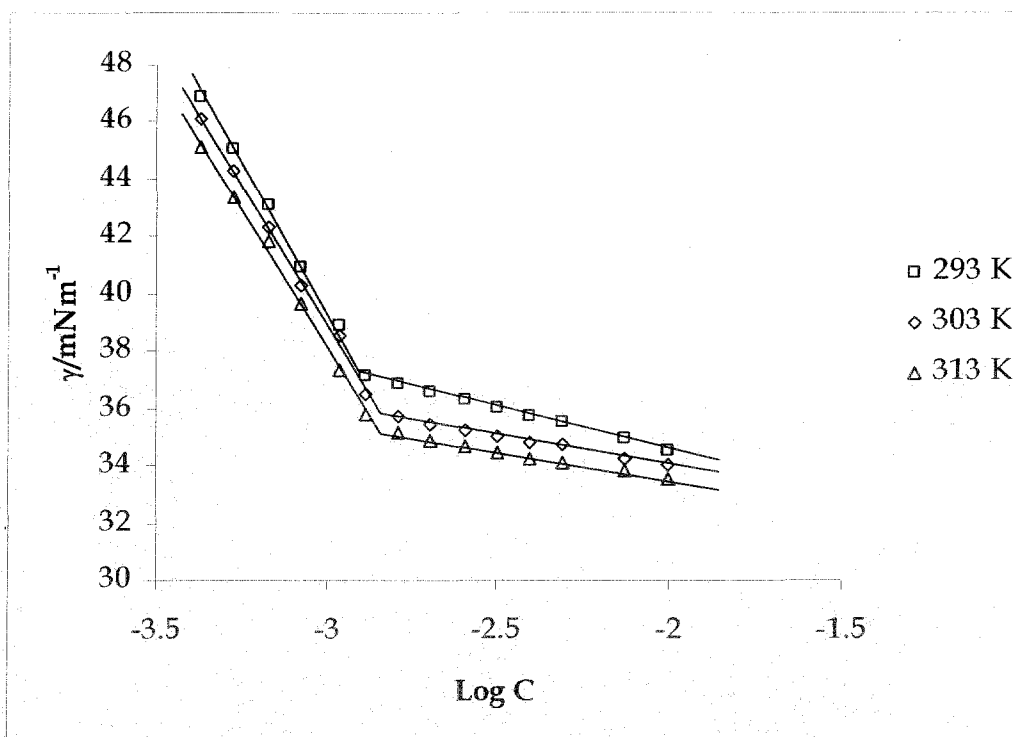
Increasing the concentration of a particular electrolyte causes a substantial decrease in the cmc. This can be accounted for by the fact that in solutions of high ionic strength, the forces of electrostatic repulsion between head groups in a micelle are considerably reduced due to charge screening. The charge screening increases the attractive force between the micellar head and the positive counterion of the electrolyte making the so-called Stern layer more densely packed, thus promoting micelle formation to be more facile. Such reduction in the cmc values of anionic surfactants is also observed in presence of all systems with corresponding bromide electrolytes. However, as has already been mentioned, due to the greater hydration in aqueous solutions, these ions cannot approach the oppositely charged micellar heads to a great extent. For example, it has been reported that the cmc of SDS is decreased from 7.8mM to 2.3mM on the addition of 0.05M of NaCl [9], while the identical concentration of TBAB could lower the cmc to as low as 0.23mM at 298K [7]. In the present study, e.g., the cmc of ADBS in water is 2.41mM at 293.15K and is lowered to 1.82mM, 1.66mM, 1.59mM, 1.49mM, 1.40mM and 1.33mM in presence of 0.0005M, 0.001M, 0.002M, 0.003M, 0.004M and 0.005M Ammonium Bromide solution respectively at the same temperature. The cmc values of all the DBS moiety with different counterions in the presence of symmetrical bromide salts are given in Table 4.1.1 - 4.1.4. From these results one may be able to examine the role of the positive ions in modifying the aggregation properties of aqueous DBS moiety. This large decrease in cmc value probably indicates the existence of strong hydrophobic interaction between the alkyl groups of the corresponding positive ions with the hydrocarbon tails of surfactant molecules along with the strong electrostatic interaction (due to weak hydration) with the surfactant head groups.



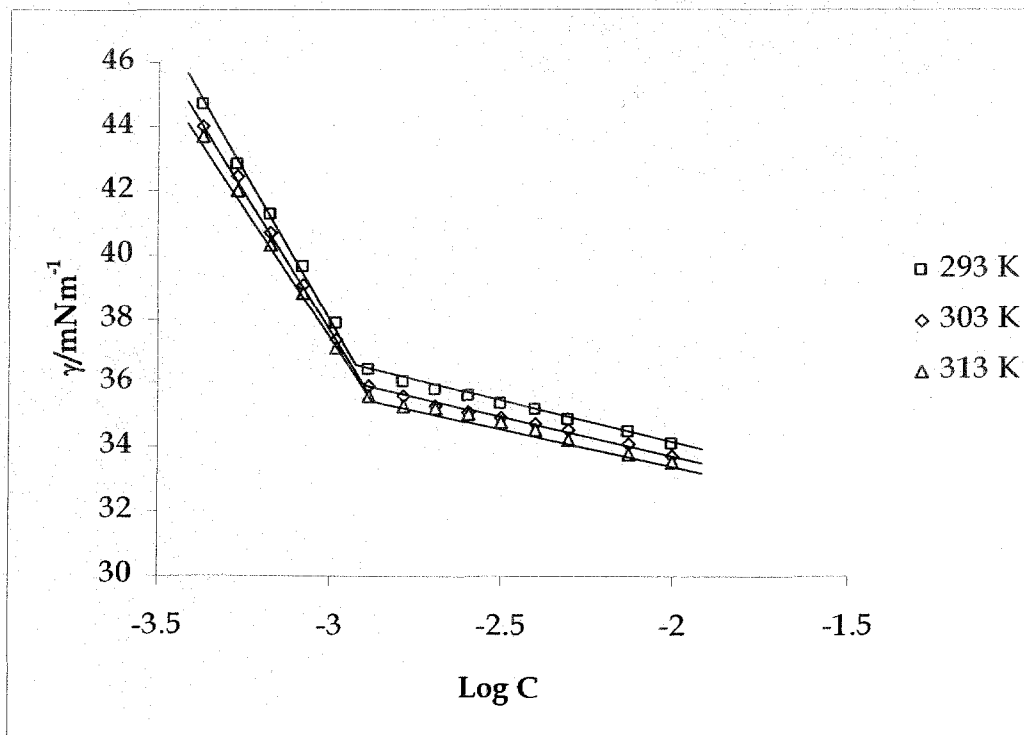
**Figure 4.1:** Surface Tension,  $\gamma$ , vs.  $\text{Log C}$  (mM) plot of SDBS in temperature range 293 – 313 K at 10 K intervals in the NaBr concentration 0.0005 M.



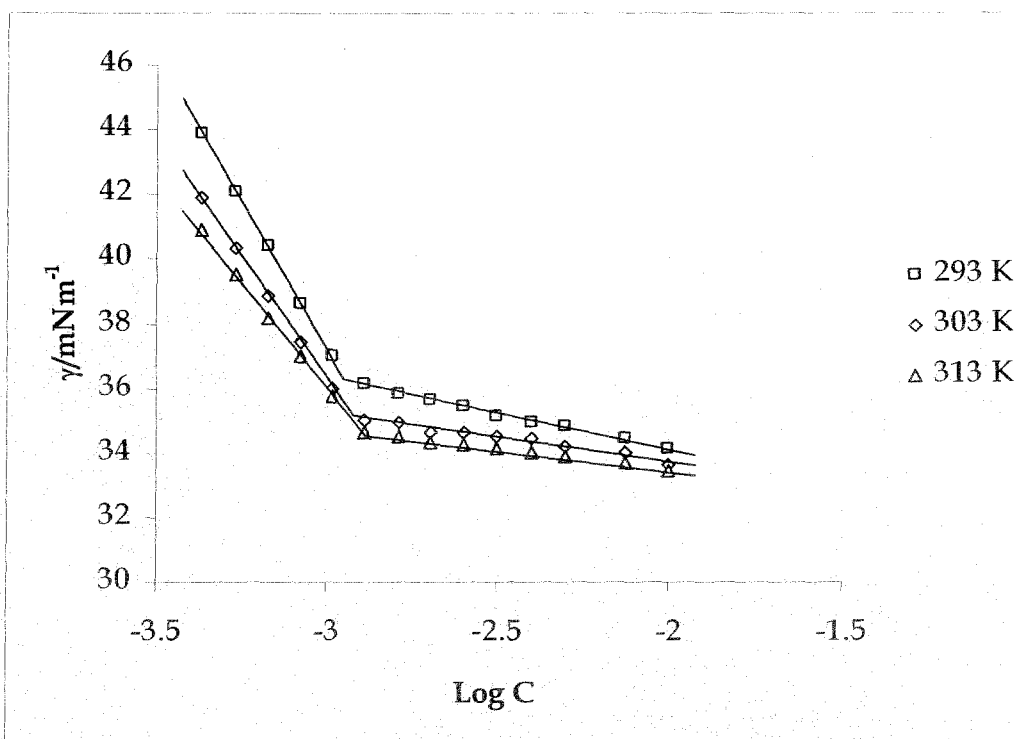
**Figure 4.2:** Surface Tension,  $\gamma$ , vs.  $\text{Log C}$  (mM) plot of SDBS in temperature range 293 – 313 K at 10 K intervals in the NaBr concentration 0.001 M.



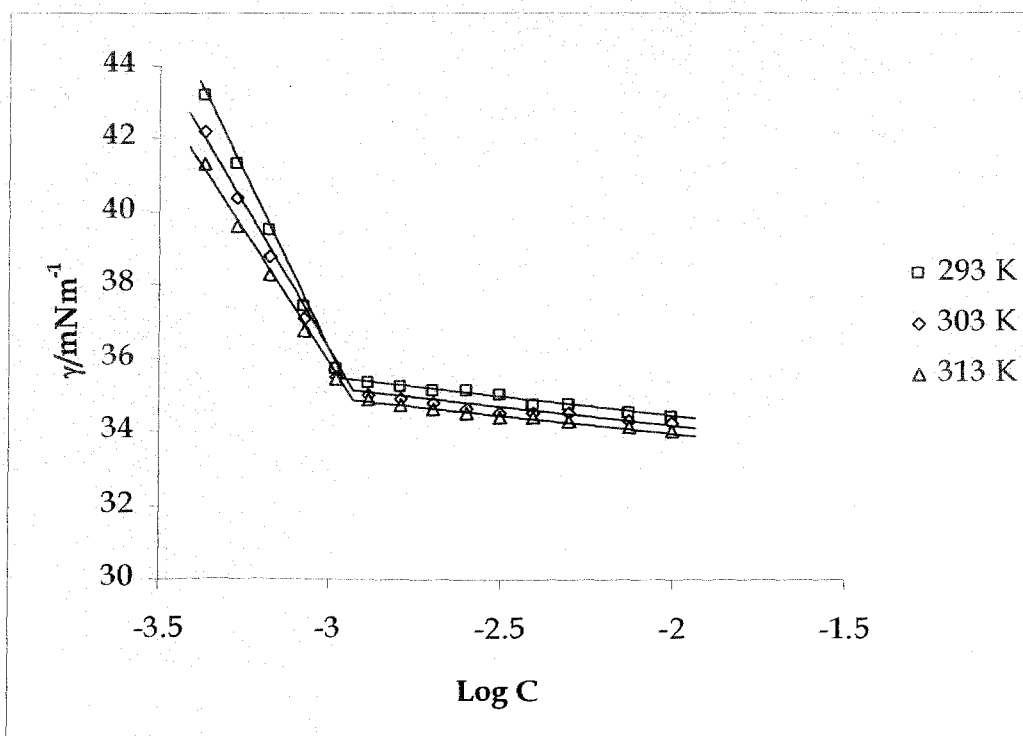
**Figure 4.3:** Surface Tension,  $\gamma$ , vs.  $\text{Log } C$  (mM) plot of SDBS in temperature range 293 – 313 K at 10 K intervals in the NaBr concentration 0.002 M.



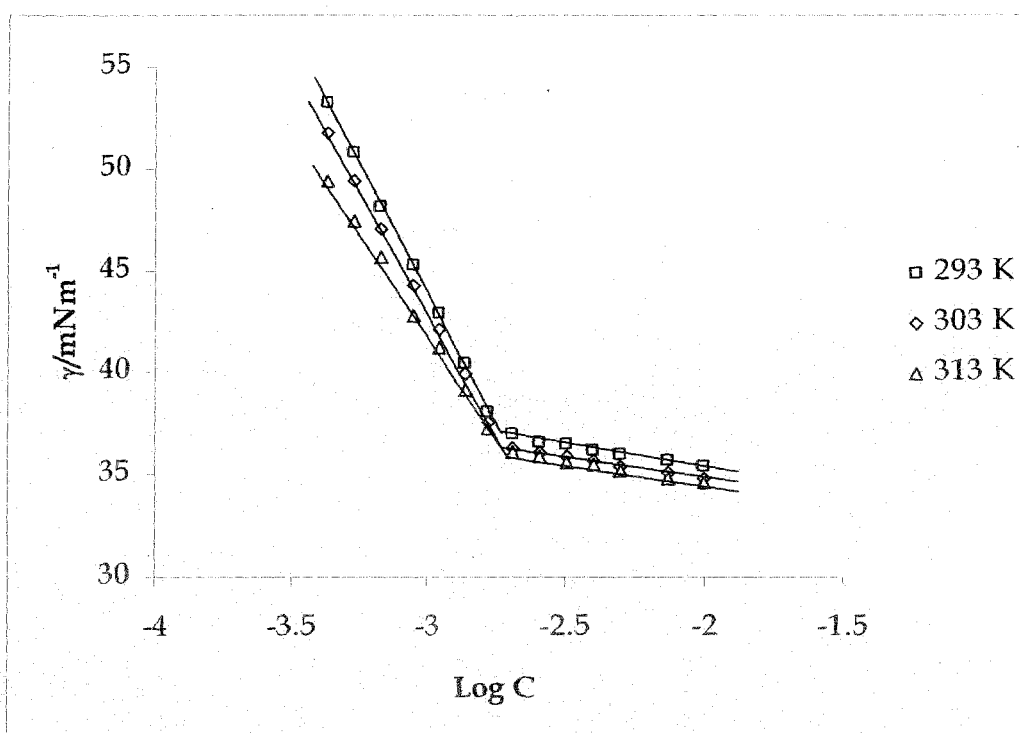
**Figure 4.4:** Surface Tension,  $\gamma$ , vs.  $\text{Log } C$  (mM) plot of SDBS in temperature range 293 – 313 K at 10 K intervals in the NaBr concentration 0.003 M.



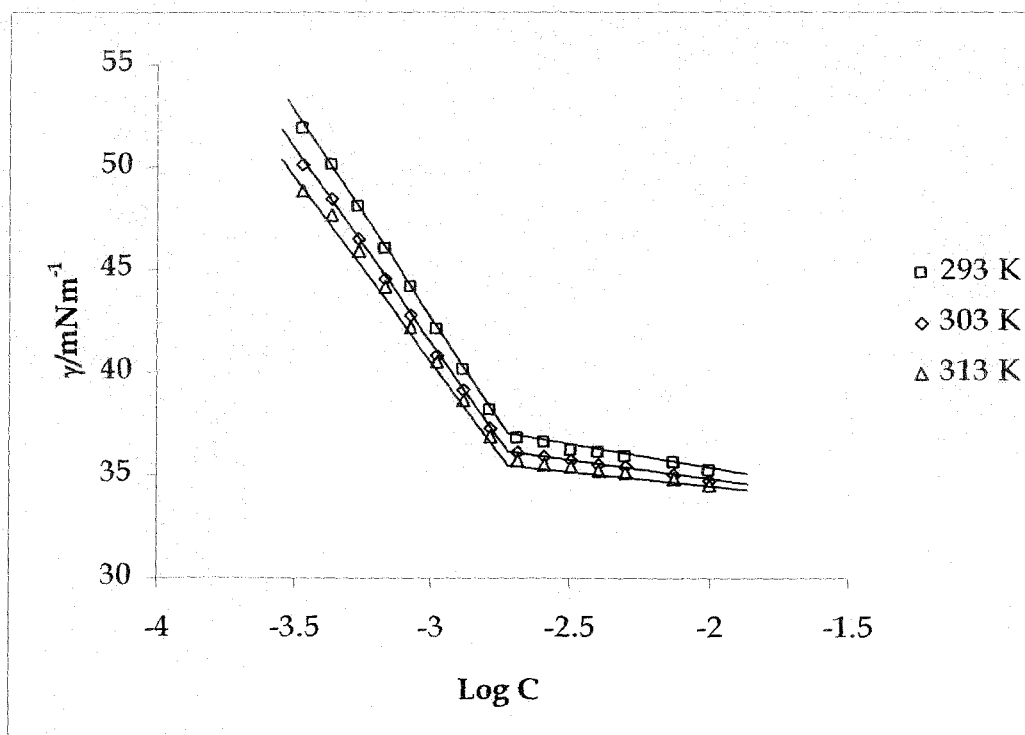
**Figure 4.5:** Surface Tension,  $\gamma$ , vs.  $\text{Log C}$  (mM) plot of SDBS in temperature range 293 – 313 K at 10 K intervals in the NaBr concentration 0.004 M.



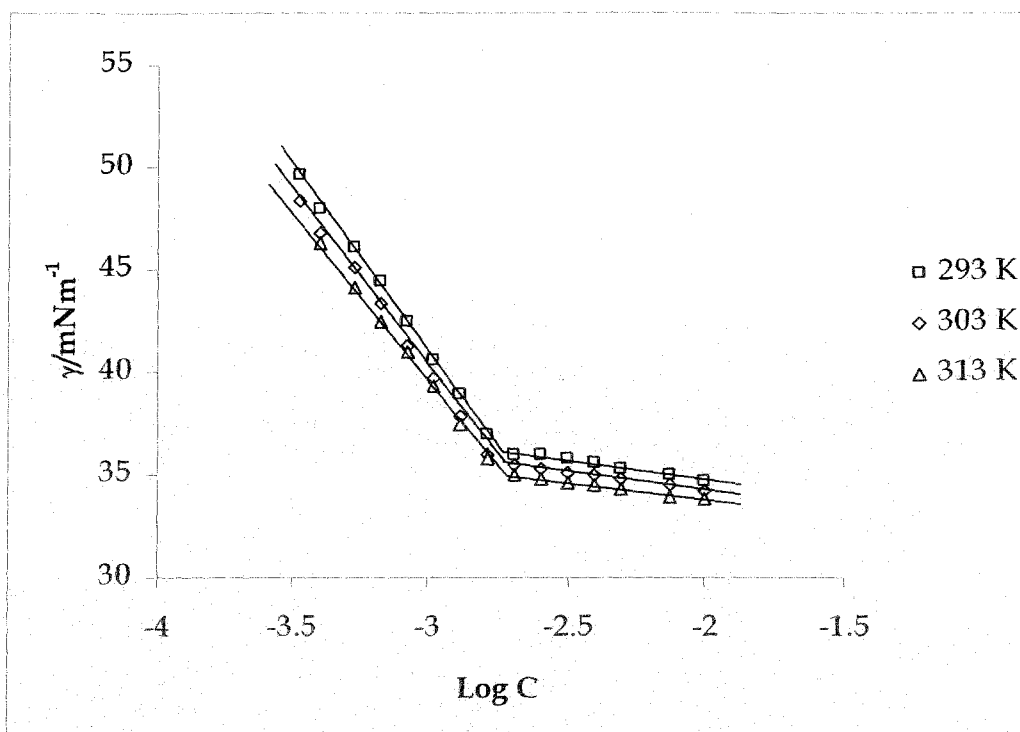
**Figure 4.6:** Surface Tension,  $\gamma$ , vs.  $\text{Log C}$  (mM) plot of SDBS in temperature range 293 – 313 K at 10 K intervals in the NaBr concentration 0.005 M.



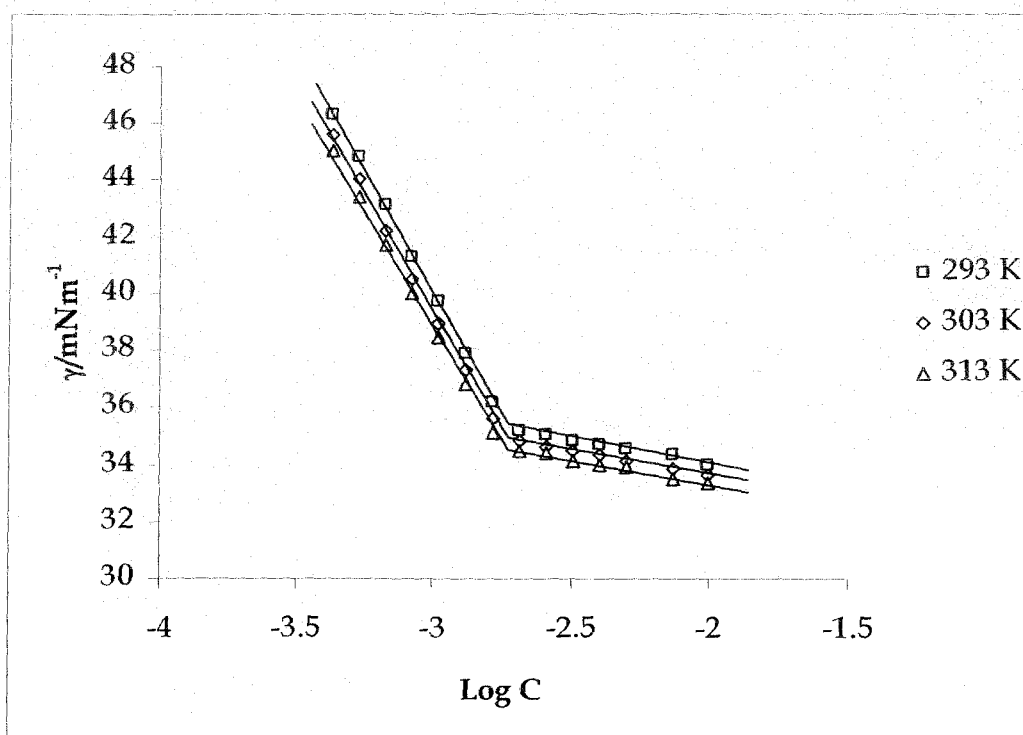
**Figure 4.7:** Surface Tension,  $\gamma$ , vs.  $\text{Log C}$  (mM) plot of LDBS in temperature range 293 – 313 K at 10 K intervals in the LiBr concentration 0.0005 M.



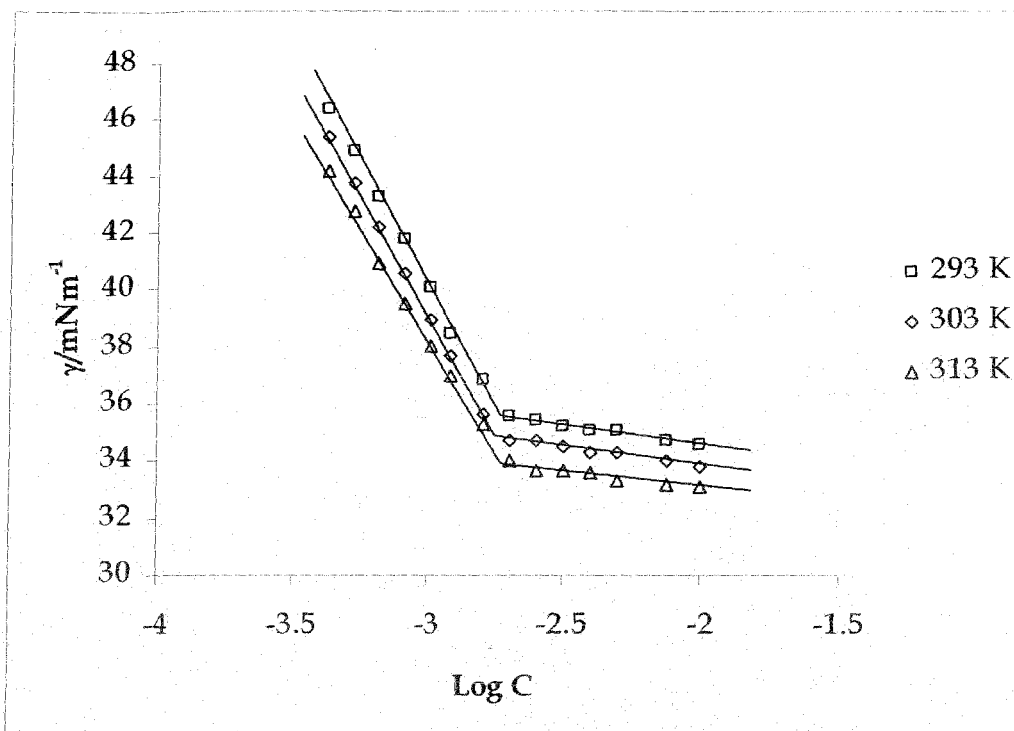
**Figure 4.8:** Surface Tension,  $\gamma$ , vs.  $\text{Log C}$  (mM) plot of LDBS in temperature range 293 – 313 K at 10 K intervals in the LiBr concentration 0.001 M.



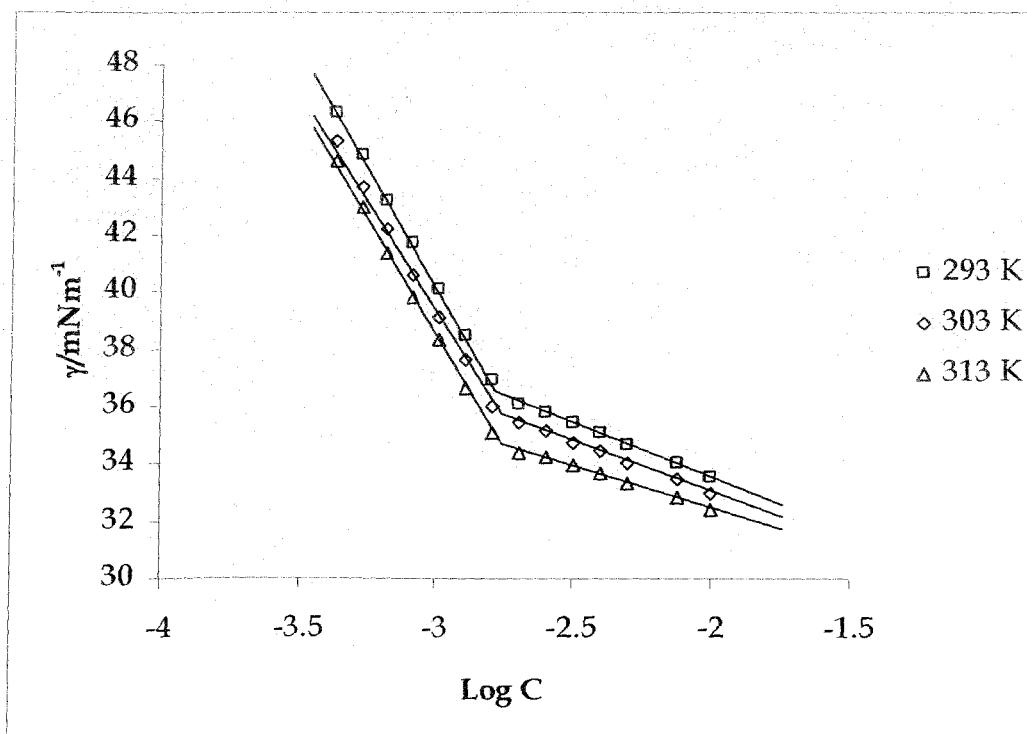
**Figure 4.9:** Surface Tension,  $\gamma$ , vs.  $\text{Log } C$  (mM) plot of LDBS in temperature range 293 – 313 K at 10 K intervals in the LiBr concentration 0.002 M.



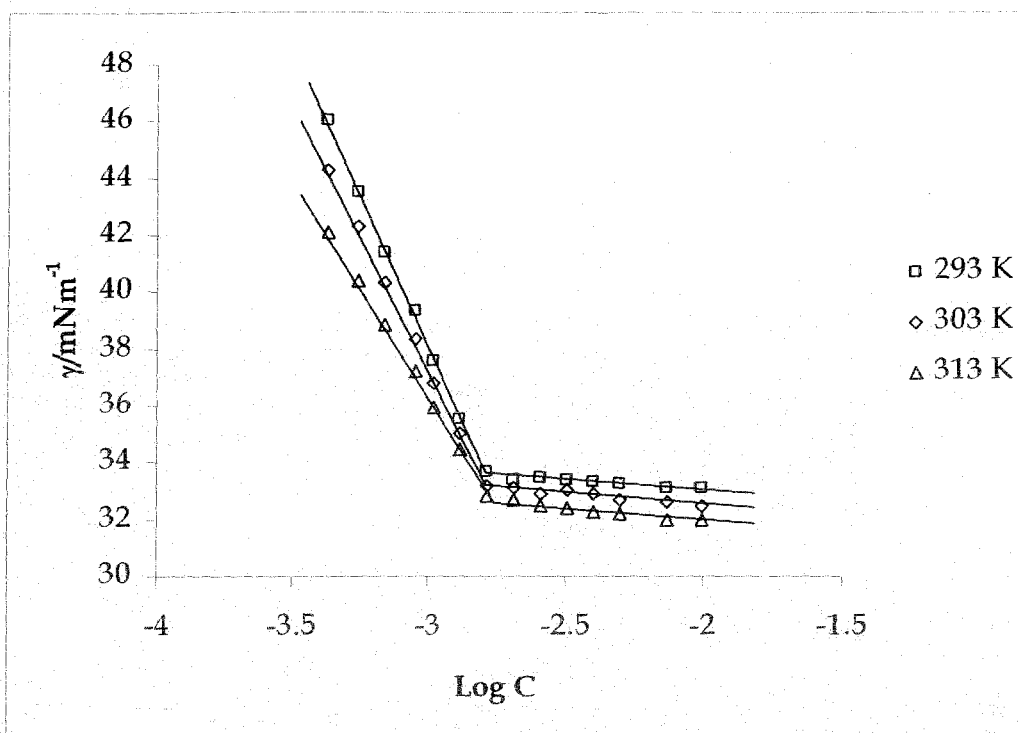
**Figure 4.10:** Surface Tension,  $\gamma$ , vs.  $\text{Log } C$  (mM) plot of LDBS in temperature range 293 – 313 K at 10 K intervals in the LiBr concentration 0.003 M.



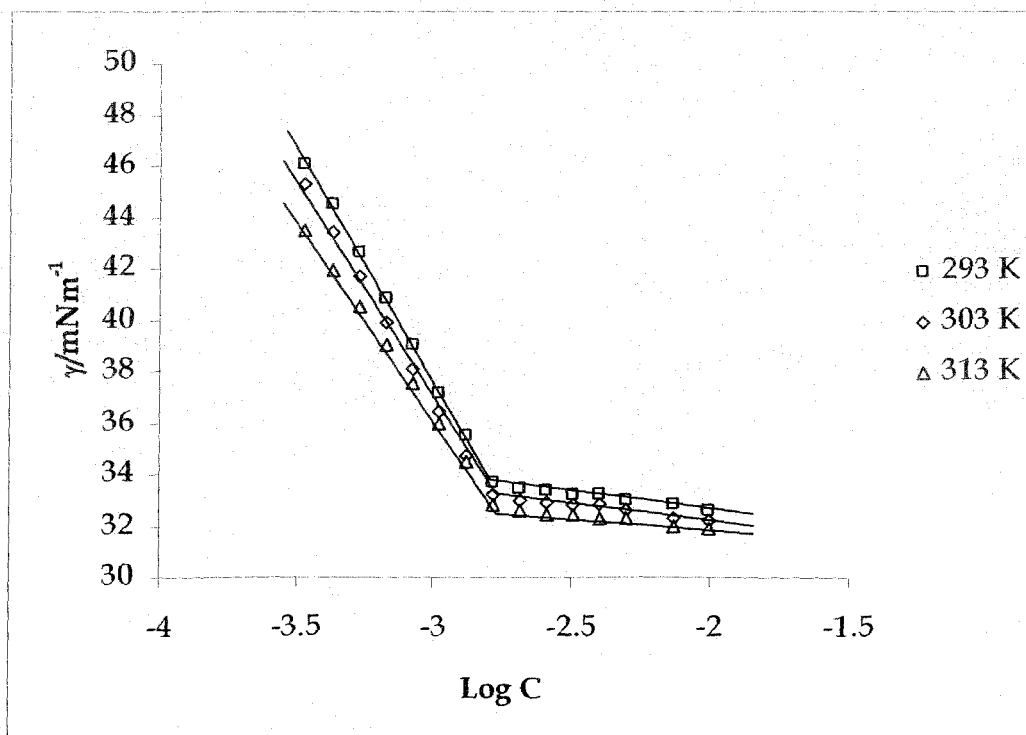
**Figure 4.11:** Surface Tension,  $\gamma$ , vs.  $\text{Log } C$  (mM) plot of LDBS in temperature range 293 – 313 K at 10 K intervals in the LiBr concentration 0.004 M.



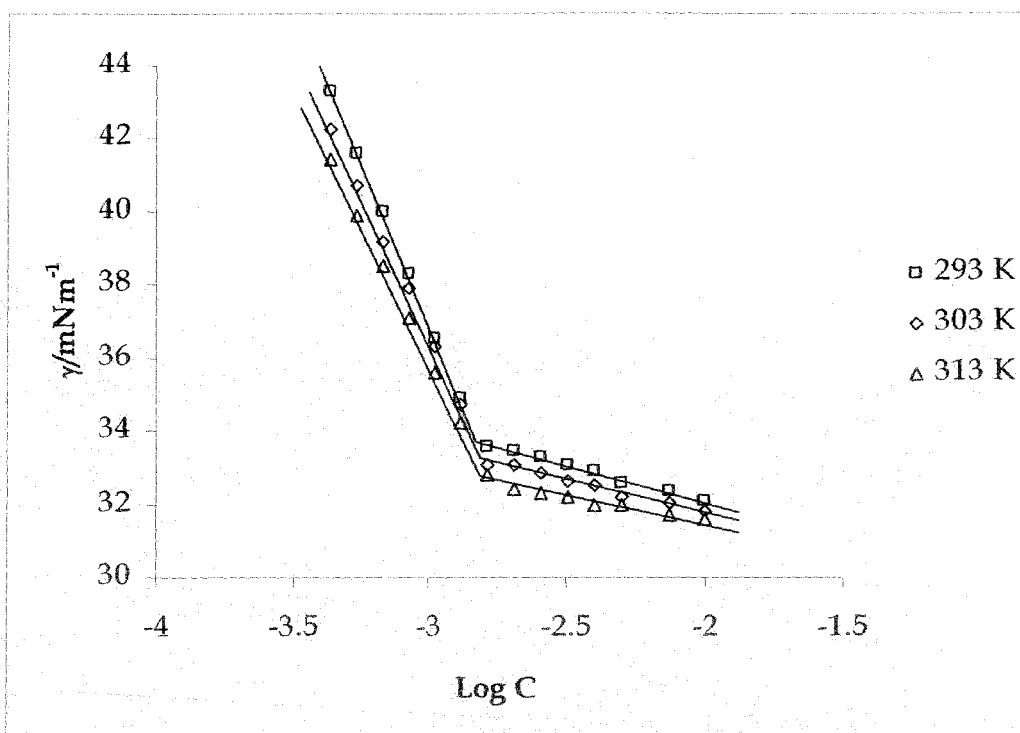
**Figure 4.12:** Surface Tension,  $\gamma$ , vs.  $\text{Log } C$  (mM) plot of LDBS in temperature range 293 – 313 K at 10 K intervals in the LiBr concentration 0.005 M.



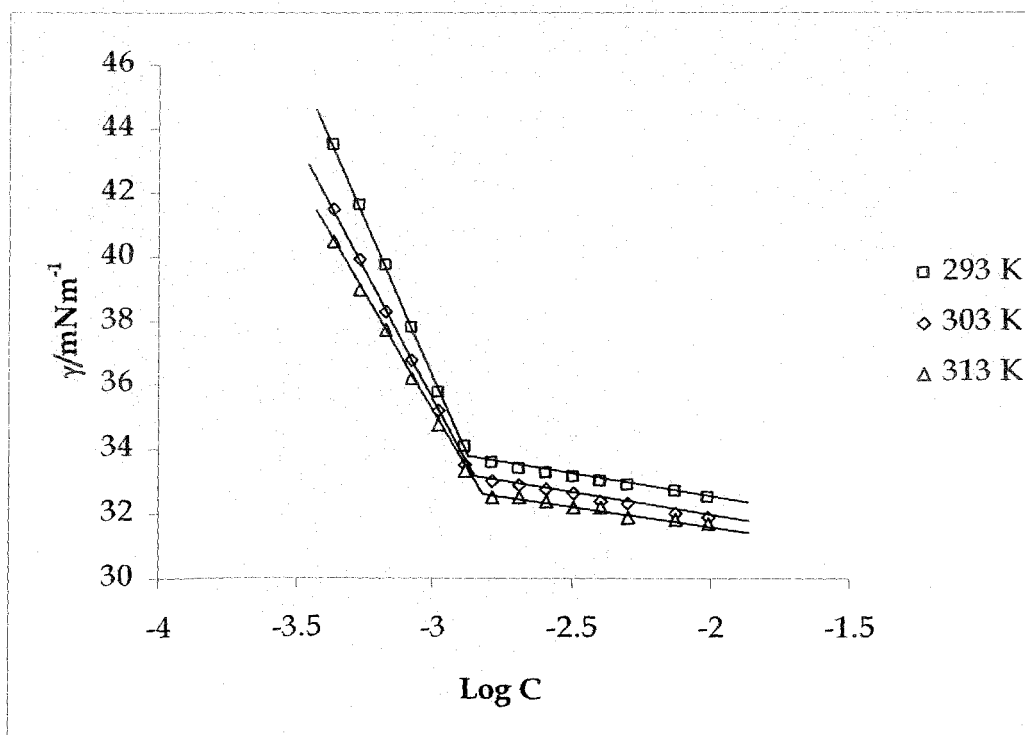
**Figure 4.13:** Surface Tension,  $\gamma$ , vs.  $\text{Log } C$  (mM) plot of PDBS in temperature range 293 – 313 K at 10 K intervals in the KBr concentration 0.0005 M.



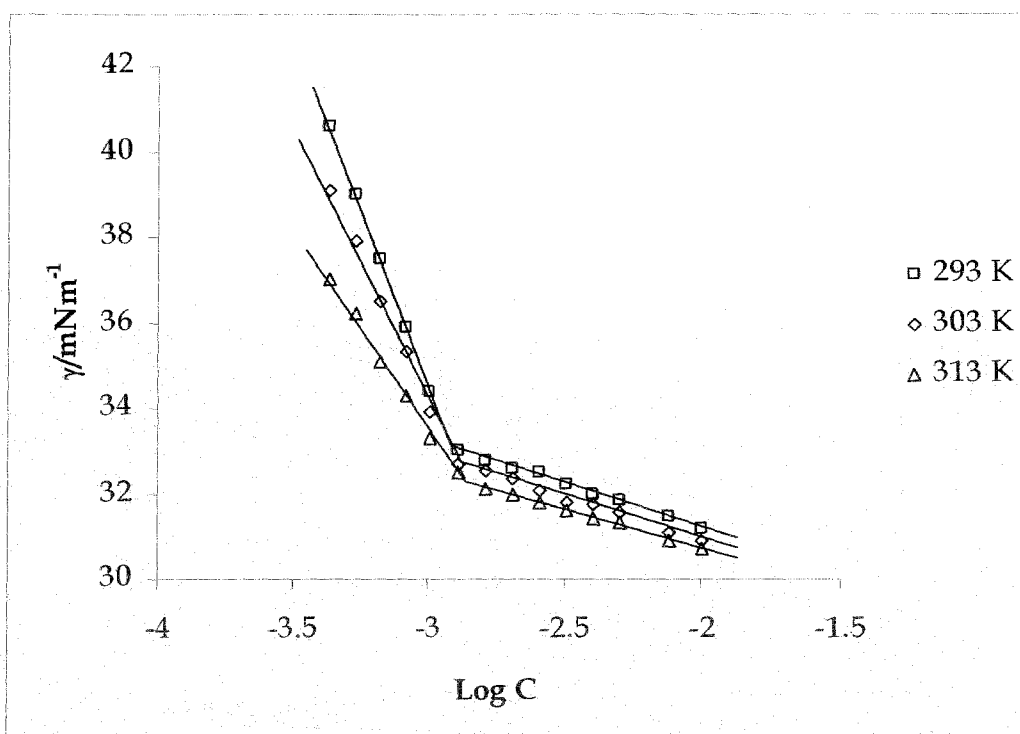
**Figure 4.14:** Surface Tension,  $\gamma$ , vs.  $\text{Log } C$  (mM) plot of PDBS in temperature range 293 – 313 K at 10 K intervals in the KBr concentration 0.001 M.



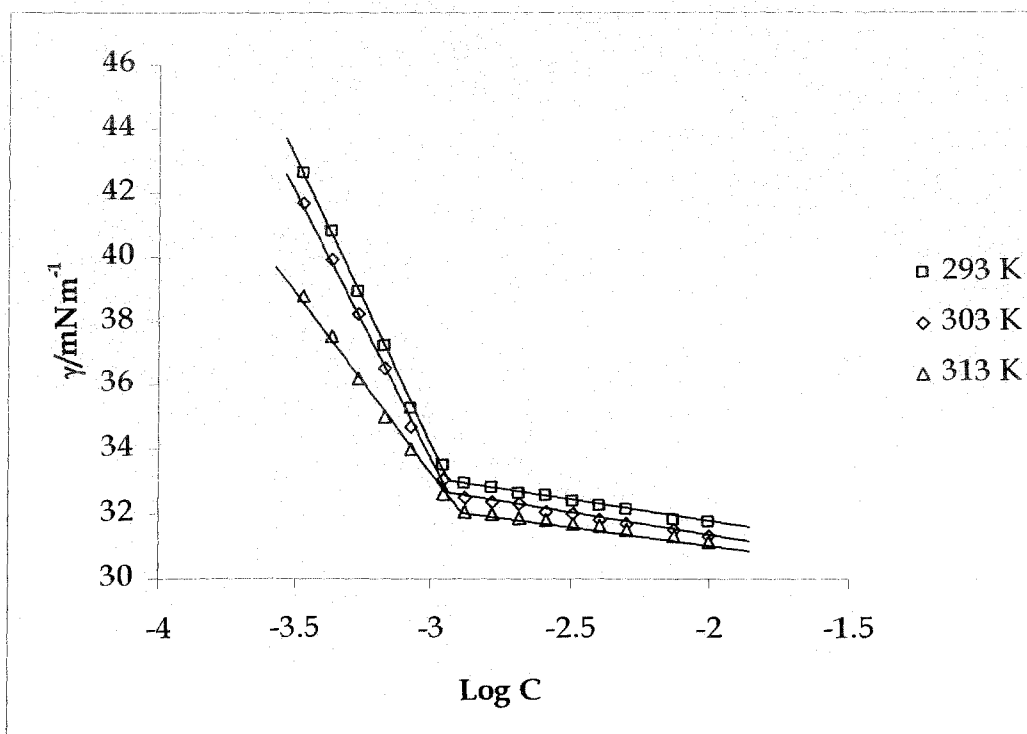
**Figure 4.15:** Surface Tension,  $\gamma$ , vs.  $\text{Log } C$  (mM) plot of PDBS in temperature range 293 – 313 K at 10 K intervals in the KBr concentration 0.002 M.



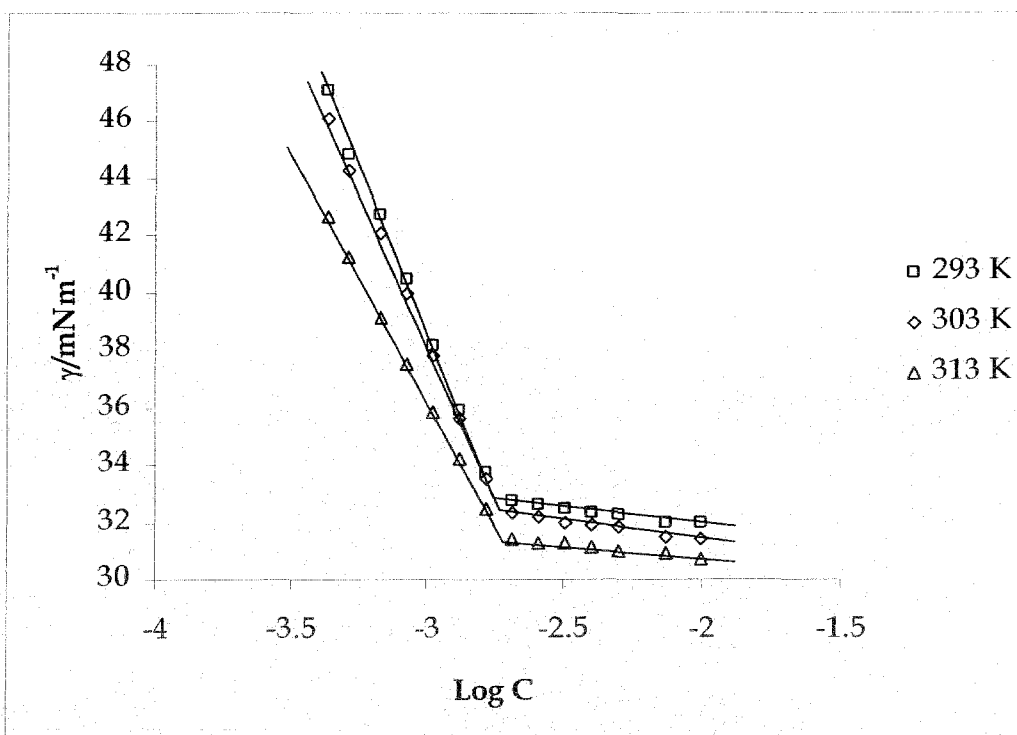
**Figure 4.16:** Surface Tension,  $\gamma$ , vs.  $\text{Log } C$  (mM) plot of PDBS in temperature range 293 – 313 K at 10 K intervals in the KBr concentration 0.003 M.



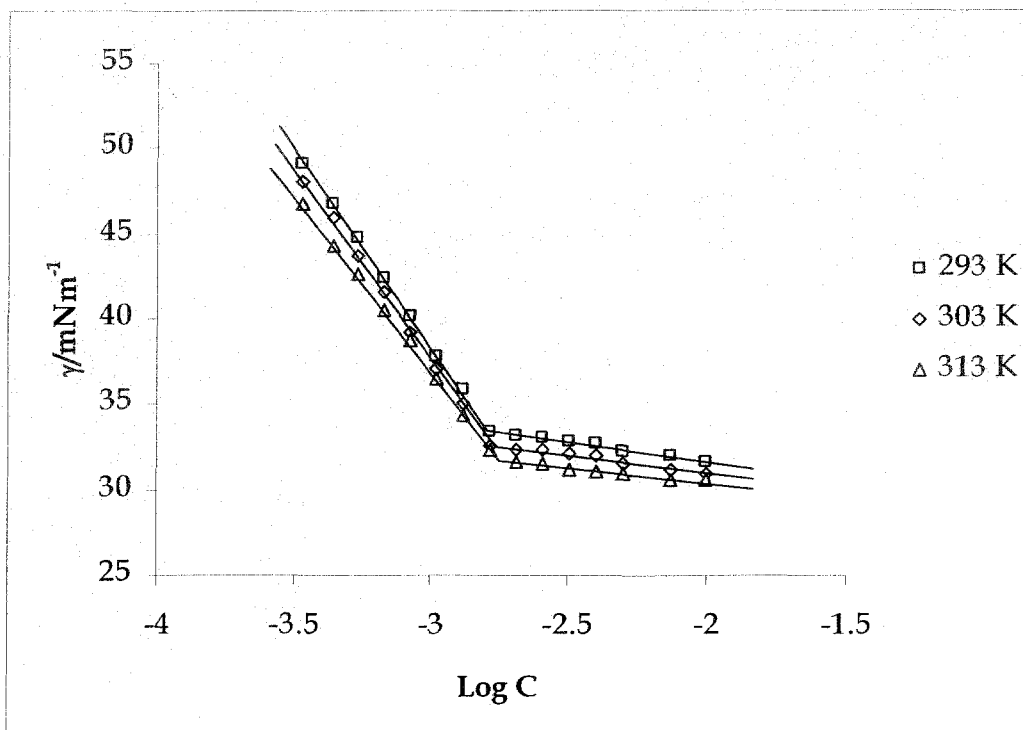
**Figure 4.17:** Surface Tension,  $\gamma$ , vs.  $\text{Log } C$  (mM) plot of PDBS in temperature range 293 – 313 K at 10 K intervals in the KBr concentration 0.004 M.



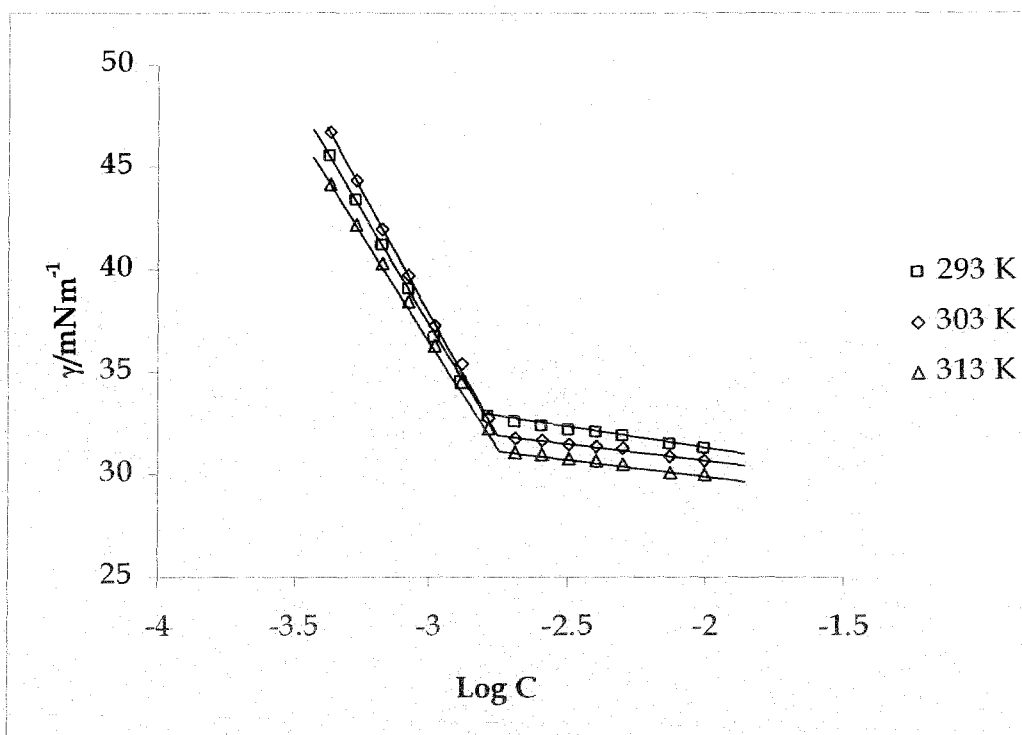
**Figure 4.18:** Surface Tension,  $\gamma$ , vs.  $\text{Log } C$  (mM) plot of PDBS in temperature range 293 – 313 K at 10 K intervals in the KBr concentration 0.005 M.



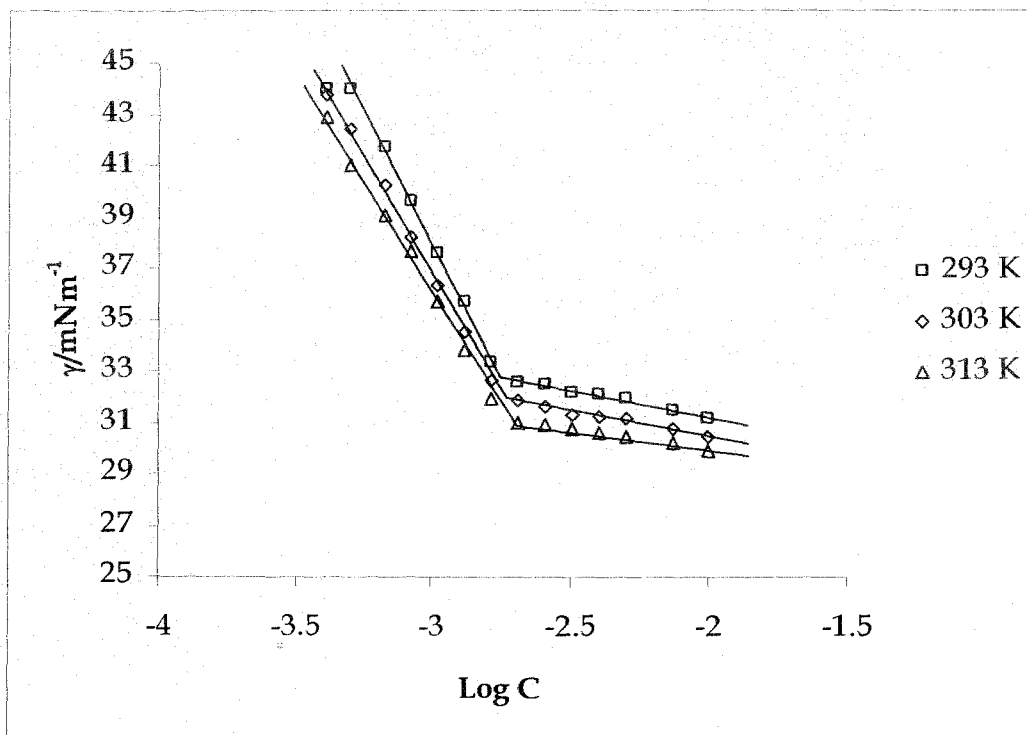
**Figure 4.19:** Surface Tension,  $\gamma$ , vs.  $\text{Log C}$  (mM) plot of ADBS in temperature range 293 – 313 K at 10 K intervals in the  $\text{NH}_4\text{Br}$  concentration 0.0005 M.



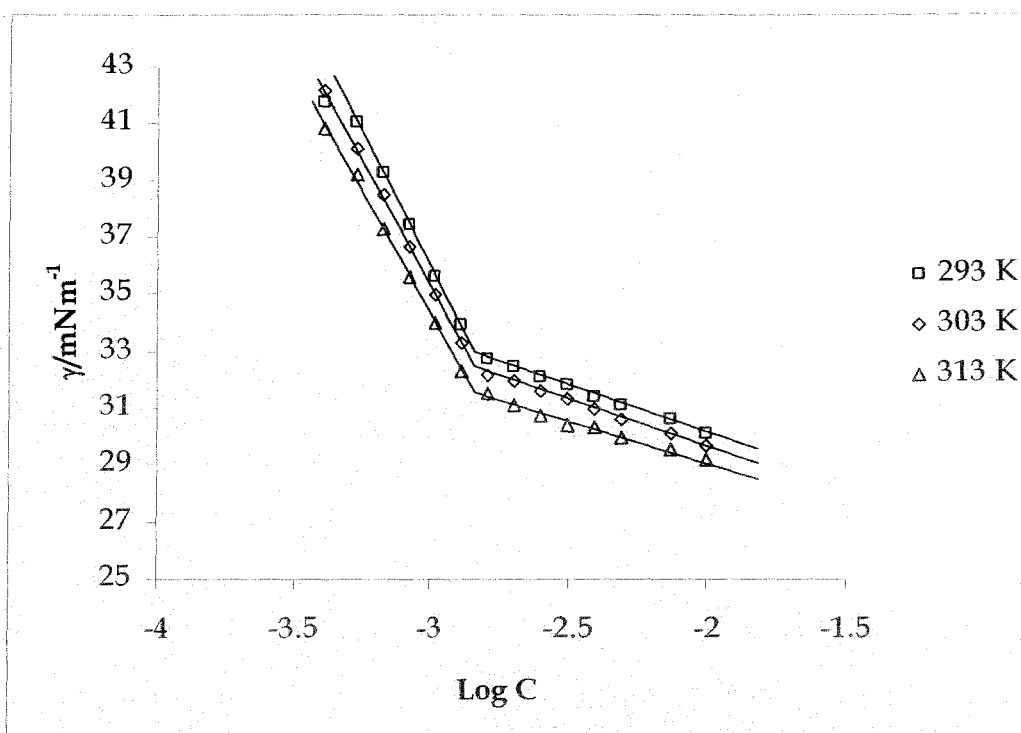
**Figure 4.20:** Surface Tension,  $\gamma$ , vs.  $\text{Log C}$  (mM) plot of ADBS in temperature range 293 – 313 K at 10 K intervals in the  $\text{NH}_4\text{Br}$  concentration 0.001 M.



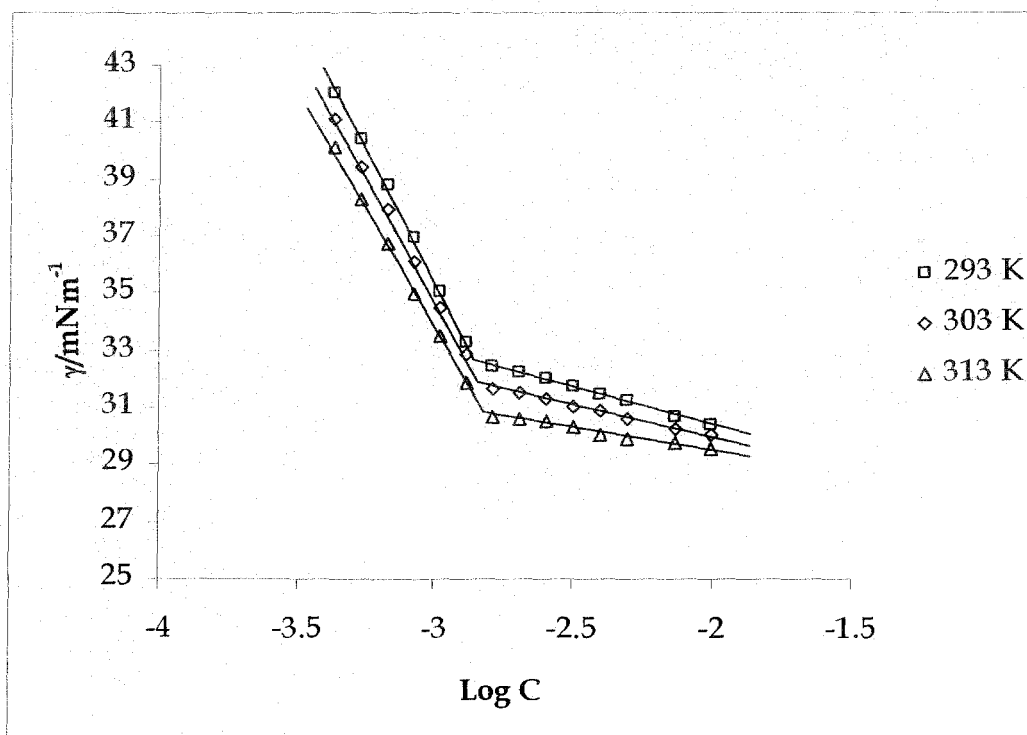
**Figure 4.21:** Surface Tension,  $\gamma$ , vs.  $\text{Log C}$  (mM) plot of ADBS in temperature range 293 – 313 K at 10 K intervals in the  $\text{NH}_4\text{Br}$  concentration 0.002 M.



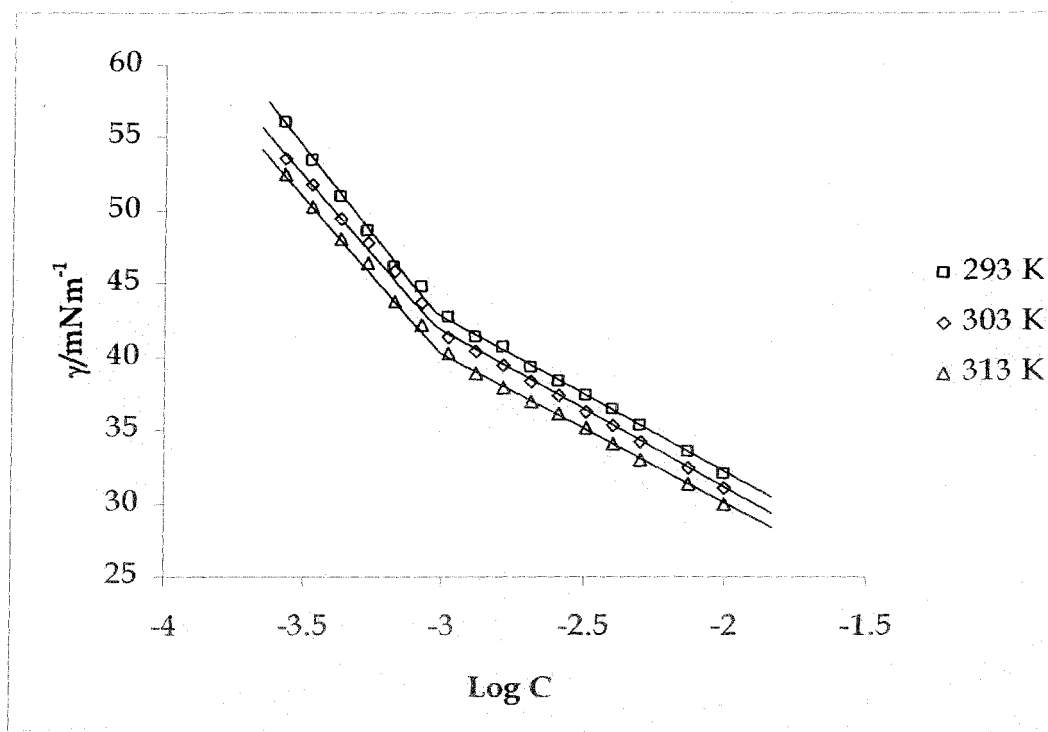
**Figure 4.22:** Surface Tension,  $\gamma$ , vs.  $\text{Log C}$  (mM) plot of ADBS in temperature range 293 – 313 K at 10 K intervals in the  $\text{NH}_4\text{Br}$  concentration 0.003 M.



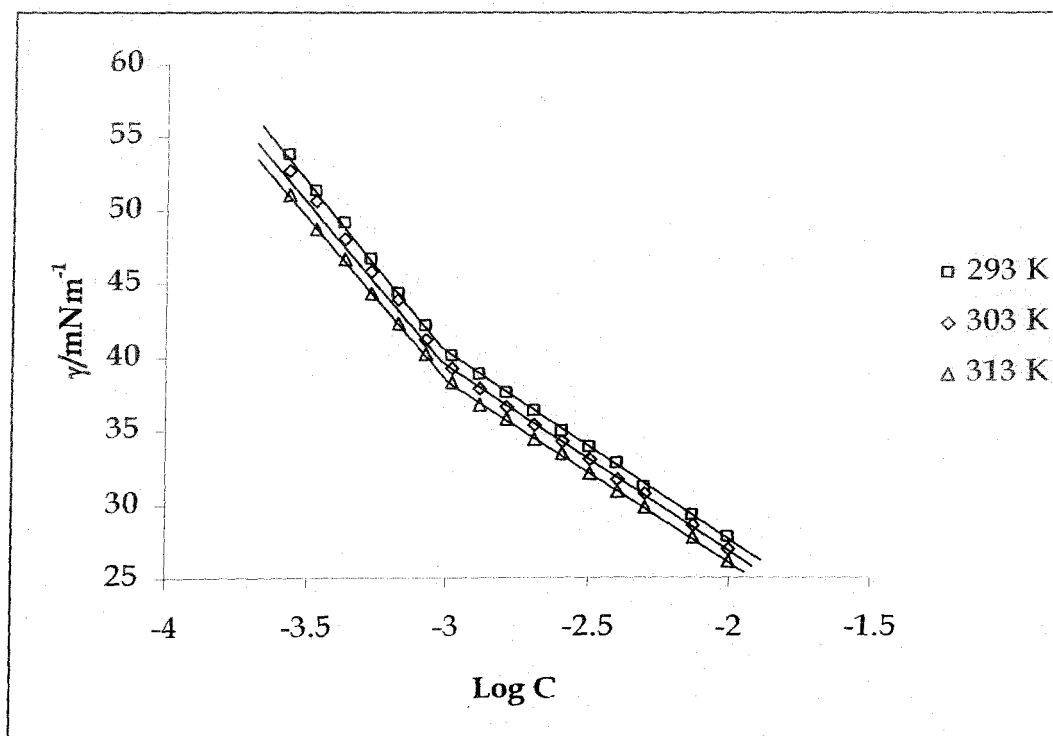
**Figure 4.23:** Surface Tension,  $\gamma$ , vs.  $\text{Log } C$  (mM) plot of ADBS in temperature range 293 – 313 K at 10 K intervals in the  $\text{NH}_4\text{Br}$  concentration 0.004 M.



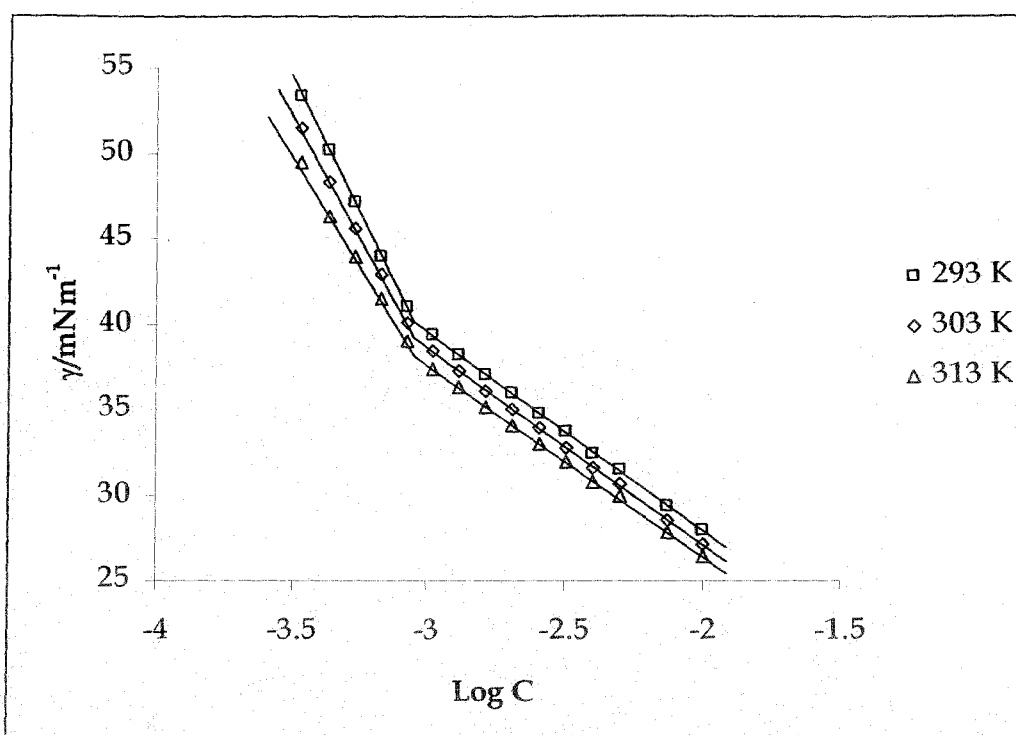
**Figure 4.24:** Surface Tension,  $\gamma$ , vs.  $\text{Log } C$  (mM) plot of ADBS in temperature range 293 – 313 K at 10 K intervals in the  $\text{NH}_4\text{Br}$  concentration 0.005 M.



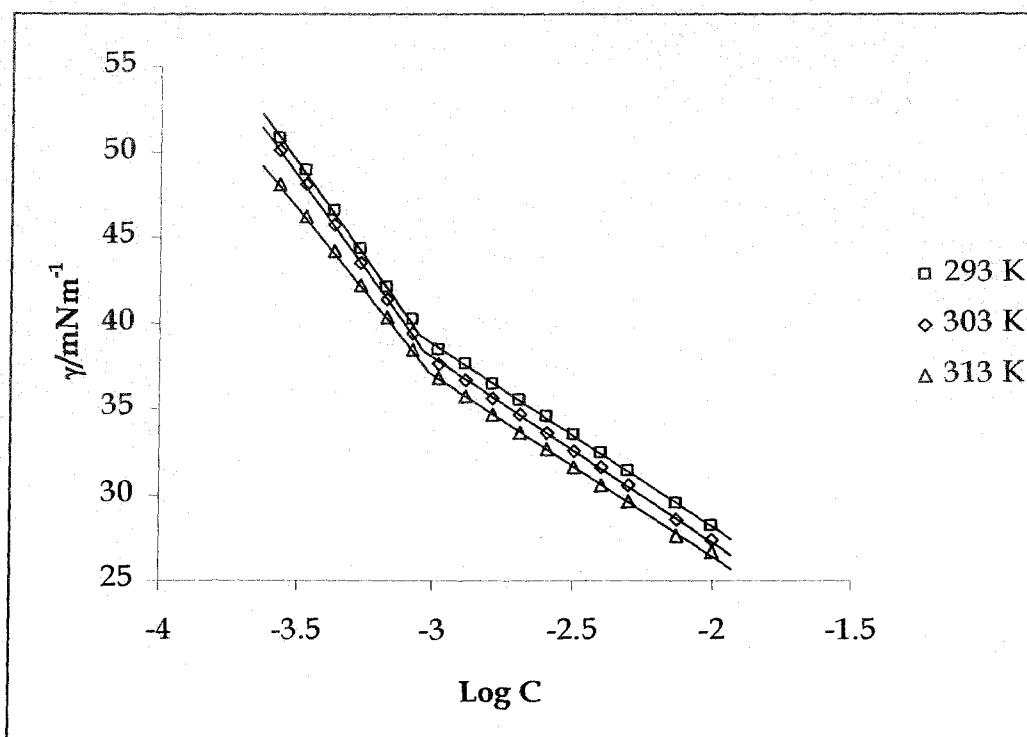
**Figure 4.25:** Surface Tension,  $\gamma$ , vs.  $\text{Log } C$  (mM) plot of TMADBS in temperature range 293 – 313 K at 10 K intervals in the TMABr concentration 0.0005 M.



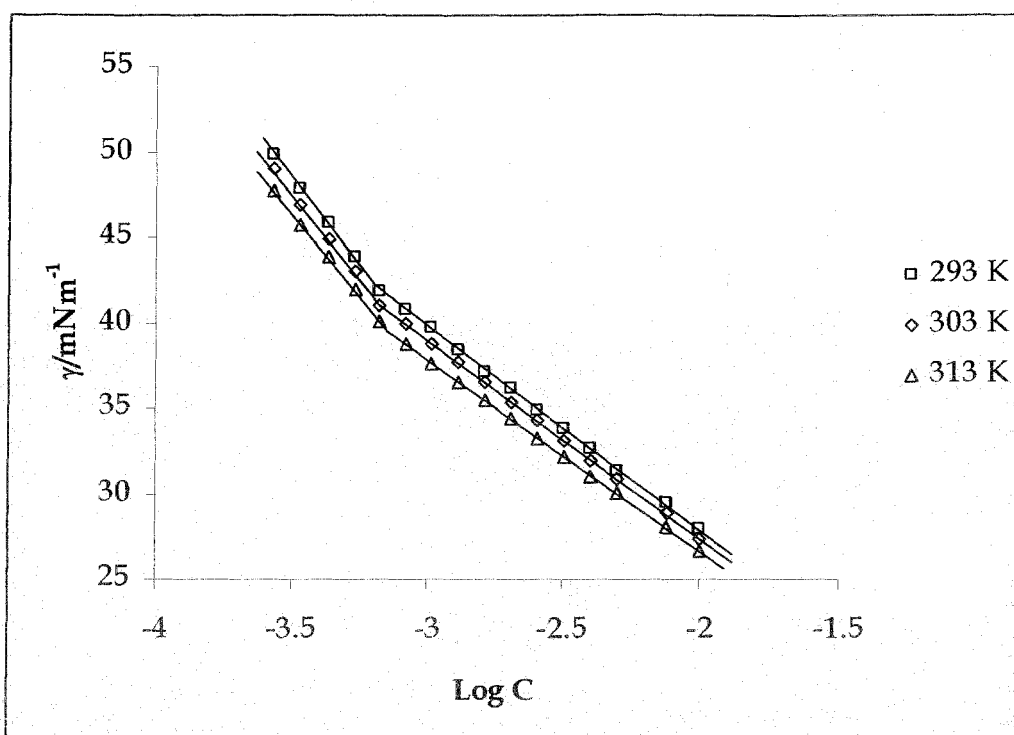
**Figure 4.26:** Surface Tension,  $\gamma$ , vs.  $\text{Log } C$  (mM) plot of TMADBS in temperature range 293 – 313 K at 10 K intervals in the TMABr concentration 0.001 M.



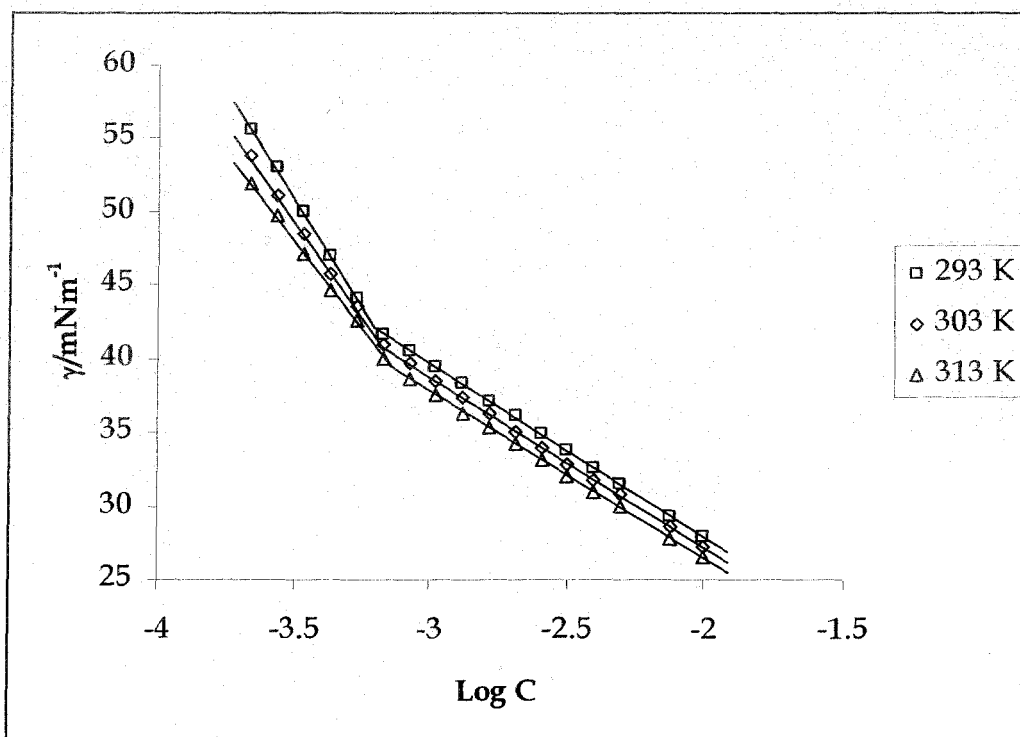
**Figure 4.27:** Surface Tension,  $\gamma$ , vs.  $\text{Log } C$  (mM) plot of TMADBS in temperature range 293 – 313 K at 10 K intervals in the TMABr concentration 0.002 M.



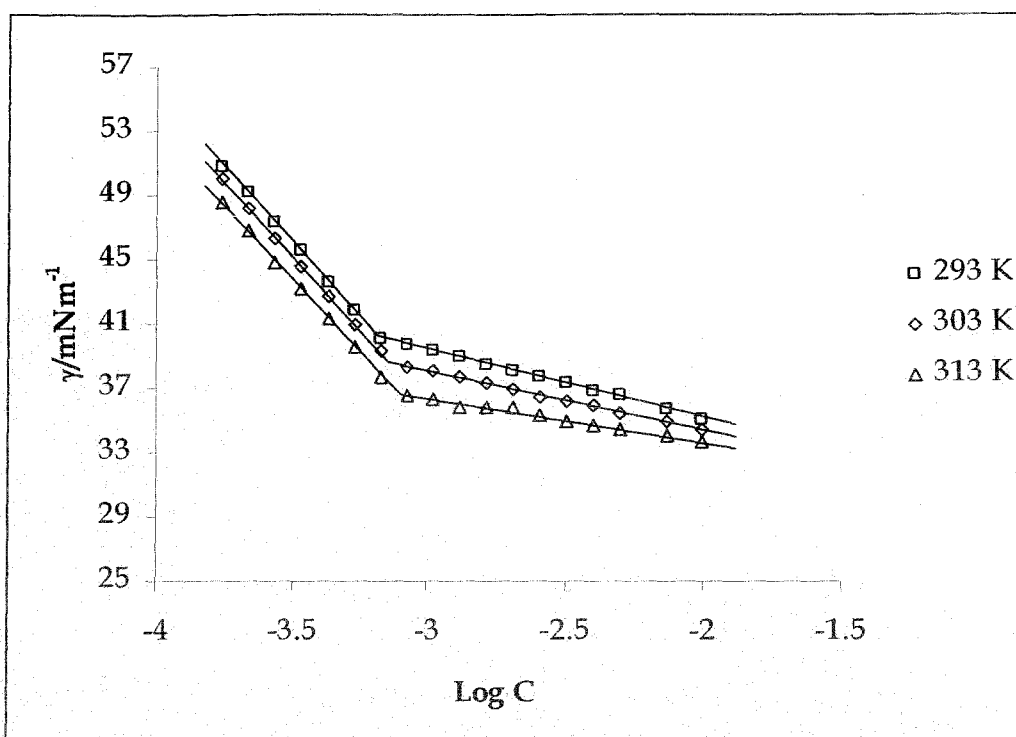
**Figure 4.28:** Surface Tension,  $\gamma$ , vs.  $\text{Log } C$  (mM) plot of TMADBS in temperature range 293 – 313 K at 10 K intervals in the TMABr concentration 0.003 M.



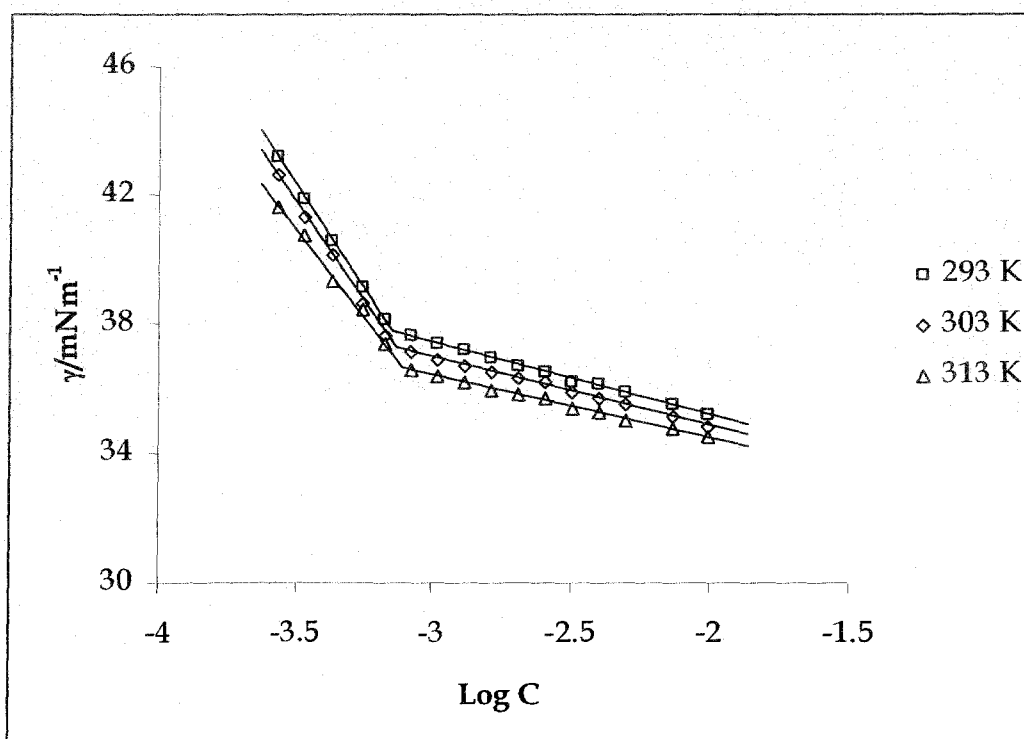
**Figure 4.29:** Surface Tension,  $\gamma$ , vs.  $\text{Log } C$  (mM) plot of TMADBS in temperature range 293 – 313 K at 10 K intervals in the TMABr concentration 0.004 M.



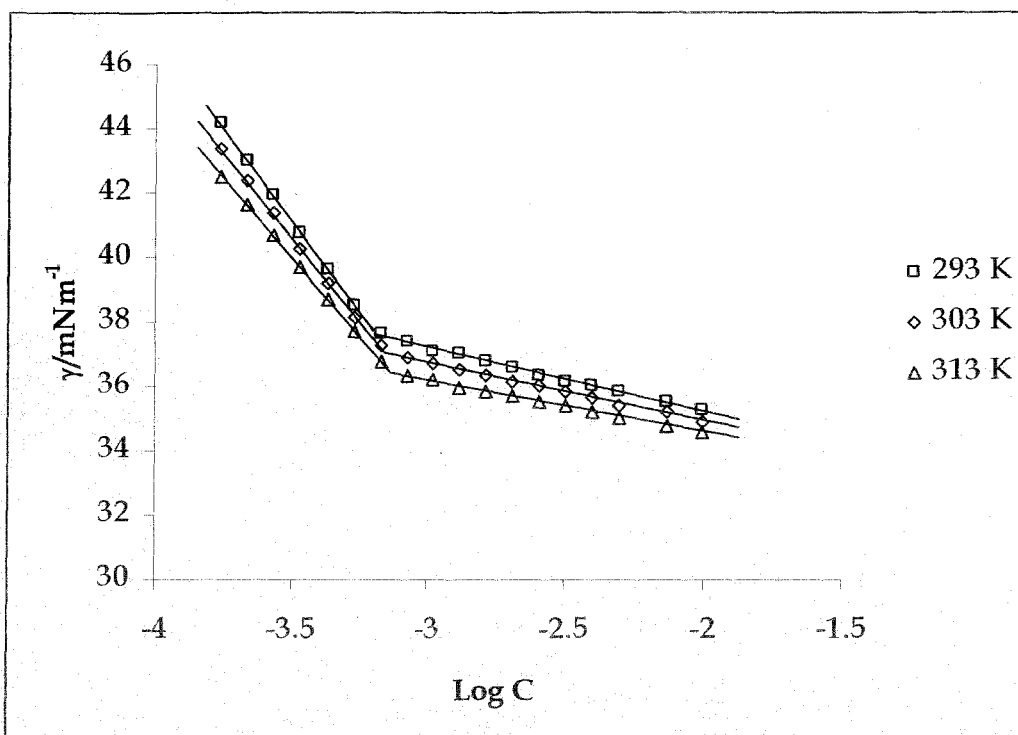
**Figure 4.30:** Surface Tension,  $\gamma$ , vs.  $\text{Log } C$  (mM) plot of TMADBS in temperature range 293 – 313 K at 10 K intervals in the TMABr concentration 0.005 M.



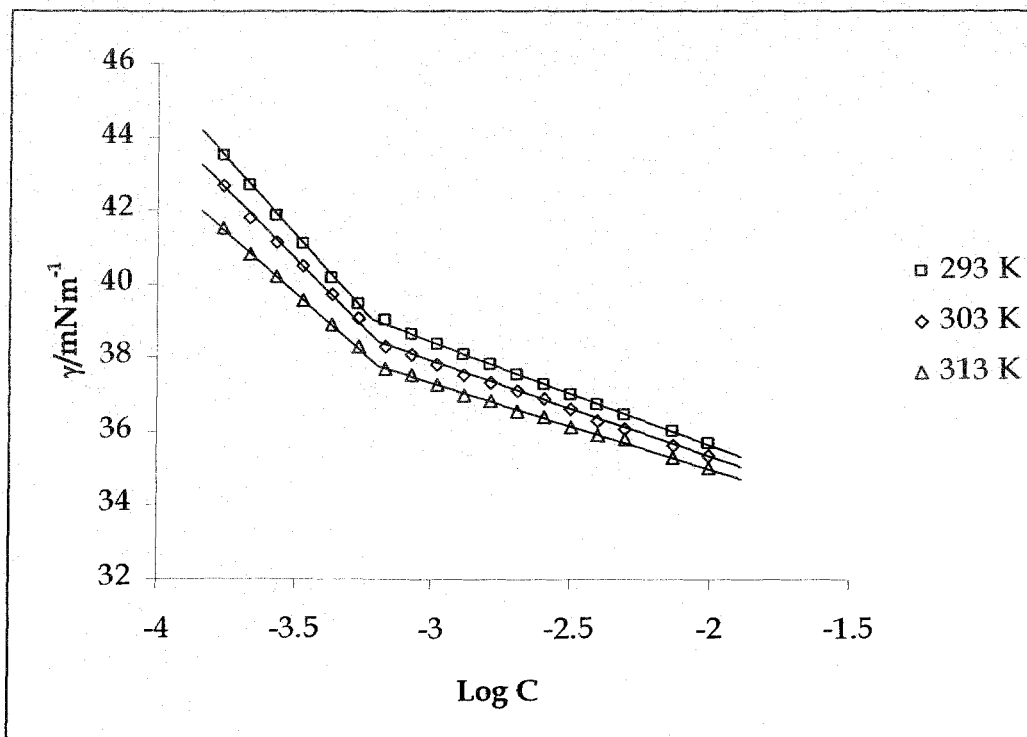
**Figure 4.31:** Surface Tension,  $\gamma$ , vs.  $\text{Log } C$  (mM) plot of TEADBS in temperature range 293 – 313 K at 10 K intervals in the TEABr concentration 0.0005 M.



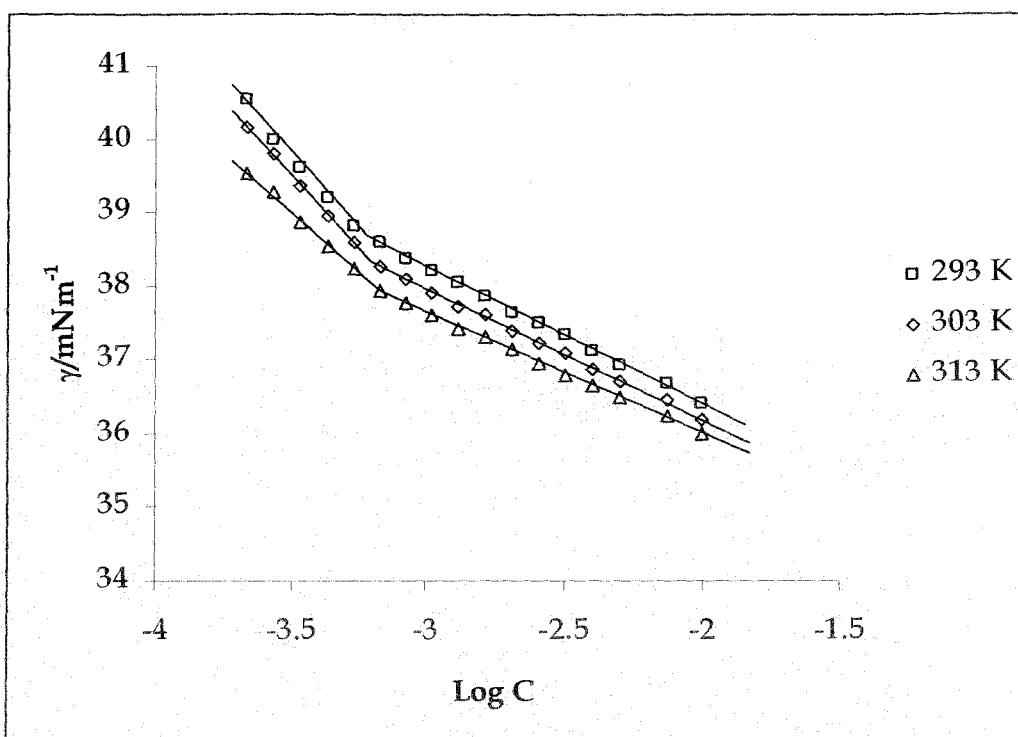
**Figure 4.32:** Surface Tension,  $\gamma$ , vs.  $\text{Log } C$  (mM) plot of TEADBS in temperature range 293 – 313 K at 10 K intervals in the TEABr concentration 0.001 M.



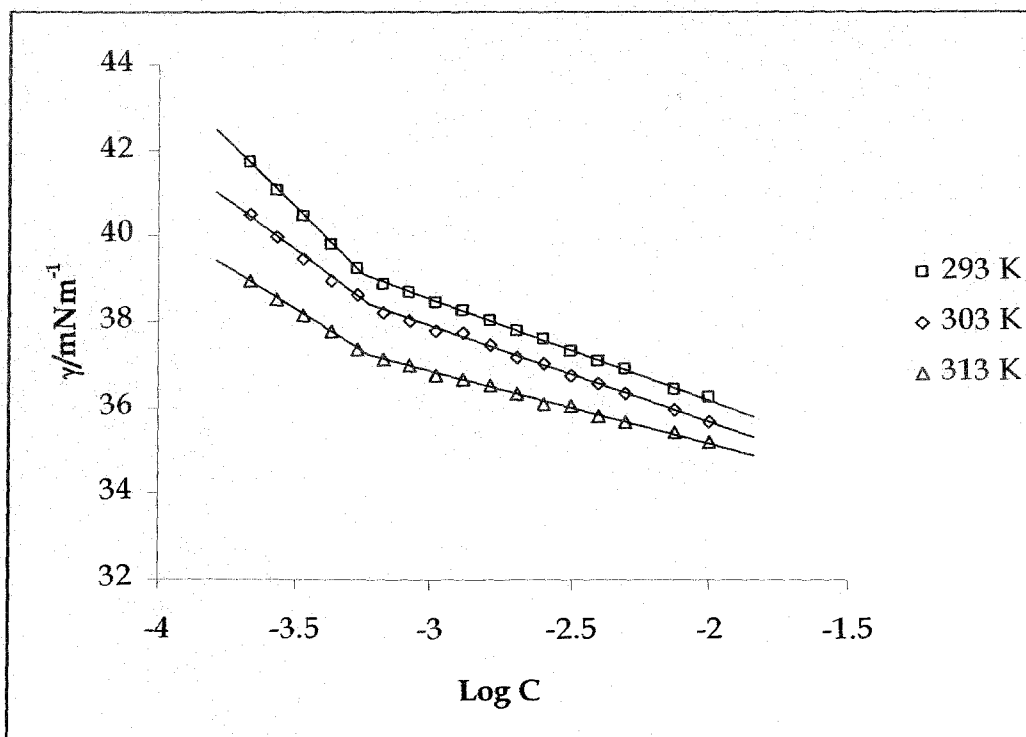
**Figure 4.33:** Surface Tension,  $\gamma$ , vs.  $\text{Log } C$  (mM) plot of TEADBS in temperature range 293 – 313 K at 10 K intervals in the TEABr concentration 0.002 M.



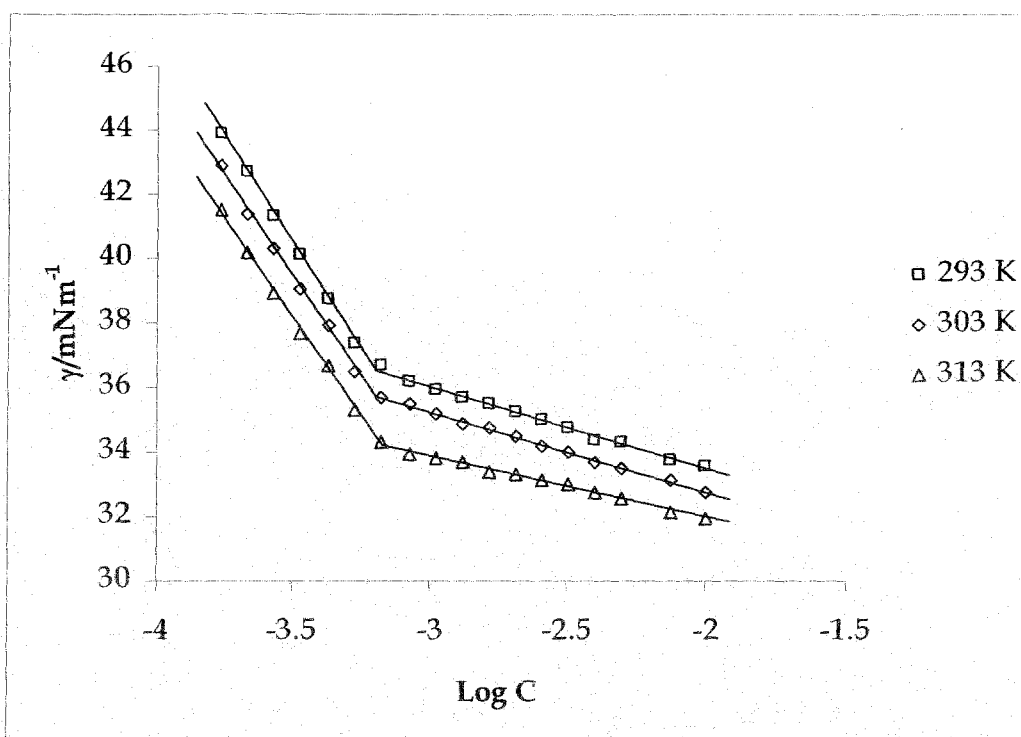
**Figure 4.34:** Surface Tension,  $\gamma$ , vs.  $\text{Log } C$  (mM) plot of TEADBS in temperature range 293 – 313 K at 10 K intervals in the TEABr concentration 0.003 M.



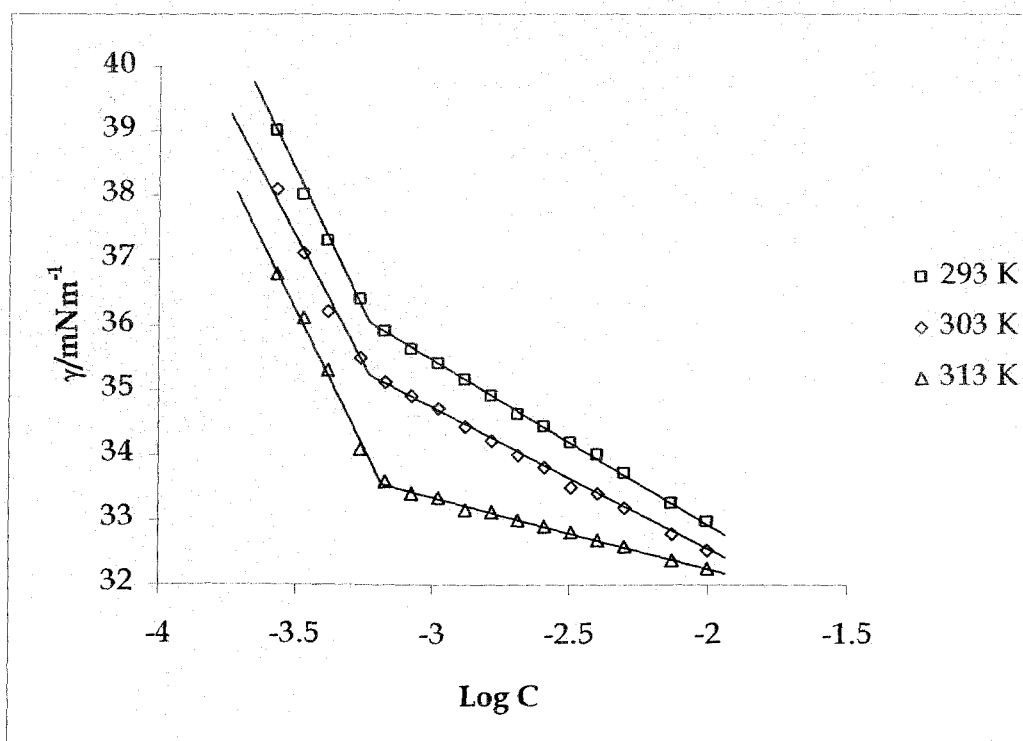
**Figure 4.35:** Surface Tension,  $\gamma$ , vs.  $\text{Log } C$  (mM) plot of TEADBS in temperature range 293 – 313 K at 10 K intervals in the TEABr concentration 0.004 M.



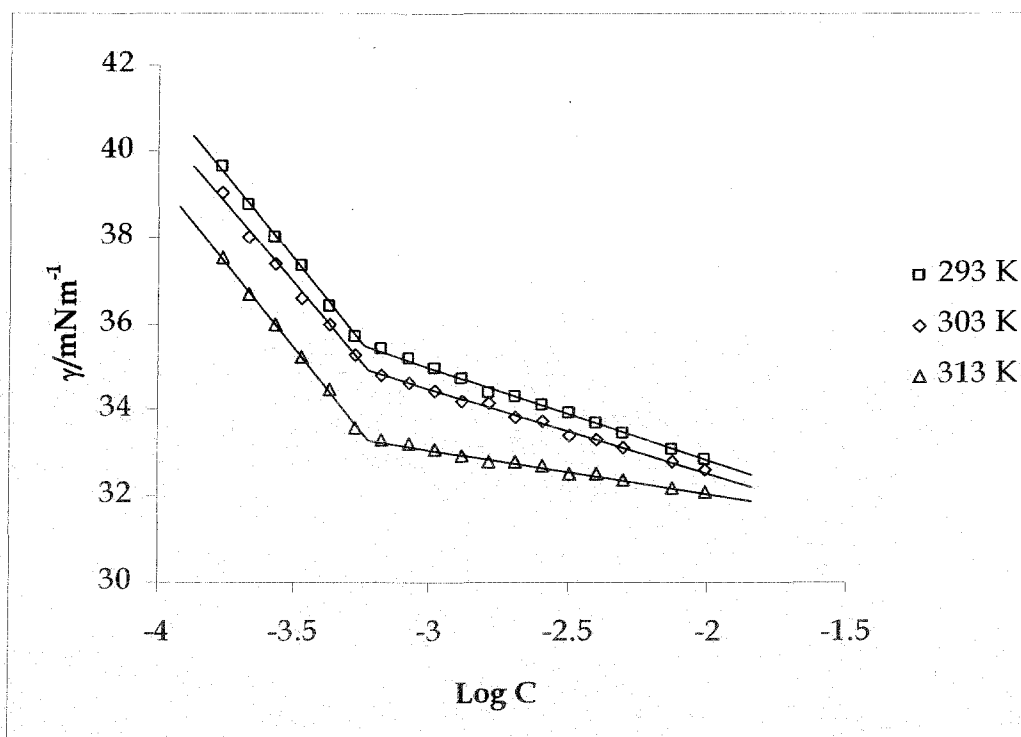
**Figure 4.36:** Surface Tension,  $\gamma$ , vs.  $\text{Log } C$  (mM) plot of TEADBS in temperature range 293 – 313 K at 10 K intervals in the TEABr concentration 0.005 M.



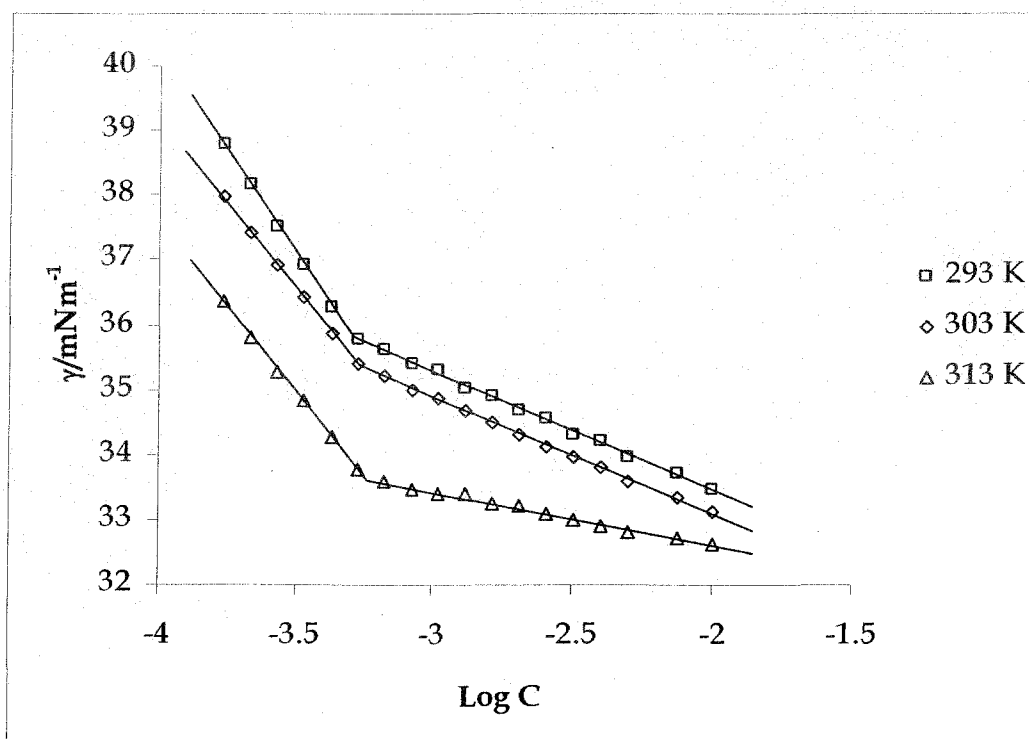
**Figure 4.37:** Surface Tension,  $\gamma$ , vs.  $\text{Log } C$  (mM) plot of TPADBS in temperature range 293 – 313 K at 10 K intervals in the TPABr concentration 0.0005 M.



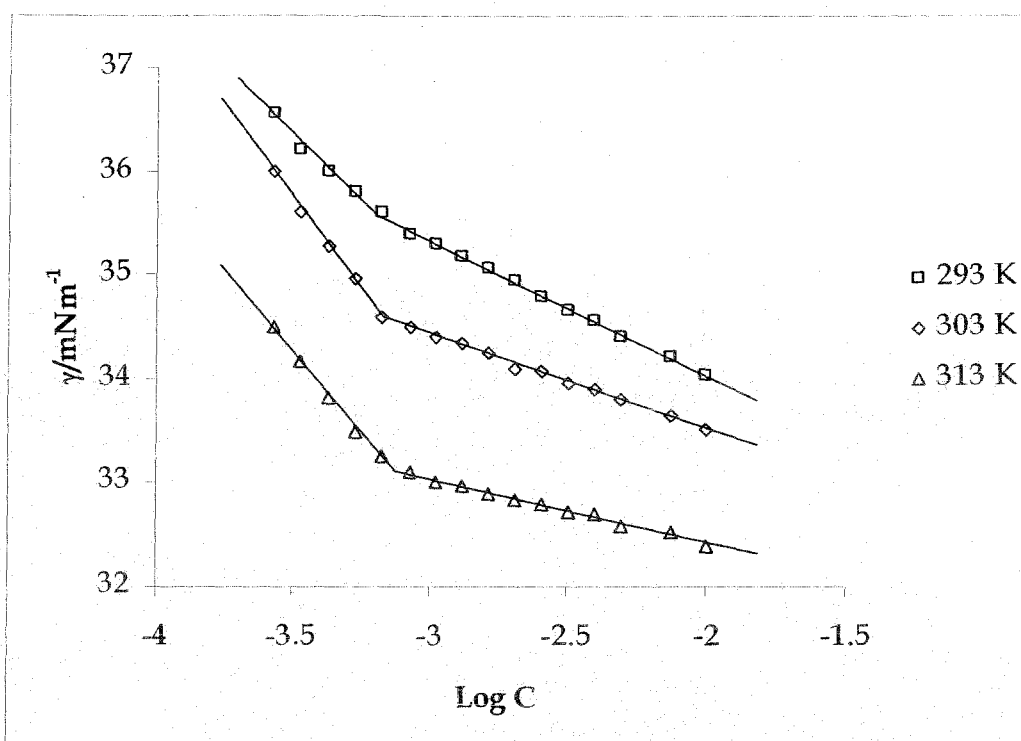
**Figure 4.38:** Surface Tension,  $\gamma$ , vs.  $\text{Log } C$  (mM) plot of TPADBS in temperature range 293 – 313 K at 10 K intervals in the TPABr concentration 0.001 M.



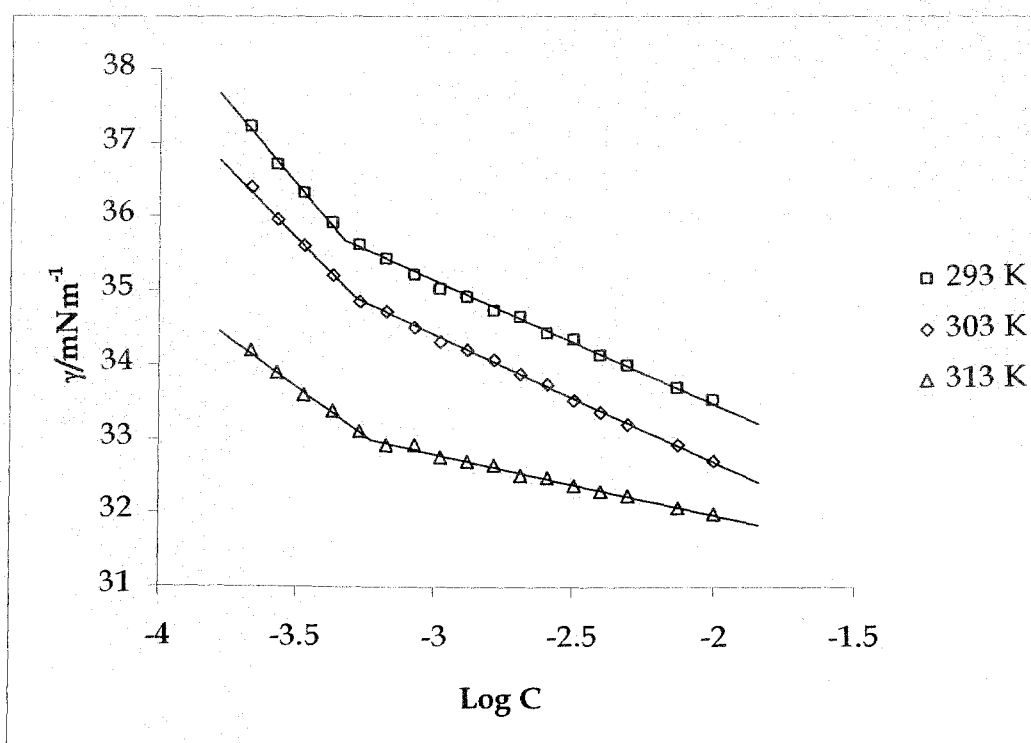
**Figure 4.39:** Surface Tension,  $\gamma$ , vs.  $\text{Log } C$  (mM) plot of TPADBS in temperature range 293 – 313 K at 10 K intervals in the TPABr concentration 0.002 M.



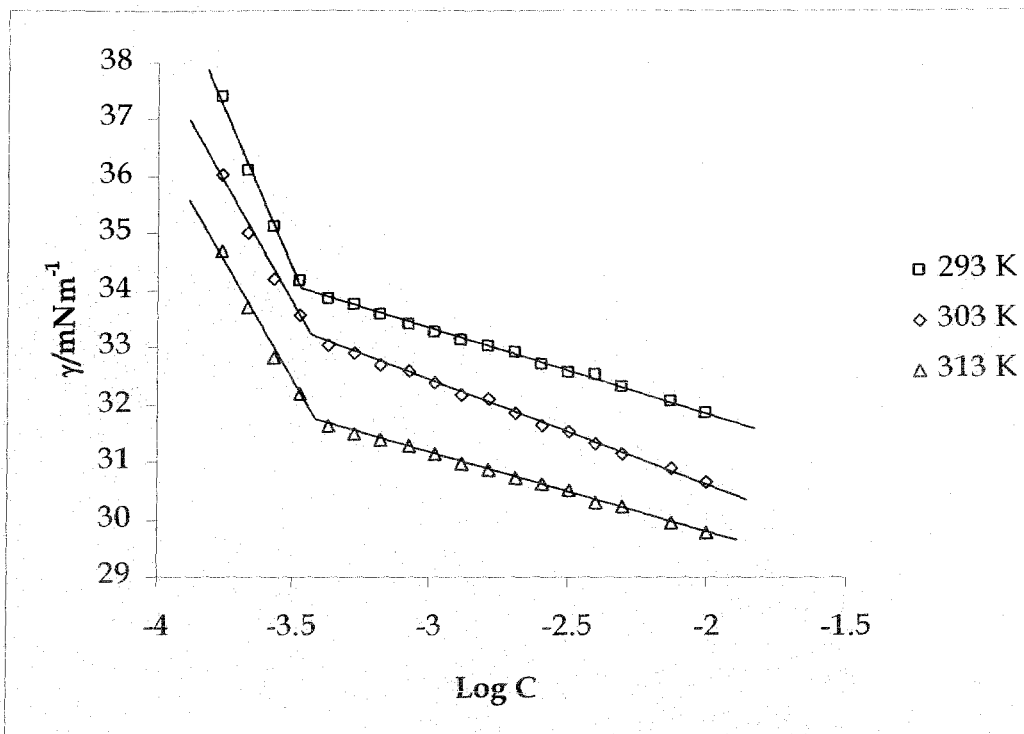
**Figure 4.40:** Surface Tension,  $\gamma$ , vs.  $\text{Log } C$  (mM) plot of TPADBS in temperature range 293 – 313 K at 10 K intervals in the TPABr concentration 0.003 M.



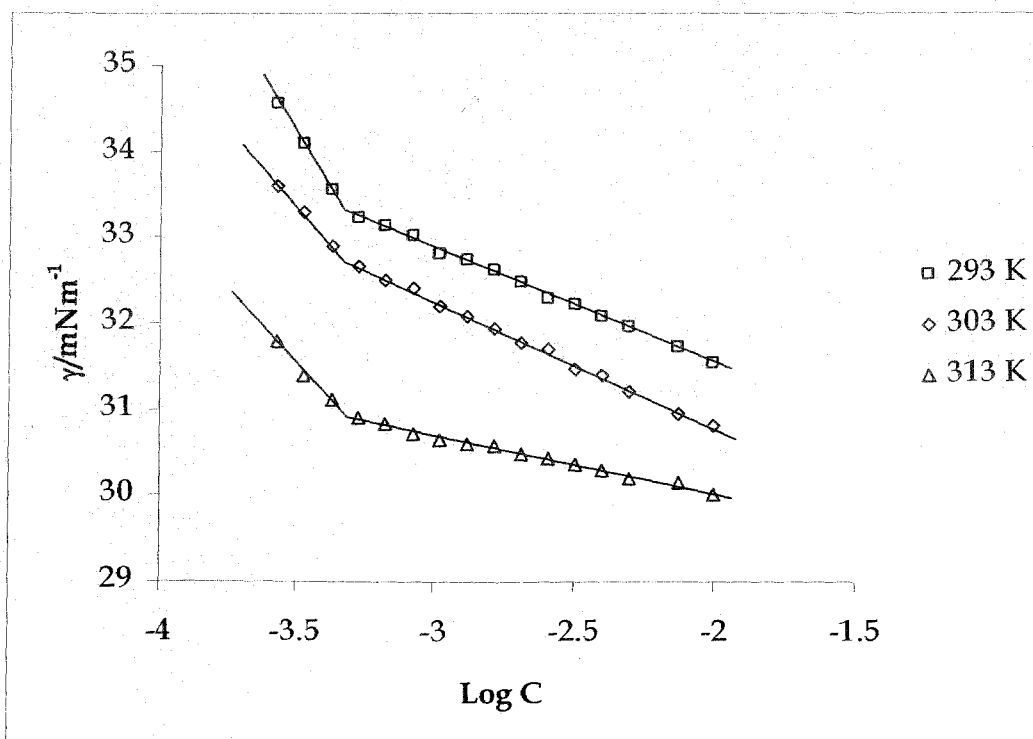
**Figure 4.41:** Surface Tension,  $\gamma$ , vs.  $\text{Log } C$  (mM) plot of TPADBS in temperature range 293 – 313 K at 10 K intervals in the TPABr concentration 0.004 M.



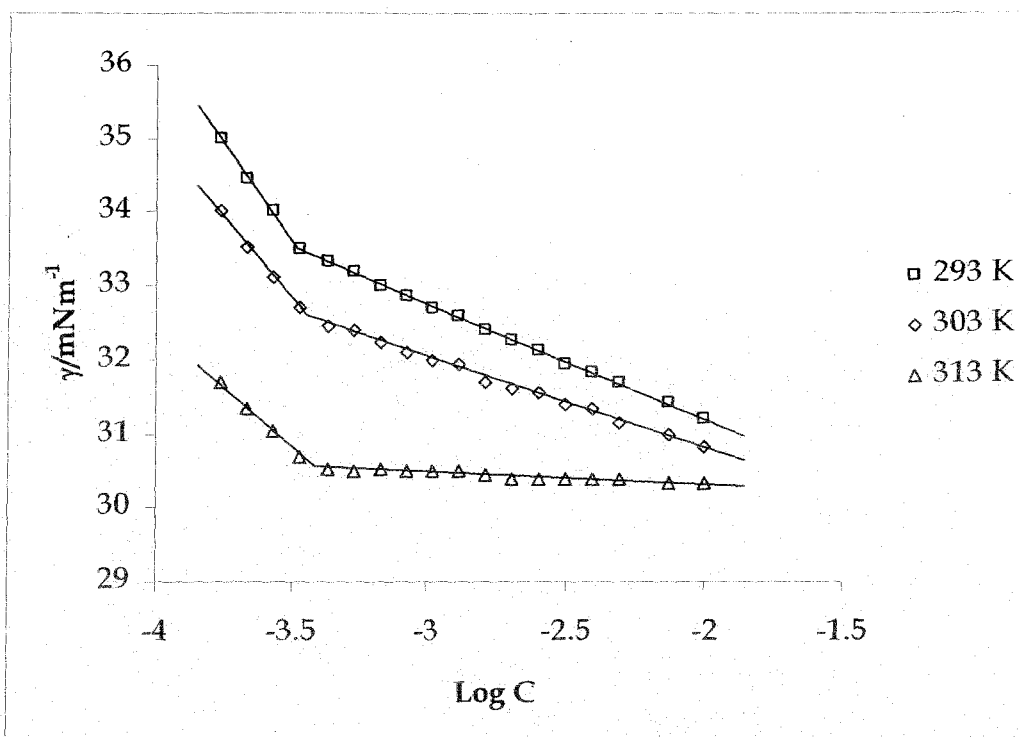
**Figure 4.42:** Surface Tension,  $\gamma$ , vs.  $\text{Log } C$  (mM) plot of TPADBS in temperature range 293 – 313 K at 10 K intervals in the TPABr concentration 0.005 M.



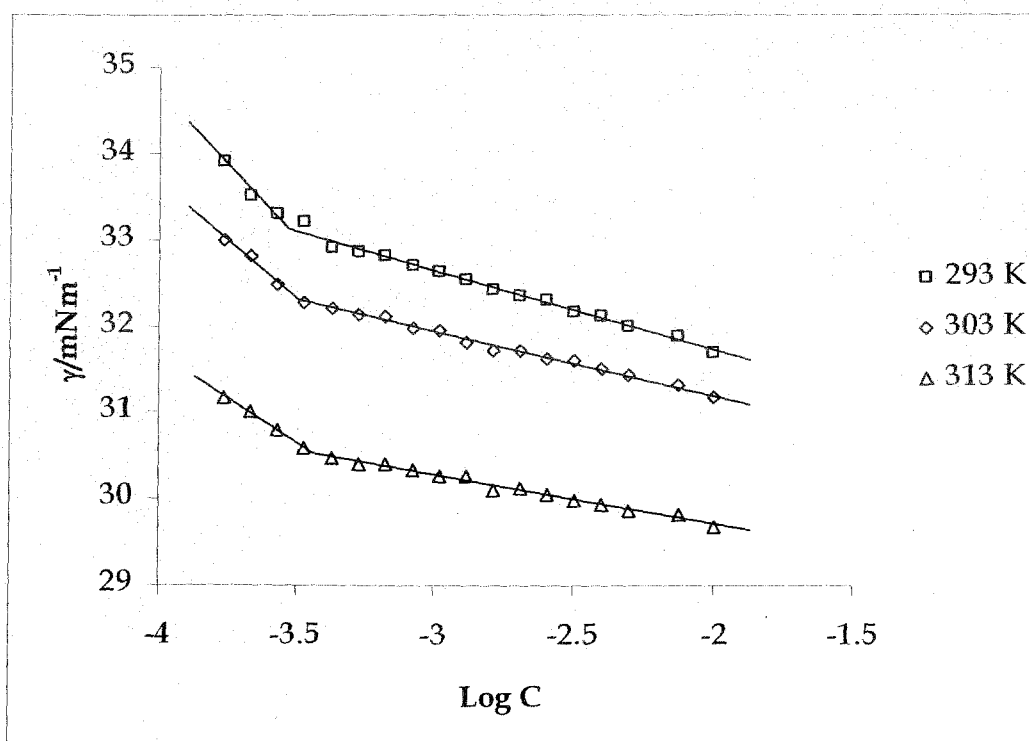
**Figure 4.43:** Surface Tension,  $\gamma$ , vs.  $\text{Log } C$  (mM) plot of TBADBS in temperature range 293 – 313 K at 10 K intervals in the TBABr concentration 0.0005 M.



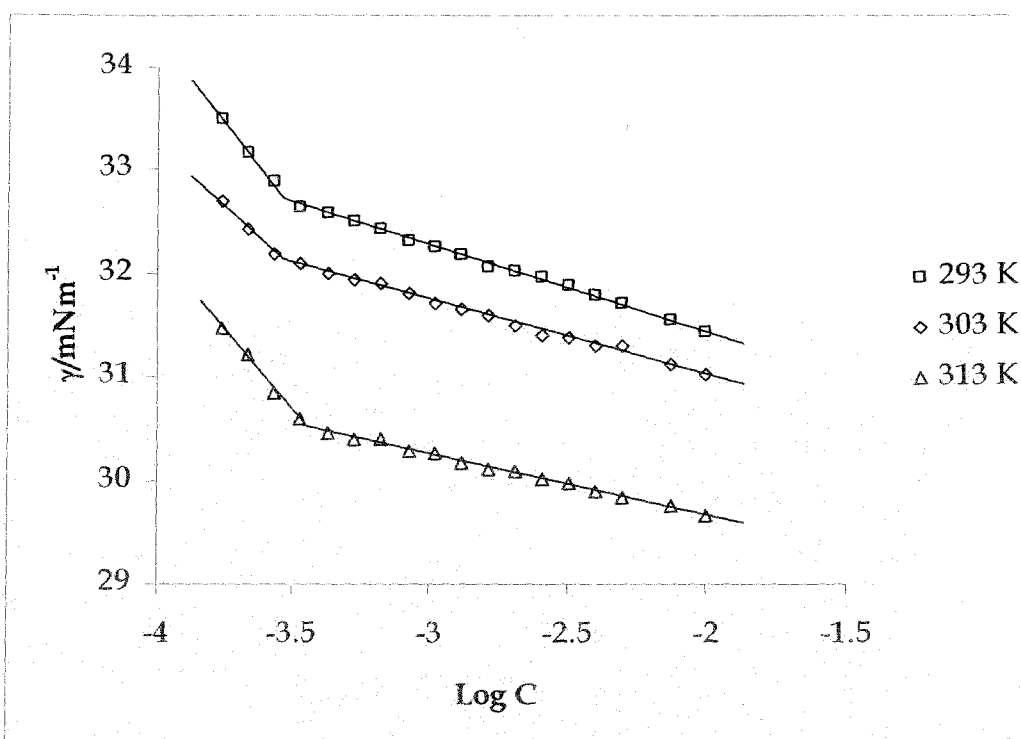
**Figure 4.44:** Surface Tension,  $\gamma$ , vs.  $\text{Log } C$  (mM) plot of TBADBS in temperature range 293 – 313 K at 10 K intervals in the TBABr concentration 0.001 M.



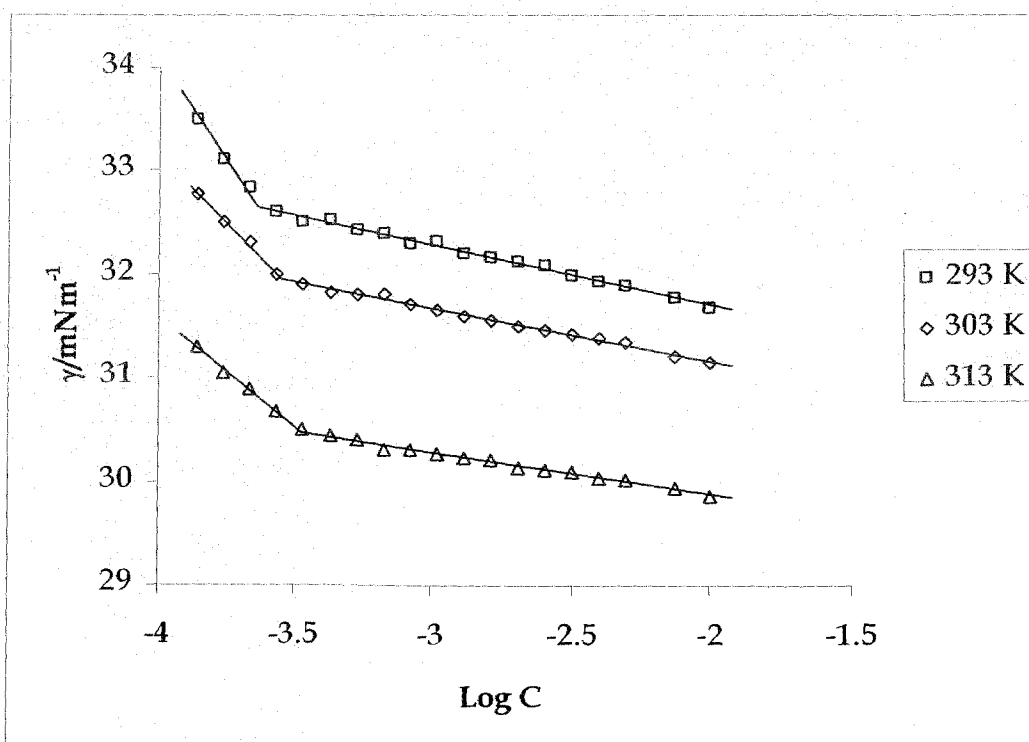
**Figure 4.45:** Surface Tension,  $\gamma$ , vs.  $\text{Log } C$  (mM) plot of TBADBS in temperature range 293 – 313 K at 10 K intervals in the TBABr concentration 0.002 M.



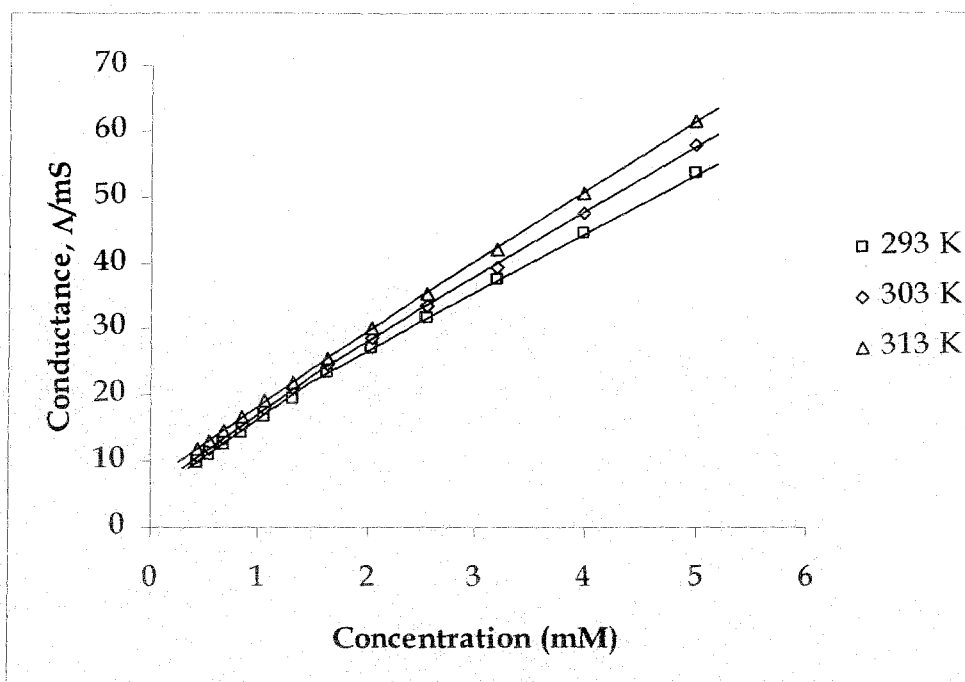
**Figure 4.46:** Surface Tension,  $\gamma$ , vs.  $\text{Log } C$  (mM) plot of TBADBS in temperature range 293 – 313 K at 10 K intervals in the TBABr concentration 0.003 M.



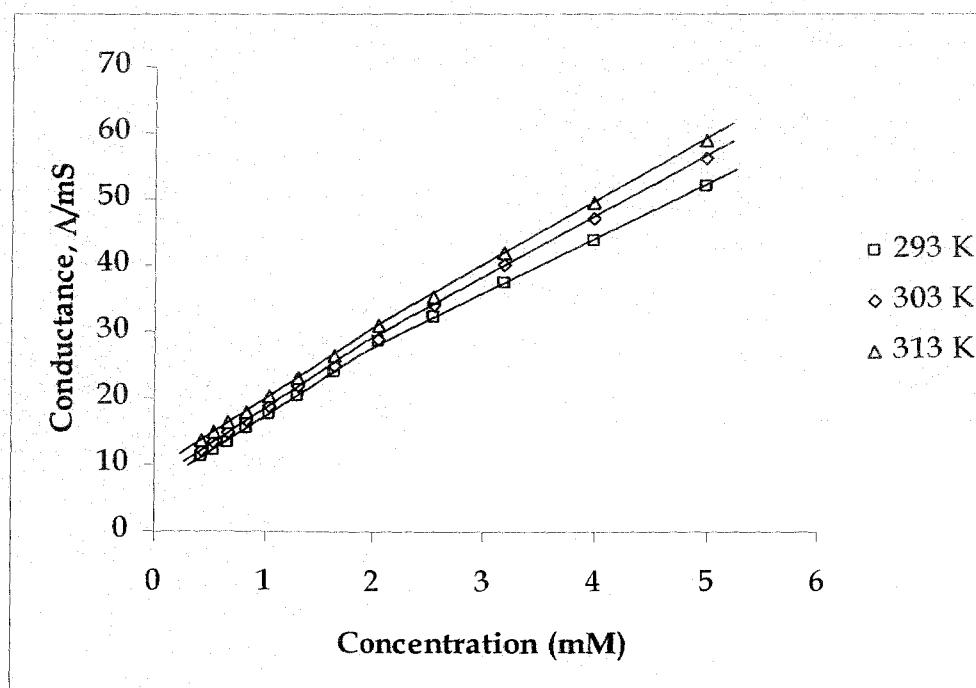
**Figure 4.47:** Surface Tension,  $\gamma$ , vs.  $\text{Log } C$  (mM) plot of TBADBS in temperature range 293 – 313 K at 10 K intervals in the TBABr concentration 0.004 M.



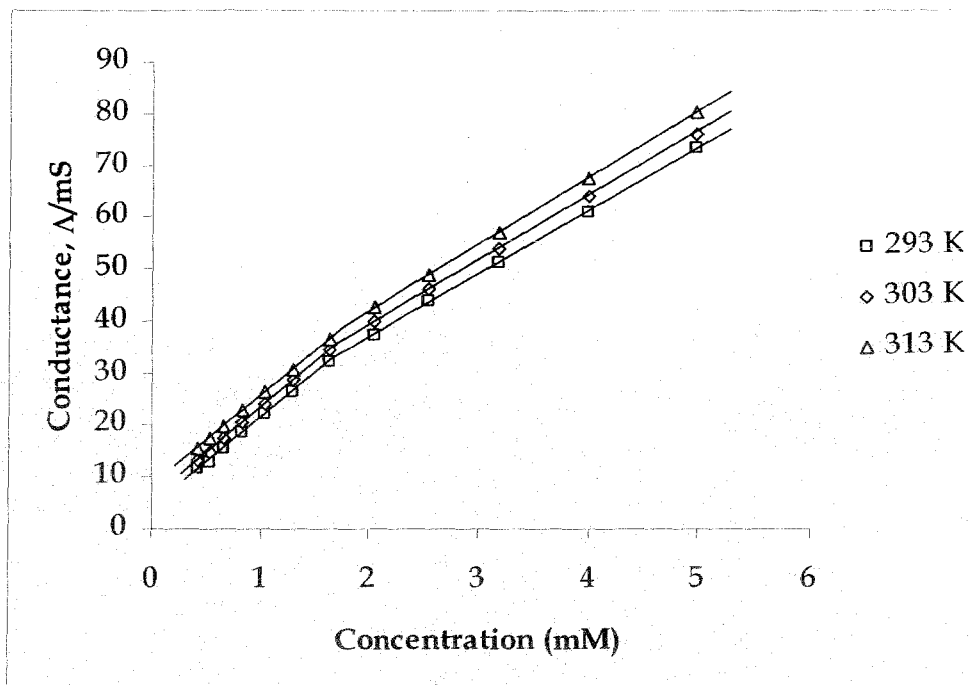
**Figure 4.48:** Surface Tension,  $\gamma$ , vs.  $\text{Log } C$  (mM) plot of TBADBS in temperature range 293 – 313 K at 10 K intervals in the TBABr concentration 0.005 M.



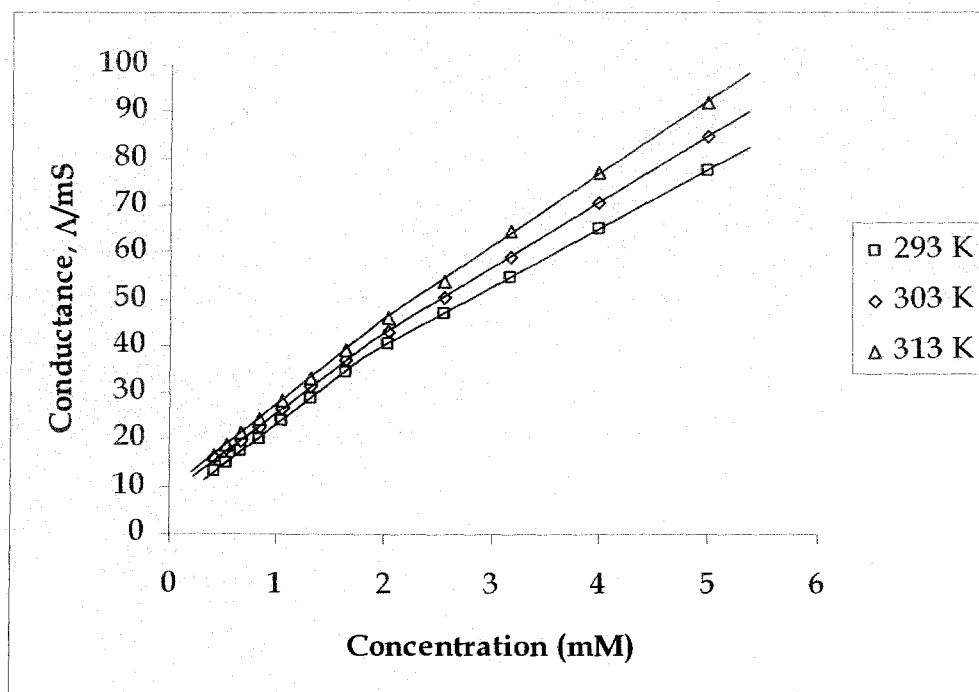
**Figure 4.49:** Conductance,  $\Lambda$ , of Sodium dodecyl benzene sulfonate (SDBS) in aqueous NaBr solution  $[\text{NaBr}] = 0.0005(\text{M})$  as a function of the surfactant concentration at different temperatures.



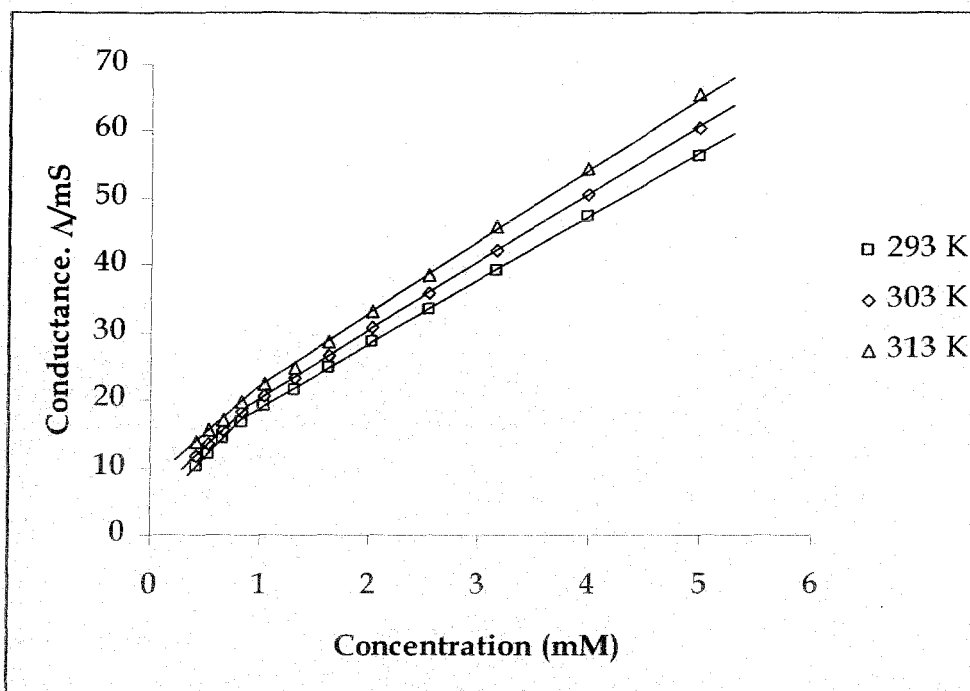
**Figure 4.50:** Conductance,  $\Lambda$ , of Lithium dodecyl benzene sulfonate (LDBS) in aqueous LiBr solution  $[\text{LiBr}] = 0.0005(\text{M})$  as a function of the surfactant concentration at different temperatures.



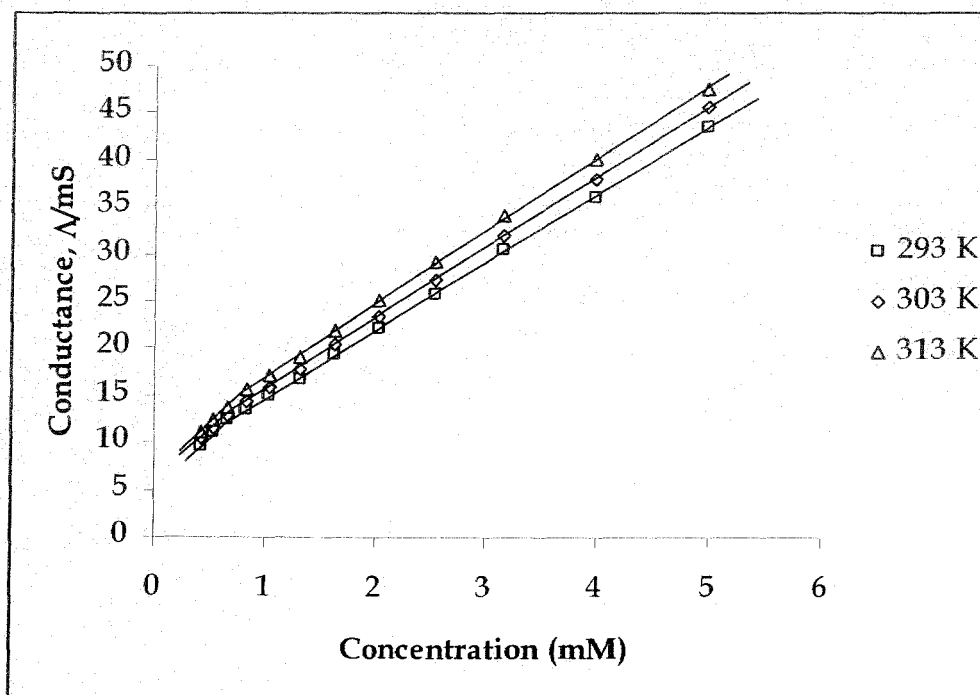
**Figure 4.51:** Conductance,  $\Lambda$ , of Potassium dodecyl benzene sulfonate (PDBS) in aqueous KBr solution  $[\text{KBr}] = 0.0005(\text{M})$  as a function of the surfactant concentration at different temperatures.



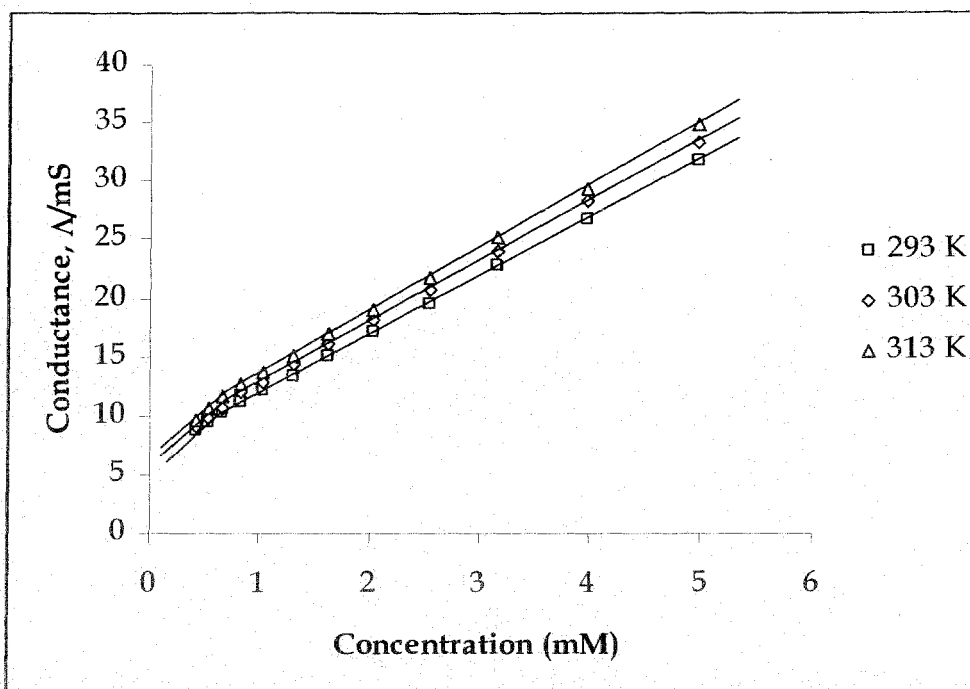
**Figure 4.52:** Conductance,  $\Lambda$ , of Ammonium dodecyl benzene sulfonate (ADBS) in aqueous  $\text{NH}_4\text{Br}$  solution  $[\text{NH}_4\text{Br}] = 0.0005(\text{M})$  as a function of the surfactant concentration at different temperatures.



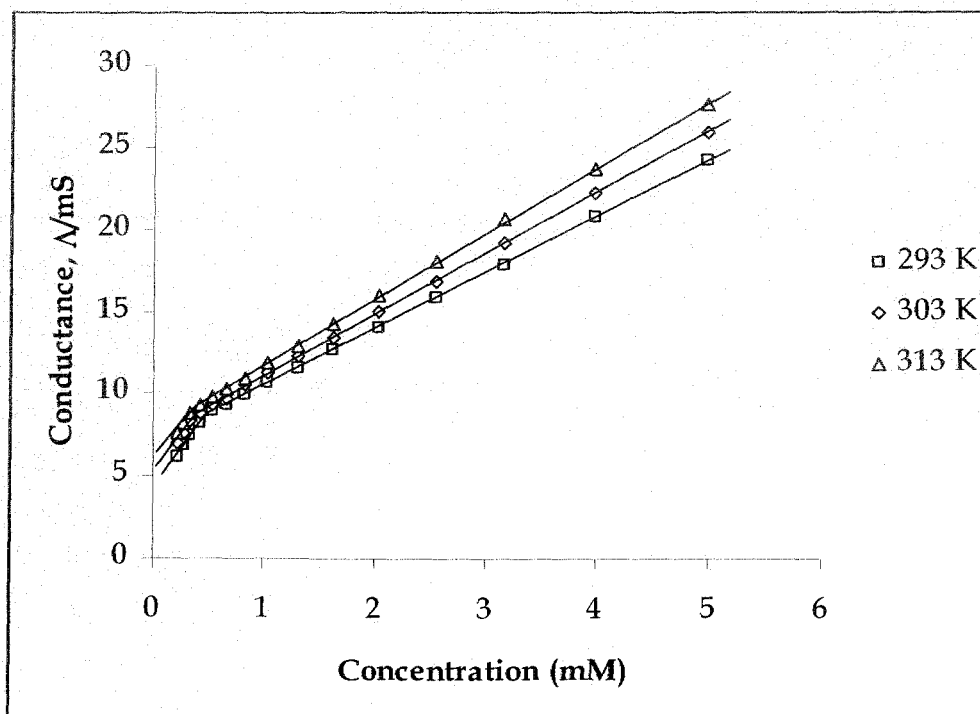
**Figure 4.53:** Conductance,  $\Lambda$ , of Tetramethylammonium dodecyl benzene sulfonate (TMADBS) in aqueous KBr solution  $[\text{TMABr}] = 0.0005(\text{M})$  as a function of the surfactant concentration at different temperatures.



**Figure 4.54:** Conductance,  $\Lambda$ , of Tetraethylammonium dodecyl benzene sulfonate (TEADBS) in aqueous TEABr solution  $[\text{TEABr}] = 0.0005(\text{M})$  as a function of the surfactant concentration at different temperatures.



**Figure 4.55:** Conductance,  $\Lambda$ , of Tetrapropylammonium dodecyl benzene sulfonate (TPADBS) in aqueous TPABr solution  $[\text{TPABr}] = 0.0005(\text{M})$  as a function of the surfactant concentration at different temperatures.



**Figure 4.56:** Conductance,  $\Lambda$ , of Tetrabutylammonium dodecyl benzene sulfonate (TBADBS) in aqueous TBABr solution  $[\text{TBABr}] = 0.0005(\text{M})$  as a function of the surfactant concentration at different temperatures.

$\text{TMA}^+$  ions with smallest ionic size are the most hydrated in aqueous solution compared to that of the others in the group, viz.,  $\text{TEA}^+$ ,  $\text{TPA}^+$  and  $\text{TBA}^+$ . Therefore, the

hydration shell of  $\text{TMA}^+$  ions limits the distance of closest approach to the micellar heads of DBS, thereby causing a small reduction in cmc as compared to  $\text{TEA}^+$ ,  $\text{TPA}^+$  or  $\text{TBA}^+$  ions. In other words it appears that this salt behaves as the common non-hydrophobic electrolytes, interacting only with the TMADBS micelle surface and screening the ionic charge around that location. The higher homologues of the series,  $\text{TPA}^+$  and  $\text{TBA}^+$ , have long hydrocarbon chains and some of these chains are supposed to penetrate in the micellar core due to hydrophobic interaction. These ions are weakly hydrated in aqueous solution because the positive charge is wrapped in the paraffin shell and are thus more hydrophobic. Therefore, the ions, in addition to the electrostatic interaction, can interact hydrophobically as well with the anionic head groups of the micelle. Hence, at a given temperature, the formation of micelles of DBS in these electrolyte media favours a cmc lowering in the order  $\text{TMAB} > \text{TEAB} > \text{TPAB} > \text{TBAB}$ . Interestingly this is also the order of their effectiveness in water structure breaking [3].

Table 4.1.1.

Micellization and surface parameters of SDBS and LDBS with symmetrical bromide salts at various temperatures (T/K): cmc, maximum surface excess concentration, minimum areas per molecule and ionization degree.

Surfactant	Salt	Temp./K	Conc. of Salt/M	Cmc <sup>a</sup> / mol dm <sup>-3</sup> ×10 <sup>3</sup>	Γ <sub>max</sub> / mol cm <sup>-2</sup> ×10 <sup>5</sup>	A <sub>min</sub> ×10 <sup>19</sup>	β
Sodium Dodecyl Benzene Sulfonate (SDBS)	NaBr	293	0.0005	1.45	2.92	0.57	0.288
			0.001	1.41	3.12	0.53	
			0.002	1.26	3.73	0.44	
			0.003	1.19	3.09	0.54	
			0.004	1.13	3.16	0.53	
		303	0.0005	1.55	3.14	0.53	0.310
			0.001	1.51	3.18	0.52	
			0.002	1.40	3.21	0.52	
			0.003	1.30	3.29	0.50	
			0.004	1.23	3.40	0.49	
		313	0.0005	1.63	3.40	0.49	0.352
			0.001	1.53	3.43	0.48	
			0.002	1.47	3.50	0.47	
			0.003	1.36	3.52	0.47	
			0.004	1.29	3.63	0.46	
Lithium dodecyl benzene sulfonate (LDBS)	LiBr	293	0.0005	1.91	2.66	0.63	0.145
			0.001	1.89	2.78	0.60	
			0.002	1.82	2.91	0.57	
			0.003	1.76	3.14	0.53	
			0.004	1.71	3.18	0.52	
		303	0.0005	1.94	3.30	0.50	0.115
			0.001	1.91	3.34	0.50	
			0.002	1.86	3.41	0.49	
			0.003	1.82	3.51	0.47	
			0.004	1.77	3.56	0.47	
		313	0.0005	1.98	3.51	0.47	0.113
			0.001	1.96	3.56	0.47	
			0.002	1.91	3.65	0.45	
			0.003	1.86	3.60	0.46	
			0.004	1.82	3.66	0.45	
		0.005	1.78	3.69	0.45		

<sup>a</sup> The cmc values determined by surface tension method.

Table 4.1.2.  
 Micellization and surface parameters of PDBS and ADBS with symmetrical  
 bromide salts at various temperatures (T/K): cmc, maximum surface excess  
 concentration, minimum areas per molecule and ionization degree.

Surfactant	Salt	Temp./K	Conc. of Salt/ M	Cmc/ mol dm <sup>-3</sup> ×10 <sup>3</sup>	Γ <sub>max</sub> / mol cm <sup>-2</sup> ×10 <sup>6</sup>	A <sub>min</sub> ×10 <sup>19</sup>	β
Potassium dodecyl benzene sulfonate (PDBS)	KBr	293	0.0005	1.70	2.68	0.62	0.420
			0.001	1.66	2.82	0.59	
			0.002	1.50	2.88	0.58	
			0.003	1.34	2.94	0.56	
			0.004	1.24	2.98	0.56	
			0.005	1.17	3.03	0.55	
		303	0.0005	1.74	2.98	0.56	0.397
			0.001	1.69	3.03	0.55	
			0.002	1.54	3.10	0.54	
			0.003	1.40	3.15	0.53	
			0.004	1.30	3.24	0.51	
			0.005	1.22	3.33	0.50	
		313	0.0005	1.79	3.32	0.50	0.368
			0.001	1.73	3.39	0.49	
			0.002	1.58	3.47	0.48	
			0.003	1.47	3.55	0.47	
			0.004	1.43	3.62	0.46	
			0.005	1.27	3.67	0.45	
Ammonium dodecyl benzene sulfonate (ADBS)	NH <sub>4</sub> Br	293	0.0005	1.82	2.73	0.61	0.306
			0.001	1.66	2.81	0.59	
			0.002	1.59	2.90	0.57	
			0.003	1.49	2.95	0.56	
			0.004	1.40	2.99	0.55	
			0.005	1.33	3.04	0.55	
		303	0.0005	1.85	2.97	0.56	0.262
			0.001	1.77	3.05	0.54	
			0.002	1.63	3.09	0.54	
			0.003	1.54	3.15	0.53	
			0.004	1.47	3.19	0.52	
			0.005	1.42	3.23	0.51	
		313	0.0005	1.89	3.18	0.52	0.254
			0.001	1.85	3.23	0.51	
			0.002	1.70	3.28	0.51	
			0.003	1.60	3.35	0.50	
			0.004	1.52	3.42	0.49	
			0.005	1.48	3.49	0.48	

<sup>a</sup> The cmc values determined by surface tension method.

Table 4.1.3.  
Micellization and surface parameters of TMADBS and TEADBS with symmetrical bromide salts at various temperatures (T/K): cmc, maximum surface excess concentration, minimum areas per molecule and ionization degree.

Surfactant	Salt	Temp./K	Conc. of Salt/ M	Cmc <sup>a</sup> / mol dm <sup>-3</sup> × 10 <sup>3</sup>	Γ <sub>max</sub> / mol cm <sup>-2</sup> × 10 <sup>6</sup>	A <sub>min</sub> × 10 <sup>19</sup>	β
Tetra methyl ammonium dodecyl benzene sulfonate (TMADBS)	(CH <sub>3</sub> ) <sub>4</sub> NBr	293	0.0005	0.93	2.66	0.62	0.326
			0.001	0.87	2.72	0.61	
			0.002	0.76	2.76	0.60	
			0.003	0.69	2.80	0.59	
			0.004	0.64	2.85	0.58	
		303	0.0005	0.95	2.90	0.57	0.302
			0.001	0.89	3.01	0.55	
			0.002	0.79	3.22	0.52	
			0.003	0.72	3.35	0.50	
			0.004	0.67	3.40	0.49	
		313	0.0005	0.98	2.83	0.59	0.306
			0.001	0.93	3.02	0.55	
			0.002	0.84	3.15	0.53	
			0.003	0.76	3.50	0.47	
			0.004	0.71	3.44	0.48	
Tetra ethyl ammonium dodecyl benzene sulfonate (TEADBS)	(C <sub>2</sub> H <sub>5</sub> ) <sub>4</sub> NBr	293	0.0005	0.71	2.67	0.62	0.163
			0.001	0.68	2.71	0.61	
			0.002	0.64	2.75	0.60	
			0.003	0.60	2.83	0.59	
			0.004	0.58	2.86	0.58	
		303	0.0005	0.75	2.91	0.57	0.169
			0.001	0.72	3.02	0.55	
			0.002	0.67	3.25	0.51	
			0.003	0.63	3.36	0.49	
			0.004	0.61	3.42	0.49	
		313	0.0005	0.79	2.86	0.58	0.204
			0.001	0.76	3.03	0.55	
			0.002	0.74	3.17	0.52	
			0.003	0.66	3.45	0.48	
			0.004	0.67	3.53	0.47	
			0.005	0.60	3.59	0.46	

<sup>a</sup> The cmc values determined by surface tension method.

Table 4.1.4.  
Micellization and surface parameters of TPADBS and TBADBS with symmetrical bromide salts at various temperatures (T/K): cmc, maximum surface excess concentration, minimum areas per molecule and ionization degree.

Surfactant	Salt	Temp./K	Conc. of Salt/ M	cmc/ mol dm <sup>-3</sup> × 10 <sup>3</sup>	Γ <sub>max</sub> / mol cm <sup>-2</sup> × 10 <sup>6</sup>	A <sub>min</sub> × 10 <sup>19</sup>	β
Tetrapropyl ammonium dodecyl sulfonate (TPADBS)	(C <sub>3</sub> H <sub>7</sub> ) <sub>4</sub> NBr	293	0.0005	0.63	2.69	0.62	0.167
			0.001	0.60	2.74	0.61	
			0.002	0.56	2.77	0.60	
			0.003	0.52	2.83	0.59	
			0.004	0.50	2.87	0.58	
			0.005	0.49	2.96	0.56	
	303	0.0005	0.65	2.92	0.57	0.147	
		0.001	0.62	3.07	0.54		
		0.002	0.58	3.20	0.52		
		0.003	0.55	3.37	0.49		
		0.004	0.53	3.45	0.48		
		0.005	0.52	3.49	0.48		
	313	0.0005	0.68	2.87	0.58	0.119	
		0.001	0.66	3.06	0.54		
		0.002	0.62	3.20	0.52		
		0.003	0.60	3.46	0.48		
		0.004	0.58	3.54	0.47		
		0.005	0.57	3.61	0.46		
Tetrabutyl ammonium dodecyl sulfonate (TBADBS)	(C <sub>4</sub> H <sub>9</sub> ) <sub>4</sub> NBr	293	0.0005	0.37	2.70	0.61	0.280
			0.001	0.36	2.75	0.60	
			0.002	0.33	2.79	0.60	
			0.003	0.30	2.84	0.58	
			0.004	0.27	2.89	0.57	
			0.005	0.24	2.97	0.56	
	303	0.0005	0.35	3.00	0.55	0.258	
		0.001	0.39	3.09	0.54		
		0.002	0.36	3.21	0.52		
		0.003	0.33	3.38	0.49		
		0.004	0.30	3.52	0.47		
		0.005	0.27	3.70	0.45		
	313	0.0005	0.39	2.96	0.56	0.142	
		0.001	0.39	3.07	0.54		
		0.002	0.38	3.21	0.52		
		0.003	0.36	3.55	0.47		
		0.004	0.34	3.60	0.46		
		0.005	0.32	3.65	0.46		

<sup>a</sup> The cmc values determined by surface tension method.

#### 4.1.3.2. Degree of counter ion binding ( $\beta$ )

In aqueous solution, the presence of electrolyte causes a change in the cmc, the effect being more pronounced for anionic and cationic than for zwitterionic surfactants and more pronounced for zwitterionic than for nonionics [3]. Experimental data indicate that for the first two classes of surfactants, the effect of the concentration of electrolyte, according to the mass action model, is given by Corrin-Harkins equation [43],

$$\text{Log}(cmc) = k - \beta \log C \quad (4.1)$$

where  $k$  is a constant,  $\beta$  is the counterion binding constant and  $C$  stands for the total counterion concentration. The decrease in the cmc values is mainly due to the decrease in the thickness of the ionic atmosphere surrounding the ionic head groups in the presence of the additional electrolyte and the consequent decrease of electrostatic repulsion between the headgroups. The Corrin-Harkins plot gives an overall value for  $\beta$  in a chosen range of electrolyte concentration. The aggregation number is known to vary with electrolyte concentration;  $\beta$  is expected to vary with cmc resulting in the nonlinearity of the above plot. However, in the study of the micellization of different dodecylbenzene sulfonate with symmetrical cations, it is observed that the plot of  $\log cmc$  vs.  $\log C$  is almost linear which envisages that both the aggregation number and the counterion binding to the DBS micelle vary in such a way that  $\beta$  remains constant. Such a rationale has also been put forward by Chatterjee et. al. for the micellization of three typical ionic surfactants, Sodium dodecyl sulphate (SDS), Cetylpyridinium chloride (CPC) and Aerosol OT (AOT) in NaCl environment [19]. Similar results were also reported by Bales et. al. for the micellization of SDS and quaternary ammonium (chloride and bromide) surfactants [44,45]. The parallel slopes of the lines corresponding to different salt concentrations also indicate that the nature of the micelles is similar within the concentration range studied. A continuous increase in the  $\beta$  values with the increase in the size of the alkyl chain length of the TAA<sup>+</sup> ions is observed from TEA<sup>+</sup> to TBA<sup>+</sup>. The largest ion, TBA<sup>+</sup>, is the most strongly bound to DBS micelle with  $\beta$  value of 0.280 at 293 K (Table 4.1.1 - 4.1.4). As discussed earlier, a different order is observed for the TMA<sup>+</sup> ion which may be due to the smallest size among all the TAA<sup>+</sup> ions. Therefore, the hydration shell of TMA<sup>+</sup> ions limits the

distance of closest approach to the micellar heads of DBS, thereby causing a small increase in  $\beta$  values as compared to  $\text{TEA}^+$ ,  $\text{TPA}^+$  or  $\text{TBA}^+$  ions. A high degree of counterion binding reduces the repulsive forces between the surfactant head groups of the ionic micelles to a great extent. As has been already mentioned, for the higher homologues of tetraalkyl ammonium ions, the increasing hydrophobic interactions between the alkyl parts of the electrolytes and the DBS micellar core results in greater charge screening of the head groups and this leads to lower cmc as well as higher  $\beta$  values. The increase in the  $\beta$  values on moving from  $\text{TEA}^+$  to  $\text{TBA}^+$  is due mainly to the increased hydrophobic interaction between the alkyl parts of both the surfactant and the added electrolyte. For inorganic ions including ammonium ions, similar result is observed due to the increase in size of the cations. The cation with largest size show highest  $\beta$  values ensures most strongly bound to DBS moiety. Here, the order of  $\beta$  values is  $\text{K}^+ > \text{Na}^+ > \text{NH}_4^+ > \text{Li}^+$ . The hydration of the inorganic ions also has a definite role in determine the counter ion binding constant values. The ions with higher degree of hydration, lesser will be the interaction with the micelle. This explains the anomalies between  $\text{Li}^+$  and  $\text{NH}_4^+$  ions in respect of the above.  $\Gamma_{\text{max}}$  is a useful measure of the effectiveness of adsorption of the surfactant at air-solution interface, since it is the maximum value that adsorption can attain. It is well known that the air-solution interface of a surfactant solution is well populated by the adsorbed molecules. The general trend of  $\Gamma_{\text{max}}$  with increase of temperature is a slight decrease in its value for both nonionic and anionic surfactants but there is some other cases are also reported where opposite trend is observed [46-49]. In the present case, slight increase in the values of  $\Gamma_{\text{max}}$  is observed which may be due to the effectiveness of adsorption. For dodecyl benzene moiety with varying counterions and in presence of symmetrical salts, a slight increase is observed which may be due to the lower hydration effect of the dodecyl benzene sulfonate part of surfactants at higher temperature and hence increasing tendency to move to the air-liquid interface. The benzene ring in the surfactants may also be partially responsible for this result causing steric inhibition during adsorption as has already been mentioned previously. The area per molecule at the air / water interface gives the information on the packing and orientation of the adsorbed surfactant molecules when compared with the dimensions of the molecule obtained from the molecular model data. The minimum area per molecule ( $A_{\text{min}}$ ) is obtained following the same procedure as described in chapter III. With increase in temperature, the  $A_{\text{min}}$  value shows the inverse trend as that of  $\Gamma_{\text{max}}$ .

### 4.1.3.3. Thermodynamics of micellization in presence of salts

#### Theory

General trend of the plot of cmc against temperature has the parabolic shape typical for ionic surfactants. The cmc decreases, reaches a shallow minimum (cmc\*) and then increases as the temperature is raised. But other trend of cmc is also observed for surfactant systems like sodium dodecyl benzene sulfonate where the cmc increases with increase in temperature, as also reported in the literature [50]. For ionic surfactants, the cmc is related to the standard Gibbs free energy change,  $\Delta G_{mic}^0$ , by the expression

$$\Delta G_{mic}^0 = (1 + \beta)RT \ln X_{cmc} \quad (4.2)$$

where  $X_{cmc}$  is the mole fraction of the surfactant in the liquid phase at the cmc and  $\beta$  is the fraction of the counterions bound to the micelles. The standard state is a hypothetical system with a unit mole fraction of the surfactant at cmc. From the knowledge of the temperature dependence of cmc, the enthalpy of micellization,  $\Delta H_{mic}^0$ , can be evaluated from the Gibbs-Helmholtz relation,

$$\Delta H_{mic}^0 = -(1 + \beta)RT^2 \left( \frac{\partial \ln X_{cmc}}{\partial T} \right)_p \quad (4.3)$$

Equation 4.3 assumes that  $\beta$  does not vary much with temperature. However,  $\beta$  is not strictly temperature independent and the more appropriate form of equation 4.3 should be,

$$\frac{-\Delta H_{mic}^0}{T^2} = (1 + \beta)R \left( \frac{\partial \ln X_{cmc}}{\partial T} \right)_p + R \ln X_{cmc} \left[ \frac{\partial(1+\beta)}{\partial T} \right] \quad (4.4)$$

Because the variation of  $\beta$  with temperature is not well defined and is devoid of any general trend, the quantity  $\left[ \frac{\partial(1+\beta)}{\partial T} \right]$  is difficult to determine experimentally [54]. Therefore, at least to gain qualitative information regarding the thermodynamics of the present system, equation 4.3 has been applied at the appropriate  $\beta$ . Moreover,

equation 4.3 has been widely used as an indirect method for the determination of  $\Delta H_{mic}^0$  as the values so calculated agree well with those obtained from the direct calorimetric measurement [51,52]. The term  $\left(\frac{\partial \ln X_{cmc}}{\partial T}\right)$  is calculated by fitting a second-order polynomial to plots of  $\partial \ln X_{cmc}$  vs temperature and taking the corresponding temperature derivative. Thus,

$$\frac{d \ln X_{cmc}}{dT} = b + 2aT \quad (4.5)$$

The entropies of micelle formation,  $\Delta S_{mic}^0$ , are determined from the equation

$$\Delta S_{mic}^0 = \frac{\Delta H_{mic}^0 - \Delta G_{mic}^0}{T} \quad (4.6)$$

Table 4.5  
Thermodynamic parameters of micellization for DBS with different counterions in presence of symmetrical bromide salts at various temperatures: cmc, Standard Gibb's free energy, Enthalpy and Entropy.

Surfactant	Salt	Conc/ M	T/K	cmc <sup>b</sup> / mol dm <sup>-3</sup> ×10 <sup>3</sup>	α	-ΔG <sub>m</sub> <sup>0</sup> /(kJm ol <sup>-1</sup> )	-ΔH <sub>m</sub> <sup>0</sup> /(kJm ol <sup>-1</sup> )	ΔS <sub>m</sub> <sup>0</sup> /(JK <sup>-1</sup> mol <sup>-1</sup> )
Sodium dodecyl benzene sulfonate	NaBr	0.0005	293	1.53	0.7922	31.1	22.4	29.67
			303	1.60	0.8378	30.7	23.7	23.06
			313	1.64	0.8795	30.4	25.1	16.94
Lithium dodecyl benzene sulfonate	LiBr	0.0005	293	1.89	0.8442	28.9	20.1	30.14
			303	1.94	0.9077	28.2	20.8	24.48
			313	1.97	0.7945	32.1	25.1	22.42
Potassium dodecyl benzene sulfonate	KBr	0.0005	293	1.69	0.6913	33.1	29.0	14.16
			303	1.70	0.9233	28.1	26.2	6.50
			313	1.76	0.7770	32.9	32.5	1.31
Ammonium dodecyl benzene sulfonate	NH <sub>4</sub> Br	0.0005	293	1.64	0.8420	29.1	18.8	35.18
			303	1.67	0.8571	29.7	20.4	30.67
			313	1.62	0.8572	30.6	22.3	26.46
Tetra methyl ammonium dodecyl benzene sulfonate	(CH <sub>3</sub> ) <sub>4</sub> NBr	0.0005	293	0.91	0.8612	30.5	21.0	32.46
			303	0.94	0.8832	30.9	22.7	26.99
			313	0.98	0.9047	31.2	24.5	21.48
Tetra ethyl ammonium dodecyl benzene sulfonate	(C <sub>2</sub> H <sub>5</sub> ) <sub>4</sub> NBr	0.0005	293	0.73	0.8075	32.7	13.0	67.52
			303	0.74	0.8027	33.8	14.3	64.52
			313	0.79	0.7973	34.9	15.7	61.48
Tetra propyl ammonium dodecyl benzene sulfonate	(C <sub>3</sub> H <sub>7</sub> ) <sub>4</sub> NBr	0.0005	293	0.60	0.8260	32.6	9.0	80.39
			303	0.65	0.8183	33.8	9.9	78.96
			313	0.69	0.8347	34.3	10.6	75.76
Tetrabutyl ammonium dodecyl benzene sulfonate	(C <sub>3</sub> H <sub>7</sub> ) <sub>4</sub> NBr	0.0005	293	0.29	0.6913	38.0	22.3	56.58
			303	0.27	0.7278	38.4	23.8	48.23
			313	0.31	0.8023	37.7	24.5	40.02

<sup>b</sup> The cmc values determined by conductivity method.

This theory is very much applicable for surfactant with high cmc value where the temperature dependence of cmc shows the parabolic nature. But in the present study, the surfactant with different counterions does not show this type of parabolic nature as a function of temperature. Furthermore, the cmc of the dodecyl benzene sulfonate is very low (for sodium-DBS ~ 3.0 mM) and it further decreases with the addition of electrolyte and So, the determination of cmc in high salt concentration with the help of conductivity is very difficult as because the conductivity due to the

electrolyte may merge that of the surfactant. In this chapter, we are mainly concerned with the surface activity of the surfactant at the air/water interface only in presence of the electrolyte and also presented a general view of the different thermodynamic parameters with the help of mass-action model as described in the previous chapter only due to the fact that these are the systems which are not available in the literature except sodium dodecyl benzene sulfonate. At the time of calculating by the previous model, the concentration of the electrolyte is kept very low, viz., 0.0005 (M) so that the effect of conductivity of electrolyte is very small and we can get the general overview of the parameters of micellization of the surfactant. The values of  $\Delta G_{mic}^0$ ,  $\Delta H_{mic}^0$  and  $\Delta S_{mic}^0$  in the presence of 0.0005 M corresponding bromide salts have been presented in table 4.1.5.

The temperature dependence of micellization of DBS with different counterions in presence of bromide salts (0.0005 M) has been studied to determine the thermodynamic parameters of micellization. The change in cmc of DBS with different counterions in pure aqueous solution as a function of temperature is small. Such weak temperature dependence of cmc in aqueous solution has been observed for all the dodecyl benzene sulfonate surfactant and already mentioned in the previous chapter. Recently it has been shown that the double tailed anionic surfactant, AOT, also display similar characteristics in presence of electrolytes [29]. The dependence of cmc on temperature further weakens in solutions of symmetrical ions suggesting the solubilization of the additives in the hydrocarbon environment of the surfactant micelle.

Addition of bromide salts to the corresponding surfactant show substantial decrease in the critical micellar concentration. The variation of  $\Delta G_{mic}^0$  with temperature is small for all the systems investigated. According to the pseudo-phase model the minimum in the cmc in the  $\ln X_{cmc}$  vs. T plot should correspond to a minimum in the  $(\Delta G_{mic}^0/T)$  curve. However, the absence of such a minima for the present dodecyl benzene sulfonate system may be due to the dominance of the RT term over  $\ln X_{cmc}$  in equation 4.3 [53].

The value of  $\Delta H_{mic}^0$  increases with the increase in temperature in all the case. The enthalpy of micellization shows negative values in all the cases indicating that the formation of micelles is an exothermic process. The higher negative values of enthalpy at higher temperatures probably suggest the importance of London-dispersion interactions as an attractive force contribution for micellization.

The entropy of micellization for different systems are all large and positive except potassium dodecyl benzene sulfonate, indicating that the micellization process is entropy dominated. The large positive values of  $\Delta S_{mic}^0$ , which increases with the increase in the size of the added electrolyte, suggests that the micellization process in these salty solutions are governed primarily by the entropy gain and the driving force for the process is the tendency of the hydrophobic groups of dodecyl benzene sulfonate to transfer from the TAA<sup>+</sup> rich solvent to the interior of the micelle. Studies on the effect of counterions on clouding of charged surfactants are rare in the literature the present study gives a brief introduction in this direction.

#### 4.1.3.4. Thermodynamic properties

A critical examination of the Table 4.1.1 - Table 4.1.4 in dodecyl benzene sulfonate moiety, it is observed that the headgroups (-SO<sub>3</sub><sup>-</sup>) are hydrated due to their polar nature. Water molecules can form stable hydrogen bonds with the head group of the surfactants, and the counterions are distributed close to the air/water interphase. Presence of salt may screen electrostatic repulsion between headgroups and decrease the thickness of the interfacial water layer. The counterions may penetrate into the hydration shell of the surfactant headgroups and restrict the mobility of the water molecules situated in this area. It is known that the inorganic ions and also the ammonium ions interact very strongly with an anionic surfactant. Therefore, it is meaningful to investigate the interaction between an anionic surfactant and inorganic salt and also ammonium salts. It is observed by theoretical measurements of sodiumdodecylbenzene sulfonate that the counter ions are distributed close to the air/water interface, near the oppositely charged sulfonate headgroups on the addition of salts to the surfactant systems. The headgroups are hydrated and localized in the water layer, whereas the tail groups (carbon chain) are excluded from the interface. In dodecylbenzene sulfonate, most of the sulfonate group is hydrated due to its polar nature. Only a small fraction of water molecules penetrate into the hydrocarbon tail part of the surfactants, suggesting that headgroups and benzene ring groups help water molecules penetrate into the monolayer film. In the bulk phase, water is a highly structured liquid due to an extensive network of hydrogen bonds, whereas water molecules at the interface region undergo volume expansion and a decrease of its density. The thickness of the interfacial layer is decreased when salts are added into

surfactant systems. The reason is that the positive ions of the salt can enter into the interfacial region and destroy the hydrated layer. Water molecules in the interfacial layer are displaced into the bulk phase. The volume effect is also important on the addition of salt to surfactant systems. Smaller positive ions may enter easily more into the region of headgroups as compared with larger ones.

## **4.2. Dodecyl Benzene Sulfonate in presence of Ethylene glycol in aqueous medium**

### **4.2.1 Introduction and review of the previous work**

The most interesting aspects of these microheterogeneous entities are their ability to accommodate organic molecules [54-57]. As we know, the London dispersion forces are the main attractive forces in the formation of the micelle and the micelle formation is supposed to be the result of hydrophobic interaction. So, it is understood that the ionic surfactants form micelle by self-association due to the hydrophobic and electrostatic forces. Alcohols have the ability to solubilize hydrophobic molecules very easily due to the increased flexibility of the micellar membrane [58]. Several works on the effect of alcohols on the surfactant micellization have been carried out by different researchers with different types of alcohols. Also, the size and shape of micelle formed by a number of commonly used surfactants and co-surfactants have been investigated earlier [59,60].

The structural changes in presence of different alcohols are very interesting and are performed by many researchers for the surfactant sodium dodecyl sulfate. Førland et al. reported that propanol successively breaks down the micelles while pentanol brings about a structural change towards large worm like aggregates of sodium dodecyl sulfate. Butanol shows a highly complex behaviour on the structure of the micelles and can decrease and increase the size of the aggregates, depending on the added alcohol concentration [61]. Many researchers became interested in mixed alcohol-water systems particularly due to their importance in the preparation of microemulsions [62,63]. Reports of Onori et al. [64-66] showed that the effects due to alcohols on two very different systems and processes, the thermal denaturation of t-RNA (transfer ribonucleic acid) and the micellization of several surfactant molecules were strikingly similar and were closely paralleled in simpler properties of alcohol-water mixtures themselves. These results support the hypothesis that the dominant

mechanism by which an alcohol affects this process is through its effect on structure of water. At higher concentrations some other effects like the alteration in the dielectric constants of the solvent or the partition of the alcohol molecules between bulk and the micellar phase may be more important. The behaviour of sodium dodecyl benzene sulfonate (SDS) and Triton X-100 micelles in the presence of alcohol was investigated by previous workers [67-72] but the works on the behaviour of sodium dodecyl benzene sulfonate with ethylene glycol are rare. Micellization studies with diols having the same number of carbons but different molecular structure have also been carried out [73,74]. Carnero Ruiz [75] reported the thermodynamics of micellization in tetradecyltrimethylammonium bromide in a dihydric alcohol, ethylene glycol-water binary mixtures, and showed that with increasing the percentage of alcohol in the solvent mixture both the cmc and counter ion dissociation constant ( $\alpha$ ) increased to a considerable extent. But in case of other progressively long chain alcohols, (e.g. n-heptanol to n-decanol) opposite observations were reported in recent studies [76]. Similar reports are available for middle and short chain alcohols also [77-79]. It was suggested that for ionic surfactants, the cmc is related by the following equation [80]:

$$\log(\text{cmc}) = Z(1 - \beta) \left[ \log \frac{2000\pi\sigma^2}{\epsilon_r RT} - \log c_i \right] + \left[ \frac{\Delta G(-CH_2-)}{2.303RT} \right] n + B \quad (4.7)$$

where  $Z$  is the charge of the surfactant ion,  $\beta$  is the fraction of counter ions bound by the micelle in the case of ionic surfactants,  $\sigma$  is the surfactants charge density on the micelle,  $\epsilon_r$  is the dielectric constant of the solvent,  $c_i$  is the concentration of counter ions in the polar solution,  $n$  is the carbon number of the surfactant and  $B$  is an arbitrary constant depending upon the system.

Equation 4.7 suggests that it is difficult to predict the effect of temperature on the cmc. But an increase in temperature may also decrease  $\beta$ , so the overall effect for an increase in temperature is to increase the cmc. When the  $\beta$  parameter of the system increases with an increment in carbon number of alcohol, it also indicates that the cmc of surfactant will also decrease.

But when the fraction of long-chain alcohol increases, the extent of counterion binding to the micelle also increases and as a result cmc is lowered. But due to the presence of alcohol the dielectric constant of the solvent decreases considerably, which predicts an easier denaturation of micelles and the cmc of the surfactant should be

increased. In general all the factors mentioned above are reflected in the resulting cmc and related thermodynamic parameters of micellization process in water-alcohol binary mixtures. In this respect ethylene glycol (EG) showed the reverse effect compared to the other alcohols and this may be explained by its higher dielectric constant, small hydrophobic surface and greater capability of hydrogen bond formation. Sjöberg [79] also observed that in strong polar solvents, such as formamide and EG, micelles are found with qualitatively the same features as in water. It was found that the cmc of hexadecyl -trimethylammonium bromide ( $C_{16}TAB$ ) is much higher in formamide (100 mM) than water (1mM) at 333K temperature. Recently, there has been a considerable amount of research dealing with the effects of nonaqueous polar solvents on the micellization process [81,82]. It is a general feature, also exemplified by smaller micelle radii and aggregation numbers, that self-assembly is much less co-operative in alternative polar solvents.

It has been proposed that the ability of a solvent to form hydrogen bonds is a necessary condition for the formation of micelles. However, the ability of water to form unique hydrogen-bonded networks is not a necessary condition for the aggregation process [83]. Ethylene glycol (EG) is of particular interest in that it has many characteristics similar to those of water. The molecule is small and can form hydrogen-bonded networks similar in nature to those of water but considerably different in the details of the structure. Ethylene glycol also possesses a high cohesive energy and a fairly high dielectric constant. Because of the similarities between water and ethylene glycol, the study of the latter is important from the point that it provides a better understanding of the structure of liquids on the micellization process [84]. In this connection the influence of very common short chain alcohols, viz. ethylene glycol on the micellization of DBS with different counterions in aqueous medium are studied in the present investigation within the temperature range of 293-313K. Though it is said that the highly water-soluble alcohols such as ethylene glycol dissolve mainly in the aqueous bulk solution [85-86], there are number of reports [87-88] supporting the influence of these short chain alcohols on micellization. The results of the investigation are relevant to several applied topics in colloids where micelles and microemulsions in alcohol-water mixtures have been used as an elution medium in micellar liquid chromatography [89]. In recent times, some surface active drugs are in use. The understanding of the thermodynamic aspects of the surface active drug is important from both fundamental as well as practical standpoints because the thermodynamic parameters governing the aggregate formation are the key to effective physical processing [90]. To elucidate the effects of ethylene glycol on the micellization process,

it is useful to study the behaviour of the molecule as a cosolvent on model compounds. Most of the investigation in recent times using ethylene glycol as a cosolvent or as a pure solvent were carried out with ionic surfactants [84,91-103]. Micellization of nonionic surfactants in non-aqueous polar solvents, and in particular ethylene glycol, has been less frequently investigated [104-108]. Sometimes, the size is also increased due to mixing of cosolvents which is due to decrease hydration of the polar head groups for the interaction between water and cosolvents resulting in a reduction of the curvature of the aggregate [108].

#### 4.2.2. Materials and Methods

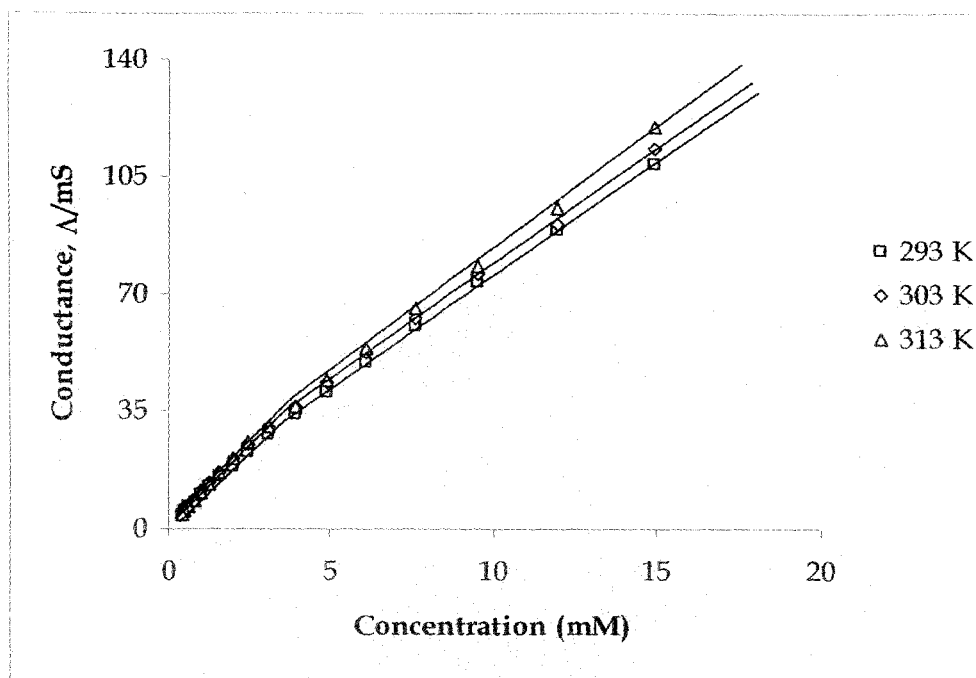
As discussed earlier, to investigate the micellization properties conductivity measurements of the solutions containing different proportion of alcohols and surfactants are performed within the temperature range of 293K to 313K. The temperature was maintained in a thermostated double-glass water jacket by the flow of constant temperature with in  $\pm 0.01$ K. The alcohol (Merck) associated in the experiments are used after necessary distillation as described elsewhere [109]. To check the reproducibility of the results, SDBS with different proportion of the alcohols are performed in spectro-photometrically by an UV-visible Spectrophotometer. Absorption spectra were recorded on a double beam Jasco V-530 uv/vis spectrophotometer (Japan). The spectra were recorded with a quartz cell having 1mm optical path length. The temperature of the whole experiment was maintained at 20<sup>0</sup>C with a thermostatic arrangement coupled with the spectrophotometer.

#### 4.2.3. Results and discussion

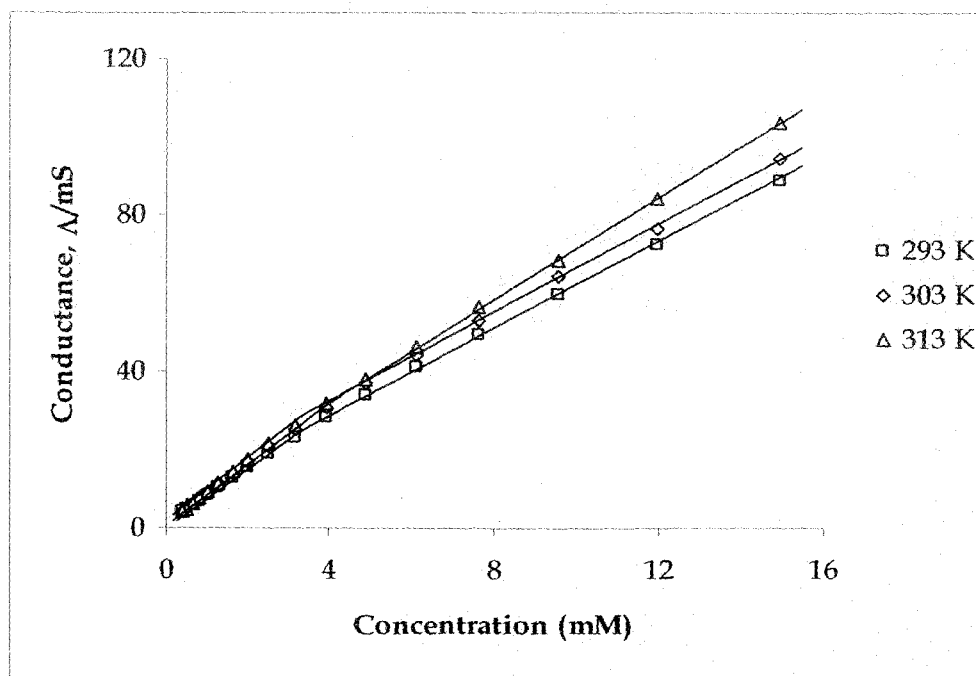
Similar to the previous measurements the cmc values of the DBS with different counterions in the presence of ethylene glycol, a hydrophilic alcohol, were determined by the 'break points' of the conductance vs. concentration plots (figure 4.57 - 4.80). The cmc and the other related thermodynamic parameters of DBS with different counter ions are given in Table 4.2.1 and Table 4.2.2 respectively. All the thermodynamic parameters including cmc are determined by similar procedure as described in the previous section (chapter III). As expected, the cmc values increase considerably upon addition of ethylene glycol. The larger cmc at higher ethylene glycol content is a result of the presence of a structure-breaking solute. Structure breaking solutes in the

aqueous phase may disturb the hydrophobic group causing a decrease in hydrophobic effect. Ethylene glycol in the present study is acting as a cosolvent and a structure-breaking solute, decreases the hydrophobic effect and possibly that is the driving force for micellization. The increase in cmc values with temperature at a given concentration of ethylene glycol is attributed to the disruption of the solvent structure with the increase in temperature. For SDBS-ethylene glycol-water system [10%, 20% and 30% ethylene glycol (w/w)], the cmc was determined conductometrically. At alcohol concentrations lower than 0.1mM, the change in conductivity is less pronounced. As presented out above, to explain the deviations observed in the micellization parameters two factors, viz., lowering of dielectric constant with addition of alcohol and the effective hydrophobic area of the alcohol molecule must be considered.

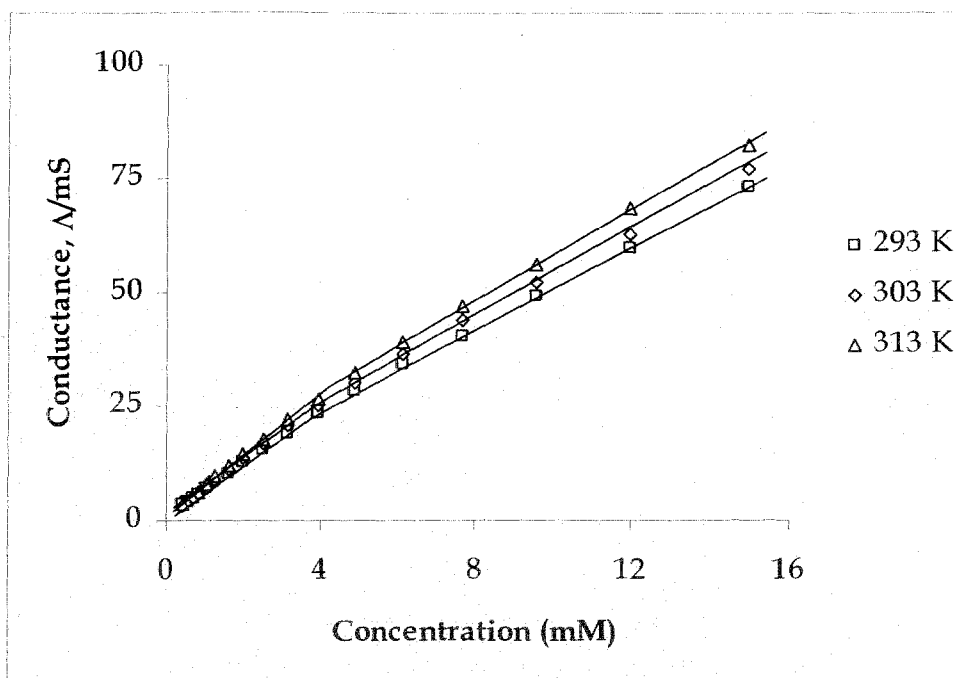
In all the cases the process of micelle formation is energetically favoured and this is supported by effective negative value of  $\Delta G_m^0$ . With increase in temperature, the  $\Delta G_m^0$  value becomes more negative, which is a general trend as found in Table 4.2.1 and Table 4.2.2. This indicates that the micellization process is more favourable with increase in temperatures. With increase in temperature the cmc values increases with the present additives. This indicates that the change in the magnitude of the logarithm of the cmc term is more than compensated by the change in the values of the RT term. The other two thermodynamic parameters viz.  $\Delta H_m^0$  and  $\Delta S_m^0$  also show their necessary contribution in favour of micellization process. The entropy of micellization is positive in water and becomes less positive in the presence of increasing amounts of ethylene glycol. In a prewater medium, the presence of hydrated ionic groups of the surfactant introduces structure in the liquid water phase. Removal of the surfactant monomers due to micellization results in an overall increase in randomness and high entropy values. In the presence of the additive, the entropy changes are not as pure water indicating that the additives lowers the energy of the three-dimensional water structure due to its structure breaking ability. Based on the relation between cmc and the thermodynamic functions the effect of alcohols on micellization can also be well explained. Table 4.2.1 and Table 4.2.2 suggests that in aqueous-alcohol medium comparatively greater negative values of  $\Delta H_m^0$  contributes to the negative  $\Delta G_m^0$  for the micellization of DBS moiety with different counterions when compared with aqueous medium (Table 4.2.3). But this phenomenon is somehow comparatively less pronounced than other anionic surfactants due to its more hydrophobic benzene moiety [109].



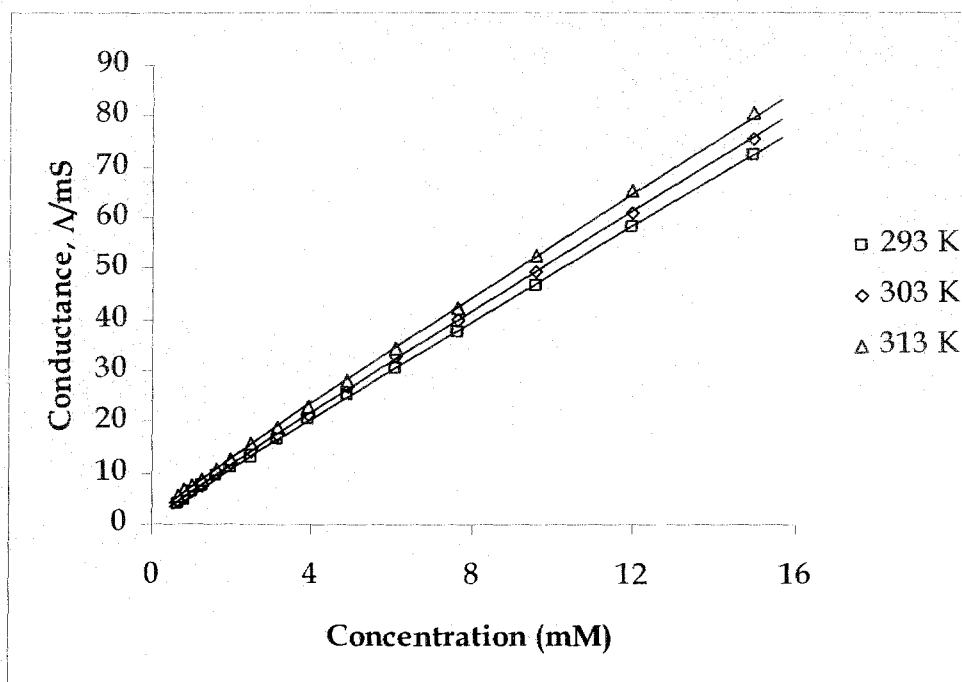
**Figure 4.57:** Conductance,  $\Lambda$  of SDBS in 10% ethylene glycol-water (w/w) solution as a function of the surfactant concentration (mM) at different temperatures ranging 293 K to 313 K with 10 K intervals.



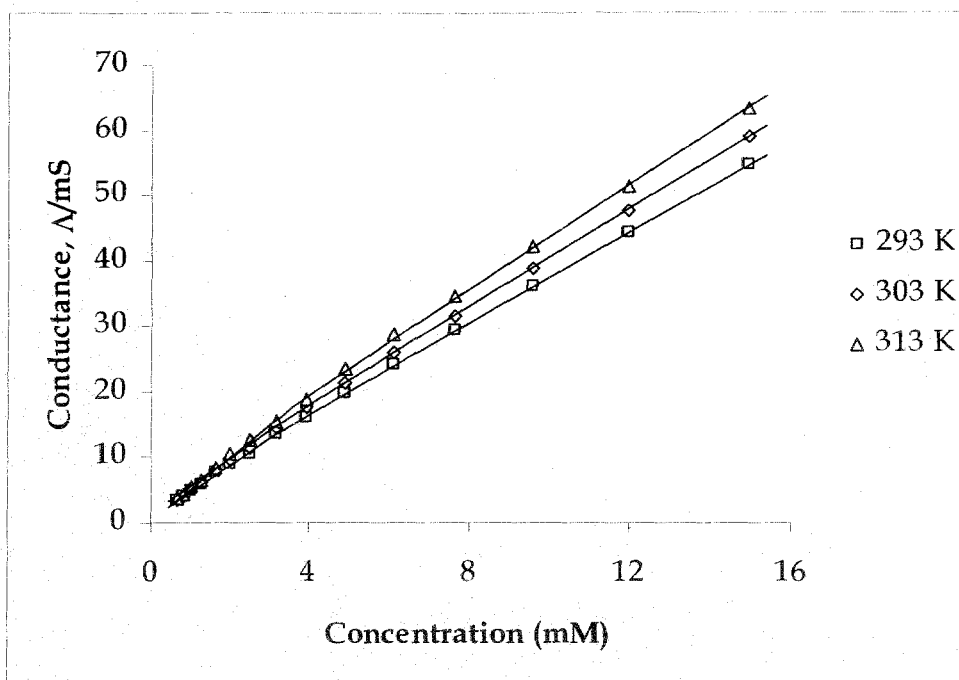
**Figure 4.58:** Conductance,  $\Lambda$  of SDBS in 20% ethylene glycol-water (w/w) solution as a function of the surfactant concentration (mM) at different temperatures ranging 293 K to 313 K with 10 K intervals.



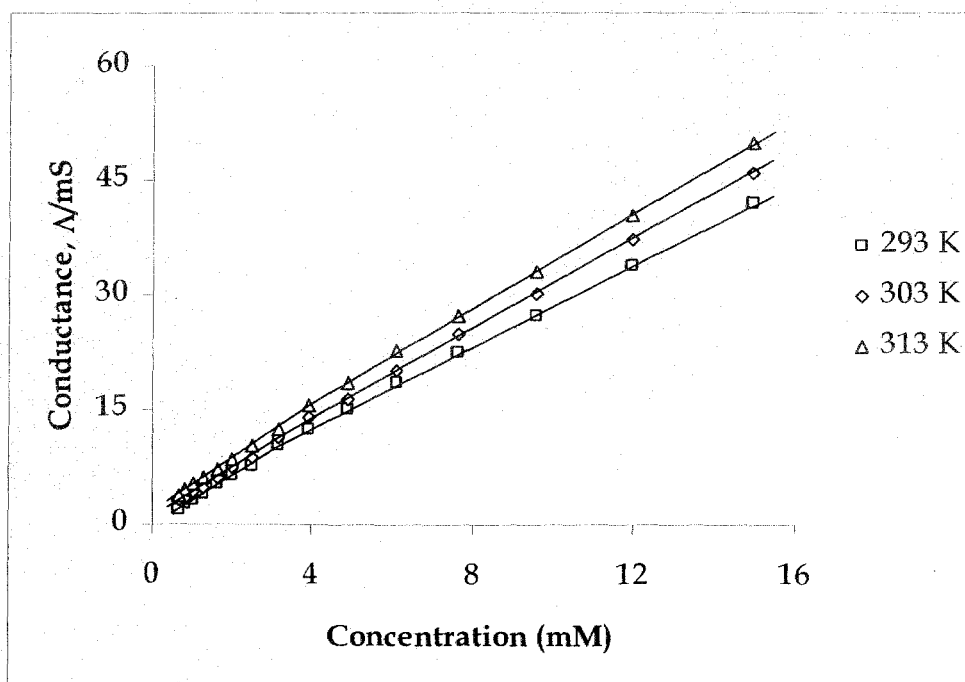
**Figure 4.59:** Conductance,  $\Lambda$  of SDBS in 30% ethylene glycol-water (w/w) solution as a function of the surfactant concentration (mM) at different temperatures ranging 293 K to 313 K with 10 K intervals.



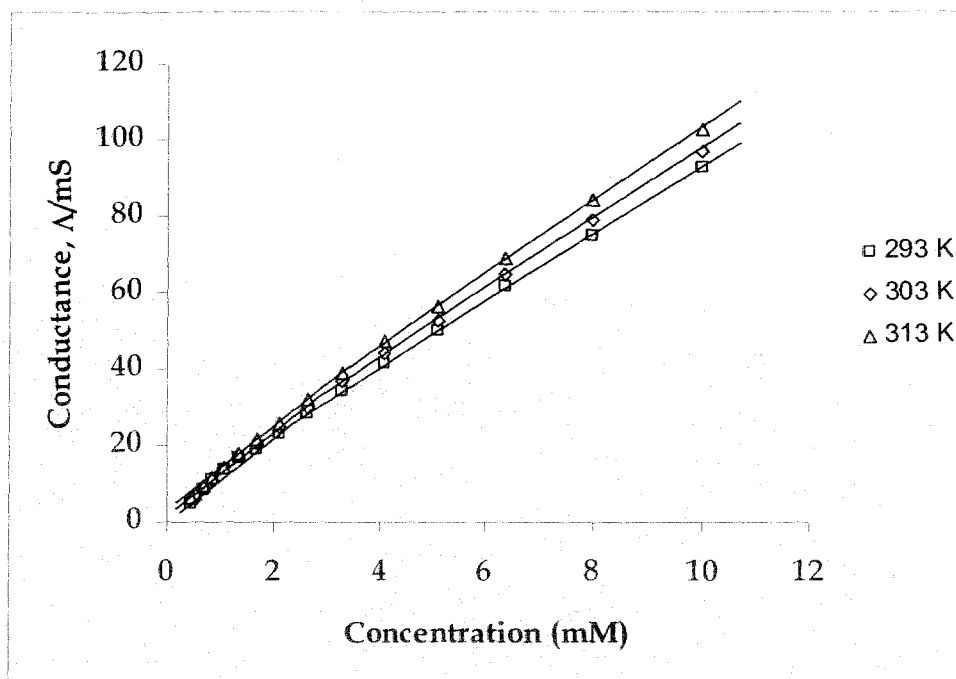
**Figure 4.60:** Conductance,  $\Lambda$  of LDBS in 10% ethylene glycol-water (w/w) solution as a function of the surfactant concentration (mM) at different temperatures ranging 293 K to 313 K with 10 K intervals.



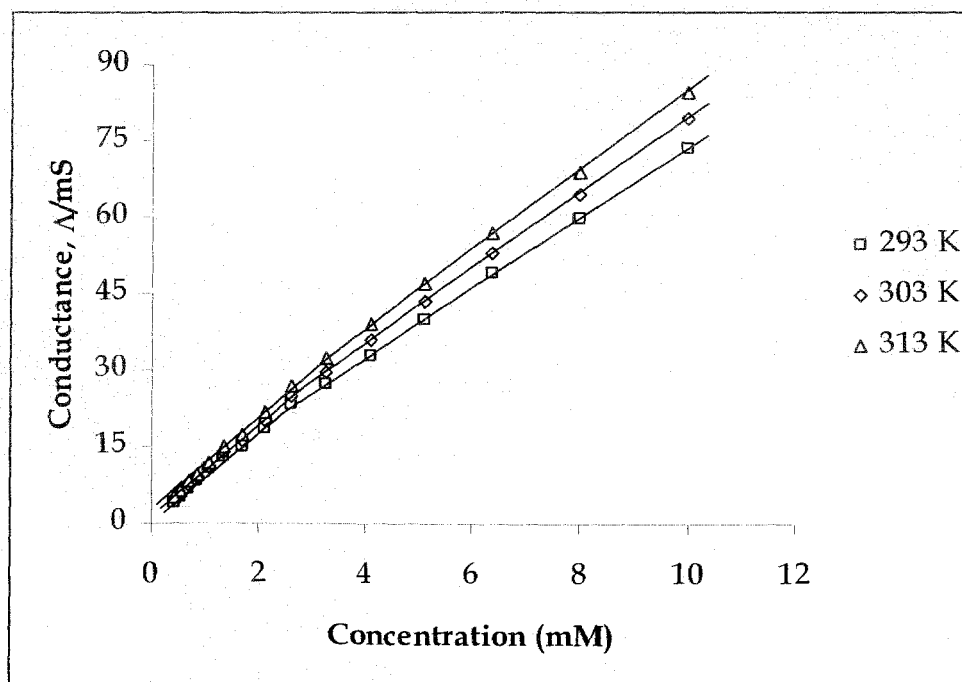
**Figure 4.61:** Conductance,  $\Lambda$  of LDBS in 20% ethylene glycol-water (w/w) solution as a function of the surfactant concentration (mM) at different temperatures ranging 293 K to 313 K with 10 K intervals.



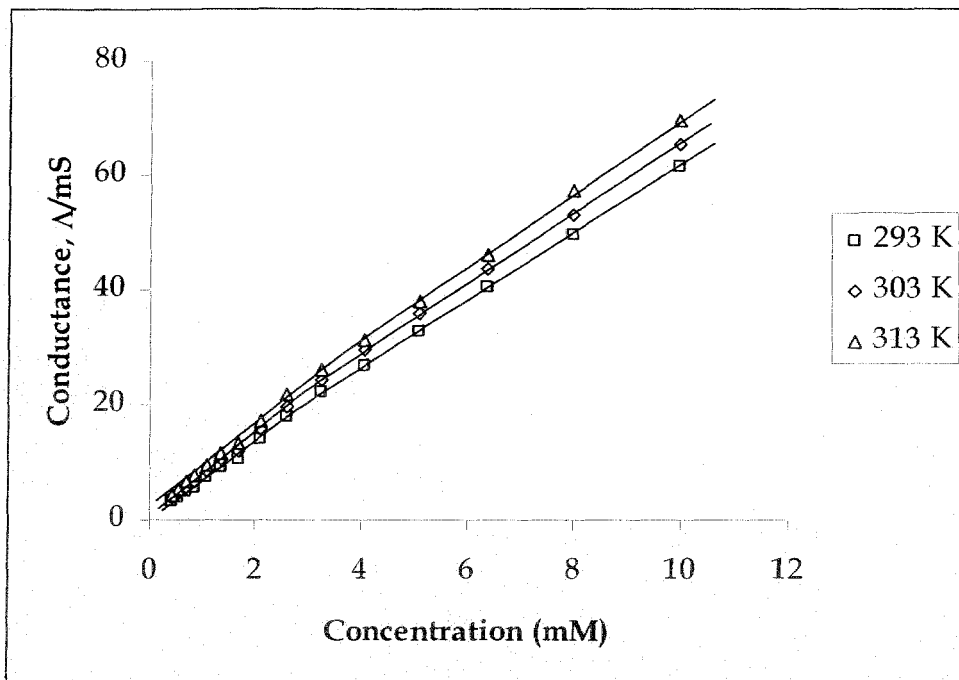
**Figure 4.62:** Conductance,  $\Lambda$  of LDBS in 30% ethylene glycol-water (w/w) solution as a function of the surfactant concentration (mM) at different temperatures ranging 293 K to 313 K with 10 K intervals.



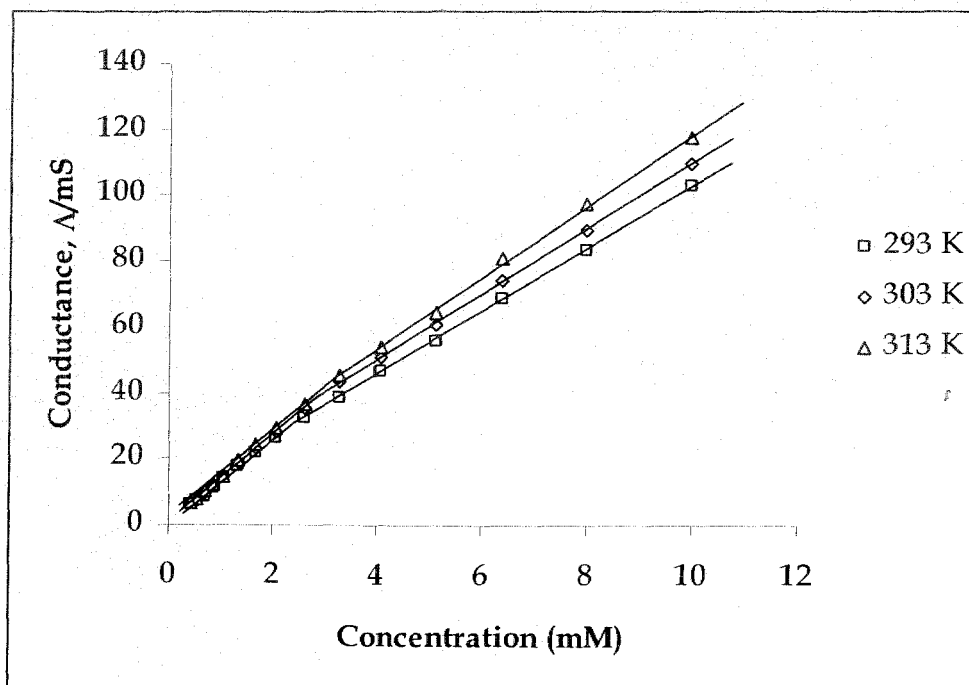
**Figure 4.63:** Conductance,  $\Lambda$  of PDBS in 10% ethylene glycol-water (w/w) solution as a function of the surfactant concentration (mM) at different temperatures ranging 293 K to 313 K with 10 K intervals.



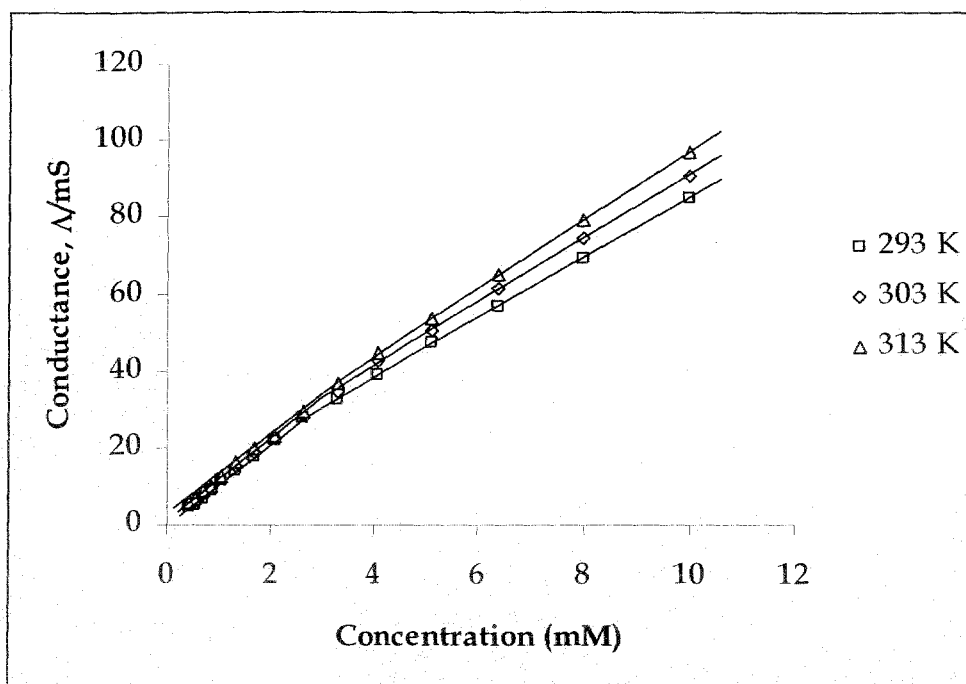
**Figure 4.64:** Conductance,  $\Lambda$  of PDBS in 20% ethylene glycol-water (w/w) solution as a function of the surfactant concentration (mM) at different temperatures ranging 293 K to 313 K with 10 K intervals.



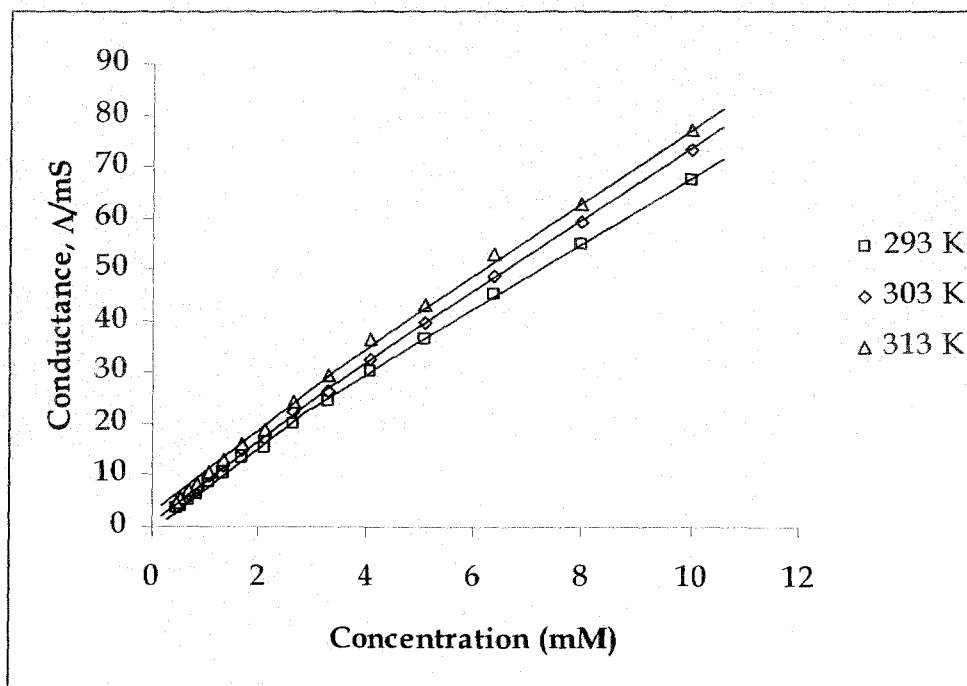
**Figure 4.65:** Conductance,  $\Lambda$  of PDBS in 30% ethylene glycol-water (w/w) solution as a function of the surfactant concentration (mM) at different temperatures ranging 293 K to 313 K with 10 K intervals.



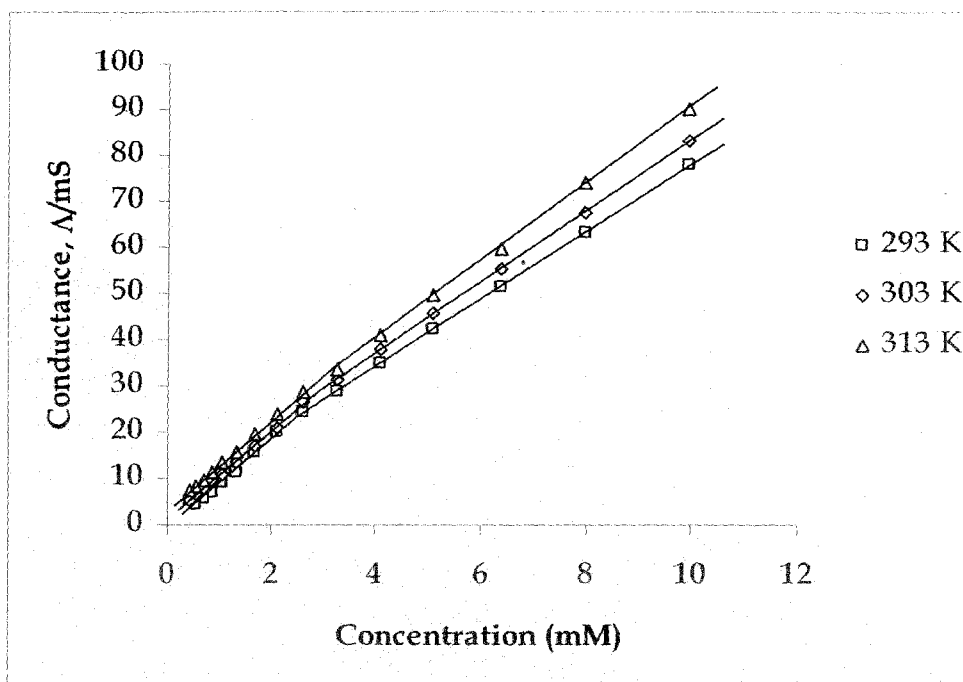
**Figure 4.66:** Conductance,  $\Lambda$  of ADBS in 10% ethylene glycol-water (w/w) solution as a function of the surfactant concentration (mM) at different temperatures ranging 293 K to 313 K with 10 K intervals.



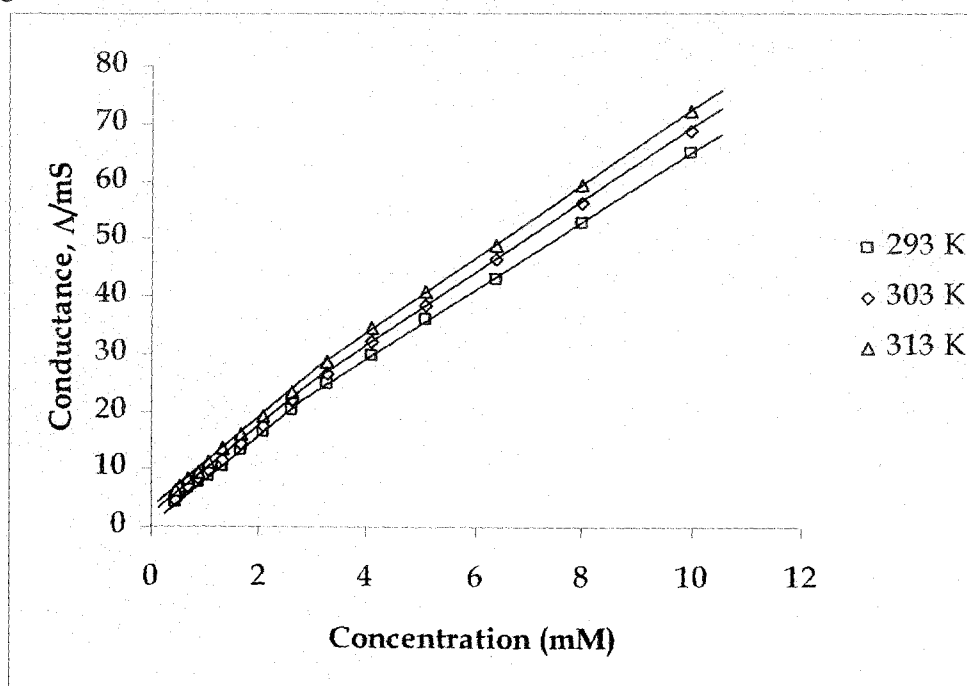
**Figure 4.67:** Conductance,  $\Lambda$  of ADBS in 20% ethylene glycol-water (w/w) solution as a function of the surfactant concentration (mM) at different temperatures ranging 293 K to 313 K with 10 K intervals.



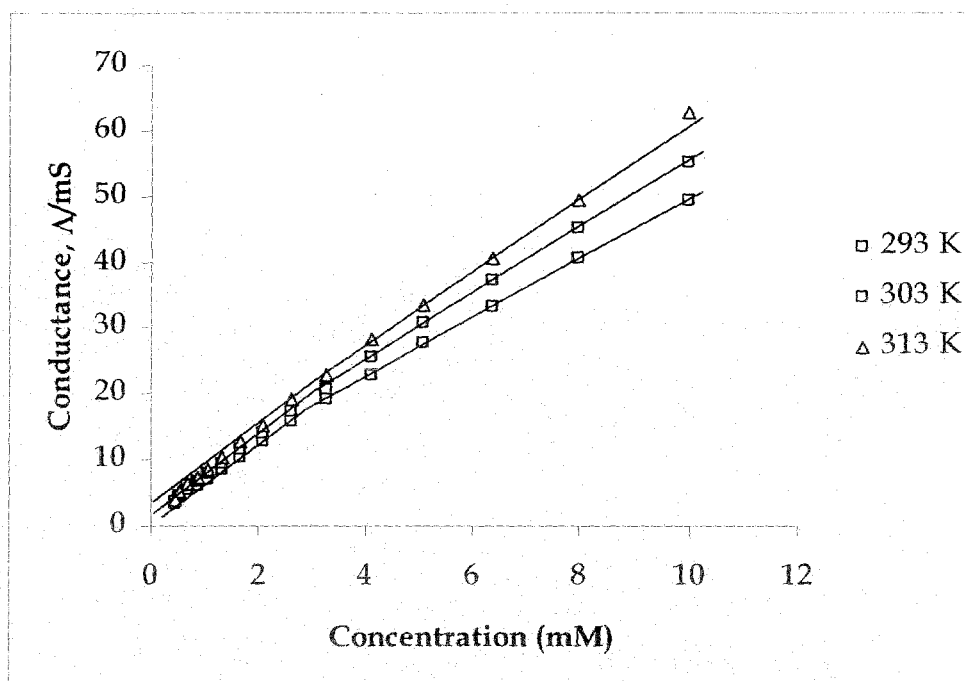
**Figure 4.68:** Conductance,  $\Lambda$  of ADBS in 30% ethylene glycol-water (w/w) solution as a function of the surfactant concentration (mM) at different temperatures ranging 293 K to 313 K with 10 K intervals.



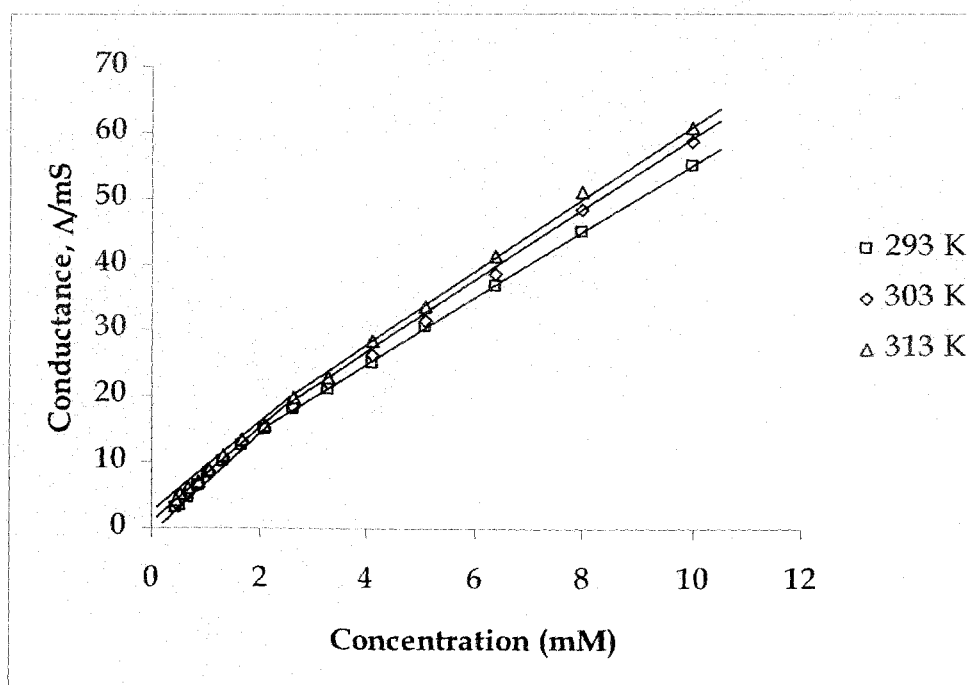
**Figure 4.69:** Conductance,  $\Lambda$  of TMADBS in 10% ethylene glycol-water (w/w) solution as a function of the surfactant concentration (mM) at different temperatures ranging 293 K to 313 K with 10 K intervals.



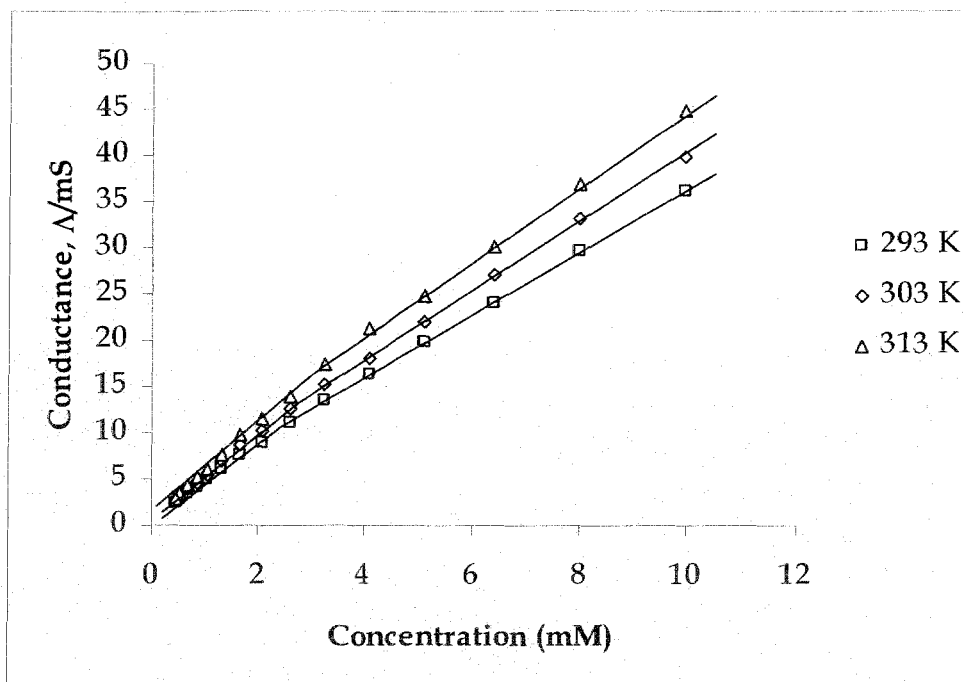
**Figure 4.70:** Conductance,  $\Lambda$  of TMADBS in 20% ethylene glycol-water (w/w) solution as a function of the surfactant concentration (mM) at different temperatures ranging 293 K to 313 K with 10 K intervals.



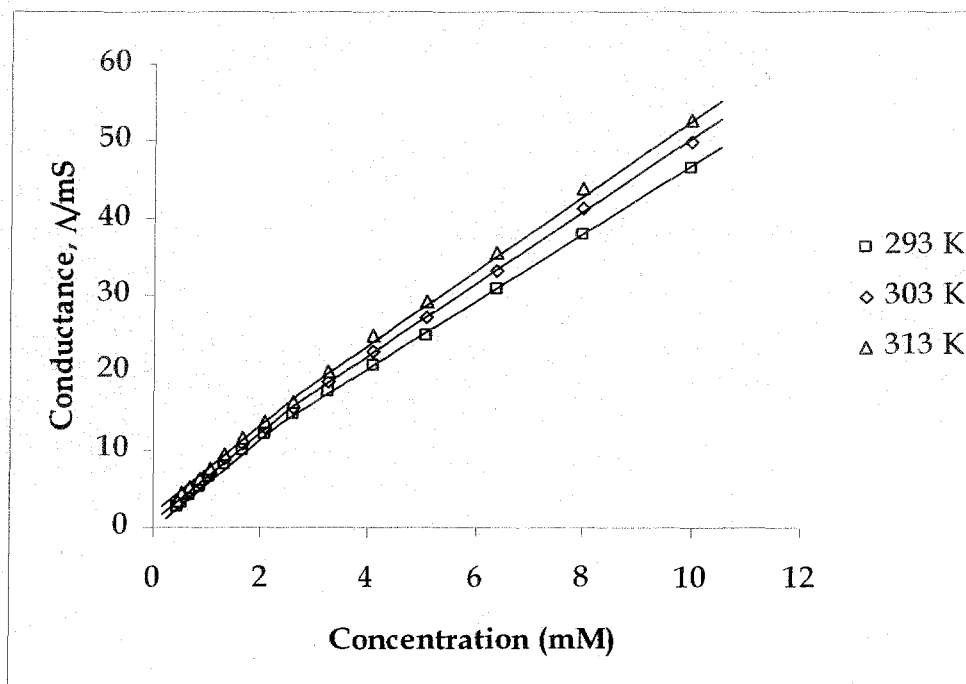
**Figure 4.71:** Conductance,  $\Lambda$  of TMADBS in 30% ethylene glycol-water (w/w) solution as a function of the surfactant concentration (mM) at different temperatures ranging 293 K to 313 K with 10 K intervals.



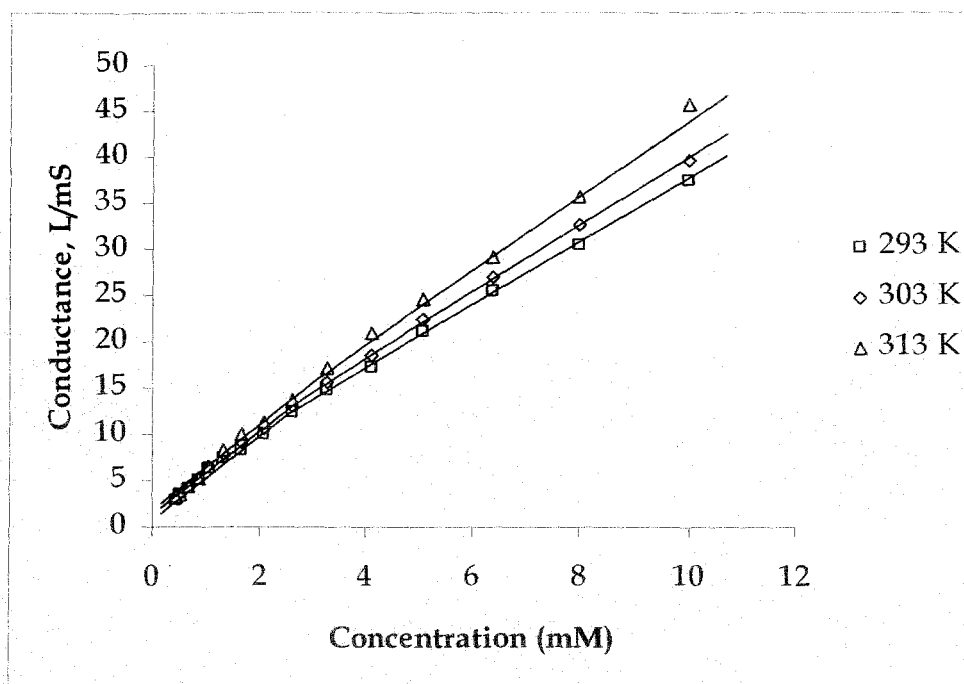
**Figure 4.72:** Conductance,  $\Lambda$  of TEADBS in 10% ethylene glycol-water (w/w) solution as a function of the surfactant concentration (mM) at different temperatures ranging 293 K to 313 K with 10 K intervals.



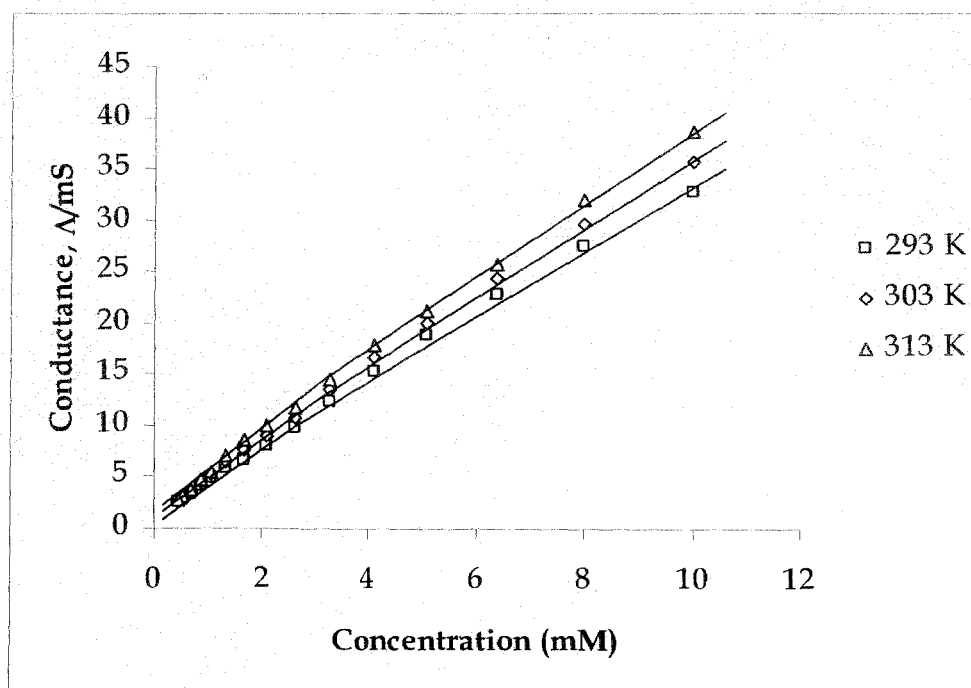
**Figure 4.73:** Conductance,  $\Lambda$  of TEADBS in 20% ethylene glycol-water (w/w) solution as a function of the surfactant concentration (mM) at different temperatures ranging 293 K to 313 K with 10 K intervals.



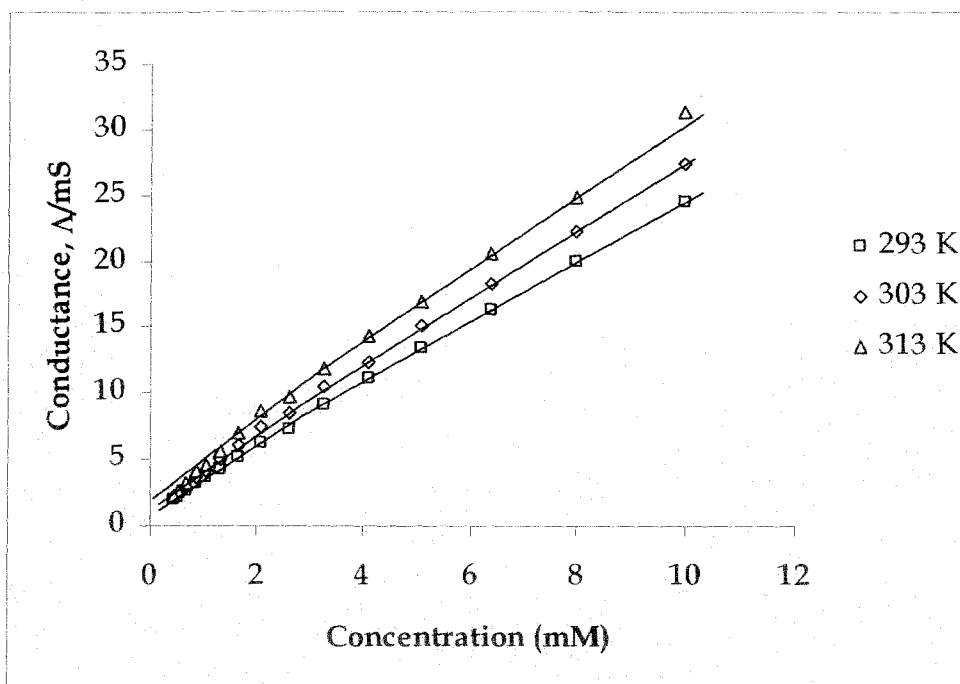
**Figure 4.74:** Conductance,  $\Lambda$  of TEADBS in 30% ethylene glycol-water (w/w) solution as a function of the surfactant concentration (mM) at different temperatures ranging 293 K to 313 K with 10 K intervals.



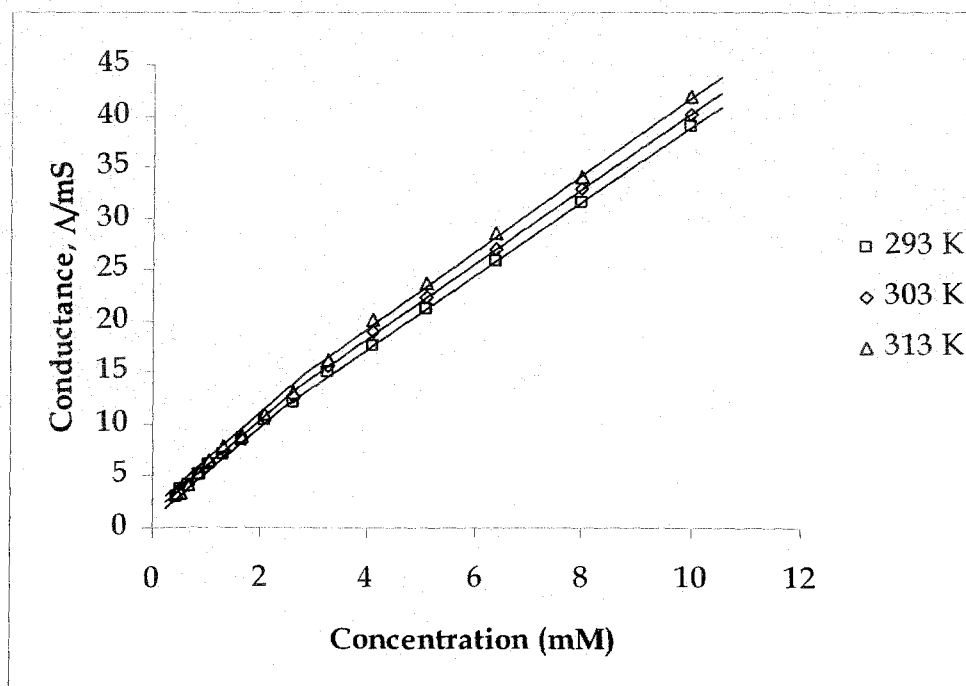
**Figure 4.75:** Conductance,  $\Lambda$  of TPADBS in 10% ethylene glycol-water (w/w) solution as a function of the surfactant concentration (mM) at different temperatures ranging 293 K to 313 K with 10 K intervals.



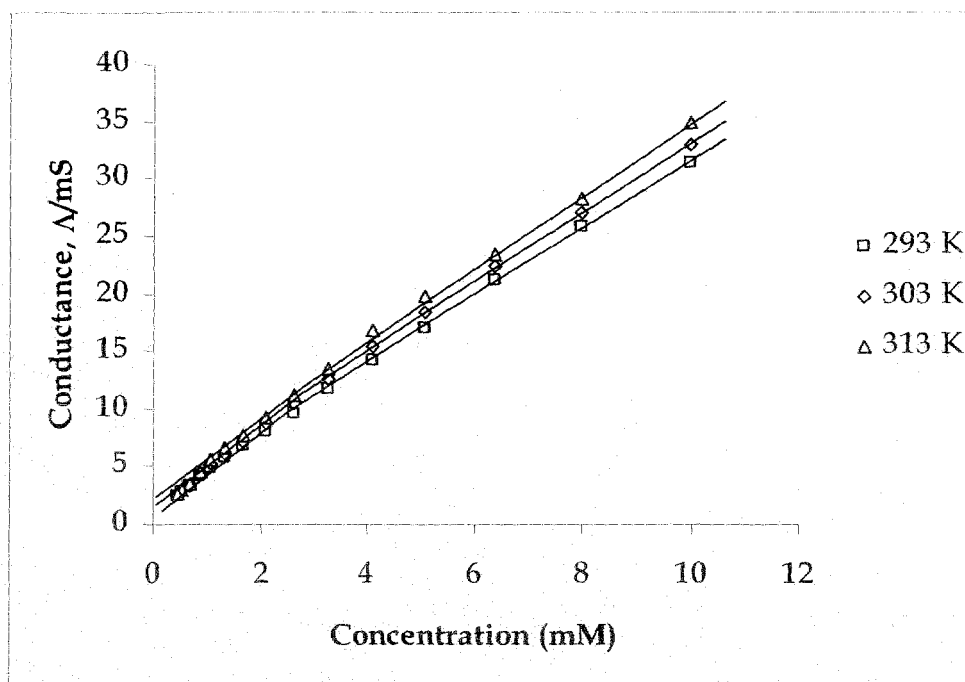
**Figure 4.76:** Conductance,  $\Lambda$  of TPADBS in 20% ethylene glycol-water (w/w) solution as a function of the surfactant concentration (mM) at different temperatures ranging 293 K to 313 K with 10 K intervals.



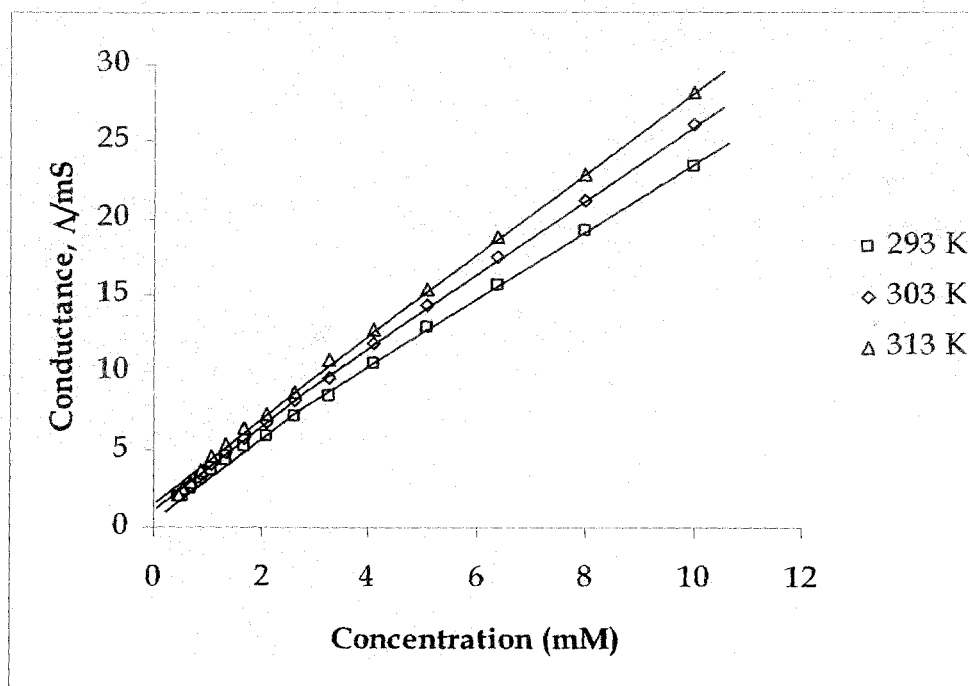
**Figure 4.77:** Conductance,  $\Lambda$  of TPADBS in 30% ethylene glycol-water (w/w) solution as a function of the surfactant concentration (mM) at different temperatures ranging 293 K to 313 K with 10 K intervals.



**Figure 4.78:** Conductance,  $\Lambda$  of TBADBS in 10% ethylene glycol-water (w/w) solution as a function of the surfactant concentration (mM) at different temperatures ranging 293 K to 313 K with 10 K intervals.



**Figure 4.79:** Conductance,  $\Lambda$  of TBADBS in 20% ethylene glycol-water (w/w) solution as a function of the surfactant concentration (mM) at different temperatures ranging 293 K to 313 K with 10 K intervals.



**Figure 4.80:** Conductance,  $\Lambda$  of TBADBS in 30% ethylene glycol-water (w/w) solution as a function of the surfactant concentration (mM) at different temperatures ranging 293 K to 313 K with 10 K intervals.

The effect of alcohol on the micellization process, given by  $\Delta G_t^0$ , was calculated using the following equation:

$$\Delta G_t^0 = \Delta G_{m(\text{alcohol-water})}^0 - \Delta G_{m(\text{water})}^0 \quad (4.8)$$

It may be noted that, micellization process of DBS with different counterions are more favourable in water-alcohol binary mixture as compared to pure aqueous solvent, which is well supported by the positive values of  $\Delta G_t^0$ , i.e., the positive values of  $\Delta G_t^0$  can be understood on the basis of a reduction of the hydrophobic interactions caused by improved solvation. The overall exothermicity of the present system indicates that both the structure-breaking ability of ethylene glycol and its interaction with the hydrophilic groups of the surfactants are dominating factors. Depending upon the temperature and the proportion of ethylene glycol present, small negative  $\Delta G_t^0$  as observed are there in different surfactants, may be due to a reduction of the micelle solvation in the mixed solvent. MacManus et. al. [110] showed that the position of the solubilized alcohol depends on the alkyl chain length. More hydrophobic alcohols seem to penetrate deeper into the hydrocarbon interior of the micelles than the hydrophilic ones. The solubilization of alcohol leads to a decrease in the electrostatic interaction between the surfactant head groups, and makes the surfactant molecules more energetically favorable for being a part of the micelles. Although the short-chain alcohols are highly hydrophilic, they undergo partitioning between the micellar pseudophase and the aqueous phase which can be supported by enhancement of the degree of ionization ( $\alpha$ ) with addition of alcohols. The decrease of local polarity of the micelle was reported [110] upon addition of allyl alcohol may also favors micellization at the lower concentration of surfactants.

In order to quantify the solubilization or association of alcohol in the micelles, the fraction ( $a$ ) of alcohol which is present in the micellar pseudophase may be expressed with self-diffusion coefficients [111]:

$$D_A = (1 - a)D_A^{free} + aD_A^{mic} \quad (4.9)$$

where  $D_A$  is the measured self-diffusion coefficient of the alcohol,  $D_A^{free}$  is the self-diffusion coefficient of the free alcohol molecules, and  $D_A^{mic}$  is the self-diffusion coefficient of the alcohol molecules bound in the micelles. In solutions where the cmc is low and the concentration of the surfactant is large compared to the cmc, the  $D_A^{mic}$  may be considered equal to the measured self-diffusion coefficient of the surfactant.

Table 4.2.1  
Micellization parameters of DBS with different counterion in different proportions  
of ethylene glycol-water mixtures

Surfactant	Wt% EG	T/K	cmc <sup>a</sup> /(mol dm <sup>-3</sup> ×10 <sup>3</sup> )	α	-ΔG <sub>m</sub> <sup>o</sup> / (kJ mol <sup>-1</sup> )	-ΔH <sub>m</sub> <sup>o</sup> / (kJ mol <sup>-1</sup> )	ΔS <sub>m</sub> <sup>o</sup> / (J K <sup>-1</sup> mol <sup>-1</sup> )
Sodium dodecyl benzene sulfonate (SDBS)	10%	293	3.43	0.7568	29.4	10.9	63.13
		303	3.62	0.7231	31.0	13.7	57.18
		313	3.81	0.7671	30.8	15.9	47.47
	20%	293	3.65	0.7563	29.2	10.9	62.51
		303	3.75	0.7154	31.1	13.8	57.15
		313	3.96	0.7353	31.4	16.3	48.29
	30%	293	3.85	0.7584	29.0	10.8	61.86
		303	3.95	0.7283	30.6	13.6	56.03
		313	4.12	0.7385	31.2	16.3	47.75
Lithium dodecyl benzene sulfonate (LDBS)	10%	293	2.65	0.8657	27.5	10.2	58.87
		303	3.19	0.8856	27.4	10.9	54.39
		313	3.55	0.8506	28.9	12.4	52.65
	20%	293	3.12	0.8466	27.5	10.4	58.30
		303	3.28	0.8656	27.8	11.1	55.10
		313	3.57	0.8289	29.4	12.6	53.59
	30%	293	3.15	0.8390	27.7	10.5	58.59
		303	3.44	0.8216	28.8	11.6	56.77
		313	3.76	0.8349	29.1	12.6	52.81
Potassium dodecyl benzene sulfonate (KDBS)	10%	293	2.42	0.8046	29.2	9.9	65.98
		303	2.83	0.7188	31.9	12.7	63.29
		313	3.25	0.9286	27.2	12.6	46.63
	20%	293	2.62	0.7596	30.1	10.3	67.64
		303	2.92	0.7711	30.5	12.2	60.39
		313	3.43	0.8883	28.0	13.1	47.89
	30%	293	2.79	0.8502	27.7	9.5	62.10
		303	2.96	0.8081	29.6	11.8	58.43
		313	3.71	0.8545	28.7	13.5	48.59
Ammonium dodecyl benzene sulfonate (ADBS)	10%	293	2.52	0.6940	31.8	13.7	61.72
		303	2.81	0.8955	27.5	13.9	44.83
		313	3.32	0.8282	29.7	17.5	38.84
	20%	293	2.75	0.7480	30.2	13.2	58.25
		303	3.01	0.7923	29.9	15.2	48.33
		313	3.33	0.8351	29.5	17.4	38.58
	30%	293	2.81	0.7626	29.8	13.0	57.35
		303	3.16	0.8088	29.3	15.0	47.19
		313	3.35	0.8681	28.6	16.9	37.43

<sup>a</sup> cmc values are calculated by conductivity method.

**Table 4.2.2**  
**Micellization parameters of DBS with different counterion in different proportions**  
**of ethylene glycol-water mixtures**

Surfactant	Wt% EG	T/K	Cmc <sup>a</sup> /(mol dm <sup>-3</sup> ×10 <sup>3</sup> )	α	-ΔG <sub>m</sub> <sup>o</sup> / (kJ mol <sup>-1</sup> )	-ΔH <sub>m</sub> <sup>o</sup> / (kJ mol <sup>-1</sup> )	ΔS <sub>m</sub> <sup>o</sup> / (J K <sup>-1</sup> mol <sup>-1</sup> )
Tetra methyl ammonium dodecyl benzene sulfonate (TMADBS)	10%	293	2.55	0.9241	26.2	19.8	21.75
		303	2.95	0.8992	27.3	22.4	16.34
		313	3.15	0.8550	29.1	25.6	11.45
	20%	293	2.80	0.8860	26.9	20.5	21.65
		303	3.01	0.9534	25.9	21.2	15.36
		313	3.20	0.9128	27.6	24.3	10.73
	30%	293	2.90	0.8729	27.1	20.8	21.58
		303	3.10	0.8695	27.9	23.0	16.31
		313	3.30	0.8914	28.1	24.7	10.66
Tetra ethyl ammonium dodecyl benzene sulfonate (TEADBS)	10%	293	2.20	0.7670	30.5	13.4	58.28
		303	2.45	0.7567	31.4	14.8	54.83
		313	2.65	0.7747	31.7	16.0	50.37
	20%	293	2.40	0.8051	29.3	13.0	55.61
		303	2.55	0.8254	29.6	14.0	51.41
		313	3.10	0.8308	29.8	15.2	46.54
	30%	293	2.42	0.7851	29.7	13.2	56.46
		303	2.62	0.6933	32.8	15.6	56.89
		313	3.20	0.9048	27.8	14.3	43.30
Tetra propyl ammonium dodecyl benzene sulfonate (TPADBS)	10%	293	2.58	0.8238	28.6	9.1	66.64
		303	2.82	0.8416	28.9	9.7	63.15
		313	2.94	0.7950	30.9	11.0	63.55
	20%	293	2.61	0.9023	26.7	8.5	62.09
		303	2.85	0.8591	28.4	9.58	62.10
		313	3.20	0.8125	30.2	10.8	61.79
	30%	293	2.80	0.8980	26.6	8.49	61.69
		303	2.93	0.7546	30.9	10.5	67.50
		313	3.26	0.9010	27.9	10.0	57.01
Tetra butyl ammonium dodecyl benzene sulfonate (TBADBS)	10%	293	2.47	0.9119	26.6	18.6	27.32
		303	2.71	0.8867	27.8	20.8	23.20
		313	2.82	0.7598	31.9	25.4	20.97
	20%	293	2.62	0.8721	27.4	19.2	27.77
		303	2.76	0.8248	29.3	22.0	24.31
		313	2.83	0.8096	30.6	24.3	20.09
	30%	293	2.71	0.8399	28.1	19.8	28.23
		303	2.79	0.8340	29.1	21.8	24.02
		313	2.85	0.7888	31.1	24.8	20.37

<sup>a</sup>cmc values are calculated by conductivity method.

Table 4.2.3.  
Effect of ethylene glycol and water mixtures on the micellization of DBS with different counterions

Surfactant	Wt% EG	T/K	$\Delta G^0_t$ (kJ mol <sup>-1</sup> )	Surfactant	Wt% EG	T/K	$\Delta G^0_t$ (kJ mol <sup>-1</sup> )
Sodium dodecyl benzene sulfonate (SDBS)	10%	293	2.44	Tetra methyl ammonium dodecyl benzene sulfonate (TMADBS)	10%	293	6.72
	20%	303	-0.01		20%	303	6.40
	30%	313	0.33		30%	313	5.56
	10%	293	2.62		10%	293	6.04
	20%	303	-0.08		20%	303	7.80
	30%	313	-0.33		30%	313	7.08
	10%	293	2.83		10%	293	5.82
	20%	303	0.40		20%	303	5.80
	30%	313	-0.12		30%	313	6.62
Lithium dodecyl benzene sulfonate (LDBS)	10%	293	3.30	Tetra ethyl ammonium dodecyl benzene sulfonate (TEADBS)	10%	293	0.85
	20%	303	4.08		20%	303	0.78
	30%	313	1.81		30%	313	1.27
	10%	293	3.30		10%	293	2.04
	20%	303	3.67		20%	303	2.64
	30%	313	1.28		30%	313	3.20
	10%	293	3.14		10%	293	1.58
	20%	303	2.73		20%	303	-0.60
	30%	313	1.59		30%	313	5.17
Potassium dodecyl benzene sulfonate (KDBS)	10%	293	2.95	Tetra propyl ammonium dodecyl benzene sulfonate (TPADBS)	10%	293	2.51
	20%	303	1.09		20%	303	3.04
	30%	313	6.62		30%	313	1.82
	10%	293	2.09		10%	293	4.45
	20%	303	2.49		20%	303	3.51
	30%	313	5.75		30%	313	2.53
	10%	293	4.47		10%	293	4.53
	20%	303	3.45		20%	303	0.99
	30%	313	5.14		30%	313	4.83
Ammoniu m dodecyl benzene sulfonate (ADBS)	10%	293	-0.82	Tetra butyl ammonium dodecyl benzene sulfonate (TBADBS)	10%	293	4.33
	20%	303	2.97		20%	303	4.15
	30%	313	2.94		30%	313	1.38
	10%	293	0.76		10%	293	3.52
	20%	303	0.61		20%	303	2.66
	30%	313	3.12		30%	313	2.67
	10%	293	1.18		10%	293	2.84
	20%	303	1.16		20%	303	2.92
	30%	313	3.98		30%	313	2.16

However, a close look at the table 4.2.1 and 4.2.2 also shows that at a fixed proportion of alcohol the cmc and other associated thermodynamic parameters except  $\alpha$  progressively increases with temperature. This effect of temperature variation may also be explained by the dehydration of the hydrocarbon tail of the surfactant molecule at high temperature followed by the greater adherence of the alcohol molecules to the micellar pseudophase. This can also be explained by the fact that short chain alcohol like ethanol [111], ethylene glycol affects the surface properties of the surfactants to a great extent by the effective adsorption in air-aqueous interface. In general, the alcohols may be distributed among three energetically different sites. It can be dispersed in the aqueous bulk solution, oriented in the micellar surface, and located in the hydrocarbon core of the aggregates. In this respect it may be said that the alcohol content works quite similar to temperature change with respect to the effect on micelle formation at constant pressure. The structure breaking ability of ethylene glycol is a dominating factor in the micellization process. It was found that the surface activity of any surfactant decreases slightly with increasing concentration of ethylene glycol at a given temperature. It was also found previously that the change of surface area per head group of the surfactant suggested an alteration in the nature of its solvation layer, produced probably by a certain participation of cosolvent in the micellar solvation layer.

## References

1. Clint, J. H. *Surfactant Aggregation*; Blackie: Glasgow/London, 1992.
2. Moroi, Y. *Micelles, Theoretical and Applied Aspects*; Plenum: New York, 1992.
3. Rosen, M.J. *Surfactants and Interfacial Phenomena*; Third ed., John Wiley & Sons: New York, 2004
4. Shah, D.O. *Micelles, Microemulsions and Monolayers*; Boca Raton: CRC Press. 1998.
5. Umlong, I.M.; Ismail, K. *J. Colloid Interface Sci.* **2005**, 291, 529.
6. Paul, B.C.; Ismail, K. *Bull.Chem.Soc.Jpn.* **1993**, 66, 703.
7. Mata, J.; Varade, D.; Ghosh, G.; Bahadur, P. *Colloids Surf. A.* **2004**, 245, 69.
8. Shanks, P.C.; Franses, E.I. *J.Phys.Chem.* **1992**, 96, 1794.
9. Dutkiewicz, E.; Jakubowska, A. *Colloid Polym.Sci.* **2002**, 280, 1009.
10. Paul, B.C.; Islam, S.S.; Ismail, K. *J.Phys.Chem.B.* **1998**, 102, 7807.
11. Dibakar, D.; Shah, D.O. *J.Phys.Chem.B.* **2001**, 105, 7133.
12. Ikeda, S. *Colloid.Polym.Sci.* **1991**, 269, 49.
13. Ozeki, S.; Ikeda, S. *J.Phys.Chem.* **1985**, 89, 5088.
14. Paul, A.; Griffiths, P.C.; Pettersson, E.; Stilbs, P.; Bales, B.L.; Zana, R.; Heenan, R.K. *J. Phys. Chem. B* **2004**, 108, 3810.
15. Bales, B.L. *J. Phys. Chem. B* **2001**, 105, 6798.
16. Benrraou, M.; Bales, B.L.; Zana, R. *J. Phys. Chem. B* **2003**, 107, 13432.
17. Shimizu, S.; Pires, P.A.R.; El Seoud, O.A. *Langmuir* **2004**, 20, 9551.
18. Pisárčik, K.; Devínsky, F.; Lacko, I. *Acta Facult. Pherm. Univ. Comenianae* **2003**, 50, 119.
19. Chatterjee, A.; Moulik, S.P.; Sanyal, S.K.; Mishra, B.K.; Puri, P.M. *J. Phys. Chem. B* **2001**, 105, 12823.
20. Attwood, D.; Florence, A.T. *Surfactant System*, Champan and Hall Ltd. USA, 1985.
21. Degiorgio, V., Nonionic Micelles, in *Physics of Amphiphiles: Micelles, Vesicles and Microemulsions*, edited by V. Degiorgio and M. Corti, North-Holland Publishers, Amsterdam, 1983, p. 303.
22. Corti, M.; Minero, C.; Degiorgio, V. *J. Phys. Chem.* **1984**, 88, 309.
23. Shigeta, K.; Olsson, U.; Kunieda, H. *Langmuir* **2001**, 17, 4717.
24. Kumar, S.; Sharma, D.; Kabir-ud-Din. *Langmuir* **2000**, 16, 6821.
25. Kumar, S.; Sharma, D.; Khan, Z.A.; Kabir-ud-Din. *Langmuir* **2001**, 17, 5813.
26. Raghavan, S.R.; Edlund, H.; Kaler, E.W. *Langmuir* **2002**, 18, 1056.
27. Kumar, S.; Sharma, D.; Khan, Z.A.; Kabir-ud-Din. *Langmuir* **2002**, 18, 205.

28. Yu, Z.-J.; Xu, G. *J. Phys. Chem.* **1989**, *93*, 7441.
29. Chakraborty, A.; Saha, S.K.; Chakraborty, S. *Colloid. Polym. Sci.* **2008**, *286*, 927.
30. Kalur, G.C.; Raghavan, S.R. *J.Phys.Chem.B* **2005**, *109*, 8599.
31. Kumar, S.; Aswal, V.K.; Naqvi, A.Z.; Goyal, P.S.; Kabir-ud-Din. *Langmuir* **2001**, *17*, 2549.
32. Kumar, S.; Sharma, D.; Kabir-ud-Din. *Langmuir* **2003**, *19*, 3539.
28. Yu, Z.-J.; Xu, G. *J. Phys. Chem.* **1989**, *93*, 7441.
29. Chakraborty, A.; Saha, S.K.; Chakraborty, S. *Colloid. Polym. Sci.* **2008**, *286*, 927.
30. Kalur, G.C.; Raghavan, S.R. *J.Phys.Chem.B* **2005**, *109*, 8599.
31. Kumar, S.; Aswal, V.K.; Naqvi, A.Z.; Goyal, P.S.; Kabir-ud-Din. *Langmuir* **2001**, *17*, 2549.
32. Kumar, S.; Sharma, D.; Kabir-ud-Din. *Langmuir* **2003**, *19*, 3539.
33. Kim, D.H.; Oh, S.G.; Cho, C.G. *Colloid Polym. Sci.* **2001**, *279*, 39.
34. Lu, J.R.; Marrocco, A.; Su, T.J.; Thomas, R.K.; Penfold, J. *J.Colloid Interface Sci.* **1993**,
35. Sein, A.; Engberts, J.B.F.N. *Langmuir* **1995**, *11*, 455.
36. Tcacenco, C.M.; Zana, R.; Bales, B.L. *J. Phys. Chem. B* **2005**, *109*, 15997.
37. Mitra, D.; Chakraborty, I.; Bhattacharya, S.C.; Moulik, S.P. *Langmuir* **2007**, *23*, 3049.
38. Yang, J. *Curr. Opin. Colloid Interface Sci* **2002**, *7*, 276.
39. Maitland, G.C. *Curr. Opin. Colloid Interface Sci.* **2000**, *5*, 301
40. Eastoe, J.; Robinson, B. H.; Hennan, R. K. *Langmuir*, **1993**, *9*, 2820.
41. Temsamani, M. B.; Maeck, M.; Hassani, I. E.; Hurwitz, H. D. *J. Phys. Chem. B*, **1998**, *102*, 3335.
42. Benrraou, M.; Bales, B. L.; Zana, R. *J. Phys. Chem. B*, **2003**, *107*, 13432.
43. Corrin, M.; Harkins, W.D. *J.Am.Chem.Soc.* **1947**, *69*, 683.
44. Bales, B.L. *J. Phys. Chem. B* **2001**, *105*, 6798.
45. Bales, B.L.; Zana, R. *J. Phys. Chem. B* **2002**, *106*, 1926.
46. Rosen, M. J.; Cohen, A. W.; Dahanayake, M. Hua, X. *J. Phys. Chem.*, **1982**, *86*, 541.
47. Oh, S. G.; Shah, D. O. *J. Phys. Chem.*, **1993**, *97*, 284.
48. Sulthana, S. B.; Bhat, S. G. T.; Rakshit, A. K. *Langmuir*, **1997**, *13*, 4562.
49. Chakraborty, S.; Chakraborty, A.; Ali, M.; Saha, S. K. *J. Dispersion Sci. Technol.* **2010**, *31*, 209-215.
50. Hait, S. K.; Majhi, P. R.; Blume, A.; Moulik, S. P. **2003**, *J. Phys. Chem. B*, *107*: 3650-3658.
51. Kresheck, G.C.; Hargraves, W.A. *J.Colloid Interface Sci.* **1974**, *48*, 481

52. Kirilay, Z.; Dekany, I. *J. Colloid Interface Sci.* **2002**, 242, 214.
53. Ropers, M.H.; Czichocki, G.; Brezesinski, G. *J. Phys. Chem. B* **2003**, 107, 5281.
54. Das, D.; Ismail, K. *J. Colloid Interface Sci.* **2008**, 327, 198.
55. Jalali, F.; Shamsipur, M.; Alizadeh, N. *J. Chem. Thermodynamics* **2000**, 32, 755.
56. Gunaseelan, K.; Ismail, K. *J. Colloid Interface Sci.* **2003**, 258, 110.
57. Zhang, H-L.; Kong, Z.; Yan, Y-M.; Li, G-Z.; Yu, L.; Geng, F. *J. Dispersion Sci. Technol.* **2007**, 28, 958
58. Moroi, Y. *Micelles: Theoretical and Applied Aspects*, Plenum, New York, 1992.
59. Chen, S.H.; *Ann. Rev. Phys. Chem.* **1986**, 37, 351.
60. Hayashi, S.; Ikeda, S. *J. Phys. Chem.* **1980**, 84, 744.
61. Førland, G.M.; Samseth, J.; Gjerde, M.I.; Høiland, H.; Jensen, A. Ø.; Mortensen, K.; *Journal of Colloid and Interface Science*, 1998, 203, 328 – 334.
62. Sjöblom, J.; Lindberg, R.; Friberg, S.E. *Adv. Colloid Interface Sci.* **1996**, 95, 125.
63. Schwunger, M.J.; Stickdorn, K.; Shomäcker, R. *Chem. Rev.* **1995**, 95, 849.
64. Onori, G.; Passeri, S.; Cipiciani, A. *J. Phys. Chem.* **1989**, 93, 4306.
65. Cipiciani, A.; Onori, G.; Savelli, G. *Chem. Phys. Letters* **1988**, 143, 505.
66. Beneventi, S.; Onori, G. *Biophys. Chem.* **1986**, 25, 181.
67. Ruiz, C.C.; Molina-Bolívar, J.A.; Aguiar, J.; MacIsaac, G.; Moroze, S.; Palepu, R. *Langmuir*, **2001**, 17, 6831–6840.
68. Chakraborty, A.; Chakraborty, S.; Saha, S.K. *J. Dispersion Sci. Technol.* **2007**, 28, 984.
69. Førland, G.M.; Samseth, J.; Høiland, H.; Mortensen, K. *J. Colloid Interface Sci.* **1994**, 164, 163.
70. Leung, R.; Shah, D.O. *J. Colloid Interface Sci.* **1986**, 113, 484.
71. Akhter, M.S. *Colloids Surf. A* **1999**, 157, 203.
72. Zhou, M.F.; Rhue, R.D. *J. Colloid Interface Sci.* **2000**, 228, 18.
73. McMahan, C. A.; Hawrylak, B.; Marangoni, D.G.; Palepu, R., *Langmuir* **1999**, 15, 429.
74. Chauhan, M.S.; Kumar, G.; Kumar, A.; Chauhan, S. *Colloids Surf. A* **2000**, 166, 51.
75. Carnero Ruiz, C. *Colloid Polym. Sci.* **1999**, 277, 701.
76. Zhang, H-L.; Kong, Z.; Yan, Y-M.; Li, G-Z.; Yu, L.; Geng, F. *J. Dispersion Sci. Technol.* **2007**, 28, 958
77. Missel, P. J.; Mazer, N. A.; Carey, M. C.; Benedek G. B. *J. Phys. Chem.* **1989**, 93, 8354.
78. Romani, A.P.; Gehlen, M.H.; Lima, G.A.R.; F.H. Quina. *J. Colloid Interface Sci.* **2001**, 240, 335.

79. Sjöberg, M. *Ph. D. Thesis*, Department of Physical Chemistry, The Royal Institute of Technology, Stockholm, Sweden, 1992.
80. Rosen, M. J. *Surfactants and Interfacial Phenomena*, Wiley-Interscience, New York, 2004.
81. Wårnheim, T. *Curr. Opin. Colloid. Interface Sci.* **1997**, 2, 472.
82. Zana, R. *Colloids Surf., A* **1997**, 123-124, 27.
83. Beesley, A.; Evans, D.F.; Laughlin, R.G. *J. Phys. Chem.* **1998**, 92, 797.
84. Nagarajan, R.; Wang, C. C. *Langmuir* **2000**, 16, 5242.
85. Leung, R.; Shah, D.O. *J. Colloid Interface Sci.* **1986**, 113, 484.
86. Christian, S.D.; Scamehorn, J.F., Eds. *Solubilization in Surfactant Aggregates, Part VI*, Dekker, New York, 1995.
87. Brinchi, L.; Di Profio, P.; Germani, R.; Savelli, G.; Spreti, N. *J. Colloid Interface Sci.* **2002**, 247, 429.
88. Zana, R.; Yiv, S.; Strazielle, C.; Lianos, P.; *J. Colloid Interface Sci.* **1981**, 80, 208.
89. Lopez-Grio, S.; Baeza, B.J.J.; Alvarez-Coque, M.C.G. *Chromatographia* **1998**, 48, 655.
90. Mosquera, V.; Ruso, J.M.; Attwood, D.; Jones, M. N.; Prieto, G.; Sarmento, F. *Journal of Colloid and Interface Scienc*, **1999**, 210, 97 - 102.
91. Ionescu, L.G.; Fung, D.S. *J. Chem. Soc., Faraday Trans. 1* **1981**, 77, 2907.
92. Backlund, S.; Bergenstål, B.; Molander, O.; Wårnheim, T. *J. Colloid Interface Sci.* **1989**, 131, 393.
93. Binana-Limbele, W.; Zana, R. *Colloid Polym. Sci.* **1989**, 267, 440.
94. Sjöberg, M.; Henriksson, U.; Wårnheim, T. *Langmuir* **1990**, 6, 1205.
95. Gharibi, H.; Palepu, R.; Bloor, D. M.; Hall, D. G.; Wyn-Jones, E. *Langmuir* **1992**, 8, 782.
96. Bakshi, M. S. *J. Chem. Soc., Faraday Trans.* **1993**, 89, 4323.
97. Callaghan, A.; Doyle, R.; Alexander, E.; Palepu, R. *Langmuir* **1993**, 9, 3422.
98. Palepu, R.; Gharibi, H.; Bloor, D. M.; Wyn-Jones, E. *Langmuir* **1993**, 9, 110.
99. Nagarajan, R.; Wang, C.C. *J. Colloid Interface Sci.* **1996**, 178, 471.
100. Lee, D.J.; Huang, W. H. *Colloid Polym. Sci.* **1996**, 160.
101. Gracie, K.; Turner, D.; Palepu, R. *Can. J. Chem.* **1996**, 74, 1616.
102. Carnero Ruiz, C. *Colloid Polym. Sci.* **1999**, 277, 1999
103. Carnero Ruiz, C. *J. Colloid Interface Sci.* **2000**, 221, 262.
104. Ray, A. *Nature* **1971**, 231, 1971
105. Ray, A.; Némethy, G. *J. Phys. Chem.* **1971**, 75, 809

106. Cantú, L.; Corti, M.; Degiorgio, V.; Hoffman, H.; Ulbricht, W. *J. Colloid Interface Sci.* **1987**, 116, 384.
107. Jonströmer, M.; Sjöberg, M.; Wärheim, T. *J. Phys. Chem.* **1990**, 94, 7549.
108. Penfold, J.; Staples, E.; Toker, I.; Cummins, P. J. *Colloid Interface Sci.* **1997**, 185, 424.
109. Chakraborty, A. *Ph. D. Thesis*, Department of Physical Chemistry, University of North Bengal, Darjeeling, India
110. McManus, H.J.D.; Kang, Y.S.; Kevan, L. *J. Chem. Soc. Faraday Trans.* **1993**, 89, 4085.
111. Kalyanansundaram, K.; Thomas, J.K.; *J. Am. Chem. Soc.* **1977**, 99, 2039.

## **Chapter V**

**Aggregation number of dodecyl benzene sulfonate micelles with varying counterion and the interaction with oxazine dye in aqueous media: a fluorescence spectroscopic study**

## Chapter V

# Aggregation number of dodecyl benzene sulfonate micelles with varying counterion and the interaction with oxazine dye in aqueous medium: a fluorescence spectroscopic study

### 5. 1 Introduction

During the past two decades there has been a remarkable growth in the use of fluorescence in the biological sciences. Fluorescence is now used in environmental monitoring, clinical chemistry, DNA sequencing, and genetic analysis by fluorescence *in situ* hybridization (FISH). Because of the sensitivity of fluorescence detection, and the expense and difficulties of handling radioactive substances, there is a continuing development of medical tests based on the phenomenon of fluorescence. These tests include the widely used enzyme-linked immunoassays (ELISA) and fluorescence polarization immunoassays.

Luminescence is the emission of light from any substance and occurs from electronically excited states. Luminescence is formally divided into two categories, fluorescence and phosphorescence, depending on the nature of the excited state. In the singlet states, the electron in the excited orbital is paired (of opposite spin) to the second electron in the ground-state orbital. Consequently, return to the ground state is spin-allowed and occurs rapidly by emission of a photon. The emission rates of fluorescence are typically  $10^8 \text{ s}^{-1}$ , so that a typical fluorescence lifetime is near 10 ns. Phosphorescence is emission of light from triplet excited states, in which the electron in the excited orbital has the same spin orientation as the ground state electron. Transition to the ground state are forbidden and the emission rates are slow ( $10^3 - 10^0 \text{ s}^{-1}$ ). Fluorescence typically occurs from aromatic molecules. Some typical fluorescent substances (fluorophores) are quinine, fluorescein, rhodamine B etc. The first observation of fluorescence from a quinine solution in sunlight was reported by Sir John Frederick William Herschel in 1845 [1].

Within the next decade, one can anticipate the introduction of numerous point-of-care fluorescence assays for use at the bedside, in the doctor's office, or for home

health care. The essence of any experiment is the existence of an observable quantity and the correlation of the value of this observable with a phenomenon of interest. The time span between the absorption of light and its subsequent reemission allows time for several processes, each of which results in changes of fluorescence spectral observables. These processes include collisions with quencher, as discussed in this chapter, rotational and translational diffusion, formation of complexes with solvents or solutes, and reorientation of the environment surrounding the altered dipole moment of the excited state. These dynamic processes can affect the fluorescence anisotropies, quantum yields, lifetimes, and emission spectra. In addition, resonance energy transfer provides a reliable indicator of molecular proximity on the angstrom size scale. As a result, the spectral characteristics of fluorophores can provide a great deal of information on the solution behaviour of macromolecules.

## 5.2. Steady State Fluorescence

Fluorescence spectral data are generally presented as emission spectra. A fluorescence emission spectrum is a plot of the fluorescence intensity versus wavelength (nanometers) or wave number ( $\text{cm}^{-1}$ ). The processes which occur between the absorption and emission of light are usually illustrated by a Jabłoński diagram. The fluorescence lifetime and quantum yield are perhaps the most important characteristics of a fluorophore. The quantum yield is the number of emitted photons relative to the number of absorbed photons. Substances with the largest quantum yields, approaching unity, such as rhodamine, display the brightest emission. The lifetime is also important, as the lifetime determines the time available for the fluorophore to interact with or diffuse in its environment, and hence the information available from its emission.

The fluorescence quantum yield is the ratio of the number of photons emitted to the number of photons absorbed. The process governed by the rate constants  $\Gamma$  and  $k_{nr}$  both depopulate the excited state. The fraction of fluorophores which decay through emission, and hence the quantum yield, is given by

$$Q = \frac{\Gamma}{\Gamma + k_{nr}} \quad (5.1)$$

The lifetime of the excited state is defined by the average time the molecule spends in the excited state prior to return to the ground state. For the fluorophore, the lifetime is

$$\tau = \frac{1}{\Gamma + k_{nr}} \quad (5.2)$$

Here, it is important to note that the lifetime is an average value of the time spent in the excited state.

Fluorescence measurements can be broadly classified into two types of measurements, steady-state measurement and time-resolved measurements. Steady-state measurements are those performed with constant illumination and observation. This is most common type of measurement. The sample is illuminated with a continuous beam of light, and the intensity or emission spectrum is recorded. Because of nanosecond timescale of fluorescence, most measurements are steady-state measurements. When the sample is first exposed to light, steady-state is reached almost immediately. The second type of measurements, time-resolved measurements, is used for measuring intensity decays or anisotropy decays. For these measurements, the sample is exposed to a pulse of light, where the pulse width is typically shorter than the decay time of the sample. This intensity decay is recorded with a high-speed detection system that permits the intensity or anisotropy to be measured on the nanosecond timescale. It is important to understand that there exists a rather simple relationship between steady-state and time-resolved measurements. The steady-state observation is simply an average of the time-resolved phenomena over the intensity decay of the sample. Considering a fluorophore which displaying a single decay time ( $\tau$ ) and a single rotational correlation time ( $\theta$ ). The intensity and anisotropy decays are given by

$$I(t) = I_0 e^{-\frac{t}{\tau}} \quad (5.3)$$

$$r(t) = r_0 e^{-\frac{t}{\theta}} \quad (5.4)$$

where  $I_0$  and  $r_0$  are, respectively, the intensities and anisotropies at  $t = 0$ , immediately following the excitation pulse.

### 5.3 Determination of Aggregation Number by Fluorescence Spectroscopy of Dodecyl Benzene Sulfonate (DBS) Micelles with Varying Counter Ions

#### 5.3.1. Introduction and review of the previous work

One of the most fundamental and important structural parameters of micellar aggregates is the aggregation number, or the average aggregation number of detergent molecules in micelle unit [1]. Therefore, the measurement and establishment of aggregation number is of great significance in surface science. "An aggregation number is a description of the number of molecules present in a micelle once the critical micelle concentration (cmc) has been reached". The fluorescence probe technique is becoming increasingly popular in the study of surfactant micellization/adsorption [2-6], polymer-surfactant interactions [7-9], microemulsions [10] and determination of aggregation number of the micelle. The value of the aggregation number contains information on the micellar size and shape, which may be important in determining stability and practical applications of the investigated systems [1,11-12]. Methods which permits easy and reliable estimates of micelle aggregation numbers in actual experimental conditions, that is at a given surfactant concentration and in presence of additives such as electrolytes, small organic molecules, polymers or proteins are therefore great interest. Many methods have been used to determine micelle aggregation number [13]. However most of these methods are restricted to small values of the aggregation number (thermodynamic methods, NMR) or suffer from the fact that the measured property depends on the micelle aggregation number and also on the micelle shape and intermolecular interactions (scattering methods). To extract the value of the aggregation number, the result must be extrapolated to low concentration, close to the cmc. In doing so one is likely to modify the micelle size as it is concentration dependent in most surfactant systems. Small angle neutron scattering data at high scattering wave vectors permit in principle the determination of micelle aggregation numbers and also yield information on the micelle shape in the actual experimental conditions [14-15]. However the measurements use experimental setups that are available only in a few facilities in the world, in addition of being very costly. The fluorescent probing method circumvents most of the problems just discussed and permits determinations of micelle aggregation numbers under the actual experimental conditions [16-21]. Indeed, this determination is affected neither by intermicellar

interactions nor by the micellar shape. Besides, the apparatuses required for the measurements are available in most of the university campuses or industrial laboratories. Fluorescence probing methods can also yield information on the micelle polydispersity and micelle dynamics. That is why the luminescent probe technique is becoming increasingly popular in the study of determination of aggregation number of surfactants.

### 5.3.2. Theory

In the present study, the measurement of aggregation number is done by a simple process based on the quenching of a luminescent probe by a hydrophobic quencher. A typical experiment to determine the mean aggregation number would involve the use of a luminescent probe, quencher and a known concentration of surfactant. If the concentration of the quencher is varied, and the cmc of the surfactant known, the mean aggregation number can be easily determined. Here the word luminescent means the emission of light by a substance not resulting from heat; it is thus from a cold body radiation. The term "luminescence" was introduced in 1888 by Eilhard Wiedemann [22]. Quenching refers to any process which decreases the fluorescence intensity of a given substance. The excited states can be deactivated in several ways - they can emit, giving off light energy, deactivate- resulting in a "vibrationally hot" ground state (i.e., energy loss as heat) or can be quenched by other molecules. A variety of process can result in quenching, such as excited state reactions, energy transfer, complex-formation and collisional quenching. Quenching of the excited state is a significant process because it is usually a very efficient process. Quenching process can occur by two ways - electron transfer or energy transfer. In both the cases, the excited state energy of the luminophore (the luminescent species) is deactivated due to presence of the quencher. Quenching is the basis for fluorescence resonance energy transfer (FRET) assays. There are two types of quenching in fluorescence, viz., "static" and "dynamic" quenching. Static quenching occurs when the donor and acceptor molecules are in the ground state. The donor and acceptor molecules bind together to form a ground state complex, an intramolecular dimer with its unique properties, such as being nonfluorescent and having a unique absorption spectrum. However, if the quencher is somehow associated with the luminophore in solution prior to light absorption, the association may mean that the luminophore will

not emit, due to induced changes in its properties because of presence of quencher. Therefore the reduction in emission intensity will be affected by the extent to which the quencher associates to the luminophore and the number of quenchers present. Whereas, dynamic quenching which occurs by the quencher diffusing through solution and interacting with luminophore, resulting in a deactivation of the excited state. The emission intensity is reduced, because as well as other deactivation pathway in competition with luminescence. This quenching process is controlled by how fast the quencher can diffuse through solution and "collide" with luminophore, and as diffusion is usually a very fast process in solutions, it can be very efficient. The reduction in emission intensity can be quantified as follows. If the luminophore,  $M$ , associates with quencher,  $Q$  according to an equilibrium constant of association,  $K_{SV}$ , then this association constant can be quantified as the ratio of associated luminophore-quenchers moieties ( $[M-Q]$ ) to the product of unassociated luminophore and quencher;  $[M][Q]$ . Since the total concentration of luminophore,  $[M]_0$  is equal to the sum of associated and unassociated luminophore, substitution of this into the equilibrium expression, followed by rearrangement results in another equation of a straight line, very similar in form to the Stern-Volmer equation. However, while plotting  $\frac{I_0}{I}$  (as emission intensity can be said to be proportional to concentration) against  $[Q]$  will result in a straight line for static quenching, analogous to dynamic quenching, interpretation of the slope is different. In this case, the slope quantifies the association constant between quencher and luminophore - and therefore is useful in providing information on how these two species interact in the ground state. So, the derived equation for static quenching is as follows:

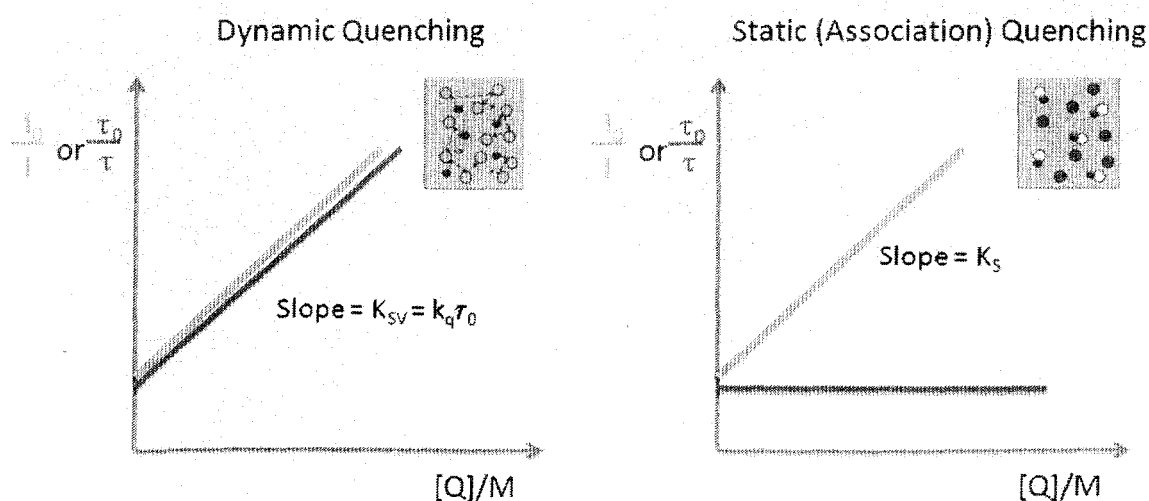
$$\frac{[M]_0}{[M]} = \frac{I_0}{I} = 1 + K_{SV} [Q] \quad (5.5)$$

If we divide the emission quantum yield in the absence of quencher by that in the presence of quencher, we can also generate an expression known as the Stern-Volmer equation for dynamic quenching. The equation is as follows:

$$\frac{\Phi_f^0}{\Phi_f} = \frac{I_f^0}{I_f} = \frac{\tau_0}{\tau} = 1 + K_q \tau_0 [Q] \quad (5.6)$$

The derivation of the Stern-Volmer Equation based on considering the rate constants of deactivation in the absence and presence of quencher in this process. So, the Stern-Volmer model is called the dynamic quenching when quenching which occurs by the quencher diffusing through solution and interacting with luminophore, resulting in a deactivation of the excited state. The Stern-Volmer equation is the equation of straight line, and hence it allows for very easy experimental determination of the quenching rate constant,  $k_q$ . If the emission intensity (or lifetime) in the absence of quencher and then in the presence of incremental amounts of quencher is measured, and the resulting ratio of emission intensities ( $I_0/I$ ) is plotted as a function of quencher concentration, the resulting graph (called a Stern-Volmer plot) will have an intercept of 1 and a slope called the Stern-Volmer constant,  $K_{SV}$ .  $K_{SV}$  is the product of the natural radiative lifetime (the lifetime in the absence of quencher),  $\tau_0$ , and the quenching rate constant,  $k_q$ . Knowing the slope and the natural radiative lifetime allows easy calculation of the quenching rate constant. So, dynamic quenching results from collisions between excited state and quencher. In an experiment there is a possibility that the reaction can occur through static quenching or dynamic quenching. The static and dynamic quenching can be represented by a very simple diagram given in figure 5.1.

**Figure 5.1:** Dynamic and Static Quenching.



In literature, there are reactions in which both the quenching process, i.e., static and dynamic quenching can occur simultaneously. We can easily understand what type of

quenching process is going on in the reaction. For dynamic quenching, all luminophores are affected by the quenching process as it is probable that they will all collide with a quencher during their excited state lifetime, so both emission intensity and life time reduced on increasing quencher concentration. For static quenching by association, only luminophore-quencher association results in reduction in emission, unassociated luminophores are free to luminescence as if there was no quencher present. Increasing quencher concentration affects emission intensity, because there are more associations, but not emission lifetime, as the unassociated luminophores can emit in the absence of quencher.

In the present experiment, the static quenching is done to measure the aggregation number of the surfactant with different counterions by steady state fluorescence quenching (SSFQ) process. This work is a part of program in our laboratory to study the dodecyl benzene sulfonate micelle as the counterion is symmetrically made more bulky and hydrophobic. It is also known that the hydration layer, so-called the Stern layer, exists in the interface between the hydrophobic micelle core and bulk water. This layer consists of the ionic head groups, counterions and hydrated water molecules. The layer should play an important role for the structural stability and dynamical property of micelle in water. Here we study sodium-, Lithium, Potassium-, Ammonium-, Tetramethyl ammonium-, Tetraethyl ammonium-, Tetrapropyl ammonium- and Tetrabutylammoniumdodecylbenzene sulfonate micelle aggregation number.

The probe was dissolved in trace amount ( $< 10^{-6}$   $\mu\text{M}$ ) in aqueous solution in a series of surfactant having different counterions. The method involves the use of a hydrophobic substance which exhibits different fluorescence characteristics depending upon the properties of the solubilising medium. For example, fluorescence probe, in our case pyrene, are sensitive to the polarity of the solubilising medium will exhibit different fluorescence behaviour in micellar and nonmicellar solutions. Such changes of behaviour as a function of surfactant concentration have been used to determine the micelle characteristics of certain surfactants. The schematic representations of pyrene and cetyl pridium chloride are given in the figure 5.2 and figure 5.3 below:

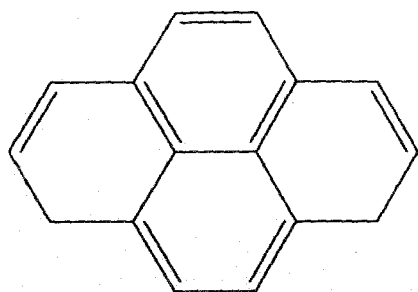


Figure 5. 2. Structure of Pyrene

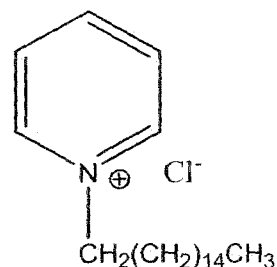


Figure 5.3 -Hexadecylpyridinium chloride (CPC)

### 5. 3.3. Materials and method

LDDBS, PDDBS, ADDBS, TMADDBS, TEADDBS, TPADDBS and TBADDBS were prepared from a sample of purified SDBS by ion exchange as described in the Chapter III. Pyrene and CPC were of puriss grade (Fluka, Switzerland) used as received.

#### Method

#### Preparation of Pyrene solution

A pyrene stock solution ( $5 \mu\text{M}$ ) is prepared as follows: About 2.02 mg of pyrene is dissolved in 10 ml absolute alcohol. 8.81 ml of this solution is added to a volumetric flask already containing 75 ml pure distilled water and the volume is made upto 100 ml with pure distilled water. Then the solution which is white in colour and turbid in nature was sonicated for 50 minutes. 0.5 ml of this turbid, white solution was then poured into another 100 ml volumetric flask containing about 50 ml pure distilled water and the volume made upto 100 ml by diluting with pure distilled water. The solution further sonicated upto 10 minutes.

The aggregation number of micelle was determined by the steady-state fluorescence quenching method using a Fluorescence Spectrophotometer, viz., Photon Technology International Co., USA (Model Q 40). Pyrene ( $5 \times 10^{-6} \mu\text{M}$ ) was used as a probe and CPC as a quencher. Emission spectra of Pyrene were obtained by exciting the samples at 332 nm and emission was measured in the range of 350-520 nm. The emission peak at 393 nm is considered for our calculation of the ratio of intensity.

### 5.3.4. Results and Discussion

The fluorescence spectrum of pyrene in water exhibits five predominant peaks. It has been shown in the case of pyrene, a quencher used to measure the aggregation number, that the ratio of intensity of the first ( $I_1$  at 373nm) and third peaks ( $I_3$  at 384 nm) is a sensitive parameter characterizing the polarity of the probe environment. For example,  $I_1/I_3$  in hydrocarbon solvents has a value of about 0.6, in ethanol about 1.1, and in water about 1.8. The value of  $I_1/I_3$  remains constant upto a certain surfactant concentration and decrease sharply above it. A lowering of the value of  $I_1/I_3$  is an indication of the solubilization of the probes in a more hydrophobic environment than water and in this case it is surfactant micelle and also with the quencher [23]. The aggregation number of the surfactant was determined by the static fluorescence quenching method using the following equation and also considering the usual following assumptions:

- (I) Static quenching occurs between the fluorescence probe and the quencher molecules so the quenching process does not affect the fluorescence lifetime of the probe.
- (II) Fluorescence lifetime of the probe is much less than the residence times of the quencher and probe inside the micelle.
- (III) The probability of finding a micelle with more than one probe molecule is negligible as because the quencher concentration is very low.

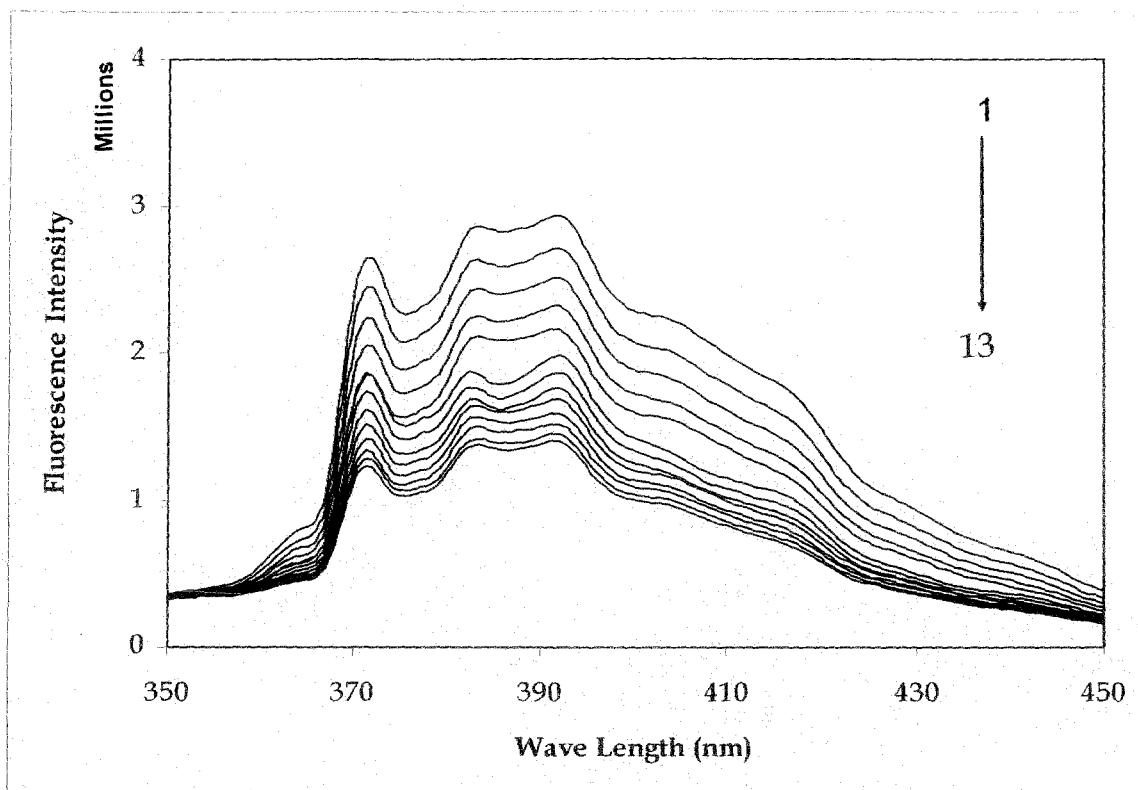
Following Poisson statistics [24] for the description of probe and the quencher among the micelles, the logarithm of  $I_0/I$  takes the form

$$\ln \frac{I_0}{I} = \frac{[Q]N}{([S]_0 - cmc)} \quad (5.7)$$

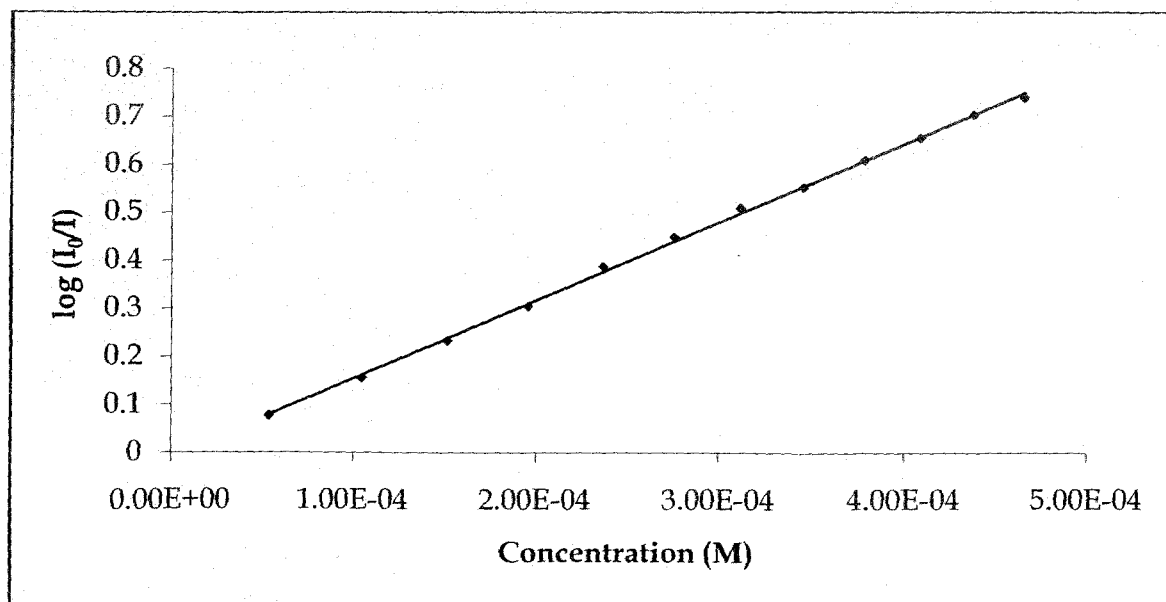
where,  $I_0$  and  $I$  are the intensities of fluorescence without and with quencher.  $[Q]$  is the bulk quencher concentration,  $N$  is the mean aggregation number and  $[S]_0$  is the total surfactant concentration. The aggregation number has been obtained by plotting  $\ln \frac{I_0}{I}$  as a function of quencher concentration.

In the present study, good linear plots for all the surfactants have been obtained satisfying the above equation suggesting constancy of both  $N$  and  $K_{SV}$ . The

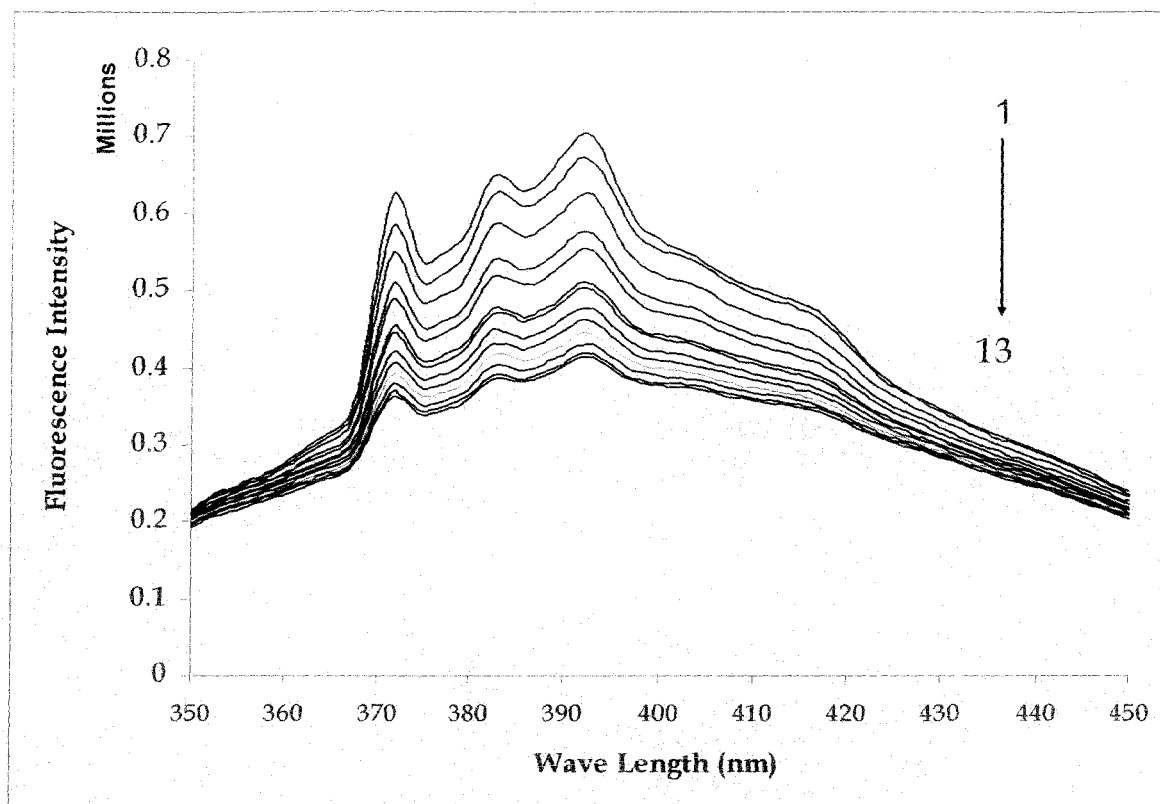
plots of fluorescence measurement for surfactant with different counter ions are shown from figure 5.4 to figure 5.11.



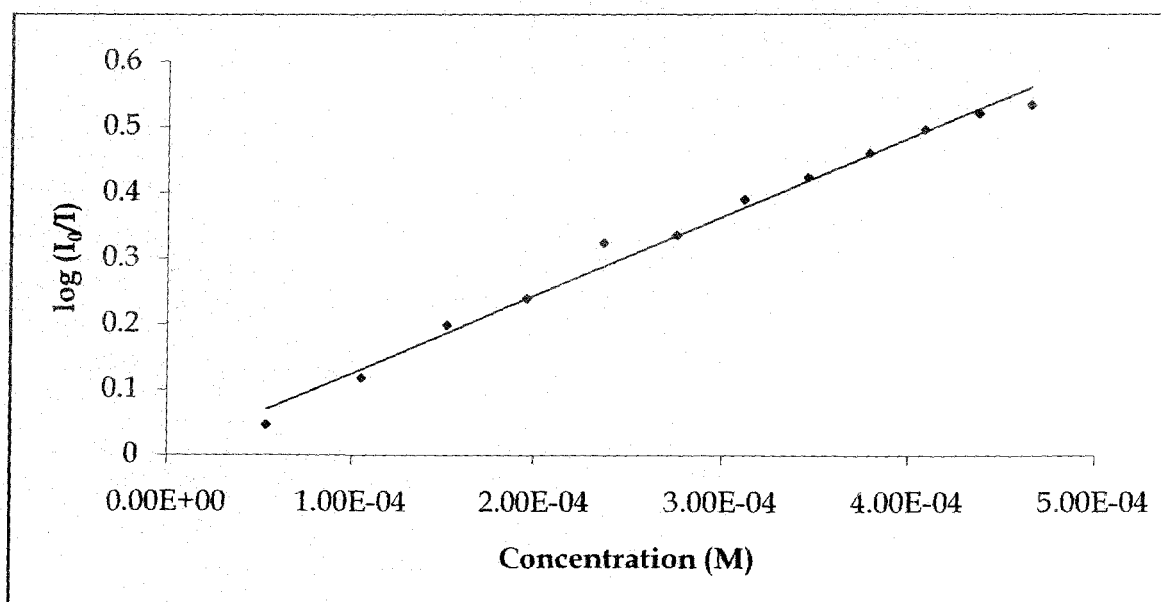
**Figure 5.4(a):** Fluorescence Spectra of pyrene in sodium dodecyl benzene sulfonate with different concentration of CPC in mM (1) 0.0 mM (2) 0.0054 mM (3) 0.105 mM (4) 0.152 mM (5) 0.196 mM (6) 0.237 mM (7) 0.276 mM (8) 0.312 mM (9) 0.346 mM (10) 0.379 mM (11) 0.409 (12) 0.438 mM (13) 0.466 mM



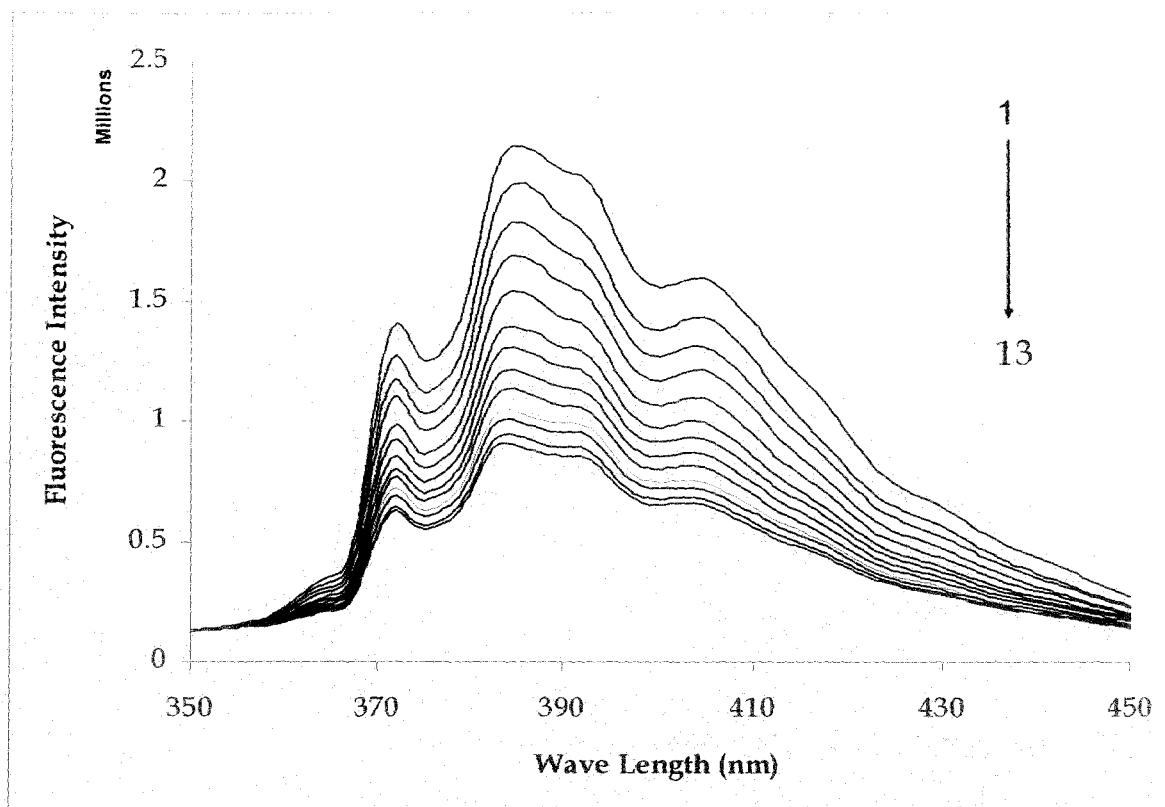
**Figure 5.4(b):** Log (I<sub>0</sub>/I) Vs Concentration (M) plot of Sodium dodecyl benzene sulfonate.



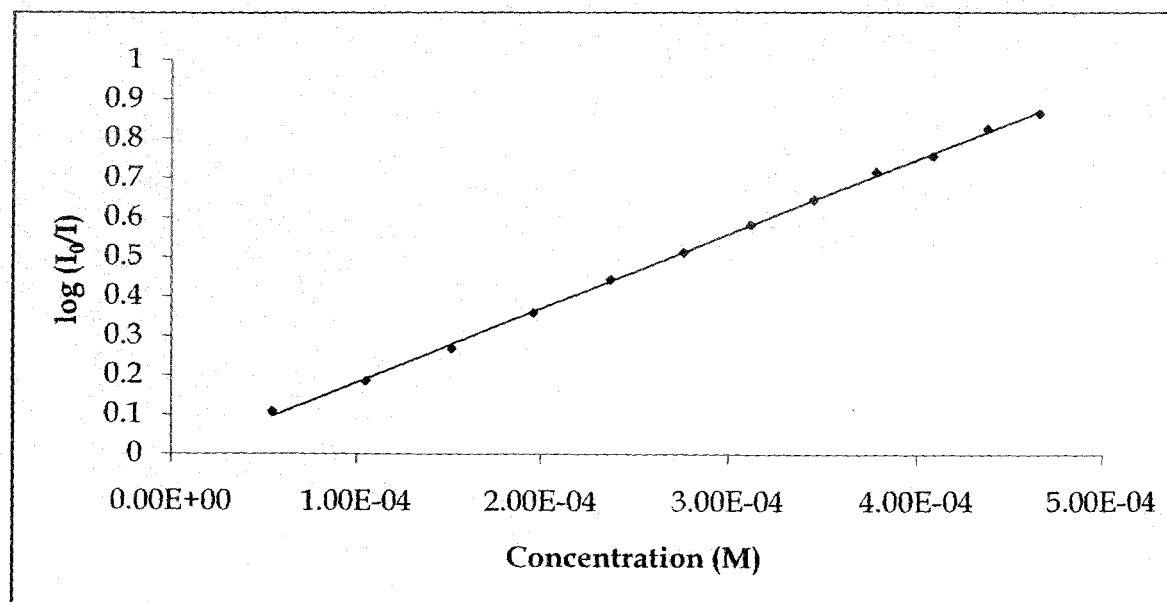
**Figure 5.5(a):** Fluorescence Spectra of pyrene in lithium dodecyl benzene sulfonate with different concentration of CPC in mM (1) 0.0 mM (2) 0.0054 mM (3) 0.105 mM (4) 0.152 mM (5) 0.196 mM (6) 0.237 mM (7) 0.276 mM (8) 0.312 mM (9) 0.346 mM (10) 0.379 mM (11) 0.409 (12) 0.438 mM (13) 0.466 mM



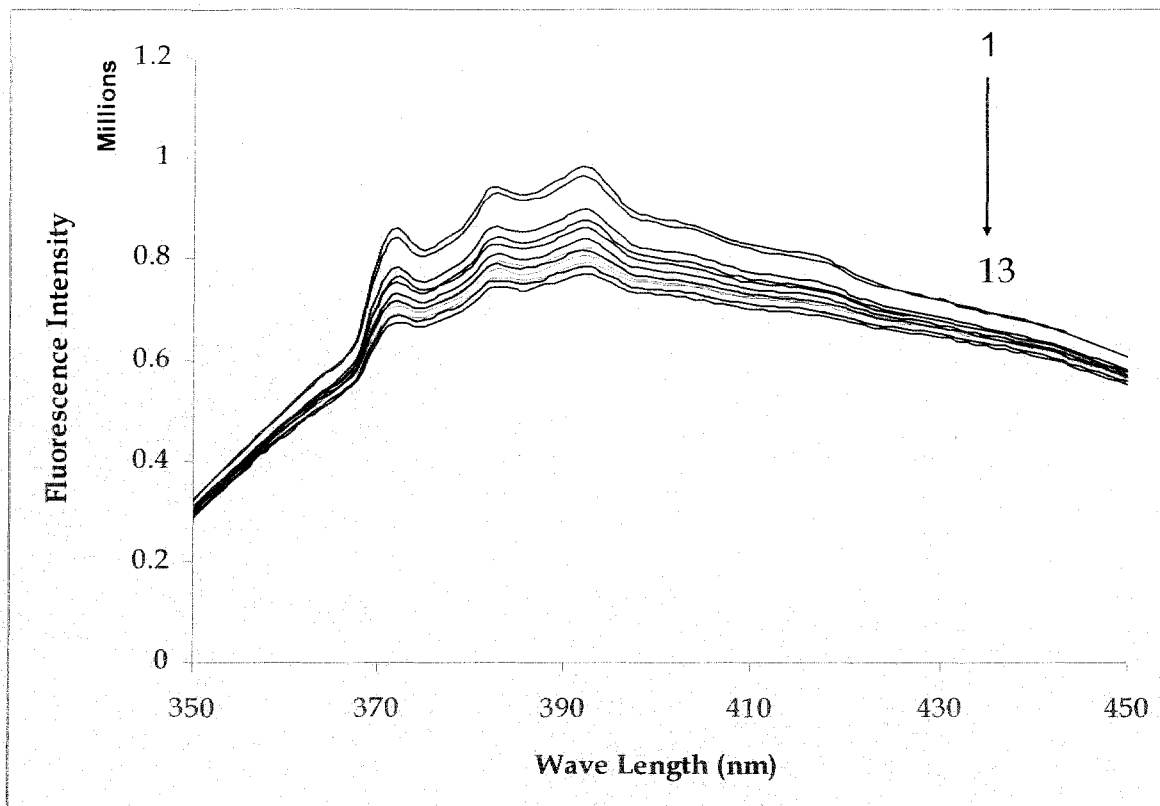
**Figure 5.5(b):** Log ( $I_0/I$ ) Vs Concentration (M) plot of Lithium dodecyl benzene sulfonate.



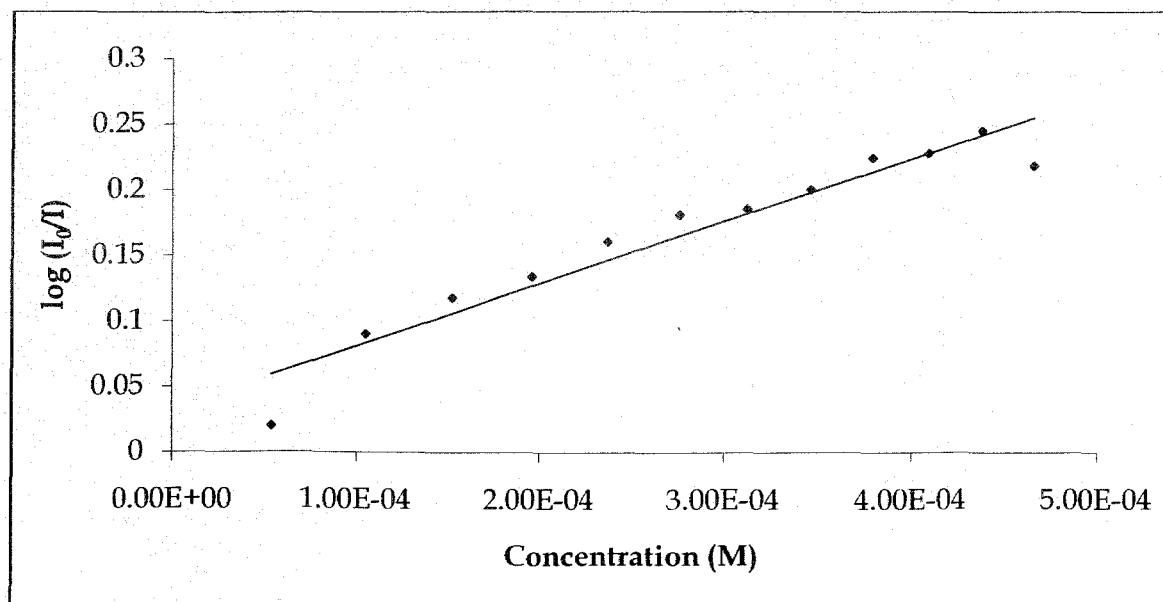
**Figure 5.6(a):** Fluorescence Spectra of pyrene in potassium dodecyl benzene sulfonate with different concentration of CPC in mM (1) 0.0 mM (2) 0.0054 mM (3) 0.105 mM (4) 0.152 mM (5) 0.196 mM (6) 0.237 mM (7) 0.276 mM (8) 0.312 mM (9) 0.346 mM (10) 0.379 mM (11) 0.409 (12) 0.438 mM (13) 0.466 mM



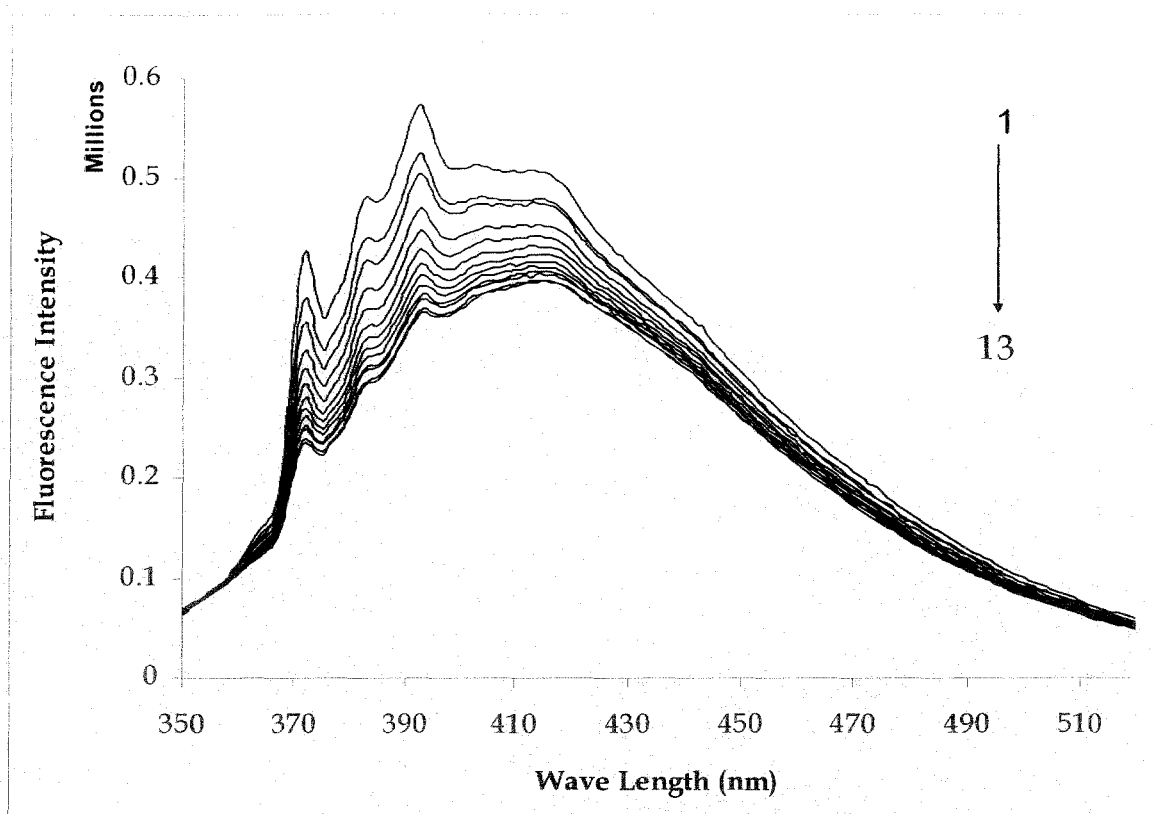
**Figure 5.6(b):** Log ( $I_0/I$ ) Vs Concentration (M) plot of Potassium dodecyl benzene sulfonate.



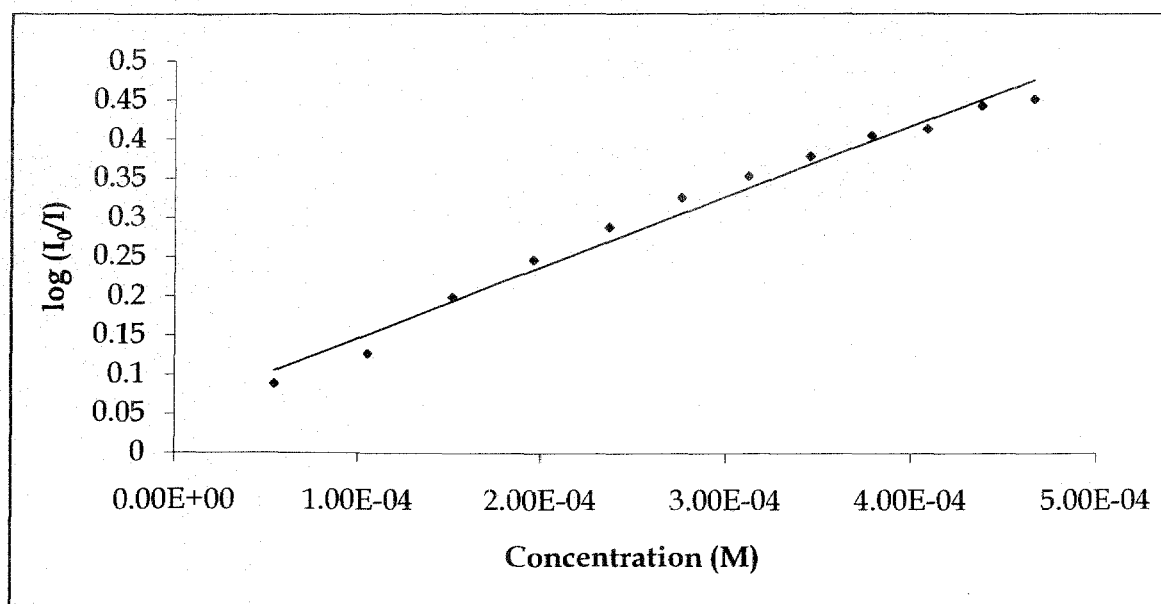
**Figure 5.7(a):** Fluorescence Spectra of pyrene in ammonium dodecyl benzene sulfonate with different concentration of CPC in mM (1) 0.0 mM (2) 0.0054 mM (3) 0.105 mM (4) 0.152 mM (5) 0.196 mM (6) 0.237 mM (7) 0.276 mM (8) 0.312 mM (9) 0.346 mM (10) 0.379 mM (11) 0.409 (12) 0.438 mM (13) 0.466 mM



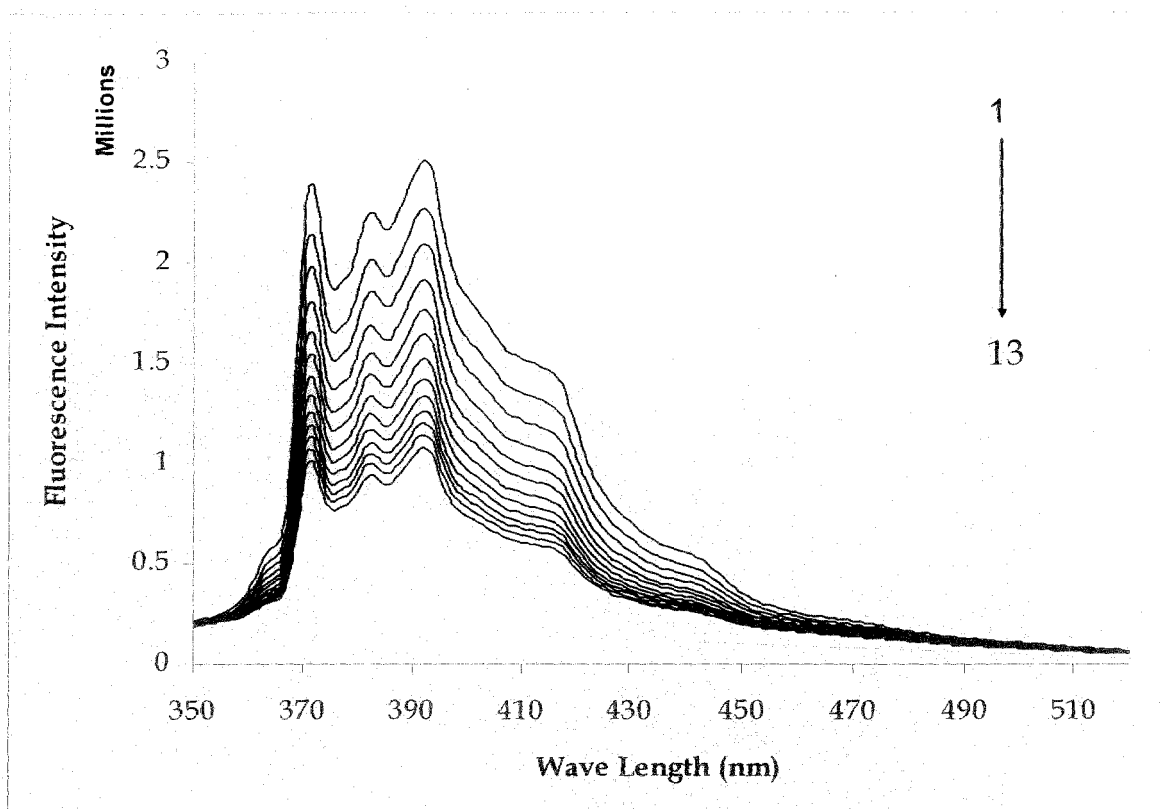
**Figure 5.7(b):** Log ( $I_0/I$ ) Vs Concentration (M) plot of Ammonium dodecyl benzene sulfonate.



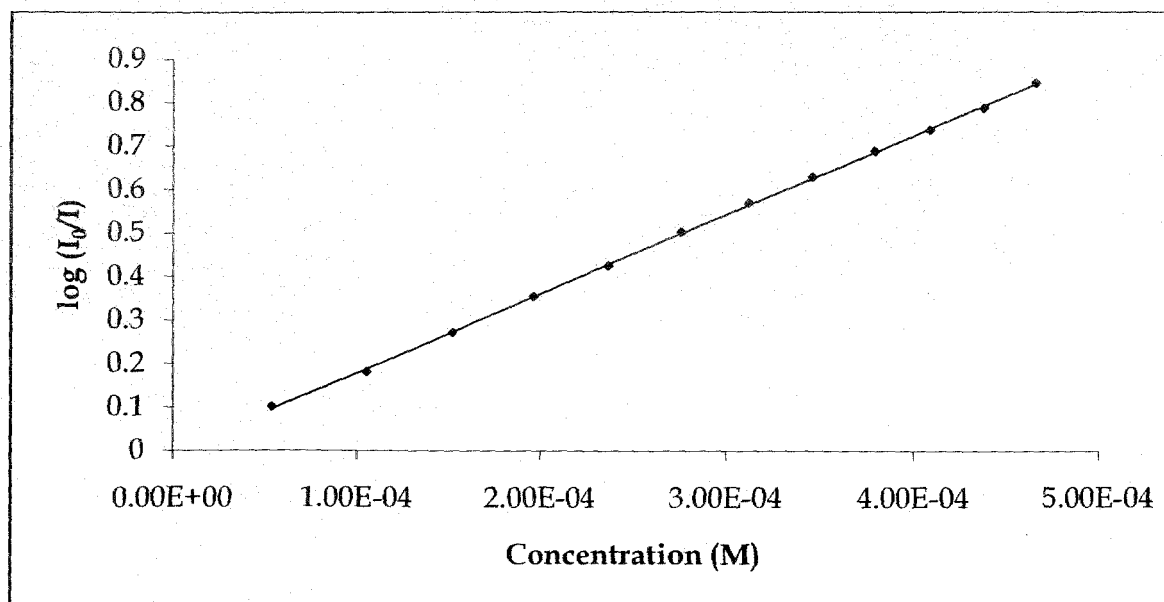
**Figure 5.8(a):** Fluorescence Spectra of pyrene in tetramethyl ammonium dodecyl benzene sulfonate with different concentration of CPC in mM (1) 0.0 mM (2) 0.0054 mM (3) 0.105 mM (4) 0.152 mM (5) 0.196 mM (6) 0.237 mM (7) 0.276 mM (8) 0.312 mM (9) 0.346 mM (10) 0.379 mM (11) 0.409 (12) 0.438 mM (13) 0.466 mM



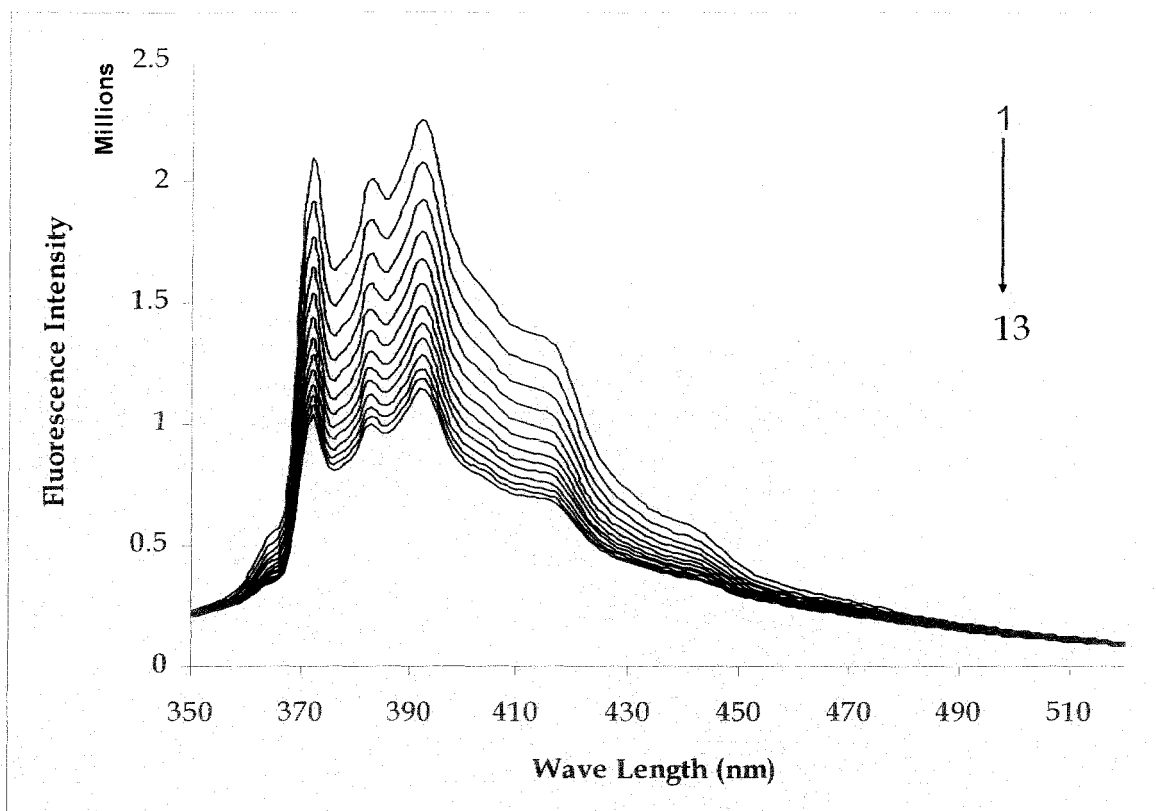
**Figure 5.8(b):** Log ( $I_0/I$ ) Vs Concentration (M) plot of Tetramethyl ammonium dodecyl benzene sulfonate.



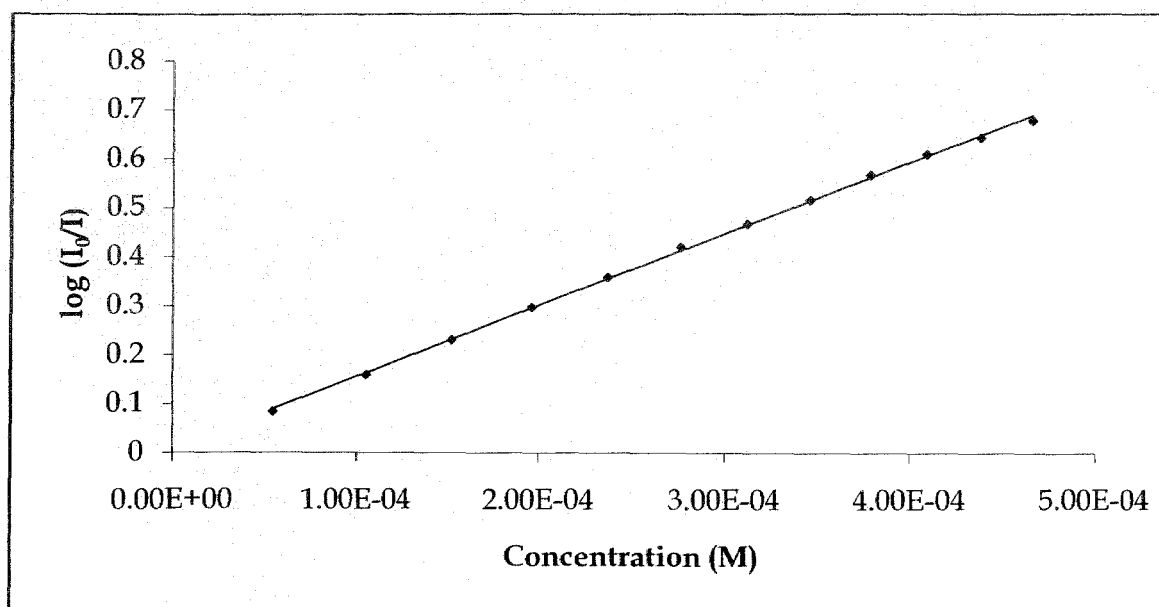
**Figure 5.9(a):** Fluorescence Spectra of pyrene in tetraethyl ammonium dodecyl benzene sulfonate with different concentration of CPC in mM (1) 0.0 mM (2) 0.0054 mM (3) 0.105 mM (4) 0.152 mM (5) 0.196 mM (6) 0.237 mM (7) 0.276 mM (8) 0.312 mM (9) 0.346 mM (10) 0.379 mM (11) 0.409 mM (12) 0.438 mM (13) 0.466 mM



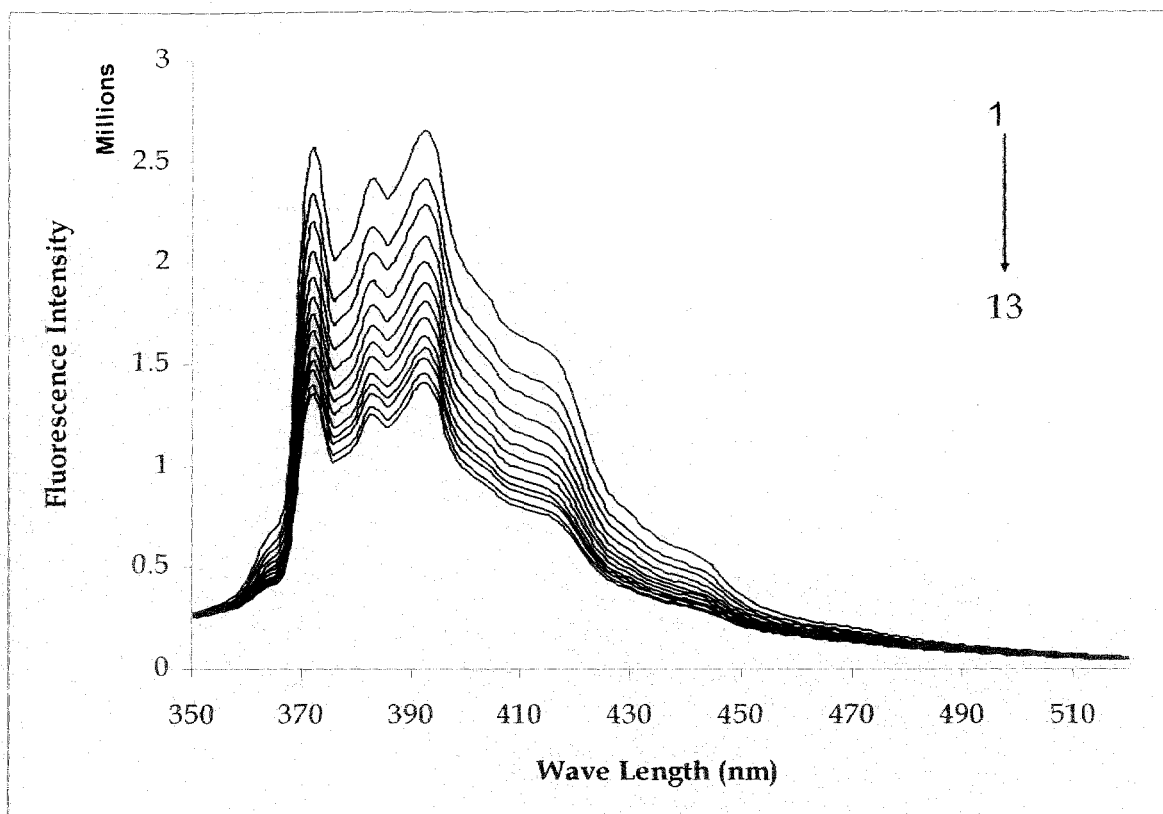
**Figure 5.9(b):** Log ( $I_0/I$ ) Vs Concentration (M) plot of Tetraethyl ammonium dodecyl benzene sulfonate.



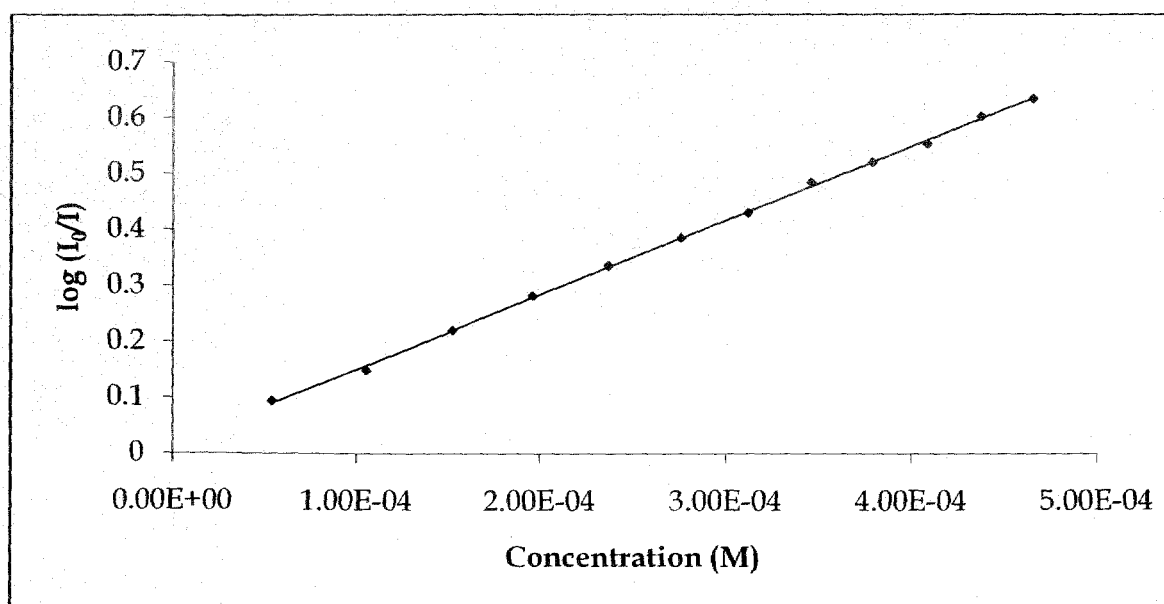
**Figure 5.10(a):** Fluorescence Spectra of pyrene in tetrapropyl ammonium dodecyl benzene sulfonate with different concentration of CPC in mM (1) 0.0 mM (2) 0.0054 mM (3) 0.105 mM (4) 0.152 mM (5) 0.196 mM (6) 0.237 mM (7) 0.276 mM (8) 0.312 mM (9) 0.346 mM (10) 0.379 mM (11) 0.409 (12) 0.438 mM (13) 0.466 mM



**Figure 5.10(b):** Log ( $I_0/I$ ) Vs Concentration (M) plot of Tetrapropyl ammonium dodecyl benzene sulfonate.



**Figure 5.11(a):** Fluorescence Spectra of pyrene in tetrabutyl ammonium dodecyl benzene sulfonate with different concentration of CPC in mM (1) 0.0 mM (2) 0.0054 mM (3) 0.105 mM (4) 0.152 mM (5) 0.196 mM (6) 0.237 mM (7) 0.276 mM (8) 0.312 mM (9) 0.346 mM (10) 0.379 mM (11) 0.409 (12) 0.438 mM (13) 0.466 mM



**Figure 5.11(b):** Log ( $I_0/I$ ) Vs Concentration (M) plot of Tetrabutyl ammonium dodecyl benzene sulfonate.

The ratio of the intensities ( $I_0/I_Q$ ) of fluorescence emission of pyrene in absence ( $I_0$ ) and presence ( $I_Q$ ) of the quencher of surfactant with different counter ions and aggregation number measured at 298 K for all the surfactants in aqueous solutions are given in table 5.1 and table 5.2.

**Table 5.1**

Ratio of the intensities ( $I_0/I_Q$ ) of fluorescence emission of pyrene in the absence ( $I_0$ ) and presence ( $I_Q$ ) of the quencher (CPC) at 373 nm in aqueous solution of dodecyl benzene sulfonate with different counterions at 298 K

[CPC] mM	Ratio of the intensities of surfactant with different counterions ( $I_0/I_Q$ )							
	Na <sup>+</sup>	Li <sup>+</sup>	K <sup>+</sup>	NH <sub>4</sub> <sup>+</sup>	TMA <sup>+</sup>	TEA <sup>+</sup>	TPA <sup>+</sup>	TBA <sup>+</sup>
0.0000	1.0000	1.0000	1.0000	1.0000	1.0000	1.0000	1.0000	1.0000
0.0540	1.0812	1.0469	1.1144	1.0204	1.0921	1.1064	1.0882	1.0882
0.1050	1.1695	1.1251	1.2034	1.0945	1.1354	1.1993	1.1739	1.1739
0.1520	1.2630	1.2194	1.3057	1.1250	1.2198	1.3125	1.2599	1.2599
0.1960	1.3570	1.2700	1.4305	1.1429	1.2784	1.4249	1.3465	1.3465
0.2370	1.4747	1.3812	1.5572	1.1739	1.3333	1.5280	1.4314	1.4314
0.2760	1.5669	1.3984	1.6663	1.1982	1.3837	1.6505	1.5209	1.5209
0.3120	1.6648	1.4765	1.7866	1.2035	1.4225	1.7655	1.5958	1.5958
0.3460	1.7383	1.5264	1.9034	1.2216	1.4593	1.8756	1.6749	1.6749
0.3790	1.8388	1.5831	2.0410	1.2515	1.4983	1.9900	1.7624	1.7624
0.4090	1.9259	1.6406	2.1240	1.2560	1.5110	2.0889	1.8390	1.8390
0.4380	2.0207	1.6814	2.2767	1.2780	1.5568	2.1966	1.9018	1.9018
0.4660	2.0936	1.7038	2.3688	1.2440	1.5703	2.3287	1.9698	1.9698

From the table, it is very clear that the ratio of emission intensity of pyrene changes with the counterions present with the dodecyl benzene sulfonate group of the surfactant.

**Table 5.2.**  
**Aggregation number of the dodecyl benzene sulfonate with different counterions at temperature 298 K.**

Surfactant	Temp./K	Agg. No. ( $N_0$ )
Sodium Dodecyl Benzene Sulfonate (SDBS)	298	27
Lithium Dodecyl Benzene Sulfonate (LDBS)	298	20
Potassium Dodecyl Benzene Sulfonate (PDBS)	298	33
Ammonium Dodecyl Benzene Sulfonate (ADBS)	298	08
Tetramethyl Ammonium Dodecyl Benzene Sulfonate (TMADBS)	298	17
Tetraethyl Ammonium Dodecyl Benzene Sulfonate (TEADBS)	298	34
Tetrapropyl Ammonium Dodecyl Benzene Sulfonate (TPADBS)	298	27
Tetrabutyl Ammonium Dodecyl Benzene Sulfonate (TBADBS)	298	25

Aggregation number increases with alkyl chain length of organic counterions and gives maximum value for tetraethylammonium ion due to hydrophobic interactions of hydrocarbon exterior of the ions with exposed hydrocarbon to the micelle surface. However, for tetrapropyl and tetrabutyl ammonium ions aggregation become increasingly unfavorable due to steric hindrance for increasing counterion size. Here, comparison of aggregation number with ionization degree might be interesting. The ionization degrees of all the surfactants are shown in table 3.2 and table 3.3. The result shows that the values are quite high which indicate that the tetraalkylammonium counter ions are strongly bound to the micelle surface. It is also observed that the counter ion ionization degree increases in the series  $\text{NH}_4^+ \leq \text{N}^+(\text{CH}_3)_4 < \text{N}^+(\text{C}_2\text{H}_5)_4 < \text{N}^+(\text{C}_3\text{H}_7)_4 < \text{N}^+(\text{C}_4\text{H}_9)_4$ . This means that, as expected, the binding increases as the counter ion becomes more and more hydrophobic in nature. The values of cmc also follow the opposite trend, i.e., as the fraction of counter ion binding increases, the micelles are formed at lower concentrations. However, the aggregation number does not follow the expected trend. At 298 K, the aggregation number become minimum in the case of  $\text{NH}_4^+$  counter ion. But as the alkyl groups are substituted for hydrogens, the aggregation number increases because of the formation of larger aggregates which is the consequences of the increased charged screening at higher counter ion binding

capacity via stronger hydrophobic interactions with the micelles. This increasing trend of aggregation number continues up to the tetraethylammonium ions. But for tetrapropyl and tetrabutyl ammonium ions, aggregation number progressively decreases as shown in the table 5.2. This is indeed interesting. Such a complex behaviour of micelle pertaining to the aggregation number with respect to the expected trend on the basis of cmc values is, however, available in the literature [25]. It has been shown that the effect of head group size of tetradecyltrialkylammonium bromide surfactant is very important pertaining to the observed reverse trend of the aggregation number with respect to its cmc. For these surfactants the values of both the cmc and aggregation number,  $N$ , decrease as the size of the tetraalkylammonium head group increases. This effect has been explained in terms of the geometric steric hindrance (overlap) between large trialkylammonium head groups at the micellar surface [26-27]. It seems apparent that in the present systems, as the hydrophobicity of the counter ions increases, the counter ion binding/condensation increases due to increased hydrophobic interactions and eventually the cmc decreases. However, enhanced electrostatic charge screening of the head groups is incapable of increasing the aggregation number of the micelles for tetrapropyl and tetrabutylammonium counter ions. On the other hand, micellar surface probably does not offer sufficient surface area to accommodate all the  $N^+R_4$  counter ions that must bind to the micelle to ensure their stability. Therefore, the micelles become smaller in size and more in number to provide larger surface area in order to pack a large number of counter ions. For alkali metal counter ions, hydration plays an important role along with ionization degree. The table 5.2 shows that among the three alkali metal counter ions, lithium yields minimum aggregation number where as potassium ion yields the maximum. However, among all the counter ions, inorganic and organic, ammonium ions display the lowest value of aggregation number of DBS micelles in aqueous medium.

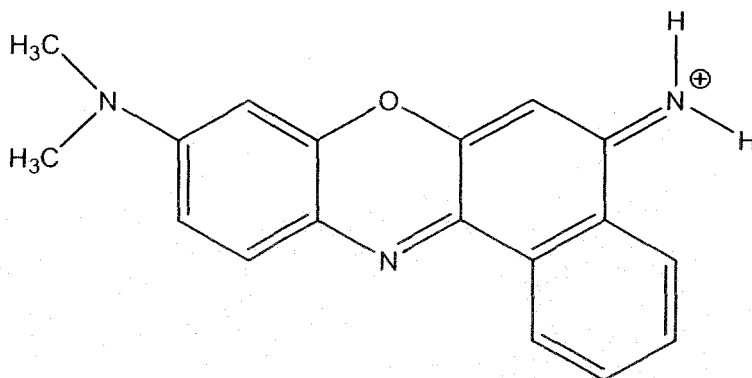
## 5.4. Studies of Interactions with oxazine dye in aqueous media

### 5.4.1. Introduction and review of the previous work

Study of the spectroscopic property of organic dyes in a micellar medium is important for understanding the thermal and light induced reactions in biomembranes (28-40). Such reactions proceed through the involvement of excited and free radical species whose behaviour in a micellar medium can be significantly different from that in a homogeneous medium. Cresyl Fast violet, an oxazine dye, has been used as a sensitizer in photo-galvanic devices [41-42]. Dye sensitization of wide band gap semiconductor particles is of current interest particularly for harnessing solar energy and for various other applications [43-47]. The dye surfactant interactions have also been the subject of many studies in view of the fact that they mimic many biological processes taking place between the large organic molecules and biomembrane and can act as a model redox system [48-51]. Further, such interaction between ionic dye and charged surfaces is of interest in numerous applications ranging from the design of electronic devices to the characterization of drug-delivery systems [52]. In view of the above, we have under taken a detailed study to understand the effects of surfactants on the spectroscopic properties of cresyl violet with anionic surfactants because only anionic surfactants have pronounced effect.

In the present experiment, we use an oxazine dye with dodecyl benzene sulfonate with varying counterions. The oxazine dyes display surprising long-wavelength absorption and emission maxima in fluorescence which makes these groups of dye an important fluorescent probe. Extended conjugated systems result in long absorption and emission wavelengths for these types of dye due to their comparatively small size [53-54]. Dyes of this class have been extensively characterized for use as long-wavelength probes and in DNA sequencing [55]. Dyes of this type are also used for staining DNA restriction fragments during capillary electrophoresis. We have studied the steady-state spectra of surfactants by a typical oxazine dye, Cresyl fast violet. This may be of interest for a number of reasons: it could give a better insight of the nature of interaction in the surfactant aggregate system; it may explain the previously observed temperature dependence of monomer spectra of some dyes [56-57] and none the less, it can test the applicability of the

exciton theory in molecular aggregate systems in further detail. Schematic representation of the dye is given in Figure 5.12.



**Figure 5.12:** Schematic representation of Cresyl Fast Violet (CFV)

#### 5.4.2. Materials and methods

##### Materials

Cresyl fast Violet (CFV) was supplied by Aldrich Chemical Co., USA and was used after recrystallization from water-ethanol mixture. SDBS was purchased from Acros Organics, USA. (Product code 325912500). Surfactants, viz., LDBS, KDBS, ADBS, TMADBS, TEADBS, TPADBS and TBADBS were prepared in our laboratory by ion-exchange method as discussed in the previous chapter.

##### Methods

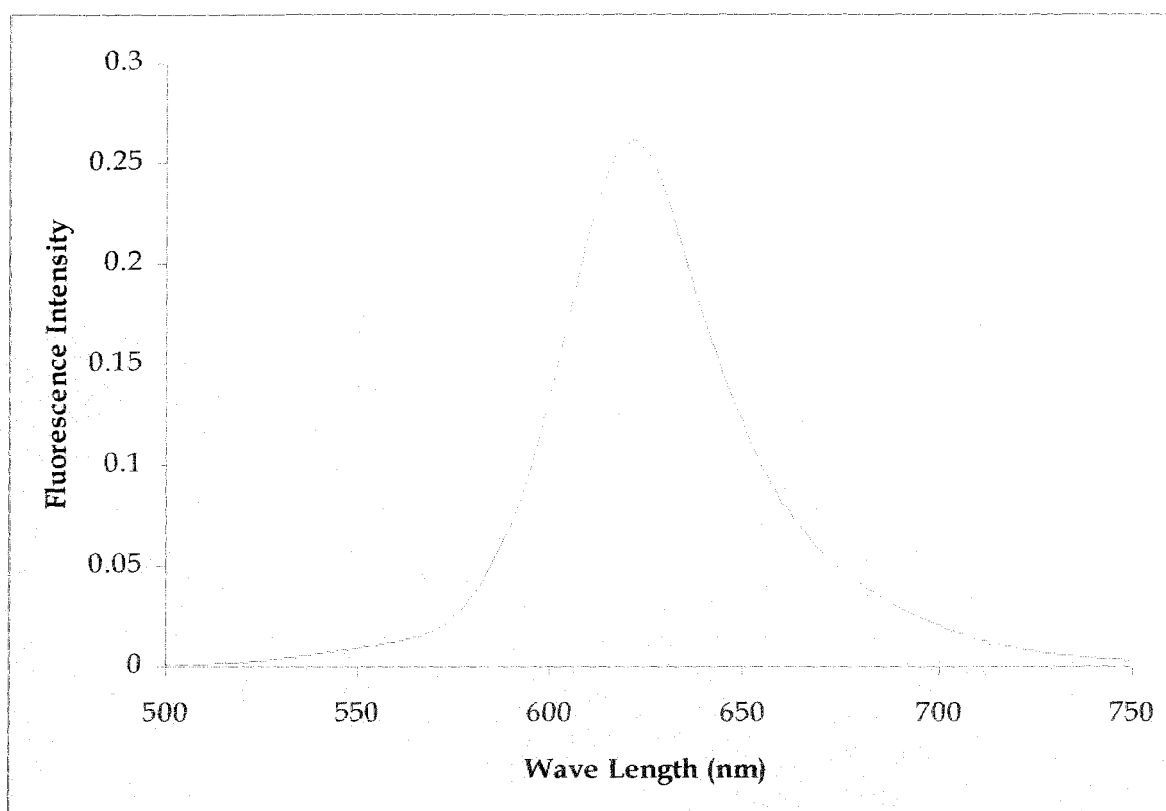
Steady-state emission spectra were done in a Fluorescence Spectrophotometer, Photon Technology Inc. Co., USA. In all the experiment, the concentration of the dye is very low,  $1 \times 10^{-6}$  (M). Quartz cuvettes and double distilled water were employed throughout the experiments. Excitation and emission slit widths were set at 0.20 nm, 0.60 nm, 0.50 nm and 1.50 nm for all the four slits respectively. The excitation wavelength was set at 584 nm for cresyl fast violet solutions. The emission spectra were recorded from 500 nm to 750 nm for all the dye & surfactant mixtures. The emission wave length for the dye is found to be 620 nm.

### 5.4.3. Results and discussions

The surfactant dodecylbenzene sulfonate consists of hydrophilic ends attached to long nonpolar organic chains. The presence of surfactants increases the free energy of a system by distorting the structure of the water molecules in aqueous solution. In aqueous solutions, micelles are usually spherical with the polar ends on their surfaces and the nonpolar organic chains on the inside. The organic micelle interiors will essentially become pockets of another solvent within the aqueous solution. Nonpolar molecules will tend to migrate into this region and will experience a much different environment there than they would in the bulk aqueous solution.

The spectral characteristics of dyes are known to change when dissolved in surfactant micelles [58-59]. Based on their structures, it is not surprising that DBS moiety and the cresyl fast violet readily interact. All the species have both organic and polar parts, so they can interact with each other through non-polar interactions, polar/ionic interactions or both. Due to these dye-surfactant interactions, the changes in spectral characteristics are observed qualitatively. In this experiment, a very low concentration of dye ( $\sim 5 \times 10^{-6}$  M) is used to overcome the effects of dye-dye interactions via possible dimer formation by the dye molecules. In addition to dye-solvent interactions, dye-surfactant and dye-micelle interactions are possible in solutions containing both dye and surfactants [59]. At concentration below the normal cmc, surfactants and dyes can interact to form a mixed micelle of the two species, lowering the resultant cmc. Above the cmc, a change in the molecular environment of the dye due to incorporation into the micelle interior is observed [52].

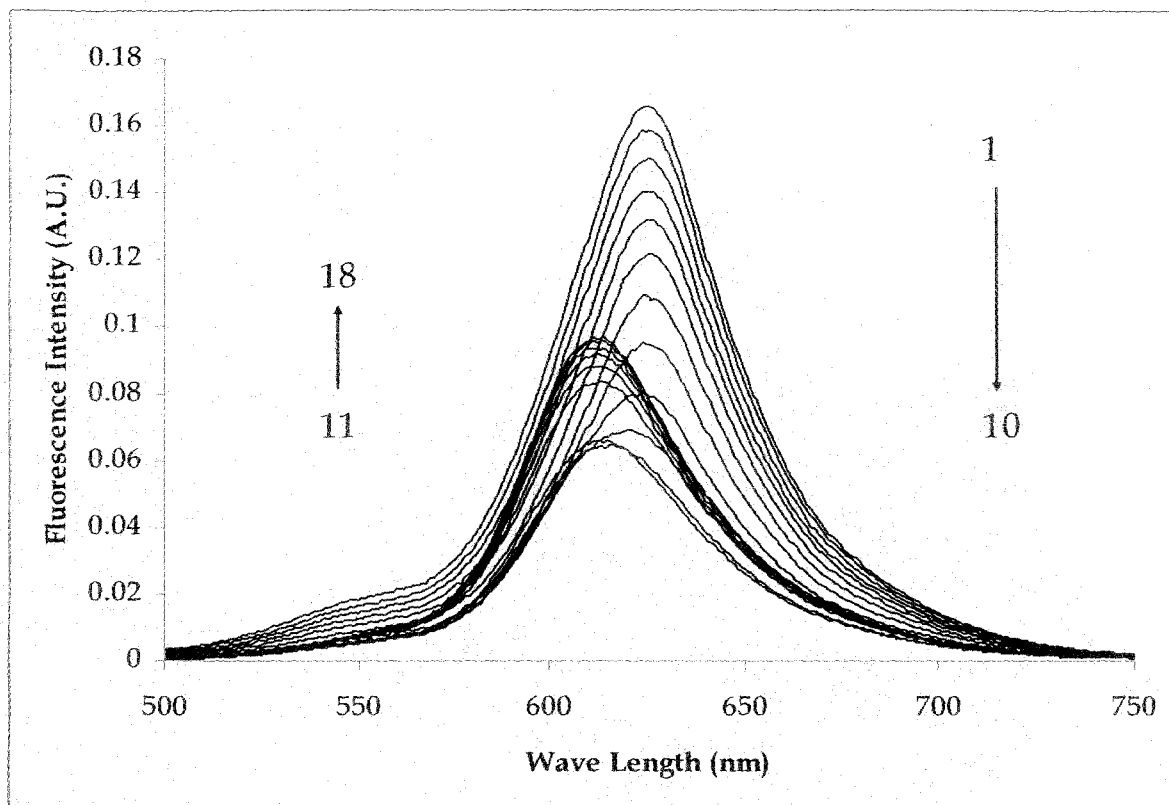
The fluorescence spectra of the cresyl fast violet vary with surfactant concentration. The spectra of cresyl fast violet without surfactants showed a single peak at 624 nm as shown in the Figure 5.13.



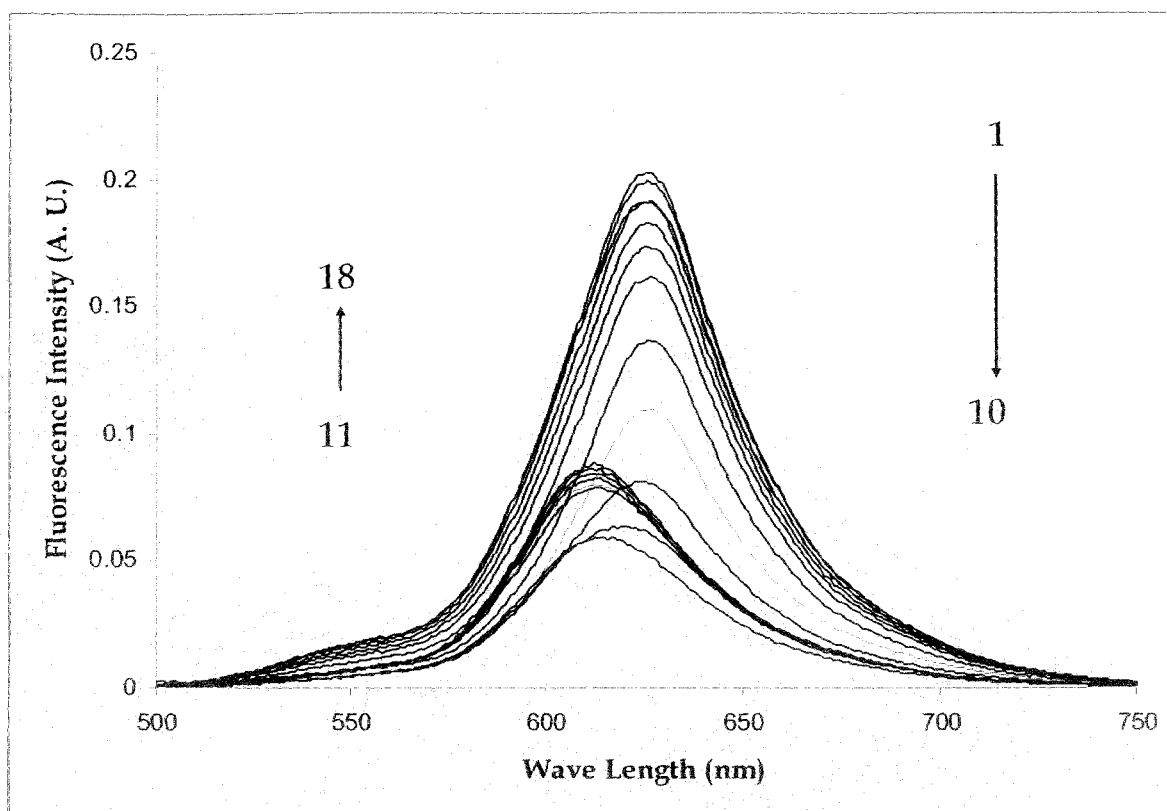
**Figure 5.13.** Fluorescence emission spectrum of cresyl fast violet (CSV), excitation wave length at 584 nm.

At concentrations of surfactants below the cmc, the fluorescence intensity decreases continuously with increase in surfactant concentration. When the surfactant concentration reaches cmc, the intensity starts increasing continuously with increase in surfactant concentration. The fluorescence spectra of dye in all the surfactant show similar behaviour with the change of surfactant concentrations. However, above cmc, the fluorescence intensities increase. The result suggests that the free monomer is tied up in ion pair or clusters. Above the cmc the fluorescence intensity increases to almost same or very close to that of the cresyl fast violet solution without the surfactant. This shows that above the cmc the dye is freed from the interaction just discussed. Since the emission intensity is same or to some extent lower as compared to the free dye, it may be argued that there was no other interaction between dye and surfactant present. Change in the absorption spectrum and decrease in fluorescence intensities below the cmc's of anionic surfactants could be attributed to the formation of ion-pair complexes of the dye with oppositely charged surfactants. At surfactant concentrations above the cmc the dye band intensity is restored with red shift. Similar result of dye surfactant interaction was also observed by other researchers [52, 58-59].

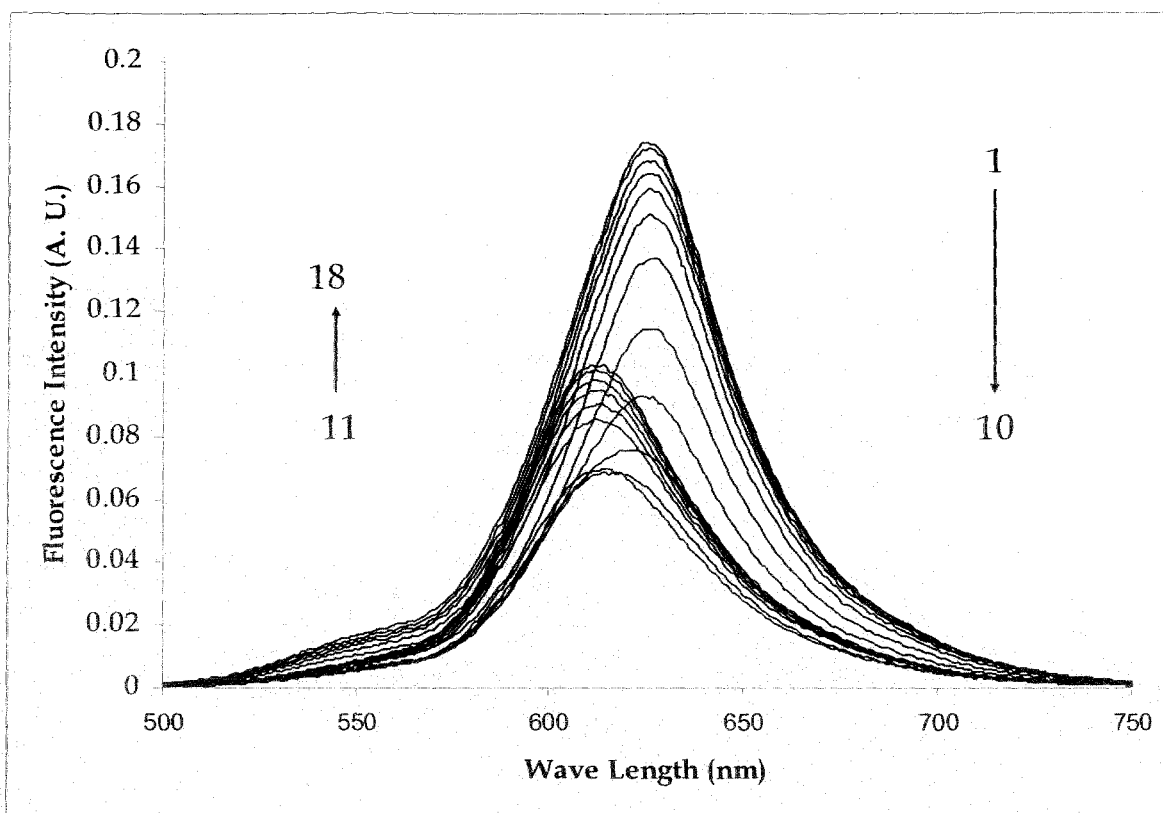
The steady-state plot of fluorescence emission intensity vs. wave length for all the surfactants are as follows (figure 5.14 to figure 5.21):



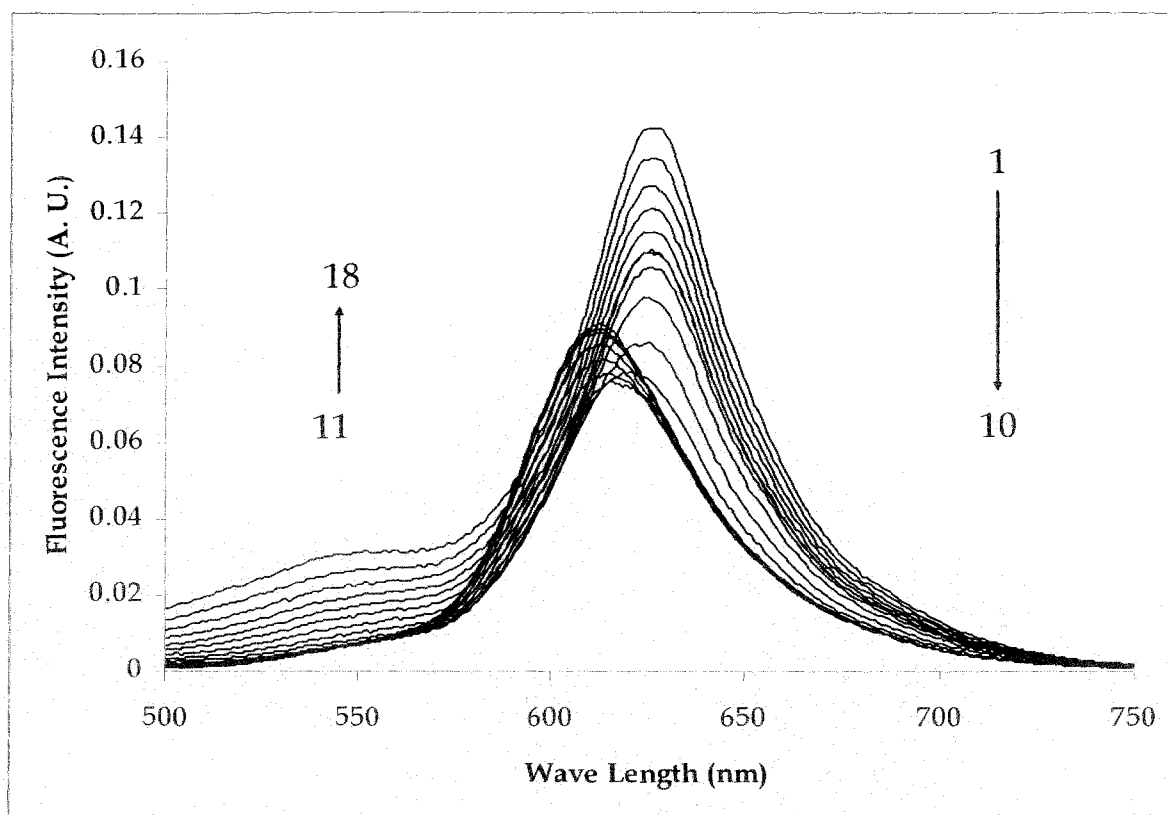
**Figure 5.14:** Fluorescence spectra of dye in lithium dodecyl benzene sulfonate having concentrations (1) 10 mM (2) 8 mM (3) 6.4 mM (4) 5.12 mM (5) 4.10 mM (6) 3.28 mM (7) 2.62 mM (8) 2.10 mM (9) 1.68 mM (10) 1.34 mM (11) 1.07 mM (12) 0.859 mM (13) 0.687 mM (14) 0.550 mM (15) 0.440 mM (16) 0.352 mM (17) 0.281 mM (18) 0.225 mM at 298 K.



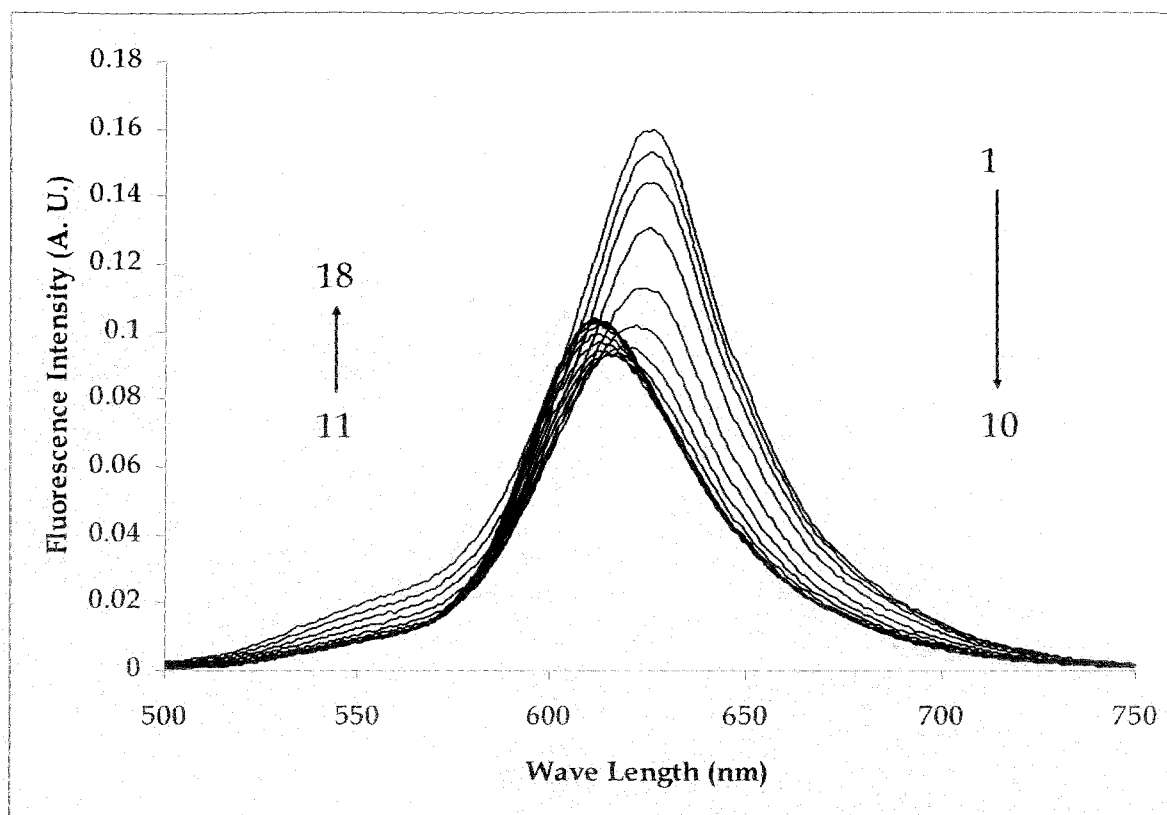
**Figure 5.15:** Fluorescence spectra of dye in sodium dodecyl benzene sulfonate having concentrations (1) 10 mM (2) 8 mM (3) 6.4 mM (4) 5.12 mM (5) 4.10 mM (6) 3.28 mM (7) 2.62 mM (8) 2.10 mM (9) 1.68 mM (10) 1.34 mM (11) 1.07 mM (12) 0.859 mM (13) 0.687 mM (14) 0.550 mM (15) 0.440 mM (16) 0.352 mM (17) 0.281 mM (18) 0.225 mM at 298 K.



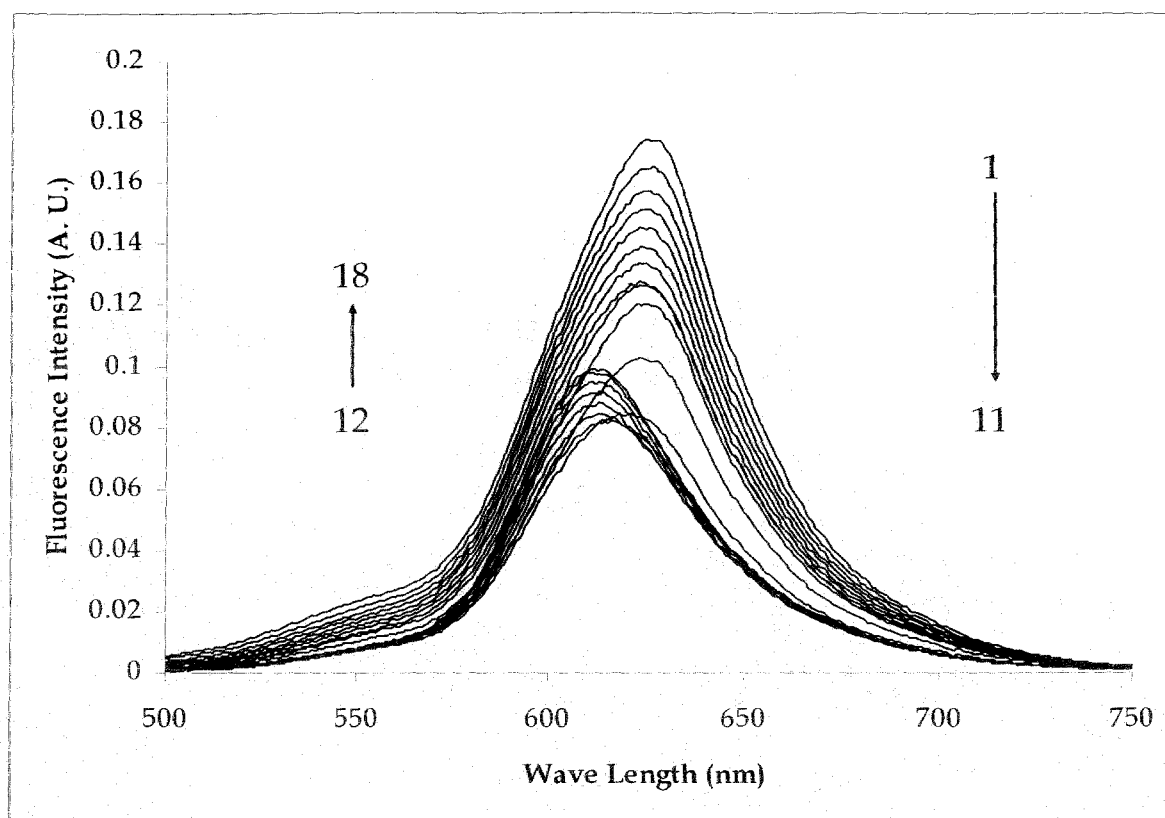
**Figure 5.16:** Fluorescence spectra of dye in potassium dodecyl benzene sulfonate having concentrations (1) 10 mM (2) 8 mM (3) 6.4 mM (4) 5.12 mM (5) 4.10 mM (6) 3.28 mM (7) 2.62 mM (8) 2.10 mM (9) 1.68 mM (10) 1.34 mM (11) 1.07 mM (12) 0.859 mM (13) 0.687 mM (14) 0.550 mM (15) 0.440 mM (16) 0.352 mM (17) 0.281 mM (18) 0.225 mM at 298 K.



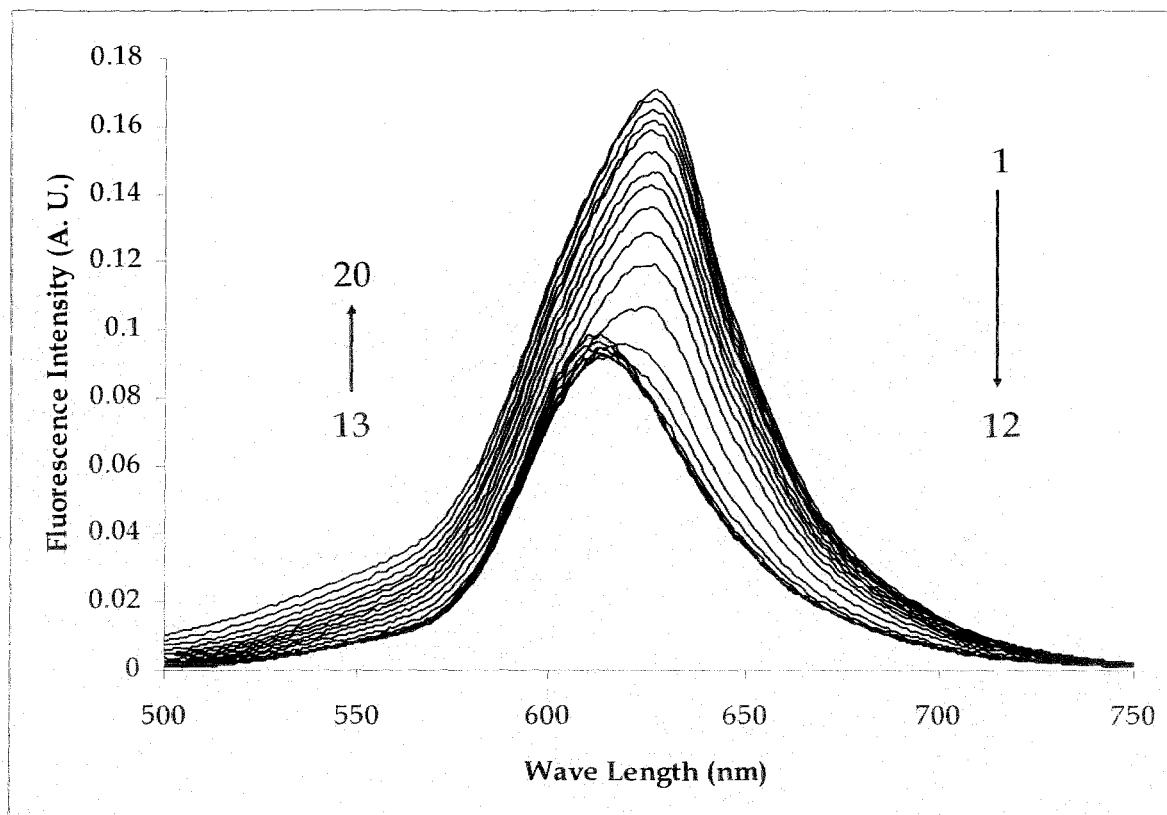
**Figure 5.17:** Fluorescence spectra of dye in ammonium dodecyl benzene sulfonate having concentrations (1) 10 mM (2) 8 mM (3) 6.4 mM (4) 5.12 mM (5) 4.10 mM (6) 3.28 mM (7) 2.62 mM (8) 2.10 mM (9) 1.68 mM (10) 1.34 mM (11) 1.07 mM (12) 0.859 mM (13) 0.687 mM (14) 0.550 mM (15) 0.440 mM (16) 0.352 mM (17) 0.281 mM (18) 0.225 mM at 298 K.



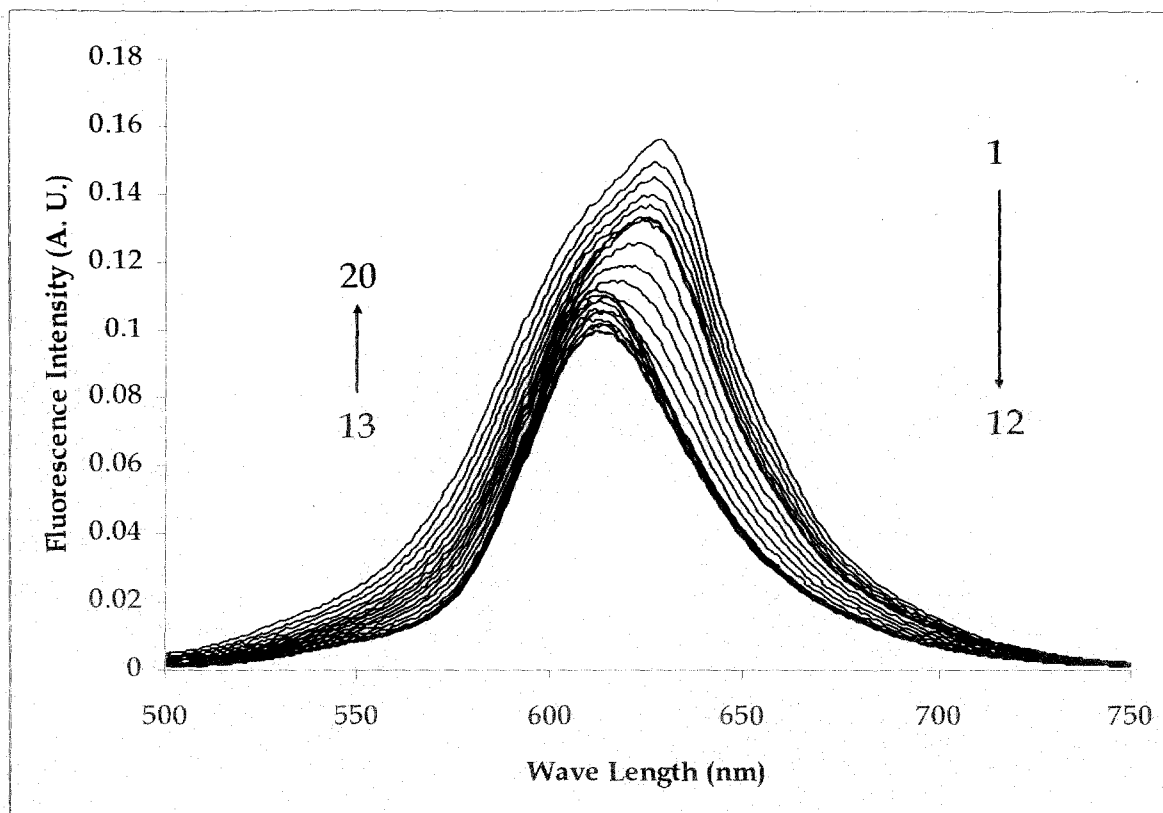
**Figure 5.18:** Fluorescence spectra of dye in tetramethyl ammonium dodecyl benzene sulfonate having concentrations (1) 10 mM (2) 8 mM (3) 6.4 mM (4) 5.12 mM (5) 4.10 mM (6) 3.28 mM (7) 2.62 mM (8) 2.10 mM (9) 1.68 mM (10) 1.34 mM (11) 1.07 mM (12) 0.859 mM (13) 0.687 mM (14) 0.550 mM (15) 0.440 mM (16) 0.352 mM (17) 0.281 mM (18) 0.225 mM at 298 K.



**Figure 5.19:** Fluorescence spectra of dye in tetraethyl ammonium dodecyl benzene sulfonate having concentrations (1) 10 mM (2) 8 mM (3) 6.4 mM (4) 5.12 mM (5) 4.10 mM (6) 3.28 mM (7) 2.62 mM (8) 2.10 mM (9) 1.68 mM (10) 1.34 mM (11) 1.07 mM (12) 0.859 mM (13) 0.687 mM (14) 0.550 mM (15) 0.440 mM (16) 0.352 mM (17) 0.281 mM (18) 0.225 mM at 298 K.



**Figure 5.20:** Fluorescence spectra of dye in tetrapropyl ammonium dodecyl benzene sulfonate having concentrations (1) 10 mM (2) 8 mM (3) 6.4 mM (4) 5.12 mM (5) 4.10 mM (6) 3.28 mM (7) 2.62 mM (8) 2.10 mM (9) 1.68 mM (10) 1.34 mM (11) 1.07 mM (12) 0.859 mM (13) 0.687 mM (14) 0.550 mM (15) 0.440 mM (16) 0.352 mM (17) 0.281 mM (18) 0.225 mM (19) 0.180 mM (20) 0.144 mM at 298 K.



**Figure 5.21:** Fluorescence spectra of dye in tetrabutyl ammonium dodecyl benzene sulfonate having concentrations (1) 10 mM (2) 8 mM (3) 6.4 mM (4) 5.12 mM (5) 4.10 mM (6) 3.28 mM (7) 2.62 mM (8) 2.10 mM (9) 1.68 mM (10) 1.34 mM (11) 1.07 mM (12) 0.859 mM (13) 0.687 mM (14) 0.550 mM (15) 0.440 mM (16) 0.352 mM (17) 0.281 mM (18) 0.225 mM (19) 0.180 mM (20) 0.144 mM at 298 K.

From all these figures, it can be concluded that at the concentration of the surfactant below cmc, there is also surfactant and dye interaction. With increase in surfactant concentration, fluorescence intensity (A.U.) dropped continuously. After this, the fluorescence intensity increases which show that the monomer is freed from ion-pair or cluster causing increase in fluorescence intensity. The order of the ion pair formation or cluster formation for alkali metal counter ions is as follows:  $\text{Li}^+ > \text{K}^+ > \text{Na}^+$  and for tetraalkyl ammonium counter ion along with ammonium ion is as follows:  $\text{NH}_4^+ > (\text{C}_4\text{H}_9)_4\text{N}^+ > (\text{C}_3\text{H}_7)_4\text{N}^+ > (\text{C}_2\text{H}_5)_4\text{N}^+ > (\text{CH}_3)_4\text{N}^+$ . The counter ion, lithium, has the smallest alkali metal ion with largest hydration sphere causing incorporation of dye into the surfactant. Recent study of this type of complex formation via charge transfer process or electron donor-acceptor complexes was also observed by some researches [60]. The fluorescence intensity of SDBS is greater than LDBS which indicates dye molecules are more free to form the ion-pair or cluster in SDBS due to its

larger size and less attraction. For potassium counter ion, the dye molecules are more free from surfactant compared to lithium but less free from sodium can be explained with increase size of alkali metals and decreasing hydration sphere contributing to the hydrophobic effect for the formation of micelle. The size of the counter ion ammonium is greater than cesium ion but less than tetramethyl ammonium ion which is less free from surfactant compared to all the alkali metal ions due to decreasing hydration sphere contributing to the hydrophobic effect for the formation of micelle. In tetrabutyl ammonium dodecyl benzene sulfonate, the counter ion is tetrabutyl ammonium group which is most hydrophobic in nature as compared to the other groups present. Tetramethylammonium counter ion does not follow the expected trend. The trend can be explained as the consequences of the increased charged screening and higher counter ion binding capacity via stronger hydrophobic interactions with the micelles. In the present study, it is found for all the counter ion that the cmc is lowered which is due to the interactions present between the surfactant and the dye. It is clear that in every case there is a red shift of the peak intensity. This shift is not similar in all the different surfactant because the interaction of the surfactant with the dye is different with change of the counterion. As the counterion gets bulky for the group of tetraalkylammonium ions, the blue shift get increased due to the hydrophobicity present in the group.

To study the quenching of the non-fluorescent aggregates formed with increasing dye concentration, Stern - Volmer (SV) plots were obtained from steady state fluorescence data. Here, the Stern - Volmer equation is

$$\frac{F_0}{F} = 1 + K_{SV} [Q] \quad (5.8)$$

Where  $F$  is the fluorescence intensity in presence of quencher;  $F_0$  is the fluorescence intensity in absence of quencher;  $[Q]$  is the quencher concentration and  $K_{SV}$  is the Stern-Volmer constant, which is equal to  $k_q \tau_0$ ;  $k_q$  is the quenching constant and  $\tau_0$  is the life time of the fluorophore in absence of quencher. Here, the aggregates are the quenchers. Thus,  $[Q] \propto [M]$ , where  $[M]$  is the monomer concentration [59].

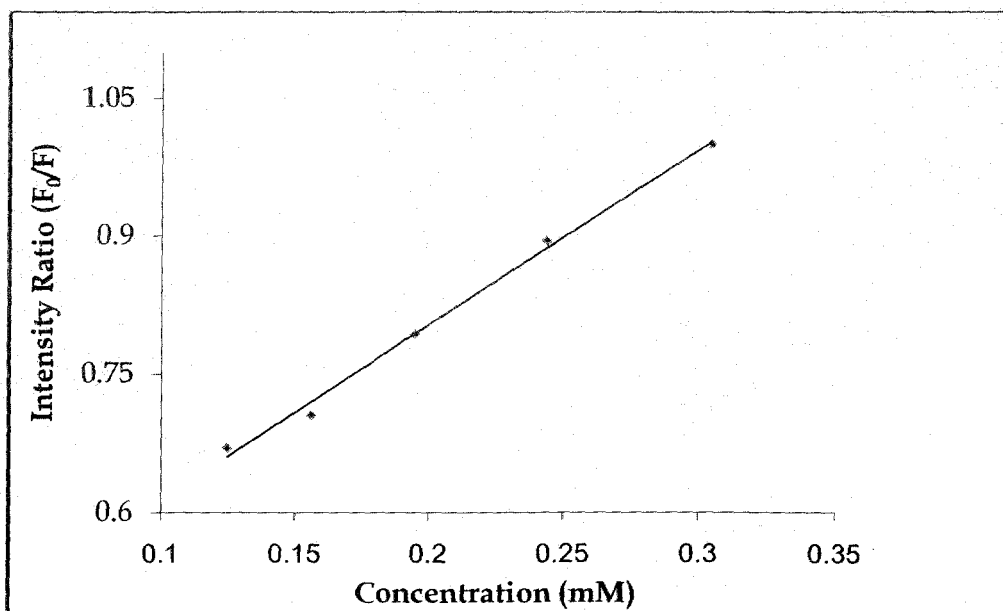
In our present case for all the surfactants, the Stern - Volmer plots deviate from linearity at high dye concentrations. Their upward curvature clearly suggests that both

static quenching and collisional quenching are present here [61]. We have calculated the Stern - Volmer constant for all the surfactants which are given in the table below:

**Table 5.3:**  
Stern-Volmer ( $K_{SV}$ ) Constants for all the surfactants

Surfactants	$K_{SV}/M^{-1}$
SDBS	$1.90 \times 10^3$
LDBS	$1.30 \times 10^3$
PDBS	$1.04 \times 10^3$
ADBS	$7.53 \times 10^4$
TMADBS	$6.19 \times 10^4$
TEADBS	$5.43 \times 10^4$
TPADBS	$4.36 \times 10^4$
TBADBS	$2.95 \times 10^4$

A representative plot for sodium dodecyl benzene sulfonate surfactant to calculate stern -volmer constant is given in figure 5.22.



**Figure 5.22:** Fluorescence intensity ratio vs. concentration (mM) of sodium dodecyl benzene sulfonate surfactant.

Here, from the Stern - Volmer constant values we see that most of the constants are of the same order. However, a closer look at the Stern-Volmer constant values, which are

the measure of the extent of the interaction of dye in the excited states with the surfactant at sub-micellar concentrations, show that such interaction is almost same for all the inorganic counter ions. For the organic counter ions, on the other hand, extent of interaction decreases as the size of the counter ion increases. Therefore, quenching of dye fluorescence due to collision and energy transfer by either the monomer or the dimer is possible though there is some discrepancies which may be due to the size and hydrophobicity of the counterion present with the dodecyl benzene sulfonate moiety.

## 5.5 Anisotropy

### 5.5.1. Theory of anisotropy

Anisotropy measurements are commonly used in the bio-chemical application of fluorescence. Anisotropy measurements provide information on the size and shape of proteins or the rigidity of various molecular environments. Anisotropy measurements have been used to measure protein-protein associations and fluidity of membranes and for immunoassays of numerous substances. Anisotropy measurements are based on the principle of photoselective excitation of fluorophores by polarized light. Fluorophores preferentially absorb photons whose electric vectors are aligned parallel to the transition moment of the fluorophore. The transition moment has a defined orientation with respect to the molecular axes. In an isotropic solution, the fluorophores are oriented randomly. Upon excitation with polarized light, one selectively excites those fluorophore molecules whose absorption transition dipole is parallel to the electric vector of the excitation. This selective excitation results in a partially oriented population of fluorophores (photoselection) and in partially polarized fluorescence emission. Emission also occurs with the light polarized along a fixed axis in the fluorophore. The relative angle between these moments determines the maximum measured anisotropy. The fluorescence anisotropy ( $r$ ) and polarization ( $P$ ) are defined by

$$r = \frac{I_{\parallel} - I_{\perp}}{I_{\parallel} + 2I_{\perp}} \quad (5.9)$$

$$P = \frac{I_{\parallel} - I_{\perp}}{I_{\parallel} + I_{\perp}} \quad (5.10)$$

where  $I_{\parallel}$  and  $I_{\perp}$  are the fluorescence intensities of the vertically and horizontally polarized emission, when the sample is excited with vertically polarized light. That is anisotropy is the absorption of light by a fluorophore along a particular direction with respect to the molecular axes.

In the present experiment, the oxazine dye with dodecyl benzene sulfonate with varying counter ions has been used. As discussed in the previous part, the oxazine dyes display surprising long-wavelength absorption and emission maxima in fluorescence which makes these groups of dye an important fluorescent probe. We have studied the anisotropy measurements of surfactants by Cresyl fast violet (CFV).

### 5.5.2 Materials and methods

#### Materials

As discussed in the previous part of this chapter.

#### Methods

Anisotropy measurement was done with the same Fluorescence Spectrophotometer, Photon Technology Inc. Co., USA. In all the experiment, the concentration of the dye is very low,  $1 \times 10^{-6}$  (M). Quartz cuvettes were employed throughout the measurements of anisotropy measurements. The data were analyzed with the software given "Felix GX" with the instruments to get the polarization values.

### 5.5.3 Results and discussions

The anisotropy/polarization data of surfactant-cresyl fast violet solution derived by the software 'Felix GX', supplied by the manufacturer with the fluorescence spectrophotometer instrument, as a function of surfactant concentration are shown in Table 5.4.

**Table 5.4.**

Polarization value for fluorescence emission of cresyl fast violet in presence of surfactant with different counterions at 298 K

[Surfactant] mM	Polarisation values due to different counter ions							
	Na <sup>+</sup>	Li <sup>+</sup>	K <sup>+</sup>	NH <sub>4</sub> <sup>+</sup>	TMA <sup>+</sup>	TEA <sup>+</sup>	TPA <sup>+</sup>	TBA <sup>+</sup>
10.00	0.1274	0.1328	0.1366	0.1347	0.1632	0.1429	0.1606	0.1961
8.000	0.1249	0.1299	0.1320	0.1309	0.1608	0.1426	0.1577	0.1876
6.400	0.1185	0.1280	0.1280	0.1299	0.1608	0.1407	0.1552	0.1804
5.120	0.1177	0.1265	0.1256	0.1292	0.1600	0.1394	0.1533	0.1745
4.100	0.1195	0.1250	0.1219	0.1271	0.1577	0.1384	0.1527	0.1697
3.280	0.1174	0.1162	0.1189	0.1247	0.1539	0.1385	0.1514	0.1665
2.620	0.1141	0.1050	0.1097	0.1222	0.1496	0.1379	0.1502	0.1634
2.100	0.1105	0.1000	0.1045	0.1197	0.1341	0.1380	0.1500	0.1607
1.680	0.1048	0.0960	0.0961	0.1120	0.1229	0.1350	0.1483	0.1579
1.340	0.0955	0.1059	0.0960	0.1052	0.1136	0.1278	0.1459	0.1545
1.070	0.0855	0.1138	0.1145	0.1084	0.1248	0.1235	0.1436	0.1497
0.859	0.0939	0.1101	0.1120	0.1159	0.1360	0.1116	0.1382	0.1462
0.687	0.1019	0.1068	0.0989	0.1049	0.1248	0.1044	0.1258	0.1399
0.550	0.1081	0.1052	0.0910	0.1186	0.1197	0.1091	0.1208	0.1350
0.440	0.1012	0.1034	0.0939	0.1089	0.1040	0.1182	0.1089	0.1269
0.352	0.0928	0.1014	0.0945	0.1096	0.0789	0.1000	0.0929	0.1336

The steady-state anisotropy or polarized fluorescence study provides a simple way of monitoring any process where the microstructure is affected in some way [62]. Further, the anisotropy is considered as an index of the micro-viscosity or rigidity in the microenvironment of the probe [63]. The polarization values from steady-state anisotropy underline the effect of hydration on the microstructure of micelle or dye - surfactant complex [64]. Actually, the degree of depolarization of the fluorescence emission of a molecular probe is a measure of its rotational diffusion during the excited life time [65-66]. So, fluorescence anisotropy ( $r$ ) is an experimental measurement of the fluorescence. The lower the anisotropy value, the faster is the rotational diffusion [62]. Polarization values for the surfactant dodecyl benzene sulfonate with varying counter ions are given in the table 5.4. The trend is normal for all the surfactant except lithium dodecyl benzene sulfonate and ammonium dodecyl benzene sulfonate due to high hydration enthalpy of lithium and intermediate size of the ammonium ion.

From table 5.4, it is also clear that at high surfactant concentration, the rotational diffusion of the probe is restrained. Consequently, the probe does not assume all possible orientations with equal probability [67]. In all the surfactant, the anisotropy value ( $r$ ) gradually decreases upto the micelle formation stage and then increases. The interpretation of the results also emerges from steady-state anisotropy of these dye-surfactant complex system is not straightforward; its value depends on various factors such as, the rotational motion and the possible dye - surfactant interactions. A plausible explanation for the decrease in polarization value with decrease in surfactant concentration is that at high surfactant concentration, the micelle hinders the rotation of the dye molecule in solution [67]. But with decrease in surfactant concentration, the packing of amphiphiles at the interface is less compact which show a decrease in polarization value. Below the cmc, the increase in polarization value can also attributed to the higher dye-surfactant interactions.

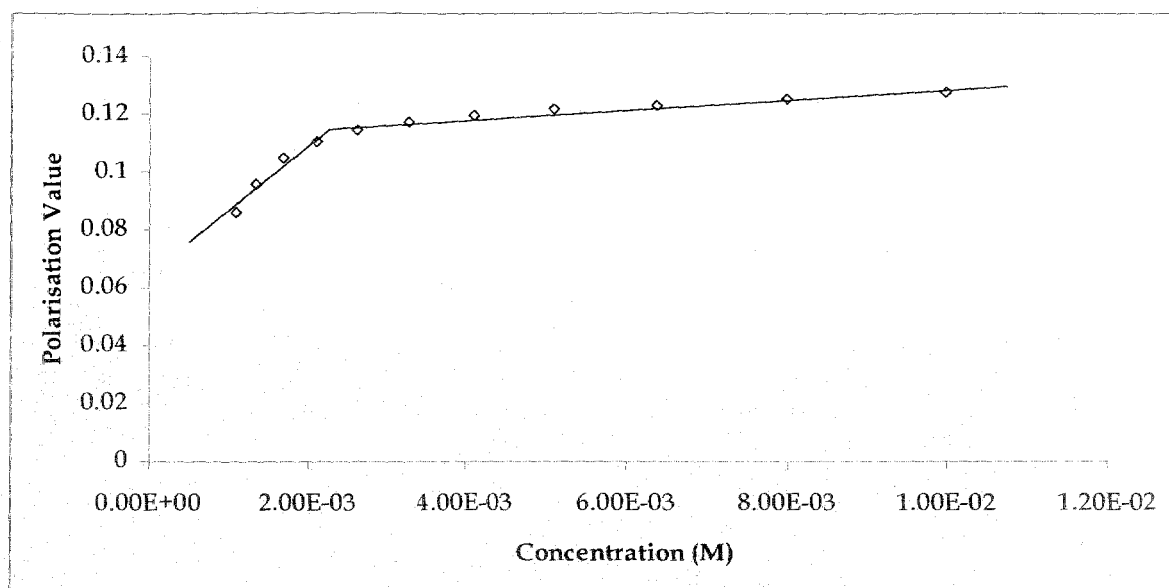
**Table 5.5.**

Table for concentration break points by polarization values.

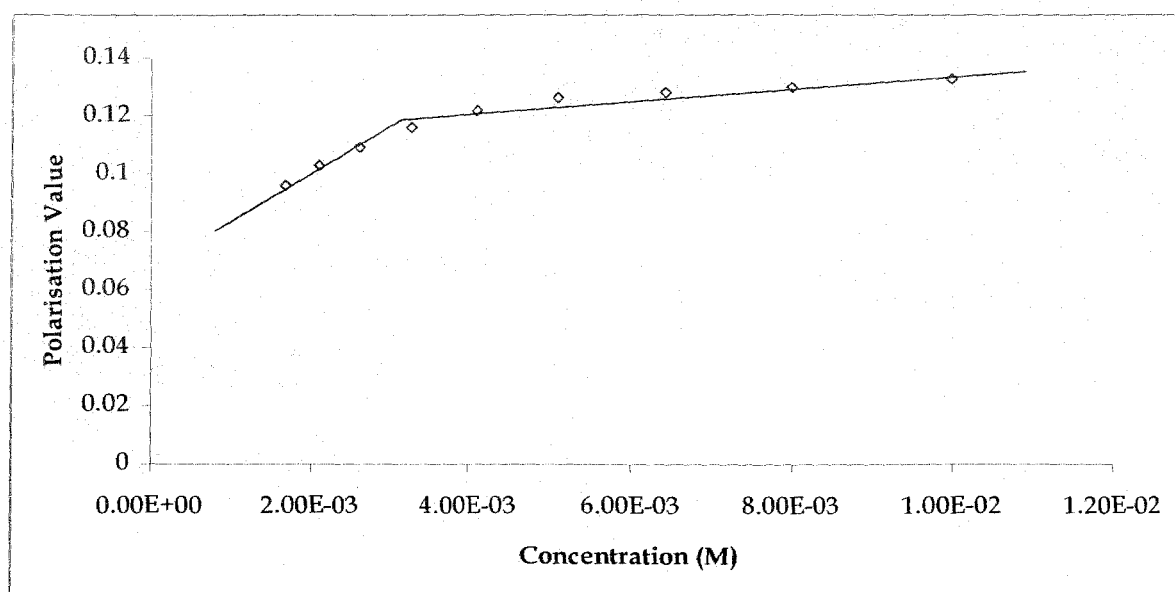
Surfactants	Concentration at break points (M)	Polarisation Value at break points
SDBS	$2.362 \times 10^{-3}$	0.1144
LDBS	$3.015 \times 10^{-3}$	0.1189
KDBS	$2.912 \times 10^{-3}$	0.1195
ADBS	$2.310 \times 10^{-3}$	0.1423
TMADBS	$2.810 \times 10^{-3}$	0.1524
TEADBS	$1.620 \times 10^{-3}$	0.1362
TPADBS	$0.825 \times 10^{-3}$	0.1475
TBADBS	$1.120 \times 10^{-3}$	0.1560

The anisotropy of the cresyl fast violet increases gradually for all the surfactant and it levels off at the value of  $1 \times 10^{-2}$  (M) concentration of the surfactant. The observed changes in anisotropy of cresyl fast violet as function of surfactant concentration also provide evidence of different types of interactions above and below the cmc. Upon addition of surfactant, the anisotropy initially increases fast, but this increase in a range of very low surfactant concentration and below the cmc. This is the evidence of interactions that reduce the dye's ability to rotate freely. A dye-surfactant ionic pair or cluster would result in such a decreased ability to rotate because of its larger size than an individual dye ion. The increase polarization value with increasing surfactant concentration probably means that more surfactant molecule join the clusters as the

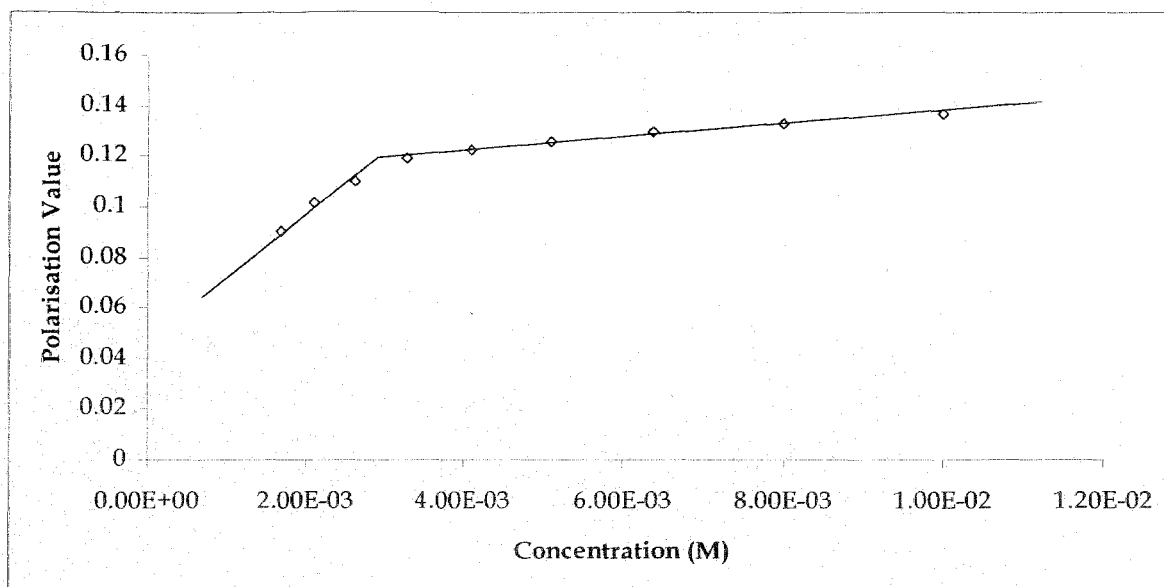
surfactant concentration increases. Around the cmc, the increase of anisotropy value drops to an extent. This point may be caused by the surfactant forming micelles preferentially to ionic interactions with the dye. This could free up some of the dye molecule from their ionic interactions with the surfactant monomers. Above the cmc, the anisotropy increases to a very little before leveling off at two or three times the anisotropy of cresyl fast violet. This shows that the dye is less free to rotate in the micellar environment. Micelles contain a large number of surfactant monomers, so they rotate slowly. A dye molecule trapped within such a micelle would also rotate slowly, causing a high anisotropy. The dye's lower ability to rotate above the cmc shows that it is within the micelle in a more rigid formation. This may be because the positively charged end of the dye is interacting with the negatively charged ends of the surfactant ions. The value of the cmc derived from polarization value is in good agreement with the value determined by surface tension and conductometrically for each of the surfactant. The slight difference between two is due to the two other methods applied to explain the facts and also dye surfactant interactions present in the latter system, with only exception in tetrabutyl ammonium dodecyl benzene sulfonate. For the case of TBADBS surfactant, apart from hydrophobic effect the alkyl chain length is also a predominating factor for its properties. Due to its chain length, hydrophobicity increases, and as a result the dye surfactant interactions increases, and so the cmc increases. The plots for polarization values vs. concentration plots for all the surfactants are given in below (figure 5.23 - 5.30).



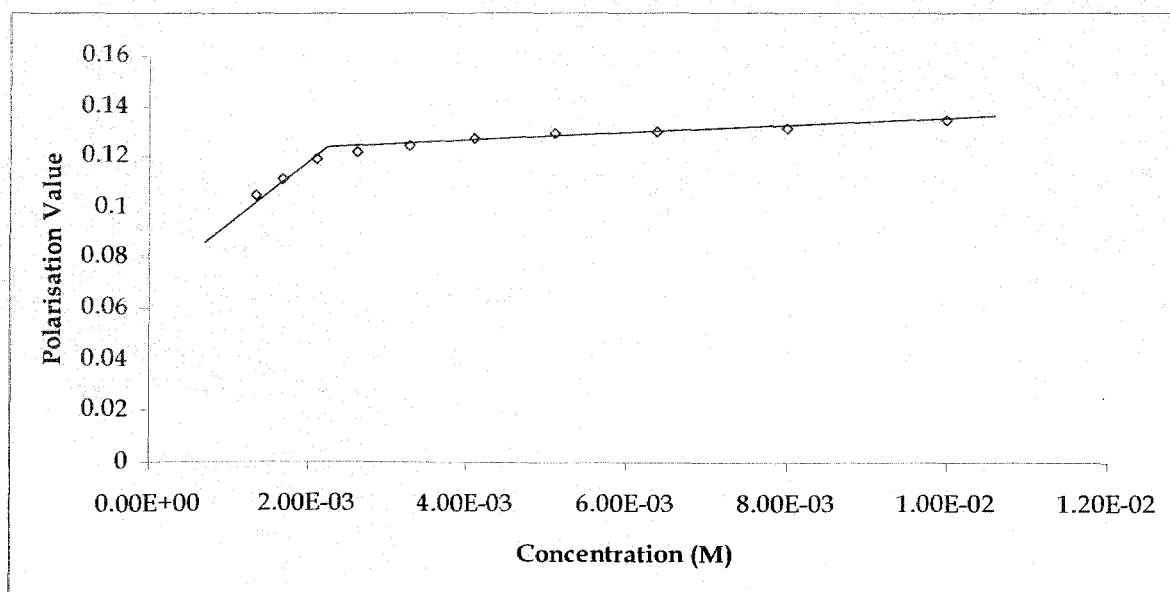
**Figure 5.23:** Polarisation value vs. concentration of the surfactant plot of sodium dodecyl benzene sulfonate



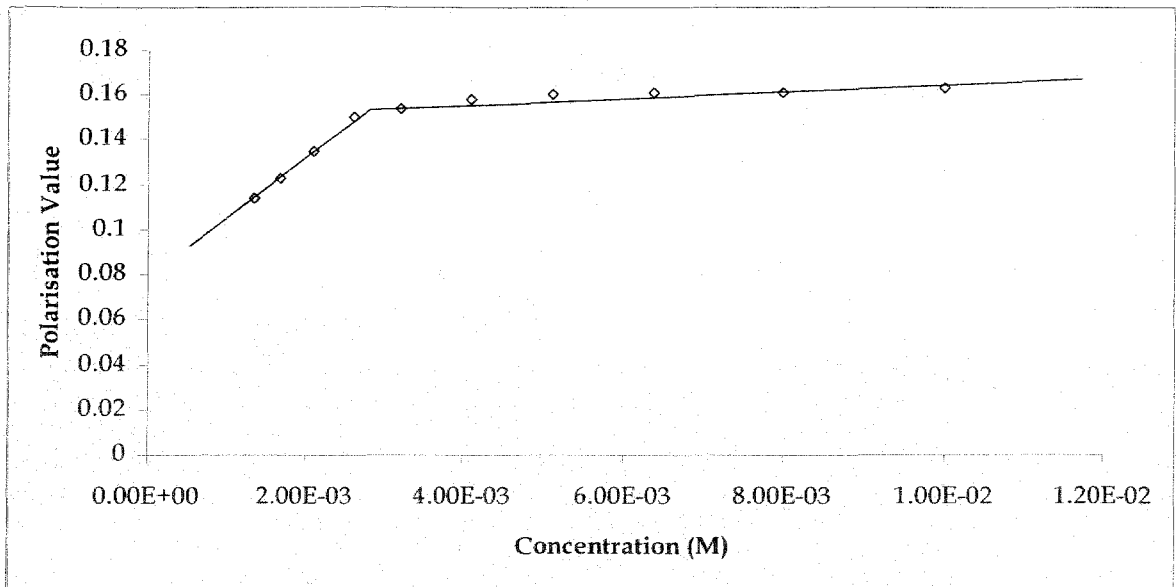
**Figure 5.24:** Polarisation value vs. concentration of the surfactant plot of lithium dodecyl benzene sulfonate



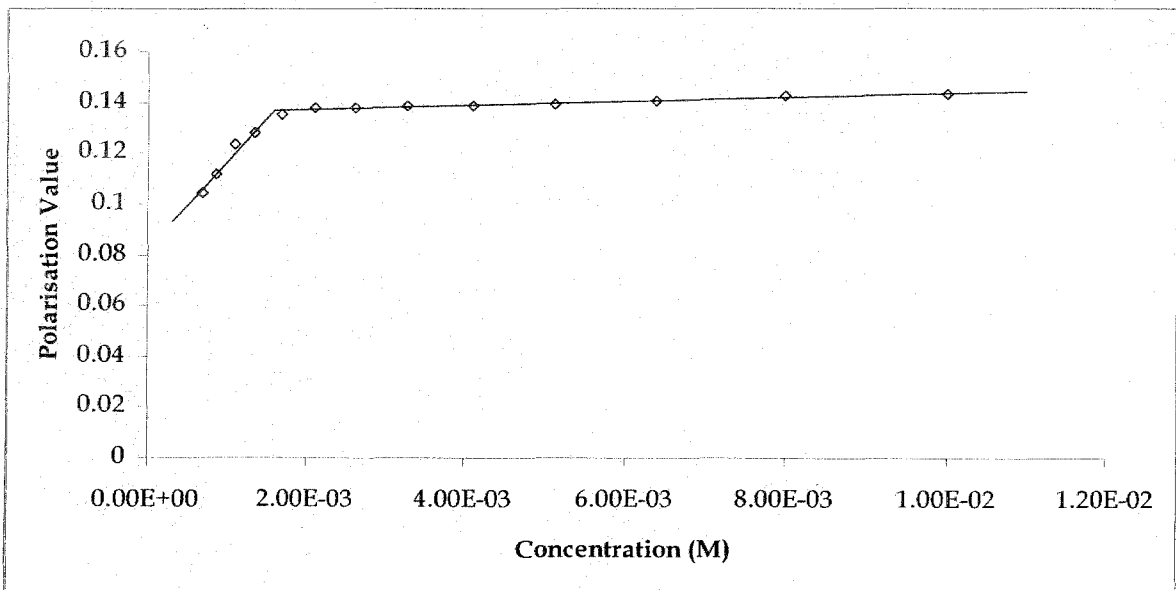
**Figure 5.25:** Polarization value vs. concentration of the surfactant plot of potassium dodecyl benzene sulfonate.



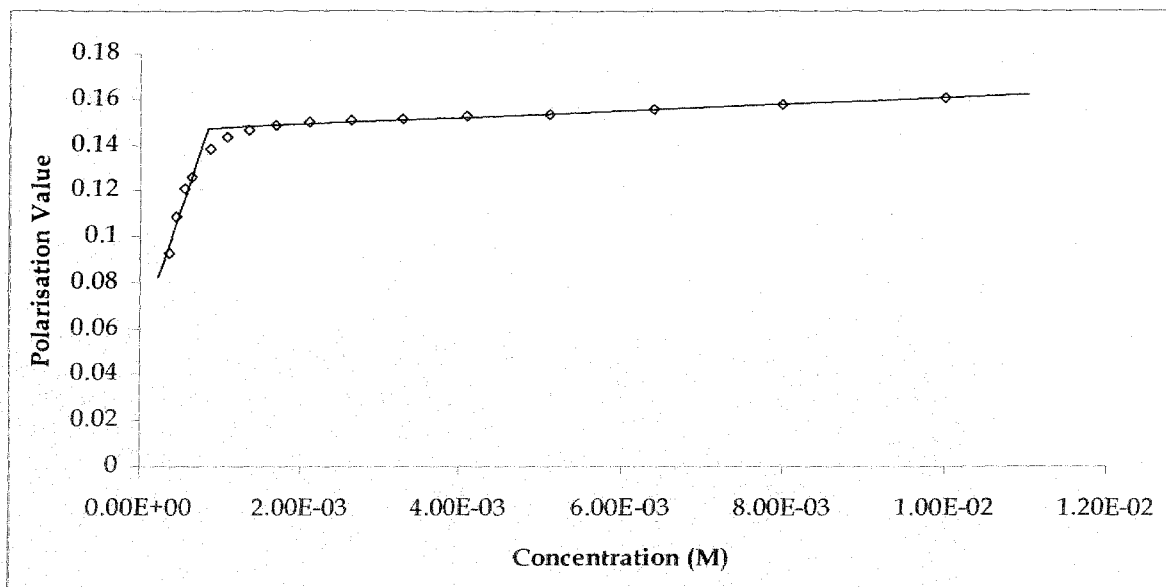
**Figure 5.26:** Polarization value vs. concentration of the surfactant plot of ammonium dodecyl benzene sulfonate.



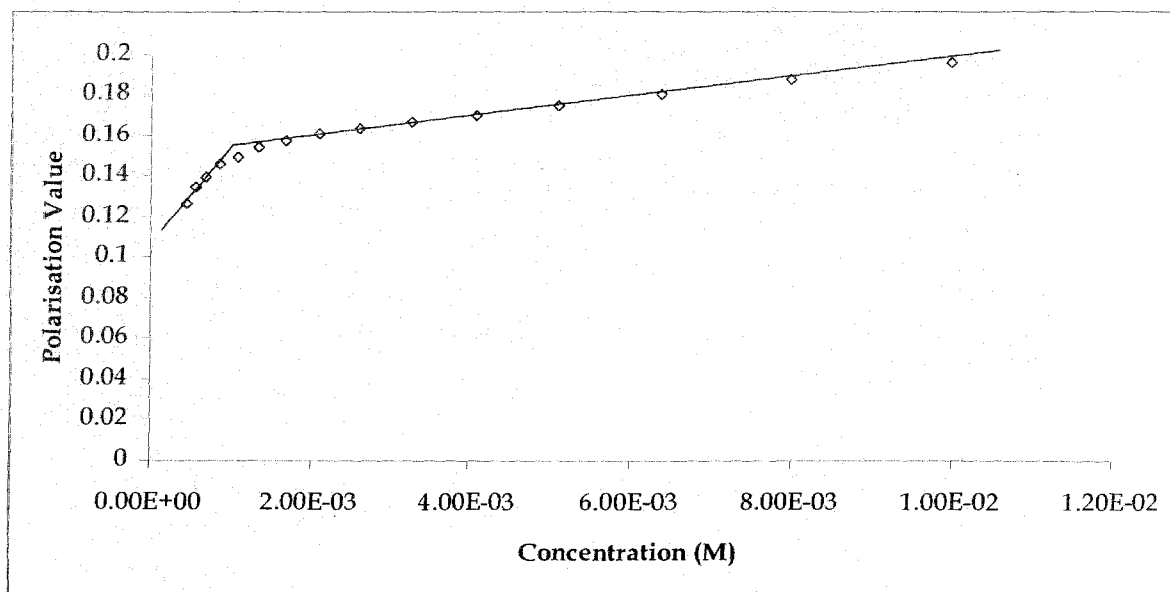
**Figure 5.27:** Polarization value vs. concentration of the surfactant plot of tetramethyl ammonium dodecyl benzene sulfonate.



**Figure 5.28:** Polarisation value vs. concentration of the surfactant plot of tetraethyl ammonium dodecyl benzene sulfonate.



**Figure 5.29:** Polarisation value vs. concentration of the surfactant plot of tetrapropyl ammonium dodecyl benzene sulfonate.



**Figure 5.30:** Polarisation value vs. concentration of the surfactant plot of tetrabutyl ammonium dodecyl benzene sulfonate.

## 5. 6. Lifetime measurements

Time-resolved measurements are widely used in fluorescence spectroscopy, particularly for studies of biological macromolecules. This is because time-resolved data frequently contain more information than is available from steady-state data. Two methods of measuring time-resolved fluorescence are in widespread use, the time-domain and frequency-domain methods. In time-domain or pulse fluorometry, the sample is excited with a pulse of light. The width of the pulse is made as short as possible and is preferably much shorter than the decay time  $\tau$  of the sample. The time-dependent intensity is measured following the excitation pulse, and the decay time  $\tau$  is calculated from the slope of a plot of  $\log I(t)$  versus  $t$ , or from the time at which the intensity decreases to  $1/e$  of the value at  $t = 0$ . The intensity decays are often measured through a polarizer oriented at  $54.7^\circ$  from the vertical  $z$ -axis [28].

In the present experiment, time resolved fluorescence studies were carried out to determine the emission decay parameters of all the surfactants with different surfactant concentrations. The concentration of the dye used was  $5 \times 10^{-6}$  (M). As a nanosecond set up was used, very fast decay could not be recorded. Thus, high dye concentrations could not be used, as at these concentrations lifetime values may be drastically decreased due to fluorescence quenching. Another experimental restriction is that, the 0.5 cm path length cell could not be inserted into the cell holder for lifetime studies. With a cell of larger path length, inner filter effects interfere with the fluorescence studies for very concentrated solutions [52,61]. So, only four set of concentrations for each dye have been taken for study and the values are given on the table 5.6. The lifetime values did not change significantly or in a regular manner with the change in surfactant concentration suggesting single exponential fluorescence decay curve for all the surfactants.

**Table5.6.**  
Life time for all the surfactant with varying counter ions

Surfactant/ Concentration	0.01M	0.005M	0.0005M	0.0001M
<b>LDBS</b>	2.9 ns	3.0 ns	2.9 ns	2.5 ns
<b>SDBS</b>	3.2 ns	3.6 ns	3.5 ns	1.5 ns
<b>KDBS</b>	3.4 ns	3.3 ns	1.9 ns	4.3 ns
<b>NH<sub>4</sub>DBS</b>	2.9 ns	3.3 ns	2.5 ns	2.9 ns
<b>TMADBS</b>	4.4 ns	2.5 ns	3.4 ns	4.9 ns
<b>TEADBS</b>	3.8 ns	2.8 ns	3.3 ns	2.5 ns
<b>TPADBS</b>	3.5 ns	4.8 ns	3.7 ns	2.4 ns
<b>TBADBS</b>	4.3 ns	2.6 ns	2.5 ns	2.2 ns

## References:

1. Tanford, C. *'The Hydrophobic Effect: Formation of Micelles and Biological Membranes'*, Wiley, New York, N. Y., 1973.
2. Kalyanasundaram, K.; Thomas, J. K. *J. Am. Chem. Soc.* **1977**, *99*, 2039-2044.
3. Kalyanasundaram, K.; Thomas, J. K. *J. Phys. Chem.* **1977**, *81*, 2176-2180.
4. Turro, N. J.; Okubo, T. *J. Phys. Chem.* **1982**, *86*, 159-161.
5. Turro, N. J.; Okubo, T. *J. Am. Chem. Soc.* **1981**, *103*, 7224-7230.
6. Levitz, P.; Van Damme, H.; Keravis, D. *J. Phys. Chem.* **1984**, *88*, 2228-2235.
7. Turro, N. J.; Pierola, I. F.; *Macromolecules* **1983**, *16*, 906-910.
8. Turro, N. J.; Baretz, B. H.; Kuo, P. C.; *Macromolecules*, **1984**, *17*, 1321-1324.
9. Ananthapadmanabhan, K. P.; Leung, P. S.; Goddard, E. D. *Colloids Surf.* **1985**, *13*, 63-72.
10. Zana, R.; Yiv, S.; Strazielle, C.; Lianos, P. *J. Coll. Interface Sci.* **1981**, *80*, 208-232.
11. Rosen, M. J. *Surfactants and Interfacial Phenomena*; John Wiley: New York, **1989**.
12. Mizusaki, M.; Morishima, Y.; Dubin, P. L. *J. Phys. Chem. B* **1998**, *102*, 1908.
13. Zana, R.; Ed.; M. Dekker Inc.: *Surfactant Solution. New Methods of Investigation*. Newyork, **1987**.
14. Cabane, B. In ref 12, Chapter 2, p 57
15. Zana, R.; Ed.; M. Dekker Inc.: *Surfactant Solution. New Methods of Investigation*. Newyork, **1987**.
16. Zana, R. In ref 12; Chapter 5 and references therein.
17. Almgren, M. *Adv. Colloid Interface Sci.* **1992**, *41*, 9
18. Gehlen, M.; De Schryver, F. C. *Chem. Rev.* **1993**, *93*, 199.
19. Barzykin, A. V.; Tachiya, M. *Heterog. Chem. Rev.* **1996**, *3*, 105.
20. Infelta, P. *Chem. Phys. Lett.* **1979**, *61*, 88
21. Yekta, A.; Aikawa, M.; Turro, N. *Chem. Phys. Lett.* **1979**, *63*, 543.
22. Valeur, B.; Berberan-Santos, M. N. *J. Chem. Educ.*, 2011, *88* (6), 731 - 738.
23. Anathapadmanabhan, K. P.; Goddard, E. D.; Turro, N. J.; Kuo, P. L. *Langmuir* **1985**, *1*, 352-355.
24. E. Rodenas and E. Perez-Benito, *J. Phys. Chem*, **1991**, *95*, 4552-4556.
25. Hait, S.K.; Majhi, P. R.; Blume, A. and Moulik, S. P., *J. Phys. Chem. B*, **2003**, *107*, 3650-3658.
26. Chakraborty, A.; Saha, S. K. and Chakraborty, S. *Colloid Polym. Sci.*, **2008**, *286*, 927-934.

27. Benrraou, M.; Bales, B. L. and Zana, R., *J. Phys. Chem. B*, **2003**, 107, 13432-13440.
28. Lakowicz, J. R., *Principles of Fluorescence Spectroscopy*, Plenum Publishers, 2<sup>nd</sup> Edition, **1999**,
29. Singhal, G. S., Rabinowich, E., and Hevesi, J. *Photochem. Photobiol.* **1970**, 11, 530.
30. Kundu, K.; Bardhan, S.; Banerjee, S.; Chakraborty, G.; Saha, S. K.; Paul, B. K., *Colloid and Surf.*, **2015**, 469, 117 - 131.
31. Snavely, in: J. B. Birks (Ed.), *Organic molecular photophysics*, Wiley, New York, **1973**.
32. Valdes-Aguilera, O.; Necbees, *Acc. Chem. Res.* **1989**, 22, 171 - 177.
33. Lopez Arbeloa, I., P. Ruiz Ojeda, P. *Chem. Phys. Lett.* **1982**, 87, 556.
34. Lopez Arbeloa, I., Rohatgi Mukherjee, K. K., *Chem. Phys. Lett.*, **1986**, 128, 474.
35. Lopez Arbeloa, I., Gonzalez, I. L., Ojeda, P. R.; Lopez Arbeloa, N., *J. Chem. Soc. Faraday Trans. 2*, **1982**, 78, 989.
36. Lopez Arbeloa, I., *Dyes and Pigments*, **1983**, 4, 213.
37. Lopez Arbeloa, I., *An. Quim.* **1984**, 80, 7.
38. Lopez Arbeloa, I., *JCS Faraday Trans.2*, **1981**, 77, 1725 - 1735.
39. Rohatgi, K. K., Mukhopadhyay, A. K., *Chem, Phys. Lett.* **1971**, 12, 259.
40. Rohatgi, K. K., Mukhopadhyay, A. K., *J. Phys. Chem.* **1972**, 76, 3970.
41. Kamat, P. V., Karkhanavala, M. D., and Moorthy, P. N., *Indian J. Chem. A*, **1977**, 15, 342.
42. Kamat, P. V., Karkhanavala, M. D., and Moorthy, P. N., *Solar Energy*, **1978**, 20, 171.
43. Liu, D., and Kamat, P. V., *J. Chem. Phys.*, **1996**, 105, 965.
44. Martini, I., Hartland, G. V., and Kamat, P. V., *J. Phys. Chem. B*, **1997**, 101, 4826.
45. Anfinrud, P., Crackel, R. L., and Struve, W. S., *J. Phys. Chem.*, **1984**, 88, 5873.
46. Liu, D., Fessenden, R. W., Hug, G., and Kamat, P. V., *J. Phys. Chem. B*, **1997**, 101, 2583.
47. Liu, D., and Kamat, P. V., *Langmuir*, **1996**, 12, 2190.
48. Dutta, R. K., and Bhat, S. N., *Bull. Chem. Soc. Jpn.*, **1992**, 65, 1089.
49. Dutta, R. K., and Bhat, S. N., *Colloids Surf. A*, **1996**, 106, 127.
50. Shah, S. S., Ahmad, R., Shah, S. W. H., Asif, K. M., and Naeem, K., *Colloids Surf. A*, **1998**, 137, 301.
51. Chibisov, A. K., Prokhorenko, V. I., and Gomer, H., *Chem. Phys.*, **1999**, 250, 47.
52. Gawandi, V. B.; Guha, S. N., Priyadarsini, K. I. and Mohan, H. *J Colloid and Interface Science*, **2001**, 242, 220 - 229.

53. Herschel, Sir J. F. W., 1845, *Phil. Trans. R. Soc. London* 135: 143 - 145
54. Rahavendran, S. V., Karnes, H. T., 1996, *J. Pharm. Biomed. Anal.* 15: 83-98.
55. Flanagan, J. H.; Romeo, S. E.; Legendre, B. L.; Hammer, R. P.; Soper, A.; 1997, *SPIE*, 2980: 328-337.
56. Selwyn, J. E.; Steinfeld, J. I.; *J. Phys. Chem.* 1972, 76: 762.
57. Hinckly, D. A.; Seybold, P. G.; Borris, D. P.; *Spectrochim. Acta. A.* 1986, 42, 747.
58. Chakraborty, M.; Panda, A. K., *Spectrochimica Acta Part A*, 2011, 81, 458 - 465.
59. De, S.; Das, S.; Girigoswami, A.; *Spectrochimica Acta Part A*, 2005, 61, 1821 - 1833.
60. R. Adhikari, *Ph.D. Thesis*, 2004.
61. Lakowicz, J. R. *Principles of fluorescence Spectroscopy*, Kluwer, 1999, Ch. 8
62. Paul, S.; Panda, A. K., *Colloids Surf. A*, 2013, 419, 113-124.
63. Jana, B.; Ghosh, S.; Chattapadhaya, Nj. *Photochem. Photobiol. B*, 2013, 126, 1 - 10.
64. Wittouck, N., Negri, R. M., Ameloot, M., De Schryver, F. C., *J. Am. Chem. Soc.* 1994, 116, 10601-10611.
65. Bardhan, S., Kundu, K., Saha, S. K., Paul, B. K., *Colloids Surf. A*, 2014, 450, 130 - 140.
66. Ruiz, C. C., Aguiar, J., *Langmuir*, 2000, 16, 7946 - 7953.
67. Valeur, B., Keh, E., *J. Phys. Chem. B.* 1979, 83, 3305 - 3307.

## **Chapter VI**

**Effect of Cetyltrimethylammonium bromide  
on the aggregation behaviour of  
Sodiumdodecylbenzene sulfonate**

## Chapter VI

# Effect of cetyltrimethylammonium bromide on the aggregation behaviour of Sodiumdodecylbenzene sulfonate

### 6.1 Introduction and review of the previous work

Molecular self-assembly provides a powerful tool for the creation of well-organized structures in the nanometre or micrometer length scale, such as micelles, vesicles, fibres, discs and tubes [1 - 6]. Conventional micelles are fluid aggregates of surfactants with shape and size, controlled by packing of individual surfactants. The main characteristics of such micelles are: (a) These micelles, especially the charged micelles, are stabilized by hydrophobic forces and head group repulsions (electrostatic and steric), (b) Each surfactant moves as in a fluid and the size and shape and aggregation numbers are decided by the packing parameter as mentioned above, (c) Length scales of these micelles are in 10 - 1000 Å (d) The life times of these micelles are often in milliseconds. On dilution below critical micelle concentration the aggregates disappear in milliseconds. The realization that there could be micelles and aggregates of different type is recent [7 - 8]. Surfactant solutions represent a well-documented class of self-assembled systems that can offer diverse organized structures [9 - 11]. Above the critical micelle concentration (cmc), hydrophilic surfactants form small globular micellar aggregates and the solutions show Newtonian flow behaviour. Compared to single surfactant, the mixed surfactant exhibits superior interfacial properties such as higher surface activity and lower critical micelle concentration (cmc). The mixtures of surfactants which have been studied include cationic/anionic, non ionic/non ionic, cationic/non ionic, anionic/non ionic, cationic/cationic etc. Surfactant mixtures are commonly preferred in medicinal and pharmaceutical formulations and industrial preparations due to the purpose of suspension, solubilization and dispersion. Ionic surfactants can also self assembled to long thread-like or worm-like micelles in presence of certain organic ions e.g., sodium salicylate. Under certain conditions such as concentration, salinity, temperature, presence of counterions, etc., the globular micelles may undergo uniaxial growth and form very

long and highly flexible aggregates, referred to as "wormlike" or "threadlike" micelles [12 - 19]. Wormlike micelles [13] are long, self-assembled, semi-flexible, breakable polymer-like materials with surfactant heads on the outside and tails in the core. They display a striking range of dynamical properties, including anomalous relaxation, shear banding, and rheological chaos [20, 21]. Due to this reason, wormlike micelles have received considerable attention from theoretician and experimentalist during the past few decades. Earlier, an extensive study on the dynamics and rheological behaviour of wormlike micelles began in long-chain ionic surfactant systems in the presence of a salt [22-25]. Above a threshold concentration  $c^*$ , wormlike micelles may entangle into a transient network, which displays remarkable viscoelastic properties. The rheological behaviour observed for wormlike micelles in the surfactant solution is similar to that for flexible polymers, and therefore, aqueous solutions of entangled wormlike micelles are often called "living polymer systems". The research of wormlike micelles has drawn considerable interest owing to their superior properties and wide applications as has been already mentioned [26-29]. Viscoelastic wormlike micelles or threadlike micelles have been observed in various surfactant systems, including mixtures of cationic and anionic surfactants [30-32], nonionic surfactants [32-34], zwitterionic surfactants [35-37] and ionic surfactants with different activities [38-43]. Hydrotopes were also found to promote the formation of viscoelastic wormlike micelles in ionic surfactant solutions, in which the surfactant interact strongly with hydrotrope due to electrostatic attraction and hydrophobic effect. Salicylate, tosylate, chlorobenzoate, hydroxynaphthalenecarboxylates and nitrobenzoate (all containing an aromatic group) were reported to induce wormlike micelle formation in a cationic surfactant solution. Unlike surfactant molecules, hydrotropes are a class of amphiphilic compounds that cannot form well-organized structures, such as micelles, but do increase the solubility of organic molecules in water by several orders of magnitude. The common structural characteristics of hydrotropes are the coexistence of an unsaturated hydrocarbon ring and an ionic group within one molecule. Strong synergistic effects are often observed when hydrotropes are added to aqueous surfactants or polymer solutions. In particular, various hierarchically self-assembled structures such as tubes, ribbons, vesicles and lamellar structures can be fabricated in mixtures of surfactants and hydrotropes.

Mixtures of cationic and anionic surfactants show not only synergistic effect of the aggregation properties but also triggered micellar grow in one dimension to form

long worm-like micelles. A dramatic influence on the viscosity of wormlike micelles in aqueous solutions of CTAB was shown for *trans-ortho*-methoxycinnamic acid [44]. While some works in this field is available in the literature, report on the effect of the aggregation properties of SDBS and CTAB mixture is rare. In this chapter, the results of the study on their mixing behaviour, synergism, and one dimensional grow to worm-like micelles and rheological characteristics of this system are reported. Through this development it became clear that by mixing surfactants (hydrotropes) of opposite charges, cationic and anionic, but with varying chain lengths one can control the degree of precipitation of the surfactants to produce different supramolecular structures like vesicles and polymeric micelles [45]. The transition from one structure to another is also well known facts in recent studies. A temperature-induced vesicle to micelle transition has been observed in the system of a new cationic surfactant cetyltrimethylammonium 3-hydroxy naphthalene 2-carboxylate [8]. Some researchers have also shown that the vesicle-to-micelle transition occurs in this system at 45°C and is induced by melting of vesicle surfaces using calorimetry and conductivity measurements. At melting the ions are released from surfaces, giving a jump in conductivity at this point and if there are trapped ions in vesicles they are also released [46]. The vesicle to micelle transition in different systems has been characterized by several techniques like rheology, light scattering, NMR, fluorescence, small angle neutron scattering (SANS), etc. Present study is divided in two major parts. In the first part, the synergistic effect of the mixing of cetyltrimethylammonium bromide (CTAB, a cationic surfactant) with SDBS (an anionic surfactant) is studied under Newtonian flow regime. In the second part, the formation of viscoelastic worm-like micelles is examined and the rheological behavior of the system is investigated under non Newtonian flow regime.

## 6. 2. Theoretical models for analyzing mixing behaviour of surfactants

### Ideal and non-ideal mixture models under Newtonian flow regime.

The process of assembling free surfactant monomers to generate aggregates is, of course, entropically unfavourable as the entropy of mixing surfactant and solvent molecules then decreases. This unfavourable change in entropy of mixing decreases

with increasing surfactant concentration,  $C_{surf}$  or, otherwise expressed, the chemical potential of free surfactant monomers increases with increasing  $C_{surf}$  and, when the chemical potential of the free monomers becomes equal to the corresponding quantity in the surfactant aggregates, the latter start to form. The surfactant concentration where aggregates start to appear is known as the cmc; above this concentration aggregates and free surfactant monomers coexists.

When two surfactants or a surfactant and cosurfactants are mixed, mixed aggregates are formed and the cmc becomes a function of the surfactant concentration. For a mixture of two different surfactants, the cmc has been observed to depend linearly on the composition of the micelles, i.e.

$$cmc(x_1) = x_1 cmc_1 + (1 - x_1) cmc_2 \quad (6.1)$$

where  $x_1$  denotes the mole fraction of one of the surfactants in the aggregates, and  $cmc_1$  and  $cmc_2$  are the cmcs of pure surfactants 1 and 2 respectively. Surfactant systems for which the cmc is seen to obey equation 6.1 are often referred to as ideal surfactant mixtures. The overall mole fraction of surfactant 1 at the cmc equals

$$y_1 \equiv \frac{cmc_1^m}{(cmc_1^m + cmc_2^m)} \quad (6.2)$$

where  $cmc_1^m$  and  $cmc_2^m$  the free monomer concentrations of surfactant 1 and 2 at  $cmc(x_1) = cmc_1^m + cmc_2^m$ , since by definition, the amount of surfactant existing as free monomers is much larger than the amount of aggregated surfactant at cmc. As a result, we can also write,

$$\frac{1}{cmc(y_1)} = \frac{y_1}{cmc_1} + \frac{(1-y_1)}{cmc_2} \quad (6.3)$$

However, for a number of surfactant mixtures synergistic effects are important which means that the cmc deviates appreciably from the behaviour predicted by above equation [47]. To account for these synergistic effects it is customary to write

$$cmc(x_1) = x_1 f_1(x_1) cmc_1 + (1 - x_1) f_2(x_1) cmc_2 \quad (6.4)$$

where, in accordance with the theory of regular mixtures, activity factor functions are introduced by setting

$$f_1(x_1) = \exp[(1 - x_1)^2 \beta] \quad (6.5)$$

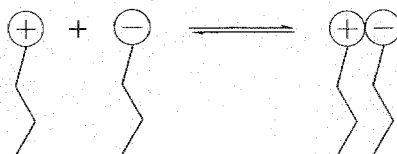
and

$$f_2(x_1) = \exp(x_1)^2 \beta] \quad (6.6)$$

In analogy with the treatment of regular mixtures,  $\beta$  is mostly referred to as the interaction parameter, and its deviation from zero (and, consequently, the deviation of  $f_1$  and  $f_2$  from unity) is commonly assumed to result from specific interactions between the surfactant headgroups (discussed in further detail under results and discussion section).

Formation of worm-like micelles and the study of viscoelastic characteristics under non-Newtonian flow regime is an interesting field, which have also been investigated and reported in the present thesis. Different theoretical models have also been proposed for micelle-vesicle transition mainly in lipid-detergent mixtures. These molecular approaches model was on the concept of curvature elasticity of thin films [48-50]. These models can take into account the basic characteristics of these transitions, in particular the presence of a two-phase region consisting of coexisting

vesicles and micelles. A similar model has also been proposed for vesicle to micelle transition in cationic anionic mixtures and the key concept is shown in the figure below [51-52]. Cationic and anionic surfactants, in view of their strong interaction in polar region, form dimers and higher n-mers even at low concentrations.



**Figure 6.1:** Strong coulomb interactions between the polar heads of cationic - anionic surfactants force them to form dimers, trimers, n-mers at interfaces of aggregates. Depending on the numbers, the bend elastic constant of the interface changes leading to formation of vesicles, worms, etc.

At any given temperature, these are in thermal equilibrium. The relative concentrations of these species decide whether the system forms worms, vesicles or crystals. The relative concentrations can be estimated from extensions of the concepts of Bjerrum transitions in two dimensions. Few of recent wide angle X- rays scattering studies have shown evidence to such melting of ion-pairs with temperature in cationic surfactant solutions [53].

### 5.3 Experimental

Conductivity measurements were carried out on a Mettler Toledo digital conductometer (Model no. MC226), using a dip cell (specific conductance  $1413 \text{ S.cm}^{-1}$ ). The experiments were performed at desired temperatures maintained within  $\pm 0.5 \text{ K}$ . Constant temperature was maintained by flowing water from the constant temperature water bath by an automatic motor to the double wall vessel containing the experimental solution. Surface tension was measured with a Kruss K9 tensiometer (Hamburg, Germany, accuracy  $\pm 0.01 \text{ mN.m}^{-1}$ ) using the platinum ring detachment method. The temperature was controlled adopting the same arrangement as mentioned above. The surface tension was determined with a single measurement method. All measurements were repeated until the difference between two values was less than  $0.2 \text{ mNm}^{-1}$ . The rheological measurements were done using cone-plate

geometry with  $40^\circ$  truncation angle, with diameter 25 mm and 0.105 mm sample gap on a dynamic compact rheometer (Anton Paar, USA, Model MCR 302), equipped with Peltier temperature control system.

#### 6.4. Preparation of solution of SDBS-CTAB mixed micelle system

A volume of 10 ml of water was taken in a beaker at room temperature ( $25^\circ\text{C}$ ) into which a stock solution of SDBS-CTAB mixed micelle system of desired concentration (4-6 times cmc) at the fixed composition was stepwise added with a micropipette as required. At each step of addition (concentration varies with every addition, the conductivity/surface tension was measured keeping the mole-fraction of SDBS and CTAB constant.

#### 6.5 Results and discussion

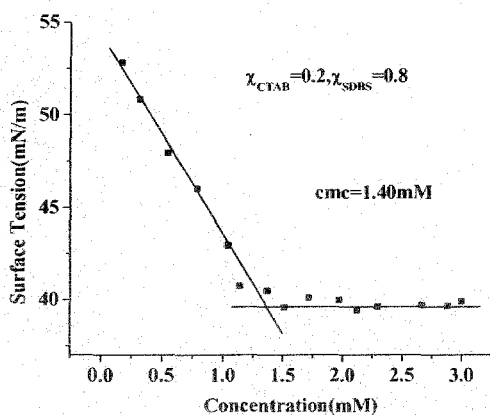
Micellar aggregates are also formed in an aqueous solution containing mixed surfactants. The cmc values obtained from the conductivity and surface tensiometry measurements are rendered in table 6.1. The individual cmc values of these two surfactants in pure water, measured by the above two techniques, are in agreement with the literature data.

**Table 6.**

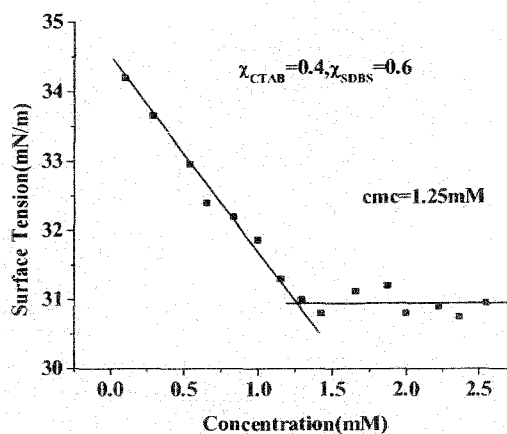
**Experimental cmc values of SDBS-CTAB mixed micelle system at different mol fractions of SDBS and CTAB measured by conductometrically and surface tensiometrically.**

$\chi_{SDBS}$	$\chi_{CTAB}$	$cmc_{\text{Conductance}} / \text{mM}$	$cmc_{\text{Surface Tension}} / \text{mM}$
1.0	0.0	2.78	2.82
0.8	0.2	1.49	1.40
0.6	0.4	1.25	1.25
0.4	0.6	1.15	1.10
0.2	0.8	0.94	0.93
0.0	1.0	0.90	0.90

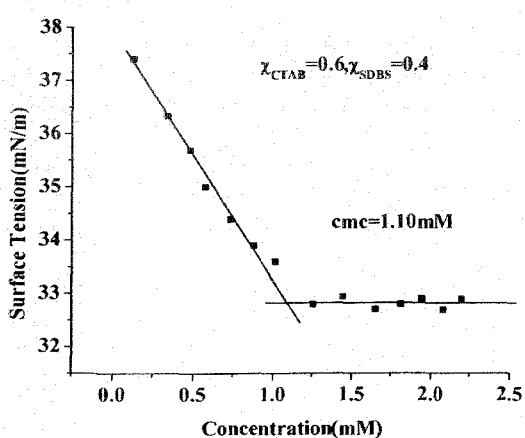
The plots for determination of cmc's (surface tension and conductometry) at different mole-fraction of CTAB and SDBS are shown in figure 6.2 to figure 6.13.



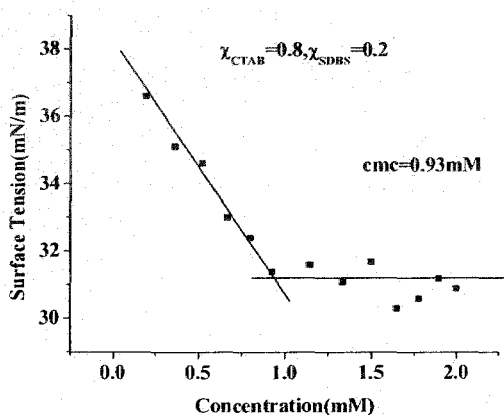
**Figure 6.2:** Surface tension vs. concentration plot at  $\chi_{CTAB} = 0.2$ ;  $\chi_{SDBS} = 0.8$ .



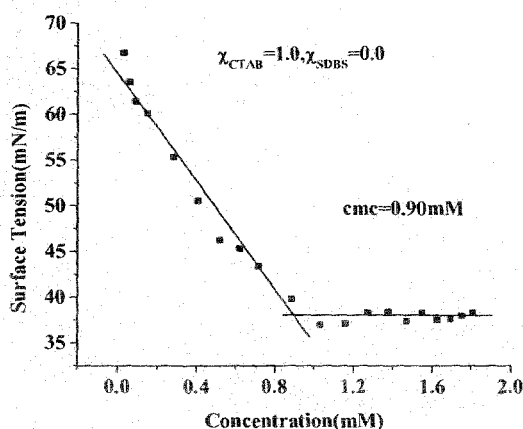
**Figure 6.3:** Surface tension vs. concentration plot at  $\chi_{CTAB} = 0.4$ ;  $\chi_{SDBS} = 0.6$ .



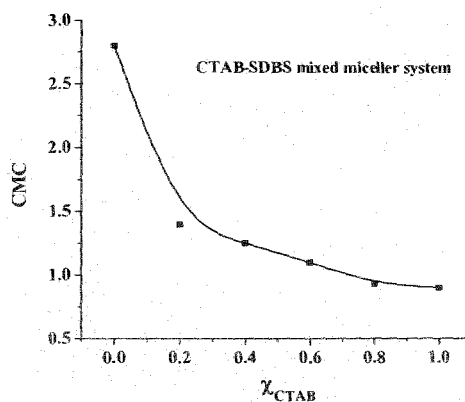
**Figure 6.4:** Surface tension vs. concentration plot at  $\chi_{CTAB} = 0.6$ ;  $\chi_{SDBS} = 0.4$ .



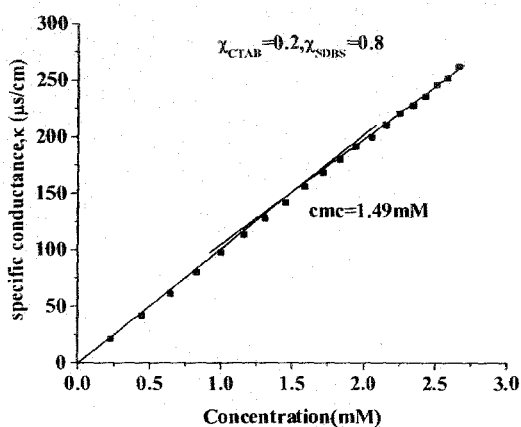
**Figure 6.5:** Surface tension vs. concentration plot at  $\chi_{CTAB} = 0.8$ ;  $\chi_{SDBS} = 0.2$ .



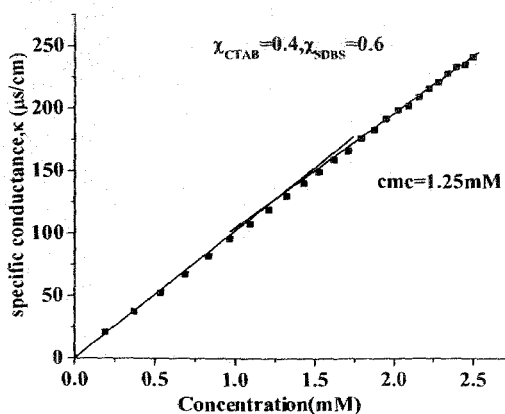
**Figure 6.6:** Surface tension vs. concentration plot at  $\chi_{CTAB} = 1.0$ ;  $\chi_{SDBS} = 0.0$ .



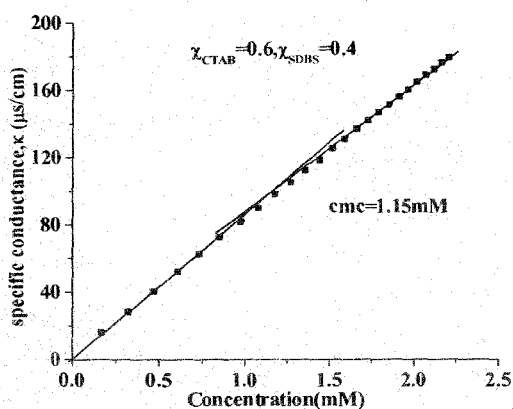
**Figure 6.7:** CTAB - SDBS mixed micelle system at different mol fraction and variation of cmc with mol fraction determined by surface tension method.



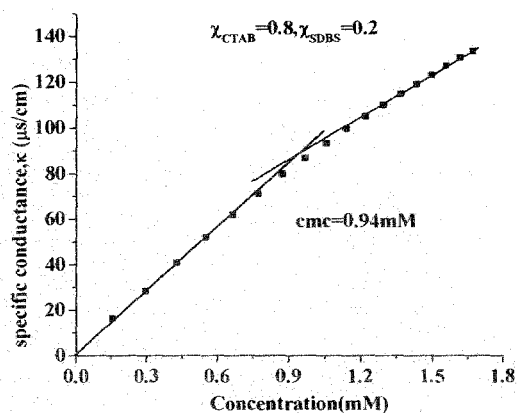
**Figure 6.8:** Conductance vs. concentration plot at  $\chi_{CTAB} = 0.2$ ;  $\chi_{SDBS} = 0.8$ .



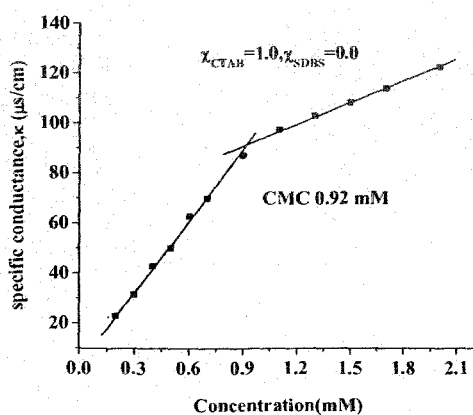
**Figure 6.9:** Conductance vs. concentration plot at  $\chi_{CTAB} = 0.4$ ;  $\chi_{SDBS} = 0.6$ .



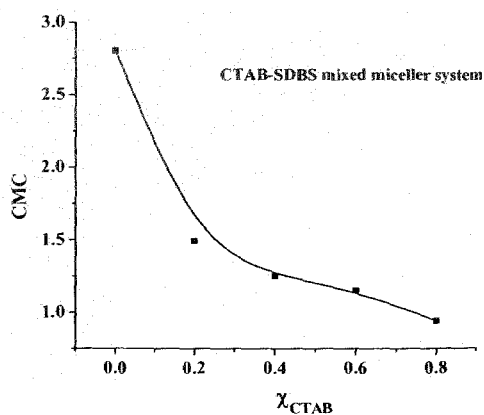
**Figure 6.10:** Conductance vs. concentration plot at  $\chi_{CTAB} = 0.6$ ;  $\chi_{SDBS} = 0.4$ .



**Figure 6.11:** Conductance vs. concentration plot at  $\chi_{CTAB} = 0.8$ ;  $\chi_{SDBS} = 0.2$ .



**Figure 6.12:** Conductance vs. concentration plot at  $\chi_{CTAB} = 1.0$ ;  $\chi_{SDBS} = 0.0$ .



**Figure 6.13:** CTAB – SDBS mixed micelle system at different mol fraction and variation of cmc with mol fraction by conductivity method.

Here the cmc's were determined for the mixed surfactant systems of various mole ratios at a particular temperature. The break points in the surface tension vs. concentration or conductivity vs. concentration plots were taken as cmc. The values for CTAB and SDBS surfactants in pure water are in fair agreement with published data. Micellar aggregates are also formed in an aqueous solution containing SDBS and CTAB. But, the tendency of aggregation is different from that of the pure surfactants. Due to hydrophobic effect, the micellization process is a function of temperature, additive and solvent because the solvent property gets modified in the presence of an additive. However, the aggregation characteristic is found to be interesting because the cmc is a function of mole fraction of each component of the surfactant mixture. In general, the cmc values were found to decrease with the increase in mole fraction of the CTAB suggesting less ionic repulsive forces and stronger hydrophobic effect (figure 6.9 and 6.15). The results indicate that the added cationic surfactant (CTAB in this experiment) is assisting in the micelle formation of the anionic surfactants. This type of variation is also found in presence of increasing mole fraction of hydrotropes [47].

Rewriting equation 6.3 for ideal conditions (with changed notations for CTAB and SDBS), which is also called Clint equation [1], we have equation 6.7.

$$\frac{1}{cmc^*} = \frac{\alpha_1}{C_{c.1}^{mic}} + \frac{\alpha_2}{C_{c.2}^{mic}} \quad (6.7)$$

Where,  $cmc^*$  is the cmc of the mixed system,  $\alpha_1$  and  $\alpha_2$  are the stoichiometric mole fraction of components (CTAB, 1, and SDBS, 2) in binary mixtures are  $C_1^{mic}$  and  $C_2^{mic}$  are the cmc's of CTAB and SDBS respectively. The  $cmc^*$  values obtained from the above equation employing surface tension data are given in the table 6.2 for all the mixtures.

Table 6. 2.  
Mole fraction of different surfactants with  $cmc^*$ .

$X_{CTAB} (\alpha_1)$	$X_{SDBS} (\alpha_2)$	$cmc^*$
0.2	0.8	1.96
0.4	0.6	1.52
0.6	0.4	1.23
0.8	0.2	1.04

The differences in the experimental values of the  $cmc$  and  $cmc^*$  value shows the deviation from ideality. It is indeed interesting to note that the non-ideality of the CTAB and SDBS mixtures is not large. However, the charge neutralization between the head groups of the two components and the interaction of hydrophobic part of CTAB is the SDBS micelles improve the hydrophobic environment in the mixed state in comparison to the pure state. As a result,  $cmc$ 's of the mixture is lower compared to that of pure SDBS micelles. While strong non-ideality is usually expected for anionic / cationic mixtures where strong attractive columbic forces exist, the weak non-ideal behaviour shown by present mixture is indeed interesting. To analyse the synergistic effect of mixed surfactant, different methods are mentioned in literature to calculate interaction parameter. Among these methods, Rubingh's regular solution model is often applied [54].

### Interaction parameter

Interaction parameters for mixed micelle system have been calculated by applying Rubingh's model [54]. According to this model,  $\alpha_1$ ,  $cmc (C_c^{mic})$  and  $x_1$  (mole fraction of component 1, i.e., CTAB) in mixed micelles are related according to the following equation.

$$\frac{[x_1^2 \ln(C_c^{mic} \alpha_1 / C_c^{mic} x_1)]}{(1-x_1)^2 \ln[C_c^{mic} (1-\alpha_1) / C_{c,2}^{mic} (1-x_1)]} = 1 \quad (6.8)$$

The values of  $x_1$  were obtained by solving above equation by successive approximation method. The micelle mole fraction in the ideal state ( $x_1^{ideal}$ ) has been computed using

$$x_1^{ideal} = \left[ \frac{(\alpha_1 C_{c.2}^{mic})}{(\alpha_1 C_{c.2}^{mic} + (1 - \alpha_1) C_{c.1}^{mic})} \right] \quad (6.9)$$

The micellar molecular interaction parameter ( $\beta$ ) is given by the equation:

$$\beta = \frac{\left[ \ln \left( \frac{C_c^{mic} \alpha_1}{C_{c.1}^{mic} x_1} \right) \right]}{(1-x_1)^2} \quad (6.10)$$

The  $\beta$  values may vary from negative to positive through zero. This demonstrates the extent of interaction between the two components which leads to the deviation from ideality. Various theoretical methods are available to interpret the formulation of mixed micelles. The final model given by Lange, and used by Clint, is based on the phase separation model and assumes ideal mixing of the surfactants in the micellar phase. Rubingh proposed a treatment based on 'regular solution theory' (RST) for non ideal mixed systems which have been extensively used. The reason for the non-ideal behaviour among surfactant molecules upon mixing are then various types of molecular interactions. These interactions (either synergistic or antagonistic) can be analysed by RST which allows the evaluation of micelle mole fraction ( $x_1$ ) and interaction parameter ( $\beta^m$ ). According to RST, the molecules of mixing components should be of comparable size, completely interchangeable, and the interaction energy could be expressed as seem of pair wise neighbour interactions. The value of  $\beta$  is proportional to the free energy of mixing, a negative  $\beta$  value means synergism in the system. Thus, a negative deviation from ideal behaviour, corresponding to negative  $\beta$  values is believed to result from a net attraction between the two different surfactant molecules. It indicates that the attractive interactions between the two component molecules are stronger than the interaction among molecules of same components. Positive  $\beta$  values have been ascribed to antagonistic behaviour. It means that the repulsive forces between two mixing components are stronger than the repulsions among similar molecules. A  $\beta^m$  value close to zero means the mixing is almost ideal [55].

Table 6.3.

The computed values of  $\alpha_1$  and  $\beta$  parameters for the present mixture of SDBS and CTAB [Interaction Parameters of CTAB/SDBS System (1) CTAB = 1; SDBS = 2]

$\alpha_{CTAB}$	$\alpha_{SDBS}$	cmc(c) <sup>a</sup> (mM)	Cmc <sup>b</sup> (ST) (mM)	cmc (avg) (mM)	$\alpha_1$	cmc* /mM	$\beta$	f <sub>1</sub>	f <sub>2</sub>
0	1.0	2.78	2.82	2.80	-	2.80	-	-	-
0.2	0.8	1.49	1.40	1.445	0.539	0.9	-2.45	0.175	0.4889
0.4	0.6	1.25	1.25	1.25	0.569	0.9	-0.128	0.916	0.959
0.6	0.4	1.15	1.10	1.125	0.749	0.9	+0.021	1.009	1.0119
0.8	0.2	0.94	0.93	0.935	0.839	0.9	-0.364	0.897	0.773
1.0	0.0	0.90	0.90	0.90	-	0.9	-	-	-

<sup>a</sup> measured from conductivity data; <sup>b</sup> measured from surface tension data.

For anionic and cationic surfactant mixture,  $\beta$  values are usually found to be highly negative. This indicates very strong synergism [56-57]. Significant synergistic effects have been observed for mixtures of two ionic surfactants with identical head groups but different hydrocarbon part [58-59]. It has also been argued that synergistic effects mostly are due to entropy contributions to the aggregation free energy rather than to specific interactions among the surfactant headgroups [55]. In the present system of CTAB and SDBS mixture,  $\beta$  values are also negative as found within the range of -2.45 to -0.364 (table 6.3). Previous results revealed that the free energy of forming a surfactant aggregate can be written as a sum of several contributions [60,61]: (i) the reduction of contact area between hydrocarbon and water, (ii) conformational entropy due to packing restrictions of the hydrocarbon chains, (iii) electrostatics for a charged aggregate surface and its diffuse layer of counterions, (iv) additional contributions related to the head groups, and (v) entropy of mixing the two surfactants. Electrostatics yields a large contribution to the aggregate free energy for mixtures consisting of ionic surfactants. According to the Poisson-Boltzmann (mean field) description, this contributions mainly due to the entropically unfavourable organization of the counterions into a diffuse layer located outside the electrically charged surface of an aggregate, whereas the purely energetic effects usually are much

smaller for surfactants mixtures like CTAB and SDBS which explains comparatively lower interactions parameter.

## **Rheology of viscoelastic worm-like micelles found in the system containing SDBS and CTAB in Water**

### **Behaviour of some surfactant mixtures under non-Newtonian flow regime**

Aqueous mixtures of anionic and cation surfactant have been found to show fundamentally different properties than the corresponding solutions of pure ionic surfactant or mixture of an ionic and a non-ionic surfactant. The spontaneous formation of rather small unilamellar vesicles has been particularly emphasized, although a number of other structures, such as small globular and large worm-like micelles as well as large lamellar sheets have also been observed [62-64].

The most conspicuous property is, however, the usually large reduction in cmc when two oppositely charged surfactants are mixed in an aqueous solvent. Whereas mixtures of an ionic and a non-ionic surfactant normally yield deviation from ideal behaviour corresponding to  $-5 < \beta < -1$ , and synergistic effects in mixtures of two non-ionic surfactants are even less, experimentally obtained  $\beta$  values for mixtures of an ionic and a cationic surfactant are usually several magnitudes larger [65]. However, the synergistic effects are observed to increase with increasing length of the surfactant tail. Accordingly,  $\beta$  values for  $C_nSO_4Na^+ / C_nTA^+Br^-$  (TA = trimethyl ammonium) mixtures have been found to be  $\beta = -25.5$  for  $n = 12$ ,  $\beta = -18.5$  ( $n = 10$ ), and  $\beta = -10.5$  ( $n = 8$ ) [66-67].

In analogy with the regular mixture theory,  $\beta$  is generally referred to as the interaction parameter and its deviation from zero has frequently been believed to be the result of specific interactions between the surfactant head groups so that it is different between surfactant 1 and 2 compared to between two identical head groups. According to this interpretation the conspicuously large magnitudes of  $\beta$  found for mixtures of most of the oppositely charged surfactants are due to very strong attractive interactions between the aggregated anionic and cationic head groups, and it has been suggested that such interactions may account for the micelle-to-vesicle transition frequently observed in aqueous cationic surfactant mixtures [52].

On the other hand, present system of cationic and anionic surfactant mixtures of CTAB and SDBS neither exhibits very large deviation from ideality nor yield high  $\beta$  values ( $\beta$  value in the present system lie between -0.364 to -2.45). This is indeed interesting. In all probabilities, the unique behaviour of this mixture stems from the very structure of SDBS molecule, where the alkyl chain is present not as linear long hydrocarbon tail but as the branched chain as shown in section 3.4.1 of this thesis. However, on account of wide industrial applications of SDBS surfactant in various fields, the behaviour of CTAB/SDBS mixture is studied in this work to further detail in non-Newtonian flow regime. Viscoelastic properties including dynamic rheology of the system at different temperature have been investigated to understand the microstructural pattern of the mixed micelles. The self-assembly of both CTAB and SDBS individually result in the formation of globular micelles near the respective cmc values. Further, when these cationic and anionic surfactants are mixed together at low concentration, the mixture synergistically leads to the formation of globular micelles again under Newtonian flow regime, as has already been discussed. On the other hand, when the concentrations of the individual component of the mixtures are increased (e.g., CTAB = 100 mM and SDBS = 20 mM), a viscoelastic gel is formed and the flow becomes non-Newtonian in nature. The observed viscoelasticity is related to worm-like micelle (WLM) formation. The structures of WLM have fascinated scientists because they are similar to polymer chain in their ability to entangle into viscoelastic networks. At the same time, micellar chains are held by weak physical bonds unlike the covalent bonds in polymer; consequently, the chain can break and recombine, and their contour length is not fixed by chemical synthesis but by solution thermodynamics [13]. From a rheological standpoint, wormlike micellar samples are interesting because they can behave as Maxwell fluids (i.e., as model viscoelastic fluids having just a single relaxation time) [68].

Therefore, in general, the experimental solutions exhibit three regions of rheological response. First, at low surfactant concentration, the solutions are Newtonian liquids with low viscosity and non-measurable elastic response. Second, with increasing surfactant concentration, they behave like polymer solutions in the semi-dilute regime, characterized by viscoelastic behaviour with a spectrum of relaxation times. Finally, with increase in the counter ion concentration, these materials enter a regime where their rheological response is similar to that of an entangled polymer or weak gel; however, unlike polymer systems, there relaxation

after shear is dominated by a single relaxation time. In the present chapter of the thesis rheology of viscoelastic worm-like micelles formed in the system of SDBS and CTAB mixtures have been studied.

### Rheology of worm-like micelles formed in SDBS and CTAB system

Modelling techniques are used to quantify rheological parameters that can be obtained from oscillating shear results. Many authors have used simple Maxwell element to fit rheological data obtained from viscoelastic surfactant solutions [69-70]. A simple Maxwell element describes the rheological behaviour of a system as a single spring connected in series to a viscous element (dashpot). In shear experiments, this results in equations from  $G'$  and  $G''$  of the form

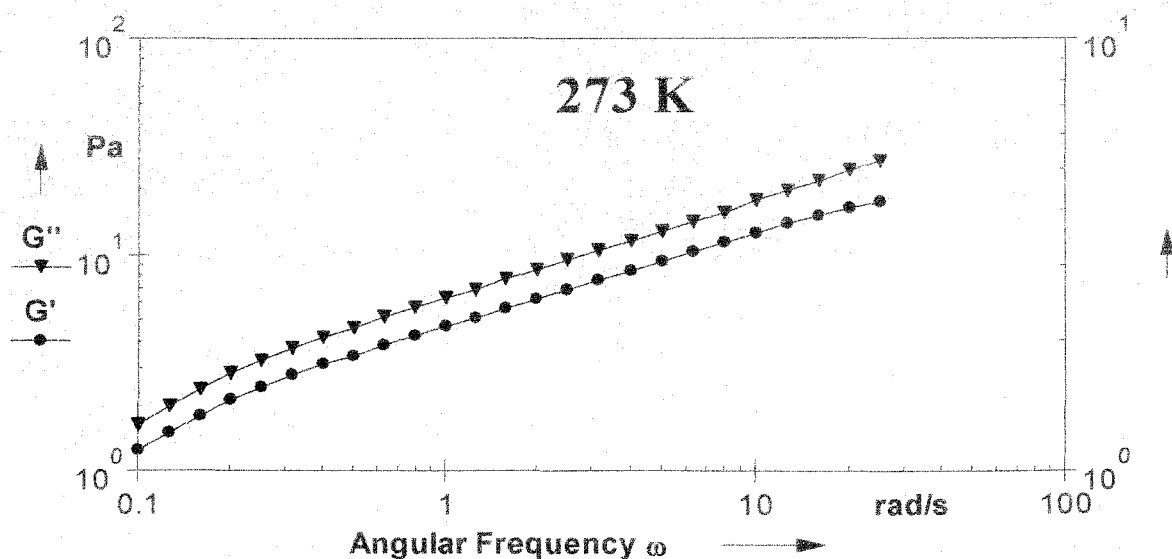
$$G'(\omega) = \frac{G_N^0 \omega^2 \tau^2}{1 + \omega^2 \tau^2} \quad (6.11)$$

$$G''(\omega) = \frac{G_N^0 \omega \tau}{1 + \omega^2 \tau^2} \quad (6.12)$$

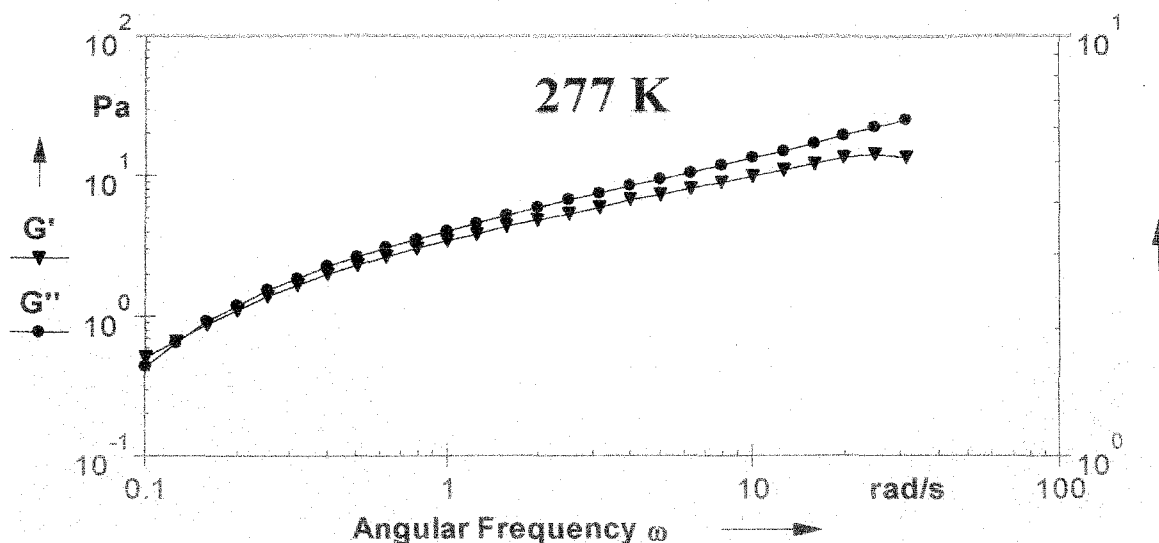
Where  $G'$  and  $G''$  are elastic modulus and viscous modulus respectively,  $\omega$  is the frequency,  $G_N^0$  is the plateau modulus, and  $\tau$  is the relaxation time. In the time domain, this type of model has single exponential decay, with  $G(t) = G_N^0 e^{-t/\tau}$ . Maxwell elements are useful in determining  $G_N^0$  and  $\tau$  of systems dominated by a single relaxation time or in a limited portion of a materials frequency response range if the relaxation times are well separated.

In our experiments, the rheological data are typical of viscoelastic wormlike micelles, with a plateau in  $G'$  at high frequencies and terminal behaviour of  $G'$  and  $G''$  at low frequencies [figure 6.14 to 6.23]. Moreover, the sample is nearly a Maxwell fluid over a short range of temperatures (303 K - 335 K). Plots are shown from temperature range 273 to 313 K. No cross over point is displayed beyond the temperature range of 303 K - 313 K, except at 281 K. We find that the Maxwell model fits the data well, especially at low and intermediate frequencies, as has been shown for normal worm in the above temperature ranges. Turning to the effect of temperature on the rheological data, we have also found that as the temperature increases, the entire frequencies move or shorter time scales, but the plateau modulus  $G_p$  remains constant which was also reported by several workers in other systems [69-71]. This shift in crossover frequency to higher values means that the relaxation time decreases with temperature.

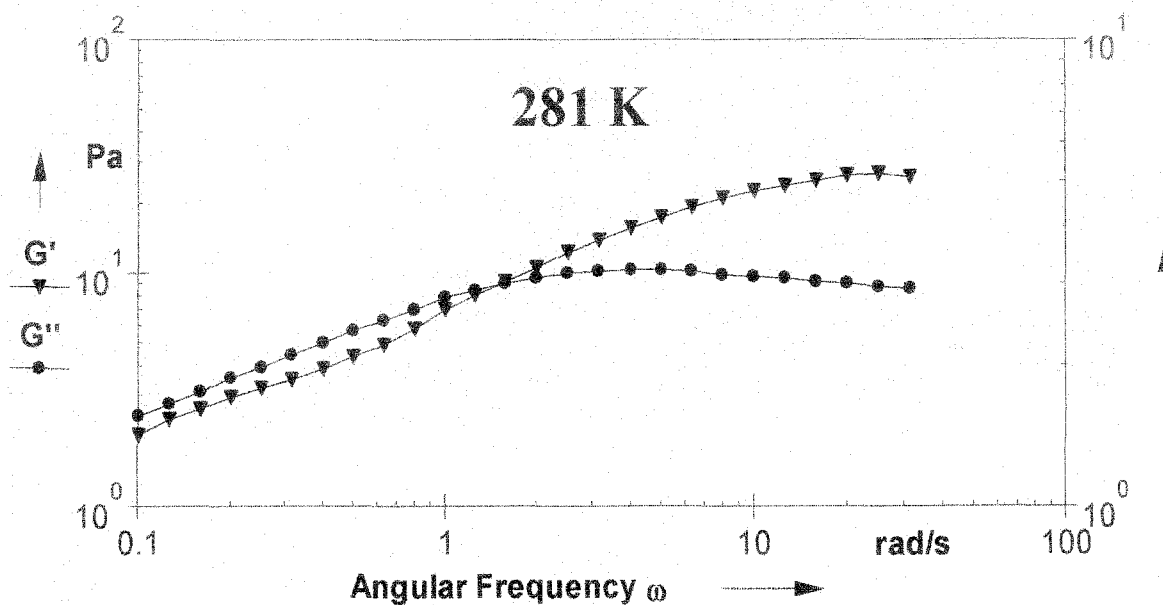
Mukherjee [54] had proposed that an additive which is surface active to a hydrocarbon-water interface will be mainly solubilized at the head group region and will promote micelle growth. Therefore, CTAB is expected to be embedded between SDBS monomers of the micelles. This embedding of CTAB may increase the volume of the micelle. This consequently modify the effective spontaneous curvature via modified packing parameter is responsible for the micelle growth in one dimension. The result is the micro-structural transformation from spherical to wormlike micelle with increasing CTAB concentrations in presence of SDBS. When micelles are sufficiently long, they are converted into more flexible wormlike micelles which can flow comparatively easily. Which reflects by a level off in the  $G'$ . At further high concentration, a micro-structural change in micelle structure results the change in rheological parameter. The increase in viscosity to a very small extent can be attributed also by micro-structural change. It is expected that a sufficient amount of CTAB will be present which will embedded between the head groups. Further with increase in temperature, the Br ion may be released and would show higher preference for the bulk phase. Such a release if occurs would increase the effective head group area, thereby driving micro-structural change of higher curvature resulting in an increase in viscosity.



**Figure 6.14:** Steady shear frequency curves of CTAB and SDBS mixture [CTAB (100 mM) + SDBS (20 mM)]: variation of  $G'$ ,  $G''$  with angular frequency (temperature = 27<sup>o</sup> C or 273 K); crossover frequency,  $\omega_c$  = not within inspected range; complex viscosity,  $\eta^* = 20.443$  Pa.s; strain,  $\gamma = 10$  %)



**Figure 6.15:** Steady shear frequency curves of CTAB and SDBS mixture [CTAB (100 mM) + SDBS (20 mM)]: variation of  $G'$ ,  $G''$  with angular frequency (temperature =  $40^\circ\text{C}$  or 277 K); crossover frequency,  $\omega_c =$  not within inspected range; complex viscosity,  $\eta^* = 7.648 \text{ Pa}\cdot\text{s}$ ; strain,  $\gamma = 10 \%$ ).



**Figure 6.16:** Steady shear frequency curves of CTAB and SDBS mixture [CTAB (100 mM) + SDBS (20 mM)]: variation of  $G'$ ,  $G''$  with angular frequency (temperature =  $80^\circ\text{C}$  or 281 K); crossover frequency,  $\omega_c = 1.499 \text{ rad}\cdot\text{s}^{-1}$ ; complex viscosity,  $\eta^* = 68.825 \text{ Pa}\cdot\text{s}$ ; strain,  $\gamma = 10 \%$ ).

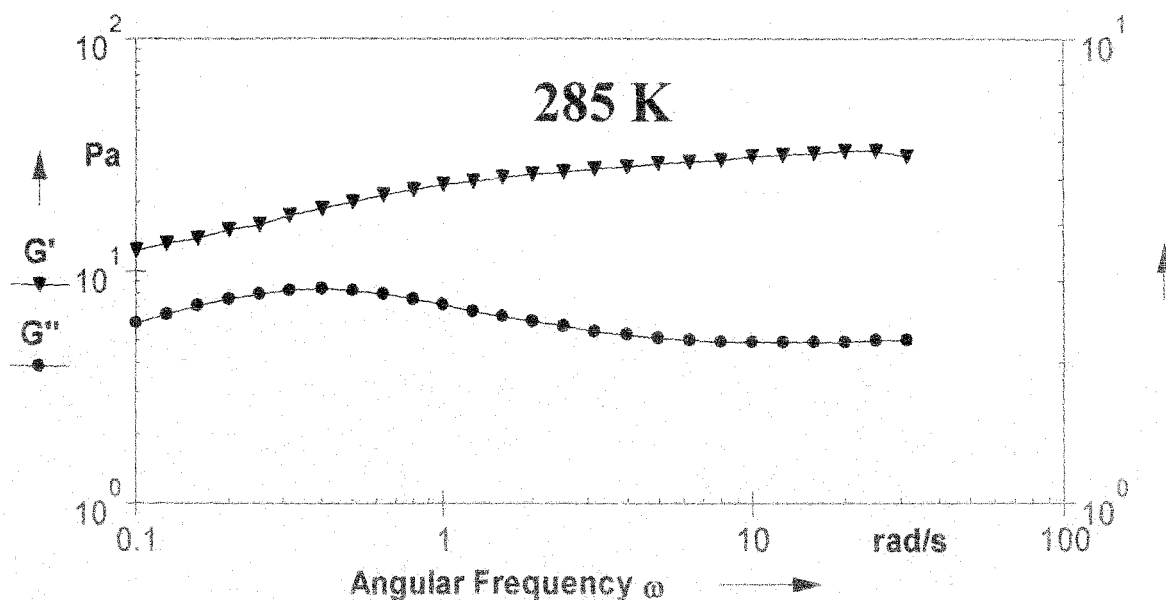


Figure 6.17: Steady shear frequency curves of CTAB and SDBS mixture [CTAB (100 mM) + SDBS (20 mM)]: variation of  $G'$ ,  $G''$  with angular frequency (temperature = 12° C or 285 K); crossover frequency,  $\omega$  = not within inspected range; complex viscosity,  $\eta^* = 258.5$  Pa.s; strain,  $\gamma = 10$  %).

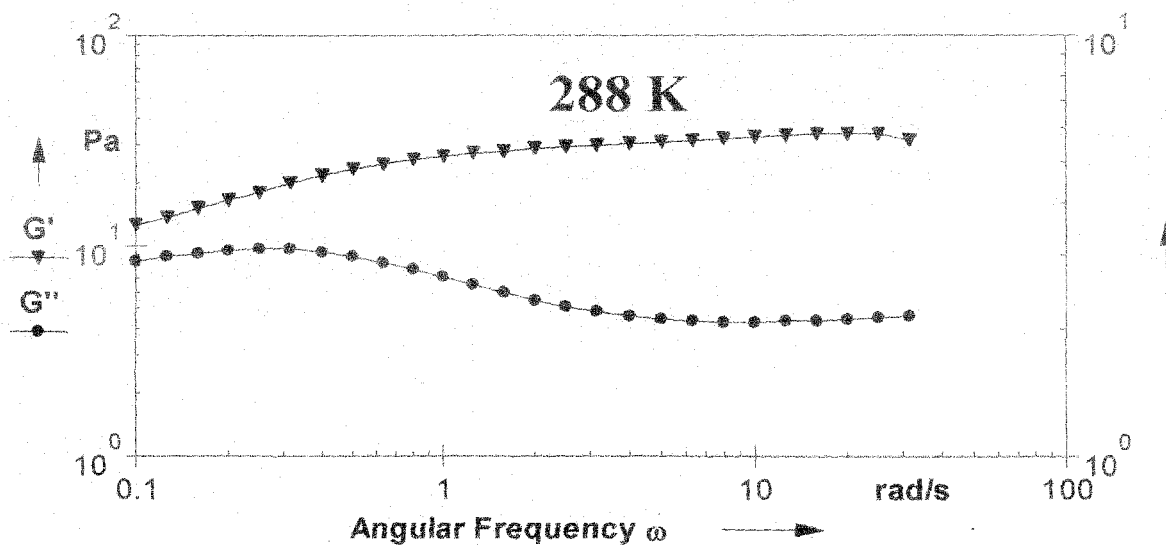


Figure 6.18: Steady shear frequency curves of CTAB and SDBS mixture [CTAB (100 mM) + SDBS (20 mM)]: variation of  $G'$ ,  $G''$  with angular frequency (temperature = 15° C or 288 K); crossover frequency,  $\omega$  = not within inspected range; complex viscosity,  $\eta^* = 253.36$  Pa.s; strain,  $\gamma = 10$  %).

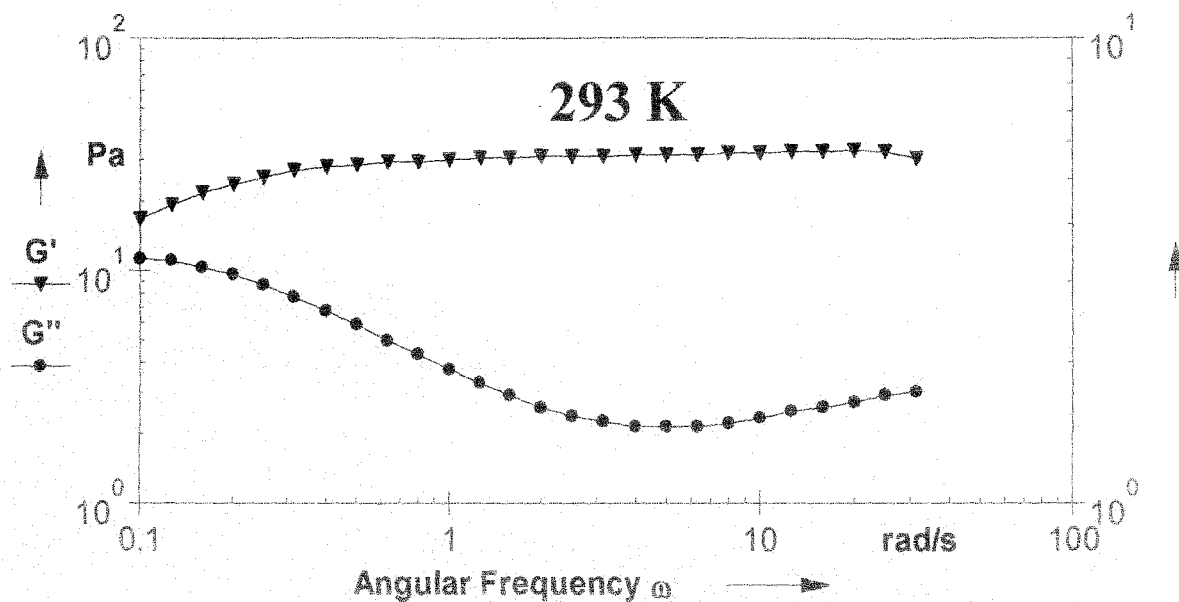


Figure 6.19: Steady shear frequency curves of CTAB and SDBS mixture [CTAB (100 mM) + SDBS (20 mM)]: variation of  $G'$ ,  $G''$  with angular frequency (temperature = 20° C or 293 K); crossover frequency,  $\omega$  = not within inspected range; complex viscosity,  $\eta^* = 247.65$  Pa.s; strain,  $\gamma = 10$  %).

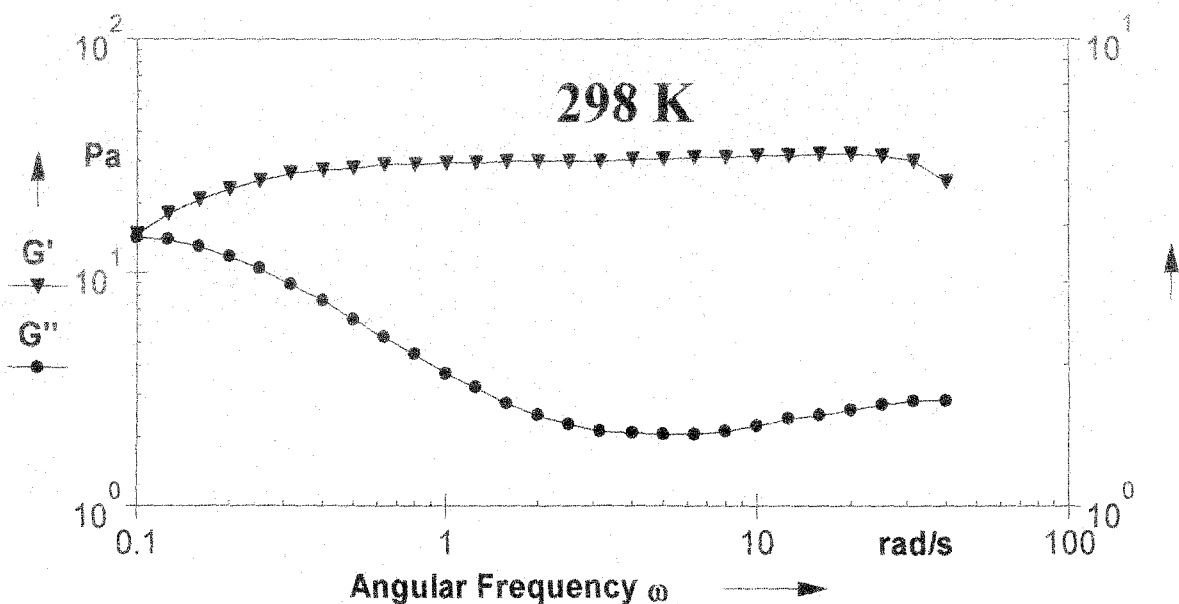


Figure 6.20: Steady shear frequency curves of CTAB and SDBS mixture [CTAB (100 mM) + SDBS (20 mM)]: variation of  $G'$ ,  $G''$  with angular frequency (temperature = 20° C or 298 K); crossover frequency,  $\omega$  = not within inspected range; complex viscosity,  $\eta^* = 232.75$  Pa.s; strain,  $\gamma = 10$  %).

A representative fitting of Maxwell model is shown, which indicates fairly good fitting at low frequencies.

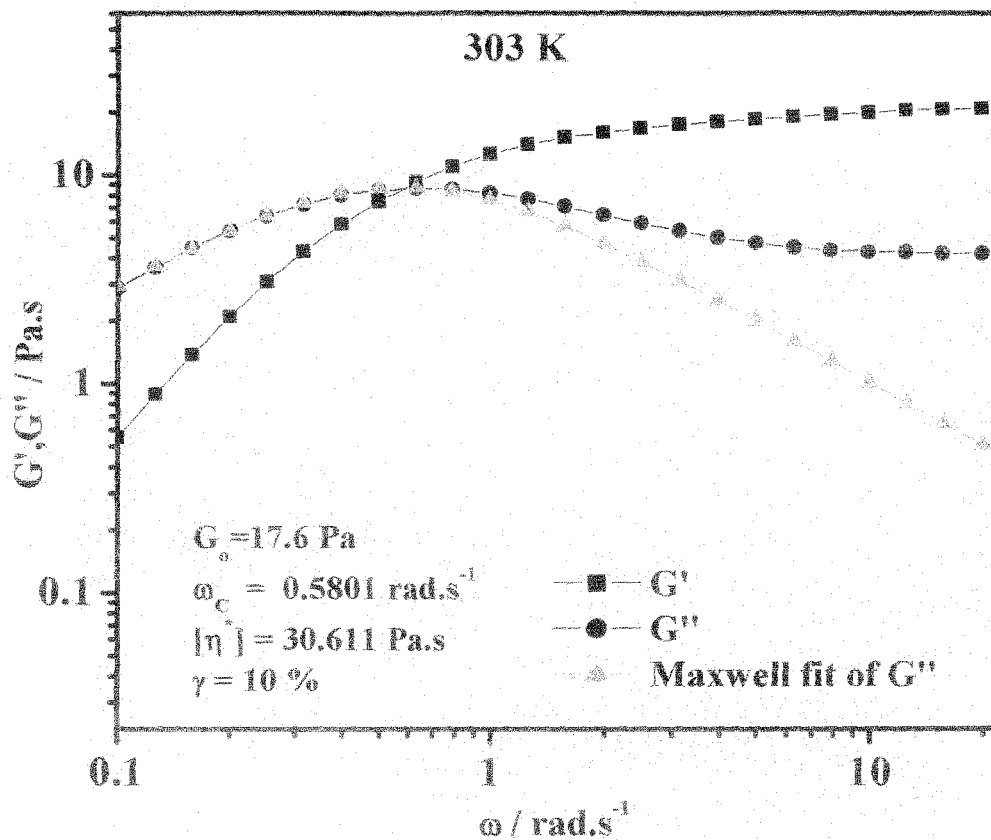


Figure 6.21: Steady shear frequency curves of CTAB and SDBS mixture [CTAB (100 mM) + SDBS (20 mM)]: variation of  $G'$ ,  $G''$  with angular frequency (temperature =  $30^\circ\text{C}$  or 303 K); crossover frequency,  $\omega = \omega_c = 0.5801 \text{ rad.s}^{-1}$ ; complex viscosity,  $\eta^* = 30.611 \text{ Pa.s}$ ; strain,  $\gamma = 10\%$ ).

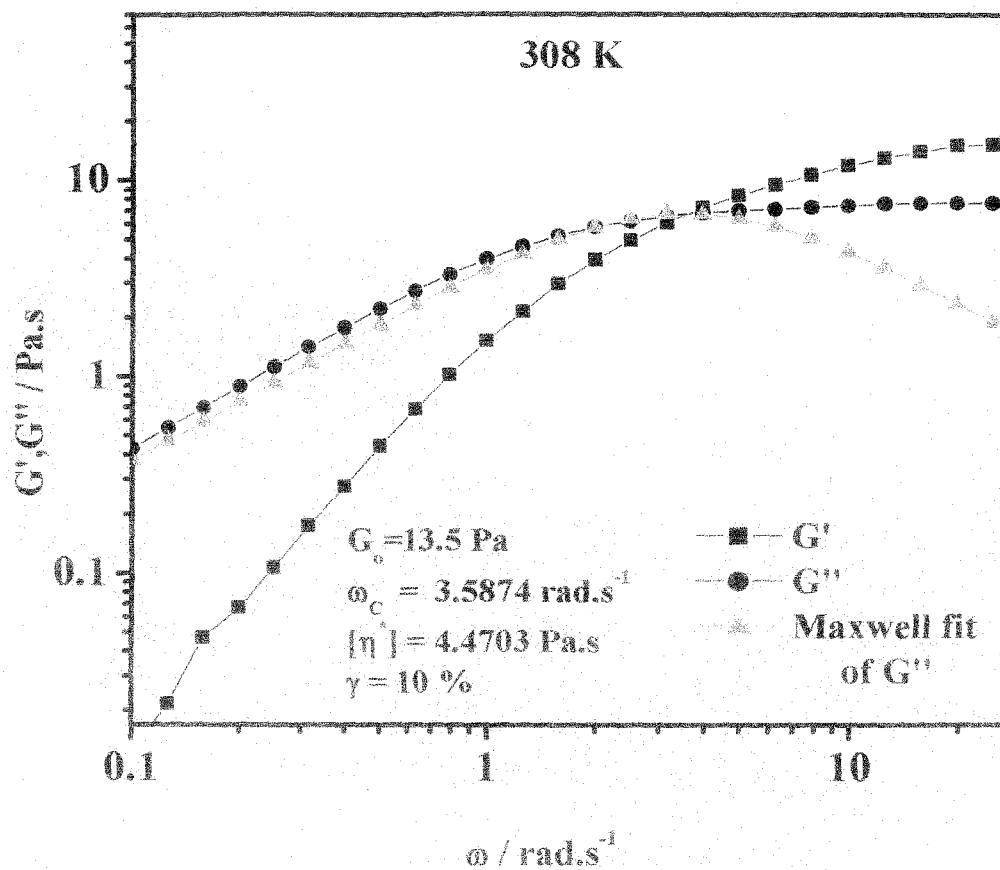


Figure 6.22: Steady shear frequency curves of CTAB and SDBS mixture [CTAB (100 mM) + SDBS (20 mM)]: variation of  $G'$ ,  $G''$  with angular frequency (temperature = 35°C or 308 K); crossover frequency,  $\omega = \omega_c = 3.5874 \text{ rad.s}^{-1}$ ; complex viscosity,  $\eta^* = 4.4703 \text{ Pa.s}$ ; strain,  $\gamma = 10\%$ ).

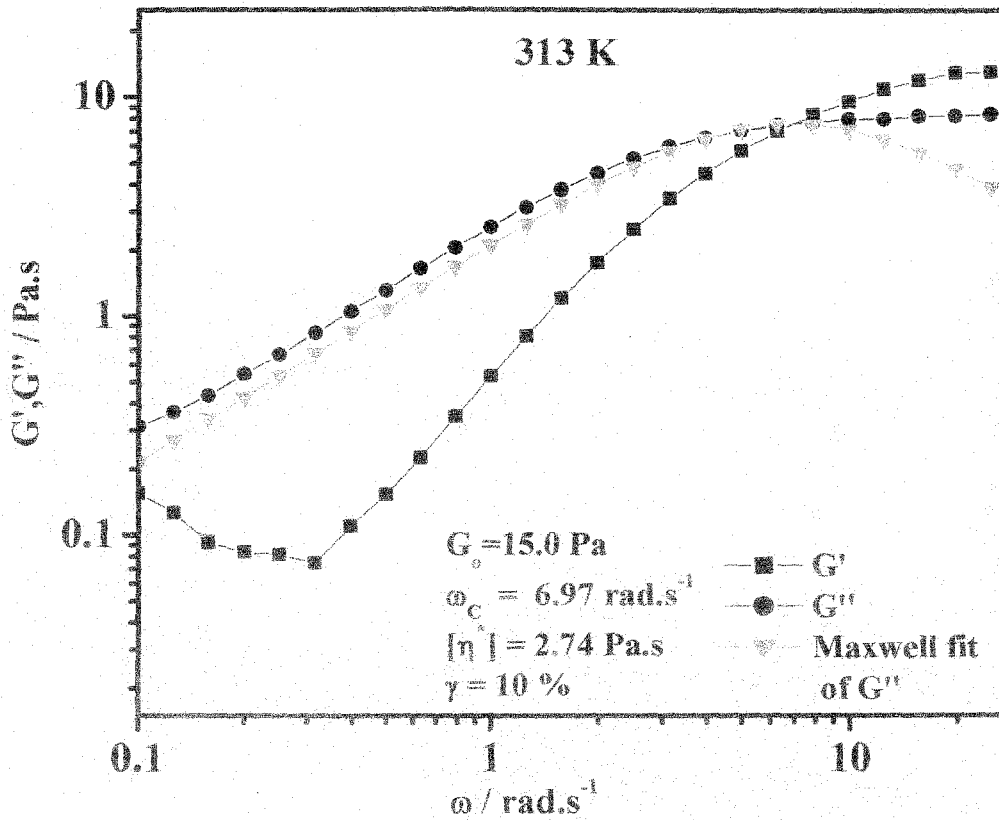


Figure 6.23: Steady shear frequency curves of CTAB and SDBS mixture [CTAB (100 mM) + SDBS (20 mM)]: variation of  $G'$ ,  $G''$  with angular frequency (temperature = 40°C or 313 K); crossover frequency,  $\omega = \omega_c = 6.9719 \text{ rad.s}^{-1}$ ; complex viscosity,  $\eta^* = 2.7426 \text{ Pa.s}$ ; strain,  $\gamma = 10\%$ ).

From the oscillatory rheometry figures 6.14 to 6.23, there is clear viscoelastic behaviour of certain SDBS and CTAB mixtures. At low frequencies the loss modulus ( $G''$ ) is higher than the storage modulus ( $G'$ ), indicating that the sample behaves as a liquid and also predominantly viscous whereas at high frequencies,  $G'$  is greater than  $G''$ , which implies that the mixtures behave like a solid which is predominantly elastic in the temperature range 303 – 313 K. As has already been mentioned that the data fits to the Maxwell model of relaxation at low frequencies but diverges at high frequencies, which is typical of worm like micellar solution with several relaxation modes [72]. The dip of the  $G''$  curve even at higher frequencies is due to the presence of further relaxation modes.

It is sometimes difficult to determine how "good" a Maxwell model fits the data from plots of  $G'$  and  $G''$  versus  $\omega$ . Systems that have a spectrum of closely spaced relaxation times may appear to be fit by a single Maxwell's element. Cole - Cole or Nyquist plots (plots of  $G''$  as a function of  $G'$ ) provide a better picture of how well this data correspond to a single relaxation time Maxwell model. A Cole - Cole plot for a perfect Maxwell element is a semicircular, where as a plot for a system with many relaxation times in a narrow range is boxlike. The curve in the present system fits to good extent to a simple Maxwell model (figure 6.24 - 6.26). The data points fit fairly well on a semicircle curve particularly at 303 K. A single exponential relaxation can be effectively explained in case of worm like micelles. According to Cates, the possibility of breaking and recombination introduces new mechanism for stress relaxation for living polymers, in addition to the reptation process [72]. Mean filled model introduces two characteristic times for this process, these are reptation time of an unbreakable chain and the average time before such a chain breaks into two pieces as a result of the reversible scission process. Several theories have been predicted depending on the relative ratio of the two characteristics time scales. From these theories, it may be concluded that when average time is very much greater than the reptation time, the micelles behave like ordinary polydisperse unbreakable polymers with exponential polydispersity and the stress relaxation function which are different from monodisperse polymers. When reptation time is greater than average time, chain breakage and recombination will both occur often for a typical chain, before it has disengaged from the tube by ordinary reptation. In this case, the reptation mechanism is short circuited and the new relaxation process will be monoexponential with a new time scale. This explains the observed single exponential behaviour of the system, because before a given tube segment relaxes, the chain occupying it typically undergoes many scission and recombination reactions, so that there is no memory of either the initial length of the chain or the position on the chain initially corresponding to the tube segment. The deviations from the half circle occur at a circular frequency  $\omega$  of the order of the inverse of the breaking time of the micelles. At higher frequencies the data deviate from the Maxwell model, which is typically the case when the systems can no longer be described by a single relaxation time. So, a Cole - Cole plot can easily visualize how well the data correspond to the Maxwell model. The large deviation from Cole - Cole plot with high angular viscosity is indicative that of a less structured system with poor viscoelastic behaviour.

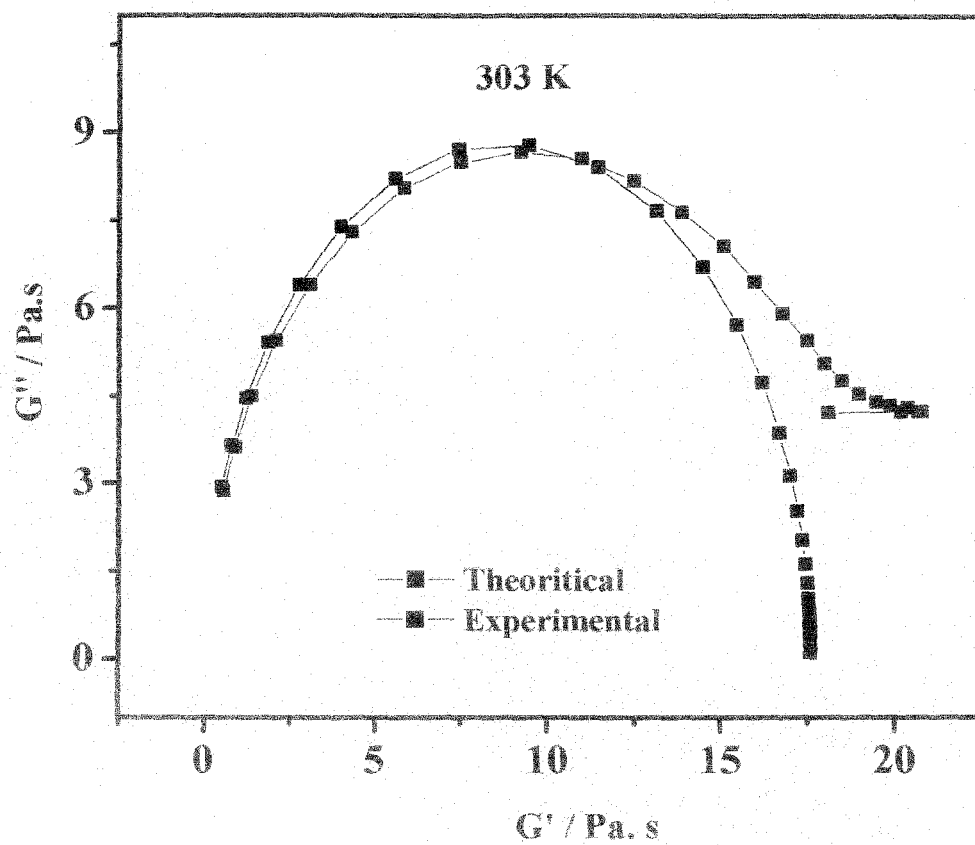


Figure 6.24: Cole - Cole Plot ( $G''$  as a function of  $G'$ ) using data presented in figure 6.23 at 303 K.

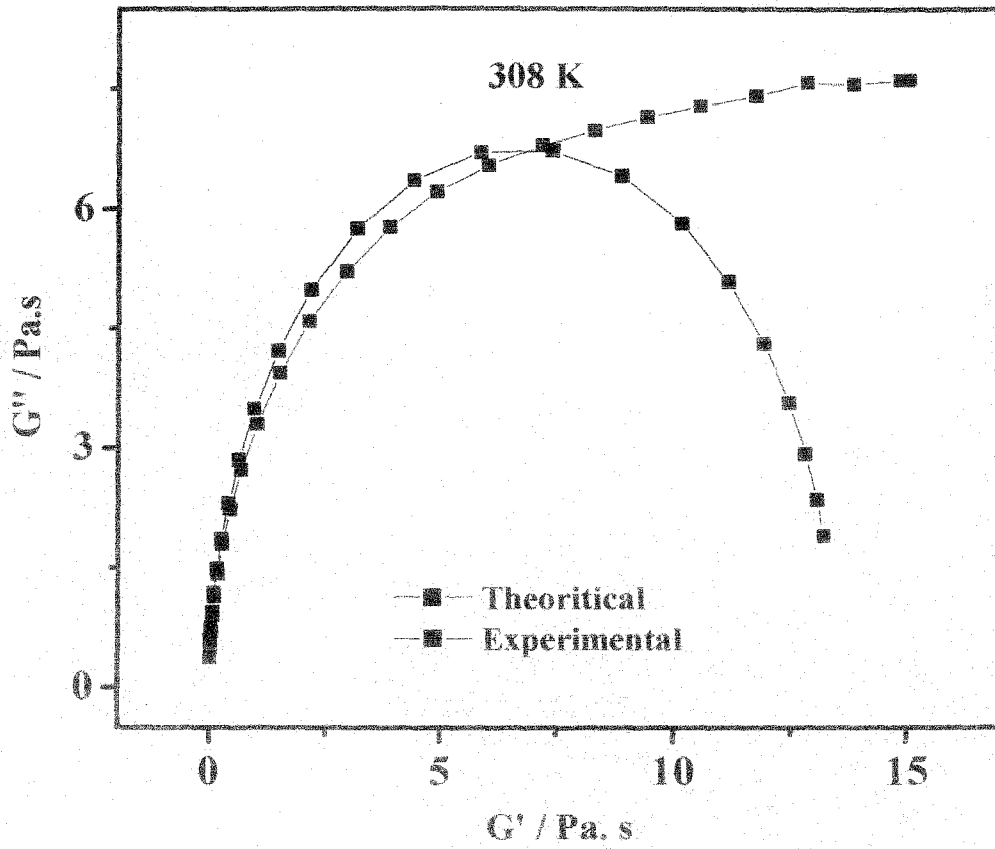


Figure 6.25: Cole - Cole Plot ( $G''$  as a function of  $G'$ ) using data presented in figure 6.24 at 308 K.

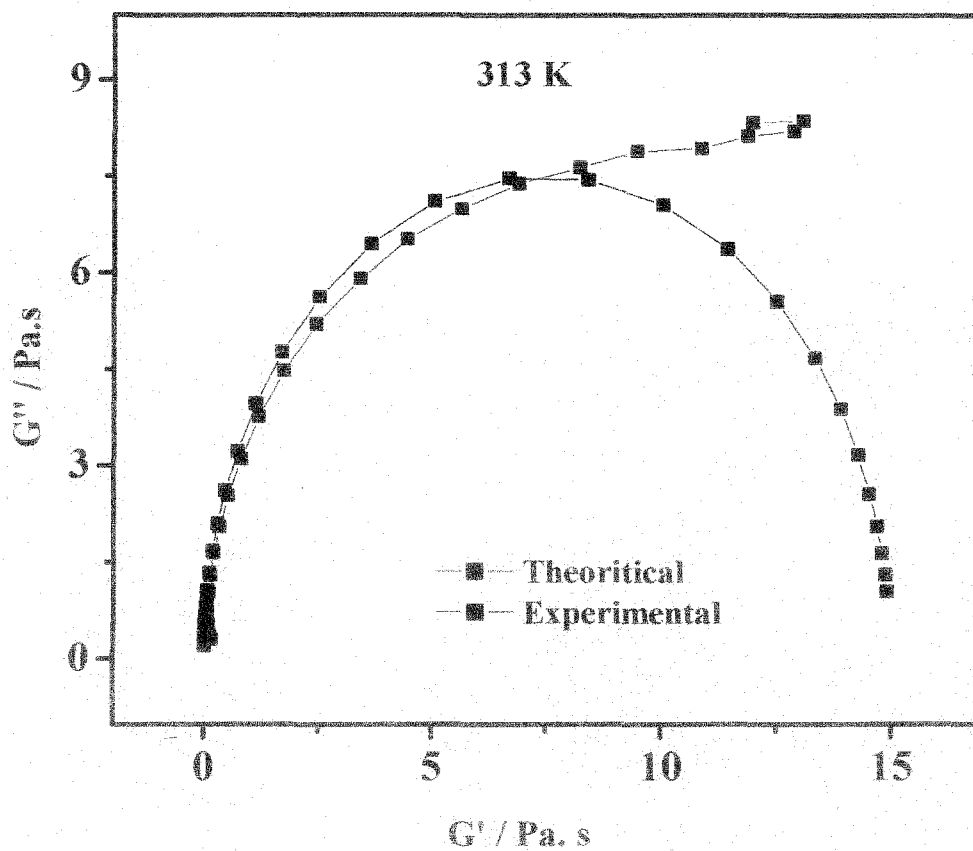


Figure 6.26: Cole - Cole Plot ( $G''$  as a function of  $G'$ ) using data presented in figure 6.25 at 313 K.

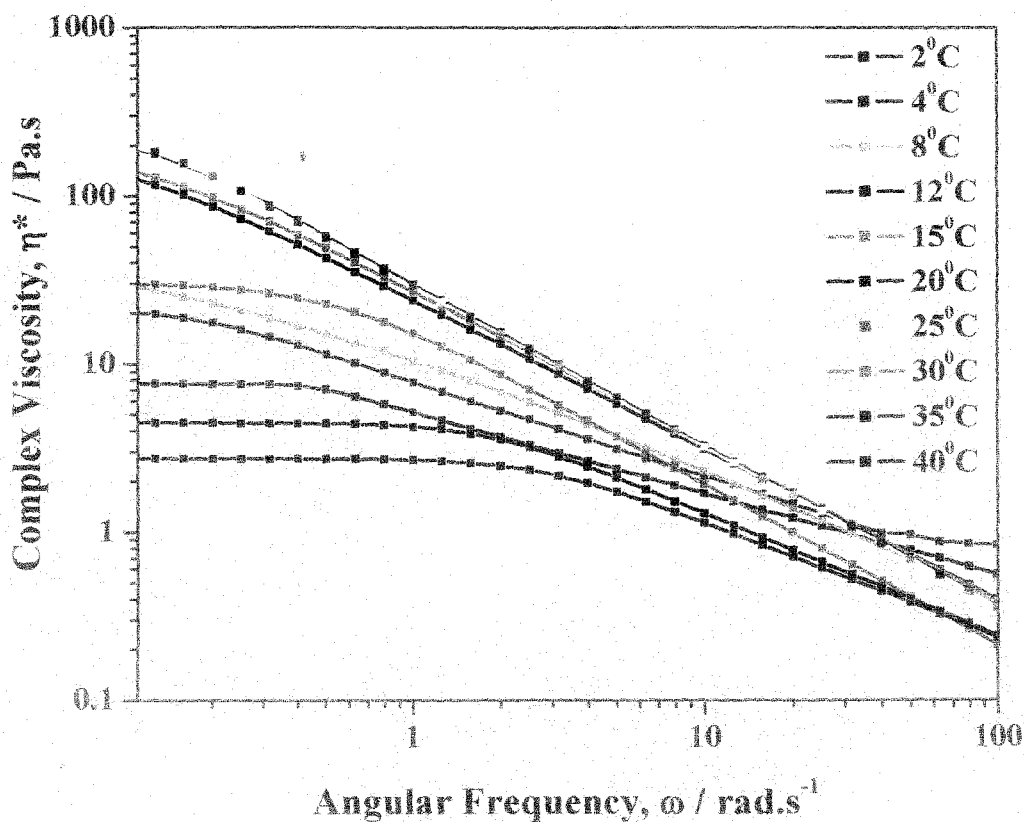


Figure 6.27: Complex viscosity Vs. Angular frequency plot

It is noteworthy that for the present surfactant mixtures the experimental data for  $G'$  and  $G''$  deviate from the Maxwell model at higher frequencies. Granek and Cates have shown that the high frequency deviations can be accounted for by the Rouse models and the primitive path fluctuations along the micelle chain [23]. Similar results were also obtained for other viscoelastic samples in the higher concentration range [73-74].

The zero-shear viscosity of the surfactant mixtures was determined from controlled-stress measurements by extrapolating the viscosity-shear stress curve to zero shear rate.

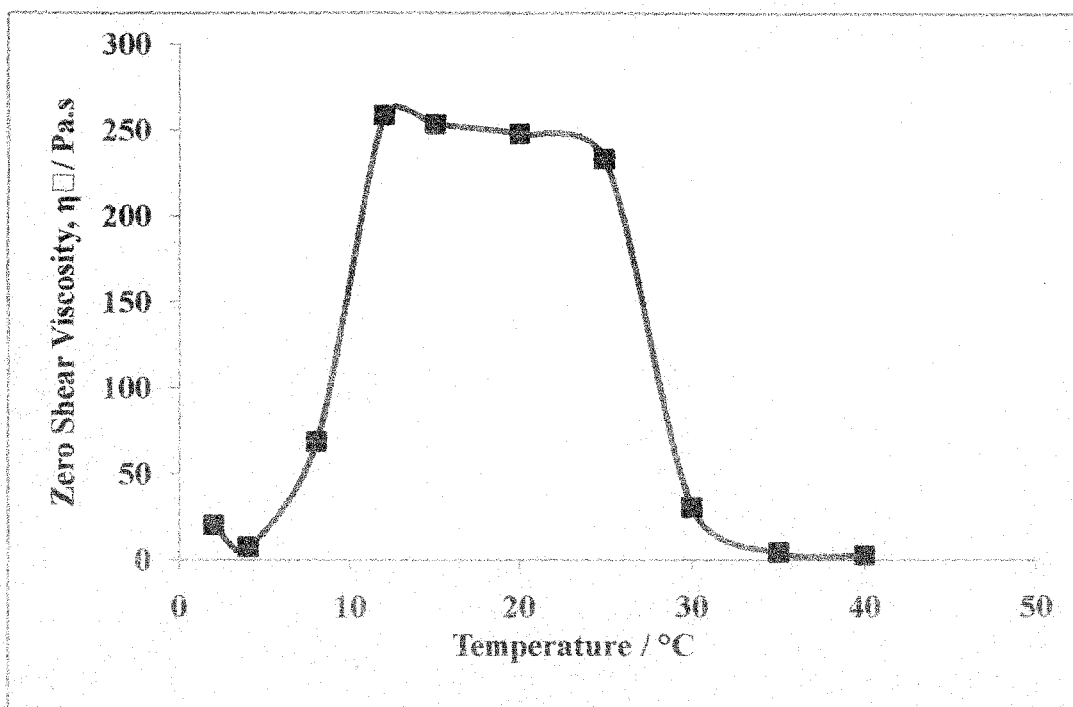
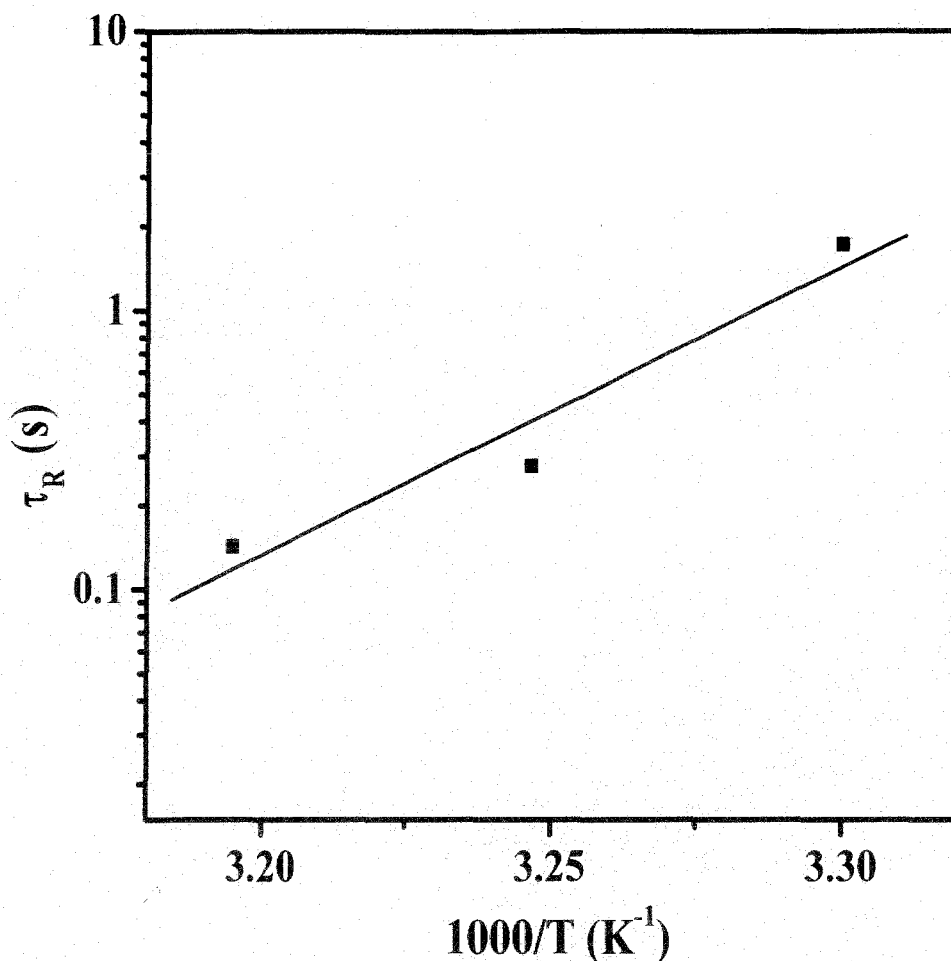


Figure 6.28: Variation of Zero Shear Viscosity,  $\eta_0$  with Temperature of the surfactant mixture {CTAB (100 mM) + SDBS (20 mM)}.

In terms of stress relaxation, it is slowest at the viscosity peak and increases at both lower and higher temperatures. Figure 6.28 shows the change in  $\eta_0$  with temperature. It is clear that with increase in temperature,  $\eta_0$  increases indicating an increase in the curvature energy for surfactant aggregates which leads to an increase in micellar length and the formation of wormlike micelles. As the temperature further increased, the zero shear viscosity exhibits a flat maximum within 10°C to 26°C temperatures. Further increase in temperature decreases the zero shear viscosity can be explained as a decrease of the micellar contour length or the formation of branched micelles as also found by other researchers [78]. In summary, all these results support a fascinating and complex rheology to exist in the present system is a structural evolution from a spherical micelle to a worm like micelle.



**Figure 6.29:** Arrhenius Semi log plot of  $\tau_R$  vs  $1/T$  for CTAB-SDBS (100 mM: 80 mM) system .

Finally, the shift in cross over frequency  $\omega$  to higher values indicate that the relaxation time  $\tau$  decreases with temperature (figure 6.22-6.24). The variation of  $\tau$  with temperature is shown in figure 6.31 on Arrhenius plot (i.e., a semilog plot of the quantities vs.  $1/T$ ). We find that the  $\tau$  values fall on a straight line, indicating an exponential decrease that can be represented by the following equation.

$$\tau = A \exp\left(\frac{E_A}{RT}\right) \quad (6.13)$$

Where  $E_A$  is the flow activation energy,  $R$  is the gas constant,  $T$  is the absolute temperature and  $A$  is the pre exponential factor. The figure shows that for the present system containing CTAB and SDBS mixture, the  $E_A$  value is 85.44 kJ/mol, which is comparable with represented values for other similar systems.

**References:**

1. J. M. Lehn, *Science*, **2002**, 295, 2400
2. G. M. Whitesides and M. Boncheva, *Proc. Natl. Acad. Sci. U. S. A.*, **2002**, 99, 4769.
3. D. Philip and J. F. Stoddart, *Angew. Chem., Int. Ed. Engl.*, **1996**, 35, 1155.
4. H. W. Jun, S. E. Paramonov and J. D. Hartgerink, *Soft Matter*, **2006**, 2, 177.
5. T. J. Deming, *Soft Matter*, **2005**, 1, 28.
6. Y. Lin, Y. Qiao, Y. Yan and J. Huang, *Soft Matter*, **2009**, 5, 3047.
7. Fuhrhop, J - H and Helfrich. W., *Chem. Rev.*, **1993**, 93, 1565 - 1582.
8. Salkar, R. A., Hassan, P. A., Samant, S. D., Valaulikar, B. S., Kuma, R. V. V., Kern, F., Candau, S. J. and Manohar, C., *J. Chem. Soc., Chem. Comm.*, **1996**, 1223 - 1224.
9. S. Svenson, *Curr. Opin. Colloid Interface Sci.*, **2004**, 9, 201
10. T. Kunitake and Y. Okahata, *J. Am. Chem. Soc.*, **1977**, 99, 3860.
11. J. C. Hao and H. Hoffmann, *Curr. Opin. Colloid Interface Sci.*, **2004**, 9, 279.
12. S. J. Candau, E. Hirsch and R. Zana, *J. Colloid Interface Sci.*, **1985**, 105, 521.
13. M. E. Cates and S. J. Candau, *J. Phys.: Condens. Matter*, **1990**, 2, 6869.
14. M. E. Cates, *J. Phys. Chem.*, **1990**, 94, 371.
15. S. J. Candau, A. Khatory, F. Lequeux and F. Kern, *J. Phys. IV*, **1993**, 3, 197.
16. E. J. Magid, *J. Phys. Chem. B*, **1998**, 102, 4064.
17. C. A. Dreiss, *Soft Matter*, **2007**, 3, 956.
18. S. Ezrahi, E. Tuval and A. Aserin, *Adv. Colloid Interface Sci.*, **2006**, 128, 77.
19. H. Rehage and H. Hoffmann, *Mol. Phys.*, **1991**, 74, 933.
20. Bandyopadhyay, R., Basappa, G and Sood, A. K., *Phys. Rev. Lett.*, **2000**, 84, 2022.
21. Ganapathy, R.; Sood, A. K. and Ramaswamy, S. *EPL*, **2007**, 77, 18007.
22. Granek, R., Cates, M. E., *J. Chem. Phys.*, **1992**, 96, 4758 - 4767.
23. Torres, M.F.; Gonzalez, J. M.; Rojas, M.R.; Muller, A. J.; Saez, A. E.; Lof, D.; Schillen, K. *J. Colloid Interface Sci.* **2007**, 307, 221 - 228.
24. Mishic, J. R.; Fisch, M. R., *J. Chem. Phys.* **1990**, 92, 3222 - 3229.
25. Lin, Z.; Cai, J.; Scriven, L. E.; Davis, H. T., *J. Phys. Chem.* **1994**, 98, 5984 - 5993.

26. L. M. Walker, *Curr. Opin. Colloid Interface Sci.*, **2001**, 6, 451.
27. G. C. Maitland, *Curr. Opin. Colloid Interface Sci.*, **2000**, 5, 301.
29. J. Yang, *Curr. Opin. Colloid Interface Sci.*, **2002**, 7, 276.
29. J. L. Zakin and H. W. Bewersdorff, *Rev. Chem. Eng.*, **1998**, 14, 2533.
30. R. D. Koehler, S. R. Raghavan and E. W. Kaler, *J. Phys. Chem. B*, **2000**, 104, 11035.
31. S. R. Raghavan, G. Fritz and E. W. Kaler, *Langmuir*, **2002**, 18, 3797.
32. B. A. Schubert, E. W. Kaler and N. J. Wagner, *Langmuir*, **2003**, 19, 4079.
33. A. Bernheim-Groswasser, E. Wachtel and Y. Talmon, *Langmuir*, **2000**, 16, 4131.
34. K. Imanishi, Y. Einaga, *J. Phys. Chem. B*, **2007**, 111, 62.
35. D. P. Acharya, S. C. Sharma, C. Rodriguez-Abreu and K. Aramaki, *J. Phys. Chem. B.*, **2006**, 41, 20224.
36. H. Hoffmann, A. Rauschera, M. Gradzielski, S. F. Schulz, *Langmuir*, **1992**, 8, 2140.
37. P. Fischer, H. Rehage and B. Gruning, *J. Phys. Chem. B*, **2002**, 106, 11041.
38. R. Kumar, G. Kalur, L. Ziserman, D. Danino and S. Raghavan, *Langmuir*, **2007**, 23, 12849.
39. P. A. Hassan, S. R. Raghavan, E. W. Kaler, *Langmuir*, **2002**, 18, 2543.
40. S. Imai, T. Shikata, *J. Colloid Interface Sci.*, **2001**, 244, 399.
41. K. Bijma, M. J. Blandamer, J.B.F.N. Engberts, *Langmuir*, **1997**, 13, 4843.
42. C. Oelschlaeger, G. Watson, S. J. Candau, *Langmuir*, **2003**, 19, 10495.
43. R. Abdel-Rahem, M. Gradzieski, H. Hoffmann, *J. Colloid Interface Sci.*, **2005**, 288, 570.
46. A. M. Ketner, R. Kumar, T. S. Davies, P. W. Elder and S. R. Raghavan, *J. Am. Chem. Soc.*, **2007**, 129, 1553.
45. Hassan, P. A., Narayanan, J., Manohar, C., *Curr. Sci.*, **2001**, 80, 8, 980.
46. Horbaschek, K., Hoffmann, H. and Thunig, C., *J. Colloid. Int. Sci.*, **1998**, 206, 439-456.
47. Khan, I. A.; Khanam, A. J.; Khan, Z. A.; Kabir-ud-Din, *J. Chem. Eng. Data.*, **2010**, 55, 4775 - 4779.
48. Andelman, D., Kozlov, M. M. and Helfrich, W. *Europhys. Lett.*, **1994**, 25, 231 - 236.
49. Fattal, D. R., Andelman, D. and Ben-Shaul, A. *Langmuir*, **1995**, 11, 1154 - 1161.

50. Kozlov, M. M., Lichtenberg, D. and Andelman, D. *J. Phys. Chem.*, **1997**, 101, 6600 – 6606.
51. Menon, S. V. G., Manohar, C. and Lequeux, F., *Chem. Phys. Lett.*, **1996**, 263, 727 – 732.
52. Salkar, R. A., Mukesh, D., Samant, S. D. and Manohar, C., *Langmuir*, **1998**, 14, 3778 – 3782.
53. Zemb, T., Dubois, M., Deme, B. and Gulikkrzywicki, T. , *Science*, **1999**, 283, 816 – 819.
54. Mukherjee, P.; Mittal, K. L. *Solution Chemistry of Surfactants*, Plenum Press, New York, **1979**.
55. Bergstrom, M. and Eriksson, J. C., *Langmuir*, **2000**, 16, 7173 – 7181.
56. Holland, P. M. *Mixed Surfactant Systems*, Chapter 2, **1992**, pp 40.
57. Jonsson, B.; Lindman, B.; Holmberg, K.; Kronberg, B. *Surfactant and Polymers in Aqueous Solution*, Wiley, Chichester, **1998**, Chapter 5.
58. Garcia-Mateos, I.; Velazquez, M. M.; Rodriguez, L. J. *Langmuir*, **1990**, 6, 1078.
59. Lopez-Fontan, J. L.; Suarez, M. J.; Mosquera, V.; Sarmiento, F. *Phys. Chem. Chem. Phys.* **1999**, 1, 3583.
60. Eriksson, J. C.; Ljunggren, S.; Henriksson, U. *J. Chem. Soc., Faraday Trans. 2*, **1985**, 81, 833
61. Eriksson, J. C.; Ljunggren, S.; *J. Chem. Soc., Faraday Trans. 2*, **1985**, 81, 1209.
62. Kamenka, N.; Chorro, M.; Talmon, Y.; Zana, R. *Colloid Surf.* **1992**, 67, 213.
63. Kaler, E. W.; Herrington, K. L.; Murthy, A. K.; Zasadzinski, J. A. N. *J. Phys. Chem.* **1992**, 96, 6698.
64. Bergström, M.; Pedersen, J. S. *J. Phys. Chem. B*, **2000**, 104, 4155.
65. Holland, P. M. *In Mixed Surfactant systems*, Holland, P. M.; Rubingh, D. N. Eds.; ACS Symposium Series 501; ACS, Washington DC; **1992**, Chapter 2, p 40.
66. Zhu, B. Y.; Rosen, M. J. *J. Colloid Interface Sci.* **1984**, 99, 435.
67. Rosen, M. J. *In Phenomena in Mixed Surfactant Systems*; Scamehorn, J. F., Ed.; ACS Symposium Series 311; ACS, Washington DC, **1986**, p 144.
68. Berret, J. F. *In Molecular Gels*, Weiss, R.G.; Terech, P. Eds. Springer Dordrecht, The Netherlands, **2005**, p 235.
69. Kem, F.; Zana, R.; Candau, S. J. *Langmuir*, **1991**, 7, 1344.

70. Raghavan, S. R.; Kaler, E. W. *Langmuir*, **2001**, *17*, 300.
71. Fischer, P.; Rehage, H. *Langmuir*, **1997**, *13*, 7012.
72. Cates, M. E., *Macromolecules*, **1987**, *20*, 2289 – 2296.
73. Shrestha, R. G.; Shrestha, L. K.; Matsunga, T.; Shibayama, M.; Aramaki, K. *Langmuir*, **2011**, *27*, 2229.
74. Shrestha, R. G.; Shrestha, L. K.; Aramaki, K. *Colloid. Polym. Sci.* **2009**, *287*, 1305.

# **Chapter VII**

## **Summary and Conclusion**

## Chapter VII

### Summary and conclusion

#### Chapter I

In chapter 1, a general introduction covering the description of different types of surfactants, their properties and their molecular assemblies, viz., micelles are presented. Self-assemble surfactants or surfactant aggregates become popular to the researchers in recent years due to a huge benefit achieved in many industries producing detergents, cosmetics and pharmaceuticals which have surfactants as one of their constituents. Added electrolyte has great influence on the shape of ionic micelles and also as the counterion concentration is increased, the shape of ionic micelles changes in the sequence spherical - cylindrical - hexagonal - lamellar.

(Page No. 1 - 21)

#### Chapter II

The scope and object of the present investigation has been incorporated in chapter II. Recently the role of the counterion binding has been recognized in the evaluation of the energetics of micellization process. The study of the effect of counterions eliminates some of the complications by leaving the properties of the amphiphilic ion as a constant factor and thus simplifies some of the interpretation of the experimental results. But, it often leads to complications connected with limited stability and preparative difficulties of the surfactant containing different counterions. Further, the literature of dodecyl benzene sulfonate moiety with different counterions is very rare.

The micellar structure of sodium dodecyl benzene sulfonate changes to bilayers in presence of added electrolyte. Compounds with polar groups such as alcohols can be expected to solubilize in the hydrophilic regions. Addition of alcohol can strongly influence the behaviour of the micelle and changes the micellar size depending on the hydrophilic/hydrophobic character of the alcohol.

Dye-micelle interaction is effective to determine the cmc of the surfactant. On the other hand self aggregation of the dyes is important to understand the self-quenching phenomena occurring in the different instruments and also the phenomena of energy transfer in biological systems. Surfactant mixtures are commonly preferred in medicinal and pharmaceutical formulations and industrial preparations due to the purpose of suspension, solubilization and dispersion as compared to single surfactant. The mixed surfactant exhibits superior interfacial properties such as higher surface activity and lower critical micelle concentration (cmc). Generally, it has been observed that with anions that associate strongly with the surfactant cations, worm-like micellar growth occurs rapidly at low surfactant and salt concentrations. The rheological behaviour exhibited by these system is viscoelastic and analogous to that observed in solution of flexible polymers. These surfactant solutions undergo similar rheological behaviour whether they are prepared directly from surfactant salts with a strongly associating anion or by addition of strongly associating anions to solutions prepared from surfactant salts with weakly associating anions. The rheological behaviour observed for wormlike micelles in the surfactant solution is similar to that for flexible polymers, and therefore, aqueous solutions of entangled wormlike micelles are often called "living polymer systems". The research of wormlike micelles has drawn considerable interest owing to their superior properties and wide applications.

(Page No. 29 - 35)

### Chapter III

Surfactants with different counterions were prepared from purified SDBS by ion-exchange techniques using a strong ion-exchange resin. The cmc and other thermodynamic parameters were determined from the temperature dependence surface tension as well as specific conductance data.

(Page No. 39 - 51)

At a specific temperature, the cmc values of the surfactants follow the order  $\text{Na}^+ > \text{Li}^+ > \text{NH}_4^+ > \text{K}^+ > \text{N}^+(\text{CH}_3)_4 > \text{N}^+(\text{C}_2\text{H}_5)_4 > \text{N}^+(\text{C}_3\text{H}_7)_4 > \text{N}^+(\text{C}_4\text{H}_9)_4$ . Among tetraalkyl ammonium cations along with ammonium cations, the binding ability is highest for  $\text{N}^+(\text{C}_4\text{H}_9)_4$  and decreases in the following order  $\text{N}^+(\text{C}_4\text{H}_9)_4 > \text{N}^+(\text{C}_3\text{H}_7)_4 > \text{N}^+(\text{C}_2\text{H}_5)_4 > \text{N}^+(\text{CH}_3)_4 > \text{NH}_4^+$ . As a result, the reduction of the electrostatic

intermicellar repulsive force occurs which leads to the formation of the micelle in the lower concentration range.

(Page No. 52 - 73)

The maximum surface excess concentrations ( $\Gamma_{\max}$ ) is a useful measure of the effectiveness of adsorption of the surfactant at air-solution interface, since it is the maximum value that adsorption can attain. For dodecyl benzene moiety with varying counterions, a slight increase may be due to the lower hydration effect of the dodecyl benzene sulfonate surfactants at higher temperature and hence increasing tendency to move the molecules to the air-liquid interface. The benzene ring in the surfactants may also be partially responsible for this result via steric inhibition during adsorption process. With increase in temperature, amphiphilic molecule tend to form a closely packed monolayer film of the hydrocarbon chain at the air / solution interface owing to the decreased repulsion between the oriented head groups indicated by the value of  $A_{\min}$ .

(Page No. 73 - 74)

The temperature dependency of DBS micelles having different counterions also enables one to determine the thermodynamic parameters of micellization. Negative sign of  $\Delta H_m^0$  suggests that surfactant aggregation is an endothermic process. The tetraalkyl ammonium surfactants have their enthalpy of micellization relatively close to each other. The enthalpy value first decreases with increase in chain length, reaches a shallow minimum for tetrapropyl ammonium counterions and then increases. A close look on the thermodynamic parameters support the view that in order to form micelle the gain in entropy is the major factor leading to negative change in Gibb's free energy. But for the alkali metals counterions, the fact that though the free energy changes are not very different, the entropy change is significantly higher and the enthalpy changes are much lower for  $K^+$  counterion containing DBS compared to all other systems. This suggests that the entropy contributes as a major driving force in micellization. With increasing temperature,  $\Delta S_m^0$  decreases systematically for a particular type of counterion, suggesting a disruption of ordered arrangement of water dipoles around the amphiphilic part of the surfactant molecules. Though the free energy change is not very different for all the systems, the enthalpy change is relatively higher.

The effective interactions associated with hydrocarbon chains may be expressed by standard heat capacity of micelle formation,  $\Delta_{mic}C_p^0$ . The calculated values of  $\Delta_{mic}C_p^0$  for DBS with varying counterions fall between a wide range of value viz., -67 to -934 J mol<sup>-1</sup> K<sup>-1</sup>, for the variation of temperature between 283 K and 313 K. For the tetraalkyl ammonium counterions, the order of  $\Delta_{mic}C_p^0$  values at a particular temperature is as follows: (CH<sub>3</sub>)<sub>4</sub>N<sup>+</sup> > (C<sub>4</sub>H<sub>9</sub>)<sub>4</sub>N<sup>+</sup> > (C<sub>2</sub>H<sub>5</sub>)<sub>4</sub>N<sup>+</sup> > (C<sub>3</sub>H<sub>7</sub>)<sub>4</sub>N<sup>+</sup>. At high temperatures,  $\Delta_{mic}C_p^0$ 's give large negative values due to solvation of ions upon demicellization, and this is quite reasonable because as the temperature is increased cmc value also increases in all the present systems.

Enthalpy and entropy change in the micellization process show a linear relationship for all the surfactant systems at a particular temperature and this is known as the enthalpy-entropy compensation. The slope and intercept of the straight line has different meanings, slope interprets a measure of desolvation part of micellization which means a characteristic of solute-solute and solute-solvent interaction whereas the intercepts interprets solute-solute interactions. The intercepts ( $\Delta H_m^*$ ) has been found to be -32.6 kJ mol<sup>-1</sup> for DBS which correspond to the driving force of micellization where the entropy does not contribute the process at that particular temperature.

(Page No. 75 - 85)

The literature concerning DBS surfactant is not so huge as compared to SDS or AOT and this may be due to the presence of several isomeric forms of DBS moiety. The range of cmc values of the following three surfactants with varying counterions are 3.33 mM to 0.79 mM, 9.21 mM to 1.10 mM and 3.55 mM to 0.75 mM for DBS, DS and AOT respectively. For all the surfactant systems with tetraalkyl ammonium counterions, cmc decreases with increase in tetraalkyl ammonium chain length. The order of cmc for alkali metal counter ions and ammonium ion is not same for the three surfactants. The orders are: NH<sub>4</sub><sup>+</sup> > Li<sup>+</sup> > Na<sup>+</sup> for dodecyl sulfate, NH<sub>4</sub><sup>+</sup> > Na<sup>+</sup> > Li<sup>+</sup> > K<sup>+</sup> for AOT and Na<sup>+</sup> > Li<sup>+</sup> > NH<sub>4</sub><sup>+</sup> > K<sup>+</sup> for DBS. This trend can be explained by the counterion binding to micelles. The general tendency of cmc change with temperature is parabolic in nature. However, the present DBS with different counterions show linear types of temperature dependency.

Among the  $\Gamma_{max}$  values of DS, DBS and AOT, only the DS follows the general trend with temperature. The order of  $\Gamma_{max}$  values is lower in the case of DBS as compared to DS and AOT suggesting effectiveness of adsorption of this surfactant at air-solution interface is low. The lower  $A_{min}$  values for DS and AOT suggest that these amphiphiles tend to form a closely packed monolayer film of the hydrocarbon chain at air / liquid interface as compared to DBS with same counterions.

In between the DS and DBS systems, the  $\Delta G_m^0$  value is higher for DS systems particularly more pronounced for the alkyl ammonium counterions. The enthalpy of micellization is negative for all the counterions in case of AOT and DBS. But for DS, there are both positive and negative value of enthalpy change of micellization suggests that both exothermic and endothermic process occurs at the micellization process. The less enthalpy values are shown by potassium counterions for both AOT and DBS surfactants with higher enthalpy values.

The effective interaction associated with hydrocarbon chains may be expressed by standard heat capacity of micelle formation,  $\Delta_{mic}C_p^0$ . The  $\Delta_{mic}C_p^0$  values for comparison are calculated for only SDBS and SDS systems due to their very similar molecular formula and also contain a dodecyl moiety in hydrocarbon chains. The calculated values of  $\Delta_{mic}C_p^0$  for SDBS fall between a wide range of value viz., -381.8 to -933.8 J mol<sup>-1</sup> K<sup>-1</sup> for the temperature range 283-293 K. On the other hand, SDS which also yields  $\Delta_{mic}C_p^0$  values between -607 and -644 J mol<sup>-1</sup> K<sup>-1</sup> in the same temperature range.

(Page No. 85 - 97)

## Chapter IV

Added electrolytes are known to affect the aggregation behaviour of ionic surfactants. In the present study, the surfactant chosen is again dodecyl benzene sulfonate (DBS) with different counterions, viz., Na<sup>+</sup>, Li<sup>+</sup>, K<sup>+</sup>, NH<sub>4</sub><sup>+</sup>, (CH<sub>3</sub>)<sub>4</sub>N<sup>+</sup>, (C<sub>2</sub>H<sub>5</sub>)<sub>4</sub>N<sup>+</sup>, (C<sub>3</sub>H<sub>7</sub>)<sub>4</sub>N<sup>+</sup> and (C<sub>4</sub>H<sub>9</sub>)<sub>4</sub>N<sup>+</sup> and the electrolytes are the symmetrical tetraalkyl bromides. The critical micellization concentrations of DBS with different counter ions in presence of corresponding aqueous bromide salt solutions in the concentration range of (5-0.5) mM were determined mainly by surface tension and partly also by the electrical conductivity method. Increasing the concentration of a particular electrolyte causes a substantial decrease in the cmc. This can be accounted for by the fact that in

solutions of high ionic strength, the forces of electrostatic repulsion between head groups in a micelle are considerably reduced due to charge screening. Such reduction in the cmc values of anionic surfactants is also observed in presence of all systems with corresponding bromide electrolytes. TMA<sup>+</sup> ions with smallest ionic size are the most hydrated in aqueous solution compared to that of the others in the group, viz., TEA<sup>+</sup>, TPA<sup>+</sup> and TBA<sup>+</sup>. The higher homologues of the series, TPA<sup>+</sup> and TBA<sup>+</sup>, have long hydrocarbon chains and some of these chains are supposed to penetrate in the micellar core due to hydrophobic interaction. Hence, at a given temperature, the formation of micelles of DBS in these electrolyte media favours a cmc lowering in the order TMAB > TEAB > TPAB > TBAB.

(Page No. 104 - 141)

The increase in the  $\beta$  values on moving from TEA<sup>+</sup> to TBA<sup>+</sup> is due mainly to the increased hydrophobic interaction between the alkyl parts of both the surfactant and the added electrolyte. For inorganic ions including ammonium ions, similar result is observed due to the increase in size of the cations. Here, the order of  $\beta$  values is K<sup>+</sup> > Na<sup>+</sup> > NH<sub>4</sub><sup>+</sup> > Li<sup>+</sup>. In the present case, slight increase in the values of  $\Gamma_{\max}$  is observed which may be due to the effectiveness of adsorption. With increase in temperature, the  $A_{\min}$  value shows the inverse trend as that of  $\Gamma_{\max}$ .

(Page No. 142 - 143)

The values of  $\Delta G_{mic}^0$ ,  $\Delta H_{mic}^0$  and  $\Delta S_{mic}^0$  in the presence of 0.0005 M corresponding bromide salts have been calculated. The variation of  $\Delta G_{mic}^0$  with temperature is small for all the systems investigated. The values of  $\Delta H_{mic}^0$  increase with the increase in temperatures in all case. The higher negative values of enthalpy at higher temperatures probably suggest the importance of London-dispersion interactions as an attractive force contribution for micellization. The entropy of micellization for different systems are all large and positive except potassium dodecyl benzene sulfonate, indicating that the micellization process is entropy dominated. Presence of salt may screen electrostatic repulsion between head groups and decrease the thickness of the interfacial water layer. The thickness of the interfacial layer is decreased when salts are added into surfactant systems. The reason is that the positive ions of the salt can enter into the interfacial region and destroy the hydrated layer.

(Page No. 144 - 149)

The most interesting aspects of these microheterogeneous entities are their ability to accommodate organic molecules. In this respect ethylene glycol (EG) showed the reverse effect compared to the other alcohols and this may be explained by its higher dielectric constant, small hydrophobic surface and greater capability of hydrogen bond formation. Influence of very common short chain alcohols, viz. ethylene glycol on the micellization of DBS with different counterions in aqueous medium are studied in the present investigation within the temperature range of 293-313K. For SDBS-ethylene glycol-water system [10%, 20% and 30% ethylene glycol (w/w)], the cmc was determined conductometrically. The cmc values increase considerably upon addition of ethylene glycol. The larger cmc at higher ethylene glycol content is a result of the presence of a structure-breaking solute which in the aqueous phase adversely influences the hydrophobic group causing the micellization process unfavourable. The increase in cmc values with temperature at a given concentration of ethylene glycol is attributed to the disruption of the solvent structure with the increase in temperature.

With increase in temperature, the  $\Delta G_m^0$  value becomes more negative, which is a general trend. The other two thermodynamic parameters viz.  $\Delta H_m^0$  and  $\Delta S_m^0$  also show their necessary contribution in favour of micellization process. The entropy of micellization is positive in water and becomes less positive in the presence of increasing amounts of ethylene glycol. The overall exothermicity of the present system indicates that both the structure-breaking ability of ethylene glycol and its interaction with the hydrophilic groups of the surfactants are dominating factors. Depending upon the temperature and the proportion of ethylene glycol present, small negative  $\Delta G_t^0$  as observed are there in different surfactants, may be due to a reduction of the micelle solvation in the mixed solvent.

(Page No. 149 - 171)

## Chapter V

One of the most fundamental and important structural parameters of micellar aggregates is the aggregation number, or the average aggregation number of detergent molecule in micelle unit. The value of the aggregation number contains information on the micellar size and shape, which may be important in determining stability and practical applications of the investigated systems. In the present study, the measurement of aggregation number is done by a simple process based on the

quenching of a luminescent probe by a hydrophobic quencher. In the present experiment, the static quenching is done to measure the aggregation number of the surfactant with different counterions by steady state fluorescence quenching (SSFQ) process.

In the case of pyrene, a quencher is used to measure the aggregation number, the ratio of intensity of the first ( $I_1$  at 373nm) and third peaks ( $I_3$  at 384 nm) is a sensitive parameter characterizing the polarity of the probe environment. In the present study, good experimental result for all the surfactants have been obtained suggesting constancy of both  $N$  and  $K_{SV}$ . At 298 K, the aggregation number become minimum in the case of  $\text{NH}_4^+$  counter ion. But as the alkyl groups are substituted for hydrogens, the aggregation number increases because of the formation of larger aggregates which is the consequences of the increased charged screening at higher counter ion binding capacity via stronger hydrophobic interactions with the micelles. This increasing trend of aggregation number continues up to the tetraethylammonium ions. But for tetrapropyl and tetrabutyl ammonium ions, aggregation number progressively decreases. It seems apparent that in the present systems, as the hydrophobicity of the counter ions increases, the counter ion binding/condensation increases due to increased hydrophobic interactions and eventually the cmc decreases. However, enhanced electrostatic charge screening of the head groups is incapable of increasing the aggregation number of the micelles for tetrapropyl and tetrabutylammonium counter ions. For alkali metal counter ions, hydration plays an important role along with ionization degree and hydrophobic interactions. As the size of the counter ion increases, the degree of hydration decreases due to more hydrophobicity of the counter ions and also enhanced electrostatic charge screening of the head groups.

(Page No. 177 - 197)

In the chapter, we also use an oxazine dye with dodecyl benzene sulfonate with varying counterions to characterize qualitatively the dye-surfactant interactions. The oxazine dyes display surprising long-wavelength absorption and emission maxima in fluorescence which makes these groups of dye an important fluorescent probe. We have studied the steady-state spectra of surfactants by a typical oxazine dye, Cresyl fast violet. Due to these dye-surfactant interactions, the changes in spectral characteristics are observed qualitatively. At concentration below the normal cmc,

surfactants and dyes can interact to form a mixed micelle of the two species, lowering the resultant cmc. Above the cmc, a change in the molecular environment of the dye due to incorporation into the micelle interior is observed.

At concentrations of surfactants below the cmc, the fluorescence intensity decreases continuously with increase in surfactant concentration. When the surfactant concentration reaches cmc, the intensity starts increasing continuously with increase in surfactant concentration. The result suggests that the free monomer is tied up in ion pair or clusters at sub-micellar region. The order of the ion pair formation or cluster formation for alkali metal counter ions is as follows:  $\text{Li}^+ > \text{K}^+ > \text{Na}^+$  and for tetraalkyl ammonium counter ion and ammonium ion the trend is as follows:  $\text{NH}_4^+ > (\text{C}_4\text{H}_9)_4\text{N}^+ > (\text{C}_3\text{H}_7)_4\text{N}^+ > (\text{C}_2\text{H}_5)_4\text{N}^+ > (\text{CH}_3)_4\text{N}^+$ . These trends are probably observed as the consequences of the increased charged screening and higher counter ion binding capacity via stronger hydrophobic interactions with the micelles.

(Page No. 198 - 212)

Anisotropy measurement was done with the same dye in presence of surfactants. The data were analyzed with the software "Felix GX", supplied by the manufacturer with the fluorescence spectrophotometer instrument. The lower the anisotropy value, the faster is the rotational diffusion. The trend is normal for all the surfactant except lithium dodecyl benzene sulfonate and ammonium dodecyl benzene sulfonate due to high hydration enthalpy of lithium and intermediate size of the ammonium ion.

The interpretation of the results emerges from steady-state anisotropy of these dye-surfactant complex system is not straightforward; its value depends on various factors such as, the rotational motion and the possible dye - surfactant interactions. With decrease in surfactant concentration, the packing of amphiphiles at the interface is less compact which show a decrease in polarization value. Below the cmc, the increase in polarization value can also attributed to the higher dye-surfactant interactions. Upon addition of surfactant, the anisotropy initially increases fast, but this increase in a range of very low surfactant concentration and below the cmc. This is the evidence of interactions that reduce the dye's ability to rotate freely. A dye-surfactant ionic pair or cluster would result in such a decreased ability to rotate because of its larger size than an individual dye ion. The increase polarization value with increasing surfactant

concentration probably means that more surfactant molecule join the clusters as the surfactant concentration increases. Around the cmc, the increase of anisotropy value drops to an extent. This could be the result of the release some of the dye molecule from their ionic interactions with the surfactant monomers. Above the cmc, the anisotropy increases little before leveling off. This shows that the dye is less free to rotate in the micellar environment. The dye's lower ability to rotate above the cmc shows that it is within the micelle in a more rigid formation. The value of the cmc derived from polarization value is in good agreement with the value determined by surface tension and conductometrically for each of the surfactant. The slight difference in the cmc values observed in these two methods may be due to the fairly strong interaction of dye molecules with the surfactants.

(Page No. 212 - 220)

In the present experiments, time resolved fluorescence studies were also carried out to determine the emission decay parameters of all the surfactants with different surfactant concentrations. The concentration of the dye used was  $5 \times 10^{-6}$  (M). Thus, high dye concentrations could not be used, as at these concentrations lifetime values may be drastically decreased due to fluorescence quenching. So, only four set of concentrations for each dye have been taken for. The lifetime values did not change significantly in a regular manner with the change in surfactant concentration and indicates single exponential fluorescence decay characteristics in presence of all the surfactants.

(Page No. 221)

## Chapter VI

Compared to single surfactant, the mixed surfactant exhibits superior interfacial properties such as higher surface activity and lower critical micelle concentration (cmc). Surfactant mixtures are commonly preferred in medicinal and pharmaceutical formulations and industrial preparations due to the purpose of suspension, solubilization and dispersion. Wormlike micelles are long, self-assembled, semi-flexible, breakable polymer-like materials with surfactant heads on the outside and tails in the core. They display a striking range of dynamical properties, including anomalous relaxation, shear banding, and rheological chaos. Above a threshold concentration  $c^*$ , wormlike micelles may entangle into a transient network, which

displays remarkable viscoelastic properties. Mixtures of cationic and anionic surfactants show not only synergistic effect of the aggregation properties but also triggered micellar grow in one dimension to form long worm-like micelles. In this chapter, the results of the study on their mixing behaviour, synergism, and one dimensional grow to worm-like micelles and rheological characteristics of this system are reported. Present study is divided in two major parts. In the first part, the synergistic effect of the mixing of cetyltrimethylammonium bromide (CTAB, a cationic surfactant) with SDBS (an anionic surfactant) is studied under Newtonian flow regime. In the second part, the formation of viscoelastic worm-like micelles is examined and the rheological behavior of the system is investigated under non Newtonian flow regime.

(Page No. 225 - 227)

Here the cmc's were determined for the mixed surfactant systems of various mole ratios at a particular temperature. Micellar aggregates are also formed in an aqueous solution containing SDBS and CTAB. But, the tendency of aggregation is different from that of the pure surfactants. Due to hydrophobic effect, the micellization process is a function of temperature, additive and solvent because the solvent property gets modified in the presence of an additive. The results indicate that the added cationic surfactant (CTAB in this experiment) is assisting in the micelle formation of the anionic surfactants.

(Page No. 227 - 235)

It is indeed interesting to note that the non-ideality of the CTAB and SDBS mixtures is not large. The charge neutralization between the head groups of the two components and the interaction of hydrophobic part of CTAB with the SDBS micelles improve the hydrophobic environment in the mixed state in comparison to the pure state. To analyse the synergistic effect of mixed surfactant, Rubingh's methods are applied.

The reason for the non-ideal behaviour among surfactant molecules upon mixing are then various types of molecular interactions. These interactions (either synergistic or antagonistic) can be analysed by RST which allows the evaluation of micelle mole fraction ( $x_1$ ) and interaction parameter ( $\beta^m$ ). A negative deviation from ideal behaviour, corresponding to negative  $\beta$  values is believed to result from a net

attraction between the two different surfactant molecules. In this system of CTAB and SDBS mixture,  $\beta$  values are also negative as found within the range of -2.45 to -0.364. Electrostatics yields a large contribution to the aggregate free energy for mixtures consisting of ionic surfactants. According to the Poisson-Boltzmann (mean field) description, this contributions mainly due to the entropically unfavourable organization of the counterions into a diffuse layer located outside the electrically charged surface of an aggregate, whereas the purely energetic effects usually are much smaller for surfactants mixtures like CTAB and SDBS which explains comparatively lower interactions parameter.

**(Page No. 235 – 239)**

Viscoelastic properties including dynamic rheology of the system at different temperature have been investigated to understand the microstructural pattern of the mixed micelles. The self-assembly of both CTAB and SDBS individually result in the formation of globular micelles near the respective cmc values. On the other hand, when the concentrations of the individual component of the mixtures are increased (e.g., CTAB = 100 mM and SDBS = 20 mM), a viscoelastic gel is formed and the flow becomes non-Newtonian in nature. The observed viscoelasticity is related to worm-like micelle (WLM) formation.

Therefore, in general, the experimental solutions exhibit three regions of rheological response. First, at low surfactant concentration, the solutions are Newtonian liquids with low viscosity and non-measurable elastic response. Second, with increasing surfactant concentration, they behave like polymer solutions in the semi-dilute regime, characterized by viscoelastic behaviour with a spectrum of relaxation times. Finally, with increase in the counter ion concentration, these materials enter a regime where their rheological response is similar to that of an entangled polymer or weak gel; however, unlike polymer systems, there relaxation after shear is dominated by a single relaxation time. In this chapter of the thesis rheology of viscoelastic worm-like micelles formed in the system of SDBS and CTAB mixtures have been studied.

**(Page No. 239 – 241)**

In our experiments, the rheological data are typical of viscoelastic wormlike micelles, with a plateau in  $G'$  at high frequencies and terminal behaviour of  $G'$  and  $G''$  at low frequencies. Moreover, the sample is nearly a Maxwell fluid over a short range

of temperatures (303 K - 335 K). No cross over point is displayed beyond the temperature range of 303 K - 313 K, except at 281 K. We find that the Maxwell model fits the data well, especially at low and intermediate frequencies, as has been shown for normal worm in the above temperature ranges. When micelles are sufficiently long, they are converted into more flexible wormlike micelles which can flow comparatively easily. Which reflects by a level off in the  $G'$ . At further high concentration, a micro-structural change in micelle structure results the change in rheological parameter. The increase in viscosity to a very small extent can be attributed also by micro-structural change. It is expected that a sufficient amount of CTAB will be present which will be embedded between the head groups. Further with increase in temperature, the Br<sup>-</sup> ion may be released and would show higher preference for the bulk phase. Such a release if occurs would increase the effective head group area, thereby driving micro-structural change of higher curvature resulting in an increase in viscosity.

At low frequencies the loss modulus ( $G''$ ) is higher than the storage modulus ( $G'$ ), indicating that the sample behaves as a liquid and also predominantly viscous whereas at high frequencies,  $G'$  is greater than  $G''$ , which implies that the mixtures behave like a solid which is predominantly elastic in the temperature range 303 - 313 K. The dip of the  $G''$  curve even at higher frequencies is due to the presence of further relaxation modes.

**(Page No. 241 - 248)**

The curve in the present system fits to good extent to a simple Maxwell model. The data points fit fairly well on a semicircle curve particularly at 303 K. A single exponential relaxation can be effectively explained in case of worm like micelles. In this case, the reptation mechanism is short circuited and the new relaxation process will be monoexponential with a new time scale. The deviations from the half circle occur at a circular frequency  $\omega$  of the order of the inverse of the breaking time of the micelles. At higher frequencies the data deviate from the Maxwell model, which is typically the case when the systems can no longer be described by a single relaxation time. The large deviation from Cole - Cole plot with high angular viscosity is indicative that of a less structured system with poor viscoelastic behaviour.

The zero-shear viscosity of the surfactant mixtures was determined from controlled-stress measurements by extrapolating the viscosity-shear stress curve to zero

shear rates. In terms of stress relaxation, it is slowest at the viscosity peak and increases at both lower and higher temperatures. It is clear that with increase in temperature,  $\eta_0$  increases indicating an increase in the curvature energy for surfactant aggregates which leads to an increase in micellar length and the formation of wormlike micelles. As the temperature further increased, the zero shear viscosity exhibits a flat maximum within 10°C to 26°C temperatures. Further increase in temperature decreases the zero shear viscosity and this can be explained due to the decrease of the micellar contour length or the formation of branched micelles. In summary, all these results support a fascinating and complex rheology to exist in the present system. This occurs due to structural evolution from a spherical micelle to a worm like micelle. Finally, the shift in cross over frequency  $\omega$  to higher values indicate that the relaxation time  $\tau$  decreases with temperature.

**(Page No. 249 – 255)**

# Reprints

## List of Publications:

1. Temperature Dependent Micellization of AOT in Aqueous Medium: Effect of Nature of Counterions.

Amitabha Chakraborty, Subrata Chakraborty, Swapan K. Saha.

*Journal of Dispersion Science and Technology*, 2007, 28, 984 – 989.

2. Effect of Size of Tetraalkylammonium Counterions on the Temperature Dependent Micellization of AOT in Aqueous Medium.

Amitabha Chakraborty, Swapan K. Saha, Subrata Chakraborty.

*Colloid and Polymer Science*, 2008, 286, 927 – 934.

3. Surface and Bulk Properties of Dodecylbenzenesulphonate in Aqueous Medium: Role of the Nature of Counterions.

Subrata Chakraborty, Amitabha Chakraborty, Moazzam Ali and Swapan K. Saha

*Journal of Dispersion Science and Technology*, 2010, 31, 209 – 215.

4. Tuning of physico-chemical characteristics of charged micelles by controlling head group interactions via hydrophobically and sterically modified counter ions.

Subrata Chakraborty, Amitabha Chakraborty and Swapan K. Saha

*RSC Adv.*, 2014, 4, 32579 - 32587.

This article was downloaded by: [Tufts University]

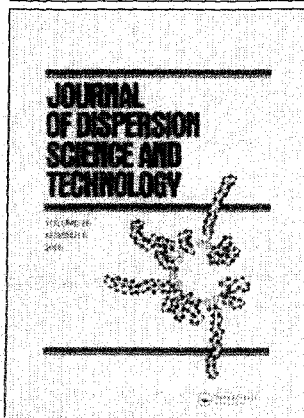
On: 30 August 2007

Access Details: [subscription number 768416767]

Publisher: Taylor & Francis

Infoma Ltd Registered in England and Wales Registered Number: 1072954

Registered office: Mortimer House, 37-41 Mortimer Street, London W1T 3JH, UK



## Journal of Dispersion Science and Technology

Publication details, including instructions for authors and subscription information:

<http://www.informaworld.com/smpp/title-content=t713597266>

### Temperature Dependant Micellization of AOT in Aqueous Medium: Effect of the Nature of Counterions

Online Publication Date: 01 August 2007

To cite this Article: Chakraborty, Amitabha, Chakraborty, Subrata and Saha, Swapan K. (2007) 'Temperature Dependant Micellization of AOT in Aqueous Medium: Effect of the Nature of Counterions', *Journal of Dispersion Science and Technology*, 28:6, 984 - 989

To link to this article: DOI: 10.1080/01932690701463175

URL: <http://dx.doi.org/10.1080/01932690701463175>

PLEASE SCROLL DOWN FOR ARTICLE

Full terms and conditions of use: <http://www.informaworld.com/terms-and-conditions-of-access.pdf>

This article may be used for research, teaching and private study purposes. Any substantial or systematic reproduction, re-distribution, re-selling, loan or sub-licensing, systematic supply or distribution in any form to anyone is expressly forbidden.

The publisher does not give any warranty express or implied or make any representation that the contents will be complete or accurate or up to date. The accuracy of any instructions, formulae and drug doses should be independently verified with primary sources. The publisher shall not be liable for any loss, actions, claims, proceedings, demand or costs or damages whatsoever or howsoever caused arising directly or indirectly in connection with or arising out of the use of this material.

© Taylor and Francis 2007

# Temperature Dependant Micellization of AOT in Aqueous Medium: Effect of the Nature of Counterions

Amitabha Chakraborty, Subrata Chakraborty, and Swapan K. Saha

Department of Chemistry, University of North Bengal, Darjeeling, India

The lithium, potassium, and ammonium salts of bis (2-ethylhexyl) sulphosuccinic acid have been prepared from the sodium salt (AOT) by applying ion-exchange technique. The critical micellization concentrations (cmc) of the surfactants with four different counterions have been determined at a temperature range of 10°C to 40°C using surface tension as well as electrical conductivity measurements. Observed data have been utilized to evaluate the ionization degree (counter ion association constant),  $\alpha$ , and various thermodynamic parameters of micellization viz, free energy, enthalpy, entropy changes of micelle formation, and also the surface parameters ( $\Gamma_{max}$ ,  $A_{min}$ ) in aqueous media. The value of cmc decreases with hydrated ionic size of the counter ions (except  $K^+$ ) and follows the order  $NH_4^+ > Na^+ > Li^+ > K^+$ . While large negative free energy change ( $\Delta G_m^0$ ) and the positive entropy change ( $\Delta S_m^0$ ) favor the micellization process thermodynamically, nature of their variation with counterion supports the involvement of counterion size factor in micellization process via a change in the hydrophilicity of surfactant head group.

**Keywords** Critical micelle concentration, counter ion, thermodynamic parameters, aerosol-OT

## 1 INTRODUCTION

Self-aggregation of amphiphiles in water forming micelles or bilayers (viz. vesicles) is an important phenomenon in view of its relevance in biology and industry.<sup>[1,2]</sup> In recent technological developments, such phenomena as emulsification, foaming, detergency, etc. are highly important, and are dependent on the stability of the micelles.<sup>[3]</sup> One of the most important parameters of self-assembly of amphiphiles, the critical micellization concentration (cmc), has been determined by numerous researchers using different techniques.<sup>[10–19,21,26]</sup> A survey of literature shows that the studies of the effect of the nature of counterion on self-assembly of cationic surfactants in aqueous media are quite heavy, while similar studies on anionic surfactants are not large in number. As the surface of a micelle possesses an array of charged head groups, for example  $-OSO_3^-$  groups in AOT, the attraction experienced by a single counterion, for example  $Na^+$ , near this surface is greater than that when near an isolated surfactant anion. As a result, the degree of dissociation of surfactants is much lower in the micelle than for monomers in solution. In cationic

surfactants the nature of counterions display dramatic effects on various physicochemical properties such as micellar growth, viscoelasticity, and shear-thickenings behavior.<sup>[4,5]</sup>

On the other hand, counterion effect is apparently not much dramatic in the case of anionic surfactants. There is a little variation in the value of cmc of dodecyl sulfate when a counterion varies within different alkaline metals viz. from lithium to cesium ion.<sup>[6]</sup> Even when the monovalent alkali metals counterion are replaced by divalent ions such as  $Mg^{+2}$ ,  $Co^{+2}$ ,  $Cd^{+2}$  the effect is not very strong. In these cases the cmc (expressed in moles per liter) values decreases by a factor 2 and there is an increase in micellar aggregation number.<sup>[7,8]</sup> Therefore, very accurate measurement of cmc as a function of counterion variation is necessary for quantification of the forces involved in the above phenomena.

The thermodynamic quantities of micellization like the Gibbs free energy  $\Delta G_m^0$ , the enthalpy  $\Delta H_m^0$  or the entropy  $\Delta S_m^0$  can be derived from either the direct measurement of the enthalpy by microcalorimetry<sup>[16–19]</sup> or from the studies of the temperature dependence of critical cmcs.<sup>[16,10,11,20]</sup> The availability of these parameters at various temperatures can give rise to the valuable insight into the principles, which govern the formation and stability of micelles. The formation of micelles was always found to be connected with a large, negative change in  $\Delta G_m^0$ , which suggests that the aggregation process is thermodynamically favored and spontaneous.<sup>[10,11,21]</sup> The major driving forces for micelle

Received 15 August 2006; Accepted 26 August 2006.  
Financial support from the UGC, New Delhi under SAP (DRS) is gratefully acknowledged.

Address correspondence to Swapan K. Saha, Department of Chemistry, University of North Bengal, Darjeeling 734 013, India. E-mail: ssahanbu@hotmail.com

formation are hydrophobic interactions of amphiphiles. Near room temperature that lead to a large gain of entropy when water molecules in the hydration shells around the hydrophobic parts of the monomeric amphiphiles are released during the micellization process. At elevated temperature, however, the increase in entropy cannot account for the large  $\Delta G_m^0$  value.<sup>[26,28,29]</sup> For many hydrophobic compounds  $\Delta S_m^0$  approaches zero at higher temperatures and it becomes negative at temperatures above 130°C. In this case the  $\Delta H_m^0$  contribute the major portion to  $\Delta G_m^0$ , which should become large and negative in order to compensate for the change in  $\Delta S_m^0$ . There are a few studies covering a border temperature range, which may confirm the idea of enthalpy-entropy compensation.<sup>[31-35]</sup>

Aerosol-OT is a well-known and versatile anionic surfactant having two hydrophobic tails. The typical molecular structure of AOT may be responsible for its ability to form microemulsion and showing rich phase behavior. We present in this work some studies with a series of surfactants derived from AOT (the sodium salt of the diester) by varying the counterions. Thus a series of alkali metal ions, viz.  $\text{Li}^+$ ,  $\text{Na}^+$ ,  $\text{K}^+$ , and the  $\text{NH}_4^+$  are investigated. Note that the cmc, along with other thermodynamic parameters related with micellization of these surfactants, have not yet been reported in the literature. Our aim, therefore, is to determine the cmc with high accuracy within a temperature range of 10°C to 40°C of AOT surfactants having different counter cations in aqueous medium and to calculate different thermodynamic parameters of micellization, viz. changes in standard Gibbs free energy ( $\Delta G_m^0$ ), standard enthalpy ( $\Delta H_m^0$ ), standard entropy ( $\Delta S_m^0$ ), maximum surface excess concentration ( $\Gamma_{\text{max}}$ ), and the minimum areas per molecule ( $A_{\text{min}}$ ) at the surface in order to examine the effect of ionic sizes on the micellization.

## 2 EXPERIMENTAL

### 2.1 Materials

The ion exchange technique of Eastoe et al.<sup>[22]</sup> and the extended work of Tamsamani et al.<sup>[23]</sup> have been applied for the preparation of anhydrous AOT having different counterions as described below.

A 10 gm sample of high purity grade AOT (>99% from Fluka, Switzerland) was dissolved in 20 ml of a 1:1 (v/v) mixture of water and ethanol. The solution was passed (2-3 drops) through a column (40 cm × 2 sq. cm) of a strong ion exchanger in the  $\text{H}^+$  form slowly (Amberlite IR-120, 20-50 mesh, Loba Cheme, India). The resin was put in the acid form by using a large excess of a 0.20 M aqueous hydrochloric acid solution and washed with water until the complete removal of the excess acid takes place. The free sulphonic acid formed on passing the AOT ( $\text{Na}^+$  salt) through the resin was immediately neutralized with an aqueous solution of the hydroxides of the desired counterion (viz.  $\text{K}^+$ ,  $\text{Li}^+$ ,  $\text{NH}_4^+$ ). All the hydroxides of high purity were procured from

Across Chem, Belgium. The solvent water was then removed fast by freeze drying and then keeping under vacuum (bath temperature 40°C) for several days, and the waxy solid was finally dried in vacuum over  $\text{P}_2\text{O}_5$ . This material contains residual water, which was finally removed by the action of  $\text{P}_2\text{O}_5$  (from Loba Cheme, India) on a solution of surfactant in isooctane ( $\geq 99.5\%$  from Merck, India). All surfactants were obtained as waxy solid. The extent of  $\text{Na}^+/\text{H}^+$  ion exchange step was optimized by examining  $\text{H}^+$  content of the  $\text{AOT}^-\text{H}^+$  solution by titration with  $\text{NaOH}$ , and the overall yield of cation exchange was found in >99%.

### 2.2 Methods

The cmc can be obtained as a break in the plot of the (i) surface tension ( $\gamma$ ) against the logarithmic value of the surfactant concentration  $C$  and also (ii) by plotting conductance  $\Lambda$  against the concentration of the surfactant. The surface tension experiments were done by measuring the surface tension of different surfactant solutions by platinum ring detachment method using a Tensiometer (K9, KRÜSS; Germany), at different temperatures. Temperature was maintained by circulating autothermostated water through a double-wall glass vessel containing the solution. The steady state at the required temperature was checked by taking a number of measurements after 15-minute intervals until no significant change occurred. Similar studies were also done conductometrically by using an electrical conductivity bridge (Mettler Toledo, Switzerland). Each measurement was repeated several times at each temperature in the range of 10 to 40°C.

## 3 RESULTS AND DISCUSSION

### 3.1 Critical Micelle Concentration

Chemical structure of the anionic part of AOT, that is, bis (2-ethylhexyl) sulphosuccinate, is shown in Figure 1. The typical experimental curves are obtained in both cases and the cmc values determined by surface tension as well as by conductance measurements are in well agreement with one another. Figures 2 and 3 illustrate the type of plots obtained in surface tension and conductance measurements respectively. The results are recorded in Table 1.

Examination of Table 1 reveals that for a particular type of surfactant at low temperature (below 30°C) the cmc values follow the order  $\text{NH}_4^+ > \text{Na}^+ > \text{Li}^+ > \text{K}^+$ . At high

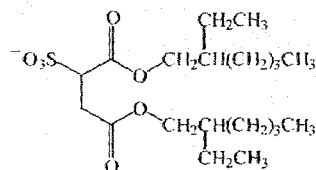


FIG. 1. Molecular structure of bis (2-ethylhexyl) sulfosuccinate; Anionic part of AOT.

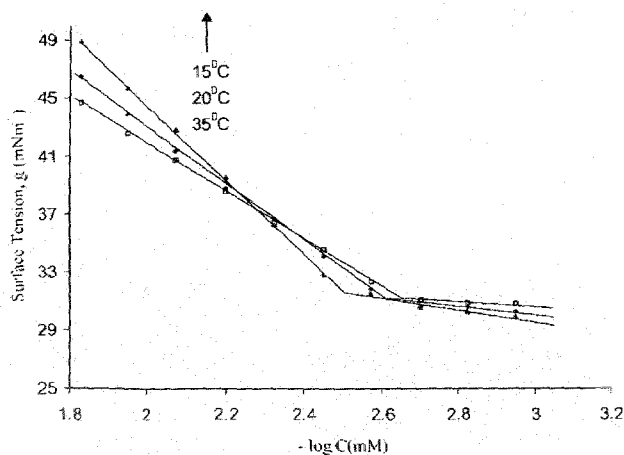


FIG. 2. Surface tension,  $\gamma$ , of AOT (sodium salt) in aqueous solution as a function of the logarithm of the surfactant concentration (M) at 15°C, 20°C, 25°C.

temperature (above 50°C) AOT micelles are rather insensitive to temperature variation. It seems apparent that the size of hydrated counterion is important; bigger the size of counterion, that is, low is its accessibility toward the head group, greater is the chance for micellization at lower concentration. The hydration number derived from the corrected ionic radii of above four ions are given below.<sup>[39]</sup>

It is well known that hydrophobic property of the tail and the hydrophilic property of the head group of a surfactant molecule are together responsible in forming micelles in water. It,

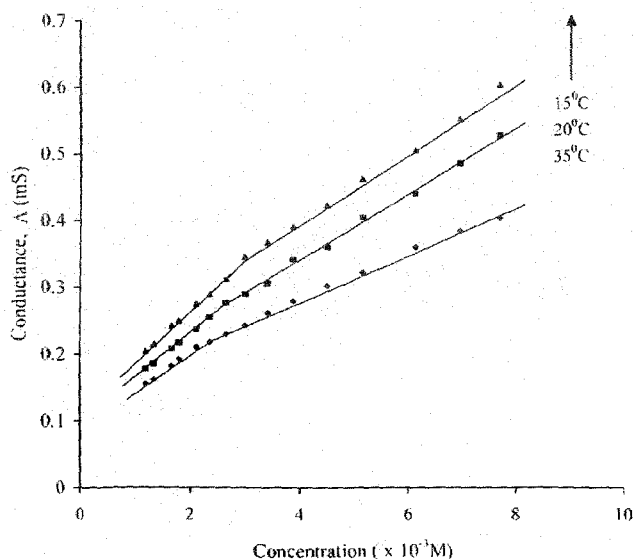


FIG. 3. Conductance,  $\Lambda$ , of AOT (sodium salt) in aqueous solution as a function of the surfactant concentration (M) at 15°C, 20°C, 25°C.

TABLE I  
Temperature dependence of cmc, maximum surface excess concentration ( $\Gamma_{\max}$ ), and minimum areas per molecule ( $A_{\min}$ ) of different AOT surfactants

Counter ions of different AOT surfactants	Temp/°C	cmc <sup>a</sup> mol dm <sup>-3</sup> × 10 <sup>3</sup>	$\Gamma_{\max}$ /mol cm <sup>-2</sup> × 10 <sup>8</sup>	$A_{\min}$ /nm <sup>2</sup> × 10 <sup>2</sup>
Li <sup>+</sup>	10	3.35 (3.40)	1.63	1.02
	15	2.98 (3.15)	1.60	1.04
	20	2.82 (2.90)	1.59	1.04
	25	2.66 (2.63)	1.59	1.44
	30	2.40 (2.37)	1.56	1.06
	35	2.24 (2.19)	1.61	1.03
	40	2.39 (2.23)	1.60	1.05
Na <sup>+</sup>	10	3.55 (3.53)	1.42	1.17
	15	3.16 (3.20)	1.45	1.14
	20	2.88 (2.77)	1.49	1.11
	25	2.63 (2.40)	1.57	1.06
	30	2.24 (2.20)	1.76	0.94
	35	2.37(2.26)	1.70	0.98
	40	2.80 (2.69)	1.71	0.97
K <sup>+</sup>	10	2.97 (3.11)	1.84	0.90
	15	2.90 (3.01)	2.01	0.83
	20	2.82 (2.90)	2.22	0.75
	25	2.70 (2.62)	2.25	0.74
	30	2.44 (2.35)	2.30	0.72
	35	2.42(2.32)	2.44	0.68
	40	—	—	—
NH <sub>4</sub> <sup>+</sup>	10	3.87 (3.85)	1.56	1.06
	15	3.31 (3.20)	1.58	1.05
	20	3.09 (3.12)	1.45	1.14
	25	2.70 (2.65)	1.55	1.07
	30	2.59 (2.52)	1.80	0.92
	35	2.65 (2.60)	1.72	0.96
	40	2.82 (2.75)	1.76	0.94

<sup>a</sup>The values in the parenthesis represent cmc determined by conductivity method.

therefore, is not surprising that as the hydrocarbon chain length is increased, micelles are formed at lower concentrations due to increased hydrophobicity of the hydrocarbon tail.<sup>[40]</sup> Similarly it is quite obvious that as the hydrated ionic size is increased from NH<sub>4</sub><sup>+</sup> to Na<sup>+</sup>, cmc value is decreased due to increasing hydrophilicity. The K<sup>+</sup>, however, give anomalous result due to its strong tendency for ion pair formation. The cmc of surfactants shows a characteristic temperature dependence with a shallow minimum around 25–35°C as shown in Figure 4. In case of K-AOT the cmc can not be determined at 40°C due to the very low solubility of the particular

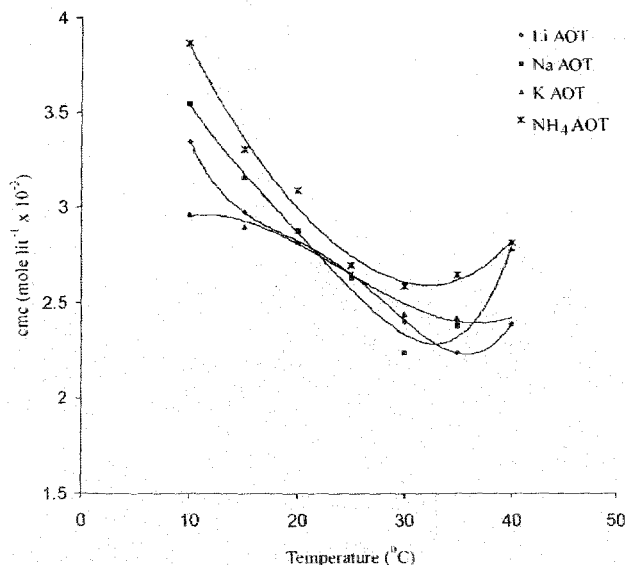


FIG. 4. Variation of cmc with temperature of AOT having different counter cation (viz.  $\text{Na}^+$ ,  $\text{Li}^+$ ,  $\text{K}^+$ ,  $\text{NH}_4^+$ ).

surfactant at that temperature, which may be hardly sufficient to make micelle. The decrease in the cmc with temperature at lower temperatures is possibly due to the hydration of the monomers, while further temperature increase causes a disruption of the structured water around the hydrophobic groups that opposes micellization. The temperature and cmc curve can be expressed according to the polynomial equation:

$$\ln \text{cmc}(T) = a - bT^2 + cT^3 - dT^4 + \dots \quad [1]$$

Our results also follow the temperature dependency, given by La Mesa, in his empirical equation of cmc:<sup>[37]</sup>

$$(\text{cmc} - \text{cmc}^*)/\text{cmc}^* = |(T - T^*)/T^*|^\gamma, \quad [2]$$

where  $\text{cmc}^*$  is the minimal value of cmc and  $T^*$  the temperature at the minimum with  $\gamma = 1.74 \pm 0.03$ . The exponent  $\gamma$  has no obvious physical meaning. The position of the minimum has thermodynamic significance also. The minimum in cmc represents minimum in free energy of micellization (Table 3).

### 3.2 Thermodynamic Parameters

The temperature dependence of the cmc of AOT surfactants having different counterion have been investigated to obtain the corresponding thermodynamic parameters of micellization. On the basis of the mass action or phase separation model,<sup>[36]</sup> the standard free energy of micelle formation per mole of monomer of nonionic surfactants is simply:

$$\Delta G_m^0 = RT \ln X_{\text{cmc}}, \quad [3]$$

where  $X_{\text{cmc}}$  is the value of cmc expressed in mole fraction. But in case of ionic surfactant the situation is somehow different due to the counterion dissociation and  $\Delta G_m^0$  should not be

TABLE 2  
Hydration number of ions derived from corrected ionic radii

Ion	Hydration number
$\text{NH}_4^+$	4.6
$\text{K}^+$	5.1
$\text{Na}^+$	6.5
$\text{Li}^+$	7.4

equivalent only to  $\Delta G_m^0$ . The Standard Gibbs free energy of micellization ( $\Delta G_m^0$ ) then may be expressed by the relation:<sup>[6]</sup>

$$\Delta G_m^0 = (2 - \alpha)RT \ln X_{\text{cmc}} \quad [4]$$

The ionization degree or counterionic association constant  $\alpha = p/n$ , of the micelle, where  $p$  and  $n$  are the effective charge and the aggregation number of the micelle respectively, can be determined from the ratio of the slope of the two linear fragments of conductivity concentration curve above and below cmc.<sup>[6]</sup> The values of  $\Delta G_m^0$  calculated for each surfactant in different temperatures are used to calculate the entropy of the same system. Similar arguments allow the standard enthalpy ( $\Delta H_m^0$ ) and entropy ( $\Delta S_m^0$ ) of micellization to be obtained from simple equations:

$$\Delta H_m^0 = -(2 - \alpha)RT^2 (\partial \ln X_{\text{cmc}} / \partial T)_p \quad [5]$$

$$\Delta S_m^0 = (\Delta H_m^0 - \Delta G_m^0) / T \quad [6]$$

All thermodynamic properties calculated for the micellization of AOT (having different counterions) in various temperatures are listed in Table 3. From these data it is obvious that the micellization process is spontaneous as indicated by the large negative values of  $\Delta G_m^0$ . The magnitude and the signs of  $\Delta G_m^0$  and  $\Delta S_m^0$  suggest the stability of the micelle which also may support the destruction of hydrophobic hydration in the process of micelle formation. The variation of all standard thermodynamical parameters with different counterions at a certain temperature can also be explained by the size along with the hydration of the counterion as stated earlier in case of cmc. At a particular temperature, for example, at 20°C, AOT with  $\text{Na}^+$  ion has the largest  $\Delta H_m^0$ , 25.4 kJ/mol while with  $\text{K}^+$  ion the least  $\Delta H_m^0$  indicates the lowest hydration of  $\text{K}^+$  during micellization though the cmc values are almost similar for all AOT with different counterions. Like cmc, the  $\Delta G_m^0$  and  $\Delta H_m^0$  also are dependent on temperature and the profile passes through minima for the surfactant containing each counterion type. The experimental  $\Delta G_m^0$  and  $\Delta H_m^0$  values can also be satisfactorily fitted with the polynomials as described by Majhi et al.<sup>[38]</sup>

$$\Delta G_m^0 = a' + b'T + c'T^2 + d'T^3 + \dots \quad [7]$$

$$\Delta H_m^0 = a'' + b''T + c''T^2 + d''T^3 + \dots \quad [8]$$

TABLE 3

Different thermodynamic parameters (viz. changes in standard Gibbs free energy,  $\Delta G_m^0$ , standard enthalpy,  $\Delta H_m^0$ , standard entropy,  $\Delta S_m^0$ ) of micellization

Counter ions of different AOT surfactants	Temp/ °C	$-\Delta G_m^0/$ (kJ mol <sup>-1</sup> )	$-\Delta H_m^0/$ (kJ mol <sup>-1</sup> )	$\Delta S_m^0/$ (J mol <sup>-1</sup> )
Li <sup>+</sup>	10	29.0	09.9	63.4
	15	35.1	12.1	80.0
	20	36.3	12.6	80.9
	25	34.9	12.3	76.0
	30	32.8	11.6	69.9
	35	34.3	12.3	71.5
	40	32.1	12.0	73.3
Na <sup>+</sup>	10	44.4	23.5	73.8
	15	37.2	25.3	41.3
	20	37.0	25.4	39.7
	25	32.1	22.1	33.3
	30	33.5	23.1	34.1
	35	33.6	23.8	32.0
	40	34.2	24.3	34.4
K <sup>+</sup>	10	29.2	5.7	83.4
	15	32.4	6.4	90.5
	20	34.1	6.8	93.2
	25	31.3	6.3	84.0
	30	29.2	5.9	76.8
	35	32.3	6.7	83.3
	40	34.2	6.7	83.3
NH <sub>4</sub> <sup>+</sup>	10	35.0	16.5	61.3
	15	33.0	15.6	56.9
	20	32.0	14.3	50.2
	25	32.5	15.9	56.6
	30	30.9	15.8	52.0
	35	34.1	16.0	50.0
	40	33.2	16.3	53.5

A close look on the thermodynamic parameters (Table 3) support the view that in order to form micelle the gain in entropy is the major factor leading to negative change in Gibbs free energy<sup>[26-31]</sup> when the temperature is not very high. The maximum surface excess concentration ( $\Gamma_{\max}$ ) and minimum areas per molecule ( $A_{\min}$ ) in the aqueous/air interface is calculated by using the following relations:<sup>[24,25]</sup>

$$\Gamma_{\max} = \frac{1}{2.303n'RT} \left( \frac{-\partial\gamma}{\partial \ln C} \right) \quad [9]$$

$$A_{\min} = 1/(N\Gamma), \quad [10]$$

where  $\gamma$  is the surface tension,  $N$  is the Avogadro number,  $C$  and  $n'$  are the concentration and number particles per molecule of the surfactant. Since the AOT surfactants behave

like a uni-univalent electrolyte in aqueous solution at the concentration less than cmc, the value of  $n'$  has been taken as 2 in all cases. Generally for the ionic surfactants  $\Gamma_{\max}$  values slightly decreases with temperature. But in the case of present AOT surfactants with four different counterions, the change of  $\Gamma_{\max}$  is rather complex. Unlike Li<sup>+</sup>, an increase in  $\Gamma_{\max}$  with temperature is observed for all the other three counterions. This may be due to the effect of lower hydration of the sulfosuccinate of AOT at higher temperature and, an increasing tendency to move to the air-liquid interface. The typical double chain "conelike molecular structure" also may be partially responsible for this result. The moderate increase in the effectiveness of adsorption with temperature is due to increased thermal motion, and  $A_{\min}$  display an inverse trend with temperature, as expected. At a particular temperature  $\Gamma_{\max}$ , however, shows anomalous behavior as the counterion of the surfactant changes. It may be attributed to the enhanced hydrophobicity of the anionic part of the surfactant molecules. Lithium ion, however, shows some different behavior, which may be due its smaller size and larger hydration number of the ion.

## REFERENCES

- [1] Delbene, J.E. (1979) An ab initio molecular orbital study of 2- and 4-monosubstituted pyridines. *J. Am. Chem. Soc.*, 107: 6184-6189.
- [2] Shah, D.O. (1991) *Surface Phenomena in Enhanced Oil Recovery*; Plenum Press: New York.
- [3] Jha, B.K., Patist, A., and Shah, D.O. (1999) Effect of antifoaming agents on the micellar stability and foamability of sodium dodecyl sulfate solutions. *Langmuir*, 15: 3042-3044.
- [4] Rehak, H. and Hoffmann, H. (1991) Viscoelastic surfactant solutions: Model systems for rheological research. *Mol. Phys.*, 74: 933.
- [5] Hoffmann, S., Rauscher, A., and Hoffmann, H. (1991) Shear induced micellar structures. *Ber. Bunsen-Ges. Phys. Chem.*, 95: 153-164.
- [6] Mukerjee, P. (1961) The nature of the association equilibria and hydrophobic bonding in aqueous solutions of association colloids. *Adv. Colloid Interface Sci.*, 1: 242-275.
- [7] Baumuller, W., Hoffmann, H., Ulbricht, W., Tondre, C., and Zana, R. (1978) Chemical relaxation and equilibrium studies of aqueous solutions of laurylsulfate micelles in the presence of divalent metal ions. *J. Colloid Interface Sci.*, 64: 418-437.
- [8] Satake, I., Iwamatsu, I., Hosokawa, S., and Matuura, R. (1963) The surface activities of bivalent metal alkyl sulfates. I. On the micelles of some metal alkyl sulfates. *Bull. Chem. Soc. Jpn.*, 36: 204-209.
- [9] Benraou, M., Bales, B.L., and Zana, R. (2003) Effect of the nature of the counterion on the properties of anionic surfactants. 1. cmc, ionization degree at the cmc and aggregation number of micelles of sodium, cesium, tetramethylammonium, tetraethylammonium, tetrapropylammonium, and tetrabutylammonium dodecyl sulfates. *J. Phys. Chem. B*, 107: 13432-13440.

- [10] Nusselder, J.J.H. and Engberts, J.B.F.N. (1992) Toward a better understanding of the driving force for micelle formation and micellar growth. *J. Colloid Interface Sci.*, 148: 353–361.
- [11] Paredes, S., Tribout, M., Ferreira, J., and Leonis, J. (1976) A microcalorimetric method of determination of critical micellar concentration and enthalpy of micellization. *Colloid Polym. Sci.*, 254: 637–642.
- [12] Shanks, P.C. and Franses, E.I. (1992) Estimation of micellization parameters of aqueous sodium dodecyl sulfate from conductivity data. *J. Phys. Chem.*, 96: 1794–1805.
- [13] Goddard, E.D. and Benson, G.C. (1957) Conductivity of aqueous solutions of some paraffin chain salts. *Can. J. Chem.*, 35: 986–991.
- [14] Kameyama, K. and Toshio, T. (1990) Micellar properties of octylglucoside in aqueous solutions. *J. Colloid Interface Sci.*, 137: 1–10.
- [15] Tanford, C. (1980) *The Hydrophobic Effect: Formation of Micelles and Biological Membranes*, 2nd edn.; Wiley: New York.
- [16] Paula, S., Süss, W., Tuchtenhagen, J., and Blume, A. (1995) Thermodynamics of micelle formation as a function of temperature: A High sensitivity titration calorimetry study. *J. Phys. Chem.*, 99: 11742–11751.
- [17] Onori, G. and Santucci, A. (1997) Calorimetric study of the micellization of *n*-butoxyethanol in water. *J. Phys. Chem. B.*, 101: 4662–4666.
- [18] Birdi, K.S. (1983) Calorimetric determination of the enthalpy of micelle formation in aqueous media. *Colloid Polym. Sci.*, 261: 45–48.
- [19] von Os, N.M., Daane, G.J., and Haandrekman, G. (1991) The effect of chemical structure upon the thermodynamics of micellization of model alkylarenesulfonates: III. Determination of the critical micelle concentration and the enthalpy of demicellization by means of microcalorimetry and a comparison with the phase separation model. *J. Colloid Interface Sci.*, 141: 199–217.
- [20] Barry, B.W. and Russel, G.F.J. (1972) Prediction of micellar molecular weights and thermodynamics of micellization of mixtures of alkyltrimethylammonium salts. *J. Colloid Interface Sci.*, 40: 174–194.
- [21] Emerson, M.F. and Holtzer, A. (1967) Hydrophobic bond in micellar systems. Effects of various additives on the stability of micelles of sodium dodecyl sulfate and of *n*-dodecyltrimethylammonium bromide. *J. Phys. Chem.*, 71: 3320–3330.
- [22] Eastoe, J., Robenson, B.H., and Heenan, R.K. (1993) Water-in-oil microemulsions formed by ammonium and tetrapropylammonium salts of Aerosol OT. *Langmuir*, 9: 2820–2822.
- [23] Tamsamani, M.B., Maeck, M., Hassani, I.E., and Hurwitz, H.D. (1998) Fourier transform infrared investigation of water states in aerosol-OT reverse micelles as a function of counterionic nature. *J. Phys. Chem. B.*, 102: 3335–3340.
- [24] Rosen, M.J., Cohen, A.W., Dahanayake, M., and Hua, X. (1982) Relationship of structure to properties in surfactants. 10. Surface and thermodynamic properties of 2-dodecyloxypropyl (ethoxyethanol)s,  $C_{12}H_{25}(OC_2H_4)_xOH$ , in aqueous solution. *J. Phys. Chem.*, 86: 541–545.
- [25] Oh, S.G. and Shah, D.O. (1993) Effect of counterions on the interfacial tension and emulsion droplet size in the oil/water/dodecyl sulfate system. *J. Phys. Chem.*, 97: 284–286.
- [26] Moroni, A. (1992) *Micelles: Theoretical and Applied Aspects*; Plenum Press: New York.
- [27] Weckström, K., Hanu, K., and Rosenholm, J.B. (1994) Enthalpies of mixing a non-ionic surfactant with water at 303.15 K studied by calorimetry. *J. Chem. Soc., Faraday Trans.*, 90: 733–738.
- [28] Evans, D.F. and Ninham, B.W. (1986) Molecular forces in the self-organization of amphiphiles. *J. Phys. Chem.*, 90: 226–234.
- [29] Evans, D.F. and Ninham, B.W. (1983) Ion binding and the hydrophobic effect. *J. Phys. Chem.*, 87: 5025–5032.
- [30] Lumry, R. and Rajender, S. (1970) Enthalpy-entropy compensation phenomena in water solutions of proteins and small molecules: A ubiquitous property of water. *Biopolymers.*, 9: 1125–1227.
- [31] Privalov, P.L. and Gill, S.J. (1989) The hydrophobic effect: a reappraisal. *Pure Appl. Chem.*, 61: 1097–1104.
- [32] Jolicœur, C. and Philip, P.R. (1974) Enthalpy-entropy compensation for micellization and other hydrophobic interactions in aqueous solutions. *Can. J. Chem.*, 52: 1834–1839.
- [33] Lee, B. (1991) Solvent reorganization contribution to the transfer thermodynamics of small nonpolar molecules. *Biopolymers*, 31: 993–1008.
- [34] Lee, B. (1994) Enthalpy-entropy compensation in the thermodynamics of hydrophobicity. *Biophys. Chem.*, 51: 271–278.
- [35] Madau, B. and Lee, B. (1994) Role of hydrogen bonds in hydrophobicity: the free energy of cavity formation in water models with and without the hydrogen bonds. *Biophys. Chem.*, 51: 279–289.
- [36] Myers, D. (1992) *Surfactant Science and Technology*; VCH: New York.
- [37] La Mesa, C. (1990) Dependence of critical micelle concentration of intensive variables: A reduced variables analysis. *J. Phys. Chem.*, 94: 323–326.
- [38] Majhi, P.R. and Blume, A. (2001) Thermodynamic characterization of temperature-induced micellization and demicellization of detergents studied by differential scanning calorimetry. *Langmuir*, 17: 3844–3851.
- [39] Marcus, Y. (1985) *Ion Solvation*; Wiley-Interscience: New York.
- [40] Nakagaki, M. and Handa, T. (1984) Effect of structure on activity at the critical micelle concentration and on the free energy of micelle formation. *ACS Symposium Series*, 253: 73.

# Effect of size of tetraalkylammonium counterions on the temperature dependent micellization of AOT in aqueous medium

Amitabha Chakraborty · Swapan K. Saha ·  
Subrata Chakraborty

Received: 9 September 2007 / Accepted: 10 February 2008  
© Springer-Verlag 2008

**Abstract** Different tetraalkylammonium, viz.  $N^+(\text{CH}_3)_4$ ,  $N^+(\text{C}_2\text{H}_5)_4$ ,  $N^+(\text{C}_3\text{H}_7)_4$ ,  $N^+(\text{C}_4\text{H}_9)_4$  along with simple ammonium salts of bis (2-ethylhexyl) sulfosuccinic acid have been prepared by ion-exchange technique. The critical micelle concentration of surfactants with varied counterions have been determined by measuring surface tension and conductivity within the temperature range 283–313 K. Counterion ionization constant,  $\alpha$ , and thermodynamic parameters for micellization process viz.,  $\Delta G_m^0$ ,  $\Delta H_m^0$ , and  $\Delta S_m^0$  and also the surface parameters,  $\Gamma_{\text{max}}$  and  $A_{\text{min}}$ , in aqueous solution have been determined. Large negative  $\Delta G_m^0$  of micellization for all the above counterions supports the spontaneity of micellization. The value of standard free energy,  $\Delta G_m^0$ , for different counterions followed the order  $N^+(\text{CH}_3)_4 > \text{NH}_4^+ > \text{Na}^+ > N^+(\text{C}_2\text{H}_5)_4 > N^+(\text{C}_3\text{H}_7)_4 > N^+(\text{C}_4\text{H}_9)_4$ , at a given temperature. This result can be well explained in terms of bulkiness and nature of hydration of the counterion together with hydrophobic and electrostatic interactions.

**Keywords** Aerosol-OT · Critical micelle concentration · Counterion · Thermodynamic parameters

## Introduction

The colligative properties of surfactants do not vary in a simple way with concentration due to self assembly of amphiphiles forming micelles or vesicles [1]. The formation of an ionic micelle from monomeric ions results a balance between hydrophobic interactions between the hydrophobic part of the micelle-forming ions, electrostatic interactions between their hydrophilic charged parts, as well as with and between the counterions. In addition, the changes in hydration energies and specific interactions with counterions may also be important [2–6]. The strength and importance of these various interactions depend upon externally controllable factors, such as temperature and ionic strength on the properties of the particular ions involved. Moreover, the structure of the resulting micelle, in particular, its aggregation number,  $n$ , its shape, and the compactness of its electrical double layer show some kind of dependency [5]. Even the molecular conformation of some dimeric surfactants (known as Gemini surfactants) affects the micellization to a large extent [6]. Obviously, the actually existing micelles correspond to the lowest free-energy state of the system. Thus, the knowledge of critical micelle concentration (cmc) and thermodynamic quantities of micellization like Gibbs free energy  $\Delta G_m^0$ , the enthalpy  $\Delta H_m^0$ , or the entropy  $\Delta S_m^0$  at various temperatures have utmost importance from the view point of formation and stability of micelles.

A survey of phase diagram of ionic surfactants, in aqueous and in the presence of a cosolvent such as a long-chain alcohol, has demonstrated clearly that the valency of the counterion plays an important role in determining phase stability as well as the aggregation shape [7, 8]. It was shown that the swelling tendency of a lamellar interface is reduced considerably with a divalent counterion as com-

A. Chakraborty · S. K. Saha (✉) · S. Chakraborty  
Department of Chemistry, University of North Bengal,  
Darjeeling 734 013, India  
e-mail: ssahanbu@hotmail.com

A. Chakraborty  
e-mail: acnbu@rediffmail.com

pared to a monovalent one, which was explained in terms of a more extensive binding of the divalent counterions to the polar head groups of the surfactant lamellae. A substantial amount of work has already been carried out on the binding of monovalent counterions to micelle [4, 9, 10] for single tail anionic surfactant like dodecyl sulfate. The study of the effect of counterions eliminates some of the complications by leaving the properties of the amphiphilic ion as a constant factor and, thus, simplifies some of the interpretation of the experimental results. But, it often leads to complications connected with limited stability and preparative difficulties of the surfactant containing different counterions. Compared to cationic surfactants, the counterionic effect in micellization is less dramatic in anionic surfactants. However, when compared with  $\text{Na}^+$  counterions, polyvalent ions usually markedly reduces the cmc [11] by several order of magnitude and lead the formation of large micelles that may be confirmed from the increase in micellar aggregation number [10, 12]. In aqueous solution, the micelles are known to be charged due to a fraction,  $\alpha$ , of their counterion dissociates into the aqueous pseudophase. The value of  $\alpha$  for a given pure surfactant is important because both the physical [13, 14] and chemical [15] properties of the micelle are influenced by surface charges.

Aerosol-OT (AOT, Sodium bis-(2-ethyl-1-hexyl) sulfosuccinate), having two hydrophobic tails, is an important anionic surfactant in the field of surface chemistry as well as in industry due to its rich phase behavior and the ability to form microemulsion [16]. This work is a part of a program to study the cmc and thermodynamic parameters of bis-(2-ethyl-1-hexyl) sulfosuccinate micelle within a wide range of temperature as the counterion is systematically made more bulky and hydrophobic. There are some evidences [4–6, 10] that the counterions exhibit mainly electrostatic interaction or, no chemical interaction is to be expected on the structural grounds. Therefore, it is the system where the cmc differences are rather small and the effect of ionic size and of physical adsorption can be best investigated. Thus, we investigate a series of tetraalkylammonium ion, such as  $\text{N}^+(\text{CH}_3)_4$ ,  $\text{N}^+(\text{C}_2\text{H}_5)_4$ ,  $\text{N}^+(\text{C}_3\text{H}_7)_4$ ,  $\text{N}^+(\text{C}_4\text{H}_9)_4$  along with  $\text{NH}_4^+$  and  $\text{Na}^+$ . It should be mentioned that the cmc and thermodynamic parameters of the AOT having different tetraalkylammonium counterion have not yet been reported in the literature. Hence, our experimental goal is to determine the cmc of AOT with different counterions within the temperature range of 283–313 K and to determine the associated thermodynamic parameters of micellization, such as changes in standard Gibbs free energy ( $\Delta G_m^0$ ), standard enthalpy ( $\Delta H_m^0$ ), standard entropy ( $\Delta S_m^0$ ), maximum surface excess concentration ( $\Gamma_{\text{max}}$ ), and the minimum areas per molecule ( $A_{\text{min}}$ ) at the surface in order to examine the effect of counterionic sizes on the micellization.

## Experimental section

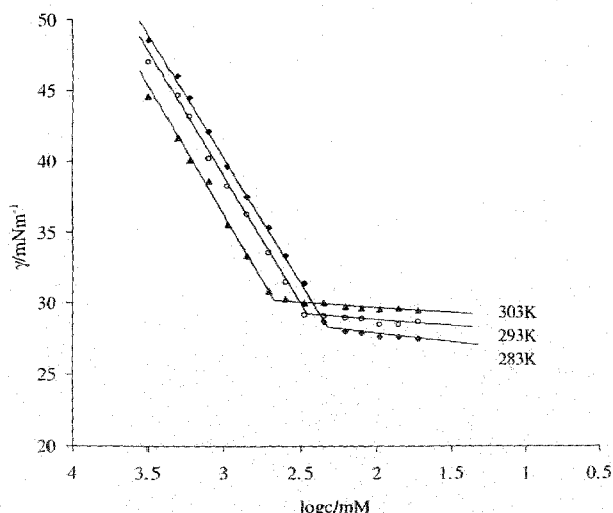
### Materials

Surfactants with the desired counterions were prepared by following the technique of Eastoe et al. [17] and the extended work of Tamsamani et al. [4, 18]. A high-grade purified sample of AOT (>99% from Fluka, Switzerland) was converted into the surfactants bearing different counterions by ion-exchange technique using a strong ion exchange resin (Amberlite IR-120, 20–50 mesh, Loba Cheme, India). The process is described below:

A 10-g sample of AOT was dissolved in 20 mL of a 1:1 (v/v) mixture of water and ethanol. The solution was passed through a column (40 cm  $\times$  2 cm<sup>2</sup>) of a strong ion exchanger in the  $\text{H}^+$  form slowly. The resin was put in the acid form by using a large excess of a 0.20 M aqueous hydrochloric acid solution and washed with water until the complete removal of the excess acid takes place. The free sulfonic acid formed on passing the AOT ( $\text{Na}^+$  salt) through the resin was, then, immediately neutralized with an aqueous solution of the hydroxides of the desired counterions (viz.  $\text{NH}_4^+$ ,  $\text{N}^+(\text{CH}_3)_4$ ,  $\text{N}^+(\text{C}_2\text{H}_5)_4$ ,  $\text{N}^+(\text{C}_3\text{H}_7)_4$ ,  $\text{N}^+(\text{C}_4\text{H}_9)_4$ ). All the hydroxides of high purity were procured from Across Chem., Belgium. The solvent water was then removed fast by freeze drying and then keeping under vacuum (bath temperature 313 K) for several days, and the waxy solid was finally dried in vacuum over  $\text{P}_2\text{O}_5$ . These materials contain residual water, which were finally removed by the action of  $\text{P}_2\text{O}_5$  (from Loba Cheme, India) on a solution of surfactant in isooctane ( $\geq 99.5\%$  from Merck, India). The extent of  $\text{Na}^+/\text{H}^+$  ion exchange was optimized by controlling the flow rate of the solution; finally,  $\text{H}^+$  content of the AOT solution (acid form) was measured by titrating with standard NaOH. The extent of exchange was found to be more than 99%. Among all the ion-exchanged surfactants, tetrabutylammonium-AOT did not crystallize at room temperature even after keeping at low temperature for several months. It appeared as a highly viscous, colorless, semi-solid material. Doubly distilled water having conductivity of 2  $\mu\text{S cm}^{-1}$  was used throughout experiment.

### Methods

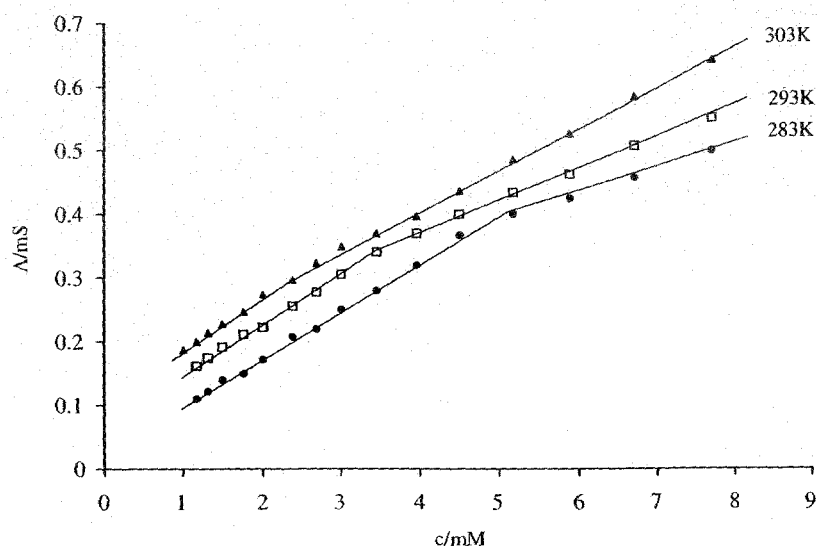
The cmc values were determined from the surface tension as well as specific conductance data. It is customary to plot the (1) surface tension  $\gamma$  against the logarithmic value of the surfactant concentration  $C$  and the (2) conductance  $\Lambda$  against the concentration of the surfactant, where the break indicates the cmc of a particular system. The surface tension experiments were done by platinum ring detachment method using a Tensiometer (K9,



**Fig. 1** Surface tension,  $\gamma$ , of AOT (Tetramethylammonium salt) in aqueous solution as a function of the logarithm of the surfactant concentration at 283, 293, and 303 K

KRÜSS; Germany) at different temperatures. The accuracy of the measurement was within  $\pm 0.1 \text{ m Nm}^{-1}$ . Temperature of the system was maintained by circulating auto-thermostated water through a double-wall glass vessel containing the solution. Similar studies were also done conductometrically by using an electrical conductivity bridge (METTLER TOLEDO, Switzerland). The conductance values were uncertain within the limit of  $\pm 1\%$ . Each measurement was repeated several times at each temperature in the ranges 283–313 K. Measurements were made at 5 K intervals of temperatures.

**Fig. 2** Conductance,  $\Lambda$ , of AOT (Tetramethylammonium salt) in aqueous solution as a function of the surfactant concentration at 283, 293, and 303 K



## Results and discussion

### Critical micelle concentration

The cmc corresponds to a concentration at which a very small but, often, clearly detectable concentration of the micelles exists. Typical experimental curves of salt-free systems are obtained in both surface tension and conductance measurements, and the cmc values determined for surfactant with each counterion are in close agreement with one another. The cmc of Na-AOT is also in good agreement with the literature value [19, 38]. The sharpness of the “break-point” is an indication of the purity of the surfactant used. Figures 1 and 2 are the representative plots obtained in the surface tension and conductivity measurements. Further results of surface tension experiments are presented in Table 1.

A critical examination of Table 1 shows that in all instances, the change of cmc with temperature is small. However, at a particular temperature, cmc depends upon the nature of the counterion following the order  $\text{N}^+(\text{CH}_3)_4 > \text{NH}_4^+ > \text{Na}^+ > \text{N}^+(\text{C}_2\text{H}_5)_4 > \text{N}^+(\text{C}_3\text{H}_7)_4 > \text{N}^+(\text{C}_4\text{H}_9)_4$  (at temperature range  $< 298 \text{ K}$ ). It seems that the hydrodynamic size of the counterion plays an important role along with the hydrophobicity of tetraalkylammonium ions. Measurement of partial molar volumes [20, 21] and calculation of hydration of micelles [22] by previous workers indicated that there was little loss of hydration water for this system during micellization. Therefore, the tightly bound hydration shell would limit the distance of closest approach. It is well known that the increase of the number of carbon atoms of hydrocarbon tail of a surfactant allows micellization to occur at a lower concentration due

**Table 1** Surface properties of AOT surfactants having different counterions ( $I^c$ ) at various temperatures ( $T/K$ ): cmc, maximum surface excess concentration, minimum areas per molecule at the surface

$I^c$	$T/K$	cmc <sup>a</sup> /(mol dm <sup>-3</sup> × 10 <sup>3</sup> )	$\Gamma_{\max}/\text{mol cm}^{-2} \times 10^8$	$A_{\min}/\text{nm}^2 \times 10^2$
Na <sup>+</sup>	283	3.55 (3.53)	1.42	1.17
	288	3.16 (3.20)	1.45	1.14
	293	2.88 (2.77)	1.49	1.11
	298	2.63 (2.40)	1.57	1.06
	303	2.24 (2.20)	1.76	0.94
	308	2.37 (2.26)	1.70	0.98
	313	2.80 (2.69)	1.71	0.97
NH <sub>4</sub> <sup>+</sup>	283	3.87 (3.85)	1.56	1.06
	288	3.31 (3.20)	1.58	1.05
	293	3.09 (3.12)	1.45	1.14
	298	2.70 (2.65)	1.55	1.07
	303	2.59 (2.52)	1.80	0.92
	308	2.65 (2.60)	1.72	0.96
	313	2.82 (2.75)	1.76	0.94
(CH <sub>3</sub> ) <sub>4</sub> N <sup>+</sup>	283	4.76 (4.61)	1.68	0.99
	288	3.82 (4.10)	1.65	1.01
	293	3.24 (3.40)	1.53	1.08
	298	2.90 (2.90)	1.60	1.04
	303	2.05 (2.35)	1.80	0.92
	308	2.10 (2.20)	1.72	0.96
	313	2.26 (2.31)	1.67	0.99
(C <sub>2</sub> H <sub>5</sub> ) <sub>4</sub> N <sup>+</sup>	283	1.88 (2.10)	1.44	1.15
	288	1.78 (2.00)	1.33	1.25
	293	2.95 (1.85)	1.46	1.14
	298	2.45 (2.50)	1.43	1.16
	303	2.31 (2.43)	1.76	0.94
	308	2.37 (2.50)	1.31	1.27
	313	2.56 (2.63)	1.41	1.12
(C <sub>3</sub> H <sub>7</sub> ) <sub>4</sub> N <sup>+</sup>	283	1.18 (1.34)	1.67	0.99
	288	1.05 (1.20)	1.71	0.97
	293	0.93 (0.98)	1.85	0.89
	298	0.97 (0.95)	1.71	0.97
	303	0.92 (0.85)	1.77	0.94
	308	0.87 (0.90)	1.69	0.98
	313	0.74 (0.80)	1.93	0.86
(C <sub>4</sub> H <sub>9</sub> ) <sub>4</sub> N <sup>+</sup>	283	1.04 (1.11)	1.32	1.26
	288	0.87 (0.91)	1.40	1.18
	293	0.80 (0.83)	1.42	1.17
	298	0.77 (0.80)	1.63	1.02
	303	0.75 (0.78)	1.82	0.91

<sup>a</sup>The values in the parenthesis represent cmc determined by conductivity method

<sup>b</sup>Values are taken from [25]

to increased hydrophobicity of the hydrocarbon tail [23]. But, the increased ionic size from N<sup>+</sup>(CH<sub>3</sub>)<sub>4</sub> to N<sup>+</sup>(C<sub>4</sub>H<sub>9</sub>)<sub>4</sub> enhances the micellization tendency and eventually reduces the cmc. Here, the hydrocarbon exterior of the tetraalkyl ions undergoes hydrophobic interactions with the exposed hydrocarbon of the micelle surface and overcome steric hindrance. However, such a phenomenon is little or absent

in the set of counterions viz., N<sup>+</sup>(CH<sub>3</sub>)<sub>4</sub>, NH<sub>4</sub><sup>+</sup> and Na<sup>+</sup>. In the absence of any appreciable hydrophobic interaction, NH<sub>4</sub><sup>+</sup> and Na<sup>+</sup> ions interact with the micellar head groups more strongly than N<sup>+</sup>(CH<sub>3</sub>)<sub>4</sub> ions due to their smaller sizes (hydration number 4.6 and 6.5, respectively [25]). Eventually, they lead to form micelle more readily via efficient charge screening than that of N<sup>+</sup>(CH<sub>3</sub>)<sub>4</sub> ions, and the systems yield low cmc values. But, in case of other tetraalkylammonium ions, as the bulkiness of the ion increases due to the presence of large alkyl groups, the hydrophobicity plays an important role causing increasingly micellization to occur at lower concentrations as has already been mentioned.

Figure 3 shows that the cmc of the surfactants follows a characteristic temperature dependency and passes through a minimum at the temperature range 298–308 K. With increasing temperature, the dehydration of N<sup>+</sup>(CH<sub>3</sub>)<sub>4</sub> ion perhaps becomes most pronounced among all the counterions and results in the highest slope in Fig. 3 at temperature <298 K. The variation of cmc with temperature shows good agreement with the empirical equation given by La Mesa [26]:

$$(\text{cmc} - \text{cmc}^*)/\text{cmc}^* = \{(T - T^*)/T^*\}^{\gamma'} \quad (1)$$

Where cmc\* is the minimum value of cmc and T\* the temperature at the minimum with  $\gamma' = 1.74 \pm 0.03$ . It should be mentioned that the exponent  $\gamma'$  has no obvious physical meaning, but both cmc\* and the related temperature, in case of a particular surfactant, are the measure of the hydrophobic–hydrophilic balance of micelle. The position of the minimum has thermodynamic significance also. The minimum in cmc represents minimum in free energy of micellization.

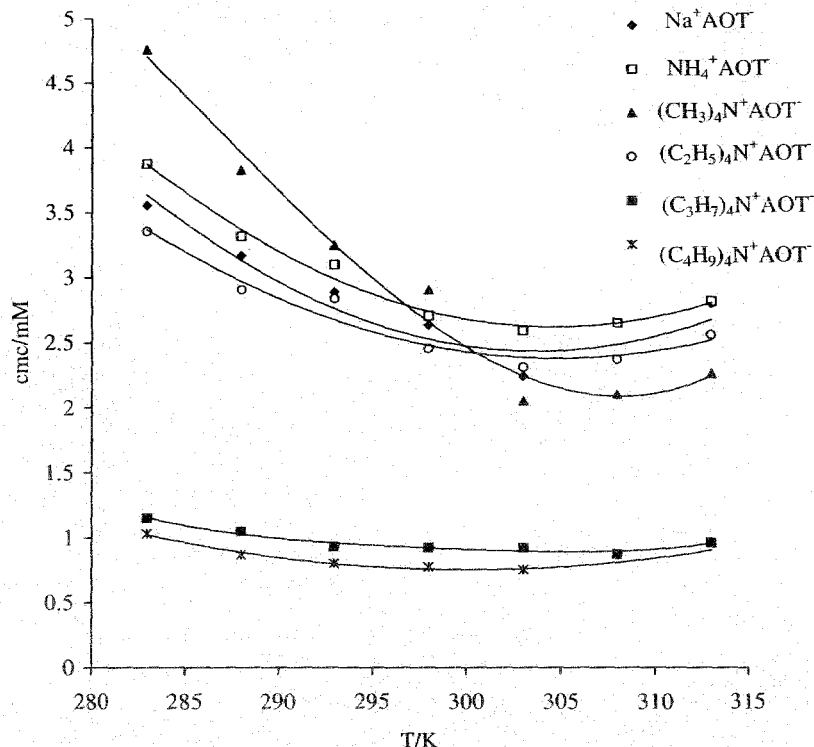
#### Thermodynamic parameters

The temperature dependency of AOT micelles having different counterions also enables to determine the corresponding thermodynamic parameters of micellization. According to mass action or phase separation model [27, 28, 36], the standard free energy of micelle formation per mole of monomer of nonionic surfactants is expressed by well-known equation:

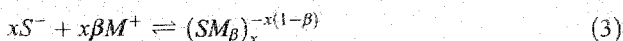
$$\Delta G_m^0 = RT \ln X_{\text{cmc}} \quad (2)$$

Where  $X_{\text{cmc}}$  is the value of cmc expressed in mole fraction. But, in case of ionic surfactant, the situation is somewhat different due to the counterion dissociation, and  $\Delta G_m^0$  should not be equivalent to that of the nonionic surfactant.

Fig. 3 Variation of cmc with temperature (K) of AOT having different counter cation



According to the theoretical mass action model, the micellization equilibrium for ionic surfactant can be expressed as:



Where  $(SM_\beta)_x$  is the micelle composed of  $x$  surfactant monomers and  $x\beta$  counterions bearing  $S^-$  and  $M^+$  as the monomer and counterion of the surfactant forming micelles. The value of  $\beta$  may correspond the fraction of bound counterion in the micelle. But, for nonionic surfactants, monomers and micelles are obviously uncharged,  $M^+$  does not enter to the equation, and the model approaches to a limiting case having  $\beta=0$ . However, applying the mass action law to the monomer-micelle equilibrium for the ionic surfactant and taking into account the charges of counterion along with the other parameters, the Standard Gibbs free energy,  $\Delta G_m^0$  can be expressed as [29, 36]:

$$\Delta G_m^0 = (2 - \alpha)RT \ln X_{cmc} \quad (4)$$

for an ionic uni-univalent surfactant. Here,  $X_{cmc}$  is the cmc expressed in mole fraction scale and  $\alpha = 1 - \beta = p/n$ , is the ionization degree or counterionic ionization constant of the micelle, where  $p$  and  $n$  are the effective charge and the aggregation number of the micelle, respectively. The value of  $\alpha$  can be determined from the ratio of the slope of the two linear fragments of conductivity-concentration plot above and below cmc [11, 30]. The values of  $\Delta G_m^0$  determined for

each surfactant-counterion pair at different temperatures eventually give the standard enthalpy ( $\Delta H_m^0$ ) and entropy ( $\Delta S_m^0$ ) of micellization from the simple thermodynamic relations:

$$\Delta H_m^0 = -(2 - \alpha)RT^2(\partial \ln X_{cmc}/\partial T)_p \quad (5)$$

The Eq. 5 is obtained from the well-known Gibbs-Helmholtz relation and Eq. 4 assumes that  $\alpha$  does not vary much with temperature. However,  $\alpha$  is not strictly temperature independent and the more appropriate form of Eq. 5 should be

$$-\Delta H_m^0/T^2 = (2 - \alpha)R(\partial \ln X_{cmc}/\partial T)_p + R \ln X_{cmc}(\partial(2 - \alpha)/\partial T) \quad (6)$$

Because the variation of  $\alpha$  with temperature is not well defined and is devoid of any general trend, the quantity  $\partial(2 - \alpha)/\partial T$  is difficult to find out experimentally [44]. Therefore, at least to gain qualitative information regarding the thermodynamics, Eq. 5 has been applied at the appropriate  $\alpha$ .

$$\Delta S_m^0 = (\Delta H_m^0 - \Delta G_m^0)/T \quad (7)$$

The  $\ln X_{cmc}$  vs  $T$  plot is not linear. To evaluate  $\Delta H_m^0$ , following polynomial form of variation of  $\ln X_{cmc}$  with temperature has been considered.

$$\ln X_{cmc} = a + bT + cT^2 \quad (8)$$

Where a, b, c are respective polynomial constants. Thus,

$$(\partial \ln X_{\text{cmc}} / \partial T) = b + 2cT \quad (9)$$

The polynomial constants b and c were evaluated from the fitting of experimental data. For all AOT surfactants with different counterions, the calculated thermodynamic parameters of micellization are listed in Table 2. Spontaneity of the micellization process is well explained from the large negative values of  $\Delta G_m^0$ . Micelles containing the same amphiphile but different counterions show different values of thermodynamic parameters because of the counterions, which could be bound to a different extent and with different energy. Micellization in aqueous medium usually

leads to a positive entropy change, which is mainly due to the melting of the "flickering cluster" that arises out of the hydrophobic effect of amphiphilic part of the surfactant molecules [24]. During formation of a micelle, the endothermic melting of the ordered polar solvent molecules around the nonpolar tail of AOT is greater than the subsequent exothermic association of the molecules. The resulting disordered state is actually reflected the positive entropy change. The variation of the standard thermodynamic parameters with different counterions at a certain temperature can also be explained by the size and the hydration of the counterion as has been already discussed. Like cmc, the  $\Delta G_m^0$  and  $\Delta H_m^0$  also show temperature

**Table 2** Thermodynamic parameters of micellization for AOT surfactants with different counterions ( $I^c$ ) at various temperatures: Standard Gibb's free energy, Enthalpy, and Entropy

$I^c$	T/C	$-\Delta G_m^0 / (\text{kJ mol}^{-1})$	$-\Delta H_m^0 / (\text{kJ mol}^{-1})$	$\Delta S_m^0 / (\text{J K}^{-1} \text{mol}^{-1})$	
Na <sup>+</sup> <sup>a</sup>	283	44.4	23.5	73.8	
	288	37.2	25.3	41.3	
	293	37.0	25.4	39.7	
	298	32.1	22.1	33.3	
	303	33.5	23.1	34.1	
	308	33.6	23.8	32.0	
	313	34.2	24.3	34.4	
	NH <sub>4</sub> <sup>+</sup> <sup>b</sup>	283	35.0	16.5	61.3
		288	33.0	15.6	56.9
293		32.0	14.3	50.2	
298		32.5	15.9	56.6	
303		30.9	15.8	52.0	
308		34.1	16.0	50.0	
313		33.2	16.3	53.5	
(CH <sub>3</sub> ) <sub>4</sub> N <sup>+</sup>		283	33.0	29.1	13.7
		288	34.2	30.0	14.6
	293	31.7	27.9	13.3	
	298	30.8	27.2	12.1	
	303	33.0	28.6	14.5	
	308	32.3	28.5	12.2	
	313	33.1	29.0	12.8	
	(C <sub>2</sub> H <sub>5</sub> ) <sub>4</sub> N <sup>+</sup>	283	35.0	12.2	80.6
		288	33.0	11.7	74.0
293		32.0	12.2	67.6	
298		32.5	12.3	67.8	
303		30.9	11.9	62.7	
308		34.1	13.3	67.5	
313		35.2	13.7	67.7	
(C <sub>3</sub> H <sub>7</sub> ) <sub>4</sub> N <sup>+</sup>		283	36.4	8.5	98.7
		288	34.7	8.1	92.3
	293	35.8	8.5	93.3	
	298	36.6	8.8	93.1	
	303	36.6	8.9	91.2	
	308	35.4	8.7	86.5	
	313	36.8	8.8	90.6	
	(C <sub>4</sub> H <sub>9</sub> ) <sub>4</sub> N <sup>+</sup>	283	36.6	14.4	78.4
		288	37.6	14.9	78.8
293		38.2	15.3	78.2	
298		34.4	15.2	64.4	
303		37.7	15.5	73.3	

<sup>a</sup> Values are taken from [25]

dependency, and the profile passes through minima when these parameters are plotted against temperature for all the surfactant-counterion systems.

A close look on the thermodynamic parameters (Table 2) support the view that in order to form micelle, the gain in entropy is the major factor leading to negative change in Gibbs free energy [32–34] if the temperature is not very high. But the fact that though the free energy changes are not very different, the enthalpy change is significantly higher and the entropy changes are much lower for  $N^+$   $(CH_3)_4$  counterion containing AOT compared to all other systems. This leads one to interpret that the enthalpy contributes major driving force in micellization. Loosely bound water dipole with the  $N^+(CH_3)_4$  ion may cause lower contribution of  $\Delta S_m^0$  in aggregation process. However, like a variety of processes such as oxidation–reduction, hydrolysis, protein unfolding, etc., micellization process also exhibit a linear relationship between the enthalpy and entropy change, which is known as enthalpy–entropy compensation [35–37]. This is important in connection with the hydrophobicity of surfactant which leads to stable micelle formation. In general, the compensation phenomenon between the enthalpy change  $\Delta H_m^0$  and the entropy change  $\Delta S_m^0$  in various processes can be described in the form of [36, 42]

$$\Delta H_m^0 = \Delta H_m^* + T_c \Delta S_m^0 \quad (10)$$

In a plot of  $\Delta H_m^0$  vs  $\Delta S_m^0$ , the slope  $T_c$  has a dimension of temperature and is known as compensation temperature. This can be interpreted as a measure of desolvation part of micellization, that means a characteristic of solute–solute and solute–solvent interaction, and the intercept characterizes the solute–solute interaction. Our experimental results also show a good agreement with the enthalpy–entropy compensation linearity for all AOT surfactants having different counterions. Figure 4 represents enthalpy–entropy compensation plot at 298 K. The calculated compensation temperature value of 295.6 K satisfactorily follows the characteristic range of other ionic surfactants [36–38]. The intercept,  $\Delta H_m^*$ , has been calculated as  $-32.8 \text{ kJ mol}^{-1}$ , which corresponds the driving force of micellization where the entropy does not contribute the process at a particular temperature (298 K).

It is well known that the air–solution interface of a surfactant solution is well populated by the adsorbed molecules. The  $\Gamma_{\max}$  and  $A_{\min}$  in the aqueous–air interface are calculated by using the following relations [39–41].

$$\Gamma_{\max} = (1/2.303n'RT)(-\partial\gamma/\partial\log C) \quad (11)$$

$$A_{\min} = 1/(N\Gamma) \quad (12)$$

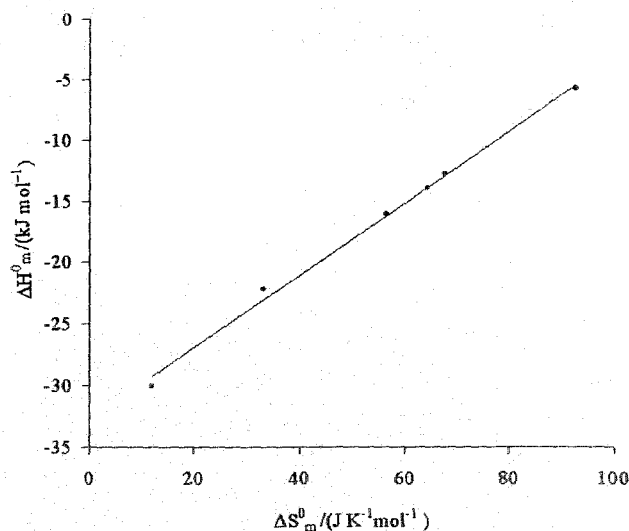


Fig. 4 Enthalpy–entropy compensation plots for AOT surfactants having different counterions at 298 K

Where  $\gamma$  expresses the surface tension,  $N$  is the Avogadro number,  $C$  and  $n'$  are the concentration and number particles per molecule of the surfactant, respectively. Because in aqueous solution at concentrations less than cmc, the AOT behaves like a uni-univalent electrolyte, the thermodynamic treatment requires  $n'=2$ , states an equimolar ratio of surfactant anion and counterion in the interface. Similar to analysis of  $\ln X_{\text{cmc}}$  vs  $T$  plot,  $\gamma$  vs  $\ln C$  plot was also fitted to a second order polynomial to measure  $\Gamma_{\max}$ . It is well known that for both nonionic [40] and anionic [41] surfactants,  $\Gamma_{\max}$  values slightly decreases with temperature while in some other cases, an increase of the surface excess quantity has been reported [43] in presence of additives. In the case of present AOT surfactant with six different counterions, the change of  $\Gamma_{\max}$  does not follow the regular trend. A critical examination of Table 2 shows a slight increment in  $\Gamma_{\max}$  with temperature for all the counterions, which may be due to the effect of lower hydration of the sulfosuccinate of AOT at higher temperature and, hence, an increasing tendency to move to the air–liquid interface. It is quite obvious that the standard state for the adsorbed surfactant is a hypothetical monolayer at its minimum surface area per molecule but at zero surface pressure. The typical double chain of the amphiphile may also partially be responsible for this result causing “steric inhibition” during adsorption. The moderate increase in the effectiveness of adsorption at the air–water interface with temperature is due to increased thermal motion, and therefore,  $A_{\min}$  displays an inverse trend with temperature, as expected. With increasing bulkiness of the counterions of the amphiphiles, the increase of  $\Gamma_{\max}$  are quite noticeable. At a particular temperature,  $\Gamma_{\max}$  shows anomalous behavior as the counterion of the surfactant changes. It may be attributed

to the enhanced hydrophobicity of the anionic part of the surfactant molecules depending upon accessibility of their corresponding counterions. A study of the behavior of tetramethylammoniumdodecyl sulfate at the air–solution interface indicated to a penetration of a part of the  $N^+(CH_3)_4$  ions in the dodecyl sulfate layer [31]. A similar phenomenon may also partially be responsible for the observed surface behavior in the present system.

## Conclusion

The sizes of tetraalkylammonium counterions influence cmc of AOT surfactant in aqueous solution significantly. As the size of counterion increases from  $N^+(C_2H_5)_4$  to  $N^+(C_4H_9)_4$ , the cmc value decreases due to increase in the hydrophobic interaction of counterions with the exterior of the micelle. The set of counterions viz.,  $NH_4^+$ ,  $Na^+$ , and  $N^+(CH_3)_4$  yield higher cmc value due to little or no hydrophobic interaction with the micelle. The  $NH_4^+$  and  $Na^+$  ions, on the other hand, interact with micellar head group more strongly than  $N^+(CH_3)_4$  ion for their small sizes, and consequently, the cmc values of  $NH_4$ -AOT and  $Na$ -AOT are low compared to  $N(CH_3)_4$ -AOT due to efficient charge screening of the head group. The values of standard thermodynamic parameters indicate spontaneity of micelle formation, and their order could be well explained in terms of bulkiness and nature of hydration of the counterion together with hydrophobic and electrostatic interactions. Characteristic temperature dependency of cmc is observed in almost all the systems with the appearance of a shallow minimum in each case. The striking steep fall of cmc's of  $N(CH_3)_4$ -AOT with temperature manifests in the large  $\Delta H_m^0$  values, which leads to low entropy changes. Loosely bound water dipoles with the  $N^+(CH_3)_4$  counterions may cause lower contribution of  $\Delta S_m^0$  to the aggregation process.

**Acknowledgement** Financial support from the University Grants Commission, New Delhi, India, under Special Assistance Program (SAP, No. F/540/6/DRS/2002) is gratefully acknowledged.

## References

- Yin H, Lei S, Zhu S, Huang J, Ye J (2006) *Chem Eur J* 12:2825
- Paul A, Griffiths PC, Pettersson E, Stilbs P, Bales BL, Zana R, Heenan RK (2004) *J Phys Chem B* 108:3810
- Griffiths PC, Paul A, Heenan RK, Penfold J, Ranganathan R, Bales BL (2005) *J Phys Chem B* 109:15775
- Benraou M, Bales BL, Zana R (2003) *J Phys Chem B* 107:13432
- Shimizu S, Pires PAR, El Seoud OA (2004) *Langmuir* 20:9551
- Pisárčik K, Devinsky F, Lacko I (2003) *Acta Facult Pherm Univ Comenianae* 50:119
- Tiddy GJT (1980) *Phys Rev* 57:1
- Khan A, Fontell K, Lindman B (1984) *J Colloid Interface Sci* 101:193
- Lindman B, Puyal M-C, Kamenka N, Rymden R, Stilbs P (1984) *J Phys Chem* 88:5048
- Mukerjee P (1967) *Adv Colloid Interface Sci* 1:241
- Corkill JM, Goodman JF (1962) *Trans Faraday Soc* 58:206
- Baumuller W, Hoffmann H, Ulbricht W, Tondre C, Zana R (1978) *J Colloid Interface Sci* 64:418
- Wang Y, Dubin PL, Zang H (2001) *Langmuir* 17:1670
- Oda R, Narayanan J, Hassan PA, Manohar C, Salkar RA, Kern F, Candau S (1998) *Langmuir* 14:4364
- Soldi V, Keiper J, Romsted LS, Cuccovia IM, Chaimovich H (2000) *Langmuir* 16:59
- Kawai T, Yasuda Y, Kon-no K (1995) *Bull Chem Soc Jpn* 68:2175
- Eastoe J, Roberson BH, Heenan RK (1993) *Langmuir* 9:2820
- Temsamani MB, Maeck M, Hassani IE, Hurwitz HD (1998) *J Phys Chem B* 102:3335
- Acosta E, Bisceglia M, Fernandez JC (2000) *Colloids Surf A* 161:417
- Moroni MA, Minardi RM, Schulz PC, Puig JE, Rodriguez JL (1998) *Colloid Polym. Sci.* 276:738
- Stokkeland I, Skauge A, Høiland H (1987) *J Soln Chem* 16:45
- Heuvelsland W, de Visser C, Somsen G (1978) *J Phys Chem* 82:29
- Nakagaki M, Handa T (1984) *ACS Symposium Series* 253:73
- Tanford C (1980) *The Hydrophobic Effect: Formation of Micelles and Biological Membranes*, vol. 2. Wiley, New York
- Chakraborty A, Chakraborty S, Saha SK (2007) *J Dispersion Sci Technol* 28:984
- La Mesa C (1990) *J Phys Chem* 94:323
- Suarez MJ, Lopez-Fontan JL, Sarmiento F, Mosquera V (1999) *Langmuir* 15:5265
- Myers D (1992) *Surfactant science and technology*. VCH, New York
- Zana R (1996) *Langmuir* 12:1208
- Mukhim T, Ismail K (2005) *J Surface Sci Technol* 21:113
- Su TJ, Lu JR, Thomas RK, Penfold J (1997) *J Phys Chem B* 101:937
- Weckström K, Hanu K, Rosenholm JB (1994) *J Chem Soc. Faraday Trans* 90:733
- Moroni A (1992) *Micelles: Theoretical and applied aspects*. Plenum, New York
- Evans DF, Ninham BW (1986) *J Phys Chem* 90:226
- Bedo Z, Berecz E, Laktos I (1992) *Colloid Polym Sci* 270:799
- González-Pérez A, Czapkiewicz J, Del Castillo JL, Rodríguez JR (2004) *Colloid Polym Sci* 282:1359
- Galán JJ, González-Pérez A, Rodríguez JR (2003) *J Therm Anal Cal* 72:465
- Shugihara G, Nakano TY, Sulthana SB, Rakshit AK (2001) *J Oleo Sci* 50:29
- Umlong IM, Ismail K (2005) *J Colloid Interface Sci* 291:529
- Rosen MJ, Cohen AW, Dahanayake M, Hua X (1982) *J Phys Chem* 86:541
- Oh SG, Shah DO (1993) *J Phys Chem* 97:284
- Carnero Ruiz C, Diaz-López L, Aguiar J (2007) *J Colloid Interface Sci* 305:293
- Sulthana SB, Bhat SGT, Rakshit AK (1997) *Langmuir* 13:4562
- Kang K, Kim H, Lim K (2000) *Colloids Surfaces A* 189:113

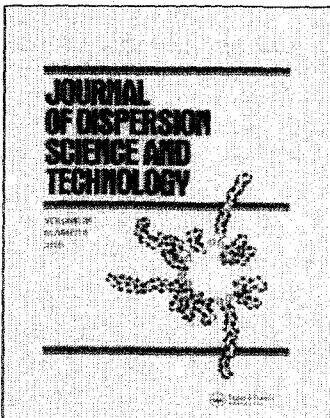
This article was downloaded by: [INFLIBNET India Order]

On: 23 January 2010

Access details: Access Details: [subscription number 909277354]

Publisher Taylor & Francis

Informa Ltd Registered in England and Wales Registered Number: 1072954 Registered office: Mortimer House, 37-41 Mortimer Street, London W1T 3JH, UK



## Journal of Dispersion Science and Technology

Publication details, including instructions for authors and subscription information:

<http://www.informaworld.com/smpp/title-content=t713597266>

### Surface and Bulk Properties of Dodecylbenzenesulphonate in Aqueous Medium: Role of the Nature of Counterions

Subrata Chakraborty <sup>a</sup>; Amitabha Chakraborty <sup>a</sup>; Moazzam Ali <sup>a</sup>; Swapan K. Saha <sup>a</sup>

<sup>a</sup> Department of Chemistry, University of North Bengal, Darjeeling, India

Online publication date: 19 January 2010

**To cite this Article** Chakraborty, Subrata, Chakraborty, Amitabha, Ali, Moazzam and Saha, Swapan K.(2010) 'Surface and Bulk Properties of Dodecylbenzenesulphonate in Aqueous Medium: Role of the Nature of Counterions', Journal of Dispersion Science and Technology, 31: 2, 209 -- 215

**To link to this Article:** DOI: 10.1080/01932690903110392

**URL:** <http://dx.doi.org/10.1080/01932690903110392>

PLEASE SCROLL DOWN FOR ARTICLE

Full terms and conditions of use: <http://www.informaworld.com/terms-and-conditions-of-access.pdf>

This article may be used for research, teaching and private study purposes. Any substantial or systematic reproduction, re-distribution, re-selling, loan or sub-licensing, systematic supply or distribution in any form to anyone is expressly forbidden.

The publisher does not give any warranty express or implied or make any representation that the contents will be complete or accurate or up to date. The accuracy of any instructions, formulae and drug doses should be independently verified with primary sources. The publisher shall not be liable for any loss, actions, claims, proceedings, demand or costs or damages whatsoever or howsoever caused arising directly or indirectly in connection with or arising out of the use of this material.

# Surface and Bulk Properties of Dodecylbenzenesulphonate in Aqueous Medium: Role of the Nature of Counterions

Subrata Chakraborty, Amitabha Chakraborty, Moazzam Ali,  
and Swapan K. Saha

Department of Chemistry, University of North Bengal, Darjeeling, India

The lithium, potassium, and ammonium salts of dodecylbenzenesulphonic acid have been prepared from the pure sodium salt by applying ion-exchange technique. The critical micellization concentrations (CMC) of the surfactants with four different counterions have been determined in a temperature range of 10°C to 40°C using surface tension as well as electrical conductivity measurements. The counterion ionization constant,  $\alpha$ , and various thermodynamic parameters of micellization viz.  $\Delta G_m^0$ ,  $\Delta H_m^0$ ,  $\Delta S_m^0$ ,  $\Delta_{mic} C_m^0$  along with the surface parameters ( $\Gamma_{max}$ ,  $A_{min}$ ) in aqueous media have been determined. The CMC value of dodecylbenzenesulphonate (DBS) having different counterions followed the order  $Na^+ > Li^+ > NH_4^+ > K^+$ . While large negative free energy change ( $\Delta G_m^0$ ) and the positive entropy change ( $\Delta S_m^0$ ) favor the micellization process thermodynamically, nature of their variation with counterion supports the importance of hydrated counterion size factor in micellization process via a change in the hydrophilicity of surfactant head group along with the structure of branched chain of hydrocarbon tail.

**Keywords** Counterion, critical micelle concentration, dodecylbenzenesulphonate, thermodynamic parameters

## INTRODUCTION

Amphiphilic systems involving surfactants have generated great interest due to their wide-ranging applications especially in detergent and pharmaceutical industries, food technology and petroleum recovery processes.<sup>[1–3]</sup> The functions and properties of surfactants in water are interesting because they form organized assemblies of various types, for example, micelles and bilayer lamellae<sup>[4,5]</sup> depending on their concentration and composition in addition to environmental conditions such as pH, temperature, pressure, and presence and absence of additives. Favorable polarity of the solvent often leads to formation of reverse micelles as well.<sup>[3]</sup> The effect of increasing temperature on the solubilizing capacity of surfactant solutions is related to the corresponding effects on the properties of the micellar aggregate and the partition coefficient of the solute into aggregate.<sup>[6]</sup> When a surfactant is dissolved in a solvent, it disrupts the interactions between the solvent molecules distorting the structure of the solvent and thus increases the free energy

of the system. The distortion of the solvent structure can be decreased by the aggregation of the surface-active species into clusters (micelles) with their hydrophobic groups directed toward the interior of the micelle and the hydrophilic groups towards the solvent. Micellization can thus be considered as a mechanism alternative to adsorption at the interfaces for removing hydrophobic groups from contact with the solvent. The energetics of adsorption and micelle formation are usually discussed in terms of the dispersion, attractions between the hydrocarbon chains, the electrostatic and van der Waals interactions between the head groups, and the hydrophobic interaction between hydrocarbon chains and water molecules. Even the molecular conformation of some dimeric surfactants affects the micellization to a large extent.<sup>[6]</sup> It has generally been accepted that a fraction,  $\alpha$ , of the counterions of an ionic surfactant are dissociated from the micelles, leaving the micelles charged.<sup>[8,9]</sup> In addition, a number of recent studies<sup>[7,10–14]</sup> show that the changes in hydration energies and specific interactions with counterions may also be important. The formation of an ionic micelle from monomeric ions results in a balance between hydrophobic interactions between the hydrophobic part of the micelle-forming ions, electrostatic interactions between their hydrophilic charged parts, as well as with and between the counterions. It is also evident that the aggregation number of ionic micelles, at a constant temperature, depends only on the concentration of counterions,  $C_{aq}$  in the aqueous

Received 27 September 2008; accepted 11 November 2008.

Financial support from the University Grants Commission, New Delhi, India, under Special Assistance Program (SAP, No. F/540/6/DRS/2002) is gratefully acknowledged.

Address correspondence to Swapan K. Saha, Department of Chemistry, University of North Bengal, Darjeeling 734 013, India. E-mail: ssahanbu@hotmail.com

phase.<sup>[15]</sup> Ionic micelles grow in response to increase in the value of whether the counterions are provided by the surfactant alone or by the surfactant plus any added electrolyte.<sup>[15]</sup> Thus  $C_{aq}$  can be written as<sup>[10]</sup>

$$C_{aq} = F(S_t)[\alpha S_t + (1 - \alpha)S_m], \quad [1]$$

where  $S_m$  and  $S_t$  are the monomeric and the total concentration of the surfactant, respectively. The factor  $F(S_t) = 1/(1 - \theta)$ , where  $\theta$  is related to the volume fraction occupied by the micelles.

The study of the effect of temperature on micellization provides information on the relative characterization of surfactant solutions. This information is most readily obtained from the thermodynamic parameters of micelle formation, viz., changes in standard Gibbs free energy ( $\Delta G_m^0$ ), enthalpy ( $\Delta H_m^0$ ), and the entropy ( $\Delta S_m^0$ ) that quantify the relative importance of hydrophobic and electrostatic interactions. It is also necessary to note that the knowledge of complete thermodynamic characterization is important for proper understanding of micellization process.

This article is a part of a series<sup>[12,14]</sup> that deals with the effect of the nature of the counterion of anionic surfactants on their self-association behavior and micellar properties of anionic micelles. It is observed that the accessibility of the counterion to the head group of the amphiphile influences CMC along with other thermodynamic parameters in a fascinating way.<sup>[10,12,14-17]</sup> Sodium dodecylbenzenesulphonate (SDBS), a well-known anionic surfactant has attracted researches during the past few years.<sup>[18-22]</sup> This work is concerned with dodecylbenzenesulphonate (DBS) micelles with a view to investigate the effect of a series of counterions, such as  $Li^+$ ,  $Na^+$ ,  $K^+$  and  $NH_4^+$  on the micellization of DBS. It may be mentioned that the CMC and thermodynamic parameters of the DBS having different counterions have not yet been reported in the literature. Therefore, the present aim is to determine the CMC of DBS with different counterions within the temperature range of 10°C to 40°C and to determine the relevant thermodynamic parameters of micellization, such as  $\Delta G_m^0$ ,  $\Delta H_m^0$ ,  $\Delta S_m^0$ ,  $\Delta_{mic}C_p^0$  along with the maximum surface excess concentration ( $\Gamma_{max}$ ), and the minimum areas per molecule ( $A_{min}$ ) at the surface as a function of hydrated counterion size.

## EXPERIMENTAL

### Materials

Surfactants with the desired counterions were prepared from a sample of purified SDBS by ion-exchange as described elsewhere.<sup>[12,14]</sup> SDBS sample is dissolved in mixture of a 1:1 (v/v) water and ethanol. The solution was passed slowly through a column (40 cm × 2 sq. cm) of

a strong ion exchanger in the  $H^+$  form. The free sulphonic acid formed on passing the aqueous DBS ( $Na^+$  salt) solution through the resin was then immediately neutralized with an aqueous solution of the hydroxides of the desired counterions (viz.  $Li^+$ ,  $K^+$ ,  $NH_4^+$ ). All the hydroxides required for the respective ion exchange experiment were of AR grade and procured from Fluka, Switzerland and Merck, India. The solvent water was then removed fast by freeze drying and then keeping under vacuum (bath temperature 313 K) for several days and the waxy solid was finally dried in vacuum over  $P_2O_5$ . The residual water of the sample was finally removed by the action of  $P_2O_5$  (from Loba Cheme, India) on a solution of surfactant in isooctane ( $\geq 99.5\%$  from Merck, India). Controlling the flow rate of the solution through the ion exchange column had optimized the extent of  $Na^+/H^+$  ion exchange and  $H^+$  content of the surfactant solution (acid form) was measured by titrating with standard NaOH to determine the extent of exchange. The extent of exchange was found to be more than 99%. Doubly distilled water having conductivity  $2 \mu S cm^{-1}$  was used throughout experiment.

Commercial SDBS may contain five different isomers viz.  $2\phi C_{12}$ ,  $3\phi C_{12}$ ,  $4\phi C_{12}$ ,  $5\phi C_{12}$  and  $6\phi C_{12}$  depending upon the number of carbon atoms in the branched chain.<sup>[20]</sup> However the supplier of the product which was used in the present study (sodium dodecylbenzenesulphonate, 88%; Acros, USA, product code 325912500) did not mention the isomeric identification of their product. While the separation of isomers from their mixtures and their identification are difficult, the CMC and other parameters indicate the presence of  $6\phi C_{12}$  as the major component of the present surfactant system. Further, the recrystallised product of SDBS was subjected to ion exchange treatment in order to prepare surfactant with different counterions, followed by repeated recrystallization to ensure adequate purification. Therefore, it may be argued that the major component of each of SDBS, LDBS, ADBS and PDBS was essentially  $6\phi C_{12}$  isomers as shown in Figure 1.<sup>[39]</sup>

### Methods

The CMC and other thermodynamic parameters were determined from the surface tension as well as specific conductance data. The surface tension experiments were done by a calibrated Tensiometer (K9, KRÜSS; Germany), to measure the surface tension at the air/water interface of the solution by the platinum ring detachment method at

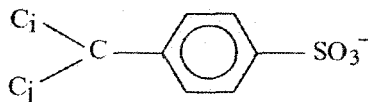


FIG. 1. Structure of DBS ( $6\phi C_{12}$  isomer) where  $i = 5$ ,  $j = 6$ .

different temperatures. The ring was cleaned by washing with doubly distilled water followed by burning in an alcohol flame. Solutions of known concentration were progressively diluted in water solutions. The accuracy of the measurement was within  $\pm 0.1 \text{ mNm}^{-1}$ . Temperature of the system was maintained by circulating auto-thermostated water through a double-wall glass vessel containing the solution to keep the temperature constant within  $\pm 0.1 \text{ K}$ . Similar studies were also done conductometrically by using an electrical conductivity bridge (METTLER TOLEDO, Switzerland). The conductance values were uncertain within the limit of  $\pm 1\%$ . Each measurement was repeated several times at each temperature in the range of  $10^\circ\text{C}$  to  $40^\circ\text{C}$ . Measurements were made at  $5^\circ\text{C}$  intervals of temperature.

## RESULTS AND DISCUSSION

Figures 2 and 3 illustrate the typical representative plots obtained by measuring conductance and surface tension, respectively, for the surfactant containing a particular type of counterion at various temperatures. Two linear fragments of each curve with different slopes correspond to premicellar and postmicellar region respectively, where the break point identifies the CMC. The CMC values determined by potentiometrically and conductometrically for each counterion are in close agreement with one another.

Table 1 bears the CMC values of the present surfactant systems along with the surface parameters. Similar to previous observations<sup>[12,14]</sup> we measure CMC, corresponds to a concentration at which a very small but often clearly detectable concentration of the micelles exists. A critical examination of Table 1 shows that in all instances the change of CMC with temperature is small. But, at a certain

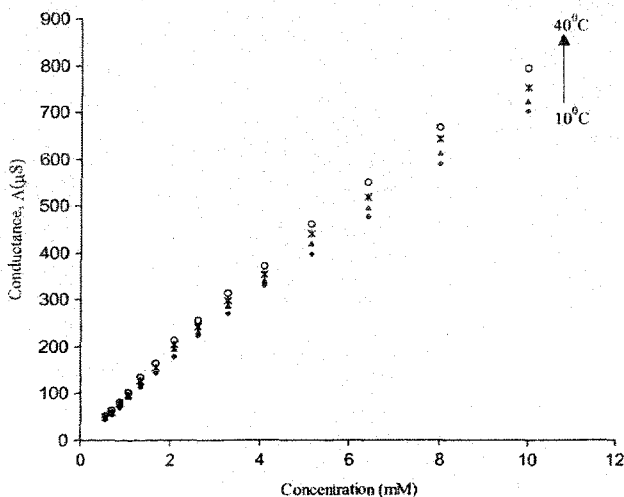


FIG. 2. Conductance,  $\Lambda$ , of LDBS in aqueous solution as a function of the surfactant concentration (M) at  $10^\circ\text{C}$ ,  $20^\circ\text{C}$ ,  $30^\circ\text{C}$ ,  $40^\circ\text{C}$ .

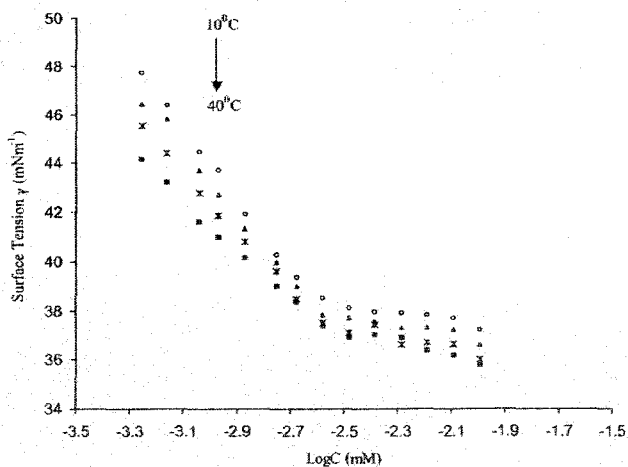


FIG. 3. Surface tension,  $\gamma$ , of LDBS in aqueous solution as a function of the logarithm of the surfactant concentration (M) at  $10^\circ\text{C}$ ,  $20^\circ\text{C}$ ,  $30^\circ\text{C}$ ,  $40^\circ\text{C}$ .

temperature, CMC of DBS depends upon the nature of the counterion following the order  $\text{Na}^+ > \text{Li}^+ > \text{NH}_4^+ > \text{K}^+$ . It is apparent that the hydrodynamic radii along with the accessibility of the counterion toward the head group of the amphiphile play an important role in micellization. However, the experimental CMCs of DBS do not follow the trend of a previous observation of counterion accessibility to AOT (Bis (2-ethylhexyl) sulfosuccinate, sodium salt) head groups.<sup>[12]</sup> This deviation may be due to the special double strand structure of bis (2-ethylhexyl) sulfosuccinate ion. Unlike present surfactant systems, AOT offers a different hydrophobic environment along with the orientation of associated water molecules during cluster formation. It has also been reported<sup>[23]</sup> that  $\text{NH}_4^+$  binds more strongly to dodecylsulfate head group compared to  $\text{Na}^+$  and reduces the electrostatic intermicellar repulsive force. This leads micellization to occur in lower concentrations and for anionic surfactant, dodecylsulfate having different counterions, CMC follows the order  $\text{Li}^+ > \text{Na}^+ > \text{NH}_4^+$ . However in the present case of dodecylbenzenesulphonate there is a branched carbon chain in the molecular structure of the anion. Though the actual nature of dependency of hydrophobic tail on the interaction of the hydrated counterions is not still well understood, it can be said that, "branched chain molecular structure" of DBS makes the environment around more hydrophobic in nature, where  $\text{Li}^+$  along with its large hydrated volume binds more readily than that of  $\text{Na}^+$  with the hydrophilic head. But  $\text{NH}_4^+$ , which has the lowest hydration number<sup>[11]</sup> shows anomalous behavior toward its accessibility to the head group. It was also reported<sup>[24]</sup> that the binding tendency of alkali metal cation to polyethyleneoxide (PEO) follows the order  $\text{K}^+ > \text{Cs}^+ > \text{Na}^+$ . However, among the

TABLE 1  
Temperature dependence of CMC, maximum surface excess concentration ( $\Gamma_{\max}$ ) and minimum areas per molecule ( $A_{\min}$ ) of different DBS surfactants

Counterion of DBS	Temp./°C	CMC mol dm <sup>-3</sup> × 10 <sup>3</sup>	$\Gamma_{\max}$ /mol cm <sup>-2</sup> × 10 <sup>6</sup>	$A_{\min}$ /nm <sup>2</sup>
Li <sup>+</sup>	10	2.50 (2.41)	3.10	0.54
	15	2.60 (2.54)	2.98	0.57
	20	2.83 (2.76)	3.18	0.52
	25	2.82 (2.80)	3.22	0.52
	30	2.79 (2.84)	3.22	0.51
	35	2.91 (2.90)	3.27	0.51
Na <sup>+</sup>	10	2.82 (2.77)	2.99	0.56
	15	2.91 (2.86)	3.16	0.53
	20	2.98 (2.95)	3.21	0.52
	25	3.10 (3.13)	3.25	0.51
	30	3.21 (3.20)	3.27	0.51
	35	3.27 (3.31)	3.27	0.50
K <sup>+</sup>	10	2.11 (2.14)	3.40	0.49
	15	2.18 (2.19)	3.46	0.48
	20	2.25 (2.24)	3.52	0.47
	25	2.38 (2.32)	3.55	0.47
	30	2.42 (2.41)	3.54	0.47
	35	2.50 (2.52)	3.58	0.46
NH <sub>4</sub> <sup>+</sup>	10	2.28 (2.23)	3.12	0.53
	15	2.39 (2.36)	3.17	0.52
	20	2.41 (2.40)	3.23	0.51
	25	2.52 (2.48)	3.28	0.51
	30	2.68 (2.62)	3.38	0.49
	35	2.81 (2.82)	3.41	0.49
	40	2.80 (2.82)	3.49	0.47

The values in the parenthesis represent CMC determined from surface tension measurements.

all four ions, K<sup>+</sup> binds most strongly to DBS resulting in the lowest CMC at a particular temperature.

Figure 4 represents the variation of CMC with temperature for DBS containing different counterions. While most of the surfactants display a typical U-shaped curve when CMC is plotted against temperature, in the present DBS systems, having Na<sup>+</sup> and K<sup>+</sup> counterion, CMC increases almost linearly with temperature. But for the other two counterions, viz., Li<sup>+</sup> and NH<sub>4</sub><sup>+</sup>, instead of linearity CMC changes rather irregularly with temperature. Although this type of temperature dependency is not common, such a temperature dependency for anionic surfactant was previously observed by a number of workers<sup>[25]</sup> and can be explained by considering two opposite

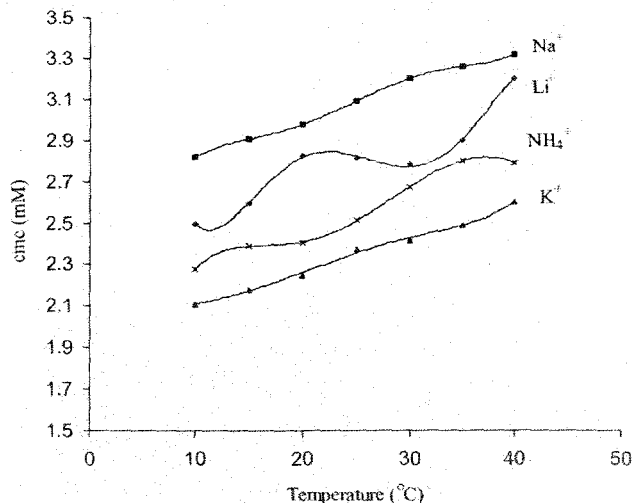


FIG. 4. Variation of CMC with temperature of DBS having different counter cation (viz. Na<sup>+</sup>, Li<sup>+</sup>, K<sup>+</sup>, NH<sub>4</sub><sup>+</sup>).

effects.<sup>[14]</sup> As the temperature increases, the degree of hydration of hydrophilic group decreases and this favors the formation of micelles more readily. On the other hand, as the temperature is increased above a certain temperature ( $T_{\min}$ ), a disruption of water cluster is brought about, and this facilitates solubilization of the surfactant monomers resulting in the increase of CMC. It appears from Figure 4 and Table 1 that the second effect is predominant for DBS micelles in the temperature range studied.

#### Thermodynamic Parameters

The temperature dependency of DBS micelles having different counterions also enables one to determine the thermodynamic parameters of micellization. According to the pseudo-phase separation model<sup>[26-28]</sup> the standard Gibbs free energy of micellization,  $\Delta G_m^0$  ionic uni-univalent surfactant can be expressed as:

$$\Delta G_m^0 = (2 - \alpha)RT \ln X_{cmc} \quad [2]$$

Here  $X_{\text{CMC}}$  is the CMC expressed in mole fraction scale and  $\alpha$ , the ionization degree or counterionic ionization constant of the micelle, can be expressed by  $\alpha = p/n$ , where  $p$  and  $n$  are the effective charge and the aggregation number of the micelle respectively. It is well known that the value of  $\alpha$  can be determined from the ratio of the slope of the two linear fragments of conductivity-concentration plot above and below CMC.<sup>[29,30]</sup>

The standard enthalpy change,  $\Delta H_m^0$  can be obtained from Gibbs-Helmholtz equation.<sup>[19]</sup>

$$\Delta H_m^0 = -RT^2 \left[ (2 - \alpha) \left( \frac{\partial \ln X_{cmc}}{\partial T} \right)_p - \ln X_{cmc} \left( \frac{\partial (2 - \alpha)}{\partial T} \right)_p \right] \quad [3]$$

However, as the variation of  $\alpha$  with temperature is not well defined due to polydispersity of micelle and does not follow any general trend,<sup>[31,32]</sup> it is difficult to estimate the second term in the parenthesis experimentally. The term, however, is small in comparison with the first one, and therefore, to gain qualitative information regarding the thermodynamics we neglect the second term of the Equation (3), and the expression now becomes:

$$\Delta H_m^0 = -(2 - \alpha)RT^2(\partial \ln X_{cmc}/\partial T)_P \quad [4]$$

The enthalpy of micellization may be obtained if the dependence of the CMC on temperature is known. The  $\Delta S_m^0$  and  $\Delta_{mic}C_p^0$  are also determined as essential thermodynamic parameters from the common expressions

$$\Delta S_m^0 = (\Delta H_m^0 - \Delta G_m^0)/T \quad [5]$$

$$\Delta_{mic}C_p^0 = (\partial \Delta H_m^0/\partial T)_P \quad [6]$$

The various thermodynamic quantities associated with micellization are reported in Table 2. The quantities calculated in the present method are seen to vary with temperature and also with the nature of the associated counterions. Negative sign of  $\Delta H_m^0$  suggests that surfactant aggregation is an endothermic process. The variation of the standard thermodynamic parameters with different counterions at a certain temperature can also be explained by the size and the hydration of the counterion as has been already discussed. Different researchers<sup>[33,34]</sup> often attempted to represent the thermodynamic variables of micellization into additive contribution of two factors: (1) interaction between hydrocarbon chains with water and (2) interactions between head groups, counterions and surfaces. It is, therefore, logical to suppose that only the

TABLE 2  
Different thermodynamic parameters (viz. changes in standard Gibbs free energy,  $\Delta G_m^0$ , standard enthalpy,  $\Delta H_m^0$ , standard entropy,  $\Delta S_m^0$ , standard heat capacity,  $\Delta_{mic}C_p^0$ ) of micellization

Counterions of different DBS surfactants	Temp./°C	$-\Delta G_m^0/$ (kJ mol <sup>-1</sup> )	$-\Delta H_m^0/$ (kJ mol <sup>-1</sup> )	$\Delta S_m^0/$ (J mol <sup>-1</sup> )	$-\Delta C_{pm}^0/$ (J mol <sup>-1</sup> K <sup>-1</sup> )
Li <sup>+</sup>	10	32.4	5.7	94.3	409
	15	31.3	7.2	83.7	480
	20	30.8	10.1	70.6	551
	25	31.1	12.9	61.1	622
	30	31.5	17.7	45.5	693
	35	31.5	20.8	34.7	764
	40	30.7	24.3	20.4	835
Na <sup>+</sup>	10	32.3	7.8	86.6	382
	15	32.0	9.0	79.9	474
	20	31.8	12.2	66.9	566
	25	32.5	14.9	59.1	658
	30	31.0	19.0	39.6	750
	35	31.0	22.9	26.3	842
	40	31.1	26.7	14.0	934
K <sup>+</sup>	10	31.2	2.1	102.8	127
	15	31.7	2.6	101.0	117
	20	32.2	3.1	99.3	107
	25	32.3	4.4	93.6	97
	30	33.0	4.7	93.4	87
	35	33.1	5.2	90.6	77
	40	33.8	5.7	89.8	67
NH <sub>4</sub> <sup>+</sup>	10	39.9	6.3	118.7	405
	15	30.3	7.7	78.5	488
	20	31.0	11.1	67.9	571
	25	31.3	13.2	60.7	654
	30	30.5	18.0	41.2	737
	35	32.0	21.1	35.4	820
	40	32.6	25.2	23.6	903

second factor is important for the present work where SDBS, LDBS, ADBS, and PDBS having different counterions form micelles. A close look on the thermodynamic parameters support the view that in order to form micelle the gain in entropy is the major factor leading to negative change in Gibbs free energy.<sup>[35-37]</sup> But the fact that though the free energy changes are not very different, the entropy change is significantly higher and the enthalpy changes are much lower for  $K^+$  counterion containing DBS compared to all other systems. This suggests that the entropy contributes as major driving force in micellization. Less hydration and higher binding capacity of  $K^+$  ion may cause higher contribution of  $\Delta S_m^0$  in aggregation process. With increasing temperature,  $\Delta S_m^0$  decreases systematically for a particular type of counterion, suggesting a disruption of ordered arrangement of water dipoles around the amphiphilic part of the surfactant molecules. The effective interaction associated with hydrocarbon chains may be expressed by standard heat capacity of micelle formation,  $\Delta_{mic}C_p^0$ . In both surfactant systems, the standard heat capacity changes linearly with temperature (Figure 5). The calculated values of  $\Delta_{mic}C_p^0$  for SDBS fall between a wide range of value viz.,  $-381.8$  to  $-933.8 \text{ Jmol}^{-1} \text{ K}^{-1}$  for the variation of temperature between  $10^\circ\text{C}$  and  $40^\circ\text{C}$ . On the other hand, SDS which also contains a dodecyl moiety yields  $\Delta_{mic}C_p^0$  values between  $-607$  and  $-644 \text{ Jmol}^{-1} \text{ K}^{-1}$  within the identical temperature range.<sup>[19]</sup> For all the counterions except  $K^+$ ,  $\Delta_{mic}C_p^0$  do not change significantly at lower temperatures ( $<25^\circ\text{C}$ ) but at higher temperatures,  $\Delta_{mic}C_p^0$  values follows the order  $\text{Na}^+ > \text{NH}_4^+ > \text{Li}^+ > \text{K}^+$ . Potassium ion, however, shows anomalous behavior which may be due to its strong tendency for ion-pair formation. Compared to that of SDS,<sup>[18]</sup> the wider variation of the specific heat capacity as a function of temperature of the present system must

be connected with the enhanced hydrophobicity due to the presence of the aromatic ring in the hydrocarbon tail of the present surfactant systems. On the other hand, counterion binding also reduces the number of water molecules in the solvation shell of the counterion as well as the negatively charged head groups of DBS. At high temperatures,  $\Delta_{mic}C_p^0$  give large negative values due to solvation of ions upon demicellization, and this is quite reasonable because as the temperature is increased CMC value also increases in all the present systems. The negative value of  $\Delta_{mic}C_p^0$  is proportional to the maximum surface excess ( $\Gamma_{max}$ ), which has been calculated following the expressions,<sup>[12,14]</sup>

$$\Gamma_{max} = (1/2.303n'RT)(-\partial\gamma/\partial\log C) \quad [7]$$

and,

$$A_{min} = 1/(NT) \quad [8]$$

where  $\gamma$  expresses the surface tension,  $N$  is the Avogadro number,  $C$  and  $n'$  are the concentration and number particles per molecule of the surfactant respectively. For a uni-univalent surfactant,  $n'$  is therefore taken as 2.  $A_{min}$  is the minimum area per molecule in the aqueous-air interface. With increasing temperature, amphiphile tends to form a closely packed monolayer film of the hydrocarbon chain at the air/aqueous solution interface owing to the decreased repulsion between the oriented head groups. This is supported by the greater  $\Gamma_{CMC}$  value (and thereby, the smaller  $A_{CMC}$  value) of the longer chain analogue.<sup>[40]</sup> However, Table 1 suggests that at a fixed temperature,  $\Gamma_{max}$  changes with the nature of counterions following the order  $\text{K}^+ > \text{NH}_4^+ > \text{Na}^+ > \text{Li}^+$ . This observation is probably associated with the hydration of DBS and the accessibility of head groups towards the counterions.  $\Gamma_{max}$  value slightly decreases with the rise of temperature and this is well known for both nonionic<sup>[37]</sup> and anionic<sup>[38]</sup> surfactants.

## CONCLUSION

The hydrodynamic size and binding capacity of the counterions to the head group along with the branching of hydrophobic chain play important roles in the process of surfactant aggregation. Critical micelle concentration (CMC) and enthalpy of micellization ( $\Delta H_m^0$ ) decreases in the order  $\text{Na}^+ > \text{Li}^+ > \text{NH}_4^+ > \text{K}^+$  at a given temperature and this may be well supported by the hydration and accessibility of the counterions to the head group of the amphiphile, dodecylbenzenesulphonate. The use of pseudo-phase separation model on the counterion binding shows that the variation of enthalpy and entropy of micellization compensate each other and the free energy,  $\Delta G_m^0$  is only slightly dependant on counterions and the temperature. Effective interaction associated with hydrocarbon chain can be well explained by  $\Delta_{mic}C_p^0$ , considering the aromatic

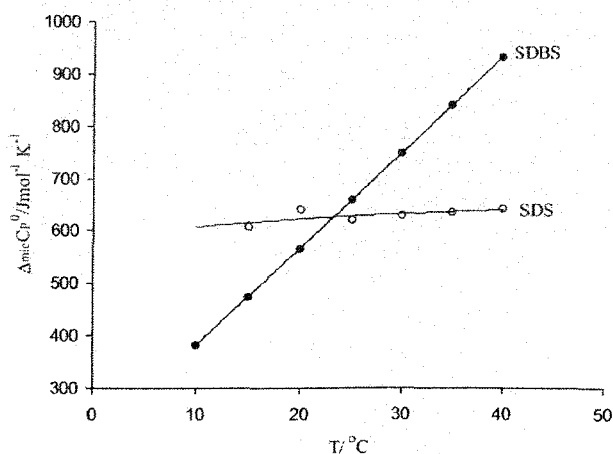


FIG. 5. Variation of standard heat capacity of micelle formation,  $\Delta_{mic}C_p^0$  as a function of temperature for SDBS and SDS.<sup>[19]</sup>

ring of SDBS and this may be compared to SDS which also contains a dodecyl moiety.<sup>[19]</sup>

## REFERENCES

- [1] Evans, D.F. and Wennerstrom, H. (1994) *The Colloidal Domain Where Physics, Chemistry, Biology and Technology Meet*; New York.
- [2] Shah, D.O. (1991) *Surface Phenomena in Enhanced Oil Recovery*; New York: Plenum Press.
- [3] Moulik, S.P. (1996) *Current Sci.*, 71: 368–376.
- [4] Saha, S.K., Jha, M., Ali, M., Chakraborty, A., Bit, G., and Das, S.K. (2008) *J. Phys. Chem. B*, 112: 4642–4647.
- [5] Yin, H., Lei, S., Zhu, S., Huang, J., and Ye, J. (2006) *Chem. Eur. J.*, 12: 2825–2835.
- [6] Yalkowsky, S.H. (1999) *Solubility and Solubilization in Aqueous Media*; New York: Oxford University Press.
- [7] Pisárčik, K., Devínsky, F., and Lacko, I. (2003) *Acta Facult. Pharm. Univ. Comeniana.*, 50: 119–131.
- [8] Bunton, C.A., Nome, F., Quina, F.H., and Romsted, L.S. (1991) *Acc. Chem. Res.*, 24: 357–364.
- [9] Jönsson, B., Lindman, B., Holmberg, K., and Kronberg, B. (1998) *Surfactants and Polymers in Aqueous Solution*; Chichester, UK: John Wiley.
- [10] Griffiths, P.C., Paul, A., Heenan, R.K., Penfold, J., Ranganathan, R., and Bales, B.L. (2004) *J. Phys. Chem. B*, 108: 3810–3816.
- [11] Paul, A., Griffiths, P.C., Pettersson, E., Stilbs, P., Bales, B.L., Zana, R., and Heenan, R.K. (2005) *J. Phys. Chem. B*, 109: 15775–15779.
- [12] Chakraborty, A., Chakraborty, S., and Saha, S.K. (2007) *J. Dispersion Sci. Technol.*, 28: 984–989.
- [13] Shimizu, S., Pires, P.A.R., and El Seoud, O.A. (2004) *Langmuir*, 20: 9551–9559.
- [14] Chakraborty, A., Saha, S.K., and Chakraborty, S. (2008) *Colloid Polym. Sci.*, 286: 927–934.
- [15] Bales, B.L.A. (2001) *J. Phys. Chem. B*, 105: 6798–6804.
- [16] Lah, J., Bester-Rogac, M., Perger, T.-M., and Vesnaver, G. (2006) *J. Phys. Chem. B*, 110: 23279–23291.
- [17] Benraou, M., Bales, B.L., and Zana, R. (2003) *J. Phys. Chem. B*, 107: 13432–13440.
- [18] Yi, H. and Huang, W. (2007) *Colloids Surf. B*, 58: 237–241.
- [19] Chatterjee, A., Moulik, S.P., Sanyal, S.K., Mishra, B.K., and Puri, P.M. (2001) *J. Phys. Chem. B*, 105: 12823–12831.
- [20] Hait, S.K., Majhi, P.R., Blume, A., and Moulik, S.P. (2003) *J. Phys. Chem. B*, 107: 3650–3658.
- [21] Šegota, S., Heimer, S., and Težak, D. (2006) *Colloids Surf. A*, 274: 91–99.
- [22] Basu Ray, G., Chakraborty, I., Ghosh, S., and Moulik, S.P. (2007) *Colloid Polym. Sci.*, 285: 457–469.
- [23] Dubin, P.L., Gruber, J.H., Xia, J., and Zhang, H. (1992) *J. Colloid Interface Sci.*, 148: 35–41.
- [24] Chaput, G., Jeminet, G., and Juillard, J. (1975) *Can. J. Chem.*, 53: 2240–2246.
- [25] Yamabe, T. and Moroi, Y. (1999) *Colloid Interface Sci.*, 215: 58–63.
- [26] Zana, R. (1996) *Langmuir*, 12: 1208–1211.
- [27] González-Pérez, A., Czapkiewicz, J., Del Castillo, J.L., and Rodriguez, J.R. (2004) *Colloid Polym. Sci.*, 282: 1359–1364.
- [28] Kim, H.-U. and Lim, K.-H. (2004) *Colloids Surf. A*, 235: 121–128.
- [29] Mukhim, T. and Ismail, K. (2005) *J. Surface Sci. Technol.*, 21: 113–127.
- [30] Perger, T.-M. and Bešter-Rogač, M. (2007) *J. Colloid Interface Sci.*, 313: 288–295.
- [31] Kang, K., Kim, H., and Lim, K. (2000) *Colloids Surf. A*, 189: 113–121.
- [32] Vautier-Giongo, C. and Bales, B.L. (2003) *J. Phys. Chem. B*, 107: 5398–5403.
- [33] Rodríguez, A., Muñoz, M., Graciani, M.M., and Moyá, M.L. (2006) *J. Colloid Interface Sci.*, 298: 942–951.
- [34] Weckström, K., Hanu, K., and Rosenholm, J.B. (1994) *J. Chem. Soc., Faraday Trans.*, 90: 733–738.
- [35] Ninham, B.W., Evans, D.F., and Wei, G.J. (1983) *J. Phys. Chem.*, 87: 5025.
- [36] Morori, A. (1992) *Micelles: Theoretical and Applied Aspects*; New York: Plenum Press.
- [37] Rosen, M.J., Cohen, A.W., Dahanayake, M., and Hua, X.Y. (1982) *J. Phys. Chem.*, 86: 541–545.
- [38] Oh, S.G. and Shah, D.O. (1993) *J. Phys. Chem.*, 97: 284–286.
- [39] van Os, N.M., Daane, D.J., and Haandrikman, G. (1991) *J. Colloid Interface Sci.*, 141: 199–217.
- [40] Clint, J.H. (1992) *Surfactant Aggregation*; New York: Blackie, Chapman and Hall.

CrossMark  
click for updatesCite this: *RSC Adv.*, 2014, 4, 32579

## Tuning of physico-chemical characteristics of charged micelles by controlling head group interactions *via* hydrophobically and sterically modified counter ions†

Subrata Chakraborty, Amitabha Chakraborty and Swapan K. Saha\*

Different tetraalkylammoniums, *viz.*,  $N^+(CH_3)_4$ ,  $N^+(C_2H_5)_4$ ,  $N^+(C_3H_7)_4$ ,  $N^+(C_4H_9)_4$  along with simple ammonium salts of dodecylbenzene sulphonic acid were prepared by an ion-exchange technique. The cmcs of dodecylbenzene sulfonate salts with various counterions were determined by electrical conductivity and surface tension measurements within the temperature range 283–313 K. The counterion ionization constant,  $\alpha$ , the surface parameters  $\Gamma_{max}$  and  $A_{min}$  and also the thermodynamic parameters of the micellization process, *viz.*,  $\Delta G_m^0$ ,  $\Delta H_m^0$  and  $\Delta S_m^0$  in aqueous solution have been determined by using a pseudo-phase model. The order of cmcs in aqueous solution is found to be  $NH_4^+ > N^+(CH_3)_4 > N^+(C_2H_5)_4 > N^+(C_3H_7)_4 > N^+(C_4H_9)_4$  at any given temperature. On the other hand, the aggregation number increases with alkyl chain length first due to increasing hydrophobic interactions and then decreases as a function of counterion size passing through a maximum for  $N^+(C_2H_5)_4$ . Spontaneity of micellization in aqueous solution is supported by large negative  $\Delta G_m^0$  as well as the positive entropy change for the micellization process for all the above counterions. At a given temperature,  $\Delta G_m^0$  for a surfactant with different counterions followed the order  $N^+(CH_3)_4 > NH_4^+ > N^+(C_2H_5)_4 > N^+(C_3H_7)_4 > N^+(C_4H_9)_4$ . Electrostatic interaction along with effective charge screening and hydrophobicity of the surfactant head group together may give an explanation for the observed variation of aggregation behaviour and the energetics as a function of the nature of the counterion.

Received 29th April 2014  
Accepted 14th July 2014

DOI: 10.1039/c4ra03937h

www.rsc.org/advances

## Introduction

Surfactants form aggregates, particularly in aqueous solutions, *via* hydrophobic and hydrophilic interactions occurring within the same molecule. These exotic molecules have generated a great deal of interests because of their various industrial applications.<sup>1–9</sup> While the formation of micelles is the consequence of interplay between hydrophobic and hydrophilic parts of the surfactant molecules with water, it is mainly triggered to avoid loss of entropy due to the formation of ordered water cages around hydrophobic part disrupting the hydrogen bonds between water molecules. There are many factors which influence critical micelle concentration (cmc), size, shape and the aggregation number of ionic micelles. These factors include temperature, geometrical structure of the surfactant molecule, the length of the hydrocarbon tail, the nature and dimension of the surfactant head group, the polarity and other characteristics of the solvent including solvent structure, ionic strength of the

medium and finally the nature of the counter ions. Among these factors, the surfactant head group characteristics, including the counter ion interactions, is perhaps the least studied facet, yet one of the pivotal issues which control the shape and size of the micellar aggregate. Strong binding counter ions favorably influence aggregate formation and decrease the cmc *via* effective charge screening of the head groups. However, the counter ion which contains fairly strong hydrophobic groups (hydro-tropes) are particularly much effective in charge screening and increase the aggregation number to a great extent and promotes micellar shape transition *via* altering micellar surface curvature. These hydro-tropes (*e.g.*, sodium salicylate) efficiently interact with the micelle core *via* hydrophobic group and facilitate the formation of rod or worm-like micelles at low surfactant concentration. The aqueous solutions of this worm like micelles behave like that of linear polymers and form shear responsive viscoelastic gel which attracts many researchers in recent years.<sup>2,3</sup> However, symmetrical tetraalkyl ammonium counter ions with varying alkyl chain length demand special attention because one can study two opposing effects in this series of ions *viz.*, the effect of progressively enhanced hydrophobicity and the effect of increasing dimension of the ions. Counter ion specific interactions (hydrophobic or hydrophilic) along with change in

Department of Chemistry, University of North Bengal, Raja Rammohanpur, Darjeeling, West Bengal 734 013, India. E-mail: ssahanbu@hotmail.com; Fax: +91-353-2699 001; Tel: +91-353-2699 425

† Electronic supplementary information (ESI) available. See DOI: 10.1039/c4ra03937h

hydration energy are also very important and this has been discussed in a number of recent reports.<sup>19–15</sup> Different types of organized assemblies are formed in surfactant systems on varying composition, concentration and environmental conditions *viz.*, pressure, temperature, additives and pH as well.<sup>1,3</sup> The fraction,  $\alpha$ , of the counterions of an ionic surfactant which are generally dissociated from the micelles, move to the bulk of the solution leaving the micelles electrically charged.<sup>16–18</sup> On the other hand, at a certain temperature, the aggregation number of ionic micelles depends only on the counterion concentrations in aqueous phase,  $C_{aq}$  which can be defined as:<sup>12</sup>

$$C_{aq} = F(S_t)[\alpha S_t + (1 - \alpha)S_m] \quad (1)$$

where  $S_t$  and  $S_m$  are the total and monomeric concentration of the surfactant molecules respectively present in the solution and the factor  $F(S_t) = 1/(1 - \theta)$ , where  $\theta$  relates to the volume fraction occupied by the micelles. The size of the ionic micelle in aqueous solution changes with the change of counterions and also with the electrolyte content of the surfactant solution.<sup>19</sup> The knowledge of the values of different thermodynamic parameters at different temperatures is also of utmost importance to understand the aggregation behaviour where the structure and interactivity of counterions also play considerable role.<sup>20</sup>

Sodiumdodecylbenzene sulfonate (SDBS) is a well known anionic surfactant widely used in the industry for manufacturing detergents, emulsions, degreaser and deinking agents and also for assisting dyeing processes in textile factories. Although the effect of the nature of counter ions of anionic surfactants is less significant than that of cationic surfactants, hydrophobic counter ions can bring about relatively stronger modification in the aggregation behaviour. Therefore a considerable number of literatures have been found<sup>2,14,15,18,21</sup> concerning micellar growth as affected by hydrotropic counter ions of both cationic and anionic surfactants. In this connection it may be anticipated that symmetrical organic counter ions might interact with the surfactant head groups more effectively *via* strong hydrophobic interaction with the terminal hydrocarbons of surfactant molecule. However, such ions with larger sizes could only approach towards the head group to a limited extent and fail to charge screen the head groups effectively and the micellization process becomes unfavourable. These two mutually opposite effects are operative in symmetrical tetraalkylammonium counter ions and the micellization process is regulated by one which prevails over the other. Therefore, for undertaking an in-depth study of the effect of size of the counter ion *vis-à-vis* its hydrophobicity on the aggregation behaviour of sodiumdodecylbenzene sulfonate, the set of symmetrical tetraalkyl ammonium counter ions with progressively larger groups may be an excellent model which one strives to investigate. This prompted us to synthesize dodecylbenzene sulfonates with tetramethyl, tetraethyl, tetrapropyl and tetrabutyl ammonium counter ions to study their aggregation properties along with the ammonium counter ion.

## Experimental

### Materials

All the surfactants with inorganic and organic counterions were prepared by the ion exchange technique starting from sodiumdodecylbenzene sulfonate following the procedure as mentioned below.<sup>17,18,23</sup> A solution of sodiumdodecylbenzene sulfonate in 1 : 1 (v/v) mixture of water and ethanol was prepared. The surfactant solution was then passed through an ion-exchange column (dimension of 40 cm by 2 sq. cm) containing strong ion exchange resin in its  $H^+$  form (Amberlite IR-120, 20–50 mesh, Loba Cheme, India). As a result, the aqueous solution of dodecylbenzene sulphonic acid is formed which then titrated immediately for neutralization with the hydroxides containing desired counterions. The above hydroxides were of AR grade procured either from Merck, India or Fluka, Switzerland. To enhance the extent of ion-exchange, flow rate was necessarily controlled in the column. To determine the extent of ion-exchange a portion of the sulphonic acid was titrated with standard NaOH solution which was quite satisfactorily found to be more than >99% in all cases. In order to prepare solid salts, water was removed from the solution by freeze drying and then keeping the solute under vacuum in a constant temperature of 313 K for 7 days and then the solid was finally dried in vacuum over  $P_2O_5$ . All the dodecylbenzene sulfonic acid salts (except tetrabutylammonium dodecyl benzene sulfonate (TBADBS)) were then purified by recrystallization twice from ethanol–water (1 : 1) mixture and finally dried in vacuum over  $P_2O_5$ . However, TBADBS salt appeared as waxy material and could not be crystallized from ethanol–water mixture. In order to remove residual water from the sample,  $P_2O_5$  was kept over the surfactant solution in isoctane ( $\geq 99.5\%$  from Merck, India) at 313 K for 7 days. The solvent was then removed and the TBADBS sample was used without further purification. Double distilled water having conductivity  $2 \mu S cm^{-1}$  were used throughout the experiment. For the determination of aggregation number, cetylpyridinium chloride (Fluka, Belgium) was used after recrystallization and puriss grade pyrene (Fluka, Switzerland) used as received.

It has already been mentioned in our earlier publication that commercial sodium dodecyl benzene sulfonate contains five different isomers<sup>22</sup> but the manufacturer did not mention any isomeric identification of the sample. The separation of isomeric forms and also their identifications are very difficult. In the present sample, however, the cmc values and the other parameters indicate the presence of  $6\phi C_{12}$  system as the major component. In order to obtain one isomeric composition with adequate purity (*viz.*,  $6\phi C_{12}$ ), repeated recrystallization was done of the ion-exchanged product. Therefore, it may be argued that the present surfactants are essentially  $6\phi C_{12}$  system of TMADBS, TEADBS, TPADBS and TBADBS.

### Methods

The critical micelle concentration (cmc) was determined by two methods *viz.*, surface tension and specific conductance methods. The Tensiometer (K9, KRÜSS; Germany) was used to

measure the surface tension at different temperatures by platinum ring detachment method at the air/water interface of the surfactant solution within the accuracy of  $\pm 0.1 \text{ mN m}^{-1}$ . The ring was cleaned several times before the measurements by double distilled water and also burning in alcohol flame and the solution was progressively diluted with water keeping the experimental solution in a double-wall container. Temperature was maintained by circulating water controlled by an auto-thermostat. Similarly, a highly calibrated electrical conductivity bridge (METTLER TOLEDO, Switzerland, uncertainty limit  $\pm 1\%$ ) was used to measure the specific conductance by progressively diluting the solution. Each measurement was repeated several times throughout the experiment to maintain the accuracy.

Steady-state fluorescence quenching method was used to determine the mean aggregation number of the surfactants by using a Fluorescence spectrophotometer (Photon Technology International Co., USA) with slit widths of 0.20 nm, 0.60 nm, 0.50 nm and 1.50 nm respectively. Pyrene solution ( $5 \mu\text{M}$ ) was used as a probe and CPC as a quencher. By exciting the samples at 332 nm, emission spectra of pyrene were obtained and the emission was measured in the range of 350–520 nm. The emission peak at 393 nm was considered for calculating micellar aggregation number.

## Results and discussion

### Critical micelle concentration (cmc)

As has been already mentioned that cmc is the most important parameter for an aqueous amphiphilic system to give the aggregation characteristics. We have determined the cmc of the systems by conductivity as well as surface tension measurements. The representative plots of surface tension and specific conductance as a function of concentration of tetramethylammonium dodecylbenzene sulfonate (TMADBS) at different temperatures are shown in Fig. 1 and 2 respectively (the plots of surface tension and specific conductance as a function of

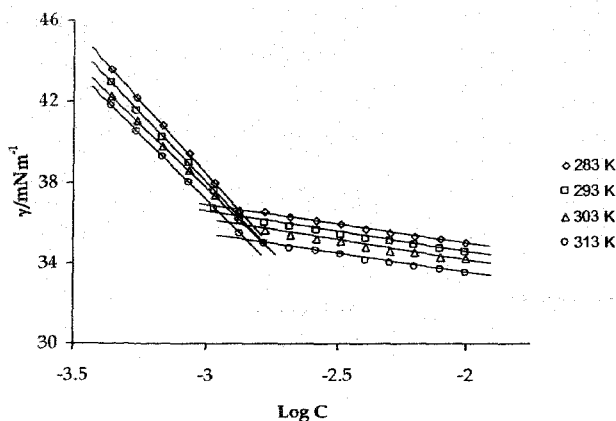


Fig. 1 Plot of surface tension vs. logarithm of concentration with different temperatures of tetramethylammonium dodecyl benzene sulfonate (TMADBS).

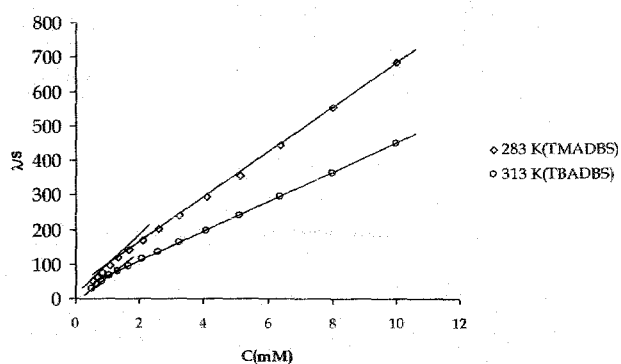


Fig. 2 Plot of specific conductance,  $\kappa$  vs. concentration with different temperatures of tetramethylammonium and tetrabutylammonium dodecyl benzene sulfonates.

concentration of TEADBS, TPADBS and TBADBS are provided as ESI†). To our knowledge, the aggregation data for TMADBS, TEADBS, TPADBS and TBADBS are recorded for the first time and, therefore, to check the reliability of the measured parameters, repeated experiments have been performed for both the measurements at least for three times and the mean values are recorded for reporting within the temperature range of 283–313 K at 5 K intervals. In Table 1, the cmc values of all the surfactant systems at various temperatures with varying counterions are shown along with different surface parameters and degree of ionization,  $\alpha$ . The values of  $\alpha$  have been determined from the ratio of the slopes of two linear fragments of conductivity-concentration plots *i.e.*, above and below the cmc. Though the values of  $\alpha$  does not change appreciably within the given temperature range (Table 1) the changes in cmc values with temperature for different surfactants are small but clearly detectable. At a given temperature, the cmc values of the surfactants follow the order  $\text{NH}_4^+ > \text{N}^+(\text{CH}_3)_4 > \text{N}^+(\text{C}_2\text{H}_5)_4 > \text{N}^+(\text{C}_3\text{H}_7)_4 > \text{N}^+(\text{C}_4\text{H}_9)_4$ . This variation of cmc can be explained in terms of the binding ability of the counterions. Among all the counter ions, the greater binding ability of  $\text{N}^+(\text{C}_4\text{H}_9)_4$  group to the polar head of DBS due to strong hydrophobic interactions reduces the electrostatic repulsive force considerably which leads to the formation of the micelle at the lowest concentration. The binding tendency decreases in the order  $\text{N}^+(\text{C}_4\text{H}_9)_4 > \text{N}^+(\text{C}_3\text{H}_7)_4 > \text{N}^+(\text{C}_2\text{H}_5)_4 > \text{N}^+(\text{CH}_3)_4 > \text{NH}_4^+$  and at a particular temperature the cmc values follow the reverse order. It shows that the result exactly follows the theoretical understanding pertaining to the micellization process. In Fig. 3, values of cmc are plotted against temperature (variation is small with temperature) for different surfactant systems. The plots give very shallow and broad minima in some cases (linear in other cases) within the given range of temperature. Similar result of linear or near linear variation of cmc with temperature for sodium dodecylbenzene sulfonate was also recorded by Hait *et al.*<sup>22</sup> and this is indeed somewhat different from the general parabolic trend of the plot with a shallow minimum shown by the surfactant like SDS, AOT *etc.*<sup>12–15</sup> In the similar range of temperature, the cmc decreases in above cases due to the

Table 1 Micellization and surface parameters of dodecyl benzene sulfonate having different tetraalkylammonium counterions at various temperatures ( $T/K$ ): cmc, maximum surface excess concentration, minimum areas per molecule and ionization degree

Counterion	$T/K$	cmc <sup>a</sup> /(mol dm <sup>-3</sup> × 10 <sup>-3</sup> )	$\Gamma_{\max}/\text{mol cm}^{-2} \times 10^6$	$A_{\min}/\text{nm}^2$	$\alpha$
<sup>b</sup> NH <sub>4</sub> <sup>+</sup>	283	2.28 (2.23)	3.12	0.53	0.74
	288	2.39 (2.36)	3.17	0.52	0.74
	293	2.41 (2.40)	3.23	0.51	0.73
	298	2.52 (2.48)	3.28	0.51	0.74
	303	2.68 (2.62)	3.38	0.49	0.78
	308	2.81 (2.82)	3.41	0.49	0.74
	313	2.80 (2.82)	3.49	0.47	0.74
(CH <sub>3</sub> ) <sub>4</sub> N <sup>+</sup>	283	1.31 (1.28)	3.11	0.53	0.71
	288	1.34 (1.29)	3.14	0.53	0.73
	293	1.34 (1.30)	3.17	0.52	0.74
	298	1.37 (1.31)	3.20	0.52	0.73
	303	1.39 (1.34)	3.28	0.51	0.74
	308	1.45 (1.37)	3.30	0.50	0.75
	313	1.49 (1.45)	3.36	0.49	0.73
(C <sub>2</sub> H <sub>5</sub> ) <sub>4</sub> N <sup>+</sup>	283	1.27 (1.27)	3.05	0.55	0.76
	288	1.28 (1.32)	3.03	0.55	0.77
	293	1.27 (1.22)	3.02	0.55	0.79
	298	1.30 (1.24)	3.10	0.54	0.79
	303	1.32 (1.25)	3.14	0.53	0.80
	308	1.32 (1.27)	3.19	0.52	0.79
	313	1.37 (1.29)	3.26	0.51	0.81
(C <sub>3</sub> H <sub>7</sub> ) <sub>4</sub> N <sup>+</sup>	283	1.08 (1.10)	3.02	0.55	0.79
	288	1.12 (1.15)	3.04	0.55	0.81
	293	1.14 (1.17)	3.07	0.54	0.81
	298	1.18 (1.19)	3.08	0.54	0.82
	303	1.23 (1.20)	3.11	0.53	0.82
	308	1.25 (1.23)	3.16	0.53	0.82
	313	1.31 (1.25)	3.19	0.52	0.82
(C <sub>4</sub> H <sub>9</sub> ) <sub>4</sub> N <sup>+</sup>	283	0.79 (0.75)	2.93	0.57	0.87
	288	0.84 (0.81)	2.96	0.56	0.84
	293	0.90 (0.96)	2.99	0.55	0.84
	298	0.93 (1.02)	2.99	0.56	0.83
	303	1.01 (1.03)	3.00	0.55	0.83
	308	1.06 (1.05)	3.01	0.55	0.82
	313	1.11 (1.12)	3.05	0.54	0.83

<sup>a</sup> The values in the parenthesis represent cmc determined by conductivity method. <sup>b</sup> The data are collected from ref. 21.

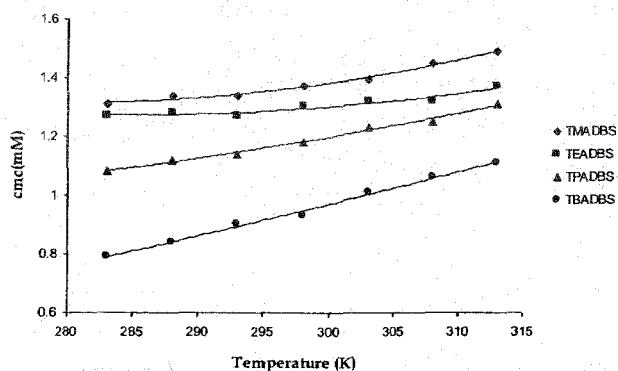


Fig. 3 Plot of cmc of different surfactants as a function of temperature.

decrease in degree of hydration of the hydrophilic group to attain the minima with increase in temperature. But for surfactants like dodecyl benzene sulfonate, this effect is not

pronounced. Here, the disruption of water cluster facilitates surfactant monomer solubilization and the result is an increase in cmc with increase in temperature.<sup>14</sup>

In fact, the effect of temperature on the cmc of surfactant in aqueous medium is quite interesting. An increase in temperature initially favours micellization process to occur at lower concentration of surfactant. This may be explained by the lower probability of the hydrogen bond formation with temperature resulting in the considerable decrease in hydrophilicity of the surfactant molecules. But further increase of temperature also causes disruption of the structured water surrounding the hydrophobic group, an effect that disfavours micellization.<sup>23,24</sup> The relative magnitude of these two opposing effects, therefore, determines whether the cmc increases or decreases over a particular temperature range. In general, from the data available, the minimum in the cmc–temperature curve appears to be around 298 K for ionics and around 323 K for nonionics.<sup>25</sup> For bivalent metal alkyl sulphates, the cmc appears to be practically independent of the temperature.<sup>26,27</sup> Though data on the effect

of temperature of zwitterionics are limited, they generally show a steady decrease in the cmc of alkyl betains with increase in temperature in the range 279–330 K.<sup>28,29</sup> Whether further increase in temperature will cause an increase in the cmc is not evident from the data.

The micellar aggregation number was determined by the fluorescence quenching method with pyrene as the probe and cetylpyridinium chloride (CPC) as the quencher. Five predominant vibronic bands are exhibited by pyrene in water in the fluorescence spectrum. It has been observed that the ratio of intensity of the first ( $I_1$  at 373 nm) and third peaks ( $I_3$  at 384 nm) is a sensitive parameter which characterizes the polarity of the probe environment. The solubilization of the probes in a more hydrophobic environment than water is indicated by a decrease in  $I_1/I_3$  values. The aggregation number of the surfactant micelles was determined by using Stern–Volmer equation and also considering the usual following assumptions:

(I) Static quenching occurs between the fluorescence probe and the quencher molecules so the quenching process does not affect the fluorescence lifetime of the probe.

(II) Fluorescent lifetime of the probe is much less than the residence times of the quencher and probe inside the micelle.

(III) The probability of finding a micelle with more than one probe molecule is negligible as because the quencher concentration is very low.

Following Poisson statistics<sup>30</sup> for the description of probe and the quencher among the micelles, the logarithm of  $I_0/I$  takes the form.

$$\ln \frac{I_0}{I} = \frac{[Q]N}{([S]_0 - \text{cmc})} \quad (2)$$

where,  $I_0$  and  $I$  are the intensities of fluorescence without and with quencher.  $[Q]$  is the bulk quencher concentration,  $N$  is the mean aggregation number and  $[S]_0$  is the total surfactant concentration. The aggregation number has been obtained by plotting  $\ln(I_0/I)$  as a function of quencher concentration.

In the present study, good linear plots for all the surfactants have been obtained satisfying the above equation. The representative plot of fluorescence measurement for the surfactant, TEADBS is shown in Fig. 4 (Similar plots of  $\ln(I_0/I)$  as a function of the concentration of CPC for TMADBS, TPADBS and TBADBS are provided as ESI†). The aggregation number measured at 298 K for all the surfactants in aqueous solutions are given in the Table 2. Fig. 5 shows the variation of aggregation number as a function of the size of the counter ions (in terms of the number of carbon atoms present in R of  $R_4N^+$ ). Aggregation number increases with alkyl chain length of counterions and gives maximum value for tetraethylammonium ion due to hydrophobic interactions of hydrocarbon exterior of the ions with exposed hydrocarbon to the micelle surface. However, for tetrapropyl and tetrabutyl ammonium ions aggregation become increasingly unfavorable due to steric hindrance for increasing counterion size. Here, comparison of aggregation number with the ionization degree might be interesting.

The ionization degrees of all the surfactants are shown in Table 1. The result shows that the values are quite high which

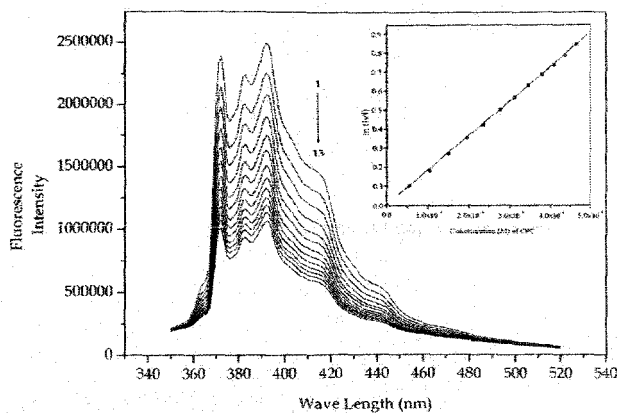


Fig. 4 Fluorescence spectra of pyrene with different concentration of CPC in mM (1) 0.0 mM (2) 0.0054 mM (3) 0.105 mM (4) 0.152 mM (5) 0.196 mM (6) 0.237 mM (7) 0.276 mM (8) 0.312 mM (9) 0.346 mM (10) 0.379 mM (11) 0.409 mM (12) 0.438 mM (13) 0.466 mM; inset – plot of  $\ln(I_0/I_3)$  vs.  $[CPC]$  to determine the aggregation number for TEADBS surfactants.

indicates that the tetraalkylammonium counter ions are strongly bound to the micelle surface. It is also observed that the counter ion ionization degree increases in the series  $NH_4^+ \leq N^+(CH_3)_4 < N^+(C_2H_5)_4 < N^+(C_3H_7)_4 < N^+(C_4H_9)_4$ . This means that, as expected, the binding increases as the counter ion becomes more and more hydrophobic in nature. The values of cmc also follow the opposite trend, i.e., as the fraction of counter ion binding increases, the micelles are formed at lower concentrations. However, the aggregation number does not follow the expected trend. At 298 K, the aggregation number becomes minimum in the case of  $NH_4^+$  counter ion. But as the alkyl groups are substituted for hydrogens, the aggregation number increases because of the formation of larger aggregates which is the consequences of the increased charged screening at higher counter ion binding capacity via stronger hydrophobic interactions with the micelles. This increasing trend of aggregation number continues up to the tetra ethylammonium ions. But for tetrapropyl and tetrabutyl ammonium ions, aggregation number progressively decreases as illustrated in Fig. 5. This is indeed interesting. Such a complex behaviour of micelle pertaining to the aggregation number with respect to the expected trend on the basis of cmc values is, however, available in the literature.<sup>22</sup> It has been shown that the effect of head group size of tetradecyltrialkylammonium bromide surfactant is very important pertaining to the observed reverse trend of the aggregation number with respect to its cmc. For these surfactants the values of both the cmc and aggregation number  $N$  decrease as the size of the tetraalkylammonium head group increases. This effect has been explained in terms of the geometric steric hindrance (overlap) between the large trialkylammonium head groups at the micellar surface.<sup>15,31</sup>

It seems apparent that in the present systems, as the hydrophobicity of counter ions increases, the counter ion binding/condensation increases due to increased hydrophobic interactions and eventually the cmc decrease. However,

Table 2 Thermodynamic parameters of micellization for dodecyl benzene sulfonate with different tetraalkylammonium counterions at various temperatures: Standard Gibbs's free energy, enthalpy, entropy and standard heat capacity and aggregation number

Counterion	T/K	$-\Delta G_m^0$ (kJ mol <sup>-1</sup> )	$\Delta H_m^0$ (kJ mol <sup>-1</sup> )	$\Delta S_m^0$ (J mol <sup>-1</sup> )	$-\Delta C_{pm}^0$ (J mol <sup>-1</sup> K <sup>-1</sup> )	Aggr. no.
NH <sub>4</sub> <sup>+</sup>	283	39.9	-6.3	118.7	405	08
	288	30.3	-7.7	78.5	488	
	293	31.0	-11.1	67.9	571	
	298	31.3	-13.2	60.7	654	
	303	30.5	-18.0	41.2	737	
	308	32.0	-21.1	35.4	820	
(CH <sub>3</sub> ) <sub>4</sub> N <sup>+</sup>	313	32.6	-25.2	23.6	903	17
	283	32.4	-21.5	38.34	141	
	288	32.5	-22.4	35.05	159	
	293	32.8	-23.3	32.21	177	
	298	33.4	-24.6	29.46	195	
	303	33.7	-25.6	26.47	213	
(C <sub>2</sub> H <sub>5</sub> ) <sub>4</sub> N <sup>+</sup>	308	33.8	-26.6	23.17	231	34
	313	34.7	-28.3	20.41	249	
	283	31.1	-12.2	66.68	108	
	288	31.5	-12.8	65.09	116	
	293	31.4	-13.1	62.50	124	
	298	31.8	-13.8	60.81	132	
(C <sub>3</sub> H <sub>7</sub> ) <sub>4</sub> N <sup>+</sup>	303	32.2	-14.3	59.08	140	27
	308	32.9	-15.1	58.02	148	
	313	33.0	-15.6	55.53	156	
	283	30.9	-8.5	79.05	81	
	288	30.9	-8.7	76.93	87	
	293	31.2	-9.1	75.34	93	
(C <sub>4</sub> H <sub>9</sub> ) <sub>4</sub> N <sup>+</sup>	298	31.6	-9.5	74.03	99	25
	303	31.9	-9.9	72.76	105	
	308	32.4	-10.3	71.64	111	
	313	32.7	-10.7	70.26	117	
	283	29.7	-17.6	43.07	245	
	288	30.9	-18.9	41.71	241	
(C <sub>4</sub> H <sub>9</sub> ) <sub>4</sub> N <sup>+</sup>	293	31.2	-19.8	38.93	237	25
	298	31.9	-20.9	36.96	233	
	303	32.1	-21.8	33.97	229	
	308	32.8	-23.1	31.74	225	
	313	33.0	-24.0	28.98	221	

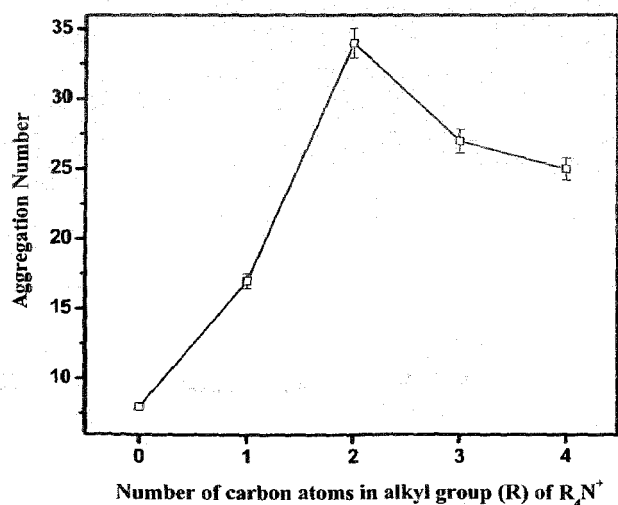


Fig. 5 Aggregation number change with the change of alkyl Chain length of R in R<sub>4</sub>N<sup>+</sup> counterion.

enhanced electrostatic charge screening of the head groups is incapable of increasing the aggregation number of the micelles for tetrapropyl and tetrabutylammonium counter ions. On the other hand, micellar surface probably does not offer sufficient surface area to accommodate all the N<sup>+</sup>R<sub>4</sub> counter ions that must bind to the micelle to ensure their stability. Therefore, the micelles become smaller in size and more in number to provide larger surface area in order to pack a large number of counter ions.

#### Energetics of micellar processes

Using pseudo-phase separation model,<sup>32-34</sup> different thermodynamic parameters have been determined by using temperature dependency of micellization. For uni-univalent ionic surfactants, the standard Gibbs free energy of micellization can be expressed as.

$$\Delta G_m^0 = (2 - \alpha)RT \ln X_{cmc} \quad (3)$$

here,  $\alpha$  is the counterion ionization constant for ionic surfactant and  $X_{cmc}$  is the cmc in the mole fraction scale. The standard enthalpy change of micellization  $\Delta H_m^0$  can also be obtained from the Gibbs-Helmholtz equation:<sup>20</sup>

$$\Delta H_m^0 = -RT^2[(2 - \alpha)(\partial \ln X_{cmc}/\partial T)_P - \ln X_{cmc}(\partial(2 - \alpha)/\partial T)_P] \quad (4)$$

The second term of the equation, which is quite small as compared to the first term, is difficult to determine because the values of  $\alpha$  do not follow any general trend of variation as a function of temperature and also due to polydispersity of the micelle.<sup>35,36</sup> Therefore, neglecting the second term of the above equation takes the form.

$$\Delta H_m^0 = -RT^2[(2 - \alpha)(\partial \ln X_{cmc}/\partial T)_P] \quad (5)$$

Further, the values of  $\partial \ln X_{cmc}/\partial T$  in eqn (5) can be obtained by fitting the curve of  $\ln X_{cmc}$  vs.  $T$  to a second order polynomial in the following way:

$$\ln X_{cmc} = a + bT + cT^2 \quad (6)$$

where  $a$ ,  $b$  and  $c$  are the polynomial coefficients respectively.

$$(\partial \ln X_{cmc}/\partial T) = b + 2cT \quad (7)$$

The free energy of micellization,  $\Delta S_m^0$  and the specific heat capacity of micellization,  $\Delta_{mic}C_p^0$  are also determined by the following expressions.

$$\Delta S_m^0 = (\Delta H_m^0 - \Delta G_m^0)/T \quad (8)$$

$$\Delta_{mic}C_p^0 = (\partial \Delta H_m^0/\partial T)_P \quad (9)$$

Here, in the Table 2, the various thermodynamic quantities are presented. All the calculated properties change with the variation in temperature and counterion present with the surfactant molecule. For all the micellization processes large negative values of  $\Delta G_m^0$  support that the micellization processes are thermodynamically favourable. On the other hand, the plot of  $\Delta G_m^0$  as a function of alkyl chain length in the Fig. 6 suggests that with increase in alkyl chain length of the counterion, the spontaneity of the process decreases first and then remains almost constants. Furthermore, with increase in temperature, the spontaneity of the process increases by increasing  $\Delta G_m^0$  values in general. The negative  $\Delta H_m^0$  values suggest that micellization is an exothermic process and for all the surfactants it can be explained in terms of the size and hydration of the counter ions.<sup>17,18,21</sup> Among the different factors proposed by researchers, the hydrocarbon chains with water molecules have the major contribution to the thermodynamic factors responsible for dodecylbenzene sulfonate aggregation.<sup>37,38</sup> Usually the micellization process results in an appreciable positive entropy change *via* (i) disruption of the hydrophobic hydration surrounding the hydrophobic tails of surfactant molecules and (ii) increased degree of freedom of the tails in the oil-like interior of micelles. Plot of  $\Delta S_m^0$  as a function of alkyl chain length

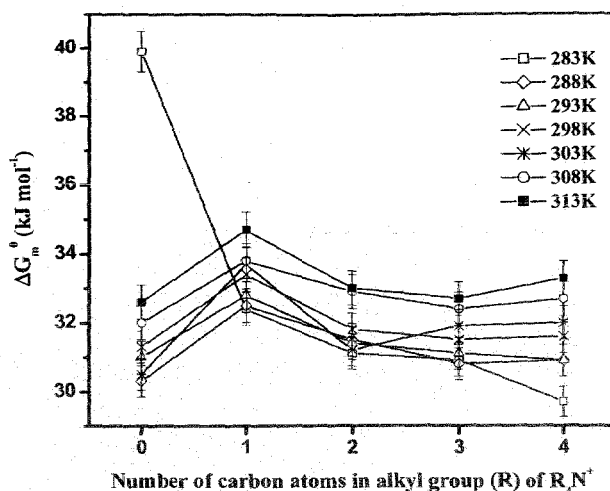


Fig. 6 Gibbs free energy change with the change of alkyl chain length of R in  $R_4N^+$  counterion.

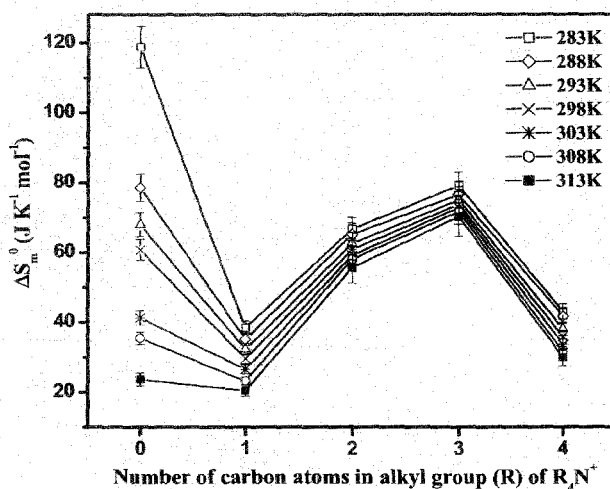


Fig. 7 Entropy change with the change of alkyl chain length of R in  $R_4N^+$  counterion.

(Fig. 7) suggests that positive entropy value first increases, reaches a maximum and then decreases with alkyl chain length which may be explained with the increase in the hydrophobic effect and the binding capabilities of the alkyl chain length and after that due to the bulkiness or large size of the tetrabutyl group, decrease in entropy is observed. An opposite effect is observed as usual for  $\Delta H_m^0$  (Fig. 8). For tetraalkylammonium counterion, the hydration number decrease effect is also a contributing factor for the micellization process. It has been observed that  $\Delta S_m^0$  decreases systematically with increasing temperature of a particular type of counterion that may be explained by the disruption of ordered arrangement of water dipoles around the amphiphilic part of the surfactant molecules. Heat capacity of micelle formation,  $\Delta_{mic}C_p^0$  is the expression for the effective interactions associated with

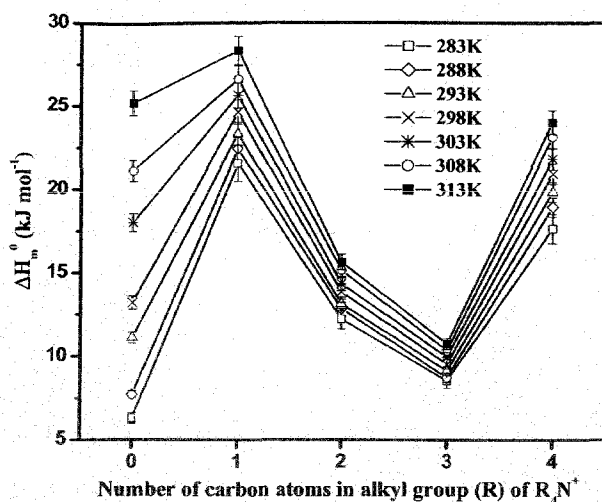


Fig. 8 Entropy change with the change of alkyl chain length of R in  $R_4N^+$  counterion.

hydrocarbon chains. The general trend in heat capacity values of a surfactant increases with increase in temperature due to solvation of ions upon micellization. Here, the dodecylbenzene sulfonate shows similar trend and the values vary from  $-81 \text{ J mol}^{-1} \text{ K}^{-1}$  to  $-249 \text{ J mol}^{-1} \text{ K}^{-1}$  which is quite similar to the other surfactants within the temperature range 283–313 K suggesting execution of hydrophobic interaction by the hydrocarbon tail followed by dehydration in greater extent<sup>15,22</sup> and with the change of counterions, the reduction of number of water molecules in counterion solvation shell occurs.

### Surface properties

The surface excess concentration maximum ( $\Gamma_{\max}$ ) and minimum areas per molecule ( $A_{\min}$ ) in the interface (aqueous/air) was calculated by the following expressions:<sup>14,15,21</sup>

$$\Gamma_{\max} = (1/2.303n'RT)(-\partial\gamma/\partial \log C) \quad (10)$$

$$A_{\min} = 1/(N\Gamma) \quad (11)$$

where  $\gamma$  expresses surface tension,  $N$  is the Avogadro's number and  $C$  and  $n'$  are the surfactant concentration and number of particles per surfactant molecules respectively. For DBS moiety with different counterions, the  $n'$  has the value of two like univalent electrolytes. Generally, the  $\Gamma_{\max}$  value decreases with increase in temperatures, but an opposite trend is also observed<sup>20</sup> especially in presence of additives. At a fixed temperature, the  $\Gamma_{\max}$  values changes in the order:  $(\text{CH}_3)_4\text{N}^+ > (\text{C}_2\text{H}_5)_4\text{N}^+ > (\text{C}_3\text{H}_7)_4\text{N}^+ > (\text{C}_4\text{H}_9)_4\text{N}^+$  which is due to the head group's accessibility towards counterions followed by hydration of the ions in reverse order. Further, with increase in temperature, the surfactant molecules try to form a closely packed monolayer film due to the decreased repulsion of the oriented head groups which is well established by the fact of decreasing  $A_{\min}$  value is also well supported in the literature.<sup>37,39</sup>

## Conclusion

Different tetraalkylammonium cation changes the cmc values of dodecyl benzene sulfonate moiety to a great extent in aqueous solution. With increase in the size of tetraalkylammonium counter ion the cmc decreases owing to the increase in hydrophobicity of the head groups. Also, with increase in size, the hydration of the head groups decreases which can effectively associate the monomer into micelle at lower surfactant concentration. However, expected reverse trend of aggregation number suffers a nudge for tetrapropyl and tetrabutylammonium counter ions because of their steric hindrance due to very large sizes, which impede their binding to the micelles and limit the values of aggregation number. The surface parameter values suggest that with increase in temperature the formation of close packed monolayer film formation occurs due to repulsion of the head groups oriented at the air/liquid interface of the surfactant solution. The thermodynamic parameters calculated by using pseudo-phase model also successfully explains the thermodynamics of micelle formation of dodecylbenzene sulfonate as a function of chain length and bulkiness of the head groups associated with the counterions.

## Acknowledgements

Financial assistance from Science & Engineering Research Board (SERB), DST, Govt. of India (Sanction no. SB/S1/PC-034/2013) is gratefully acknowledged.

## References

- H. Yin, S. Lei, S. Zhu, J. Huang and J. Ye, *Chem.-Eur. J.*, 2006, 12, 2825–2835.
- D. F. Evans and H. Wennerstrom, *The Colloidal Domain Where Physics, Chemistry, Biology and Technology Meet*, New York, 1994.
- S. K. Saha, M. Jha, M. Ali, A. Chakraborty, G. Bit and S. K. Das, *J. Phys. Chem. B*, 2008, 112, 4642–4647.
- S. P. Moulik, *Curr. Sci.*, 1996, 71, 368–376.
- H. Shi, W. Ge, H. Oh, S. M. Pattison, J. T. Huggins, Y. Talmon, S. D. J. Hart, R. Raghavan and J. L. Zakin, *Langmuir*, 2011, 27, 5806–5813.
- S. Bardhan, K. Kundu, S. Das, M. Poddar, S. K. Saha and B. K. Paul, *J. Colloid Interface Sci.*, 2014, 430, 129–139.
- B. Kar, S. Bardhan, S. Kundu, S. K. Saha, B. K. Paul and S. Das, *RSC Adv.*, 2014, 4, 21000–21009.
- R. Kaur, S. Kumar, V. K. Aswal and R. K. Mahajan, *Colloid Polym. Sci.*, 2012, 290, 127–139.
- H. Liu, F. Li, B. Xu, G. Zhang, F. Han, Y. Zhou, X. Xin and B. Xu, *J. Surfactants Deterg.*, 2012, 15, 709–713.
- M. Pisacik, F. Devinsky and I. Lacko, *Acta Facult. Pharm. Univ. Comenianae*, 2003, 53, 184–192.
- S. Shimizu, P. A. R. Pires and O. A. El Seoud, *Langmuir*, 2004, 20, 9551–9559.
- P. C. Griffiths, A. Paul, R. K. Heenan, J. Penfold, R. Ranganathan and B. L. Bales, *J. Phys. Chem. B*, 2004, 108, 3810–3816.

- 13 A. Paul, P. C. Griffiths, E. Pettersson, P. Stilbs, B. L. Bales, R. Zana and R. K. Heenan, *J. Phys. Chem. B*, 2005, **109**, 15775–15779.
- 14 A. Chakraborty, S. Chakraborty and S. K. Saha, *J. Dispersion Sci. Technol.*, 2007, **28**, 984–989.
- 15 A. Chakraborty, S. K. Saha and S. Chakraborty, *Colloid Polym. Sci.*, 2008, **286**, 927–934.
- 16 S. H. Yalkowsky, *Solubility and Solubilization in aqueous Media*, Oxford University Press, New York, 1999.
- 17 C. A. Bunton, F. Nome, F. H. Quina and L. S. Romsted, *Acc. Chem. Res.*, 1991, **24**, 357–364.
- 18 B. Jönsson, B. Lindmann, K. Holmberg and B. Kronberg, *Surfactants and Polymers in Aqueous Solution*, John Wiley, Chichester, UK, 1998.
- 19 B. L. Bales, *J. Phys. Chem. B*, 2001, **105**, 6798–6804.
- 20 A. Chatterjee, S. P. Moulik, S. K. Sanyal, B. K. Mishra and P. M. Puri, *J. Phys. Chem. B*, 2001, **105**, 12823–12831.
- 21 S. Chakraborty, A. Chakraborty, M. Ali and S. K. Saha, *J. Dispersion Sci. Technol.*, 2010, **31**, 209–215.
- 22 S. K. Hait, P. R. Majhi, A. Blume and S. P. Moulik, *J. Phys. Chem. B*, 2003, **107**, 3650–3658.
- 23 M. E. Mahmood and D. A. F. Al-Koofee, *Global J. Sci. Frontier Res. Chem.*, 2013, **13**, 1–7.
- 24 E. Mohajeri and G. D. Noudeh, *E-J. Chem.*, 2012, **9**, 2268–2274.
- 25 H.-U. Kim and K.-H. Lim, *Bull. Korean Chem. Soc.*, 2003, **24**, 1449–1454.
- 26 A. Zapf, R. Beck, G. Platz and H. Hoffmann, *Adv. Colloid Interface Sci.*, 2003, **100–102**, 349–380.
- 27 Y. Moroi, K. Motomura and R. Matuura, *J. Colloid Interface Sci.*, 1974, **46**, 111–117.
- 28 A. Morori, *Micelles: Theoretical and Applied Aspects*, Plenum Press, New York, 1992.
- 29 M. Yaseen, Y. Wang, T. J. Su and J. R. Lu, *J. Colloid Interface Sci.*, 2005, **288**, 361–370.
- 30 E. Rodenas and E. Pérez-Benito, *J. Phys. Chem.*, 1991, **95**, 4552–4556.
- 31 M. Benraou, B. L. Bales and R. Zana, *J. Phys. Chem. B*, 2003, **107**, 13432–13440.
- 32 R. Zana, *Langmuir*, 1996, **12**, 1208–1211.
- 33 H.-U. Kim and K.-H. Lim, *Colloids Surf., A*, 2004, **235**, 121–128.
- 34 A. González-Pérez, J. Czapkiewicz, J. L. Del Castillo and J. R. Rodrigues, *Colloid Polym. Sci.*, 2004, **282**, 1359–1364.
- 35 C. Vautier-Giongo and B. L. Bales, *J. Phys. Chem. B*, 2003, **107**, 5398–5403.
- 36 K.-H. Kang, H.-U. Kim and K.-H. Lim, *Colloids Surf., A*, 2001, **189**, 113–121.
- 37 K. Weckström, K. Hanu and J. B. Rosenholm, *J. Chem. Soc., Faraday Trans.*, 1994, **90**, 733–738.
- 38 A. Rodríguez, M. Muñoz, M. M. Graciani and M. L. Moyá, *J. Colloid Interface Sci.*, 2006, **298**, 942–951.
- 39 A. Chakraborty and S. K. Saha, *Surfactant Aggregation and Behavior of Dyes in the Organized Media*, VDM Verlag Dr. Müller, Germany, 2010.

